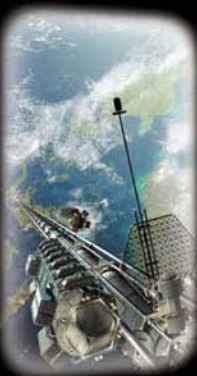




Non-Rocket Space Launch and Flight



Alexander A. Bolonkin

Non-Rocket Space Launch and Flight

Elsevier Internet Homepage

<http://www.elsevier.com>

Consult the Elsevier homepage for full catalogue information on all books, journals and electronic products and services.

Elsevier Titles of Related Interest

RELIABILITY OF LARGE SYSTEMS

Krzysztof Kolowrocki (Ed.)

2004, ISBN 0-08-044429-6

www.elsevier.com/locate/isbn/0080444296

COMPREHENSIVE STRUCTURAL INTEGRITY (10 vols.)

I. Milne, R.O. Ritchie, B. Karihaloo (Eds)

2003, ISBN 0-08-043749-4

www.elsevier.com/locate/isbn/0080437494

LONG-TERM DURABILITY OF STRUCTURAL MATERIALS

P.J.M. Monteiro, K.P. Chong, J. Larsen-Basse, K. Komvopoulos (Eds)

2001, ISBN 0-08-043890-3

www.elsevier.com/locate/isbn/0080438903

Related Journals

The following journals related to reliability and safety can all be found at

www.sciencedirect.com

Automatica

Engineering Failure Analysis

Journal of Loss Prevention in the Process Industries

Measurement

Probabilistic Engineering Mechanics

Reliability Engineering and System Safety

Safety Science

Structural Safety

To Contact the Publisher

Elsevier welcomes enquiries concerning publishing proposals: books, journal special issues, conference proceedings, etc. All formats and media can be considered. Should you have a publishing proposal you wish to discuss, please contact, without obligation, the commissioning editor responsible for Elsevier's materials science and engineering books-publishing programme:

Graham Hart

Commissioning Editor, Materials Science & Engineering

Elsevier Limited

The Boulevard, Langford Lane

Tel.: +44 1865 84 3197

Kidlington, Oxford

Fax: +44 1865 84 3987

OX5 1GB, UK

E-mail: g.hart@elsevier.com

General enquiries including placing orders, should be directed to Elsevier's Regional Sales Offices – please access the Elsevier Internet Homepage for full contact details.

Non-Rocket Space Launch and Flight

Alexander A. Bolonkin

*Dr. Sci., Professor of Russian and American Universities
Former Senior Researcher of NASA
USA Air Force and Russian Space Industry*



ELSEVIER

Amsterdam • Boston • Heidelberg • London • New York • Oxford
Paris • San Diego • San Francisco • Singapore • Sydney • Tokyo

ELSEVIER B.V.
Radarweg 29
P.O. Box 211, 1000 AE
Amsterdam The Netherlands

ELSEVIER Inc.
525 B Street, Suite 1900
San Diego, CA 92101-4495
USA

ELSEVIER Ltd
The Boulevard, Langford Lane
Kidlington, Oxford OX5 1GB
UK

ELSEVIER Ltd
84 Theobald's Road
London WC1X 8RR
UK

© 2006 Elsevier Ltd. All rights reserved.

This work is protected under copyright by Elsevier Ltd., and the following terms and conditions apply to its use:

Photocopying

Single photocopies of single chapters may be made for personal use as allowed by national copyright laws. Permission of the Publisher and payment of a fee is required for all other photocopying, including multiple or systematic copying, copying for advertising or promotional purposes, resale, and all forms of document delivery. Special rates are available for educational institutions that wish to make photocopies for non-profit educational classroom use.

Permissions may be sought directly from Elsevier's Rights Department in Oxford, UK; phone: (+44) 1865 843830, fax: (+44) 1865 853333, e-mail: permissions@elsevier.com. Requests may also be completed on-line via the Elsevier homepage (<http://www.elsevier.com/locate/permissions>).

In the USA, users may clear permissions and make payments through the Copyright Clearance Center, Inc., 222 Rosewood Drive, Danvers, MA 01923, USA; phone: (+1) (978) 7508400, fax: (+1) (978) 7504744, and in the UK through the Copyright Licensing Agency Rapid Clearance Service (CLARCS), 90 Tottenham Court Road, London W1P 0LP, UK; phone: (+44) 20 7631 5555; fax: (+44) 20 7631 5500. Other countries may have a local reprographic rights agency for payments.

Derivative Works

Tables of contents may be reproduced for internal circulation, but permission of the Publisher is required for external resale or distribution of such material. Permission of the Publisher is required for all other derivative works, including compilations and translations.

Electronic Storage or Usage

Permission of the Publisher is required to store or use electronically any material contained in this work, including any chapter or part of a chapter.

Except as outlined above, no part of this work may be reproduced, stored in a retrieval system or transmitted in any form or by any means, electronic, mechanical, photocopying, recording or otherwise, without prior written permission of the Publisher.

Address permissions requests to: Elsevier's Rights Department, at the fax and e-mail addresses noted above.

Notice

No responsibility is assumed by the Publisher for any injury and/or damage to persons or property as a matter of products liability, negligence or otherwise, or from any use or operation of any methods, products, instructions or ideas contained in the material herein. Because of rapid advances in the medical sciences, in particular, independent verification of diagnoses and drug dosages should be made.

First edition 2006

ISBN-13: 978-0-08044-731-5

ISBN-10: 0-080-44731-7

Typeset by Charon Tec Ltd, Chennai, India
www.charontec.com

Printed in Great Britain.

06 07 08 09 10 10 9 8 7 6 5 4 3 2 1

Working together to grow
libraries in developing countries

www.elsevier.com | www.bookaid.org | www.sabre.org

ELSEVIER

BOOK AID
International

Sabre Foundation

To my wife Olga Lyubavina

This page intentionally left blank

Contents

Abstract	xiii
Preface	xv
1 Space elevator, transport system for space elevator, and tether system	1
1.1 Brief history	1
1.2 Short description	2
1.3 Transport system for the space elevator	5
1.4 Free trip to space (Project 1)	8
1.5 Delivery system for free round trip to Mars (Project 2)	24
1.6 Free trip to Moon (Project 3)	29
1.7 Discussion	31
1.8 Conclusions	33
1.9 Tether system	34
2 Cable space accelerator	39
2.1 Introduction	39
2.2 Description of suggested launcher	40
2.3 Theory of the cable launcher	42
2.4 Projects	55
2.5 General discussion	58
3 Circle launcher and space keeper	59
3.1 Introduction	61
3.2 Description of circle launcher	61
3.3 Theory of circle launcher	67
3.4 Case studies	75
3.5 Discussion, summary, and conclusions	81
4 Optimal inflatable space towers	83
4.1 Introduction	83
4.2 Description of innovation and problem	85

4	Theory of inflatable towers	89
4.3	Theory of inflatable towers (all equations are given in metric system)	89
4.4	Projects	92
4.5	Conclusion	105
5	Kinetic space towers	107
5.1	Introduction	107
5.2	Description of suggested launcher	108
5.3	Theory of the kinetic tower and launcher	111
5.4	Projects	121
5.5	Discussion	122
6	Gas tube hypersonic launcher	125
6.1	Introduction	126
6.2	Description	127
6.3	Methods of estimation and results of computation	129
6.4	Production cost of delivery	138
6.5	Advantages of the proposed space launcher	143
6.6	Discussion	145
7	Earth–Moon cable transport system	147
7.1	Introduction	147
7.2	Brief history	147
7.3	Brief description, theory, and computation of innovations	148
7.4	Theory of optimal cable from earth to moon	150
7.5	Technical parameters of projects	151
7.6	Conclusion	154
8	Earth–Mars cable transport system	157
8.1	Introduction	157
8.2	Brief description	158
8.3	Theory of Earth–Mars equal stress cable	159
8.4	Project	160
8.5	Conclusion	162
9	Kinetic anti-gravitator	165
9.1	Introduction	166
9.2	Brief description of the installation	167
9.3	Theory of the kinetic anti-gravitator	171
9.4	Advantages of offered method	179
9.5	Applications	179
9.6	Discussion	184
9.7	Conclusion	185

10	Centrifugal space launchers	187
10.1	Introduction	188
10.2	Description of innovative launcher	189
10.3	Theory of the sling launcher	193
10.4	Projects	197
10.5	General discussion	205
11	Asteroids as propulsion system of space ships	209
11.1	Introduction	209
11.2	Connection method	210
11.3	Project	218
11.4	Discussion	218
11.5	Conclusion	221
12	Multi-reflex propulsion systems for space and air vehicles and energy transfer for long distance	223
12.1	Introduction	223
12.2	Description of innovation	225
12.3	Theory (estimation) of multi-reflex launching and beam transfer	230
12.4	Discussion	240
13	Electrostatic solar wind propulsion	245
13.1	Introduction	245
13.2	Brief description of the propulsion system	247
13.3	Basic theories of the solar wind installation and main estimations and computations	252
13.4	Discussion	265
13.5	Conclusion	266
14	Electrostatic utilization of asteroids for space flight	271
14.1	Introduction	271
14.2	Description of utilization	272
14.3	Theory and computation (in metric system)	273
14.4	Project	278
14.5	Discussion	279
15	Electrostatic levitation on the earth and artificial gravity for space ships and asteroids	281
15.1	Introduction	281
15.2	Brief description of innovation	282
15.3	Theory of an electrostatic lift force and results of computations (in metric system)	285

15.4	Projects	299
15.5	Discussion	301
16	Guided solar sail and energy generator	303
16.1	Description of method and innovations	303
16.2	Description of innovation and their advantages	305
16.3	Further development	307
17	Radioisotope space sail and electro-generator	309
17.1	Description of method and innovations	309
17.2	General information about the isotope sail	310
17.3	Description of new method, installation, and innovation	311
17.4	Improvements to the radioisotope sail	312
17.5	Possibility of electric power	312
17.6	Equation for computation of conventional IsoSail	313
17.7	Conclusion	315
18	Electrostatic solar sail	317
18.1	Introduction	317
18.2	Brief description of the innovations	318
18.3	Theory of estimation and computation	320
19	Utilization of space	327
19.1	Recombination space jet propulsion engine	327
19.2	Utilization of high-altitude mirror for lighting in local Earth areas	330
19.3	Electronic sail	334
19.4	In outer space without a space suit?	335
19.5	Electrostatic space radiator	336
Attachments: Non-conventional and non-rocket flight on Earth		
1	Air cable transport and bridges	341
A1.1	Introduction	341
A1.2	Short description of installation	343
A1.3	Advantages	345
A1.4	Formulas for estimation and computation (in metric system)	346
A1.5	Cable problems	349
A1.6	Data which can be used for computation	352
A1.7	Projects	352
A1.8	Conclusion	357

2	High-speed catapult aviation	359
A2.1	Introduction	359
A2.2	Brief description of the innovation	360
A2.3	Theory of KV and a general estimation of flight data (in metric system)	361
A2.4	Advantages	365
A2.5	Project	367
A2.6	Discussion of problems	368
3	Light multi-reflex engine	371
A3.1	Introduction	371
A3.2	Description of innovation	373
A3.3	Theory of the multi-reflex engine	375
A3.4	Discussion	381
4	Optimal trajectories of air and space vehicles	383
A4.1	Introduction	384
A4.2	General equations	385
A4.3	Flight with a small change of vehicle mass and flight path angle	386
A4.4	Statement of the problem	388
A4.5	Optimal wing area	397
A4.6	Estimation of flight range	401
A4.7	Optimal engine control for constant flight pass angle	405
A4.8	Solution	406
A4.9	Simultaneous optimization of the path angle and fuel consumption	408
A4.10	Application to aircraft, rocket missiles, and cannon projectiles	410
A4.11	General discussion and conclusion	418
5	High-efficiency transfer of mechanical energy	423
A5.1	Introduction	423
A5.2	Description of innovation	424
A5.3	Theory of air energy transfer (in metric system)	425
A5.4	Discussion	429
A5.5	Advantages of proposed method	430
A5.6	Defect	430
6	Optimal aircraft thrust angles	431
A6.1	Introduction	432
A6.2	General methodology	433
A6.3	OTA for takeoff and landing	435
A6.4	Optimal angle of thrust vector in horizontal flight (cruise regime)	438
A6.5	Climb and descent regimes	442
A6.6	Turning of airplane	443
A6.7	Discussion	444
A6.8	Conclusions	446

Appendix 1 System of mechanical and electrical units and other useful values	447
1.1 System of mechanical and electrical units	447
1.2 Fundamental physical constants	448
1.3 Astronomical data	448
1.4 Density of gases at normal pressure and temperature 0°C in kg/m ³	449
1.5 Parameters of earth atmosphere (relative density and temperature)	449
General references	451
Index	459

Abstract

At present, rockets are used for launches and flights into space. They have been intensively developed since World War II when the German engineer F. Von Braun designed the first long-distance rocket FAU-2. In the subsequent 60 years liquid and solid rockets reached the peak of their development. Their main shortcomings are: (1) very high cost of space launching \$20,000–50,000/kg; (2) large fuel consumption; (3) fuel storage problems because the oxidizer and fuel (for example, oxygen and hydrogen) require cryogenic temperatures, or they are poisonous substances (for example, nitric acid, N_2O_3).

In the past years the author and other scientists have published a series of new methods which promise to revolutionize space launching and flight. These include the cable accelerator, circle launcher and space keeper, space elevator transport system, space towers, kinetic towers, the gas-tube method, sling rotary method, asteroid employment, electromagnetic accelerator, tether system, Sun and magnetic sails, solar wind sail, radioisotope sail, electrostatic space sail, laser beam, kinetic anti-gravitator (repulsator), Earth–Moon or Earth–Mars non-rocket transport system, multi-reflective beam propulsion system, electrostatic levitation, etc.

There are new ideas in aviation which can be useful for flights in planet atmosphere. Some of these have the potential to decrease launch costs thousands of times, other allow the speed and direction of space apparatus to be changed without the spending of fuel.

The author summarizes some revolutionary methods for scientists, engineers, students, and the public. He seeks attention from the public, engineers, inventors, scientists for these innovations and he hopes the media, government, and the large aerospace companies will increase research and development activity in these areas.

This page intentionally left blank

Preface

The new methods are only proposals. There are a lot of problems that must be researched, modeled, and tested before these ideas can be developed, designed, built, and explored. Most of the ideas are described in the following way: there is a brief explanation of the idea including its advantages and shortcomings, then methods estimation and computations of the main system parameters, and a brief description of projects, including estimations of the main parameters.

The first (Chapters 1–19) and third (Appendix) parts are in a popular form accessible to the wider public, the second part (Attachments) requires some mathematical and scientific knowledge of technical graduate students. This book gives the main physical data and technical equations in attachment which will help researchers, engineers, students, and readers make estimations for their projects. Also inventors will find the extensive field on inventions and innovations in this book.

The author has published a lot of new ideas and articles about non-rocket launches and flights in recent years (see General references at the end of this book). That is, the way he seeks to draw more attention to new ideas than the old ideas that are covered in many publications and are well known to scientist and the public.

This book mainly contains material from the author's articles published in the last few years.



Alexander A. Bolonkin

CHAPTER 1

Space Elevator, Transport System for Space Elevator, and Tether System

Summary

This chapter brings together research on the space elevator and a new transportation system for it. This transportation system uses mechanical energy transfer and requires only minimal energy so that it provides a “Free Trip” into space. It uses the rotary energy of planets. This chapter contains the theory and results of computations for the following projects: (1) Transport System for Space Elevator. This low-cost project will accommodate 100,000 tourists annually. (2) Delivery System for Free Round Trip to Mars (for 2000 people annually). (3) Free Trips to the Moon (for 10,000 tourists annually).

The projects use artificial materials like nanotubes and whiskers that have a ratio of strength to density equal to 4 million meters. At present scientific laboratories receive nanotubes that have this ratio equal to 20 million meters.

1.1 Brief history

The concept of the space elevator first appeared in 1895 when a Russian scientist, Konstantin Tsiolkovsky, considered a tower that reached a geosynchronous orbit. The tower was to be built from the ground up to an altitude of 35,800 kilometers (geostationary orbit). Comments from Nikola Tesla suggest that he may have also conceived such a tower. His notes were sent behind the *iron curtain* after his death.

Tsiolkovsky’s tower would be able to launch objects into orbit without a rocket. Since the elevator would attain orbital velocity as it rode up the cable, an object released at the tower’s top would also have the orbital velocity necessary to remain in geosynchronous orbit.

Building from the ground up, however, proved an impossible task; there was no material in existence with enough compressive strength to support its own weight under such conditions. It took until 1957 for another Russian scientist, Yuri N. Artsutanov, to conceive of a more feasible scheme for building a space tower. Artsutanov suggested using a geosynchronous satellite as the base from which to construct the tower. By using a counterweight, a cable would be lowered from geosynchronous orbit to the surface of Earth while the counterweight was extended from the satellite away from Earth, keeping the center of mass of the cable motionless relative to Earth. Artsutanov published his idea in the Sunday supplement of *Komsomolskaya Pravda* in 1960. He also proposed tapering the cable thickness so that the tension in the cable was constant – this gives a thin cable at ground level, thickening up towards geostationary Earth orbit (GEO) (http://www.liftport.com/files/Artsutanov_Pravda_SE.pdf). An American scientist, Jerome Pearson, designed a tapered cross-section that would be better suited to building the tower. The weight of the material needed to build the tower would have been thousands of tons.

In 1975, Arthur C. Clarke introduced the concept of a space elevator to a broader audience in his 1978 novel, *The Fountains of Paradise*.

David Smitherman of National Aeronautics and Space Administration (NASA)/Marshall's Advanced Projects Office has compiled plans for an elevator. His publication, *Space Elevators: An Advanced Earth-Space Infrastructure for the New Millennium* (http://flightprojects.msfc.nasa.gov/fd02_elev.html), is based on findings from a space infrastructure conference held at the Marshall Space Flight Center in 1999.

Space elevator proponents are planning competitions for space elevator technologies (<http://msnbc.msn.com/id/5792719/>), similar to the Ansari X Prize. Elevator: 2010 (<http://www.elevator2010.org/>) will organize annual competitions for climbers, ribbons, and power-beaming systems. The Robolympics Space Elevator Ribbon Climbing (<http://robolympics.net/rules/climbing.shtml>) organizes climber–robot building competitions.

1.2 Short description

The space elevator is a cable installation which connects the Earth's surface to a GEO above the Earth 37.786 km in altitude (Fig. 1.1).

The GEO is a 24-h orbit and stays over the same point above the equator as the Earth rotates on its axis. The installation center of mass is at or above this altitude. The space elevator has a counterweight, which allows it to have its center of gravity at or above GEO, and climbers. Once sent far enough, climbers would be accelerated further by the planet's rotation. A space elevator, also known as a space bridge, is one of the technology concepts that are aimed at improving access to space. Also called a geosynchronous orbital tether, it is one kind of skyhook.

The elevator would have to be built of a material that could endure tremendous stress while also being lightweight, cost-effective, and manufacturable. A considerable

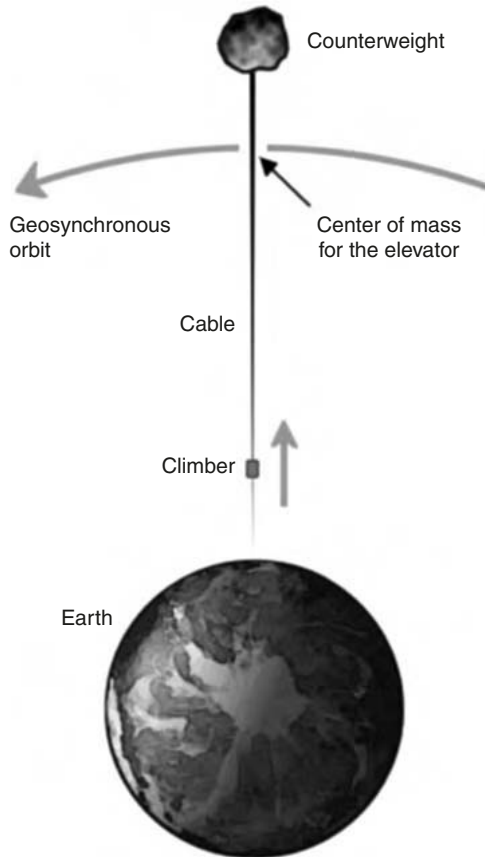


Fig. 1.1. Space elevator.

number of other novel engineering problems would also have to be solved to make a space elevator practical. Today's technology does not meet these requirements.

There are a variety of space elevator designs. Almost every design includes a base station, a cable, climbers, and a counterweight. The base station designs typically fall into two categories: mobile and stationary. Mobile stations are typically large oceangoing vessels (Fig. 1.2). Stationary platforms are generally positioned in high-altitude locations.

The building of a space elevator has two main problems: the need for material with a very high tensile stress/specific density ratio, and the very large cost of installation. But a space elevator could be made relatively economically if a cable with a density similar to graphite, with a tensile strength of around 65–120 GPa could be produced in bulk at a reasonable price.

By comparison, the strongest steels are no more than 5 GPa ($1 \text{ GPa} = 100 \text{ kg/mm}^2 = 0.1 \text{ ton/mm}^2$), but steel is heavy. The much lighter material kevlar has a tensile strength

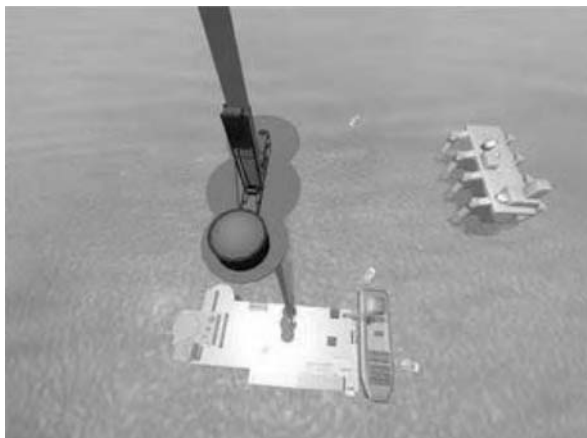


Fig. 1.2. Sea space elevator.

of 2.6–4.1 GPa, while quartz fiber can reach upwards of 20 GPa; the tensile strength of diamond filaments would theoretically be minimally higher.

Carbon nanotubes (CNT) have a theoretical tensile strength and density that lie well within the desired range for space elevator structures, but the technology to manufacture bulk quantities and fabricate them into a cable has not yet been developed. Theoretically, CNT can have tensile strengths beyond 120 GPa. Even the strongest fiber made of nanotubes is likely to have notably less strength than its components (30–60 GPa). Further research on purity and different types of nanotubes will hopefully improve this value.

Note that at present (March 2004), CNT have an approximate cost of \$100/g, and 20 million grams would be necessary to form even a seed elevator. This price is decreasing rapidly, and large-scale production would reduce it further.

Climbers cover a wide range of designs. On elevator designs whose cables are planar ribbons, some have proposed to use pairs of rollers to hold the cable with friction. Other climber designs involve magnetic levitation (unlikely due to the bulky track required on the cable).

Power is a significant obstacle for climbers. Some solutions have involved nuclear power, laser or microwave power beaming. They are very complex, or expensive, or have very low efficiency. The primary power methods (laser and microwave power beaming) have significant problems with both efficiency and heat dissipation on both the sides. Below the author offers a cable transport system which is more realistic at the present time.

There have been two methods proposed for dealing with the counterweight needed: a heavy object, such as a captured asteroid, positioned just beyond geosynchronous orbit;

and extending the cable itself well beyond geosynchronous orbit. The latter idea has gained more support, it is simpler and the long cable located out of GEO (up to 144,000 km) may be used for launching payload to other planets.

A space elevator could also be constructed on some of the other planets, asteroids, and moons (Mars, Moon). A Mars space elevator could be much shorter than one on Earth. Exotic materials might not be required to construct such an elevator. A lunar tether would need to be very long – more than twice the length of an Earth elevator. It could also be made of existing engineering materials.

There are a lot of problems in the development and design of a space elevator: corrosion of cable (cable), meteoroids, micrometeorites and space debris, Earth's weather, Earth's satellites, failure modes and safety issues, sabotage, vibrational harmonics, the event of failure, breaking of the cable, elevator pods, Van Allen belts (radiation region), political issues, economics problems, etc.

The building of a space elevator involves lifting the entire mass of the elevator into geosynchronous orbit. One cable is lowered downwards towards the Earth's surface while another cable is simultaneously deployed upwards. This method requires lifting hundreds or even thousands of tons on conventional rockets, which would be very expensive. The other way of building an elevator from the Earth's surface is offered by the author and presented in this book (see Chapter 5, Kinetic space towers).

1.3 Transport system for the space elevator*

This section proposes a new method and transportation system to fly into space, to the Moon, Mars, and other planets. This transportation system uses a mechanical energy transfer and requires only minimal energy so that it provides a “Free Trip” into space. It uses the rotary and kinetic energy of planets, asteroids, meteorites, comet heads, moons, satellites, and other natural space bodies.

This chapter contains the theory and results of computations for three projects. The projects use artificial materials like nanotubes and whiskers that have a ratio of tensile strength to density equal to 4 million meters. In the future, nanotubes will be produced that can reach a specific stress up to 100 million meters and will significantly improve the parameters of suggested projects.

The author is prepared to discuss the problems with serious organizations that want to research and develop these innovations.

*This part of the chapter was presented by the author as paper IAC-02-V.P.07 at the *World Space Congress – 2002*, 10–19 October 2002, Houston, TX, USA, and published in the *Journal of British Interplanetary Society*, Vol. 56, No. 7/8, 2003, pp. 231–249.

Nomenclature (metric system)

a	relative cross-section area of cable (cable)
a_m	relative cross-section area of Moon cable (cable)
A	cross-section area of cable [m^2]
A_0	initial (near planet) cross-section area of cable [m^2]
C	cost of delivery 1 kg
C_i	primary cost of installation [\\$]
d, D	cable diameter [mm]
E	delivery energy of 1-kg load mass [J]
g	gravity [m/s^2]
g_0	gravitation at the R_0 [m/s^2]; for Earth $g_0 = 9.81 \text{ m/s}^2$
g_m	gravitation on Moon surface [m/s^2]
F	force [N]
H	altitude [m]
H_p	perigee altitude [m]
$k = \sigma/\gamma$	ratio of cable tensile stress to density [nm/kg]
$K = k/10^7$	coefficient [million meters]
L	annual load [kg]
n	overload
n	number of working days
$N_e S_e$	annual employee salary [\\$]
$m = m_2/m_1$	relative apparatus mass. Here are m_2 is mass of apparatus, m_1 is mass of asteroid [kg]
M	equalizer mass [kg]
M_a	annual maintenance of installation [\\$]
M_e	final mass of an Installation [kg]
M_0	load mass delivered in one day
r	variable
R	radius [m]
R_0	radius of planet [m]
R_g	radius of geosynchronous orbit [m]
R_m	radius of Moon [m]
T	orbit period [h]
v	volume of a cable [m^3]
V	speed of space ship around asteroid [m/s]
V_a	initial speed of asteroid around space ship [m/s]
V_d	delivery speed [km/s]
V_r	maximum admitted cable speed [m/s]
V_1	circulate speed [m/s]
V_2	escape speed [m/s]
ΔV	ship additional speed received from asteroid [m/s]
W	mass of a cable [kg]
W_r	relative mass of cable (ratio of cable mass to ship mass W_s)
T	orbit period [h]
Y	live time [years]
σ	tensile strength [N/m^2]
ω	angle speed of a planet [rad/s]

ω_m	angle speed of the Moon [rad/s]
γ	density of cable [kg/m^3]

1.3.1 Introduction

At present, rockets are used to deliver payloads into space and to change the trajectory of space ships and probes. This method is very expensive in the requirement of fuel, which limits the feasibility of space stations, interplanetary space ships, and probes. Since 1997, the author has proposed a new revolutionary transport system for (1) delivering payloads and people into space, (2) accelerating a space ship for interplanetary flight, and (3) changing the trajectory of space probes. This method uses a mechanical energy transfer, energy of moved-down loads, and the kinetic energy of planets, of natural planet satellites, of asteroids, of meteorites, and of other space bodies. The author has not found an analog for this space mechanical energy transfer or similar facilities for transporting a payload into space in the literature and patents.

The present method does not require geosynchronous orbit (which is absent from most planets, moons, and asteroids which have weak gravitation) and instead, uses the kinetic and rotational energy of the space body to modify the trajectory and impart additional speed to the artificial space apparatus. The installation has a cable transport system and counterbalance, which is used for balancing the moving load. For this proposal, the cable, which is used for launching or modifying the speed or direction of a space vehicle or for connecting to an asteroid, is spooled after use and may be used again.

1.3.2 Brief history

There are many articles that develop a tether method for a trajectory change of space vehicles^{1,2} and there is an older idea of a space elevator (for reviews see Refs.^{3,4}). In the tether method two artificial bodies are connected by cable. The main problem with this method, which requires energy for increasing the rotation of the tether system (motorized tether²) is how to rotate it with a flexible cable and what to do with momentum after launch if the tether system is used again, etc. If this system is used only one time, it is worse than a conventional rocket because it loses the second body and requires a large source of energy.

In the suggested method, the space vehicle is connected to a natural body (planet, asteroid, moon, meteorite). The ship gets energy from the natural body and does not have to deal with the natural body in the future.

In the older idea, a space elevator is connected between a geosynchronous space station and the Earth by a cable.⁴ This cable is used to deliver a payload to the station. The main problems are the very large cable weight and delivery of the energy for movement of the load container.

In this suggested transport system, the load engine is located on the Earth and transfers energy to the load container and the space station using a very simple method

(see Project 1, capability is 100,000 tourists per year). The author also found and solved the differential equations of the cable for an equal stress for a complex Earth–Moon gravitation field which allows the cable weight to be decreased by several times.

The main difference in the offered method is the transport system for the space elevator and the use of the planet rotational energy for a free trip to another planet, for example, Mars (see Project 2, capability is 2000 people annually).

In Project 3 with in a capability of 10,000 tourists per year, the author suggests the idea of connecting the Moon and the Earth's pole by a load cable. He solves the problem of transferring the energy to the load container, finds the cable of equal stress, and shows a possibility of this project in the near future.

There are some millions of asteroids in the Sun system. In Project 4 the author suggests a way of increasing the maneuverability of space apparatus by some millions of times by using asteroid energy.

The author's other non-rocket methods are presented in publications listed in Refs.^{12–22}

1.3.3 Brief description, theory, and computation of innovations

The objective of these innovations is to: (a) provide an inexpensive means to travel to outer space and other planets, (b) simplify space transportation technology, and (c) eliminate complex hardware. This goal is obtained by new space energy transfer for long distance, by using engines located on a planet (for example, the Earth), the rotational energy of a planet (for example the Earth, the Mars, etc.), or the kinetic and rotational energy of the natural space bodies (for example asteroids, meteorites, comets, planet moons, etc.). Below is the theory and research for four projects, which can be completed in the near future.

1.4 Free trip to space (Project 1)

1.4.1 Description

A proposed centrifugal space launcher with a cable transport system is shown in Fig. 1.3. The system includes an equalizer (balance mass) located in geosynchronous orbit, an engine located on Earth, and the cable transport system having three cables: a main (central) cable of equal stress, and two transport cables, which include a set of mobile cable chains connected sequentially one to an other by the rollers. One end of this set is connected to the equalizer, the other end is connected to the planet. Such a separation is necessary to decrease the weight of the transport cables, since the stress is variable along the cable. This transport system design requires a minimum weight because at every local distance the required amount of cable is only that of the diameter for the local force. The load containers are also connected to the chain. When containers come up to the rollers, they move past the rollers and continue their motion up to the cable. The entire transport system is driven by any conventional motor *located on the planet*.

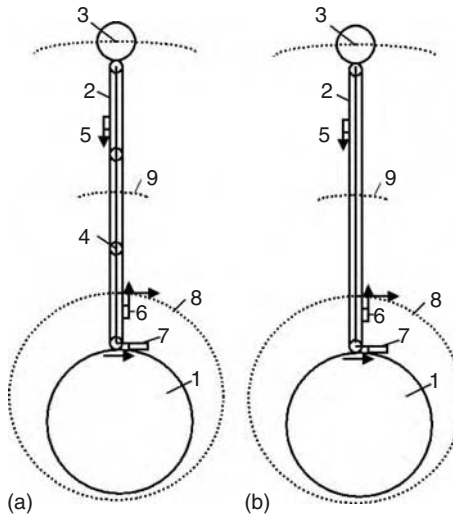


Fig. 1.3. The suggested space transport system. (a) System for low coefficient k . (b) System for high coefficient k (without rollers 4). *Notations:* (1) Rotary planet (for example, the Earth); (2) suggested space transport system; (3) equalizer (counterweight); (4) roller of transport system; (5) launch space ship; (6) a return ship after flight; (7) engine of transport system; (8) elliptic orbit of tourist vehicles; and (9) Geosynchronous orbit.

When payloads are not being delivered into space, the system may be used to transfer mechanical energy to the equalizer (load cabin, the space station). This mechanical energy may also be converted to any other sort of energy.

The space satellites released below geosynchronous orbit will have elliptic orbits and may be connected back to the transport system after some revolutions when the space ship and cable are in the same position (Fig. 1.3). If low Earth orbit satellites use a brake parachute, they can have their orbit closed to a circle.

The space probes released higher than geosynchronous orbit will have a hyperbolic orbit, fly to other planets, and then can connect back to the transport system when the ship returns.

Most space payloads, like tourists, must be returned to Earth. When one container is moved up, then another container is moved down. The work of lifting equals the work of descent, except for a small loss in the upper and lower rollers. The suggested transport system lets us fly into space without expending enormous energy. This is the reason why the method and system are named a “Free Trip”.

Devices shown on Fig. 1.4 are used to change the cable length (or chain length). The middle roller is shown in Fig. 1.5.

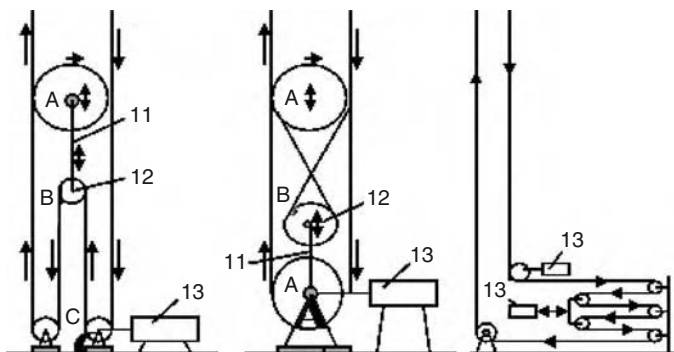


Fig. 1.4. Three mechanisms for changing the rope length in the Transport System (they are same for the space station). *Notations:* (11) The rope is connected to the axes A and B. This rope can change its length (the distance AB); and (12) additional rollers; (13) engine.

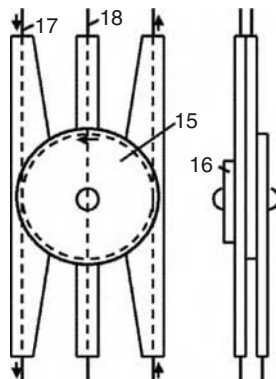


Fig. 1.5. Roller of space transport system. *Notations:* (15) Roller; (16) control; (17) transport system cable; and (18) main cable.

If the cable material has a very high ratio of safe (admissible) stress/density there may be one chain (Fig. 1.3(b)). The transport system then has only one main cable. Old design (Fig. 1.1) has many problems, for example, in the transfer of large amounts of energy to the load cabin.

1.4.2 Theory and computation (in metric system)

1. The cable of equal stress for the planet. The force active in the cable is:

$$F = \sigma A = F_0 + \int_{R_0}^R dW = F_0 + \int_{R_0}^R \gamma A dR, \quad (1.1)$$

where

$$\gamma = \gamma_0 g_0 \left[\left(\frac{R_0}{R} \right)^2 - \frac{\omega^2}{g_0} \right]. \quad (1.2)$$

If we substitute equation (1.2) in (1.1) and find the difference to the variable upper integral limit, we obtain the differential equations:

$$\frac{1}{A} dA = \frac{\gamma_0 g_0}{\sigma} \left[\left(\frac{R_0}{R} \right)^2 - \frac{\omega^2}{g_0} \right] dR. \quad (1.3)$$

Solution to equation (1.3) is:

$$a(R) = \frac{A}{A_0} = \exp \left[\frac{\gamma_0 g_0 B(r)}{\sigma} \right],$$

$$B(r) = R_0^2 \left\{ \left(\frac{1}{R_0} - \frac{1}{R} \right) - \frac{\omega^2}{2g_0} \left[\left(\frac{R}{R_0} \right)^2 - 1 \right] \right\}, \quad (1.4)$$

where a is the relative cable area and $B(r)$ is the work of lifting 1-kg mass.

The computation for different $K = \sigma/\gamma_0/10^7$ is presented in Figs. 1.6 and 1.7.

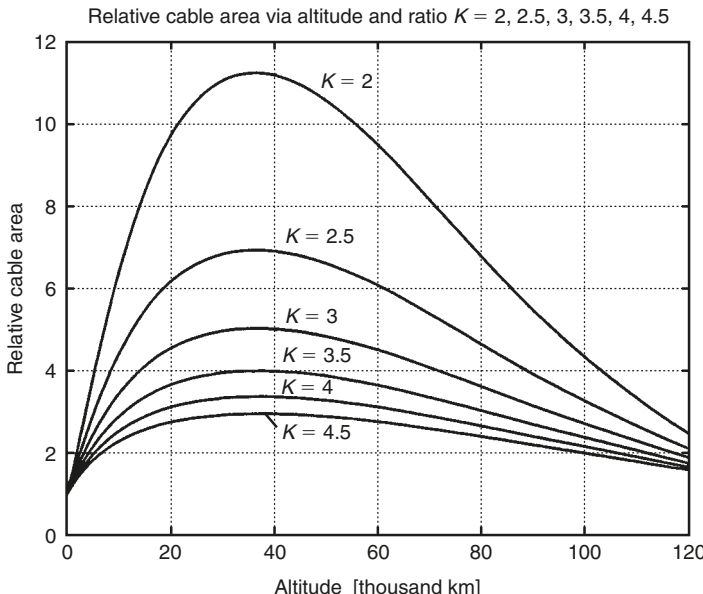


Fig. 1.6. Relative cable area via altitude [thousand km] for coefficient $K = 2-4.5$.

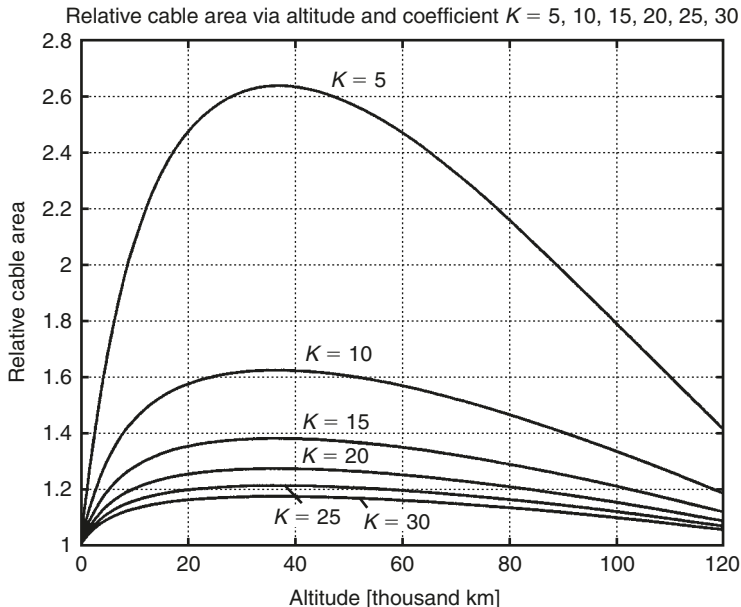


Fig. 1.7. Relative cable area via altitude [thousand km] for coefficient $K = 5\text{--}30$.

As you see for $K = 2$ the cable area changes by 11 times, but for very high $K = 30$ only by 1.19 times.

2. The mass of the cable W and a volume v can be calculated by equations:

$$v = Av_0 \int_{R_0}^R a dR = \frac{F_0}{kg_0} \int_{R_0}^R a dR, \quad W(R) = \gamma_0 v = \frac{F_0}{kg_0} \int_{R_0}^R \exp\left(\frac{\gamma g_0 B}{\sigma}\right) dR. \quad (1.5)$$

The results of the computation of the cable mass for the load mass of 3000 kg (force 3000 N) and cable density of 1800 kg/m³ is presented in Figs. 1.8 and 1.9.

3. The lift force of a mass of 1 kg, which is located over geosynchronous orbit and has speed $V > V_1$ is:

$$\Delta F = \frac{\omega^2 R}{g_0} - \left(\frac{R_0}{R}\right)^2 \text{ [kgf/kgm].} \quad (1.6)$$

The result of this computation is presented in Fig. 1.10. Every 100 kg of a mass of the equalizer gives 5 kgf of lift force at the altitude 100,000 km.

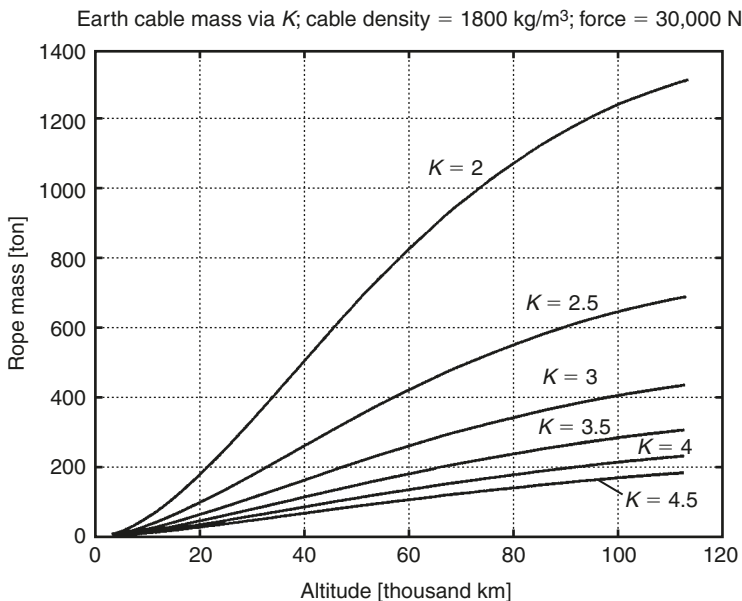


Fig. 1.8. Cable mass [tons] via counterweight altitude for Earth's surface force of 3 ton, cable density 1800 kg/m^3 , and $K = 2\text{--}4.5$.

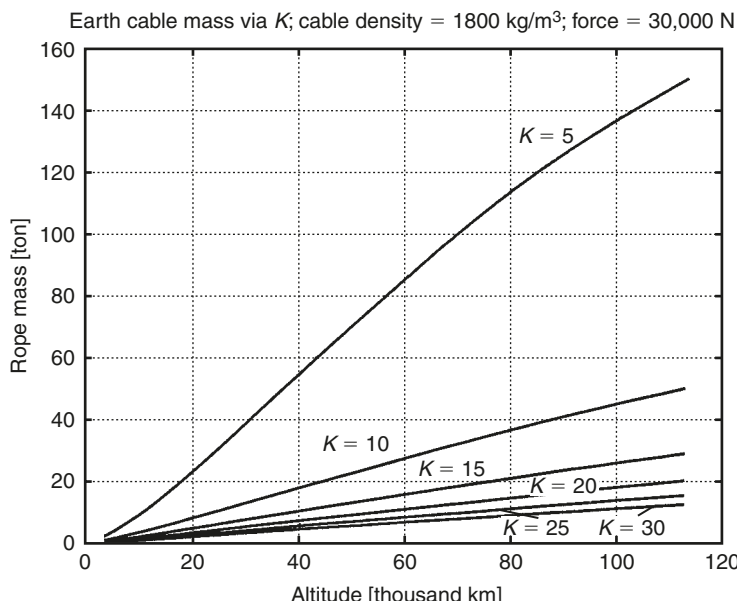


Fig. 1.9. Cable mass [tons] via counterweight altitude for Earth's surface force of 3 ton, cable density 1800 kg/m^3 , and $K = 5\text{--}30$.

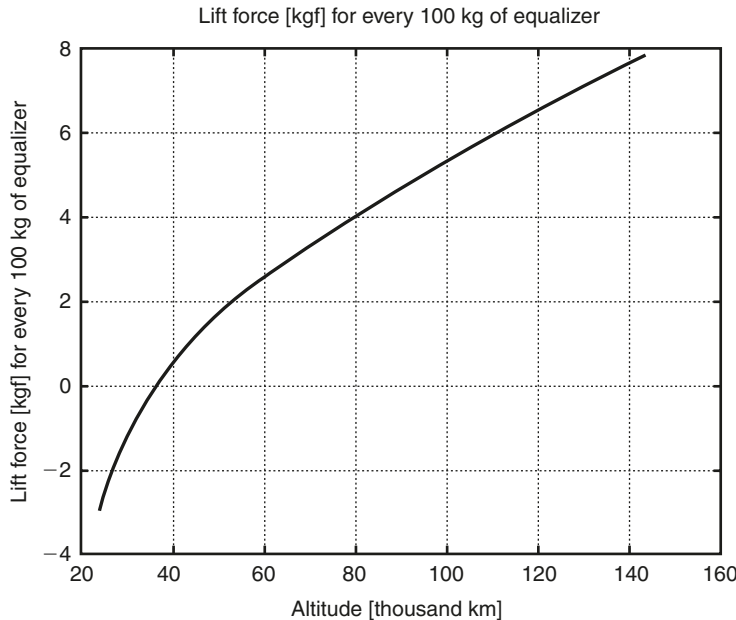


Fig. 1.10. Lift force [kgf] via altitude [thousand km] for every 100 kg of a counterweight (equalizer).

4. The equalizer mass (counterweight) M for different radius (altitudes) R and K may be computed from the equilibrium equation and (1.6):

$$F_0 a(R) + F_0 = M \left[\frac{\omega^2 R}{g_0} - \left(\frac{R_0}{R} \right)^2 \right],$$

$$M = \frac{F_0[a(R) + 1]}{\frac{\omega^2 R}{g_0} - \left(\frac{R_0}{R} \right)^2}. \quad (1.7)$$

Results of this computation are presented on Figs. 1.11–1.14. For a lift force of 10 ton at Earth (payload of 3000 kg), the equalizer mass is 570 ton for $K = 4$ and about 435 ton for $K = 10$ at the altitude 100,000 km.

5. If the balance cabin (load) to be moved down is absent, then the delivery work of 1 kg mass may be computed by the equation:

$$E(R) = R_0^2 \left\{ \left(\frac{1}{R_0} - \frac{1}{R} \right) - \frac{\omega^2}{2g_0} \left[\left(\frac{R}{R_0} \right)^2 - 1 \right] \right\}. \quad (1.8)$$

The result of this computation presented in Fig. 1.15.

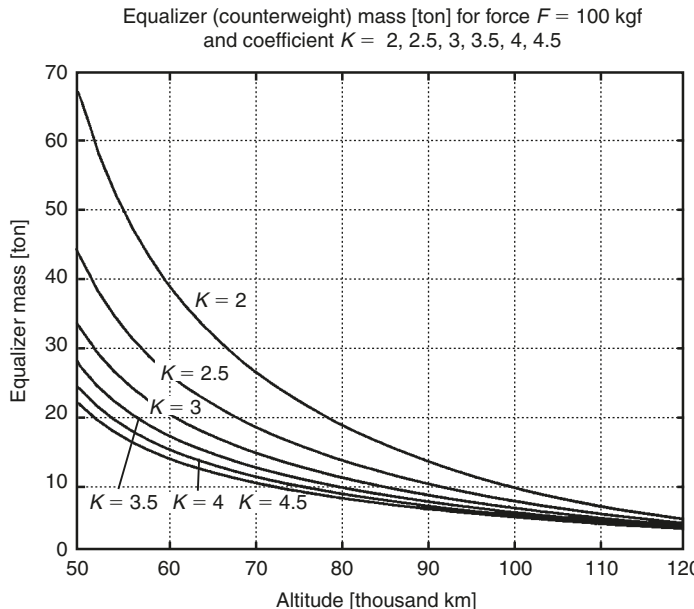


Fig. 1.11. Counterweight (equalizer mass) [tons] via altitude [thousand km] for ground force 100kgf (at Earth's surface) for $K = 2-4.5$. (It is centrifugal force without additional force, which supports the cable of equal stress.)

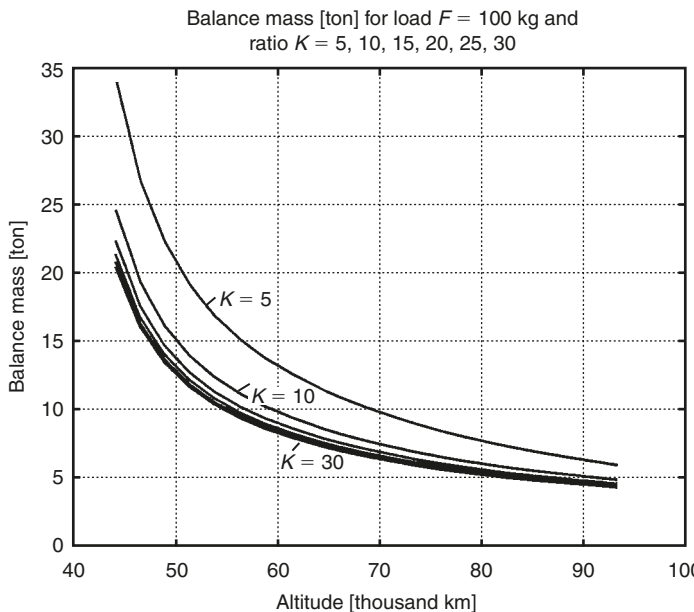


Fig. 1.12. Counterweight [tons] via altitude [thousand km] for ground force 100kgf (at Earth's surface) for $K = 5-30$. (It is centrifugal force without additional force, which supports the cable of equal stress.)

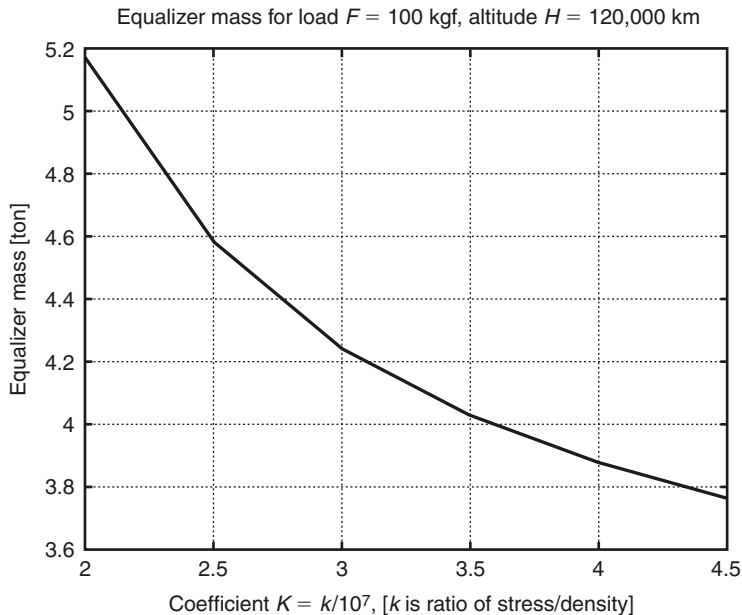


Fig. 1.13. Counterweight [tons] via altitude [thousand km] for ground force 100kgf (at Earth's surface) for $K = 2\text{--}4.5$. (It is centrifugal force without additional force, which supports the cable of equal stress.)

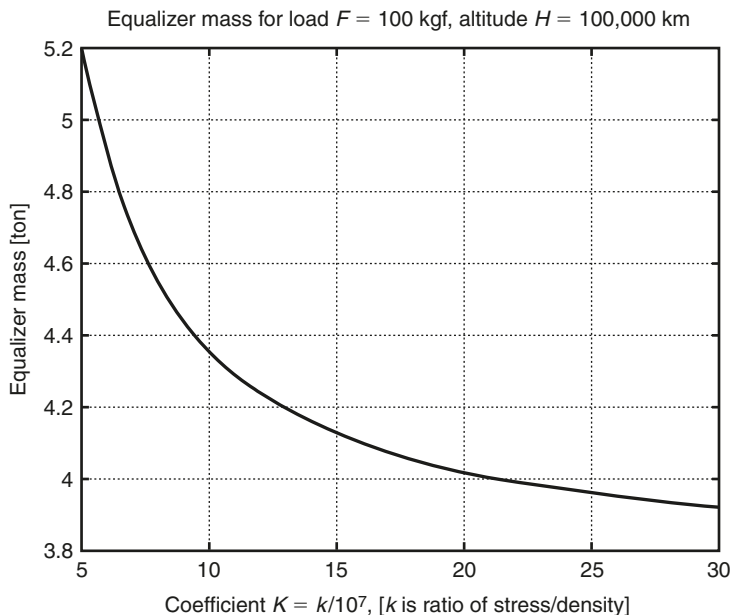


Fig. 1.14. Counterweight [tons] via altitude [thousand km] for ground force 100kgf (at Earth's surface) for $K = 5\text{--}30$. (It is centrifugal force without additional force, which supports the cable of equal stress.)

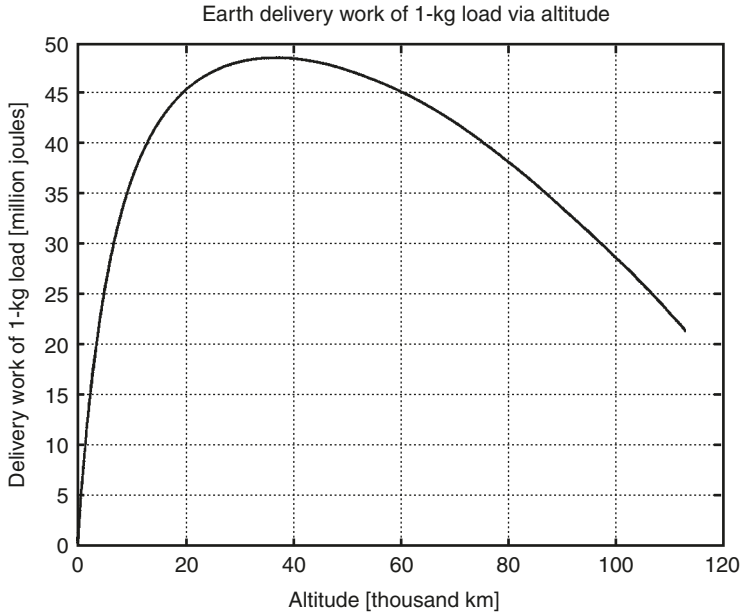


Fig. 1.15. Earth delivery work [million joules] of 1 kg load via altitude [thousand km].

6. When a space vehicle (satellite) is disconnected from the transport system before reaching geosynchronous orbit then an orbit perigee r (perigee altitude H) and period time T can be computed by the equations:

$$H = r - R_0, \quad r = \frac{uR}{2-u}, \quad T = \frac{\pi(r+R)^{3/2}}{3600\sqrt{2c}}, \quad (1.9)$$

where $u = \omega^2 R^3 / c$, $c = 3.986 \times 10^{14}$.

The result of this computation is presented in Figs. 1.16 and 1.17. When this space vehicle is in a suitable position (after the return flight), it can be connected back to the transport system.

7. When the space vehicle is disconnected from the transport system higher than the geosynchronous orbit, then the vehicle speed V , the first space speed V_1 , and the second (escape) space speed V_2 can be computed by formulas

$$V = \omega R, \quad V_1 = \frac{19.976 \times 10^6}{\sqrt{R}}, \quad V_2 = 1.414 V_1. \quad (1.10)$$

Then the result of computation are given in Fig. 1.18. Above an altitude of 50,000 km the space vehicle can go into interplanetary orbit. The necessary speed

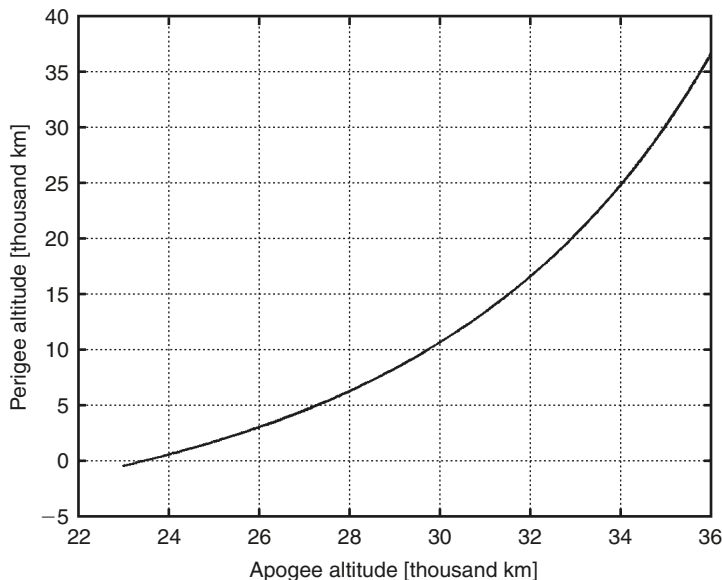


Fig. 1.16. Perigee altitude [thousand km] via disconnected (apogee) altitude of a space ship.

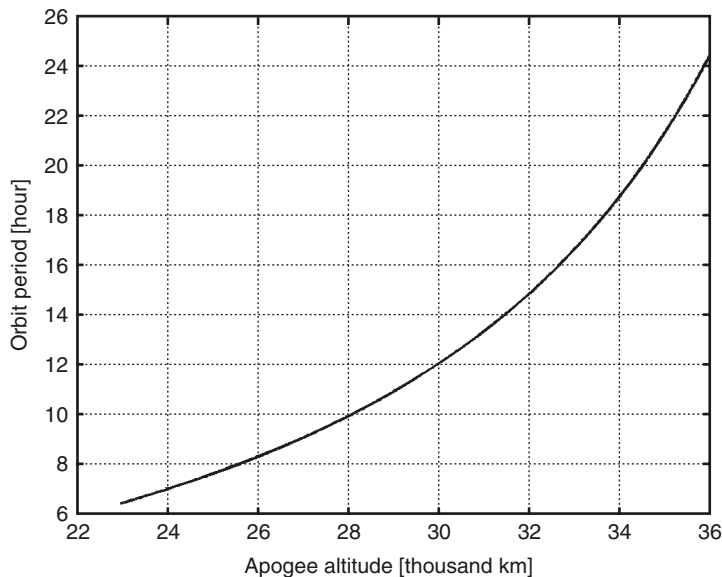


Fig. 1.17. Orbit period [h] via apogee altitude [thousand km].

and direction can be set by a choice of the disconnect point and position system in space. Additional speed over the escape velocity may reach 6 km/s. This is more than enough for a flight to the far planets. When the space vehicle returns it can also choose a point in the transport system for connection.

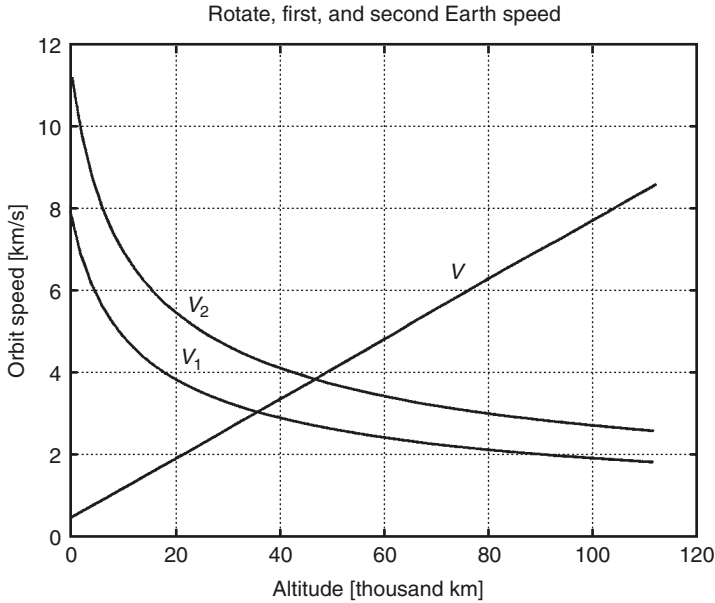


Fig. 1.18. Rotate, first, and second Earth speed [km/s] via altitude [thousand km].

8. Let us take a small part of a rotary circle and write it equilibrium:

$$\frac{2AR\alpha\gamma V^2}{R} = 2A\sigma \sin \alpha.$$

The maximum safe cable speed of chains is:

$$V_r = \sqrt{\frac{\sigma}{\gamma}} = \sqrt{10^7 K} \text{ [m/s].} \quad (1.11)$$

Results of this computation are presented in Fig. 1.19.

9. The delivery cost of 1-kg load is (Fig. 1.20):

$$C = \left(\frac{C_i}{Y} + N_e S_e + M_a \right) \frac{1}{3V_d}. \quad (1.12)$$

10. The increase of the space installation mass is a geometric progression:

$$n = 1 + \frac{\ln(M_e/M_0)}{\ln[(M_0 + M_g)/M_0]}, \quad (1.13)$$

where n is the number of working days (Fig. 1.21).

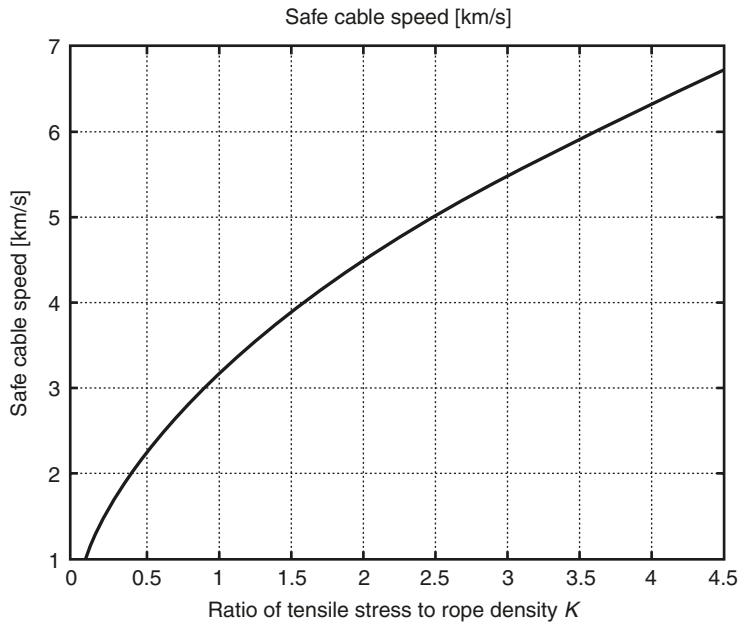


Fig. 1.19. Safe cable speed [km/s] via the ratio of tensile stress to cable density (coefficient K).

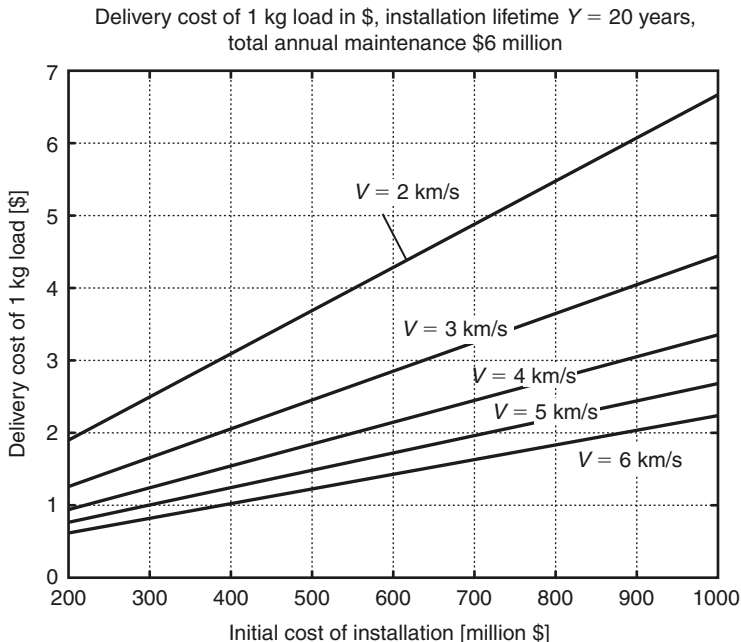


Fig. 1.20. Delivery cost of 1-kg of load [\$] via initial cost of installation [million dollars] for a delivery speed of $V = 2\text{--}6 \text{ km/s}$, for live time 20 years, total annual salary 5 million, maintenance 1 million [US dollars].

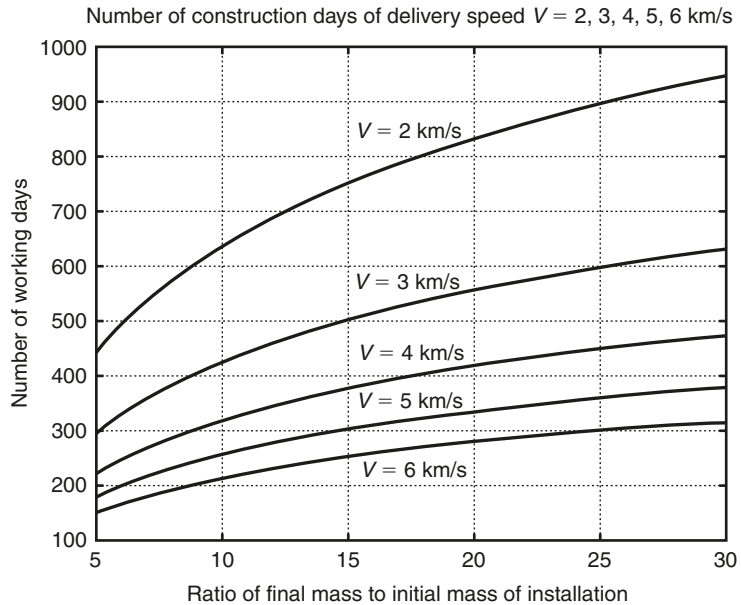


Fig. 1.21. Number of working days via the ratio of final mass to initial mass of the installation for delivery speed $V = 2\text{--}6 \text{ km/s}$.

11. The planetary parameters used for computations in all projects are shown in Table 1.1.

Table 1.1. The planetary parameters used for computations.

Planet	Radius R_0 [10^6 m]	Gravitation g_0 [m/s^2]	Angle speed ω [10^{-6} rad/s]	Geosynchronous R_g [10^6 m]
Earth	6.378	9.81	72.685	42.2
Mars	3.39	3.72	71.06	20.38
Moon	1.737	1.62	2.662	88.55

1.4.3 Transport system for space elevator (Project 1)

This is an example of an inexpensive transport system for cheap annual delivery of 100,000 tourists, or 12,000 ton of payload into Earth orbits, or the delivery up to 2000 tourists to Mars, or the launching of up to 2500 ton of payload to other planets.

1.4.3.1 Main results of computation

The suggested space transport system can be used for delivery of tourists and payloads to an orbit around the Earth, or to space stations serving as a tourist hotel, scientific laboratory, or industrial factory, or for the delivery of people and payloads to other planets.

Technical parameters: Let us take the safe cable stress 7200 kg/mm^2 and cable density 1800 kg/m^3 . This is equal to $K = 4$. This is not so great since by the year 2000 many

laboratories had made experimental nanotubes with a tensile stress of 200 GPa ($20,000 \text{ kg/mm}^2$) and a density of 1800 kg/m^3 . The theory of nanotubes predicts 100 ton/mm^2 with Young's modulus of up to 5 TPa (currently it is 1 TPa) and a density of 800 kg/m^3 for single-walled nanotubes (SWNTs). This means that the coefficient K used in our equations and graphs can be up to 125.

Assume a maximum equalizer lift force of 9 ton at the Earth's surface and divide this force between three cables: one main and two transport cables. Then it follows from Fig. 1.11, that the mass of the equalizer (or the space station) creates a lift force of 9 ton at the Earth's surface, which equals 518 ton for $K = 4$ (this is close to the current International Space Station weight of 450 ton). The equalizer is located over a geosynchronous orbit at an altitude of 100,000 km. Full centrifugal lift force of the equalizer (Fig. 1.10) is 34.6 ton, but 24.6 ton of the equalizer are used in support of the cables. The transport system has three cables: one main and two in the transport system. Each cable can support a force (load) of 3000 kgf. The main cable has a cross-section area of equal stress. Then the cable cross-section area is (see Fig. 1.6) $A = 0.42 \text{ mm}^2$ (diameter $D = 0.73 \text{ mm}$) at the Earth's surface, maximum 1.4 mm^2 in the middle section ($D = 1.33 \text{ mm}$, altitude 37,000 km), and $A = 0.82 \text{ mm}^2$ ($D = 1 \text{ mm}$) at the equalizer. The mass of main cable is 205 ton (see Fig. 1.8). The chains of the two transport cable loops have cross-section areas to equal the tensile stress of the main cable at given altitude, and the capabilities are the same as the main cable. Each of them can carry 3 ton force. The total mass of the cable is about 620 ton. The three cables increase the safety of the passengers. If any one of the cables breaks down, then the other two will allow a safe return of the space vehicle to Earth and the repair of the transport system.

If the container cable is broken, the pilot uses the main cable for delivering people back to Earth. If the main cable is broken, then the load container cable will be used for delivering a new main cable to the equalizer. For lifting non-balance loads (for example, satellites or parts of new space stations, transport installations, interplanetary ships), the energy must be spent in any delivery method. This energy can be calculated from equation (1.8) (Fig. 1.15). When the transport system in Fig. 1.3 is used, the engine is located on the Earth and does not have an energy limitation.¹¹ Moreover, the transport system in Fig. 1.3 can transfer a power of up to 90,000 kW to the space station for a cable speed of 3 km/s. At the present time, the International Space Station has only 60 kW of power.

Delivery capabilities: For tourist transportation the suggested system works in the following manner. The passenger space vehicle has the full mass of 3 ton (6667 pounds) to carry 25 passengers and 2 pilots. One ship moves up, the other ship, which is returning, moves down; then the lift and descent energies are approximately equal. If the average speed is 3 km/s, then the first ship reaches the altitude of 21.5–23 thousand km in 2 h (acceleration 1.9 m/s^2). At this altitude the ship is separated from the cable to fly in an elliptical orbit with minimum altitude 200 km and period approximately 6 h (Figs. 1.16 and 1.17). After one day the ship makes four revolutions around the Earth while the cable system makes one revolution, and the ship and cable will be in the same place with the same speed. The ship is connected back to the transport system, moves down the cable and lifts the next ship. The orbit may be also three revolutions (period 8 h) or two revolutions (period 12 h). In one day the transport system can accommodate 12 space ships (300 tourists) in both directions. This means more than 100,000 tourists annually into space.

The system can launch payloads into space, and if the altitude of disconnection is changed then the orbit is changed (see Fig. 1.17). If a satellite needs a low orbit, then it can use the brake parachute when it flies through the top of the atmosphere and it will achieve a near circular orbit. The annual payload capability of the suggested space transport system is about 12,600 ton into a geosynchronous orbit.

If instead of the equalizer the system has a space station of the same mass at an altitude of 100,000 km and the system can have space stations along cable and above geosynchronous orbit, then, these stations decrease the mass of the equalizer and may serve as tourist hotels, scientific laboratories, or industrial factories.

If the space station is located at an altitude of 100,000 km, then the time of delivery will be 9.36 h for an average delivery speed of 3 km/s. This means 60 passengers per day or 21,000 people annually in space.

Let us assume that every person needs 400 kg of food for a 1-year-round trip to Mars, and Mars has the same transport installation (see next project). This means we can send about 2000 people to Mars annually at suitable positions of Earth relative to Mars.

1.4.4 Estimations of installation cost and production cost of delivery

1.4.4.1 Cost of suggested space transport installation^{5,6}

The current International Space Station has cost many billions of dollars, but the suggested space transport system can cost a lot less. Moreover, the suggested transport system allows us to create other transport systems in a geometric progression (see equation (1.13)). Let us examine an example of the transport system.

Initially we create the transport system to lift only 50 kg of load mass to an altitude of 100,000 km. Using the Figs. 1.6–1.14 we have found that the equalizer mass is 8.5 ton, the cable mass is 10.25 ton, and the total mass is about 19 ton. Let us assume that the delivery cost of 1 kg mass is \$10,000. The construction of the system will then have a cost of \$190 million. Let us assume that 1 ton of cable with $K = 4$ from whiskers or nanotubes costs \$0.1 million then the system costs \$1.25 million. Let us put the research and development (R&D) cost of installation at \$29 million. Then the total cost of initial installation will be \$220 million. About 90% of this sum is the cost of initial rocket delivery.

After construction, this initial installation begins to deliver the cable and equalizer or parts of the space station into space. The cable and equalizer capability increase in a geometric progression. The installation can use part of the time for delivery of payload (satellites) and self-financing of this project. After 765 working days the total mass of equalizer and cables reaches the amount above (1133 ton) and the installation can work full time as a tourist launcher or continue to create new installations. In the last case this installation and its derivative installations can build 100 additional installations (1133 ton) in only 30 months (see equation (1.13) and Fig. 1.21) with a total capability of 10 million tourists/year. The new installations will be separated from the mother installations and moved to other positions around the Earth. The result of these installations allows the delivery of passengers and payloads from one continent to another across space with low expenditure of energy.

Let us estimate the cost of the initial installation. The installation needs 620 ton of cable. Let us take the cost of cable as \$0.1 million/ton. The cable cost will be \$62 million. Assume the space station cost \$20 million. The construction time is 140 days (equation (1.13)). The cost of using the mother installation without profit is \$5 million/year. In this case the new installation will cost \$87 million. In reality soon after construction the new installation can begin to launch payloads and become self-financing.

1.4.4.2 Cost of delivery

The cost of delivery is the most important parameter in the space industry. Let us estimate it for the full initial installation above.

As we calculated earlier the cost of the initial installation is \$220 million (further construction is made by self-financing). Assume that installation is used for 20 years, served by 100 officers with an average annual salary of \$50,000 and maintenance is \$1 million in year. If we deliver 100,000 tourists annually, the production delivery cost will be \$160/person or \$1.27/kg of payload. Some 70% of this sum is the cost of installation, but the delivery cost of the new installations will be cheaper.

If the price of a space trip is \$1990, then the profit will be \$183 million annually. If the payload delivery price is \$15/kg then the profit will be \$189 million annually.

The cable speed for $K = 4$ is 6.32 km/s (equation (1.11), Fig. 1.19). If average cable speed equals 6 km/s, then all performance factors are improved by a factor of 2 times.

If the reader does not agree with this estimation, then equations (1.1)–(1.13) and Figs. 1.6–1.21 are able calculations of the delivery cost for other parameters. In any case the delivery cost will be hundreds of times less than the current rocket powered method.

1.5 Delivery system for free round trip to Mars (Project 2)

A method and similar installation (Figs. 1.3–1.5) can be used for inexpensive travel to other planets, for example, from the Earth to Mars or the Moon and back (Fig. 1.22). A Mars space station would be similar to an Earth space station, but the Mars station would weigh less due to the decreased gravitation on Mars. This method uses the rotary energy of the planets. For this method, two facilities are required, one on Earth and the other on another planet (for example Mars). The Earth accelerates the space ship to the required speed and direction and then disconnects the ship. The space ship flies in space along the defined trajectory to Mars (Fig. 1.22). On reaching Mars the space ship connects to the cable of the Mars space transport system, then it moves down to Mars using the transport system.

The inverse of the process is used for the return trip. If two ships are used for descent and lifting payloads (Fig. 1.2), energy will only be required to overcome the small amount of friction losses in the lift transmission. The way back is the same. The Mars space ship chooses a cable disconnect point with a suitable speed and direction or a connect–disconnect in a special arrival–departure port.

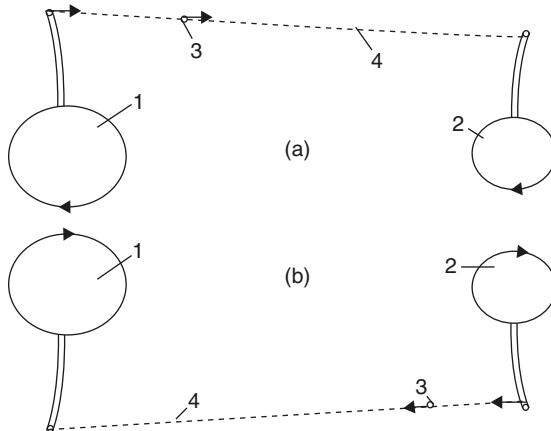


Fig. 1.22. Using the suggested transport system for space flight to Mars and back. (1) Earth; (2) Mars; (3) Space ship; and (4) Trajectory of space ship to (a) Mars and (b) back.

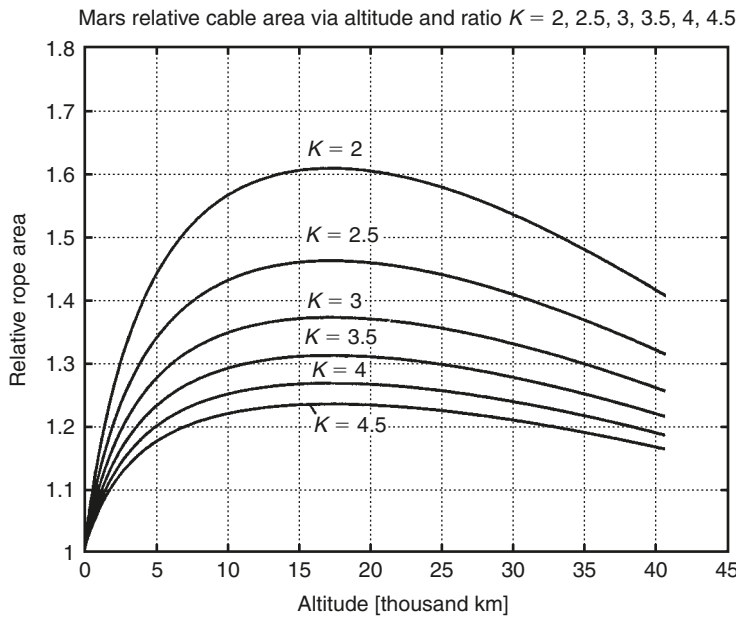


Fig. 1.23. Mars relative cable area via altitude and coefficient $K = 2-4.5$.

1.5.1 Technical parameters of Mars transport system

Equations (1.1)–(1.13) may be used for estimation main parameters of mars transport system. These computations are presented in Figs. 1.23–1.29. If we want to accept Earth space ships of 3 ton mass, then the parameters of the Mars transport system will be $K = 4$, three cables, and an equalizer altitude of 50,000 km.

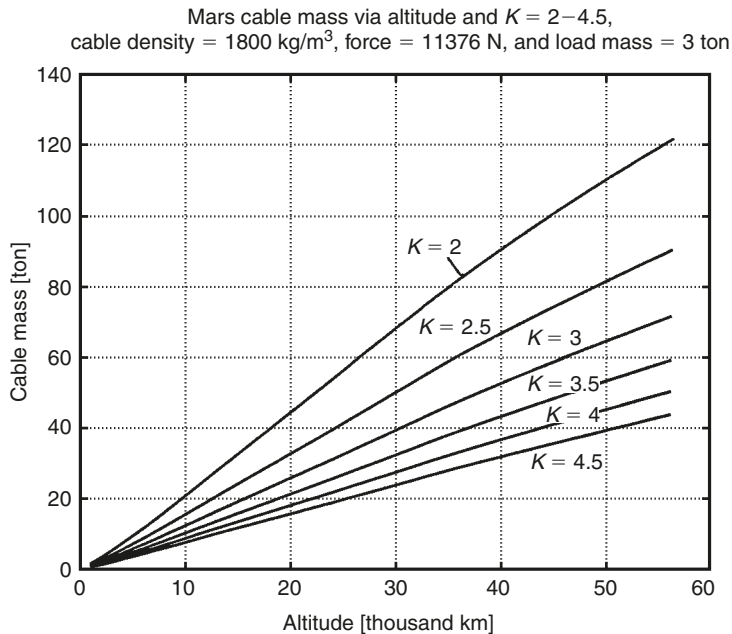


Fig. 1.24. Mars cable mass via altitude [thousand km], a cable density 1800 kg/m^3 and a load mass of 3 ton.

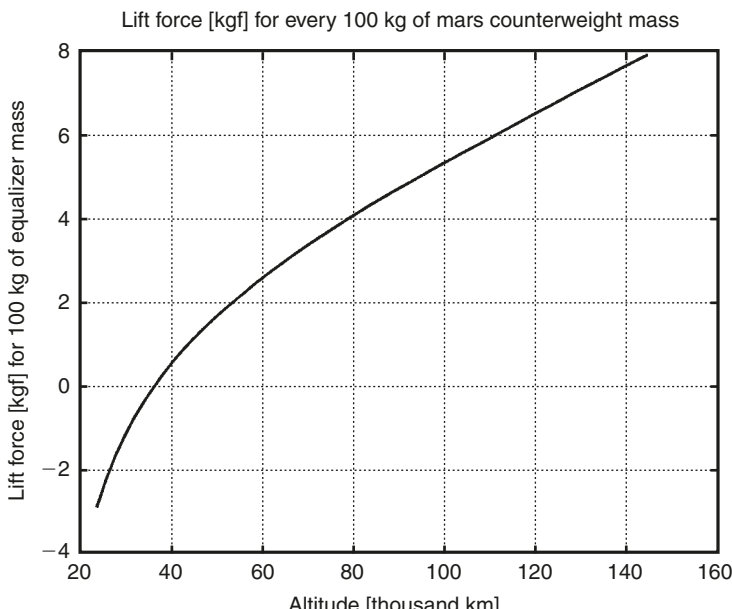


Fig. 1.25. Lift force [kgf] via altitude [thousand km] for every 100 kg of Mars equalizer mass.

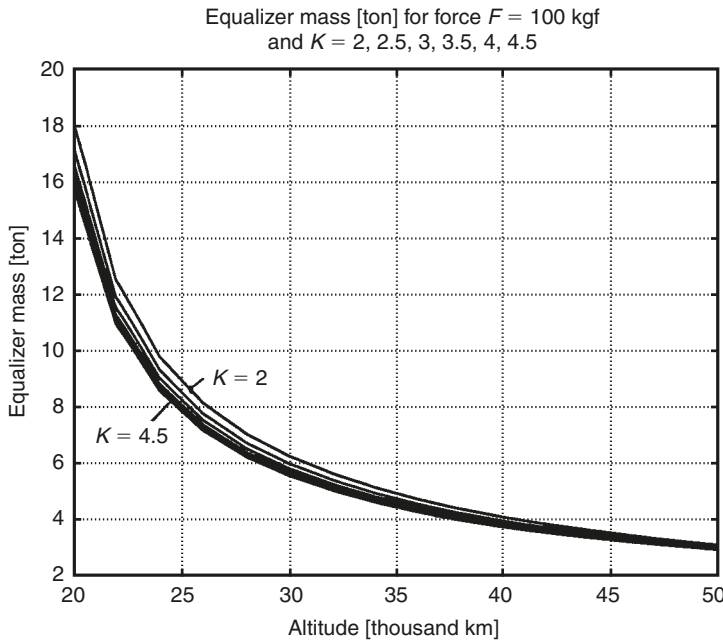


Fig. 1.26. Mars counterweight (equalizer) mass [tons] via altitude [thousand km] for the force 100 kgf and the coefficient $K = 2\text{--}4.5$.

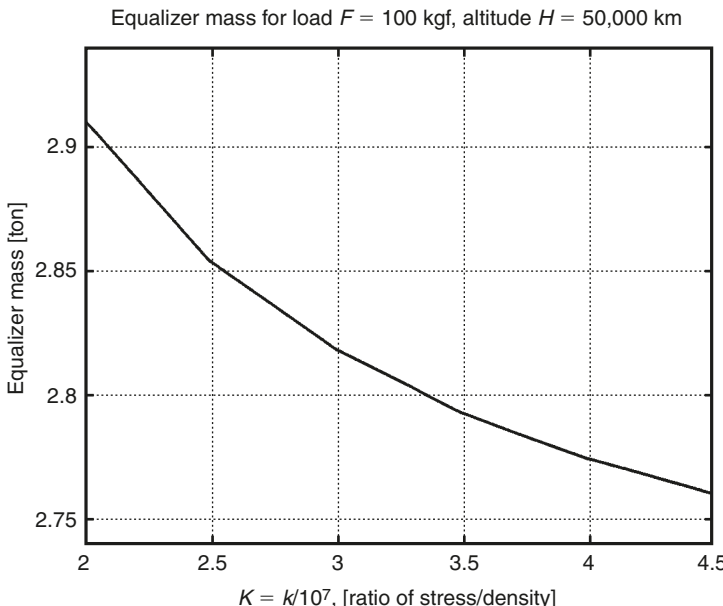


Fig. 1.27. Mars counterweight mass [tons] via the coefficient $K = 2\text{--}4.5$ for altitude 50,000 km and the force 100 kgf.

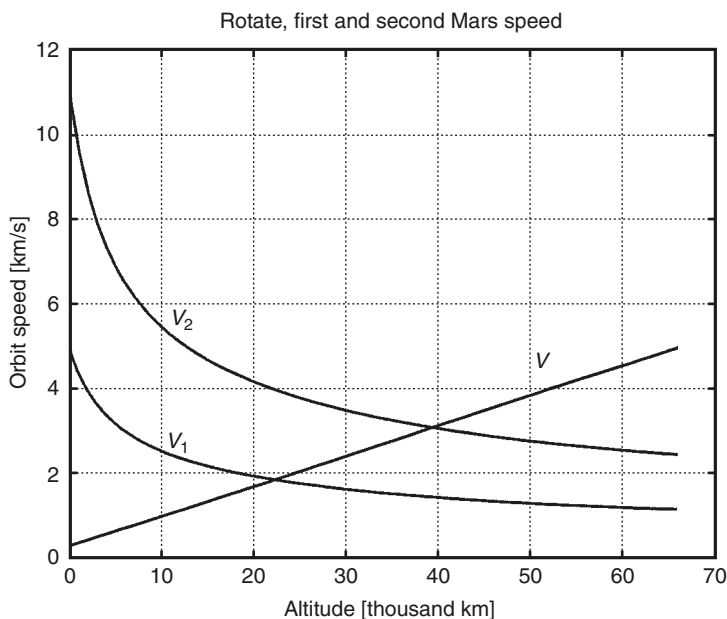


Fig. 1.28. Rotate, first, and second Mars speed via altitude [thousand km].

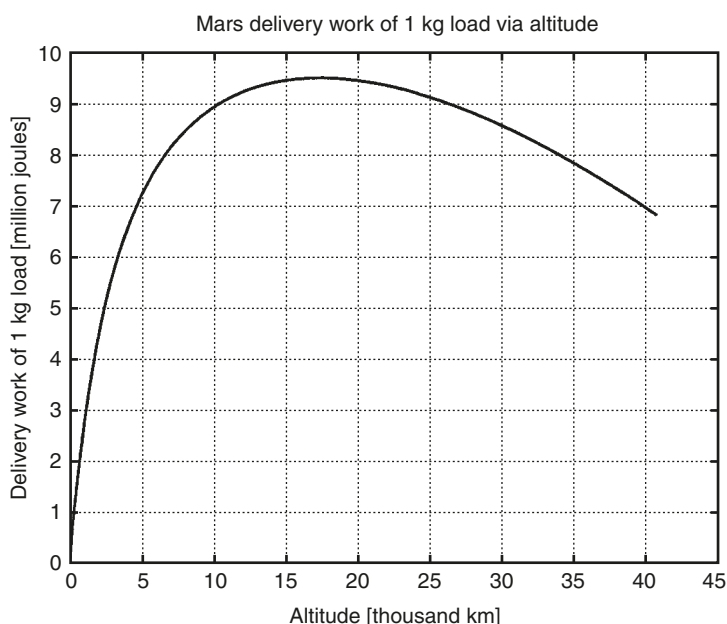


Fig. 1.29. Mars delivery work [million joules] of 1 kg of a load via altitude [thousand km].

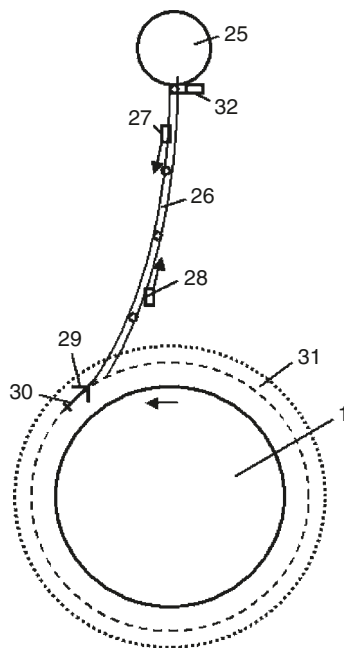


Fig. 1.30. The suggested transport system for Moon. *Notations:* (1) Earth; (25) Moon; (26) suggested Moon transport system; (27) and (28) load cabins; (29) aircraft; (30) cable control; (31) Earth's atmosphere; and (32) engine.

Equalizer mass is 94.7 ton. The total cable mass is 51 ton. Cross-section area of one cable is 0.158 mm^2 (diameter $D = 0.45 \text{ mm}$) at Mars surface, $D = 0.5 \text{ mm}$ at altitude 20,000 km, and $D = 0.47 \text{ mm}$ at altitude 50,000 km.

For construction on Mars we need to deliver only the cables. The equalizer can be made from local Mars material, for example, stones. Delivery capability is about 1000 ton, or 2000 people annually.

1.6 Free trip to Moon (Project 3)

This method may be used for an inexpensive trip to a planet's moon, if the moon's angular speed is equal to the planet's angular speed, for example, from the Earth to the Moon and back (Figs. 1.30–1.32). The upper end of the cable is connected to the planet's moon. The lower end of the cable is connected to an aircraft (or buoy), which flies (that is, glides or slides) along the planet's surface. The lower end may be also connected to an Earth pole. The aircraft (or Earth polar station, or Moon) has a device which allows the length of cable to be changed. This device would consist of a spool, motor, brake, transmission, and controller. The facility could have devices for delivering people and payloads to the Moon and back using the suggested transport system. The delivery devices include: containers, cables, motors, brakes, and controllers. If the aircraft is small and the cable is strong then the motion of the Moon can be used to move the airplane.

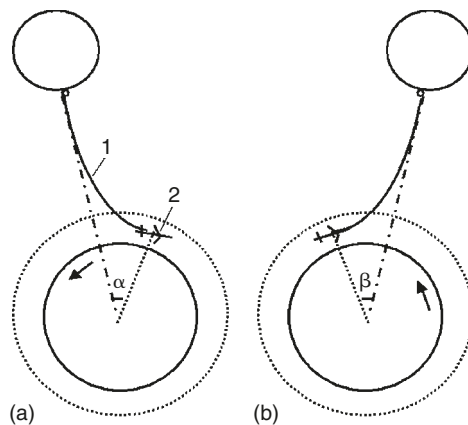


Fig. 1.31. Temporary landing of the Moon aircraft on the Earth's surface for loading: (a) Landing and (b) Takeoff.

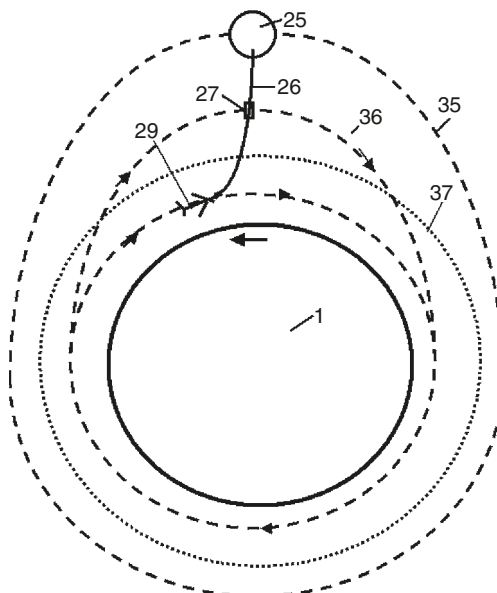


Fig. 1.32. Using the Moon's elliptical orbit for a free trip in space of up 71,000 km. *Notations:* (1) Earth; (25) Moon; (26) cable from Earth to Moon; (27) space vehicle; (29) limit of Earth's atmosphere; (35) Moon orbit; (36) elliptic orbit of a Moon vehicle; and (37) border of Earth's atmosphere.

For example, if the airplane weighs 15 ton and has an aerodynamic ratio (the lift force to the drag force) equal to 5, a thrust of 3000 kg would be enough for the aircraft to fly for infinity without requiring any fuel. The aircraft could use a small engine for maneuverability and temporary landing. If the planet has an atmosphere (as the Earth) the engine could be a turbine engine. If the planet does not have an atmosphere, a rocket engine may be used.

If the suggested transport system is used only for free thrust (9 ton), the system can thrust the three named supersonic aircraft or produce up to 40 million watts of energy.

A different facility could use a transitional space station located at the zero gravity point between the planet and the planet's moon. Fig. 1.31 shows a sketch of the temporary landing of an airplane on the planet surface. The aircraft increases the length of the cable, flies ahead of the cable, and lands on a planet surface. While the planet makes an angle turn ($\alpha + \beta = 30^\circ$, see Fig. 1.31) the aircraft can be on a planet surface. This time equals about 2 h for the Earth, which would be long enough to load payload on the aircraft.

The Moon's trajectory has an eccentricity (Fig. 1.32). If the main cable is strong enough, the moon may be used to pull a payload (space ship, manned cabin), by trajectory to an altitude of about 60,000 km every 27 days. For this case, the length of the main cable from the Moon to the container does not change and when the Moon increases its distance from the Earth, the Moon lifts the space ship. The payload could land back on the planet at any time if it is allowed to slide along the cable. The Moon's energy can be used also for an inexpensive trip around the Earth (Figs. 1.30 and 1.32) by having the moon "drag" an aircraft around the planet (using the Moon as a free thrust engine). The Moon tows the aircraft by the cable at supersonic speed, about 440 m/s (Mach number is 1.5).

The other more simple design (without aircraft) is shown in Fig. 7.1, Chapter 7. The cable is connected to one Earth pole, to a special polar station which allows to change a length of cable. Near the pole the cable is supported in the atmosphere by air balloons and wings.

1.6.1 Technical parameters

The following are some of the data for estimating the main transport system parameters for connecting to the Moon to provide inexpensive payload transfer between the Earth and the Moon (see Ch. 7, Eqs. (7.1)–(7.7), Figs. 7.2–7.4). The system has three cables, each of which can keep the force at 3 ton. Material of the cable has $K = 4$. All cables would have cross-section areas of equal stress. The cable has a minimal cross-section area A_0 of 0.42 mm^2 (diameter $d = 0.73 \text{ mm}$) and maximum cross-section area A_m of 1.9 mm^2 ($d = 1.56 \text{ mm}$). The mass of the main cable would be 1300 ton (Fig. 7.3, Ch. 7). The total mass of the main cable plus the two container cables (for delivering a mass of 3000 kg) equals 3900 ton for the delivery transport system in Figs. 1.30–1.33. An inexpensive means of payload delivery between the Earth and the Moon could thus be developed. The elapsed time for the Moon trip at a speed of 6 km/s would be about 18.5 h and the annual delivery capability would be 1320 ton in both directions.

1.7 Discussion

1.7.1 Cable problems

Most engineers and scientists think it is impossible to develop an inexpensive means to orbit to another planet. Twenty years ago, the mass of the required cable would not allow this proposal to be possible for an additional speed of more 2000 m/s from one asteroid. However, today's industry widely produces artificial fibers that have a tensile

strength 3–5 times more than steel and a density 4–5 times less than steel. There are also experimental fibers which have a tensile strength 30–60 times more than steel and a density 2–4 times less than steel. For example, in the book *Advanced Fibers and Composites* in p. 158, there is a fiber C_D with a tensile strength of $\sigma = 8000 \text{ kg/mm}^2$ and density (specific gravity) $\gamma = 3.5 \text{ g/cm}^3$. If we take an admitted strength of 7000 kg/mm^2 ($\sigma = 7 \times 10^{10} \text{ N/m}^2$, $\gamma = 3500 \text{ kg/m}^3$), then the ratio $\sigma/\gamma = 0.05 \times 10^{-6}$ or $\sigma/\gamma = 20 \times 10^6$ ($K = 2$). Although (in 1976) the graphite fibers are strong ($\sigma/\gamma = 10 \times 10^6$), they are at best still 10 times weaker than theory predicts.

Steel fiber has tensile strengths of 5000 MPa (500 kg/mm^2), but the theoretic value is $22,000 \text{ MPa}$ (1987). Polyethylene fiber has a tensile strength of $20,000 \text{ MPa}$ and the theoretical value is $35,000 \text{ MPa}$ (1987).

The mechanical behavior of nanotubes also has provided excitement because nanotubes are seen as the ultimate carbon fiber, which can be used as reinforcements in advanced composite technology. Early theoretical work and recent experiments on individual nanotubes (mostly multi-walled nanotubes, MWNTs) have confirmed that nanotubes are one of the stiffest materials ever made. Whereas carbon–carbon covalent bonds are one of the strongest in nature, a structure based on a perfect arrangement of these bonds oriented along the axis of nanotubes would produce an exceedingly strong material. Traditional carbon fibers show high strength and stiffness, but fall far short of the theoretical in-plane strength of graphite layers (an order of magnitude lower). Nanotubes come close to being the best fiber that can be made from graphite structure.

For example, whiskers made from CNT have a tensile strength of 200 GPa and Young's modulus of over 1 TPa (1999). The theory predicts 1 TPa and Young modulus $1\text{--}5 \text{ TPa}$. The hollow structure of nanotubes makes them very light (specific density varies from 0.8 g/cm^3 for SWNTs up to 1.8 g/cm^3 for MWNTs, compared to 2.26 g/cm^3 for graphite or 7.8 g/cm^3 for steel).

Specific strength (strength/density) is important in the design of our transportation system and space elevator; nanotubes have this value at least two orders of magnitude greater than steel. Traditional carbon fibers have a specific strength 40 times greater than steel. Where nanotubes are made of graphite carbon, they have good resistance to chemical attack and have high terminal stability. Oxidation studies have shown that the onset of oxidation shifts by about 100°C higher temperatures in nanotubes compared to high modulus graphite fibers. In vacuums or reducing atmospheres, nanotubes structures will be stable at any practical service temperature. Nanotubes have excellent conductivity like copper.

The price for the SiC whiskers produced by Carborundun Co. with $\sigma = 20,690 \text{ MPa}$, $\gamma = 3.22 \text{ g/cm}^3$ was $\$440/\text{kg}$ in 1989. Medicine, the environment, space, aviation, machine building, and the computer industry need cheap nanotubes. Some American companies plan to produce nanotubes in 2–3 years.

Below the author provides a brief overview of the annual research information (2000) regarding the proposed experimental test fibers.

Table 1.2. Figures for experimental whiskers and industrial fibers.

Material whiskers	Tensile strength [kg/mm ²]	Density [g/cm ³]	Fibers	Tensile strength [MPa]	Density [g/cm ³]
AlB ₁₂	2650	2.6	QC-8805	6200	1.95
B	2500	2.3	TM9	6000	1.79
B ₄ C	2800	2.5	Thorael	5650	1.81
TiB ₂	3370	4.5	Allien 1	5800	1.56
SiC	1380–4140	3.22	Allien 2	3000	0.97

1.7.2 Data that can be used for computation

Let us consider the following experimental and industrial fibers, whiskers, and nanotubes:

1. Experimental nanotubes CNT have a tensile strength of 200 GPa (20,000 kg/mm²), Young's modulus is over 1 TPa, specific density $\gamma = 1800 \text{ kg/m}^3$ (1.8 g/cm³) (year 2000).

For safety factor $n = 2.4$, $\sigma = 8300 \text{ kg/mm}^2 = 8.3 \times 10^{10} \text{ N/m}^2$, $\gamma = 1800 \text{ kg/m}^3$, $(\sigma/\gamma) = 46 \times 10^6$, $K = 4.6$. The SWNTs nanotubes have a density of 0.8 g/cm³, and MWNTs have a density of 1.8 g/cm³. Unfortunately, the nanotubes are very expensive at the present time (1994).

2. For whiskers $C_D \sigma = 8000 \text{ kg/mm}^2$, $\gamma = 3500 \text{ kg/m}^3$ (1989) (p. 158).⁷
3. For industrial fibers $\sigma = 500\text{--}600 \text{ kg/mm}^2$, $\gamma = 1800 \text{ kg/m}^3$, $\sigma/\gamma = 2.78 \times 10^6$, $K = 0.278\text{--}0.333$, figures for some other experimental whiskers and industrial fibers are give in Table 1.2.

1.8 Conclusions

The new materials make the suggested transport system and projects highly realistic for a free trip to outer space without expetion of energy. The same idea was used in the research and calculation of other revolutionary innovations such as launches into space without rockets (not space elevator, not gun); cheap delivery of loads from one continent to another across space; cheap delivery of fuel gas over long distances without steel tubes and damage to the environment; low-cost delivery of large load flows across sea streams and mountains without bridges or underwater tunnels (Gibraltar, English Channel, Bering Stream (USA–Russia), Russia–Sakhalin–Japan, etc.); new economical transportation systems; obtaining inexpensive energy from air streams at high altitudes; etc. some of these are in Refs. ^{12–21}

The author has developed innovations, estimations, and computations for the above mentioned problems. Even though these projects seem impossible for the current technology, the author is prepared to discuss the project details with serious organizations that have similar R&D goals.

Patent applications are 09/789,959 of 02/23/01; 09/873,985 of 6/4/01; 09/893,060 of 6/28/01; 09/946,497 of 9/6/01; 09/974,670 of 10/11/01; 09/978,507 of 10/18/01, USA.

1.9 Tether system

In a tether system two artificial bodies are connected by a cable. The system rotates around its common axis and the Earth. This section contains a brief description of the idea of a tether system. The reader can find details in the *Tethers in Space Handbook*¹ and special researches made in this area.

1.9.1 Short description

A space tether is a long cable used to couple masses to each other or to other spacecraft, such as a spent booster rocket of a space station (Fig. 1.33). Space tethers are usually made of strong cable. The tether can provide a mechanical connection between two space objects that enables the transfer of energy and momentum from one object to the other. They can be used to provide space propulsion without consuming propellant. Conductive space tethers can interact with the Earth's magnetic field and ionospheric plasma to generate thrust or drag forces without expending rocket fuel.

Tether propulsion uses long, strong strings (known as tethers) to change the orbits of spacecraft. Space tethers can also provide the applications as then allow momentum and energy to be transferred between objects in space. For example, the tether system enables spacecraft to be thrown from one orbit to another. Electrodynamic tethers interact with the Earth's magnetosphere to generate power or propulsion without consuming propellant.

Most current tether designs use crystalline plastics such as Spectra. A possible future material would be CNT, which have theoretical strengths up to 100 GPa.

There are four potential ways to use tethers for propulsion.



Fig. 1.33. Tether system.

1.9.1.1 Tidal stabilization for altitude control

The tether has a small mass on one end, and a satellite on the other. Tidal forces stretch the tether between the two masses, stabilizing the satellite. Its long dimension is always oriented towards the planet. Some of the earliest satellites were stabilized this way, or used mass distribution to achieve tidal stabilization. This is a simple form of stabilization that uses no electronics, rockets, or fuel. A small bottle of fluid must be mounted in the spacecraft to damp vibrations.

1.9.1.2 Electrodynamic tethers

An electrodynamic tether conducts current in order to act against a planetary magnetic field. It's a simplified, very low-budget magnetic sail. The tether inducts the Earth's magnetic field electric force to use as power and produce substantial work. When a conductive tether is trailed in a planetary or solar magnetosphere (magnetic field), it generates a current, and thereby slows the spacecraft into a lower orbit. The tether's end can be left bare. This is sufficient to make contact with the ionosphere and allow a current to flow. A circuit in electrodynamic tethers can be used as a phantom loop, with a cathode tubes placed at the ends of the tethers. A double-ended cathode tube tether will allow alternating currents.

A similar concept was used in the wireless transmission of energy.

Electrodynamic tethers build up vibrations from variations in magnetic and electric fields. One plan to control these is to vary the tether current to oppose the vibrations. In simulations, this keeps the tether together. By channelling direct current through a tether, the space ship can be moved into a higher orbit.

1.9.1.3 Rotovators

A rotovator is a rotating tether. A spacecraft in one orbit aligns with the end of the tether, latching onto it and being accelerated by its rotation. This is not free; the tether's angular momentum changes. They separate later, when the spacecraft's velocity has been changed by the rotovator. Rotovators could theoretically open up inexpensive transportation throughout the solar system, as long as the net mass flow was toward the Sun. On airless planets (such as the Moon), a rotovator in a polar orbit would provide cheap surface transport as well.

A rotovator can be an electrodynamic tether in a planetary magnetic field. Its angular momentum can be charged electrically from solar or nuclear power, by running current through a wire that goes the length of the tether. When the tether turns over, the direction of current must reverse to act against the magnetic field. Ultimately, such a tether pushes against the angular momentum of the planet.

Rotovators can also be charged by momentum exchange. Momentum charging uses the rotovator to move mass from a place that is higher in the gravity well to a place that is lower in the gravity well. The energy from the falling weight speeds up the rotation of the rotovator. For example, it is possible to use a system of two or three rotovators to implement trade between the Moon and Earth. The rotovators are charged by lunar mass (dirt, if imports are not available) dumped on Earth, and use the momentum so gained to boost Earth goods back to the Moon.

A rotovator can pick up a moving vehicle and sling it into orbit. For example, a rotovator could pick up a Mach-12 aircraft from the upper atmosphere of the Earth, and move it into orbit without using rockets. It could likewise catch such aircraft, and lower them into atmospheric flight. An important practical modification of a rotovator would be to add several latch points and to achieve different momentum transfers. This is a very valuable option, given that such performance otherwise requires extremely exotic spacecraft propulsion systems.

1.9.1.4 Space elevators

Space elevators (beanstalks) may be considered as a special case when the tether system is a rotovator powered by the spin of a planet. For example, on Earth, a beanstalk would go from the equator to geosynchronous orbit.

1.9.2 Problems

Simple tethers are quickly cut by micrometeoroids. The lifetime of a one-strand tether in space is on the order of 5 h for a length of 10 km. Several systems have been proposed to correct this. The US Naval Research Lab has successfully flown a long-term tether that used very fluffy yarn. This is reported to remain uncut several years after deployment. Another proposal is to use tape or cloth.

Rotovators are currently limited by the strengths of available materials. The ultra-high-strength plastic fibers (Kevlar and Spectra) permit rotovators to pluck masses from the surface of the Moon and Mars. Rotovators made from these materials cannot lift masses from the surface of the Earth. Tethers have many modes of vibration, and these can build to cause stresses so high that the tether breaks. Mechanical tether-handling equipment is often surprisingly heavy, with complex controls to damp vibrations. Electrodynamic tethers can be stabilized by reducing their current when it would feed the oscillations, and increasing it when it opposes oscillations.

Unexpected electrostatic discharges have cut tethers, damaged electronics, and welded tether-handling machinery.

References

1. M.L. Cosmo and E.C. Lorenzini (eds.), *Tethers in Space Handbook*, 3rd edition, Smithsonian Astrophysical Observatory, December, 1997.
2. S.W. Ziegler and M.P. Cartmell, “Using Motorized Tethers for Payload Orbital Transfer”, *Journal of Spacecraft and Rockets*, Vol. 38, No. 6, 2001.
3. B.C. Edwards, “Design and Deployment of Space Elevator”, *Acta Astronautica*, Vol. 47, No. 10, 2000, pp. 735–744.
4. D.V. Smitherman Jr., *Space Elevators*, NASA/CP-2000-210429, US National Aeronautics and Space Administration, Washington, DC.
5. M.R. Palmer, “A Revolution In Access to Space Through Spinoffs of SDI Technology”, *IEEE Transactions on Magnetics*, Vol. 27, No. 1, January 1991, pp. 11–20.

6. M.R. Palmer, "Economics and Technology Issues for Gun Launch to Space", *Space Technology*, 1996, Part 3, pp. 697–702.
7. F.S. Galasso, *Advanced Fibers and Composite*, Gordon and Branch Science Publisher, 1989.
8. *Carbon and High Performance Fibers, Directory*, 6th edition, Chapman & Hall, London and New York, 1995.
9. *Concise Encyclopedia of Polymer Science and Engineering*, Ed. J.I. Kroschwitz, 1990.
10. M.S. Dresselhous, *Carbon Nanotubes*, Springer, New York, 2001.
11. J.D. Anderson, *Hypersonic and High Temperature Gas Dynamics*, McGraw-Hill Book Co., New York, 1989.
12. A.A. Bolonkin, "Hypersonic Gas-Rocket Launch System", AIAA-2002-3927, *38th AIAA/ASME/SAE/ASEE Joint Propulsion Conference and Exhibit*, 7–10 July 2002, Indianapolis, IN, USA.
13. A.A. Bolonkin, "Inexpensive Cable Space Launcher of High Capability", IAC-02-V.P07, *53rd International Astronautical Congress, The World Space Congress – 2002*, 10–19 October 2002, Houston, TX, USA.
14. A.A. Bolonkin, "Non-Rocket Missile Rope Launcher", IAC-02-IAA.S.P.14, *53rd International Astronautical Congress, The World Space Congress – 2002*, 10–19 October 2002, Houston, TX, USA.
15. A.A. Bolonkin, "Hypersonic Launch System of Capability Up 500 tons per Day and Delivery Cost \$1 per lb". IAC-02-S.P.15, *53rd International Astronautical Congress, The World Space Congress – 2002*, 10–19 October 2002, Houston, TX, USA.
16. A.A. Bolonkin, "Employment Asteroids for Movement of Space Ship and Probes". IAC-02-S.6.04, *53rd International Astronautical Congress, The World Space Congress – 2002*, 10–19 October 2002, Houston, TX, USA.
17. A.A. Bolonkin, "Non-Rocket Space Rope Launcher for People", IAC-02-V.P.06, *53rd International Astronautical Congress, The World Space Congress – 2002*, 10–19 October 2002, Houston, TX, USA.
18. A.A. Bolonkin, "Optimal Inflatable Space Towers of High Height", COSPAR 02-A-02228, *34th Scientific Assembly of the Committee on Space Research (COSPAR), The World Space Congress – 2002*, 10–19 October 2002, Houston, TX, USA.
19. A.A. Bolonkin, "Non-Rocket Earth–Moon Transport System", COSPAR-02 B0.3-F3.3-0032-02, 02-A-02226, *34th Scientific Assembly of the Committee on Space Research (COSPAR), The World Space Congress – 2002*, 10–19 October 2002, Houston, TX, USA.
20. A.A. Bolonkin, "Non-Rocket Earth–Mars Transport System", COSPAR 02-A-02224, *34th Scientific Assembly of the Committee on Space Research (COSPAR). The World Space Congress – 2002*, 10–19 October 2002, Houston, TX, USA.
21. A.A. Bolonkin, "Transport System for Delivery Tourists at Altitude 140 km", IAC-02-IAA.1.3.03, *53rd International Astronautical Congress, The World Space Congress – 2002*, 10–19 October 2002, Houston, TX, USA.
22. A.A. Bolonkin, "Non-Rocket Transport System for Space Travel", *Journal of British Interplanetary Society*, Vol. 56, No. 7/8, 2003, pp. 231–249.

This page intentionally left blank

CHAPTER 2

Cable Space Accelerator*

Summary

A method and facilities for delivering payload and people into outer space are presented. This method uses, in general, engines and a cable located on a planetary surface. The installation consists of a space apparatus, power drive stations located along the trajectory of the apparatus, the cable connected to the apparatus and to the power stations, and a system for suspending the cable. The drive stations accelerate the apparatus up to hypersonic speed.

The estimations and computations show the possibility of making these projects a reality in a short period of time (two project examples are given: a launcher for tourists and a launcher for payloads). The launch will be very cheap at a projected cost of \$1–5/lb. The cable is made from cheap artificial fiber widely produced by modern industry.

2.1 Introduction

At present, rockets are used to carry people and payloads into space, or to deliver bombs over long distances. This method is very expensive, and requires a well-developed industry, high technology, expensive fuel, and complex devices.¹

Other than rockets, methods to reach the space velocities are the space elevator,² the hypersonic tube air rocket,³ and the electromagnetic system.⁴ Several new non-rockets methods were also proposed by author at the World Space Congress-2002, Houston, USA, 10–19 October 2002.

The space elevator requires very strong nanotubes, as well as rockets and high technology for the initial development. The tube air rocket and non-rocket systems require more detailed research. The electromagnetic transport system, suggested by Minovich,

* This chapter was presented as Bolonkin's papers IAC-02-V.P.06, IAC-02-S.P.14 at *World Space Congress-2002*, 10–19 October, Houston, TX, USA, and as variant No. 8057 at symposium *The Next 100 years*, 14–17 July 2003, Dayton, OH, USA.

is not realistic at the present time. It requires a vacuum underground tunnel 1530-km long located at a depth of 40 km. The project requires a power cooling system (because the temperature is very high at this depth), a complex power electromagnetic system, and a huge impulse of energy which is greater than the energy of all the electric-generating stations on Earth.

This chapter suggests a very simple and inexpensive method and installation for launching into space.

This is a new revolutionary space launcher system for delivering hypersonic speeds. This method uses the straight cable launcher, intermediate power (drive) stations, any conventional engines (mechanical, electrical, gas turbines), and flywheels (as storage energy) located on the ground. After completing an exhaustive literature and patent search, the author cannot find the same space method or similar facilities mentioned elsewhere.

The distinguishing features of the given research in comparison with that previously described⁵ is the installation design (single cable and short distance between drive stations) that allows the use of the cheap artificial fiber widely produced by current industry.

2.2 Description of suggested launcher

2.2.1 Brief description

The installation includes (see notations in Fig. 2.1): a cable; power drive stations; winged space apparatus (space ship, missile, probe, projectile, and so on); conventional engines and flywheels; and a launching area (airdrome). Between drive stations the cable is supported by columns. The columns can also hold additional cables for future launches and a delivery system for used cable.

The installation works in the following way. All drive station start to run. The first power station pulls the cable (1) connected to the winged space apparatus. The apparatus takes off from the start area and flies with acceleration along trajectory (5). When the apparatus

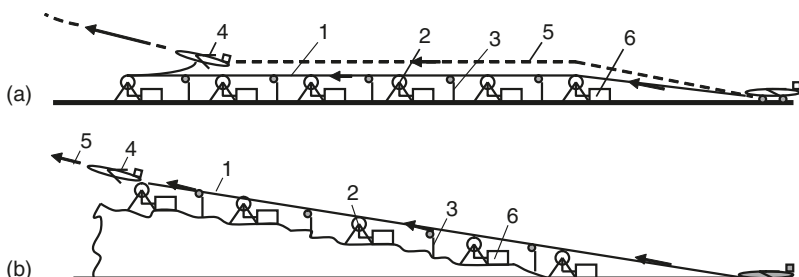


Fig. 2.1. (a) Launcher for a crewed space ship with single cable. *Notations:* (1) Cable contains three parts: main part, outlet part, and directive part; (2) power drive station; (3) cable support columns; (4) winged space apparatus (space ship, missile, probe, projectile, and so on); (5) trajectory of space apparatus; and (6) engine. (b) A fixed slope maintained small launcher for projectiles.

reaches the first drive station, this drive station disconnects from the cable and the next drive station continues the apparatus acceleration, and so on. At the end of the distance, the winged apparatus has reached hypersonic speed, disconnects from the cable, changes the horizontal acceleration into vertical acceleration (while it is flying in the atmosphere) and leaves the Earth's atmosphere.

The power stations contain the engines. The engine can be of any type, for example, gas turbines, or electric or mechanic motors. The power drive station has also an energy storage system (flywheel accumulator of energy), a type transmission and a clutch. The installation can also have a slope and launch a projectile at an angle to horizon (Fig. 2.1(b)).

The cable includes three parts (Fig. 2.2): directive part, inlet part, and main (pull) part. The lengths of the inlet and main parts equal the distance between drive stations, and the directive part controls only itself. It directs the inlet part to the drive stations. Its length equals the full acceleration distance minus the inlet and pull parts. This design allows the use of the current fibers, and minimizes the cable mass and energy.

The cables are made from light strong material such as artificial fibers, filaments, whiskers, and nanotubes. The better the cable properties the less the installation requires in terms of the drive stations, and cable mass and energy.

The rollers are made from strong matter such as a composite material.

2.2.2 Advantages

The suggested launch cable system has big advances in comparison with current rocket systems:

1. The cable launcher is cheaper by several times than the modern rocket launch system. No expensive rockets are needed.
2. The cable launcher decreases the delivery cost by some thousand times (up to \$1–2/lb).
3. The cable launcher can be made in 1 year. Modern rocket launch systems require some years for development, design, and building.
4. The cable launcher does not require high technology and can be made by any non-industrial country.

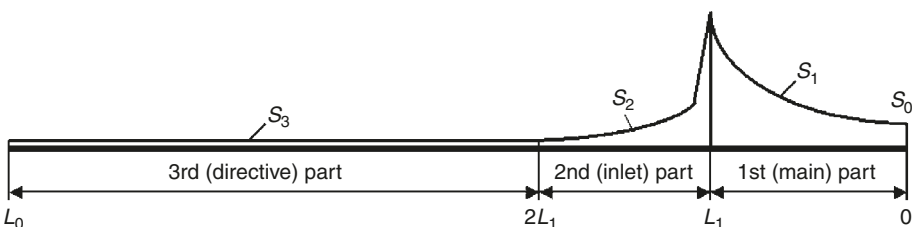


Fig. 2.2. Optimal cable cross-section area along the launch distance.

5. Rocket fuel is expensive. The cable launcher can use the cheapest sources of energy such as wind, water, or nuclear power, or the cheapest fuels such as gas, coal, peat, etc., because the engine is located on the Earth's surface. The flywheels may be used as an accumulator of energy.
6. It is not necessary to have highly qualified personnel such as rocket specialists with high salaries.
7. The fare for the space tourists is small.
8. There is no pollution of the atmosphere from toxic rocket gas.
9. Thousands of tons of useful loads can be launched annually.

2.2.3 Cable discussing

The reader can find the cable discussing in Chapter 1 and cable characteristics in Refs.^{5–9} In our projects we use only cheap artificial fibers widely produced by present industry.

2.3 Theory of the cable launcher

2.3.1 Formulas for estimation and computation (in metric system)

Below are a well-known formula from physics and formulas developed by the author. These formulas can be used for calculation of the different variants.

2.3.1.1 Relative cross-section area

Relative cross-section area, \bar{S} , and weight of an optimal cable of an equal (constant) stress can be found as a solution of the differential equation of local balance of inertia force, F , and cable stress force.

- (a) For the main part of the cable, the relative cross-section area is:

$$\begin{aligned} dF_1 &= ngdm_1 = ng\gamma S_1 dL = \sigma dS_1, \quad \frac{dS_1}{S_1} = \frac{ng\gamma}{\sigma} dL, \quad \ln S_1 \Big|_{S_0}^{S_1} = \frac{ng\gamma}{\sigma} \Big|_0^L, \\ W &= \int_0^L \gamma S_1 dL, \quad \text{or} \quad \bar{S}_1 = \frac{S_1}{S_0} = \exp \frac{ng\gamma L}{\sigma}, \quad S_0 = \frac{ngm}{\sigma}, \\ W &= m \left[\exp \left(\frac{ng\gamma L}{\sigma} \right) - 1 \right], \quad K = 10^{-7} \frac{\sigma}{\gamma} \end{aligned} \quad (2.1)$$

where S_1 is the cross-section cable area of main part [m^2]; S_0 is the cross-section area of cable near the ship [m^2]; n is the overload; $g = 9.81 \text{ m/s}^2$ is gravity; σ is the tensile stress [N/m^2]; γ is the specific density [kg/m^3]; L is the distance between power stations [m]; m is the mass of apparatus [kg]; m_1 is the mass of the main cable part [kg]; W is the cable weight [kg]; and K is the stress coefficient. The result of the computation is shown in Figs. 2.3–2.7.

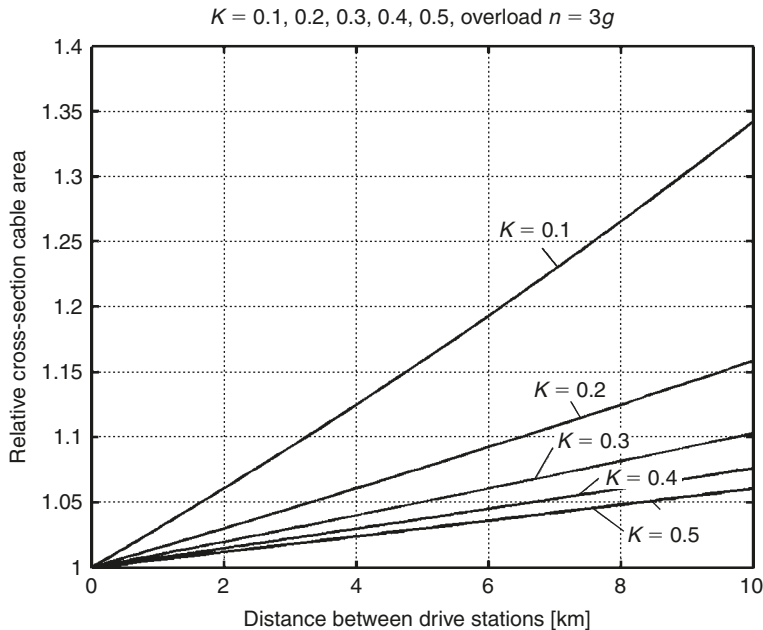


Fig. 2.3. Relative cable cross-section area versus the distance between drive stations for stress coefficient $K = 0.1–0.5$ ($K = 10^{-7}\sigma/\gamma$) and overload $3g$.

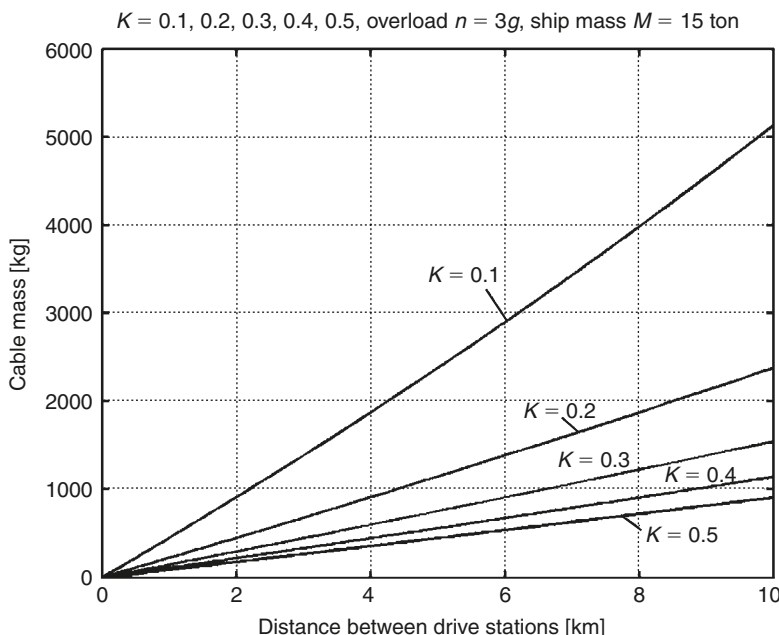


Fig. 2.4. Cable mass versus distance between drive stations for $K = 0.1–0.5$, overload $3g$, space ship mass 15 ton.

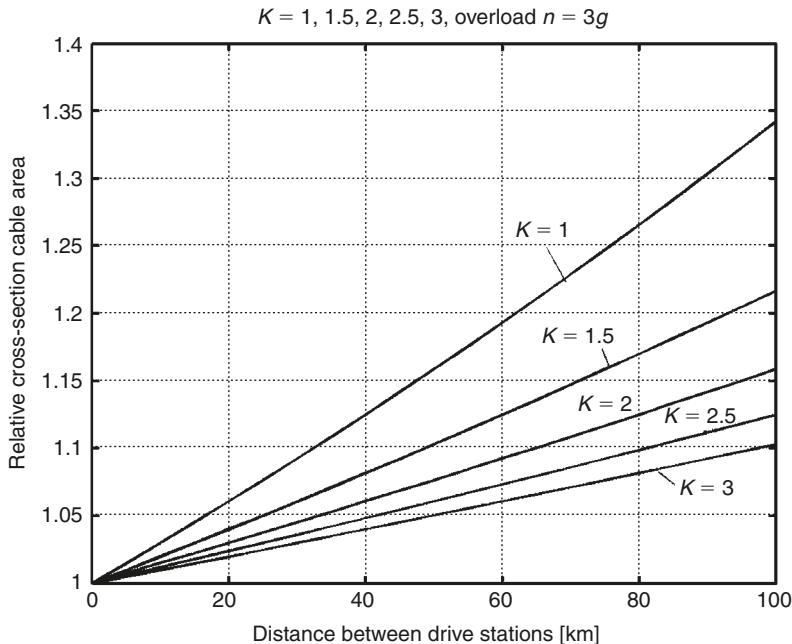


Fig. 2.5. Relative cable cross-section area versus distance between drive station for $K = 1\text{--}5$, overload $3g$. High stress coefficient allows do decrease the drive station distance (compare with Fig. 2.3).

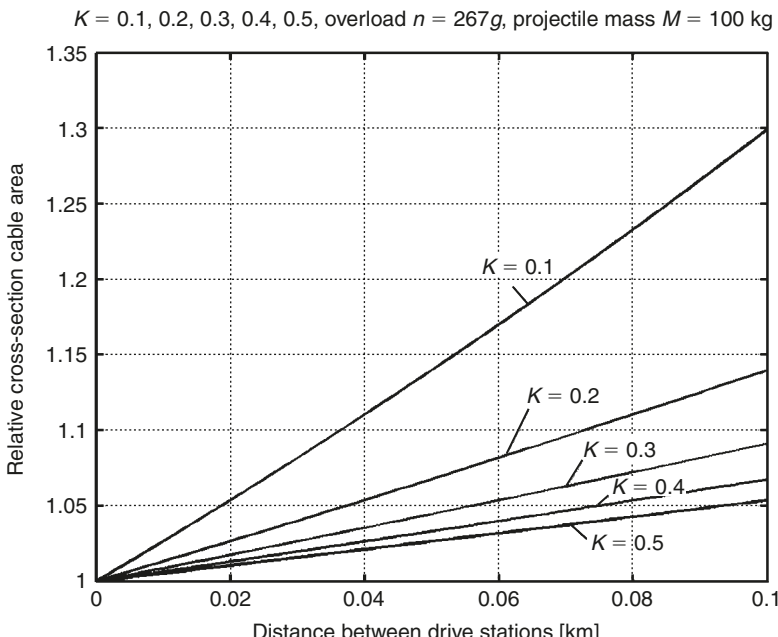


Fig. 2.6. Relative cable cross-section area versus the distance between drive stations for stress coefficient $K = 0.1\text{--}0.5$ ($K = 10^{-7}\sigma/\gamma$) and overload $267g$.

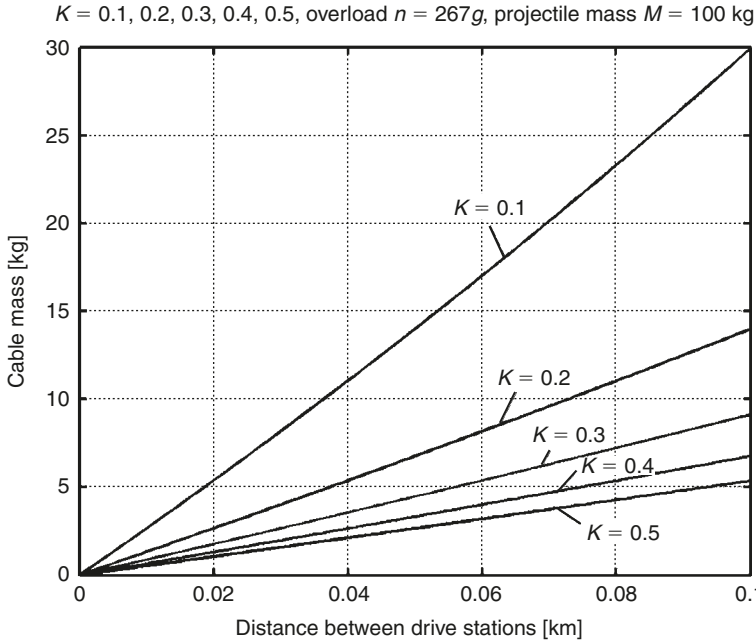


Fig. 2.7. Cable mass versus distance between drive stations for $K = 0.1-0.3$, overload $267g$, and apparatus mass 100 kg .

(b) For the inlet part of the cable the noted values are as follows:

$$\begin{aligned}
 dF_2 &= ngdm_2 = ng\gamma S_0 \exp\left[\frac{ng\gamma}{\sigma}(L_1 - L)\right] dL, \\
 F_2 &= ngm \exp\left[\frac{ng\gamma}{\sigma} L_1\right] \left[1 - \exp\left(-\frac{ng\gamma}{\sigma} L\right)\right], \\
 S_0 &= \frac{ngm}{\sigma}, \quad S_2 = \frac{F_2}{\sigma}, \quad W = \int_0^{L_1} \gamma S_2 dL, \quad \text{or} \\
 \bar{S}_2 &= \frac{S_2}{S_0} = \exp\frac{ng\gamma L_1}{\sigma} \left[1 - \exp\left(-\frac{ng\gamma}{\sigma}\right)\right], \\
 W &= \gamma S_0 \exp\frac{ng\gamma L_1}{\sigma} \left[L_1 + \frac{\sigma}{ng\gamma} \left(\exp\left(-\frac{ng\gamma L_1}{\sigma}\right) - 1\right)\right], \tag{2.1a}
 \end{aligned}$$

where L_1 is the distance between drive stations [m]; F_2 is the force in the inlet cable part [N]; and m_2 is the mass of the inlet cable part. The inlet part introduces the main part to an inlet of the drive station.

(c) The directive part directs the inlet part to an inlet of the drive station and supports only itself. This part can be thin and has a constant cross-section.

The optimal cable cross-section area is shown in Fig. 2.2.

2.3.1.2 Safety cable speed

Let us take a small part of the rotary circle and write the balance:

$$\frac{2SR\alpha\gamma V^2}{R} = 2S\sigma \sin \alpha,$$

where V is the rotary cable speed [m/s]; R is the circle radius [m]; and α is the angle between the ends of the circle part [rad.]. If $\alpha \rightarrow 0$, the relationship between maximum rotational speed V and tensile stress of the closed-loop (curve) cable is:

$$V = \sqrt{\frac{\sigma}{\gamma}}. \quad (2.2)$$

2.3.1.3 Energy

Energy, E , storage by the rotary flywheel per 1-kg cable [J/kg] can be found from the known equation of the kinetic energy and equation (2.2):

$$E = \frac{V^2}{2} = \frac{1}{2} \frac{\sigma}{\gamma}. \quad (2.3)$$

2.3.1.4 Maximum distance

The maximum distance L [km] between supports of the suspension system (without wings) for $h \ll R$, where $R = 6378$ km, and the radius of the Earth can be found from geometry. That is:

$$L \cong 2\sqrt{(R + h)^2 - R^2} \approx 2\sqrt{2Rh} = 226\sqrt{h}, \quad (2.4)$$

where h [km] is the altitude of support.

2.3.1.5 Amount of sag ΔH of the cable

The amount of sag ΔH of the cable (from its weight and the curvature of the Earth) can be found from the balance between weight and stress. The cable has a parabolic form under its weight: $y = ax^2 - b$, $a > 0$, $y' = 2ax$, $a = \operatorname{tg}\alpha/2x = \operatorname{tg}\alpha/L$. If $x = 0$, then $b = H_2$. If $y = 0$, then $x = \pm L/2$. We also have the balance equation $W = 2T \sin \alpha$ or $\sin \alpha = W/2T$. We substitute these equations and put $\operatorname{tg}\alpha \cong \sin \alpha \cong \alpha$. The cable sag, H_2 , under its weight is as follows:

$$H_2 = \frac{\tan \alpha}{L} \left(\frac{L}{2} \right)^2 = \frac{\alpha L}{4} = \frac{WL}{8T} = \frac{SL\gamma L}{8T} = \frac{S\gamma L^2}{8T}.$$

The sag from the Earth's curvature is $H_1 = L^2/8R$ from equation (2.4), and the total sag is:

$$\Delta H = H_1 + H_2 \approx \frac{L^2}{8} \left(\frac{S\gamma}{T} + \frac{1}{R} \right) = \frac{L^2}{8} \left(\frac{\gamma}{g\sigma} + \frac{1}{R} \right), \quad (2.5)$$

where ΔH is the sag of the cable [m]; L is the distance between supports [m]; T is the tension of the cable [kg]; S is the cross-section cable area [m^2]; R is the Earth's radius [m]; and W is the cable weight [kg].

2.3.1.6 Flight range

The estimation of maximum horizon *flight range*, r , of the winged projectile in the atmosphere is found from the kinetic energy:

$$Dr = \frac{m}{2}(V_2^2 - V_1^2), \quad D = gm/k_3, \quad \text{or} \quad r = \frac{k_3}{2g}(V_2^2 - V_1^2), \quad (2.6)$$

where k_3 is the projectile ratio of lift/drag ($k_3 = 3 - 6$); V_2 is the initial speed of the projectile [m/s]; and V_1 is the final speed of projectile [m/s].

2.3.1.7 Wave drag

The equation for the estimation of *wave drag*, D , of an edge-ship cable for supersonic velocity can be given from aerodynamic equations:

$$\begin{aligned} dD &= C_D \frac{\rho(H)V^2}{2} dA, \quad D = C_D \frac{\rho V^2}{2} A, \quad C_D = \frac{4c^2}{\sqrt{M^2 - 1}}, \\ V &= aM, \quad A = wH/\sin \theta, \quad c = \frac{h_1}{w} \sin \theta, \quad \rho = \rho_0 e^{bH}, \\ \text{for } M > 3 \quad \frac{M}{\sqrt{M^2 - 1}} &\approx 1, \end{aligned} \quad (2.7)$$

where D is the air drag [N]; M is the Mach number; $a = \text{const.}$ – the speed of sound [m/s]; C_D is the drag coefficient; A is the specific area [m^2]; V is the cable speed [m/s]; $c = h_1/w$ is the ratio a thickness; h_1 , to width, w , of an edge-type cable; ρ [kg/m^3] is the air density at altitude H [m]; $\theta = \text{const.}$ – the angle of the cable to the horizon; $b \approx -1.3115 \times 10^{-4}$, the coefficient of change of air density with altitude; $\rho_0 = 1.225$ – the air density at $H = 0$.

Let us substitute equation (2.7) in the first equation for D given above and integrate this for the interval of altitude from H_0 to H :

$$\begin{aligned} D &= 2c^2Vwa \sin \theta \int_{H_0}^H \rho(H)dH = \frac{2\rho_0 a V c^2 w \sin \theta}{b} (e^{bH} - e^{bH_0}) \\ &= \frac{2\rho_0 a V c^{1.5} S^{0.5} \sin \theta}{b} (e^{bH} - e^{bH_0}), \end{aligned} \quad (2.8)$$

where $S = wh_1$ [m^2] is the cable cross-section area.

2.3.1.8 Loss of speed

Loss ΔV [m/s] of speed, when a projectile passes through the atmosphere with a trajectory angle $\theta = \text{const.}$, can be found from the energy equation:

$$E = \int_{H_0}^H \frac{D}{\sin \theta} dH, \quad D = C_D \frac{\rho V^2}{2} F,$$

$$E = \frac{2c_1^2 a V A F}{\sin \theta} \int_{H_0}^H \rho_0 e^{bH} dH = \frac{2c_1^2 a V A F \rho_0}{b \sin \theta} (e^{bH} - e^{bH_0}).$$

For other cases the amount of energy lost, E , is:

$$E = \frac{m}{2} (V^2 - V_1^2), \quad V_1 = \sqrt{V^2 - \frac{2E}{m}}, \quad V_1 = V - \Delta V,$$

or

$$\Delta V = V - \sqrt{V^2 - \frac{2E}{m}}, \quad E = \frac{2c^2 a V F \rho_0}{b \sin \theta} (e^{bH} - e^{bH_0}), \quad (2.9)$$

where V is the initial speed of the projectile [m/s]; m is the mass of the projectile [kg]; $a = 300 \text{ m/s}$ – the speed of sound; F is the specific area of the projectile [m^2]; c_1 is the semi-angle of the projectile edge in radians; θ is the angle of the trajectory to the horizon; H is the altitude at which the projectile disconnects from the cable [m]; $\rho_0 = 1.225 \text{ kg/m}^3$ – air density at altitude $H = 0$. The result of this computation (for $c_1 = 0.1$, $F = 0.01 \text{ m}^2$, $a = 300 \text{ m/s}$, $H_0 = 3 \text{ km}$, $H = 50 \text{ km}$) is presented in Fig. 2.8. This loss is small.

Many people know about the “Shuttle” heating up in the atmosphere and think that a hypersonic space projectile will have a large amount of heat when it crosses the atmosphere. This is wrong. The purposes of the “Shuttle” and a hypersonic space projectile are opposed. A space ship, when it re-enters into the atmosphere, has a huge kinetic energy and must decrease its hypersonic speed (energy) to subsonic speed. The Shuttle has a special spherical body nose and pointless wing edge to increase the air drag by tens to hundreds of times. This means a lot of heating takes place. The Shuttle also has a long horizontal trajectory along the Earth’s surface. The purpose of a projectile is to save speed and energy. The projectile has a sharp body bow, and wing edge. The required head protection of launch rockets is tens of time less than re-entry apparatus.

2.3.1.9 Cable friction

Estimation of *cable friction* due to the air. This estimation is very difficult because there are no experimental data for air friction of an infinitely very thin cable (especially at hypersonic speeds). A computational method for plates at hypersonic speed as described by Anderson (Ref.¹⁰, [p. 287]) was used. The computation is made for two cases: a laminar and a turbulent boundary layer.

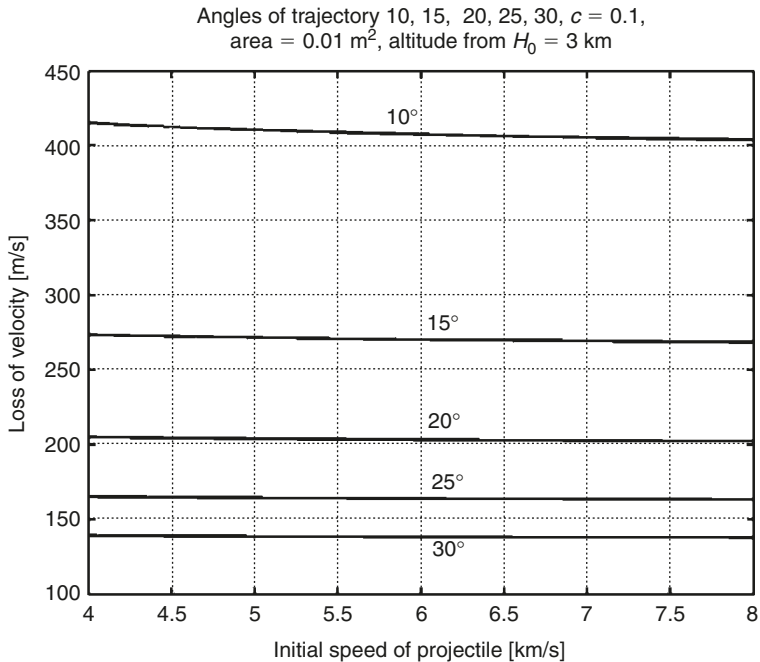


Fig. 2.8. Estimation of velocity lost by projectile in the atmosphere for different trajectory angles to the horizon.

The results of this comparison are very different. Turbulent flow has maximum friction. About 80% of the friction drag occurs in the troposphere (from 0 to 12 km). If cable end is located on a mountain at 4-km altitude the maximum air friction will be decreased by 30%.

It is postulated that half of the cable surface will have a laminar boundary layer because a small wind or trajectory angle will blow away the turbulent layer and restore the laminar flow. The blowing away of the turbulent boundary layer is studied in aviation and is used to restore laminar flow and decrease air friction. The laminar flow decreases the friction in hypersonic flow about by 280 times! If half of the cable surface has a laminar layer, it means that we must decrease the air drag calculated for full turbulent layer a minimum of 2 times.

Below, the equations from Anderson for computation of the local air friction for a two-sided plate are given¹⁰:

$$(T^*/T) = 1 + 0.032M^2 + 0.58(T_W/T - 1); \quad \mu^* = 1.458 \times 10^{-6} T^{*1.5}/(T^* + 110.4); \\ \rho^* = \rho(T/T^*); \quad Re^* = \rho^* Vx / \mu^*; \quad C_{f,l} = 0.664/(Re^*)^{0.5}; \quad C_{f,t} = 0.0592/(Re^*)^{0.2}; \\ \rho^* D_L = 0.5C_{f,l}\rho^* V^2 S; \quad D_T = 0.5C_{f,t}\rho^* V^2 S, \quad S = \pi d, \quad (2.10)$$

where T^* , Re^* , ρ^* , μ^* are reference (evaluated) temperature; Reynolds number, air density, and air viscosity, respectively. M is Mach number; V is speed; x is length of plate (distance from the beginning of the cable); T is flow temperature; T_w is body temperature; $C_{f,l}$ is a local skin friction coefficient for laminar flow; $C_{f,t}$ is a local skin friction coefficient for turbulent flow. S is area of skin [m^2] of both plate sides (this means for the cable we must take $0.5S$); and D is air drag (friction) [N]. It may be shown that the general air drag for the cable equals $D_g = 0.5D_T + 0.5D_L$, where D_T is turbulent drag and D_L is laminar drag.

From equation (2.10) we can derive the following equations for turbulent and laminar flows of a horizontal cable:

$$D_T = 0.0465\rho^{*0.8}\mu^{*0.2}V^{1.8}L^{0.8}d, \quad (2.11)$$

$$D_L = 0.521\rho^{*0.5}\mu^{*0.5}V^{1.5}L^{0.5}d, \quad (2.12)$$

where d is the diameter of the cable [m]. The laminar drag is less than the turbulent drag by 200–300 times and can be neglected.

Note: If L_0 is the full acceleration distance (initial length of cable) [m]; L_1 is the distance between drive stations [m]; and L is the variable length of cable [m], we can write the following equations for turbulent drag of the different cable parts:

1. Main cable part

- (a) If $0 < L < (L_0 - L_1)$, then $D_1 = BL_1^{0.8}d_1$,
where $B = 0.5 \times 0.0465\rho^{*0.8}\mu^{*0.2}V^{1.8}$, $V = (2ngL)^{0.5}$.

- (b) If $(L_0 - L_1) < L < L_0$, then $D_1 = B(L_0 - L)^{0.8}d_1$.

2. Inlet cable part

- (a) If $0 < L < (L_0 - 2L_1)$, then $D_2 = BL_1^{0.8}d_2$.
- (b) If $(L_0 - 2L_1) < L < (L_0 - L_1)$, then $D_2 = B(L_0 - L)^{0.8}d_2$.
- (c) If $0 < L < (L_0 - 2L_1)$, then $D_2 = 0$.

3. Directive part

- (a) If $0 < L < (L_0 - 2L_1)$, then $D_3 = B(L_0 - L)^{0.8}d_3$.
- (b) If $(L_0 - 2L_1) < L < L_0$, then $D_3 = 0$.

Here d_1 , d_2 , d_3 are average cable diameters of the main, inlet, and directive parts, respectively [m].

Full cable drag is thus:

$$D = D_1 + D_2 + D_3. \quad (2.13)$$

2.3.1.10 Mass of cable

Mass of cable is:

$$M = M_1 + M_2 + M_3 = \frac{\pi}{4} \gamma [d_1^2 L_1 + d_2^2 L_1 + d_3^2 (L_0 - 2L_1)]. \quad (2.14)$$

The accelerated cable mass is:

$$M_a \approx M_1 + M_2 + 0.125M_3, \quad (2.15)$$

where the coefficient 0.125 is the product of an average length (0.5) and an average speed (0.5^2) of the directive cable part.

2.3.1.11 Energy

The *energy* required by the cable air drag is:

$$E = \int_0^{L_0} D dL. \quad (2.16)$$

The results of computations of equations (2.13)–(2.15) are presented in Figs. 2.9–2.14 for two projects (see below) and different initial cable diameters.

2.3.1.12 Subsonic speed

For subsonic speed the formulas (2.11)–(2.12) are the same, but conventional ρ and μ must be inserted.

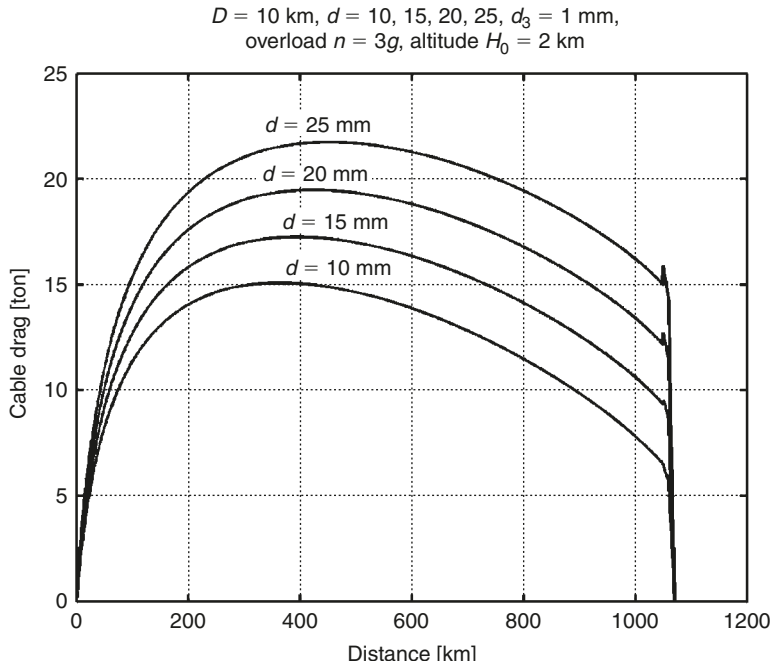


Fig. 2.9. Cable drag along the acceleration distance for initial cable diameter at ship $d_o = 10\text{--}25 \text{ mm}$, cable diameter of part 3 $d_3 = 1 \text{ mm}$, overload $3g$, at altitude 2 km .

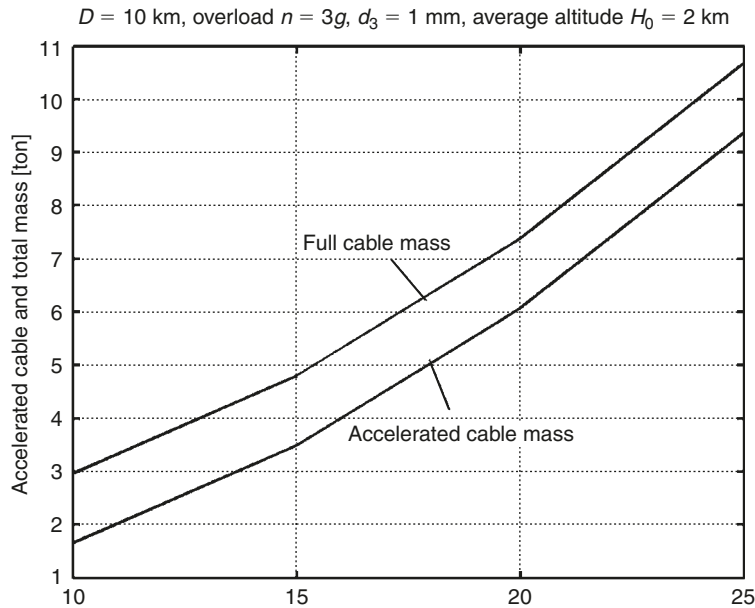


Fig. 2.10. Cable mass versus the initial cable diameter at ship 10–25 mm, for distance between drive stations $L_1 = 10 \text{ km}$, overload $n = 3g$, $d_3 = 1 \text{ mm}$.

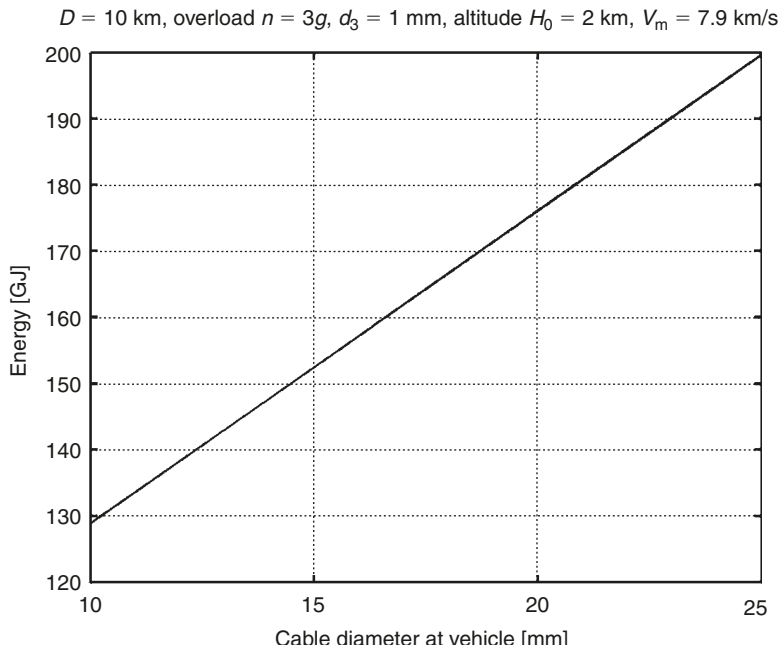


Fig. 2.11. Cable air drag energy versus the initial cable diameter at ship 10–25 mm, for distance between drive stations $L_1 = 10 \text{ km}$, overload $n = 3g$, $d_3 = 1 \text{ mm}$.

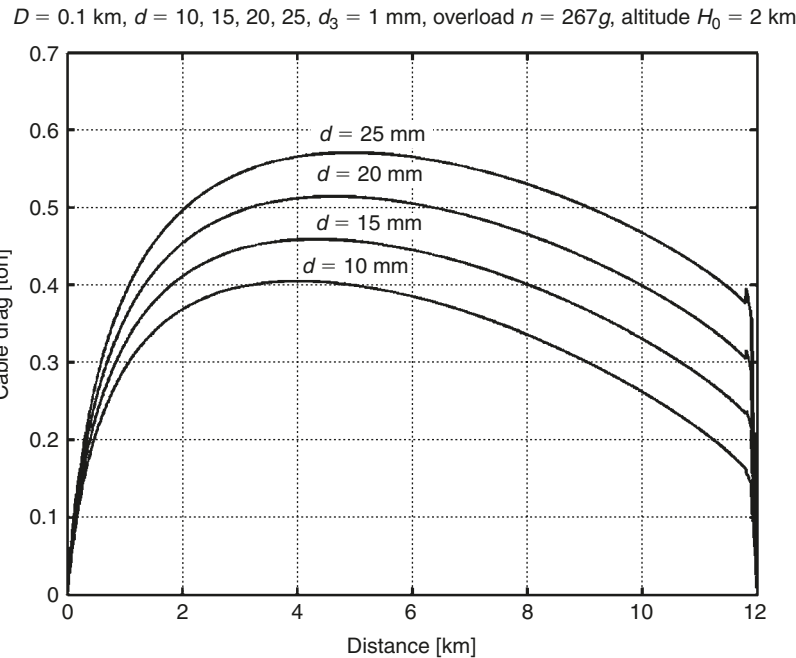


Fig. 2.12. Cable drag along the acceleration distance for initial cable diameter at ship $d_o = 10\text{--}25 \text{ mm}$, cable diameter of part 3 $d_3 = 1 \text{ mm}$, overload $267g$, at altitude 2 km .

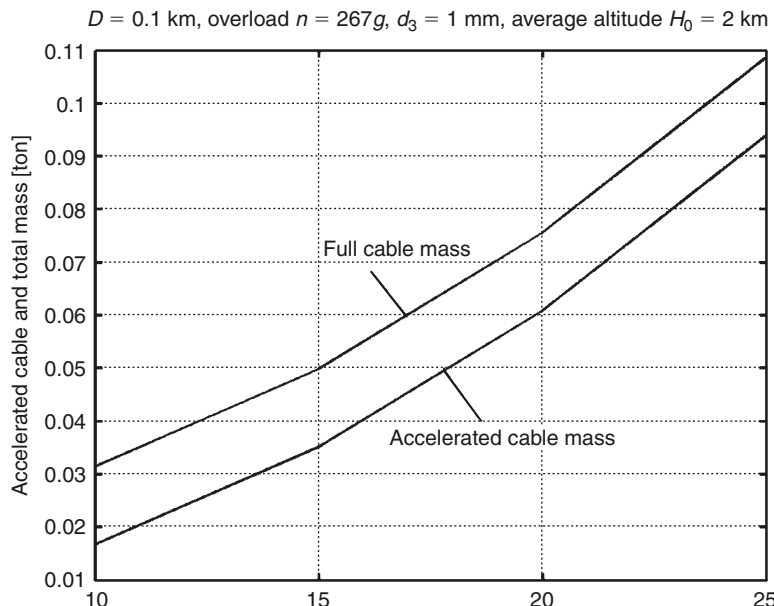


Fig. 2.13. Cable mass versus the initial cable diameter at ship $10\text{--}25 \text{ mm}$, for distance between drive stations $L_1 = 0.1 \text{ km}$, overload $n = 267g$, $d_3 = 1 \text{ mm}$.

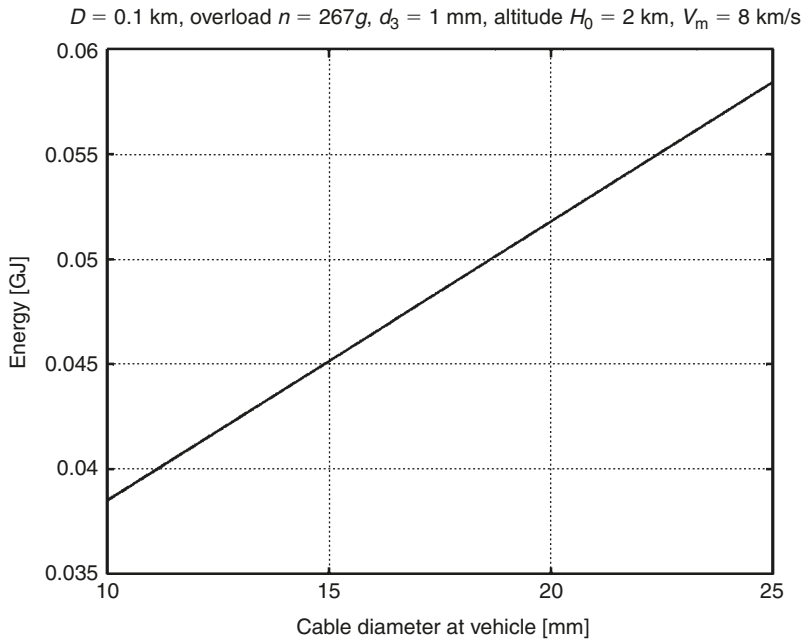


Fig. 2.14. Cable air drag energy versus the initial cable diameter at ship 10–25 mm, for distance between drive stations $L_1 = 0.1 \text{ km}$, overload $n = 267g$, $d_3 = 1 \text{ mm}$.

2.3.1.13 Last drive station

The last drive station can be located on a mountain top. The final ship trajectory will have an angle to the horizon. After disconnection from the launcher the winged ship can increase this angle while flying in the atmosphere. This additional angle, lost velocity, and time can be estimated in the following way. First write the standard ship equations of air movement:

$$\dot{H} = V \sin \theta, \quad \dot{V} = -\frac{D}{m} - g \sin \theta, \quad \dot{\theta} = \frac{L}{mV} - \frac{g}{V} \cos \theta + \frac{V \cos \theta}{R},$$

where H is the altitude; V is the speed; θ is the trajectory angle [rad]; D is the drag; L is the lift force; m is the ship's mass; and R is the Earth's radius.

If parameter changes in θ angle and time t , are small, and the speed is close to 8 km/s, we have:

$$\begin{aligned} \sin \theta &\approx \theta, \quad \cos \theta \approx 1, \quad \theta_a = 0.5(\theta + \theta_0), \quad D = ngm/k, \\ L &= ngm, \quad \frac{g}{V} - \frac{V}{R} \approx 0, \quad t = \frac{\Delta H}{V \sin \theta_a}, \quad \Delta V = -\left(\frac{ngm}{mk} + g \sin \theta_a\right)t, \\ \theta - \theta_0 &= \frac{ngm}{kmV} t, \quad k = \frac{L}{D}, \end{aligned}$$

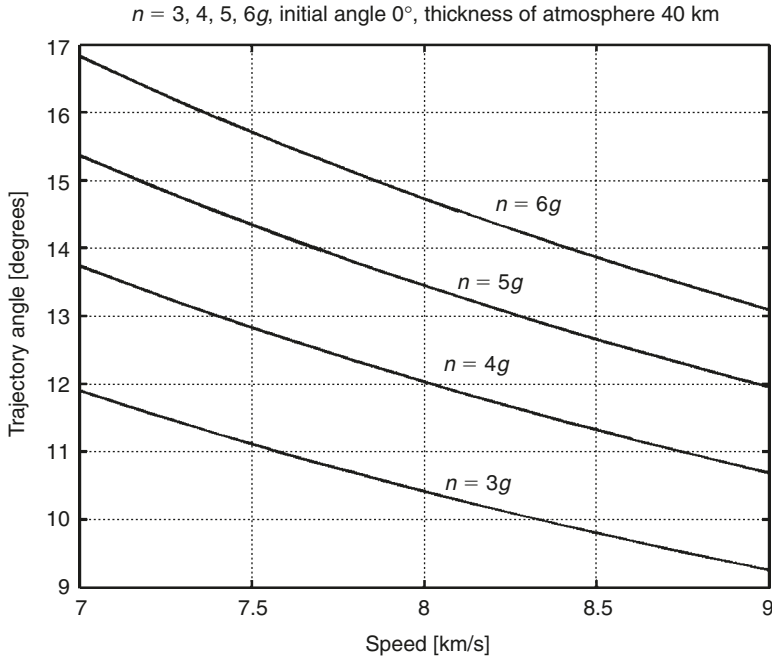


Fig. 2.15. Final trajectory angle versus speed for overload $n = 3-6g$, initial trajectory angle 0° .

or equations for estimation:

$$\theta \approx \left(\theta_0^2 + \frac{2ng\Delta H}{V^2} \right)^{0.5}, \quad \Delta V \approx -\frac{g\Delta H}{V} \left(1 + \frac{n}{k\theta_a} \right), \quad t \approx \frac{\Delta H}{V \sin \theta_a}, \quad (2.17)$$

where n is the overload; ΔH is the altitude change [m]; ΔV is the speed change (speed lost) [m/s]; $k = L/D$ – average ratio of lift/drag of the ship ($k = 3-7$); θ_0 is the initial trajectory angle [rad]; and t is time [s].

The results of the computation are presented in Figs. 2.15–2.16.

2.4 Projects

Below are estimations for two projects: (1) tourists with low acceleration ($3g$) and (2) payloads (projectiles) with high acceleration ($270g$).

2.4.1 Project 1

2.4.1.1 The launch of tourists into space (Fig. 2.1(a), single cable version)

Assume the mass of the space vehicle is $m = 15$ ton (100 tourists and 4 members of crew); overload is $n = 3$ “ g ”, the acceleration is $a = 3g \cong 30$ m/s ($g = 9.81 \cong 10$ m/s 2) (this acceleration is safe for conventional purposes); the final speed is 8 km/s.

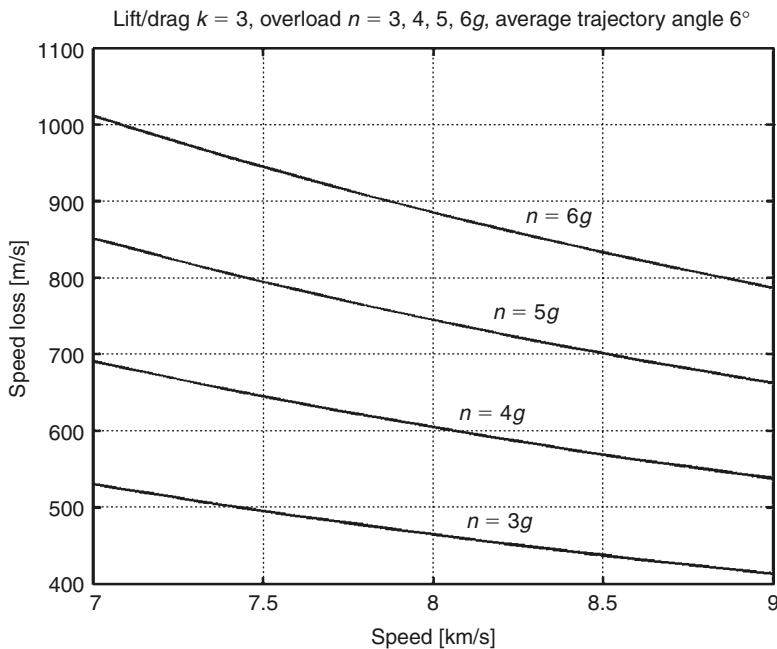


Fig. 2.16. Speed loss (method 2) versus speed for ratio lift/drag $k = 3$, overload $n = 3\text{--}6g$, and average trajectory angle $\theta_a = 6^\circ = 0.1 \text{ rad}$.

The required distance of acceleration is $L = V^2/2a \approx 1070 \text{ km}$. The time of horizontal acceleration is $t = V/a \approx 4 \text{ min } 27 \text{ s}$. (If trained cosmonauts are launched the safe acceleration can be taken as $8g$ and the required launch distance will be 400 km and the time $1 \text{ min } 40 \text{ s}$.) The time of vertical acceleration ($3g$) in the atmosphere (after disconnection) is about 50 s . The final angle is about $\theta = 12^\circ$.

Assume we use the artificial cheap fiber widely produced by current industry. Safe tensile strength of the vehicle cable is $\sigma = 180 \text{ kg/mm}^2$ (safety factor is $n_1 = 600/180 = 3.33$), density $\gamma = 1800 \text{ kg/m}^3$ ($K = 180/1800 = 0.1$). Then the cross-section area of the vehicle cable about the vehicle will be $S_0 = nmg/\sigma = 250 \text{ mm}^2$, diameter $d_o = 2(S/\pi)^{0.5} = 17.8 \text{ mm}$, average diameter is about $d_{o,a} = 19 \text{ mm}$.

Let us assume that the drive stations are located every $L_1 = 10 \text{ km}$. We need 107 drive stations. The final drive station is located at altitude $H_0 = 4 \text{ km}$. Mass of the cable is $M = 7 \text{ ton}$, accelerated cable mass is $M_a = 5.6 \text{ ton}$ (Fig. 2.10). A variable cross-section areas of main and inlet cables are included in the average diameter.

The energy required for accelerating the ship and cable is $E = (m + M_a)V^2/2 = 659 \times 10^9 \text{ J}$ (659 GJ) if $V = 8 \text{ km/s}$. The energy of air drag of the cable is 172 GJ (see Fig. 2.11). The average drag of the ship is about $D = m/k = 15/3 = 5 \text{ ton}$ (here k is the ratio of the lift force to the drag of the ship). This is $E = DL = 5 \times 10^4 \times 1,070,000 = 53.5 \text{ GJ}$. The total energy required for one launch is $E_T = 884.5 \text{ GJ}$. If the launches are made every hour the

engines must have a total power of about $P = E_T/t = 884 \times 10^9/60/60 = 246,000 \text{ kW}$ distributed between 107 drive station (that is 2300 kW each). If the engine efficiency is $\eta = 0.3$ the fuel consumption will be $F = 884 \times 10^9/\varepsilon/0.3 = 70 \text{ ton}$ per each flight. Here $\varepsilon = 42 \times 10^6 [\text{J/kg}]$ is the energy capability of diesel fuel. This means that 7001 of fuel is used for each tourist. If the safe tensile strength is 180 kg/mm^2 , then the total mass of the flywheels (as storage of energy) will be about $M_w = 2E/k = 2 \times 884 \times 10^9/10^6 = 1768 \text{ ton}$ or $1768/107 = 16.5 \text{ ton}$ for each drive station.

2.4.1.2 Economic efficiency

Assume a cost of \$500 million for the installation,¹¹ a lifetime of 10 years, and an annual maintenance cost of \$5 million. If 100 tourists are launched on every flight, and there is one flight every hour for 350 days a year, then 840,000 passengers will be launched per year. The launch cost for one passenger is $55,000,000/840,000 = \$65.5$ plus fuel cost. If 7001 of fuel are used for one passenger and the fuel price is \$0.25/l, then the fuel cost is \$175/passenger. The total production cost will then be \$241/person. If the ticket is sold for \$349, then the profit will be about \$90 million/year.

Any reader who does not agree with this estimation can recalculate for other data. In any case, the cost of delivery will be hundreds of times less than delivery by rockets. Critics must remember that the main content of this chapter is not economical estimations, but the new idea for the launch of space apparatus.

2.4.2 Project 2

2.4.2.1 The launcher for payload (projectile) with high acceleration (267g)(Fig. 2.1(b))

We can use the equations from Project 1 for the estimation of Project 2. Assume the mass of the space apparatus is 100 kg (222 lb); the escape velocity is 8 km/s, the distance of acceleration is 12 km, the height of a mountain is 3 km (a slope is about 15°) and the acceleration stations are located every 0.1 km. The acceleration will be:

$$a = V^2/2L = 8000^2/2 \times 12,000 = 2666 \text{ m/s} = 267g.$$

Assume a fiber tensile strength of $\sigma = 180 \text{ kg/mm}^2$ for all cable parts. The cross-section area of the cable is 148 mm^2 , and the average diameter 15 mm. The total mass of the cables is 50 kg. The required energy for one launch is about 5 GJ. If the engine efficiency is $\eta = 0.3$ then the required amount of fuel is 397 kg for one launch. If the frequency of launching is 0.5 h then the required total power is 2800 kW or $2800/120 \cong 23.3 \text{ kW}$ for every drive station. The total mass of flywheels is about 10 ton or 84.3 kg in every station. The loss of velocity is 275 m/s when the projectile crosses the atmosphere at an angle 15° (Fig. 2.8).

2.4.2.2 Economic efficiency

Assume the cost of installation is \$20 million, the lifetime is 10 years, and the maintenance cost is \$1 million/year, with a frequency of launching of 30 min.

We can launch 4.8 ton/day or $4.8 \times 350 = 1680 \text{ ton/year}$. The production cost will be $3,000,000/1,680,000 = \$1.78/\text{kg}$ plus fuel cost.

We take the fuel consumption as 4 kg/1 kg payload and the price as \$0.25/kg. The fuel cost is \$1. The total cost is $1.78 + 1 = \$2.78/\text{kg}$.

2.5 General discussion

Science laboratories have whiskers and nanotubes that have high tensile strength. The theory shows that these values are only one-tenth of the theoretical level. We must study how to produce a thin cable, such as the strings or threads we produce from cotton or wool, from whiskers and nanotubes.

The fiber industry produces fibers which are used for the author's projects at the present time. However, the whiskers and especially nanotubes strongly improve the possibility of this method. They decrease the required number of drive stations, and the cable mass and drag (energy). These projects are unusual (strange) for specialists and people now, but they have huge advantages, and they have a big future.

References

1. Space Technology and Application. International Forum (STAIF), Aalbuquerque, MN, USA, 1996–1997.
2. D.V. Smitherman Jr., “Space Elevators”, NASA/CP-2000-210429, 2000.
3. A.A. Bolonkin, “Earth Accelerator for Space Ships and Missiles”, *Journal of British Interplanetary Society*, Vol. 56, No. 11/12, 2003, pp. 394–404.
4. M. Minovich, “Electromagnetic Transportation System for Manned Space Travel”, US Patent 4,795,113, 3 January 1989.
5. A.A. Bolonkin, “Space Cable Launchers”, Paper No. 8057, Presented at the *Symposium “The Next 100 years”*, Dayton, OH, USA, 14–17 July 2003.
6. F.S. Galasso, *Advanced Fibers and Composites*, Gordon and Breach Scientific Publisher, 1989.
7. *Carbon and High Performance Fibers, Directory*, 6th edition, Chapman & Hall, London & New York, 1995.
8. *Concise Encyclopedia of Polymer Science and Engineering*, Ed. J.I. Kroschwitz, New York, 1990.
9. M.S. Dresselhous, *Carbon Nanotubes*, Springer, New York, 2001.
10. J.D. Anderson, *Hypersonic and High Temperature Gas Dynamics*. McGraw-Hill Book Co., 1989.
11. D.E. Koell, *Handbook of Cost Engineering*, TCS, Germany, 2000.

CHAPTER 3

Circle Launcher and Space Keeper*

Summary

This chapter proposes a new method and installation for flight in space. This method uses the centrifugal force of a rotating circular cable that provides a means to launch a load into outer space and to keep the stations fixed in space at altitudes at up to 200 km. The proposed installation may be used as a propulsion system for space ships and/or probes. This system uses the material of any space body for acceleration and changes to the space vehicle trajectory. The suggested system may also be used as a high-capacity energy accumulator.

This chapter contains the theory of estimation and computation of suggested installations and four projects. Calculations include: a maximum speed given the tensile strength and specific density of a material, the maximum lift force of an installation, the specific lift force in planet's gravitation field, the admissible (safe) local load, the angle and local deformation of material in different cases, the accessible maximum altitudes of space cabins, the speed than a space ship can obtain from the installation, power of the installation, passenger elevator, etc. The projects utilize fibers, whiskers, and nanotubes produced by industry or in scientific laboratories.

Nomenclature

a	acceleration [m/s]
$C_{f,l}$	local skin friction coefficient of a two-sided plate for laminar flow
$C_{f,t}$	local skin friction coefficient of a two-sided plate for turbulent flow
$C_{c,l} = 0.5C_{f,l}$	local skin friction coefficient of cable for laminar flow
$C_{c,t} = 0.5C_{f,t}$	local skin friction coefficient of cable for turbulent flow
D	air drag (friction) [N]
D_T	turbulent drag [N]
D_L	laminar drag [N]

* Detail manuscript was presented as Bolonkin's paper IAC-02-IAA.1.3.03 at the *World Space Congress – 2002*, 10–19 October, Houston, TX, USA (Publication⁸). The material is published in *Journal of the British Interplanetary Society*, Vol. 56, No. 9/10, 2003, pp. 314–327.

d	cable diameter [m]
E	Young's modulus
E_s	energy stored by rotary circle per 1 kg of the cable [J/kg]
F	air friction [N]
g	specific gravity of the planet [m/s^2] (for the Earth $g = 9.81 \text{ m/s}^2$ at an altitude $H = 0$)
G	local load [kg]
H	altitude [m] or [km]
H_{\max}	maximum altitude of a circle top [m] or [km]
ΔH	decrement of an altitude [m] or [km]
$k = \delta/\gamma$	ratio of tensile stress to cable density
$K = k/10^7$	strength coefficient
L	length of a cable [m]
M	Mach number
m	throwing mass [kg]
m_{ss}	mass of a space ship [kg]
n	safety factor
N	power [J/s]
p	internal pressure on the cable circle [N/m^2]
P	maximum vertical lift force of the vertical cable circle in the constant gravity field of a planet [N]
P_1	specific lift force of 1 kg of cable mass in a planet's gravity field [N]
P_L	specific lift force of 1 m of cable in a planet's gravity field [N]
P_a	full lift force of a closed-loop cable circle rotated around a planet [N]
$P_{a,1}$	specific lift force of a 1-kg closed-loop cable circle rotated around a planet [N]
$P_{a,L}$	specific lift force of a 1-m closed-loop cable circle rotated around a planet, when $g = 0$ [N]
P_{\max}	maximum lift force of the rotary closed-loop cable circle when gravity $g = 0$ [N]
r	radius of cable cross-section area or half of cable width [m]
R	cable (circular) radius [m]
R_{\max}	maximum cable radius [m]
R_0	radius of planet [m]
R_v	radius of observation [m]
Re^*	reference Reynolds number
S	cross-section area of cable [m^2]
S_c	cable surface [m^2]
S_s	area of skin [m^2] of both plate sides, which means for cable we must take $S_c = 0.5S_s$
T	air temperature [$^\circ\text{C}$]
T^*	reference (evaluated) air temperature [$^\circ\text{C}$]
T_w	temperature of wall (cable) [$^\circ\text{C}$]
T_e	temperature of flow [$^\circ\text{C}$]
T_{\max}	maximum cable thrust [kg]
t	time [s]
V	rotary cable speed [m/s]
V_a	maximum speed of a closed-loop circle around a planet [m/s]

V_{\min}	minimum speed of a closed-loop circle [m/s]
V_c	mass speed [m/s]
V_f	speed of falling from an altitude H [m/s]
W	weight (mass) of cable [kg] or [ton]
w	thickness of a boundary layer [m], for cable $w \approx 5r$
x	length of plate (distance from the beginning of the cable) [m]
Δh	cable deformation about a local load [m]
Δh_o	cable deformation about a local load for the cable circle around a planet [m]
ΔR	increase in cable radius from internal pressure [m]
ΔV	additional speed which a space ship obtains from a cable propulsion system [m/s]
α	angle of cable section [rad]
α_h	cable angle to the horizon about a local load [rad]
γ	cable density [kg/m^3]
μ	air viscosity; for standard conditions $\mu = 1.72 \times 10^{-5}$
μ^*	reference air viscosity [$\text{kg}/\text{m s}$]
ρ	air density; for standard condition $\rho = 1.225 \text{ kg}/\text{m}^3$
ρ^*	reference air density [kg/m^3]
σ	cable tensile stress [N/m^2]
ω	planet angle speed [rad/s]

3.1 Introduction

The author proposes a revolutionary new method and launch device for: (1) delivering payloads and people into space; (2) accelerating space ships and probes for space flight; (3) changing the trajectory of space probes; (4) landing and launching of space ships on space bodies with small gravity; and (5) accelerating other space apparatus. The system may be used as a space propulsion system by utilizing the material of space bodies for propelling space apparatus, as well as for storing energy. This method utilizes the centrifugal force of a closed-loop cable circle (hoop, semi-circle, double circle). The cable circle rotates at high speed and has the properties of an elastic body.

The current proposal is a unique transport system for delivering loads and energy from Earth to the space station and back. The major difficulties of the space elevator^{1,2} are in delivering the energy to the transport gondola of a space elevator and the fact that electric wire weighs a lot more than a load bearing cable. The currently proposed space transportation system solves this problem by locating a motor on the Earth and using conventional energy to provide the power to move the gondola to the space station. Moreover the present transportation system can transfer large amounts of mechanical energy from the Earth to the space station on the order of 3–10 MW.

3.2 Description of circle launcher

The installation includes (Fig. 3.1) a closed-loop cable made from light, strong material (such as artificial fibers, whiskers, filaments, nanotubes, composite material) and a main engine, which rotates the cable at a fast speed in a vertical plane. The centrifugal force makes the closed-loop cable a circle. The cable circle is supported by two pairs (or more)

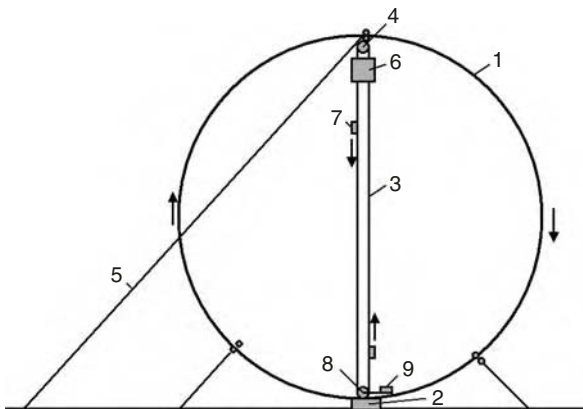


Fig. 3.1. Circle launcher (space station keeper) and space transport system. *Notations:* (1) Cable circle; (2) main engine; (3) transport system; (4) top roller; (5) additional cable; (6) a load (space station); (7) mobile cabin; (8) lower roller; and (9) engine of the transport system.

of guide cables, which connect at one end to the cable circle by a sliding connection and at the other end to the planet's surface. The installation has a transport (delivery) system comprising the closed-loop load cables (chains), two end rollers at the top and bottom that can have medium rollers, a load engine and a load. The top end of the transport system is connected to the cable circle by a sliding connection; the lower end is connected to a load motor. The load is connected to the load cable by a sliding control connection.

The installation can have an additional cables to increase the stability of the main circle, and the transport system can have an additional cable in case the load cable is damaged.

The installation works in the following way. The main engine rotates the cable circle in the vertical plane at a sufficiently high speed so the centrifugal force becomes large enough to lift the cable and transport system. After this, the transport system lifts the space station into space.

The first modification of the installation is shown in Fig. 3.2. There are two main rollers: 20 and 21. These rollers change the direction of the cable by 90° so that the cable travels along the diameter of the circle, thus creating the form of a semi-circle. It can also have two engines. The other parts are same.

The installation can be used for the launch of a payload to outer space (Fig. 3.3). The load is connected to the cable circle by a sliding bearing through a brake. The load is accelerated by the cable circle, lifted to a high altitude, and disconnected at the top of the circle (semi-circle).

The installation may also be used as transport system for delivery of people and payloads from one place to another through space (Fig. 3.4).

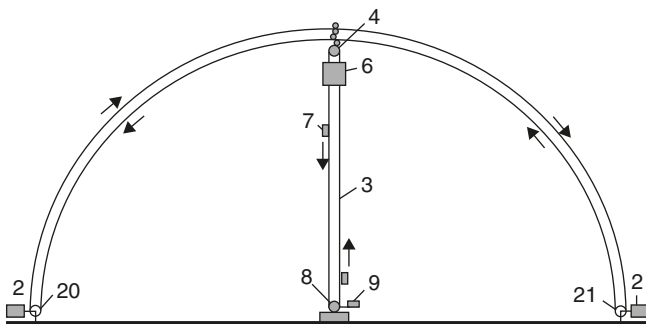


Fig. 3.2. Semi-circle launcher (space station keeper) and transport system. *Notation:* The same as in Fig. 3.1 with the additional of (20 and 21) rollers. The semi-circle is the same (see right-hand side of Fig. 3.4).

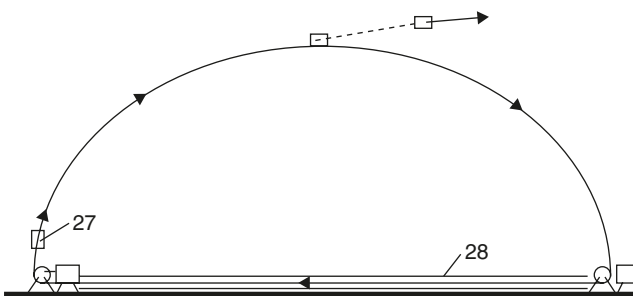


Fig. 3.3. Launching the space ship (probe) into space using the cable semi-circle. *Notations:* (27): Load and (28) vacuum tube (option).

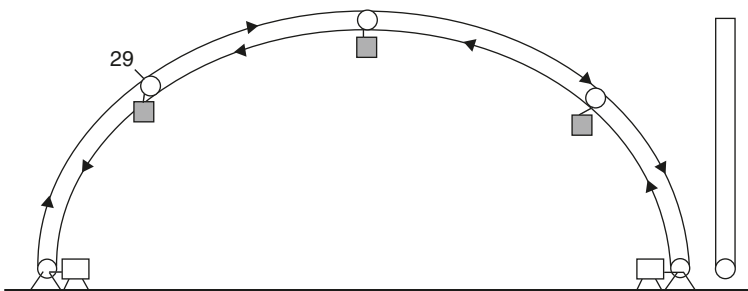


Fig. 3.4. Double semi-circle with opposed speeds for delivery of a load to another semi-circle end. *Notation:* (29) Roller.

The double cable can be used as an excellent launch system, which generates a maximum speed 3 times the speed of the cable. The launch system has a space probe (Fig. 3.5) connected to the semi-circular cable and to a launch cable. The launch cable is connected through a roller (block) to the main cable. A tackle block is used in which the maximum speed is 3 times more than the cable speed.

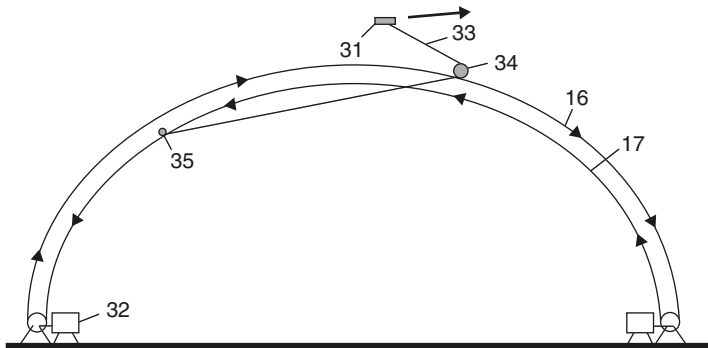


Fig. 3.5. Launching a load into space with a triple circle rope speed using the double semi-circle. *Notations:* (31) Space probe; (32) engine; (33) launch cable; (34) roller; (35) connection point of the launch cable; and (16, 17) semi-circle.

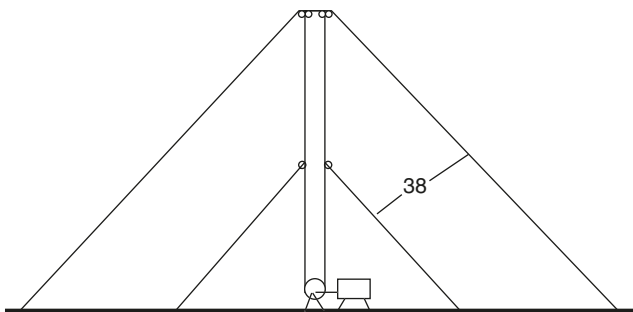


Fig. 3.6. Supporting the semi-circle in vertical position (for stability). *Notation:* (38) Guide cable.

The maximum cable speed depends on the tensile strengths of the cable material. Speeds of 4–6 km/s can be achieved using modern fibers, whiskers, and nanotubes (see attached projects).

For stability, the installation can have guide cables connected to the top of the cable circle by a sliding connection and to the ground (Fig. 3.6).

The ship installation may be used as a system for vertical landing on or taking-off (launch) from a planet or asteroid because the cable circle can work like a spring.

The cable circle of the space ship can be used as a propulsion system (Fig. 3.7). The propulsion system works in the following way. Material from asteroids or meteorites, or garbage from the ship, is packed in small packets. A packet is connected to the cable circle, then circle engine turns on and rotates at high speed. At the desired point the pack is disconnected from the circle and, as the ejected mass flies off with a velocity, the space ship gets an impulse in the required direction.

The suggested cable circle or double cable circle can be made around a planet or space body (Fig. 3.8). This system can be used for suspended objects such as space stations,

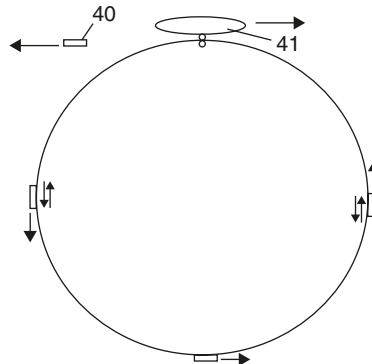


Fig. 3.7. Using the rope circle as a propulsion system. *Notations:* (40) Garbage and (41) space ship.

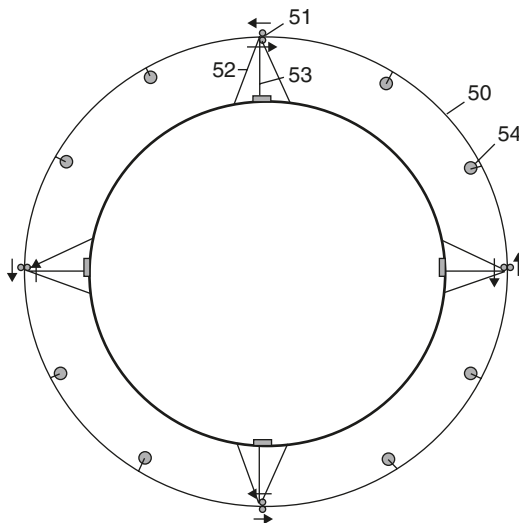


Fig. 3.8. Cable circle around the Earth for 8–10 space objects. *Notations:* (50) Double circle; (51) drive stations; (52) guide cable; (53) energy transport system; and (54) space station.

tourist cabins, scientific laboratories, observatories, or relay station for TV and radio stations.

This system works in the following way. The installation has two cable circles, which move in the opposite directions at the same speed. The space stations are connected to the cable circle through the sliding connection. They can move along the circle in any direction when they are connected to one of the cable circles through a friction clutch, transmission, gearbox, brake and engine, and can use the transport system in Figs. 3.1 and 3.2 for climbing to or descending from the station. As energy can be lost through friction in the connections, the energy transport system and drive rollers transfer energy to

the cable circle from the planet surface. The cable circles are supported at a given position by the guide cables (see Project 2). No towers for supporting the circle cable are needed.

The system can have only one cable (Figs. 3.1 and 3.3).

The installation can have a system for changing the radius of the cable circle (Fig. 3.9). When an operator moves the tackle block, the length of the cable circle is changed and the radius of the circle is also changed.

With the radius system the problem of creating the cable circle is solved very easily. Expensive rockets are not necessary. The operator starts with a small radius near the planet surface and increases it until the desired radius is achieved. This method may be used for making a semi-circle or double semi-circle system.

The small installation may be used as a crane for construction engineering, developing building, bridges, in the logging industry, and so on.

The main advantage of the proposed launch system is its very low cost for the amount of payload delivered into space and over long distances. Expensive fuels, complex control systems, expensive rockets, computers, and complex devices are not required. The cost of payload delivery into space would drop by a factor of a thousand. In addition, large amounts of payloads could be launched into space (in the order of a thousand tons a year) using a single launch system. This launch system is simple and does not require high-technology equipment. The payloads could be delivered into space at production costs of \$2–10/kg (see computations in the attached projects).

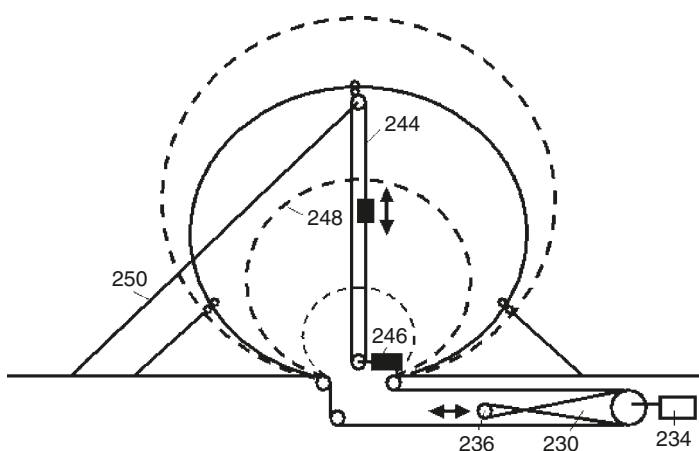


Fig. 3.9. System for changing the radius of the rope circle. Notations: (230) System for radius control; (234): engine; (236) mobile tackle block; (244) transport system; (246): engine; (248): circle; and (250) guide cable.

3.2.1 Cable problem

See in Chapters 1, 2 and Refs.^{3,5}

3.3 Theory of circle launcher

The equations developed and used for estimation and computation are provided below. All equations are in the metric system. The nomenclature was given in special section at the beginning of this chapter.

Take a small part of a rotary circle and write the equilibrium:

$$2SR\alpha\gamma V^2/R = 2S\sigma \sin \alpha.$$

When $\alpha \rightarrow 0$, the relationship between maximum rotary speed and tensile strength of a closed-loop circle cable is:

$$V = (\sigma/\gamma)^{1/2} = k^{1/2}. \quad (3.1)$$

Results of this computation are presented in Fig. 3.10.

Maximum lift force P_{\max} of the rotary closed-loop circle cable when the gravity $g = 0$ equals the cable tensile force is:

$$P_{\max} = 2V^2\gamma S = 2\sigma S. \quad (3.2)$$

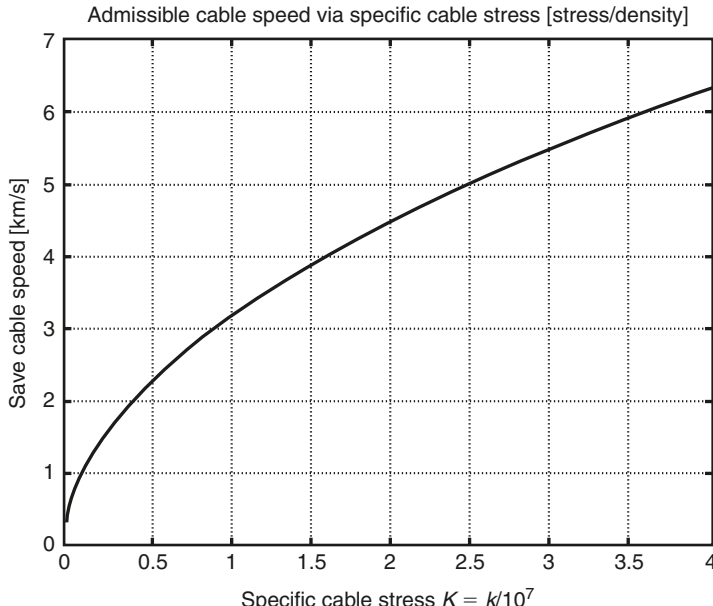


Fig. 3.10. Maximum cable speed versus safe specific cable stress.

The maximum vertical lift force P of the vertical cable circle in the constant gravity field of a planet equals the lift force in equation (3.2) minus the cable weight:

$$P = 2S(\sigma - \pi R \gamma g). \quad (3.3)$$

The maximum lift force P of the double semi-circle cable in the gravity field of a planet is:

$$P = 4S(\sigma - 0.5\pi R \gamma g). \quad (3.3a)$$

Approximately one-quarter of this force can be used. The results of computation are presented in Fig. 3.11.

The minimum speed of the cable circle can be found from equations (3.3) and (3.1) for $P = 0$:

$$V_{\min} = \sqrt{\pi R g}. \quad (3.4)$$

Example: For $R = 0.15$ m, the minimum speed is 2.15 m/s; for $R = 50$ km, the minimum speed is 1241 m/s.

The minimum speed of the double semi-circle can be found from equations (3.3a) and (3.1) for $P = 0$:

$$V_{\min} = \sqrt{0.5\pi R g}. \quad (3.4a)$$

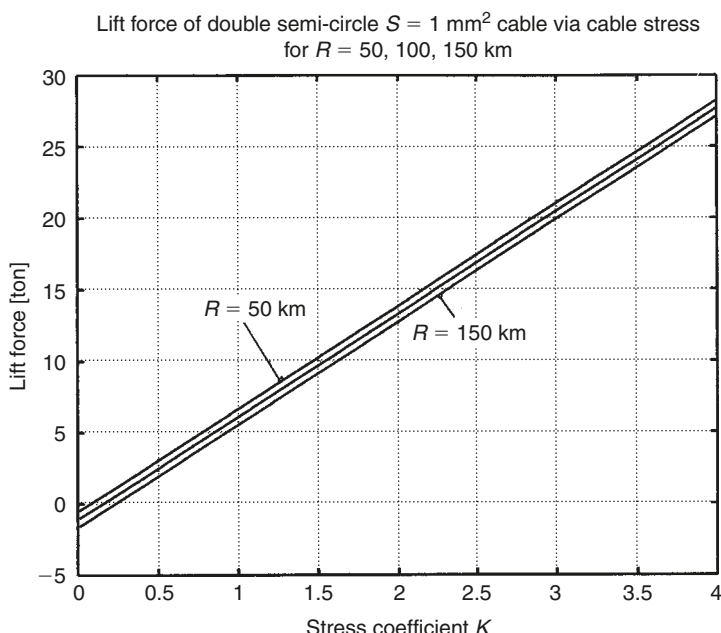


Fig. 3.11. Maximum lift force of cable $S = 1 \text{ mm}^2$ versus stress.

The specific lift force of 1 kg of cable mass P_1 in a planet's gravity field equals the lift force in equation (3.3) divided by the cable weight $2\pi RS\gamma$. For a conventional circle:

$$P_1 = (\sigma/\pi\gamma R) - g \quad (3.5)$$

while for a double semi-circle:

$$P_1 = (2\sigma/\pi\gamma R) - g. \quad (3.5a)$$

The specific lift force P_L of 1 m of cable in a planet's gravity field equals the lift force in equations (3.3) and (3.3a) divided by the cable length, respectively:

$$P_L = S[(\sigma/\pi R) - \gamma g] \quad (3.6)$$

$$P_L = 2S[(\sigma/\pi R) - 0.5\gamma g]. \quad (3.6a)$$

The length of a cable L which supports the given local load G is:

$$L = G/P_L. \quad (3.7)$$

The cable angle, α_h , to the horizon about a local load equals (from a local equilibrium):

$$\alpha_h = \arcsin(G/2\sigma S). \quad (3.8)$$

Cable deformation about a local load (decrease in altitude) for a cable semi-circle in a planet gravity's field can be found approximately:

$$\Delta h \approx GL/12\sigma S. \quad (3.9)$$

Cable deformation about a local load for the double cable circle around a planet in space is:

$$\Delta h_0 \approx \frac{\pi(R_0 + H)}{24} \left(\frac{G}{\sigma S} \right)^2. \quad (3.10)$$

The internal pressure on the cable circle can be derived from the equilibrium condition. The result is:

$$p = \pi r\sigma/2R. \quad (3.11)$$

The increase in cable radius under an internal pressure is:

$$\Delta R = \gamma V^2 R/E. \quad (3.12)$$

The maximum cable radius (maximal cable top) in a constant gravity field can be derived from the equilibrium of the lift force and a cable weight:

(a) Full circle (from equation (3.3))

$$R_{\max} = \sigma/\pi\gamma g, \quad H_{\max} = 2R_{\max}. \quad (3.13)$$

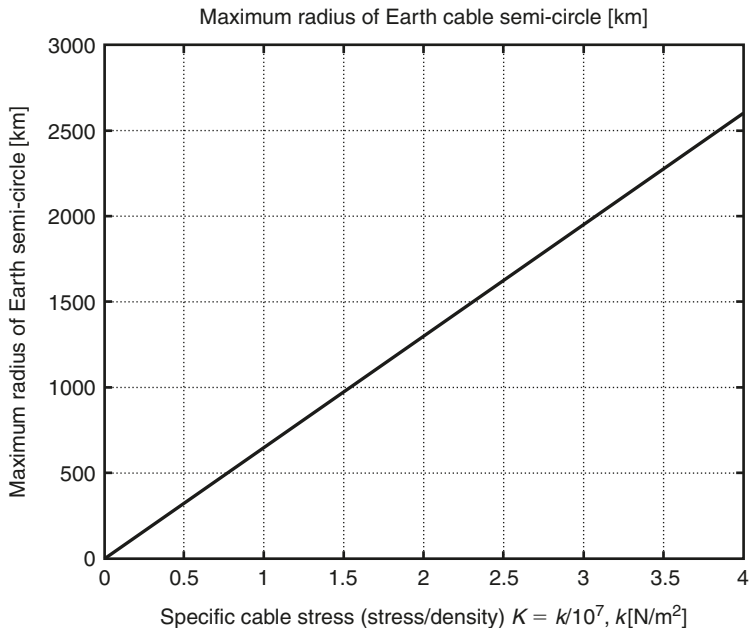


Fig. 3.12. Maximum radius of Earth semi-circle versus specific cable stress.

(b) Semi-circle (from equation (3.3a))

$$R_{\max} = 2\sigma/\pi\gamma g, \quad H_{\max} = R_{\max}. \quad (3.13a)$$

The results of this computation are presented in Fig. 3.12.

The maximum cable radius in a variable gravity field of a rotating planet can be found from the equation of a circle located on a flat equator:

$$R \left[\frac{1 + R/R_0}{(1 + 3R/R_0)^{3/2}} - \omega^2 (R_0 + R) \right] = \frac{\sigma}{\pi\gamma g}. \quad (3.14)$$

The maximum speed of a closed-loop circle rotated around a planet (Fig. 3.8) can be found from the equilibrium between centrifugal and gravity forces:

$$V_a = [(\sigma/\gamma) + Rg]^{1/2}. \quad (3.15)$$

The results of computation are presented in Fig. 3.13. The minimum value $V_a = (Rg)^{1/2}$ occurs when $k = \sigma/\gamma = 0$.

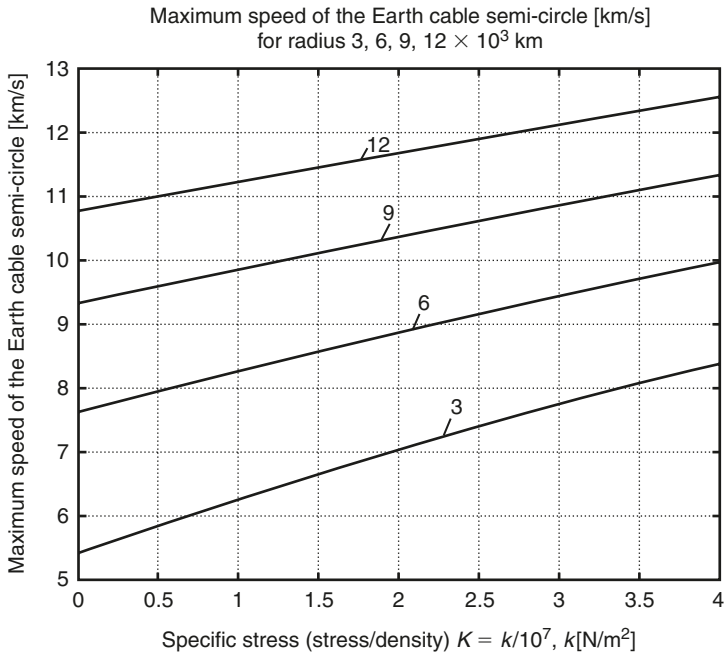


Fig. 3.13. Maximum speed of a closed-loop circle around a planet.

The lift force P_a of a double closed-loop cable circle rotated around a planet can be found from equilibrium of a small circle element:

$$P_a = 4\pi S \gamma (V_s^2 - k - Rg). \quad (3.16)$$

The full lift force of a double closed-loop cable circle rotated around a planet is found by multiplying p from equation (3.11) by a cable area $4\pi Rr$, or:

$$P_a = 2\pi\sigma S. \quad (3.16a)$$

The results of computation are presented in Fig. 3.14.

The specific lift force of a 1-kg closed-loop cable circle rotated around a planet can be found from equation (3.16), by dividing by cable weight:

$$P_{a,1} = \sigma/\gamma R. \quad (3.17)$$

The specific lift force of a 1-m closed-loop cable circle around a planet in space, when $g = 0$, can also be found from equation (3.16), if it is divided by the cable length:

$$P_{a,L} = S\sigma/R. \quad (3.18)$$

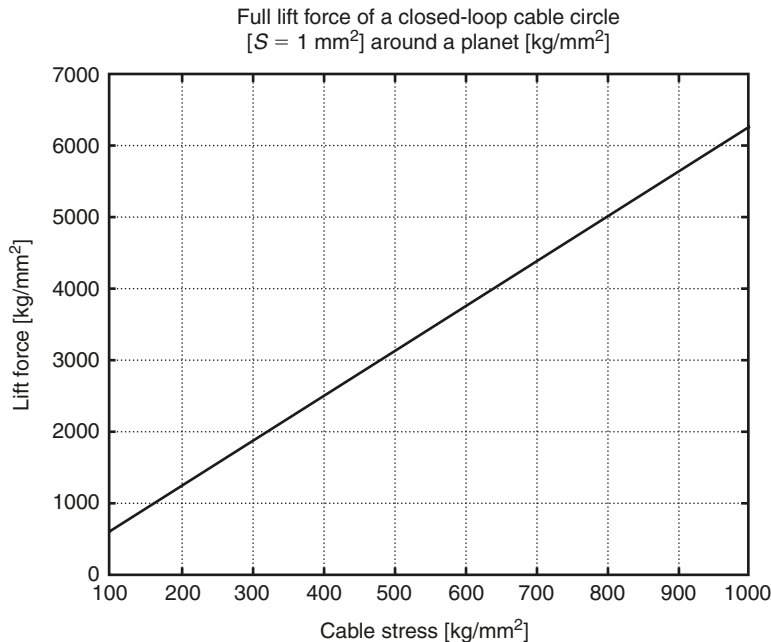


Fig. 3.14. Full lift force of the closed-loop cable circle rotated around a planet.

We can derive from momentum theory an additional speed, ΔV , which a space ship (Fig. 3.7) gets from a cable propulsion system:

$$\Delta V = V_c m / (m_{ss} - m). \quad (3.19)$$

The results of computation are presented in Fig. 3.15.

The speed of falling from an altitude H is given by:

$$V_f = (2gH)^{0.5}. \quad (3.20)$$

The energy, E_s , stored by a rotary circle per 1 kg of the cable mass can be derived from the known equation of kinetic energy. The equation is:

$$E_s = \sigma / 2\gamma. \quad (3.21)$$

The results of computation are presented in Fig. 3.16.

The radius of observation versus altitude H [km] over the Earth is approximately:

$$R_r = (2R_0H + H^2)^{0.5} [\text{km}], \quad (3.22)$$

where Earth radius $R_0 = 6378$ km. If $H = 150$ km, then $R_r = 1391$ km.

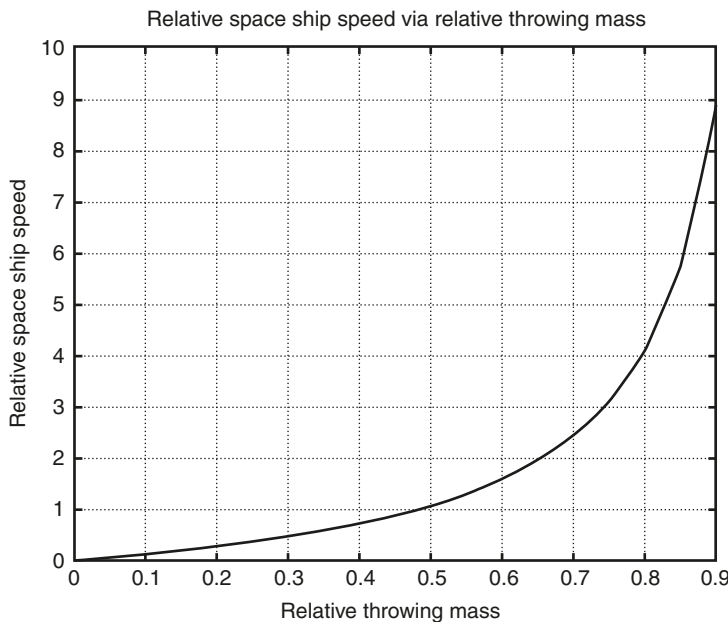


Fig. 3.15. Relative speed of space ship versus relative throwing mass.

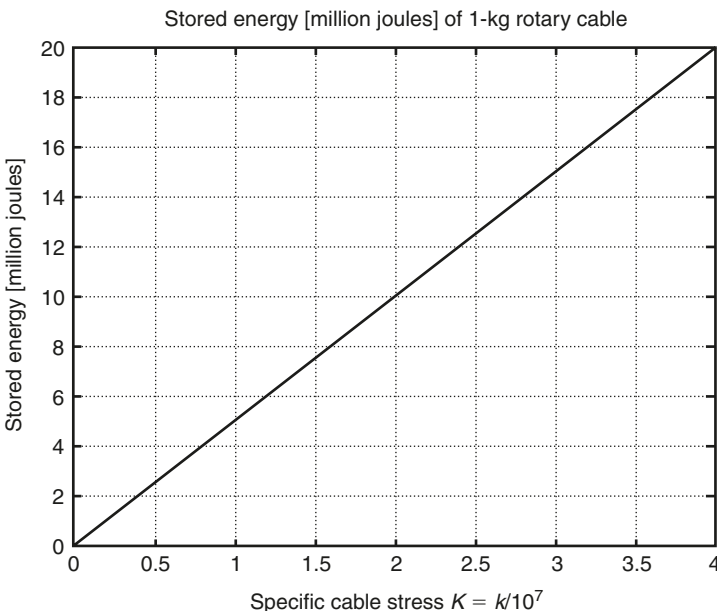


Fig. 3.16. Storage energy of 1 kg of the cable.

3.3.1 Estimation of cable friction due to the air

This estimation is very difficult because there are no experimental data for air friction of an infinitely very thin cable (especially at hypersonic speeds). A computational method for plates at hypersonic speed was used (see Ref.⁴, p. 287). The computation is made for two cases: a laminar and a turbulent boundary layer.

The results are very different. The maximum friction is for turbulent flow. About 80% of the friction drag occurs in the troposphere (from 0 to 12 km). If we locate the cable end on a mountain at an altitude of 4 km the maximum air friction decreases by 30%. So the drag is calculated for three cases: when the cable end is located on the ground $H = 0.1$ km above sea level, $H = 1$ km and when it is located on the mountain at $H = 4$ km (2200 ft).

The major part of cable will have the laminar boundary layer because a small wind will blow away the turbulent layer and restore the laminar flow. The blowing away of the turbulent boundary layer is studied in aviation and is used to restore laminar flow and decrease air friction. The laminar flow decreases the friction in hypersonic flow by 280 times! If half the cable surface has a laminar layer it means that we must decrease the air drag calculated for the full turbulent layer by a minimum of 2 times.

Below the equations from Anderson⁴ for computation of local air friction for a two-sided plate are given:

$$\begin{aligned} \frac{T^*}{T} &= 1 + 0.032M^2 + 0.58\left(\frac{T_w}{T} - 1\right), \quad M = \frac{V}{a}, \quad \mu^* = 1.458 \times 10^6 \frac{T^{*1.5}}{T^* + 110.4}, \\ \rho^* &= \frac{\rho T}{T^*}, \quad Re^* = \frac{\rho^* Vx}{T^*}, \quad C_{f,L} = \frac{0.664}{(Re^*)^{0.5}}, \quad C_{f,T} = \frac{0.0592}{(Re^*)^{0.2}}, \quad C_{c,l} = 0.5C_{f,l}, \\ C_{c,t} &= 0.5C_{f,t}, \quad D_L = 0.5C_{f,l}\rho^*V^2S, \quad D_T = 0.5C_{f,t}\rho^*V^2S, \quad D = 0.5(D_T + D_L). \end{aligned} \quad (3.23)$$

To apply the above theory to the double semi-circle case we can approximate the atmosphere density by the exponential equation:

$$\rho = \rho_0 e^{bh}, \quad (3.24)$$

where $\rho_0 = 1.225 \text{ kg/m}^3$, $b = -0.00014$, and h is the altitude [m]. Then the air friction drag is:

$$D_{T,L} = \pi dV^2 \int_{H_0}^H C_{c,t,l}(h)\rho^*(h)dh/\cos \alpha_1, \quad \alpha_1 = \arcsin \frac{h - H_0}{H_m - H_0}, \quad (3.25)$$

where $D_{T,L}$ and $C_{c,t,l}$ are the turbulent and laminar drag and drag coefficient, respectively, α_1 is the angle of the cable element to the horizon. The full drag is $D = 0.5(D_T + D_L)$. The results of computation are presented in Fig. 3.17.

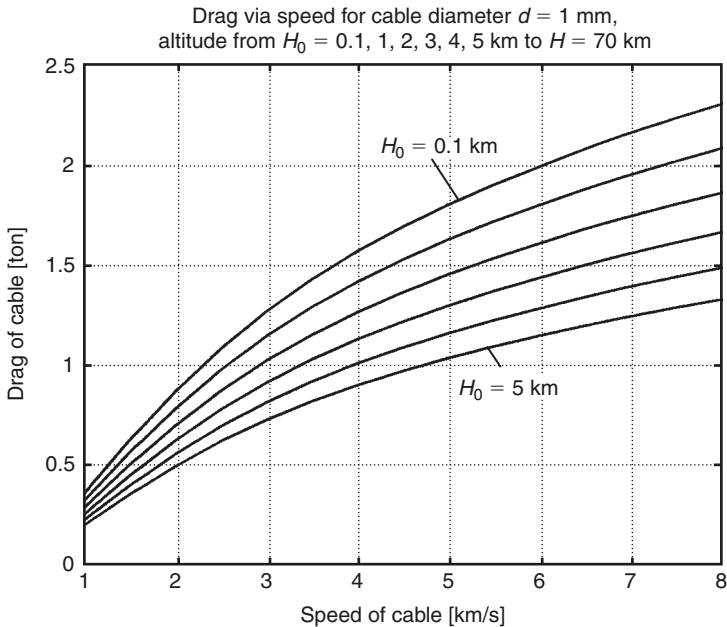


Fig. 3.17. Estimation of the friction air drag [ton] versus cable speed [km/s] and initial altitude [km] for a double semi-circle keeper.

The simplest formula for air friction F is:

$$F = \mu VS_c/w. \quad (3.26)$$

The required power, N , is:

$$N = DV. \quad (3.27)$$

The results of computations using equation (3.27) are presented in Fig. 3.18.

3.4 Case studies

Data on artificial fiber, whiskers, and nanotubes are given in Chapter 1.

3.4.1 Project 1

3.4.1.1 Space station for tourists or a scientific laboratory at an altitude of 140 km (Figs. 3.1–3.6)

The closed-loop cable is a semi-circle. The radius of the circle is 150 km. The space station is a cabin with a weight of 4 ton (9000 lb) at an altitude of 150 km (94 miles). This altitude is 140 km under load.

The results of computations for three versions (different cable strengths) of this project are given in Table 3.1.

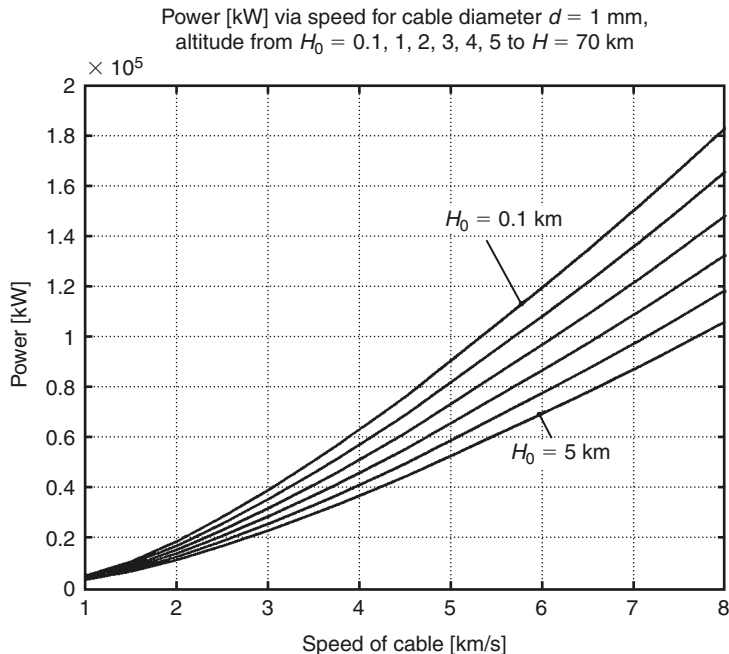


Fig. 3.18. Estimation of the drive power [kW] versus cable speed [km/s] and initial altitude [km] for a double semi-circle keeper.

Table 3.1. Results of computation Project 1.

Variant (1)	σ [kg/mm ²] (2)	γ [kg/m ³] (3)	$K = \sigma/\gamma \cdot 10^7$ (4)	V_{\max} [km/s] (5)	H_{\max} [km] (6)	S [mm ²] (7)
1	8300	1800	4.6	6.8	2945	1
2	7000	3500	2.0	4.47	1300	1
3	500	1800	0.28	1.67	180	100
P_{\max} [ton] (8)	G [kg] (9)	Lift force [kg/m] (10)	Local load [kg] (11)	L [km] (12)	α° (13)	ΔH [km] (14)
30	1696	0.0634	4000	63	13.9	5.0
12.5	3282	0.0265	4000	151	16.6	7.2
30.4	170×10^3	0.0645	4000	62	4.6	0.83
Cable thrust T_{\max} [kg] (15)	Cable drag $H = 0$ km [kg] (16)	Cable drag $H = 4$ km [kg] (17)	Power MW $H = 0$ km (18)	Power MW $H = 4$ km (19)	Maximum tourists people/ day (20)	
8300	2150	1500	146	102	800	
7000	1700	1100	76	49	400	
50,000	7000	5000	117	83.5	800	

The column numbers are: (1) the number of the variant; (2) the permitted maximum tensile strength [kg/mm^2]; (3) the cable density [kg/m^3]; (4) the ratio $K = \sigma/\gamma / 10^{-7}$; (5) the maximum cable speed [km/s] for a given tensile strength; (6) the maximum altitude [km] for a given tensile strength; (7) the cross-section area of the cable [mm^2]; (8) the maximum lift force of one semi-circle [ton]; (9) the weight of the two semi-circle cable [kg]; (10) the lift force of 1 m of cable [kg/m]; (11) the local load (4 ton or 8889 lb); (12) the length of the cable required to support the given (4 ton) load [km]; (13) the cable angle to the horizon near the local load [$^\circ$]; (14) the change of altitude near the local load; (15) the maximum cable thrust [kg]; (16) the air drag on one semi-circle cable if the driving (motor) station is located on the ground (at altitude $H = 0$) for a half turbulent boundary layer; (17) the air drag of the cable if the drive station is located on a mountain at $H = 4$ km; (18) the power of the drive stations [MW] (two semi-circles) if located at $H = 0$; (19) the power of the drive stations [MW] if located at $H = 4$ km; and (20) the number of tourists (tourist capacity) per day (0.35 h in station) for double semi-circles.

3.4.1.2 Economic estimations of these projects for space tourisms

Take the weight (mass) of the tourist cabin as 2 ton (it may be up to 4 ton), and the useful payload as 1.3 ton (16 tourists plus one operator). Acceleration (braking) is $0.5g$ ($a = 5 \text{ m/s}^2$). Then the time to climb and descend will be about 8 min ($H = 0.5at^2$) and 20 min for observation at an altitude 150 km. The common flight time will be 30 min. The passenger capability will be about 800 tourists/day.

Let us use the following equation to estimate the delivery cost, C :

$$C = \frac{I/n_1 + M + Ntc/q\eta}{n_2 n_3}, \quad (3.28)$$

where I is the installation cost [\$]; n_1 is the installation lifetime [years]; M is the yearly maintenance [\$]; N is the DV – engine power [J/s]; t – year time ($t = 3600 \times 24 \times 365$), [s]; c is the fuel cost [\$/kg]; q is the fuel heat capability [J/kg] (for benzene $q = 43 \times 10^6$ [J/kg] for coal $q = 20 \times 10^6$; for natural gas $q = 45 \times 10^6$); η is the engine efficiency, $\eta = 0.2–0.3$; n_2 is the number of tourist per day [people/day]; n_3 is the number of working days in year.

Let us take for variant 3: $I = \$100$ million; $n_1 = 10$ years; $M = \$2$ million in year; $N = DV$ – engine power [J/s], where $D = 50,000 \text{ N}$, $V = 1670 \text{ m/s}$; $t = 3600 \times 24 \times 365 = 31.5 \times 10^6 \text{ s}$; $c = 0.25$ [\$/kg]; $q = 43 \times 10^6$ [J/kg]; $\eta = 0.25$; $n_2 = 400$ people; $n_3 = 360$. Results of computations are presented in Fig. 3.19.

Then the production cost of a space trip for one tourist will be equal to \$508 (about 84% of this cost is the cost of benzene). This cost is \$363 for variant 2. If the cost of the trip ticket is \$100 more than the production cost, the installation will give a profit of about \$14–49 million/year. This profit may be larger if we design the installation especially for tourism. If our engines use natural gas (not benzene), the production cost decreases by the ratio of the cost of gas to benzene.

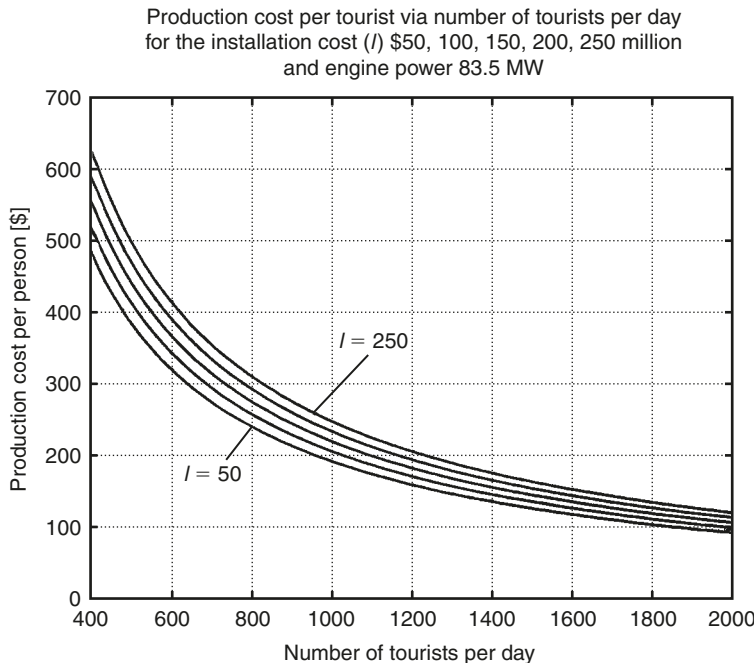


Fig. 3.19. Estimation of the production cost per tourist versus number of tourists per day for the installation cost US \$ (in million): 50, 100, 150, 200, and 250 and engine power 83.5 MW.

3.4.1.3 Discussion of Project 1

1. The first variant has a cable diameter of 1.13 mm (0.045 in.) and a general cable weight of 1696 kg (3658 lb). It needs a power (engine) station to provide from 102 to a maximum of 146 MW (the maximum amount is needed for additional research).
2. The second variant needs the engine power from 49 to 76 MW.
3. The third variant uses a cable with tensile strength near that of current fibers. The cable has a diameter of 11.3 mm (0.45 in.) and a weight of 170 ton. It needs an engine to provide from 83.5 to 117 MW.

The systems may be used for launching (up to 1 ton daily) satellites and interplanetary probes. The installation may be used as a relay station for TV, radio, and telephones.

3.4.2 Project 2

3.4.2.1 Semi-circle of a radius 1000 km (625 miles) for delivering passengers to a distance of 2000 km (1250 miles) through space (Fig. 3.4)

The two closed-loop cable is a semi-circle. The radius is 1000 km. The space cabin has a weight of 4 ton (9000 lb). The maximum altitude is 1000 km. The results of computation for two versions are given in Table 3.2.

Table 3.2. Result of computations for Project 2.

σ [kg/mm ²] (1)	γ [kg/m ³] (2)	V [km/s] (3)	S [mm ²] (4)	W [ton] (5)	P_{\max} [ton] (6)	P_{us} [kg] (7)	People/ day (8)	Time [min] (9)
8300	1800	4.6	1	11.3	11	3000	2000	27
7000	3500	2.0	1	20.2	3	750	500	27

The columns number are: (1) tensile strength [kg/mm²]; (2) density [kg/m³]; (3) cable speed [km/s]; (4) cross-section cable area [mm²]; (5) cable weight of two semi-circles [ton]; (6) maximum cable lift force [ton]; (7) useful local load [kg]; (8) maximum passenger capability in both directions [people/day]; and (9) time of flight in one direction.

3.4.2.2 Estimation of economic efficiency

Let us take the cost of installation and service as the same as the previous project. Then the delivery cost of one passenger will be same (see Fig. 3.19). If a ticket is marked up by \$50 more (from \$130 to \$180 if there are 2000 passengers), then the profit will be about \$18 million/year.

3.4.2.3 Discussion of Project 2

Version 1 has a cable diameter of 1.13 mm (0.047 in.), and a cable weight of 11.3 ton, and has a passenger capacity of 2000 people/day in two directions. The distance is 2000 km (1250 miles) and delivery time 27 min.

These transport systems may be used for launching (weight up to 1 ton) satellites. Such a system may also be the optimum way to travel between two countries that are separated by a third country which does not have an air corridor for conventional airplanes, or is an enemy country. The suggested project goes into outer space ($H = 1000$ km) and out of the atmosphere of the third country.

3.4.3 Project 3

3.4.3.1 Circle around the Earth at an altitude of 200 km (125 miles) for 8–10 scientific laboratories (Fig. 3.8)

The closed-loop cable is the circle around the Earth at an altitude H of 200 km (125 miles). The radius is 6578 km. The space stations are 8–10 cabins with a weight of 1 ton (2222 lb).

Results of computation for three versions are given in Table 3.3.

Table 3.3. Result of computations for Project 3.

Number (1)	σ [kg/mm ²] (2)	γ [kg/m ³] (3)	V [km/s] (4)	S [mm ²] (5)	P_{\max} [ton] (6)	Weight [ton] (7)	Lift force [kg/km] (8)	Angle α [°] (9)	Δh_o [km] (10)
1	8300	1800	10.53	1	52.1	74.4	1.26	3.45	12.5
2	7000	3500	9.19	1	44	145	1.06	4.1	17.2
3	500	1800	8.06	10	31.4	744	0.76	5.74	35

The numbers are: (1) the variant; (2) tensile strength [kg/mm^2]; (3) cable density [kg/m^3]; (4) cable speed [km/s]; (5) cross-section cable area [mm^2]; (6) maximum cable lift force [ton]; (7) cable weight [ton]; (8) lift force of 1 km of cable [kg/km]; (9) cable angle to the horizon near a local load [$^\circ$]; and (10) change (decrease) in altitude under a local load of 1 ton [km].

3.4.3.2 Discussion of Project 3

The variant 3 using current fibers ($\sigma = 500 \text{ kg}/\text{mm}^2$; 5000 MPa) has a cable diameter of 3.6 mm (0.15 in.), a cable weight of 744 ton, and can keep 10 space stations with useful loads (200–500 kg) for each station at an altitude of 180 km (112 miles). This may also be used for launching small (up to a weight 200 kg) satellites.

3.4.4 Project 4

3.4.4.1 Using the cable circle as a propulsion system and energy storage system (Fig. 3.7)

As presented in the main text the suggested system may be used as a space ship launch system, as a landing system for space ships on planets and asteroids, or as a delivery system for people and payloads from a space ship to the planet or asteroid's surface and back without landing the ship.

Below we consider an application of this system as a propulsion system using *any* mass (for example, a meteorites, asteroid material, ship garbage, etc.) to create the ship's thrust. The offered system may be used also for storing energy.

Let us suggest that a space ship has a nuclear energy station. The ship has a lot of energy. However, the ship cannot use this energy efficiently for thrust because known ion thrusters (electric rocket engines) produce only small amounts of thrust (from grams to kilograms). Consequently any trip would take a long time (years). Rocket engines require a lot of expensive fuel (for example, liquid hydrogen for a nuclear engine) and oxidizer (for example, liquid oxygen), which greatly increases launch costs, the ship mass, requirements for low temperatures, and difficulties for storage.

The suggested system allows any material (mass) to be used for imparting speed to a ship. For example, let the space ship have the cable system made from carbon nanotubes (tensile strength $8300 \text{ kg}/\text{mm}^2$ and density $1800 \text{ kg}/\text{m}^3$). This means (equation (3.1)) the cable system can have a maximum speed of 6800 m/s (Table 3.2, column 5). The system can throw off mass at this speed in any direction and provide thrust for the space ship. The specific impulse of the cable system, 6800 m/s, is better than the specific impulse of any modern rocket engine. For example, current rocket engines have impulses 2000–2500 m/s (solid fuel), 3000–3200 m/s (liquid kerosene–oxygen fuel), and up to 4200 m/s (hydrogen–oxygen fuel). If the ship takes 50% of its mass in asteroid material, it can achieve an additional speed of 6800 m/s (see equation (3.19)). The space ship can also use any of the ship's garbage to produce thrust.

As an energy storage system the suggested cable system allows 23 MW of energy to be stored per every kilogram of a cable (see equation (3.21)). This is more than any current kilogram of a conventional fuel (fuel and oxidizer).

3.5 Discussion, summary, and conclusions

The offered method and installations promise to decrease launch costs by a factor of thousands. They are very simple and inexpensive. As with any new system, the suggested method requires further detailed theoretical research, modeling, and development.

Science laboratories have whiskers and nanotubes that have high tensile strength.

The fiber industry produces fibers that can be used for some of the author's projects at the present time. These projects are unusual (strange) for specialists and people now, but they have huge advantages, and they have a big future. The government should support scientific laboratories and companies who can produce a cable with the given performances for a reasonable price, and who research and develop prospective methods.

References

1. *Space technology and Application. International Forum*, 1996–1997, Albuquerque, MN, USA, Parts 1–3.
2. D.V. Smitherman Jr., “Space Elevators”, NASA/CP-2000-210429, US National Aeronautics and Space Administration, Washington, DC, 2000.
3. F.S. Galasso, *Advanced Fibers and Composite*, Gordon and Branch Scientific Publisher, New York, 1989.
4. J.D. Anderson, *Hypersonic and High Temperature Gas Dynamics*, McGraw-Hill Book Co., New York, 1989.
5. *Carbon and High Performance Fibers*, 6th edition, Directory, Chapman & Hall, London, New York, 1995.
6. J.I. Kroschwitz (ed.), *Concise Encyclopedia of Polymer Science and Engineering*, 1990.
7. M.S. Dresselhous, *Carbon Nanotubes*, Springer, London, New York, 2000.
8. A.A. Bolonkin, “Centrifugal Keeper for Space Stations and Satellites”, *Journal of the British Interplanetary Society*, Vol. 56, No. 9/10, 2003, pp. 314–327.

This page intentionally left blank

CHAPTER 4

Optimal Inflatable Space Towers*

Summary

In this chapter the author provides theory and computations for building inflatable space towers up to 100 km in height. These towers can be used for tourism, scientific observation of space, the Earth's surface, weather, and the top atmosphere; as well as for radio, TV, and communication transmissions. These towers can also be used to launch space ships and Earth satellites.

These projects are not expensive and do not require rockets. They require thin strong films composed of artificial fibers and fabricated by current industry. They can be built using present technology. Towers can be used (for tourism, communication, etc.) during the construction process and provide self-financing for further construction. The tower design does not require work at high altitudes; all construction can be done at the Earth's surface.

The transport system for a tower consists of a small engine (used only for friction compensation) located at the Earth's surface. The tower is separated into sections and has special protection mechanisms in case of damage.

Problems involving security, control, repair, and stability of the proposed towers will be addressed in other publications. The author is prepared to discuss these and other problems with serious organizations desiring to research and develop these projects.

4.1 Introduction

4.1.1 Brief history

The idea of building a tower high above the Earth into the heavens is very old.^{1,9} The writings of Moses, about 1450 BC, in Genesis, Chapter 11, refer to an early civilization

* Detail manuscript was published as article "Optimal Inflatable Space Towers with 3–100 km Height", by A.A. Bolonkin, *Journal of British Interplanetary Society*, Vol. 56, No. 3/4, pp. 87–97, 2003.

that in about 2100 BC tried to build a tower to heaven out of brick and tar. This construction was called the Tower of Babel, and was reported to be located in Babylon in ancient Mesopotamia. Later in Chapter 28, about 1900 BC, Jacob had a dream about a staircase or ladder built to heaven. This construction was called Jacob's Ladder. More contemporary writings on the subject date back to K.E. Tsiolkovski in his manuscript *Speculation about Earth and Sky and on Vesta*, published in 1895.² This idea inspired Sir Arthur Clarke to write his novel, *The Fountains of Paradise*,³ about a space tower (elevator) located on a fictionalized Sri Lanka, which brought the concept to the attention of the entire world.

Today, the world's tallest construction is a TV transmitting tower near Fargo, ND, USA. It stands 629 m high and was built in 1963 for KTHI-TV. The Cable News Network (CNN) Tower in Toronto, ON, Canada is the world's tallest building. It is 553 m in height, was built from 1973 to 1975, and has the world's highest observation deck at 447 m. The tower structure is concrete up to the observation deck level. Above is a steel structure supporting radio, TV, and communication antennas. The total weight of the tower is 3,000,000 ton.

The Ostankin Tower in Moscow is 540 m in height and has an observation deck at 370 m. The world's tallest office building is the Petronas Towers in Kuala Lumpur, Malaysia. The twin towers are 452 m in height. They are 10 m taller than the Sears Tower in Chicago, IL, USA.

Current materials make it possible even today to construct towers many kilometers in height. However, conventional towers are very expensive, costing tens of billions of dollars. When considering how high a tower can be built, it is important to remember that it can be built to any height if the base is large enough. Theoretically, you could build a tower to geosynchronous Earth's orbit (GEO) out of bubble gum, but the base would likely cover half the surface of the Earth.

The proposed inflatable towers are cheaper by factors of hundreds. They can be built on the Earth's surface and their height can be increased as necessary. Their base is not large. The main innovations in this project are the application of helium, hydrogen, or warm air for filling inflatable structures at high altitude and the solution of a stability problem for tall (thin) inflatable columns, and utilization of new artificial materials.⁴⁻⁷

4.1.2 The tower applications

The inflatable high towers (3–100 km) have numerous applications for government and commercial purposes:

1. *Entertainment and observation platform.*
2. *Entertainment and observation desk for tourists:* Tourists could see over a huge area, including the darkness of space and the curvature of the Earth's horizon.
3. *Drop tower:* Tourists could experience several minutes of free-fall time. The drop tower could provide a facility for experiments.

4. *Tall tower*: A permanent observatory on a tall tower would be competitive with airborne and orbital platforms for Earth and space observations.
5. *Communication boost*: A tower tens of kilometers in height near metropolitan areas could provide much higher signal strength than orbital satellites.
6. *Solar power receivers*: Receivers located on tall towers for future space solar power systems would permit use of higher frequency, wireless, and power transmission systems (for example, lasers).
7. *Low Earth's orbit (LEO) communication satellite replacement*: Approximately six to ten 100-km tall towers could provide the coverage of a LEO satellite constellation with higher power, permanence, and easy upgrade capabilities.

Further methods proposed by the author for access to space are given in Ref.⁸ and Ch. 5.

4.2 Description of innovation and problem

4.2.1 Tower structure

The simplest tourist tower includes (Fig. 4.1): inflatable column, top observation desk, elevator, expansions, and control stability. The tower is separated into sections by horizontal and vertical partitions (Fig. 4.2), and contains entry and exit airlines, and control devices.

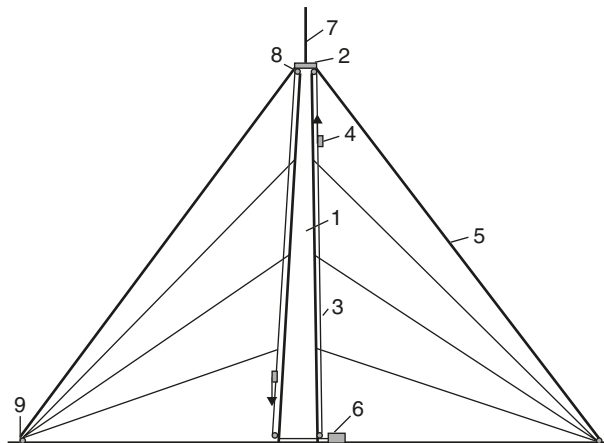


Fig. 4.1. Inflatable tower of height 3 km (10,000 ft). Notations: (1) Inflatable column of radius 5 m; (2) observation desk; (3) load cable elevator; (4) passenger cabin; (5) expansion; (6) engine; (7) radio and TV antenna; (8) rollers of cable transport system; and (9) stability control.

4.2.2 Filling gas

The compressed air filling the inflatable tower provides the weight. Its density decreases at high altitude and it cannot support a top tower load. The author suggests filling the

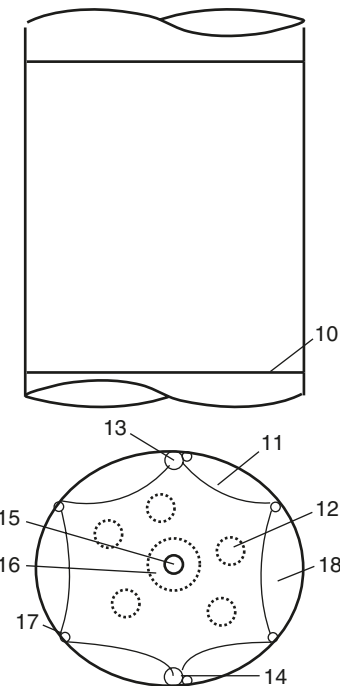


Fig. 4.2. Section of inflatable tower. *Notations:* (10) Horizontal film partitions; (11) light second film (internal cover); (12) air balls; (13) entrance line of compression air and pressure control; (14) exit line of air and control; (15) control laser beam; (16) sensors of laser beam location; (17) control cables and devices; and (18) section volume.

towers with a light gas (for example, helium, hydrogen, or warm air). The computations for changing pressure of air, helium, and hydrogen are presented in Fig. 4.3 (see equation (4.1)). If all the gases have the same pressure (1.1 atm) at Earth's surface, their columns have very different pressures at 100 km altitude. Air has 0 atm, hydrogen 0.4 atm, and helium 0.15 atm. A pressure of 0.4 atm means that every square meter of a tower top can support 4 ton of useful load. Helium can support only 1.5 ton.

Unfortunately, hydrogen is dangerous as it can burn. The catastrophes involving dirigibles are sufficient illustration of this. Hydrogen can be used only above an altitude of 13–15 km, where the atmospheric pressure decreases by 10 times and the probability of hydrogen burning is small.

The average temperature of the atmosphere in the interval from 0 to 100 km is about 240 K. If a tower is made from dark material, the temperature inside the tower will be higher than the temperature of the atmosphere at a given altitude in daytime, so that the tower support capability will be greater (equation (4.1)).

The observation radius versus altitude is presented in Figs. 4.4–4.5 (equation (4.23)).

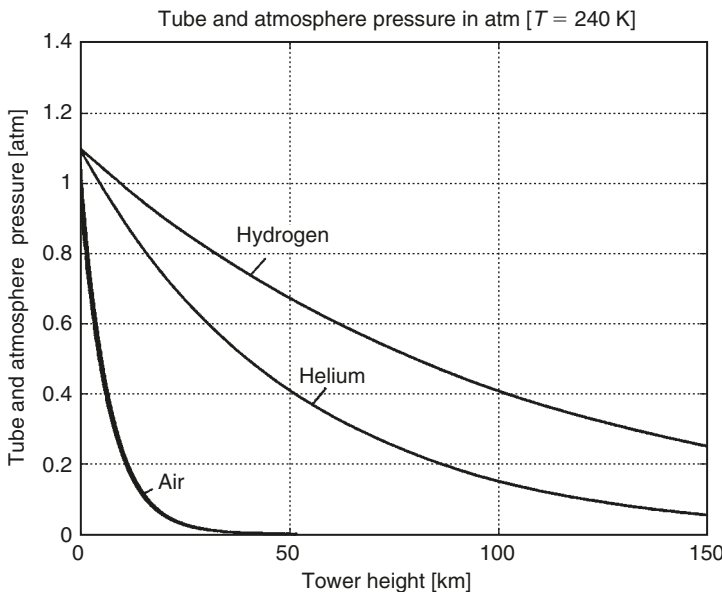


Fig. 4.3. Change in hydrogen, helium, and air pressure for intervals of 0–150 km of altitude.

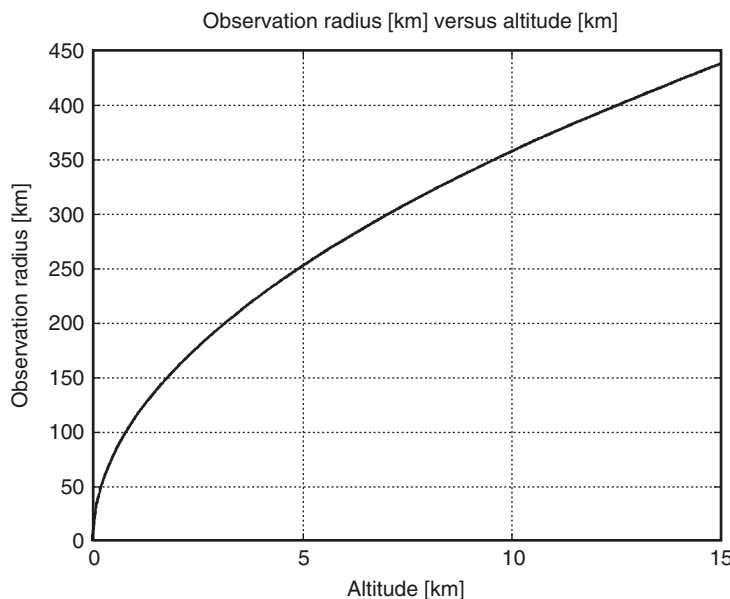


Fig. 4.4. Observation radius for altitudes up to 15 km.

4.2.3 Tower material

The author has found only old (1973) information about textile fiber for inflatable structures.⁴ This refers to DuPont textile Fiber **B** and Fiber **PRD-49** for tire cord. They

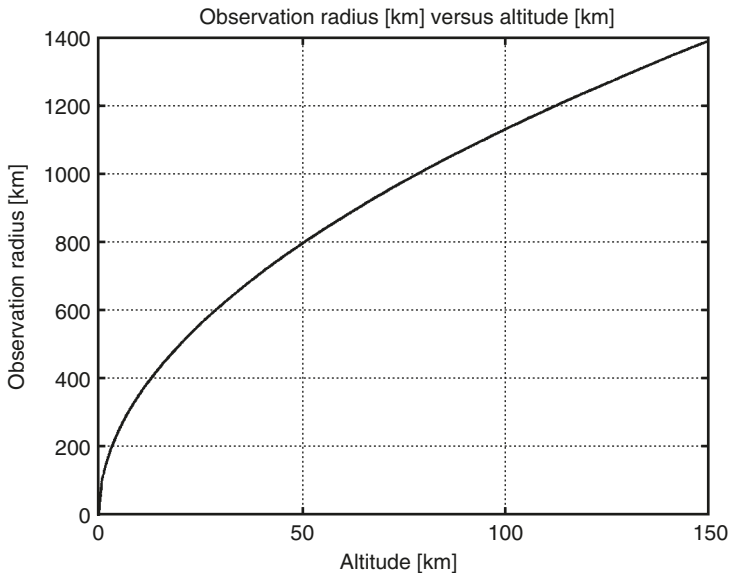


Fig. 4.5. Observation radius for altitudes up to 150 km.

are 6 times as strong as steel (psi is 400,000 or 312 kg/mm^2) with a specific gravity of only 1.5. Minimum available yarn size (denier) is 200, tensile modulus is 8.8×10^6 (**B**) and 20×10^6 (**PRD-49**), and ultimate elongation (percent) is 4 (**B**) and 1.8 (**PRD-49**).

The tower parameters vary depending on the strength of the textile material (film), specifically the ratio of the safe tensile stress σ to specific density γ . Current industry widely produces artificial fibers that have tensile stress $\sigma = 500\text{--}620 \text{ kg/mm}^2$ and density $\gamma = 1800 \text{ kg/m}^3$. Their ratio is $K = \sigma/\gamma = 0.28\text{--}0.34$. There are whiskers (in industry) and nanotubes (in scientific laboratories) with $K = 1\text{--}2$ (whisker) and $K = 5\text{--}11$ (nanotubes). Theory predicts fiber, whisker, and nanotubes could have K values 10 times greater.^{5–7}

The tower parameters have been computed for $K = 0.05\text{--}0.3$, with a recommended value of $K = 0.1$. The reader can estimate tower parameters for other strength ratios.

4.2.4 Tower safety

Many people think that inflatable construction is dangerous, on the basis that a small hole (damage) could deflate the tower. However that assumption is incorrect. The tower will have multiple vertical and horizontal sections, double walls (covers), and special devices (for example, air balls), which will temporarily seal a hole. If a tower section sustains major damage, the tower height is only decreased by one section. This modularity is similar to combat vehicles – bullets may damage its tires, but the vehicle continues to operate.

4.2.5 Tower stability

Stability is provided by expansions (tensile elements). The verticality of the tower can be checked by laser beam and sensors monitoring beam location (Fig. 4.2). If a section deviates from vertical control cables, control devices, and pressure changes restore the tower position.

4.2.6 Tower construction

The tower building will not have conventional construction problems such as lifting building material to high altitude. All sections are identifiable. New sections are put in at the bottom of the tower, the new section is inflated, and the entire tower is lifted. It is estimated that the building may be constructed in 2–3 months. A small tower (up to 3 km) can be located in a city.

4.2.7 Tower cost

The inflatable tower does not require high cost building materials. The tower will be a 100 times cheaper than conventional solid towers 400–600 m tall.

4.3 Theory of inflatable towers (all equations are given in metric system)

Equations developed and used by author for estimations and computation are provided below.

4.3.1 The pressure of any gas in a column versus altitude

The given molecular weight, μ ; temperature, T , of an atmospheric gas mixture; gravity, g , of planet; and atmospheric pressure, P , versus altitude, H , may be calculated using the equation:

$$P = P_o \exp(-\mu g H / RT) \quad \text{or} \quad P_r = P/P_o = \exp(-aH), \quad (4.1)$$

where P_o is the pressure at the planet surface (for the Earth $P_o \approx 10^5$ [N/m²]), $R = 8314$ is gas constant. For air: $\mu = 28.96$, for hydrogen: $\mu = 2$, for helium: $\mu = 4$; $a = \mu g / RT$.

4.3.2 Optimal cover thickness and tower radius

Let us consider a small horizontal cross-section of tower element. Using the known formulas for mass and stress, we write:

$$P ds = g dm, \quad dm = 2\pi r \gamma \delta dH, \quad s = \pi(R^2 - r^2), \quad R = r + dr, \quad ds = 2\pi r dr. \quad (4.2)$$

where m is the cover mass [kg]; γ is the cover specific weight [kg/m^3]; σ is the cover tensile stress [N/m^2]; d is the sign of differential; s is the tower cross-section area which supports a tower cover [m^2]; $g = 9.81$ [m/s^2] gravity; R, r is the radius of tower [m]; $\pi = 3.14$; P is the surplus internal gas pressure over outside atmosphere pressure [N/m^2].

Substituting the above formulas in the first equation, we get:

$$p \, dr = g\gamma\delta \, dH. \quad (4.3)$$

From equations for stress we find the cover thickness:

$$2\pi RP \, dH = 2\delta\sigma \, dH \quad \text{or} \quad \delta = \pi RP/\sigma. \quad (4.4)$$

If we substitute equation (4.4) in equation (4.3) and integrate, we find:

$$R = R_o \exp(-\pi g H/k) \quad \text{or} \quad R_r = R/R_o = \exp(-\pi g H/k), \quad (4.5)$$

where R_r is relative radius, R_o is base tower radius [m], and $k = \sigma/\gamma$.

4.3.3 Tower lift force F

$$F = PS, \quad S = S_r S_o, \quad S_r = \pi(R_r R_o)^2/S_o, \quad S = S_o R_r^2, \quad (4.6)$$

$$F = P S_o R_r^2, \quad (4.7)$$

where $S_o = \pi R_o^2$ is a cross-section tower area at $H = 0$, $S_r = S/S_o$ is the relative cross-section of the tower area.

If we substitute equations (4.1) and (4.5) in equation (4.7), we find:

$$F = P_o S_o \exp[-(a + 2\pi g/k)H] \quad \text{or} \quad F_r = F/P_o S_o = \exp[-(a + 2\pi g/k)H], \quad (4.8)$$

where F_r is the relative force.

4.3.4 Base area for a given top load W [kg]

The required base area S_o (and radius R_o) for given top load W may be found from equation (4.8) if $F = gW$:

$$P_o S_o = gW/F_r(H_{\max}) \quad \text{and} \quad R_o = (S_o/\pi)^{1/2}. \quad (4.9)$$

4.3.5 Mass of cover

From equation (4.2):

$$dm = 2\pi R\gamma\delta dH. \quad (4.10)$$

If we substitute equations (4.1), (4.4), and (4.5) in equation (4.10), we find:

$$dm = (2\pi/k)P_o S_o \{\exp[-(a + 2\pi g/k)H]\}dH. \quad (4.11)$$

Integrate this relation from H_1 to H_2 , we get:

$$M = [2\pi P_1 S_1 / k(a + 2\pi g/k)][F_r(H_1) - F_r(H_2)], \quad (4.12)$$

or relative mass (for $H = 0$) is:

$$M_r = M/(P_o S_o) = [2\pi/k(a + 2\pi g/k)](1 - F_r). \quad (4.13)$$

4.3.6 The thickness of a tower cover

It may be found from equations (4.4), (4.5), and (4.1):

$$\delta = (\pi/\gamma k)P_o R_o \{\exp[-(a + \pi g/k)H]\}. \quad (4.14)$$

Relative thickness is:

$$\delta_r = \delta/P_o R_o = (\pi/\gamma k)\{\exp[-(a + \pi g/k)H]\}. \quad (4.15)$$

4.3.7 Maximum safety bending moment

Maximum safety bending moment for example, from wind (see equations (4.5) and (4.8))

$$M_b = FR = R_o P_o S_o R_r F_r, \quad (4.16)$$

or relative bending moment is:

$$M_{b,r} = M_b/(R_o P_o S_o) = R_r F_r. \quad (4.17)$$

4.3.8 Gas mass M into tower

Let us write the gas mass as a small volume and integrate this expression for altitude and constant temperature:

$$dm_g = \rho dV, \quad dV = \pi R^2 dH, \quad \rho = \rho_0 P_r, \quad (4.18)$$

where V is volume, ρ is gas density at altitude H , ρ_0 is gas density at $H = 0$, R is tower radius at H . If we substitute P_r from (4.1), integrate, and substitute F_r from (4.8), we have:

$$M_g = [\pi\rho_1 R_1^2/(a + 2\pi g/k)][F_r(H_1) - F_r(H_2)], \quad (4.19)$$

where lower index “1” means values for lower end and “2” means values for top end of the tower, ρ_1 is gas density at altitude H_1 .

Relative gas mass is:

$$M_{g,r} = M_g/\rho_1 R_1^2 = [\pi/(a + 2\pi g/k)][F_r(H_1) - F_r(H_2)]. \quad (4.20)$$

4.3.9 Base tower radius

We get from equation (4.8) for $F = gW$:

$$R_1 = (gW/\pi P_1 R_r)^{1/2} \quad (4.21)$$

where W is the top load [kg].

4.3.10 Tower mass

Tower mass M [kg] is:

$$M = \pi R_1^2 P_1. \quad (4.22)$$

4.3.11 Distance L of Earth

Earth's distance view from a high tower is:

$$L \approx (2ReH + H^2)^{0.5}, \quad (4.23)$$

where $Re = 6378$ [km] is the Earth's radius. Results of computations are presented in Figs. 4.4 and 4.5.

4.4 Projects

4.4.1 Project 1: A simple air tower of 3 km height (base radius 5 m, 15 ft, and K = 0.1)

This inexpensive project provides experience in design and construction of a tall inflatable tower, and of its stability. The project also provides funds from tourism, radio, and TV. The inflatable tower has a height of 3 km (10,000 ft). Tourists will not need a special

suit or breathing device at this altitude. They can enjoy an Earth's panorama of a radius of up to 200 km. The bravest of them could experience 20 s of free-fall time followed by 2g overload.

4.4.1.1 Results of computations

Assume the additional air pressure is 0.1 atm; air temperature is 288 K (15°C , 60°F); base radius of tower is 5 m; and $K = 0.05\text{--}0.3$. Take $K = 0.1$, computations of radius are presented in Fig. 4.6. If the tower cone is optimal, the tower top radius must be 4.55 m (Fig. 4.6). The maximum useful tower top lift is 46 ton (Fig. 4.7). The cover thickness is 0.087 mm at the base and 0.057 mm at the top (Fig. 4.8). The outer cover mass is only 11.5 ton (Fig. 4.9). If we add light internal partitions, the total cover weight will be about 16–18 ton (compared to 3 million ton for the 553 m tower in Toronto). Maximum safe bending moment versus altitude (as presented in Fig. 4.10) ranges from 390 ton m (at the base) to 210 ton m at the tower top.

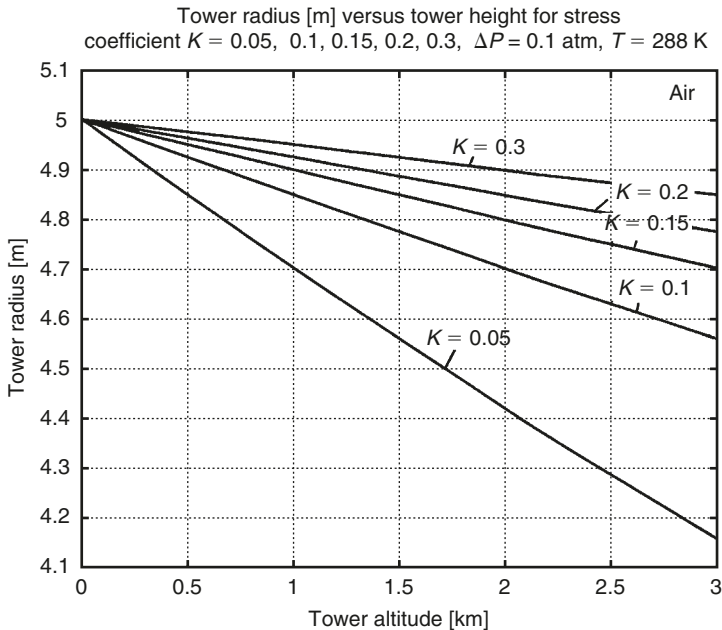


Fig. 4.6. Tower radius versus tower height for the 3-km air tower.

4.4.1.2 Economic efficiency

Assume the cost of the tower is \$5 million, its lifetime is 10 years, annual maintenance \$1 million, the number of tourists at the tower top is 200 (15 ton), time at the top is 0.5 h, and the tower is open 12 h/day. Then 4800 tourists will visit the tower per day, or 1.7 million/year. The unit cost of one tourist is $(0.5 + 1)/1.7 = \$1/\text{person}$. If a ticket costs \$9, the profit is $1.7 \times 8 = \$13.6$ million/year. If a drop from the tower (in a special cabin, for a free-fall (weightlessness) time of 20 s, followed by a overload of 2g) costs \$5 and 20% of tourists take it, the additional profit will be \$1.7 million.

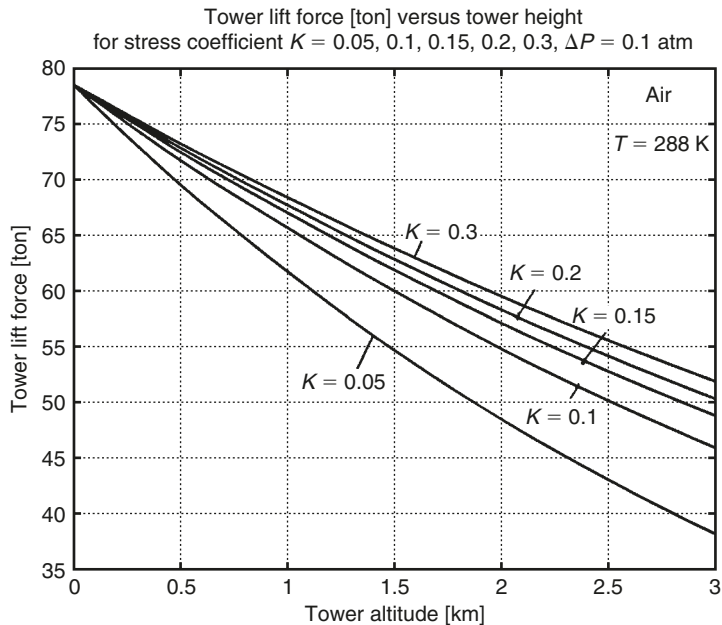


Fig. 4.7. Tower lift force versus tower height for the 3-km air tower.

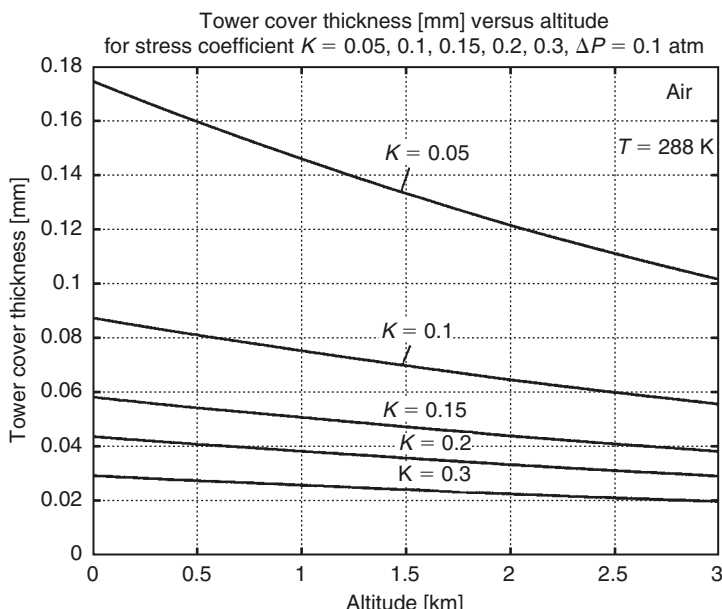


Fig. 4.8. Tower cover thickness for the 3-km air tower.

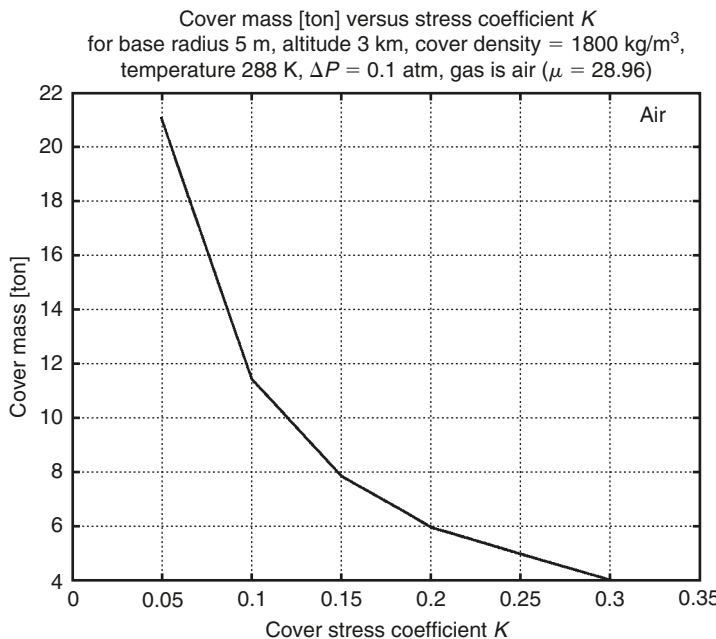


Fig. 4.9. Cover mass of the 3-km air tower versus stress coefficient.

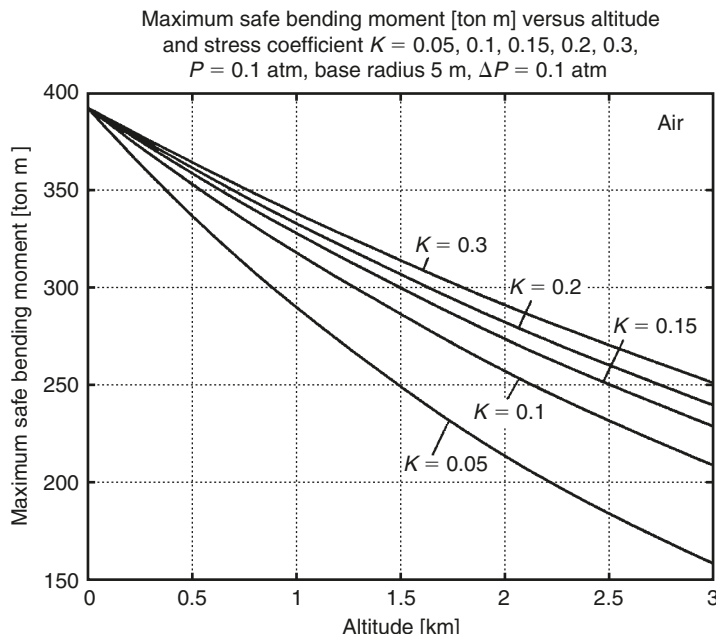


Fig. 4.10. Maximum safe bending moment.

4.4.2 Project 2: Helium tower 30 km (base radius is 5 m, 15 ft, and $K = 0.1$)

4.4.2.1 Results of computation

Let us take the additional pressure over atmospheric pressure as 0.1 atm. The change of air and helium pressure versus altitude are presented in Figs. 4.3 and 4.4. The change of radius versus altitude is presented in Fig. 4.11. For $K = 0.1$ the radius is 2 m at an altitude of 30 km. The useful lift force is presented in Figs. 4.12 and 4.15. For $K = 0.1$ it is about 75 ton at an altitude of 30 km, thus it is a factor of 2 times greater than the 3-km air tower. It is not surprising, because the helium is lighter than air and it provides a lift force. The cover thickness is presented in Fig. 4.13. It changes from 0.08 mm (at the base) to 0.42 mm at an altitude of 9 km and decreases to 0.2 mm at 30 km. The outer cover mass is about 370 ton (Fig. 4.14). Required helium mass is 190 ton (Fig. 4.16).

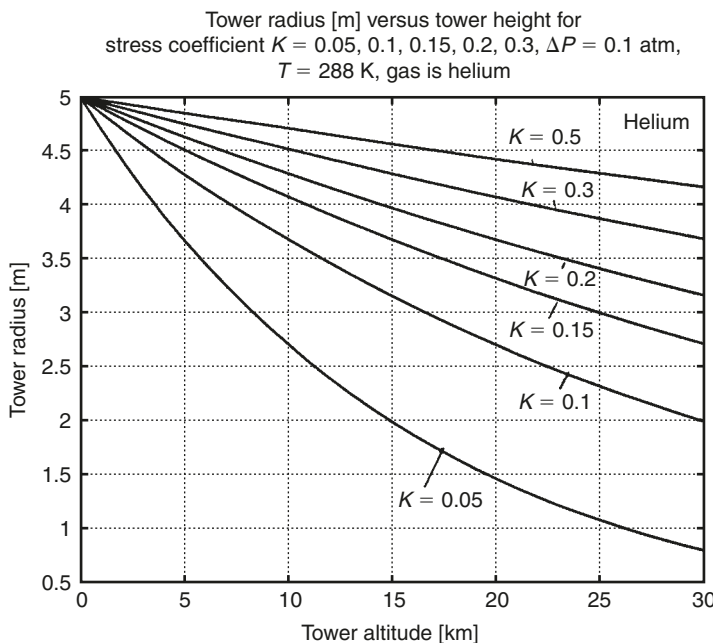


Fig. 4.11. Tower radius versus tower height for the 30-km helium tower.

The tourist capability of this tower is twice than that of the 3-km tower, but all tourists must stay in cabins.

4.4.3 Project 3: Air–hydrogen tower 100 km (base radius of air part is 35 m and the hydrogen part has base radius 5 m)

This tower is in two parts. The lower part (0–15 km) is filled with air. The top part (15–100 km) is filled with hydrogen. It makes this tower safer, because the low atmospheric pressure at high altitude decreases the probability of fire. Both parts may be used for tourists.

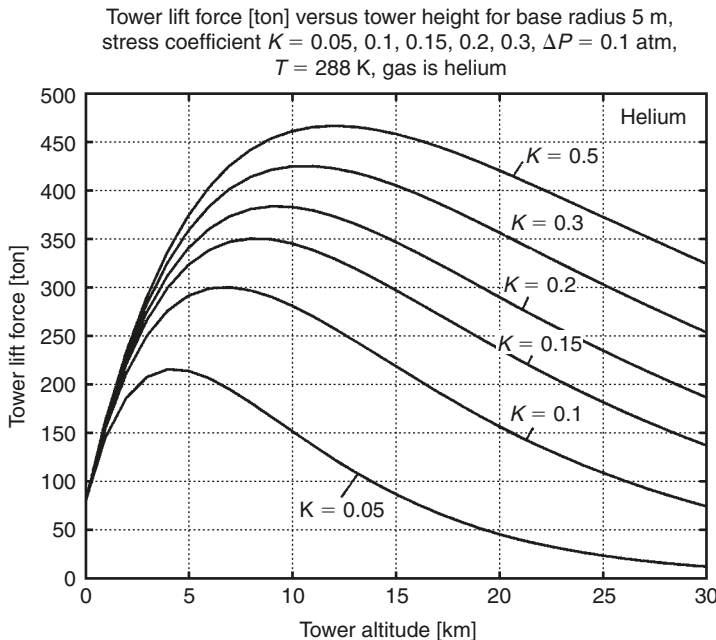


Fig. 4.12. Tower lift force versus tower height for the 30-km helium tower.

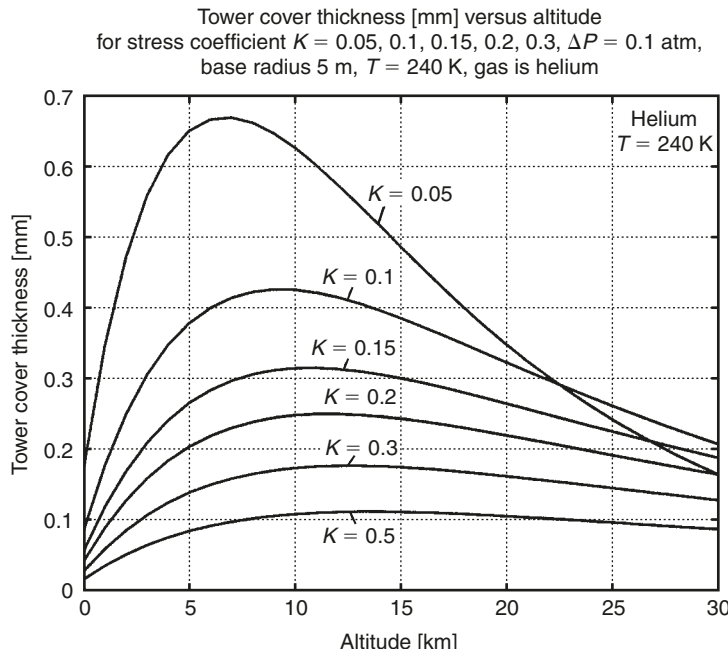


Fig. 4.13. Tower cover thickness versus tower height for the 30-km helium tower.

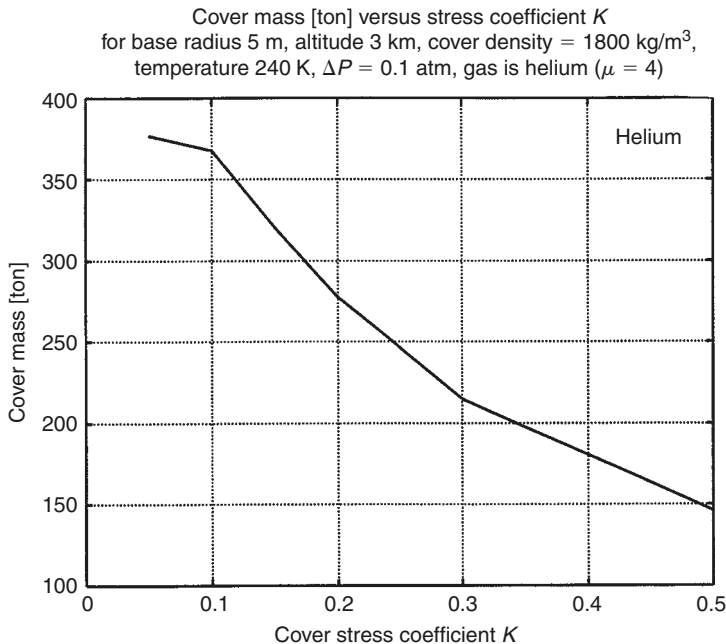


Fig. 4.14. Cover mass versus stress coefficient for the 30-km helium tower.

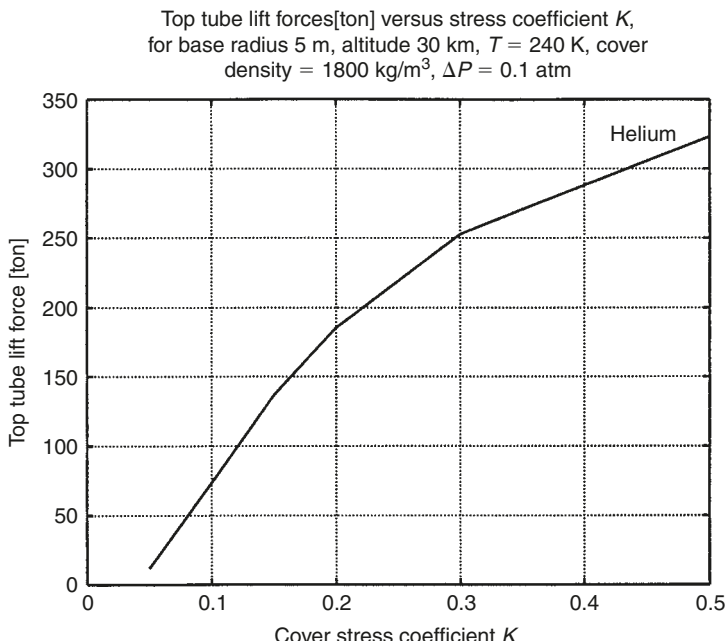


Fig. 4.15. Top lift force for the 30-km helium tower.

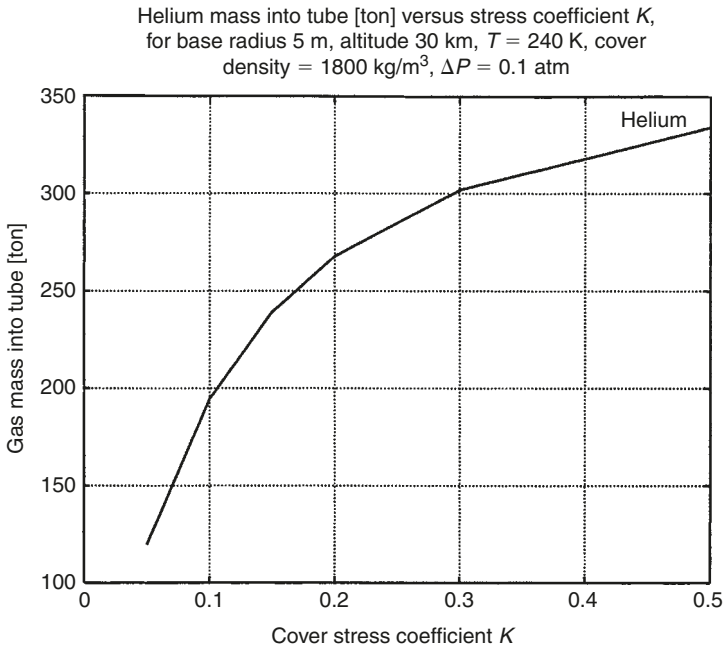


Fig. 4.16. Helium mass for the 30-km tower.

4.4.3.1 Air part (0–15 km)

The base radius is 25 m, the additional pressure is 0.1 atm, average temperature is 240 K, and the stress coefficient $K = 0.1$. Change of radius is presented in Fig. 4.17, the useful tower lift force in Fig. 4.21, the outer tower cover thickness is in Fig. 4.18, maximum safe bending moment is in Fig. 4.19, and the cover mass in Fig. 4.20. This tower can be used for tourism and as an astronomy observatory. For $K = 0.1$, the lower (0–15 km) part of the project requires 570 ton of outer cover (Fig. 4.20) and provides 90 ton of useful top lift force (Fig. 4.21).

4.4.3.2 Hydrogen part (15–100 km)

This part has base radius 5 m, additional gas pressure 0.1 atm, and requires a stronger cover with $K = 0.2$.

The results of computation are presented in the following figures: the change of air and hydrogen pressure versus altitude are in Fig. 4.3; the tower radius versus altitude is in Fig. 4.22; the tower lift force versus altitude is in Fig. 4.23; the tower thickness is in Fig. 4.24; the cover mass is in Fig. 4.25; the lift force is in Fig. 4.26; and hydrogen mass is in Fig. 4.27.

The useful top tower load can be about 5 ton, maximum, for $K = 0.2$. The cover mass is 112 ton (Fig. 4.25) and the hydrogen lift force is 37 ton. The top tower will press on the lower part with a force of only $(112 - 37) + 5 = 80$ ton. The lower part can support 90 ton.

Readers can easily calculate any variant by using the presented figures.

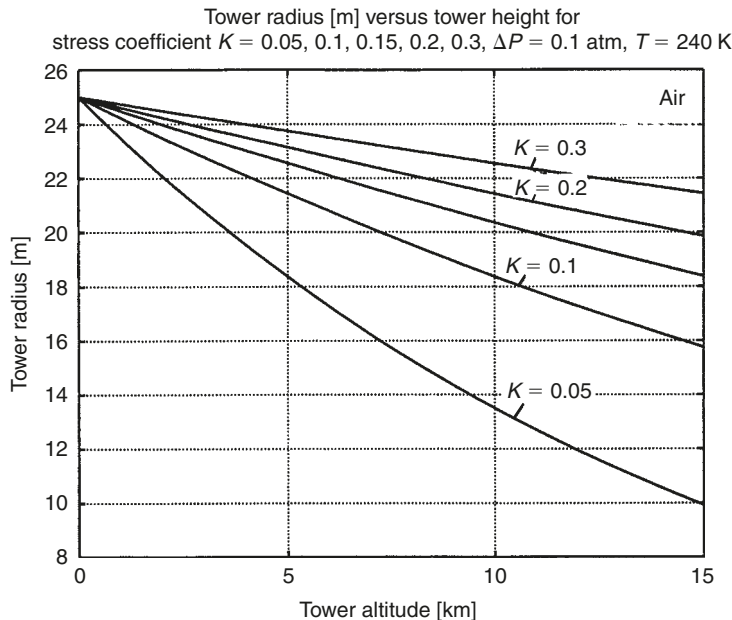


Fig. 4.17. Air lower part of 100-km tower. Tower radius versus altitude.

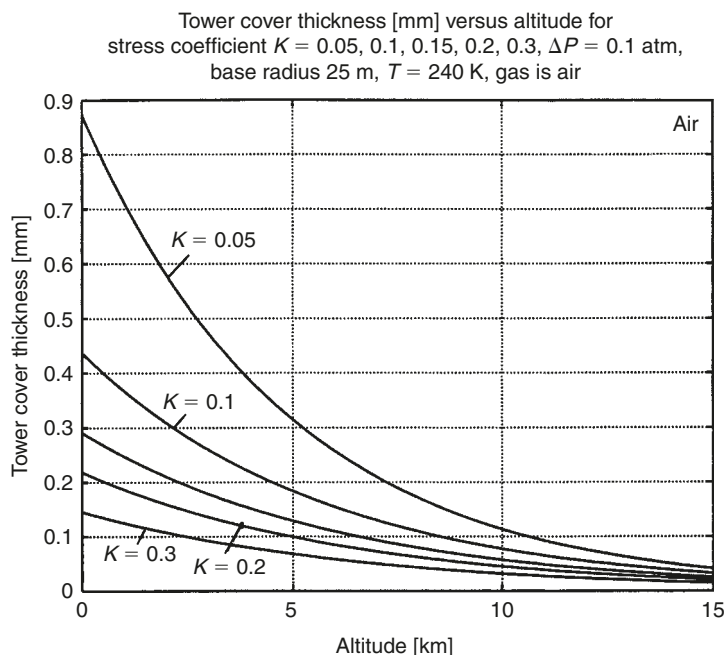


Fig. 4.18. Air lower part of 100-km tower. Tower cover thickness versus altitude.

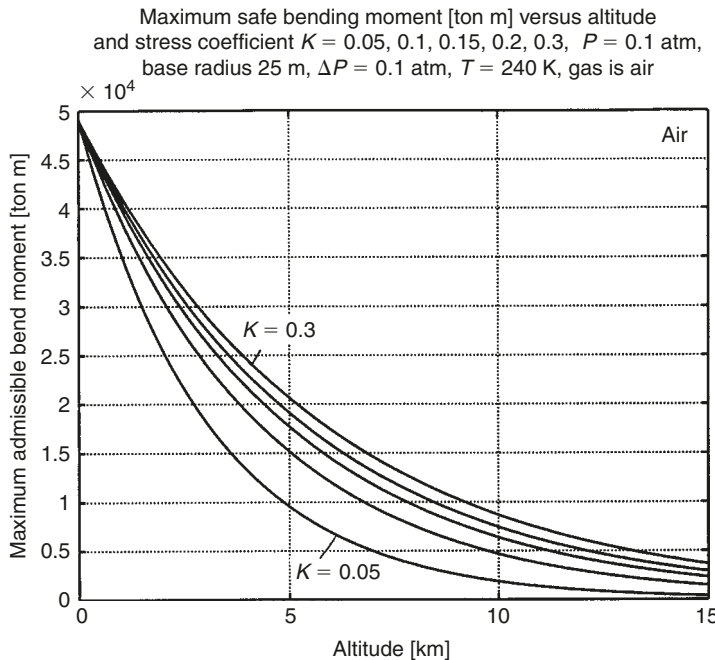


Fig. 4.19. Air lower part of 100-km tower. Maximum safe bending moment.

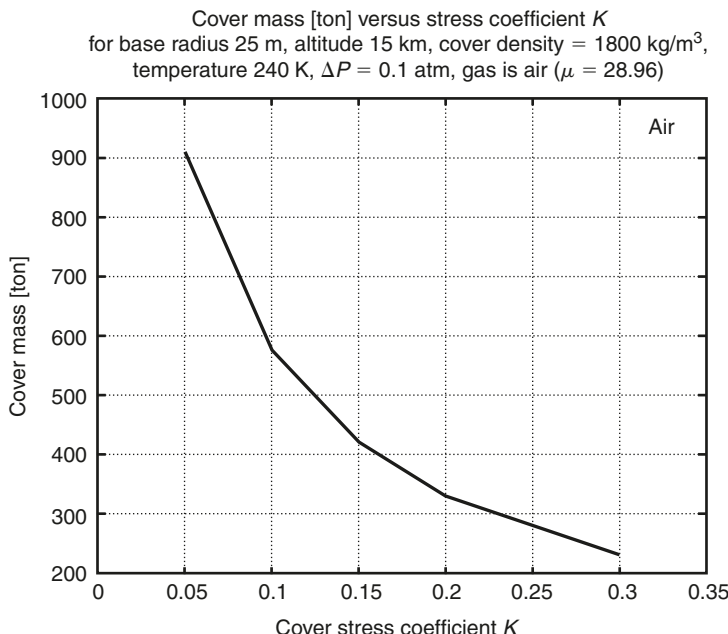


Fig. 4.20. Air lower part of 100-km tower. Cover mass.

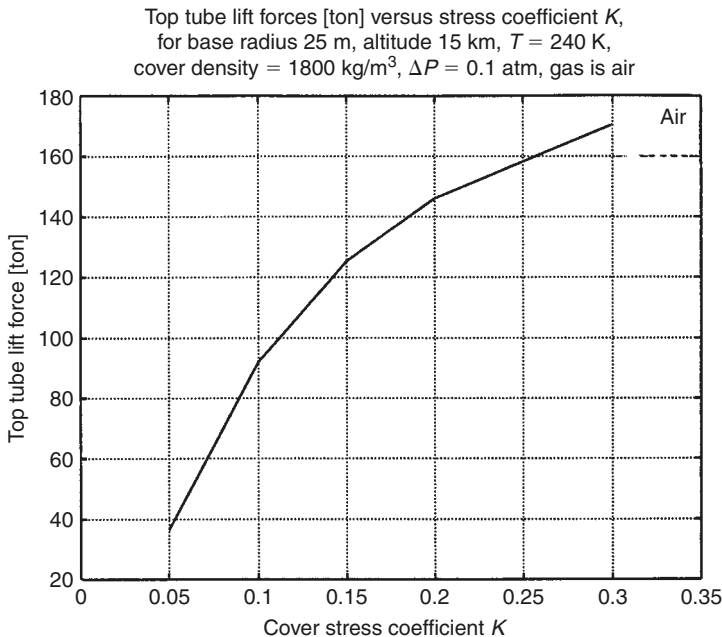


Fig. 4.21. Air lower part of 100-km tower. Top lift force.

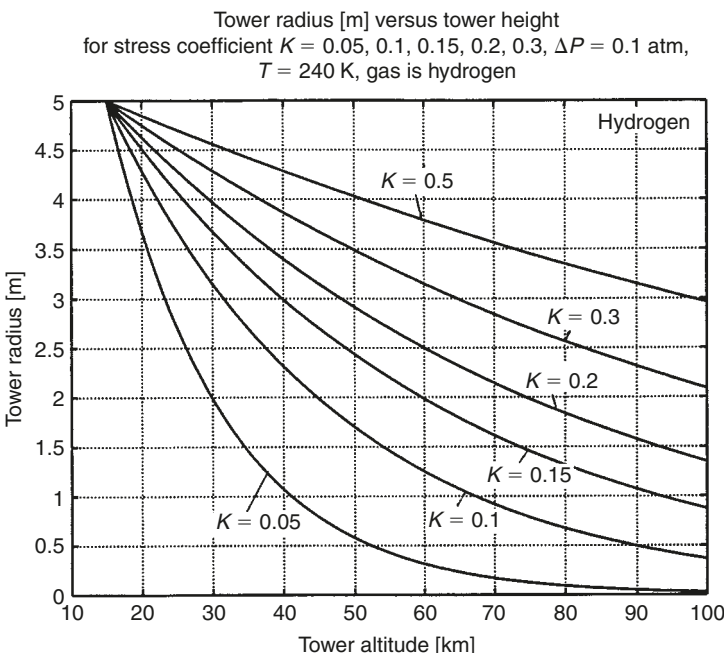


Fig. 4.22. Hydrogen top part of 100-km tower. Tower radius versus altitude.

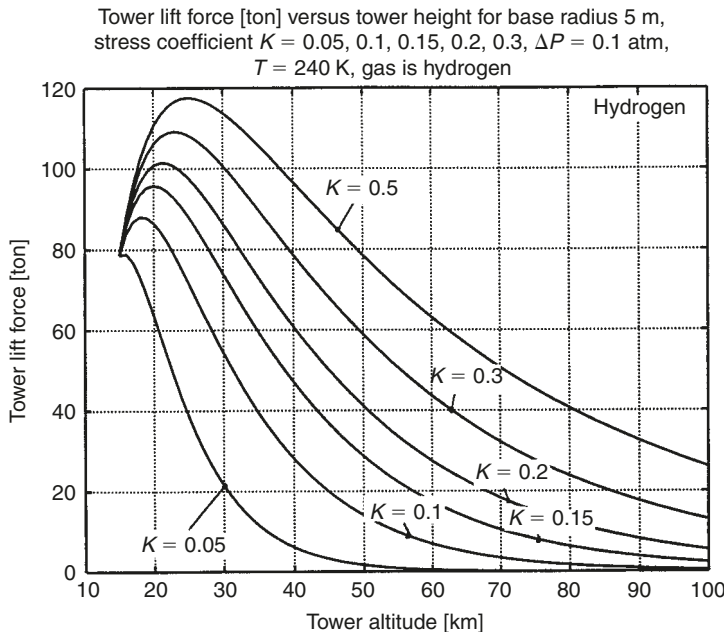


Fig. 4.23. Hydrogen top part of 100-km tower. Tower lift force versus altitude.

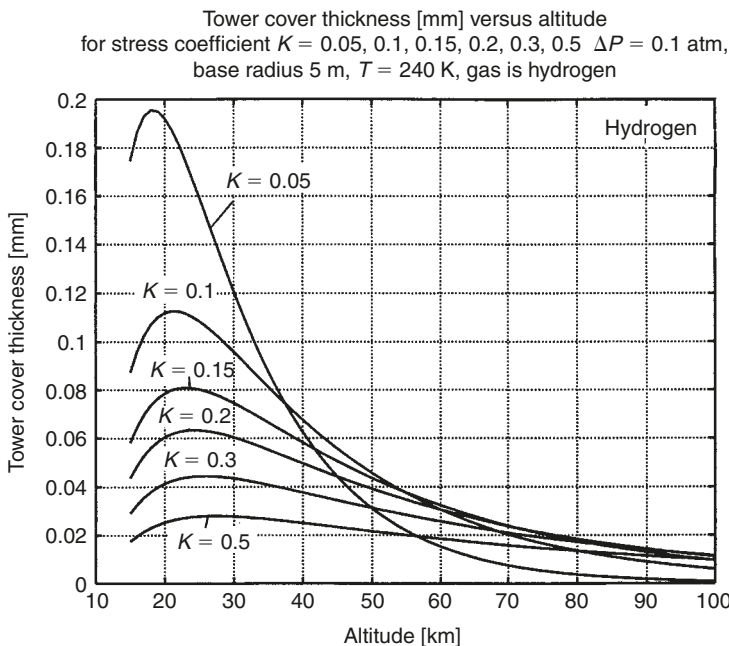


Fig. 4.24. Hydrogen top part of 100-km tower. Tower cover thickness.

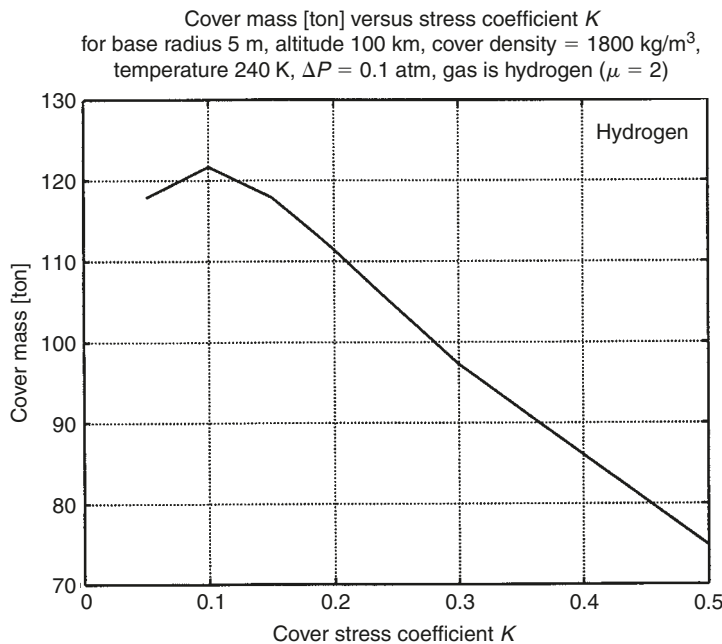


Fig. 4.25. Hydrogen top part of 100-km tower. Cover mass.

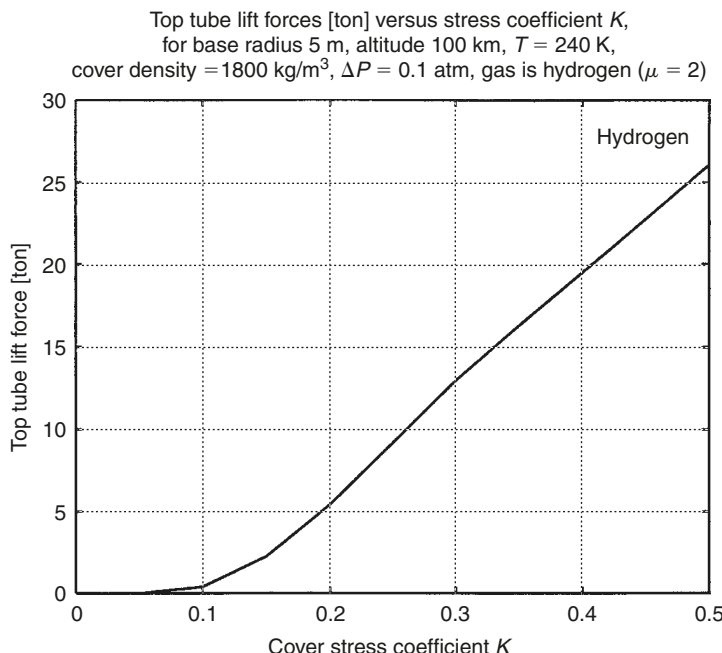


Fig. 4.26. Hydrogen top part of 100-km tower. Tower top lift force.

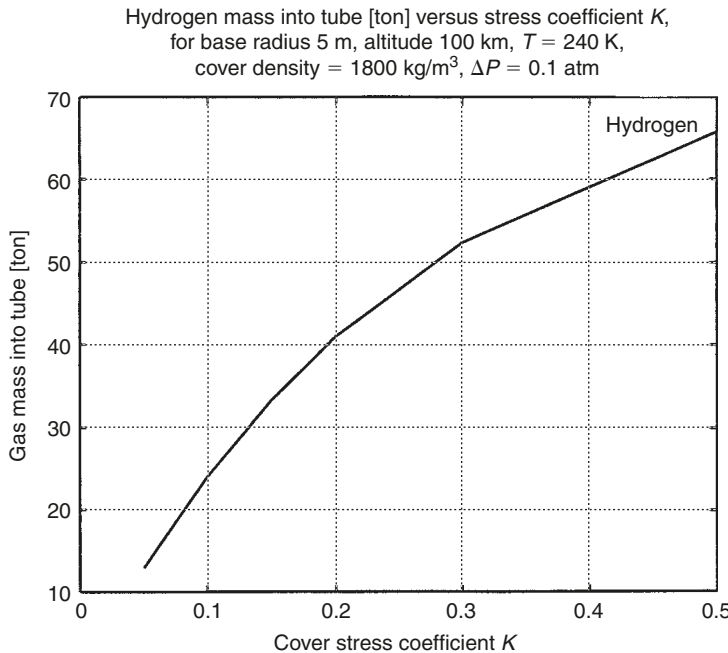


Fig. 4.27. Hydrogen top part of 100-km tower. Required hydrogen mass.

The proposed projects use the optimal change of radius, but designers must find the optimal combination of the air and gas parts.

4.5 Conclusion

The presented theory and computation show that an inexpensive tall tower can be designed and constructed, and can be useful for industry, government, and science.

The author has developed the innovation, estimation, and computations for the above mentioned problems. Even though these projects may seem impossible using current technology, the author is prepared to discuss the details with serious organizations that want to develop these projects.

References

1. D.V. Smitherman Jr., “Space Elevators”, NASA/CP-2000-210429, US National Aeronautics and Space Administration, Washington, DC, 2000.
2. K.E. Tsiolkovski, “Speculations about Earth and Sky and on Vesta”, Moscow, Izd-vo AN SSSR, 1959; Grezi o zemle i nebe (in Russian), Academy of Sciences, USSR, Moscow, 1999, p. 35.
3. A.C. Clarke, *Fountains of Paradise*, Harcourt Brace Jovanovich, New York, 1978.

4. J.T. Harris, *Advanced Material and Assembly Methods for Inflatable Structures*, AIAA, Paper No. 73-448, 1973.
5. F.S. Galasso, *Advanced Fibers and Composite*, Gordon and Branch Science Publisher, New York, 1989.
6. *Carbon and High Performance Fibers, Directory*, 6th edition, Chapman & Hall, London, New York, 1995.
7. M.S. Dresselhous, *Carbon Nanotubes*, Springer, London, New York, 2001.
8. A.A. Bolonkin, “Optimal Inflatable Space Towers with 3–100 km Height”, *Journal of British Interplanetary Society*, Vol. 56, 2003, pp. 87–97.
9. G.A. Landis and C. Cafarelli, “The Tsiolkovski Tower Re-examined”, *Journal of British Interplanetary Society*, Vol. 32, 1999, pp. 176–180.

CHAPTER 5

Kinetic Space Towers*

Summary

This chapter discusses a revolutionary new method to access outer space. A cable stands up vertically and pulls up its payload into space with a maximum force determined by its strength. From the ground the cable is allowed to rise up to the required altitude. After this, one can climb to an altitude using this cable or deliver a payload at altitude. The author shows how this is possible without infringing the law of gravity.

This chapter contains the theory of the method and the computations for four projects for towers that are 4, 75, 225, and 160,000 km in height. The first three projects use the conventional artificial fiber widely produced by current industry, while the fourth project uses nanotubes made in scientific laboratories. This chapter also shows in a fifth project how this idea can be used to launch a load at high altitude.

5.1 Introduction

Lyrical note: Many people have seen films showing trick by Indian magician. The magician arrives at an Indian village, calls the residents, and shows them the trick. He shows a flexible rope to the people, then he takes this rope, says the magic words, flips the rope, and it stands up vertically. A boy climbs up to the top of the rope and descends. The magician again says the magic words and the rope fall down.

I have asked a lot of scientists: what is the scientific explanation of this trick. This is called hypnosis. However, you can hypnotize people, but you cannot hypnotize a camcorder.

Current access to outer space is described in Refs.^{1–6,9}.

This chapter suggests a very simple and inexpensive method and installation for lifting and launching into space. This method is different from the centrifugal method⁶ in

* Presented as paper IAC-02-IAA.1.3.03 at *World Space Congress 2002*, 10–19 October, Houston, TX, USA. Detail manuscript was published as A.A. Bolonkin, “Kinetic Space Towers and Launchers”, *Journal of the British Interplanetary Society*, Vol. 57, No.1/2, 2004, pp. 33–39.

which a cable circle or semi-circle and a centrifugal force are used, which keeps the space station at high altitude. In the offered method there is a straight line vertical cable connecting the space station to the Earth's surface. The space station is held in place by reflected cable and cable kinetic (shot) energy. The offered method expends more than twice as little energy in air drag because the cable length is twice as short as in the semi-circle and has a shorter distance (vertical beeline) than a full circle.

This is a new method and transport system for delivering payloads and people into space. This method uses a cable and any conventional engine (mechanical, electrical, and gas turbines) located on the ground. After completing an exhaustive literature and patent search, the author cannot find the same space method or similar facilities.

5.2 Description of suggested launcher

5.2.1 Brief description of innovation

The installation includes (see notations in Fig. 5.1(a) and (b) and others): a strong closed-loop cable, two rollers, any conventional engine, a space station, a load elevator, and a support stabilization ropes.

The installation works in the following way. The engine rotates the bottom roller and permanently sends up the closed-loop cable at high speed. The cable reaches a top roller at high altitude, turns back and moves to the bottom roller. When cable turns back it creates a reflected (centrifugal) force. This force can easily be calculated using centrifugal theory, or as reflected mass using a reflection theory. The force keeps the space station suspended at the top roller, and the cable (or special elevator) allows the delivery of a load to the space station. The station has a parachute that saves people if the cable or engine fails.

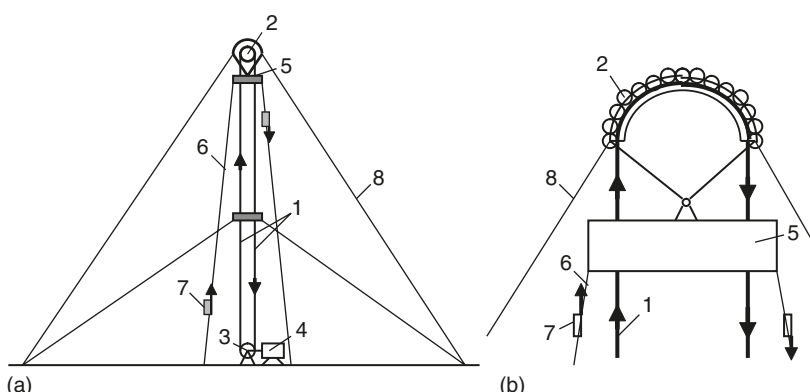


Fig. 5.1. (a) Offered kinetic tower. *Notations:* (1) Mobile closed-loop cable; (2) top roller of the tower; (3) bottom roller of the tower; (4) engine; (5) space station; (6) elevator; (7) load cabin; and (8) tensile element (stabilizing rope). (b) Design of top roller.

The theory shows that current widely produced artificial fibers (see Refs.^{4–6} for cable properties) allow the cable to reach altitudes up to 100 km (see Projects 1 and 2). If more altitude is required a multi-stage tower must be used (Fig. 5.2, see also Project 3). If a very high altitude is needed (geosynchronous orbit or more), a very strong cable made from nanotubes must be used (see Project 4).

The offered tower may be used for a horizontal launch of the space apparatus (Fig. 5.3). The vertical kinetic towers support horizontal closed-loop cables rotated by the vertical cables. The space apparatus is lifted by the vertical cable, connected to horizontal cable, and accelerated to the required velocity.

The closed-loop cable can have variable length. This allows the system to start from zero altitude, and gives the ability to increase the station altitude to a required value, and to spool the cable for repair. The device for this action is shown in Fig. 5.4. The offered spool can reel in the left and right branches of the cable at different speeds and can change the length of the cable.

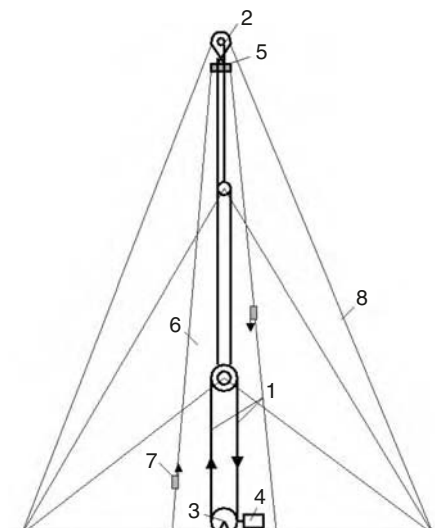


Fig. 5.2. Multi-stage kinetic tower. Notations are same as in Fig. 5.1.

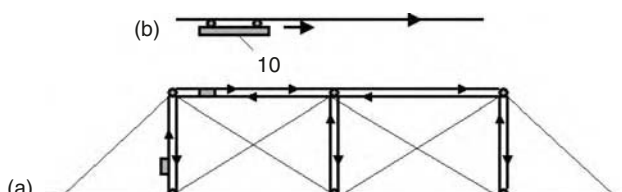


Fig. 5.3. (a) Kinetic space installation with horizontally accelerated parts. (b) *Notation:* (10) Accelerated missile.

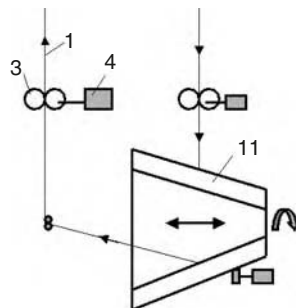


Fig. 5.4. Variable cable spool. Notations: (1) cable; (3) rollers; (4) engines; and (11) cable spool.

5.2.1.1 Advantages

The suggested towers and launch systems have made big advances in comparison with the currently available towers and rocket systems:

1. They allow a very high altitude (up to geosynchronous orbit and more) to be reached, which is impossible for solid towers.
2. They are cheaper by some thousands at times than the current low towers. No expensive rockets are required.
3. The kinetic towers may be used for tourism, power, TV, and radio signal relay over a very wide area, as a radio locator, or as a space launcher.
4. The offered towers and space launchers decrease the delivery cost by some thousand times (up to \$1–4/lb weight).
5. The offered space tower launcher can be made in a few months, whereas the modern rocket-launch system requires some years for development, design, and building.
6. The offered cable towers and space launcher do not require high technology and can be made by any non-industrial country from current artificial fibers.
7. *Rocket fuel is expensive.* The offered cable towers and space launcher can use the cheapest sources of energy (such as wind, water, or nuclear power), or the cheapest fuels (such as gaseous gas, coal, peat, etc.) because the engine is located on the Earth's surface. The flywheels may be used as an accumulator of energy.
8. There is no necessity to have highly qualified personnel such as rocket specialists with high salaries.
9. We can launch thousands of tons of useful loads annually.

The advantages of the offered method are the same as for the centrifugal launcher⁶ (see also Chapter 3). The suggested method is approximately half the cost of the semi-circle launcher⁶ because it uses only one double vertical cable. It also has approximately half the delivery cost (up to \$2–4/kg), because it has half the air drag and fuel consumption.

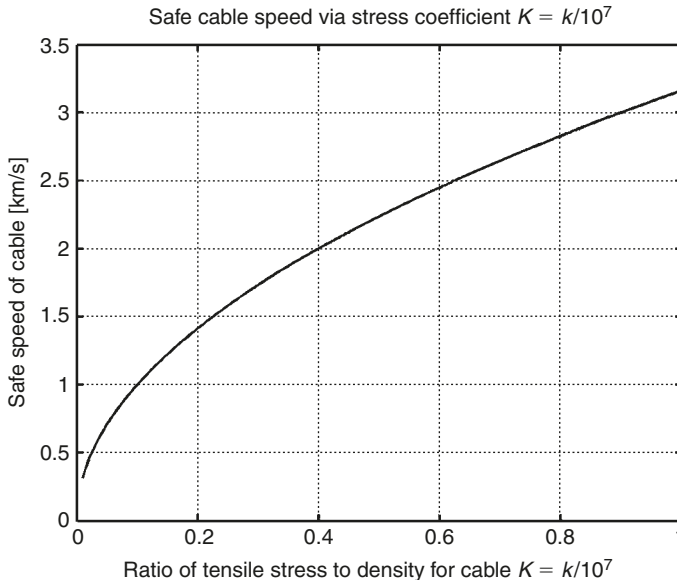


Fig. 5.5. Safe cable speed via stress coefficient $K = 0\text{--}1$.

5.2.1.2 Cable discussing

The reader can find detail of the cable discussion in Chapter 1 and cable characteristics in Refs.^{5–6}. In the Projects 1–3 we use only cheap artificial fibers widely produced by current industry.

5.3 Theory of the kinetic tower and launcher

5.3.1 Lift force of the kinetic tower

- (a) To find the lift force of the kinetic support device from centrifugal theory, take a small part of the rotary circle and write the equilibrium:

$$\frac{2SR\alpha\gamma V^2}{R} = 2S\sigma \sin \alpha, \quad (5.1)$$

where V is rotary cable speed [m/s]; R is circle radius [m]; α is angle of circle part [rad]; S is cross-section of cable areas [m^2]; σ is cable stress [n/m^2]; and γ is cable density [kg/m^3].

When $\alpha \rightarrow 0$ the relationship between the maximum rotary speed V and the tensile stress of the closed-loop (curve) cable is:

$$V = \sqrt{\frac{\sigma}{\gamma}} = \sqrt{k}, \quad F = 2\sigma S, \quad (5.2)$$

where F is the lift force [n] and $k = \sigma/\gamma$ is the relative cable stress [m^2/s^2]. The computations of the first equation for intervals $0\text{--}1K$, $1K\text{--}10K$ ($K = k/10^7$) are presented in Figs. 5.5 and 5.6.

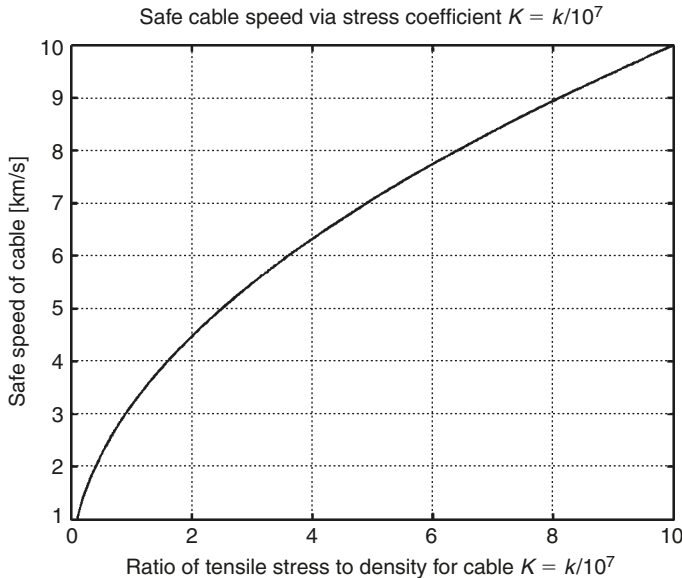


Fig. 5.6. Safe cable speed via relative stress coefficient $K = 1\text{--}10$.

- (b) We can find the lift force of the offered installation from theoretical mechanics. Writing the momentum of the reflected mass in 1 s we find:

$$F = mV - (-mV) = 2mV, \quad m = \gamma SV, \quad \text{or} \quad F = 2\gamma SV^2, \quad (5.3)$$

where m is the cable mass reflected in 1 s [kg/s].

If we substitute equation (5.2) in (5.3), the expression for lift force $F = 2\sigma S$ will be the same. The computation of equation (5.2) for intervals $0\text{--}1K$, $1\text{--}10K$ ($K = k/10^7$) is presented in Figs. 5.5 and 5.6.

5.3.2 Lift force in a constant gravity field

In a constant gravity field without air drag, the lift force of the offered device equals the centrifugal force F minus the cable weight W :

$$F_g = F - W = F - 2\gamma g SH = 2\gamma S(V^2 - gH) = 2S(\sigma - \gamma gH) = 2S\gamma(k - gH), \quad (5.4)$$

where H is the altitude of the kinetic tower [m].

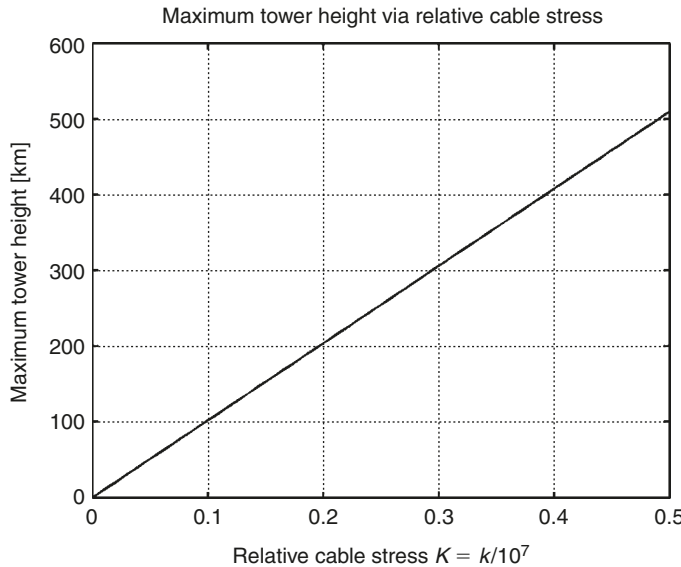


Fig. 5.7 Maximum tower height via relative cable stress.

5.3.3 Maximum tower height or minimum cable speed in a constant gravity field

They are (from equation (5.4)):

$$H_{\max} = \frac{\sigma}{g\gamma} = \frac{k}{g}, \quad V_{\min} = \sqrt{gH}. \quad (5.5)$$

Computations for $K = 0\text{--}1$ are presented in Figs. 5.7 and 5.8. In this case the installation does not produce a useful lift force and will support only itself.

5.3.4 Kinetic lift force in a variable gravity field and for the rotary Earth

$$\begin{aligned} dP &= \left(g - \frac{V^2}{R} \right) dm, \quad g = g_0 \left(\frac{R_0}{R} \right)^2, \quad \frac{V^2}{R} = \omega^2 R, \quad dm = \gamma S dR, \\ R &= R_0 + H, P = \int_{R_0}^R \left[g_0 \left(\frac{R_0}{R} \right)^2 - \omega^2 R \right] \gamma S dR = g_0 \left(R_0 - \frac{R_0^2}{R} \right) - \frac{\omega^2}{2} (R^2 - R_0^2), \\ \text{or } F &= 2\sigma S - 2P = 2\gamma Sk - 2P = 2\gamma S \left[k - g_0 \left(R_0 - \frac{R_0^2}{R} \right) + \frac{\omega^2}{2} (R^2 - R_0^2) \right], \\ k &= \frac{\sigma}{\gamma} = V^2, \end{aligned} \quad (5.6)$$

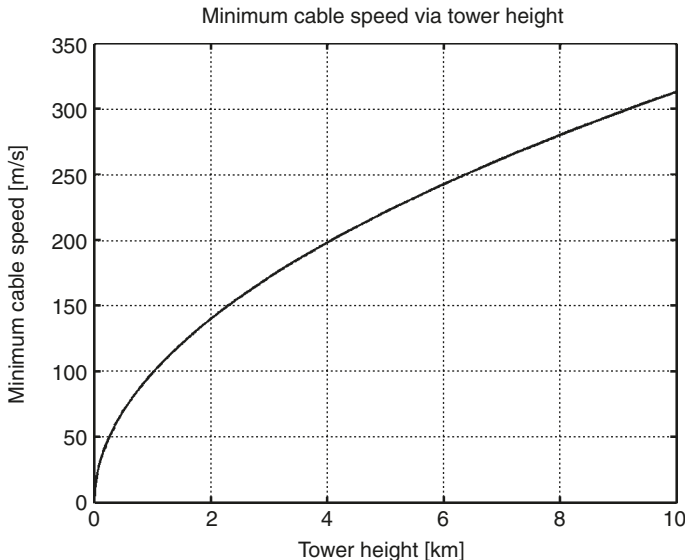


Fig. 5.8. Minimum cable speed via tower height.

where k is the relative cable stress. We will use a more convenient value for graphs of $K = 10^{-7}k$.

Minimum cable stress or minimum cable speed of a variable rotary planet equals:

$$k_{\min} = g_0 \left(R_0 - \frac{R_0^2}{R} \right) - \frac{\omega^2}{2} (R^2 - R_0^2), \quad V_{\min}^2 = g_0 \left(R_0 - \frac{R_0^2}{R} \right) - \frac{\omega^2}{2} (R^2 - R_0^2). \quad (5.7)$$

Computation of these equations for Earth is presented in Figs. 5.9 and 5.10. If $K > 5$ the height of the kinetic tower may be beyond the Earth's geosynchronous orbit. For Mars this is $K > 1$, and for the Moon it is $K > 0.3$. One point to note from Fig. 5.9 the offered tower of a height of 145,000 km can be maintained without a cable rotation, and if the tower height is more than 145,000 km, the tower has a useful lift force that allows a payload to be lifted using an immobile cable.

5.3.5 Estimation of cable friction in the air

This estimation is very difficult because there is no experimental data for air friction of an infinitely thin cable (especially at hypersonic speeds). A computational method for plates at hypersonic speed, described in the book *Hypersonic and High Temperature Gas Dynamics* by J.D. Anderson, p. 287,⁷ was used. The computation is made for two cases: laminar and turbulent boundary layers.

The results of this comparison are very different. Turbulent friction is greater than laminar friction by hundreds of times. About 80% of the friction drag occurs in the troposphere

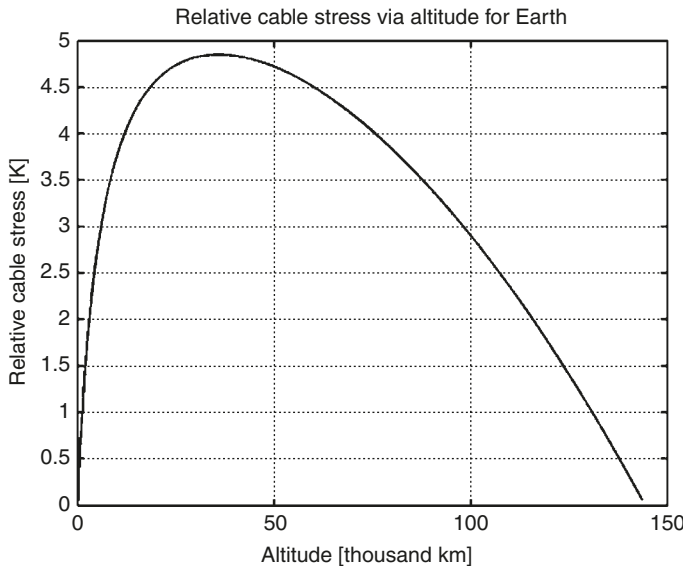


Fig. 5.9. Relative cable stress via altitude for rotary Earth with variable gravity.

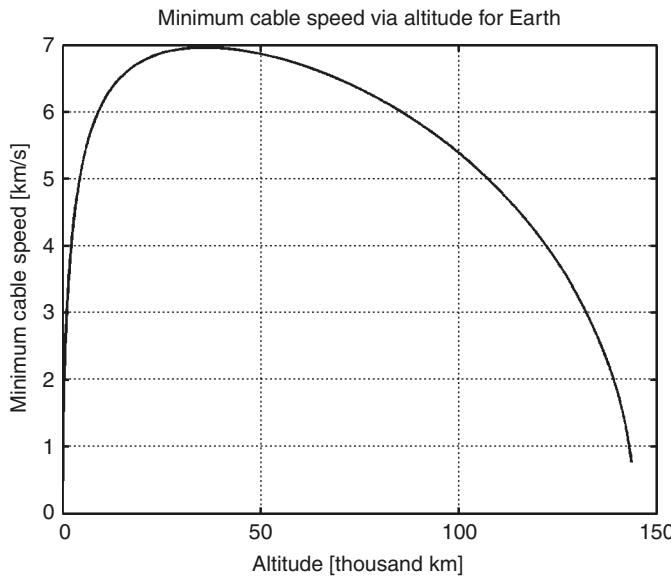


Fig. 5.10. Minimum cable speed via altitude for rotary Earth with variable gravity.

(from 0 to 12 km). If the cable end is located on the mountain at 4 km altitude the maximum air friction will be decreased by 30%.

It is postulated that half of the cable surface will have the laminar boundary layer because a small wind or trajectory angle will blow away the turbulent layer and restore the laminar flow. The blowing away of the turbulent boundary layer is studied in aviation and is used

to restore laminar flow and decrease air friction. The laminar flow decreases the friction in hypersonic flow about by 280 times! If half of the cable surface has a laminar layer, it means that we must decrease the air drag calculated for full turbulent layer by a minimum of 2 times.

Below, the equation from Anderson⁷ for computation of local air friction for a two-sided plate is given:

$$\begin{aligned} \frac{T^*}{T} &= 1 + 0.032M^2 + 0.58\left(\frac{T_w}{T} - 1\right), \quad M = \frac{V}{a}, \mu^* = 1.458 \times 10^6 \frac{T^{*1.5}}{T^* + 110.4} \\ \rho^* &= \frac{\rho T}{T^*}, \quad Re^* = \frac{\rho^* V x}{T^*}, \quad C_{f,l} = \frac{0.664}{(Re^*)^{0.5}}, \quad C_{f,t} = \frac{0.0592}{(Re^*)^{0.2}}, \\ D_L &= 0.5C_{f,l}\rho^*V^2S; \quad D_T = 0.5C_{f,t}\rho^*V^2S, \end{aligned} \quad (5.8)$$

where T^* , Re^* , ρ^* , and μ^* are the reference (evaluated) temperature, Reynolds number, air density, and air viscosity, respectively. M is the Mach number, a is the speed of sound; V is the speed; x is the length of the plate (distance from the beginning of the cable); T is the flow temperature; T_w is the body temperature; $C_{f,l}$ is a local skin friction coefficient for laminar flow; and $C_{f,t}$ is a local skin friction coefficient for turbulent flow. S is the area of skin [m^2] of both plate sides, so this means for the cable we must take $0.5S$; D is air drag (friction) [N]. It can be shown that the general air drag for the cable is $D_g = 0.5D_T + 0.5D_L$, where D_T is the turbulent drag and D_L is the laminar drag.

From equation (5.8) we can derive the following equations for turbulent and laminar flows of the vertical cable:

$$\begin{aligned} D_T &= \frac{0.0592\pi d}{4}\rho_0^{0.8}\left(\frac{T}{T^*}\right)^{0.8}\mu^{0.2}V^{1.8}\int_{H_0}^H h^{-0.2}e^{0.8bh}dh \\ &= 0.0547d\left(\frac{T}{T^*}\right)^{0.8}\mu^{0.2}V^{1.8}\int_{H_0}^H h^{-0.2}e^{0.8bh}dh, \\ D_L &= \frac{0.664\pi d}{4}\rho_0^{0.5}\left(\frac{T}{T^*}\right)^{0.5}\mu^{0.5}V^{1.5}\int_{H_0}^H h^{-0.5}e^{0.5bh}dh \\ &= 0.5766d\left(\frac{T}{T^*}\right)^{0.5}\mu^{0.5}V^{1.5}\int_{H_0}^H h^{-0.5}e^{0.5bh}dh, \end{aligned} \quad (5.9)$$

where d is the diameter of the cable [m], and $\rho_0 = 1.225$ is air density at $H = 0$. The laminar drag is less than the turbulent drag by 200–300 times and we can ignore it.

Engine power and additional cable stress can be computed by conventional equations:

$$P = 2DV, \quad \sigma = \pm \frac{D}{S} = \pm \frac{4D}{\pi d}, \quad (5.10)$$

where P is engine power [J, W]. The factor of 2 is because we have two branches of the cable: one moves up and the other moves down. The drag does not decrease the lift force because in the different branches the drag is in opposite directions.

Computations are presented in Figs. 5.11 and 5.12 for low cable speed and relative cable stress $K = 0\text{--}2$, and in Figs. 5.13 and 5.14 for high cable speed and the relative cable stress $K = 0\text{--}10$.

5.3.6 People security

If the cable is damaged, the people can be rescued using a parachute with variable area. Below the reader will find equations and computations of the possibility of saving people on the tower. The parachute area is changed so that overload does not go beyond a given value ($N < 5 \text{ g}$):

$$\begin{aligned}\frac{dH}{dV} &= -V, \quad \frac{dV}{dt} = g - \frac{D}{m}, \quad \frac{D}{m} = C_D \frac{\rho a V}{2p}, \\ p &= \frac{0.5 C_D \rho a V}{gN}, \quad p \geq 0, \quad \frac{D}{mg} \leq N, \quad \text{for } H = 0 - 10 \text{ km} \\ \rho &= 1.225e^{-H/9218}, \quad \text{for } H = 10 - \infty \quad \rho = 0.414e^{-(H-10000)/6719}\end{aligned}\quad (5.11)$$

where H is altitude [m]; V is speed [m/s]; t is time [s]; m is mass [kg]; D is drag [n]; $g = 9.81 \text{ m/s}^2$ is gravity; C_D is the drag coefficient; ρ is air density [kg/m^3]; a is speed of sound [m/s]; p is the parachutes specific load [kg/m^2]; and N is overload [g].

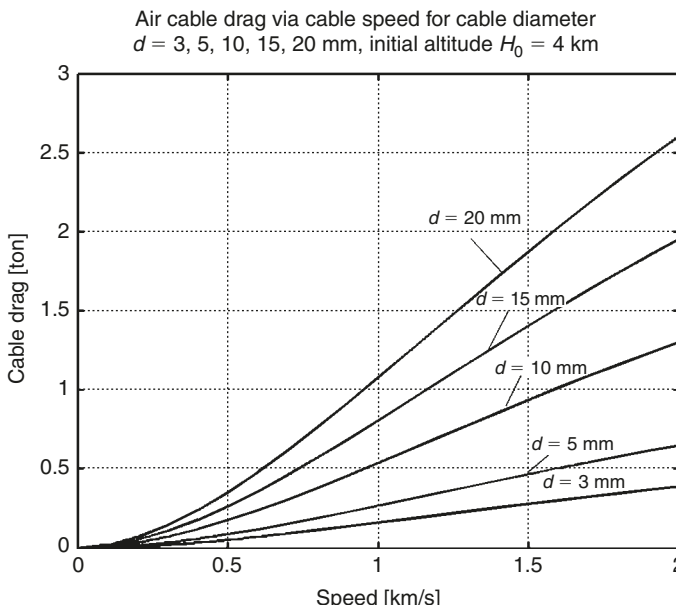


Fig. 5.11. Air cable drag via cable speed 0–2 km/s for different cable diameter.

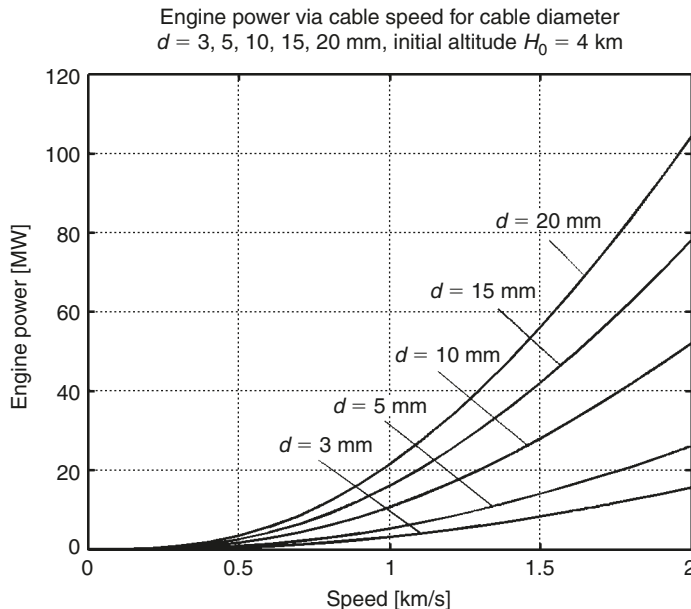


Fig. 5.12. Engine power via cable speed 0–2 km/s for different cable diameter.

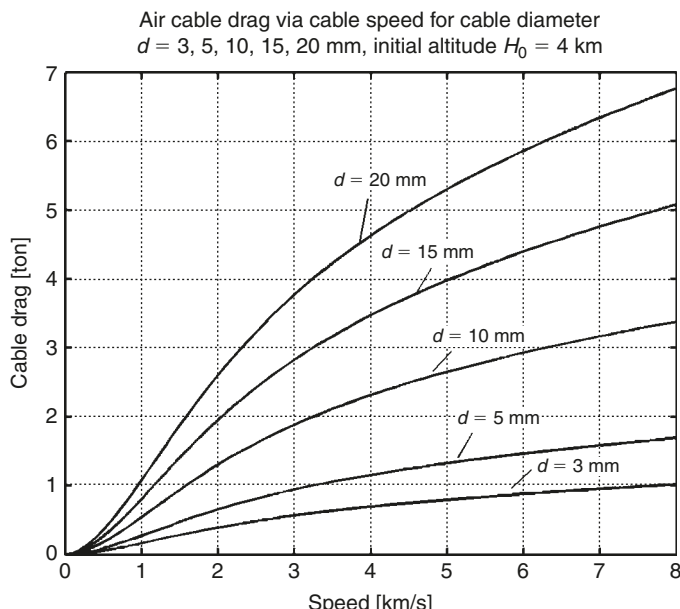


Fig. 5.13. Air cable drag via cable speed 2–8 km/s for different cable diameter.

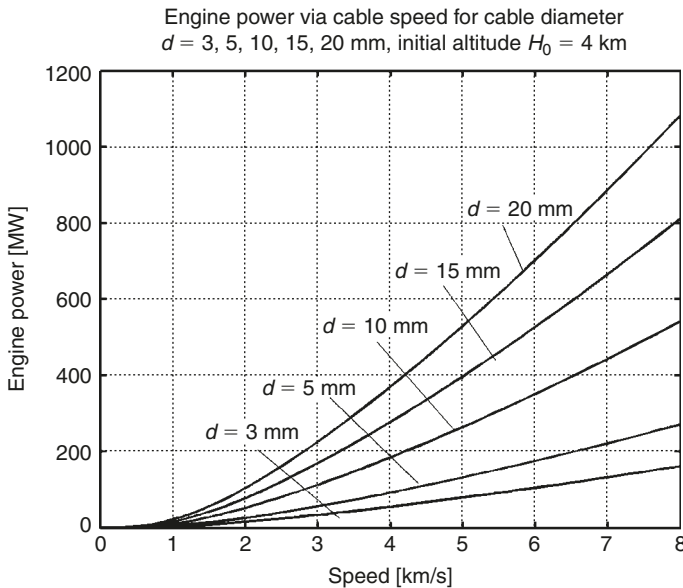


Fig. 5.14. Engine power via cable speed 2–8 km/s for different cable diameter.

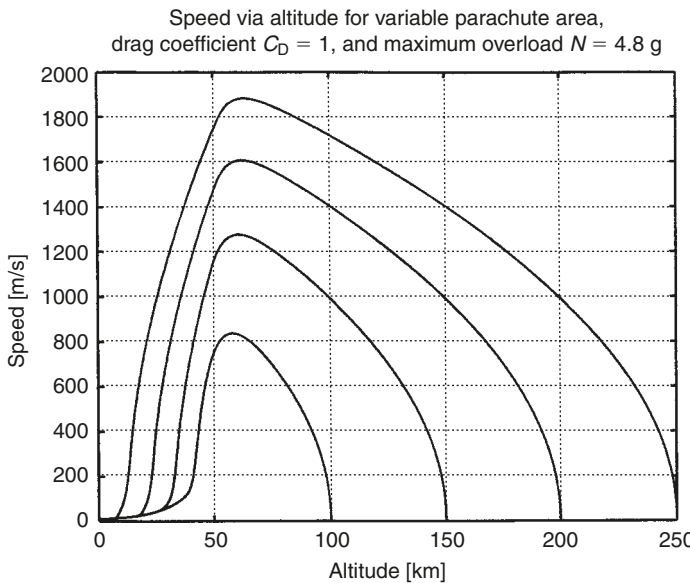


Fig. 5.15. Speed via altitude for variable parachute area.

Computations are presented in Figs. 5.15–5.17. The conventional people (tourists) can be rescued from altitudes up to 250–300 km. The cosmonauts can outstay an overload up to 8 g and may be rescued from greater altitudes.

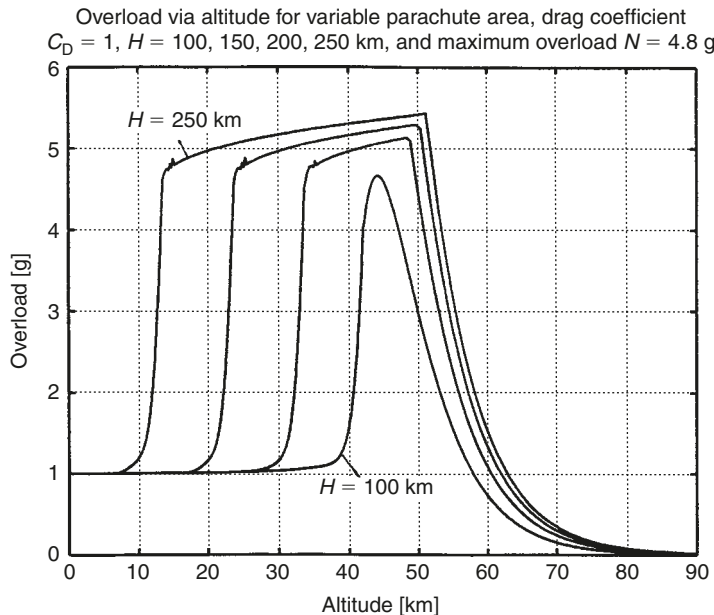


Fig. 5.16. Overload via altitude for variable parachute area.

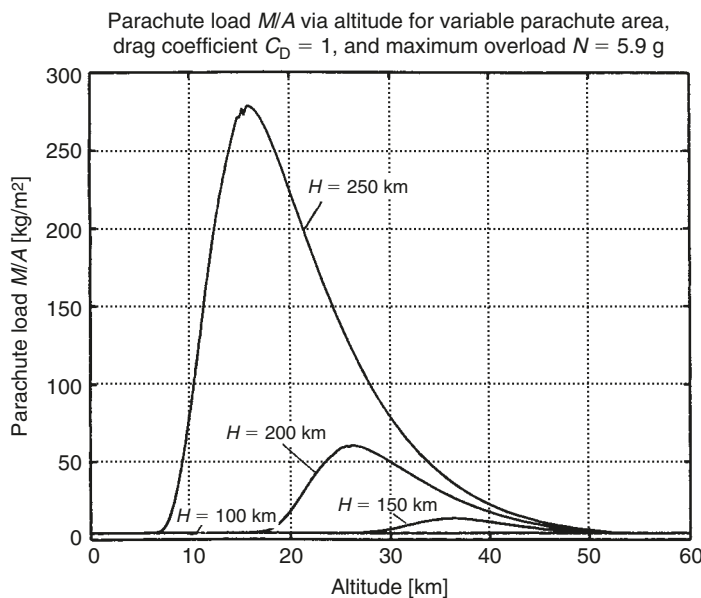


Fig. 5.17. Parachute load via altitude.

5.4 Projects

5.4.1 Project 1: Kinetic tower of height 4 km

For this we can take a conventional artificial fiber widely produced by industry with the following cable performances: admissible stress is $\sigma = 180 \text{ kg/mm}^2$ (maximum $\sigma = 600 \text{ kg/mm}^2$, safety coefficient $n = 600/180 = 3.33$), density is $\gamma = 1800 \text{ kg/m}^3$, and cable diameter $d = 10 \text{ mm}$.

The special stress is $k = \sigma/\gamma = 10^6 \text{ N/m}^2$ ($K = k/10^7 = 0.1$), admissible cable speed is $V = k^{0.5} = 1000 \text{ m/s}$, the cable cross-section area is $S = \pi d^2/4 = 78.5 \text{ mm}^2$, useful lift force is $F = 2S\gamma(k - gH) = 27.13 \text{ ton}$. Requested engine power is $P = 16 \text{ MW}$ (equation (5.10)), cable mass is $M = 2S\gamma H = 2 \times 78.5 \times 10^{-6} \times 1800 \times 4000 = 1130 \text{ kg}$.

Assume that the tower is used for tourism with a payload of 20 ton. This means $20,000/75 = 267$ tourists may be in the station at same time. We take 200 tourists every 30 min, that is $200 \times 48 = 9600 \text{ people/day}$. Let's say 9000 tourists/day which corresponds to $9000 \times 350 = 3.15 \text{ million/year}$.

Assume the cost of installation is \$15 million,⁸ the lifetime is 10 years, and the maintenance cost is \$1 million/year. The cost of an installation to service a single tourist is $2.5/3.15 = \$0.8/\text{person}$.

The required fuel $G = Pt/\varepsilon\eta = 16 \times 10^6 \times 350 \times 24 \times 60 \times 60/(42 \times 10^6 \times 0.3) = 38.4 \times 10^6 \text{ kg}$. If the fuel cost is \$0.25/kg, the annual fuel cost is \$9.6 million, or $9.6/3.15 = \$3.05/\text{person}$. Here t is annual time [s], ε is fuel heat capability [J/kg], and η is the engine efficiency coefficient.

The total production cost is $0.8 + 3.05 = \$3.85/\text{tourist}$. If a trip costs \$9, the annual profit is $(9 - 3.85) \times 3.15 = 16.22 \text{ million of US dollars}$. If readers do not agree with this estimation, calculations can be made with other data.

5.4.2 Project 2: Kinetic tower of height 75 km

For this tower take the admissible cable stress $K = 0.1$, the cross-section area $S = 90 \text{ mm}^2$ ($d = 10.7 \text{ mm}$), and the cable density $\gamma = 1800 \text{ kg/m}^3$. Then the lift force is $F = 2S\gamma(k - gH) = 7 \text{ ton}$. The required engine power is $P = 11 \text{ MW}$ (equation (5.10), Fig. 5.12), cable mass is $M = 2S\gamma H = 2 \times 90 \times 10^{-6} \times 1800 \times 75,000 = 24.3 \text{ ton}$, and the cable speed is 1000 m/s.

5.4.3 Project 3: Multi-stage kinetic tower of height 225 km

Current industry widely produces only a cheap artificial fiber with maximum stress $\sigma = 500\text{--}620 \text{ kg/mm}^2$ and density $\gamma = 1800 \text{ kg/m}^3$. We take an admissible stress $\sigma = 180 \text{ kg/mm}^2$ (safety coefficient is $n = 600/180 = 3.33$), and $\gamma = 1800 \text{ kg/m}^3$. Then $k = \sigma/\gamma = 1,000,000 \text{ N/m}^2$ or $K = k/10^7 = 0.1$. From this cable one can design a one-stage kinetic tower with a maximum height 100 km (payload = 0). Assume we want to design a tower height is 225 km high using the current material. Then we can design third-stage tower

with each stage at height $H = 75\text{ km}$ and useful load capability $M_{3,p} = 3\text{ ton}$ at the tower top.

In this case the third (top) stage ($150\text{--}225\text{ km}$) must have a cross-section area $S_3 = M_{3,p}/[2\gamma(k - gH)] = 33.3\text{ mm}^2$ ($d = 6.5\text{ mm}$), and the cable mass of the third stage is $M_{3,c} = 2S_3\gamma H = 9\text{ ton}$. Total mass of third stage is $M_3 = 9 + 3 = 12\text{ ton}$.

The second stage ($75\text{--}150\text{ km}$) must have a cross-section area $S_2 = M_3/[2\gamma(k - gH)] = 133\text{ mm}^2$ ($d = 13\text{ mm}$), and the cable mass of second stage is $M_{2,c} = 2S_2\gamma H = 36\text{ ton}$. Total mass of third + second stages is $M_2 = 12 + 36 = 48\text{ ton}$.

The first stage ($0\text{--}75\text{ km}$) must have a cross-section area $S_1 = M_2/[2\gamma(k - gH)] = 533\text{ mm}^2$ ($d = 26\text{ mm}$), and the cable mass of the first stage is $M_{1,c} = 2S_1\gamma H = 144\text{ ton}$. Total mass of third + second + first stages is $M_0 = 48 + 144 = 192\text{ ton}$.

5.4.4 Project 4: Kinetic tower with height 160,000 km

Assume that nanotube cable is used, with $K = 6$ (for this height K must be more than 5, see Fig. 5.8). This means the admissible stress is $\sigma = 6000\text{ kg/mm}^2$ and the cable density is $\gamma = 1000\text{ kg/m}^3$. At the present time (2000) scientific laboratories produce nanotubes with $\sigma = 20,000\text{ kg/mm}^2$ and density $\gamma = 0.8\text{--}1.8\text{ kg/m}^3$. Theory predicts $\sigma = 100,000\text{ kg/mm}^2$. Unfortunately, there are no widely produced industrial nanotubes and the laboratory samples are very expensive.

Take a cross-section cable area of 1 mm^2 . The required speed is $V = (k)^{0.5} = (6 \times 10^7)^{0.5} = 7.75\text{ km/s}$, the mass of cable is $M = S\gamma H = 320\text{ ton}$, and the engine power (only in an installation launch) is $P = 50\text{ kW}$ (equation (5.10)). When full altitude is reached the engine can be turned off and the centrifugal force of the Earth's rotation will support the cable. Moreover, the installation has a lift force of about 1000 kg , so a useful load can be connected to the cable, the engine can be turned on or slow speed, and the load can be delivered into space.

5.4.5 Project 5: Kinetic tower as space launcher

The suggested installation of Fig. 5.3 can be used as a space launcher. The space apparatus is lifted to high altitude by the left kinetic tower, connected to the horizontal line and accelerated. The required acceleration distance depends on the admissible acceleration. For a projectile it may be $10\text{--}50\text{ km}$ ($N = 64\text{--}320g$), for cosmonauts it may be 400 km ($N = 8g$), for tourists it may be 1100 km ($N = 3g$).

5.5 Discussion

The proposed method offers a new, simpler, cheaper, more realistic method for space launcher than many others. It is impossible to demand immediately solutions to all problems. This is only the start of much research and development of the associated problems. The purpose here is to offer a new idea and show that it has good prospects, but it needs further research.

It is thought that this method has a big future. It does not need expensive rockets as current methods do, or rockets to launch a counterbalance into space and thousands of tons of nanotube cable as the space elevator does. It only needs conventional cable and a conventional engine located on a planet. It is very important not to dismiss new ideas when they are first contained.

References

1. Space Technology and Application. International Forum, Parts 1–3, Albuquerque, MN, 1996–1997.
2. D.V. Smitherman Jr., *Space Elevators*, NASA/CP-2000-210429, US National Aeronautics and Space Administration, Washington, DC, 2000.
3. A.A. Bolonkin, “Hypersonic Gas-Rocket Launch System”, AIAA-2002-3927, *38th AIAA/ASME/SAE/ASEE Joint Propulsion Conference and Exhibition*, 7–10 July, 2002. Indianapolis, IN, USA; IAC-02-S.P.15, *World Space Congress 2002*, 10–19 October 2002, Houston, USA; *Journal Actual Problems of Aviation and Aerospace Systems*, Vol. 8, No. 1, 2003, pp. 45–58, Kazan, Daytona Beach.
4. A.A. Bolonkin, “Asteroids as Propulsion Systems of Space Ships”, *Journal of the British Interplanetary Society*, Vol. 58, No. 3–4, pp. 98–107.
5. A.A. Bolonkin, “Space Cable Launchers”, Paper 8057 at *Symposium on “The Next 100 Years”*, 14–17 July 2003, Dayton, OH, USA.
6. A.A. Bolonkin, “Centrifugal Keeper for Space Stations and Satellites”, *Journal of the British Interplanetary Society*, Vol. 56, September–October 2003, pp. 314–322.
7. J.D. Anderson, *Hypersonic and High Temperature Gas Dynamics*, McGraw-Hill Book Co., New York, 1989.
8. D.E. Koell, *Handbook of Cost Engineering*, TCS, Germany, 2000.
9. A.A. Bolonkin, “Kinetic Space Towers and Launchers”, *Journal of the British Interplanetary Society*, Vol. 57, No. 1/2, 2004, pp. 33–39.

This page intentionally left blank

CHAPTER 6

Gas Tube Hypersonic Launcher*

Summary

The present chapter describes a hypersonic gas rocket, which uses tube walls as a moving compressed air container. Suggested burn programs (fuel injection) enable use of the internal tube components as a rocket. A long tube (up to 0.4–0.8 km) provides mobility and can be aimed in water. Relatively inexpensive oxidizer and fuel are used (compressed air or gaseous oxygen and kerosene). When a projectile crosses the Earth's atmosphere at an angle more than 15°, loss of speed and the weight of the required thermal protection system are small. The research shows that the launcher can give a projectile a speed of up to 5–8 km/s. The proposed launcher can deliver up to 85,000 ton of payloads to space annually at a cost of \$1–2/lb of payload. The launcher can also deliver about 500 ton of mail or express parcels per day over continental distances and may be used as an energy station and accumulator. During war, this launch system could deliver military munitions to targets thousands to tens of thousands of kilometers away from the launch site.

Nomenclature (metric system)

C_p	heat capability at constant pressure $C_p = 1.115$ [kJ/kg K] for air, $C_p = 1.069$ for oxygen
C_v	heat capability at constant volume
G_p	mass of the projectile (payload)[kg]
$K = C_p/C_v$	coefficient, $k = 1.34$ for air, $k = 1.2$ for rocket gas
L	length of launch tube [m]
L_r	length of rocket air column [m]

* This chapter is based on a paper presented at the *38th AIAA Propulsion Conference*, 7–10 July 2002, Indianapolis, USA (AIAA-2002-3927) and *The World Space Congress*, 10–19 October 2002, Houston, USA (IAC-02-S.P.15). Detailed material is published as A.A. Bolonkin, “Hypersonic Gas-Rocket Launcher of High Capacity”, *Journal of the British Interplanetary Society*, Vol. 57, No. 5/6, 2004, pp. 162–172; *Actual Problems of Aviation and Aerospace Systems*, Kazan, Vol. 1, No. 15, 2003, pp. 45–69.

M	mass of rocket [N]
M_k	rocket mass at the end of acceleration [N]
M_0	rocket mass at the beginning of acceleration [N]
V	speed of rocket [m/s]
V_0	speed of the rocket after initial acceleration [m/s]
V_p	projectile speed after being shot at sea level [m/s]
ΔV	increment of rocket velocity [m/s]
w	speed of gas after nozzle [m/s]
P	pressure of gas from nozzle [atm]
P_0	initial pressure of gas in tube
Q	amount of heat [J]
R	gas low constant, $R = 287$ for air, $R = 325$ for rocket gas
t	time [s]
T	absolute temperature [K]
θ	trajectory angle to a horizon [°]
β	fuel rate [kg/s]
$\mu = M_k/M_0$	relative mass of rocket

6.1 Introduction

Unfortunately, most specialists, when they see projectiles in tubes, think of a gun (cannon). They know very well that a gun cannot give a projectile speed of more than 1–2 km/s.^{1–5} They also know that a gas gun using hydrogen can give a speed of up to 3–4 km/s, which however is still not enough for space flight.

A high-speed ground-based gun is very large, complex and expensive, and can shoot only from one point on the Earth or in space,^{6–12} therefore they do not want to read or hear about a new revolutionary method.

As is shown in Ref.¹² the offered installation is a gas rocket in a tube. It looks like the solid traveling charge gun,^{13–14} but the offered tube rocket uses air and kerosene as fuel (not powder as in the traveling charge gun).

6.1.1 Short history of the high-speed gun

The first high-speed gun was the Krupp gun in World War I. After World War II research into a big high-speed gun was made in project HARP.¹¹

The cannon had a caliber of 16.4 in. (417 mm), with a barrel length at 45–126 calipers (18.8–52.5 m), and the weight of the gunpowder was 780 lb (351 kg). Maximum pressure reached 340 MPa (3400 atm). The projectile weighing 38 lb (17 kg) had speeds up to 6000–6135 ft/s (2 km/s). Iraq made the most recent attempt to create a big cannon, which was destroyed by the UN.

A gun with a solid traveling charge was studied by the Ballistic Research Laboratory.^{13,14} They used solid gunpowder as rocket fuel and a small bore (5/8 in.) (9.5 mm). The traveling charge gun was initiated at the Ballistic Research Laboratories, Aberdeen Proving Group, Maryland. The objective of their paper¹³ is to show that it is possible to

build a device capable of accelerating small projectiles (weight range of 1–5 g) to velocities in excess of 20,000 ft/s (6 km/s) without subjecting the projectile to severe acceleration force. Their result is as follows.

In theory there is no upper limit to the velocity that can be attained. All that is required is more propellant and a longer barrel. However, the shot time is about 4 ms and the required fast burning rate of 2000 in./s is three orders of magnitude greater than the burning rate of solid gun propellants. This problem could not be solved by using a porous (grains) propellant (gunpowder). It was noted that it could be possible for the propellant to detonate. Some experiments with ball powder in a long tube (analogous to a long grain of porous propellant) have indicated that rapid burning of the propellant may change over a detonation.

The suggested method and installation^{15,16} uses conventional compressed air (as oxidizer) and conventional kerosene (as fuel). The barrel is long (up to 0.4–1 km) and the time of the shot is long (up to 0.5–1.2 s). The injection fuel program keeps constant pressure in the rocket (constant thrust) and avoids detonation. Other differences and advantages are shown later.

6.2 Description

Fig. 6.1(a) shows a design of the tube of the suggested hypersonic gas-rocket system. The system is made up of a tube, a piston with a fuel tank and payload, and nozzle connected to the piston, and valves.

The tube rocket engine can be made without a special nozzle (Fig. 6.1(b)). In this case, the fuel efficiency of the gas-rocket engine will decrease but its construction becomes simpler.

The tube may be placed into a frame (Fig. 6.1(c)). The frame is placed into water and connected to a ship for mobility and aiming.

The launch sequence is as follows. First the movable piston with the fuel tank (containing liquid fuel), and payload are loaded into the tube. The piston is held in place by the fasteners or closed valve 17 (Fig. 6.1). The direction and angle of the launch tube are set.

Valve 19 (Fig. 6.1) is closed and a vacuum (about 0.005 atm) is created in the launch tube space above the payload/piston to reduce the drag imparted to the payload/piston as it moves along the launch tube. The tube, of a length of 630 m and a diameter of 10 m, contains 61 ton of air at atmospheric pressure. If this air is not removed, the payload must be decreased by the same value. If air pressure is decreased down to 0.005 atm, the parasitic air mass is decreased to 300 kg. This is an acceptable parasitic load.

Valve 17 is closed and an oxidizer (air, oxygen, or a mixture) is pumped into the space below the payload/piston.

Liquid fuel (benzene, kerosene) is injected into the space below nozzle 6 through the launch tube injectors (item 15, Fig. 6.1) and ignited. Valve 17 (Fig. 6.1) is opened. The hot combustion gas expands and pushes the payload/piston system along the launch tube together with the air column (item 7) between the piston and nozzle.

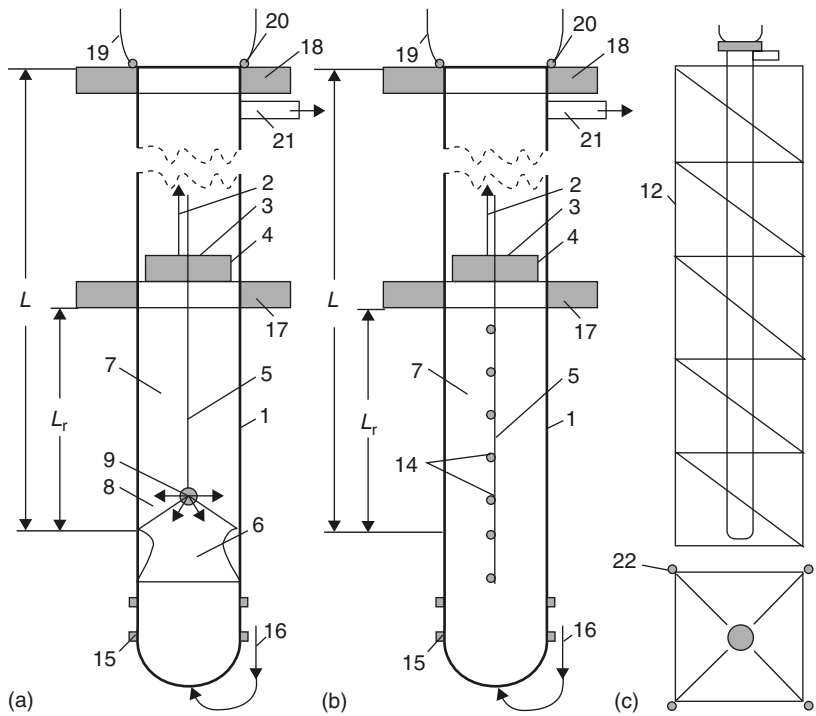


Fig. 6.1. (a) Space launcher with the gas rocket and rocket nozzle in the tube. Notations: (1) tube; (2) payload (projectile); (3) fuel tank; (4) piston; (5) fuel pipeline; (6) nozzle connected to piston; (7) rocket air column; (8) combustion chamber; (9) injectors of the combustion chamber; (12) tube frame; (14) additional injectors; (15) lower tube injectors; (16) air pipeline; (17) lower valve; (18) upper valve; (19) top valve; (20) airlock; (21) gas pipe; and (22) electric engines. (b) Space launcher without the rocket nozzle. (c) Launcher in frame.

When the piston reaches the maximum gun speed (about 1 km/s), the compressed air column begins to work as a rocket engine using one of the special injection fuel programs (see Ref.¹²).

As the payload/piston approaches the end of the launch tube, valve 19 is opened and the airlock (item 20) begins to operate. After the payload/piston has left the launch tube, valve 18 closes the end of the launch tube and re-directs the hot combustion gases down the bypass tube (item 21) to various turbo-machines preparing compressed air for the next shot and electricity for customers.

If a high launch frequency is required, then internal tube water injectors are used to quickly cool the launch tube.

After the payload/piston system leaves the launch tube, the payload (projectile) separates from the piston and the empty fuel tank. The payload continues to fly along a ballistic trajectory. At apogee, the payload may use a small rocket engine to reach orbit or to fly to any point on Earth.

The method by which the fuel is injected and ignited within the launch tube is critical to high-speed (hypersonic) acceleration of the payload. The author has developed the five fuel injection programs for the launch system.¹²

In these programs the thrust (force) is constant at all times, which means that pressure and all parameters in the rocket engine are constant. Parts of the programs have two steps. In the first step, the fuel is injected into compressed air at the lower part of the tube to support a constant pressure and provide the initial acceleration of the rocket (together with air column L_r) to the velocity V_0 . In the second step, the rocket engine begins to thrust and support the constant pressure and temperature in the rocket combustion chamber. The result is that the thrust force of the gas-rocket engine remains constant. In the reference article the author considered only a simplified model (Fig. 6.1(b)) when a rocket nozzle is absent.

6.3 Methods of estimation and results of computation

6.3.1 Estimation of missile velocity

Take the well-known rocket equation:

$$M \frac{dV}{dt} = \beta w + P, \quad (6.1)$$

and its solution,

$$\Delta V = - \left(w + \frac{P}{\beta} \right) \ln \mu, \quad (6.2)$$

where ΔV is the increment of speed [m/s]; $\mu = M_k/M_0$ is the relative mass of rocket; M_k is the rocket mass at the end of acceleration [kg]; M_0 is the rocket mass at the beginning of acceleration [kg]; β is the fuel (gas consumption) rate [kg/s] (constant); w is the speed of gas at nozzle exit [m/s] (constant); and P is the force of pressure at nozzle exit [N] (constant).

From the theory of nozzle expansion the following relations are known:

$$P = 10^4 g P_n S_n, \quad \beta = \rho_c w_c S_c, \quad p_c = p_0 \left(\frac{2}{k+1} \right)^{\frac{k}{k-1}},$$

$$\rho_c = \frac{10^4 g P_0}{RT} \left(\frac{2}{k+1} \right)^{\frac{1}{k-1}}, \quad w_c = \sqrt{\frac{2kRT}{k+1}},$$

where subscript “c” denotes parameters in a critical (most narrow) nozzle area; subscript “0” denotes the gas parameters in tube rocket before combustion; subscript “n” denotes parameters in the nozzle exit; S is the cross-section area of the tube [m^2]; T is the gas temperature in the combustion chamber [K]; p is the gas pressure in the rocket [kg/cm^2], k , R are gas constants; and $g = 9.81 m/s^2$ is gravity.

In this chapter the computations are given only for the simplest case: the rocket without a special nozzle (the tube is used as a nozzle of constant cross-section area), where: $S = S_n = S_c$, $w = w_c$, $P_n = P_c$.

Let us substitute the above expressions in equation (6.2):

$$w = \sqrt{\frac{2kRT}{k+1}}, \quad \frac{P}{\beta} = \sqrt{\frac{2RT}{k(k+1)}}, \quad w + \frac{P}{\beta} = \sqrt{\frac{2(k+1)RT}{k}}, \quad \rho_c = \rho_0 \left(\frac{2}{k+1} \right)^{\frac{1}{k-1}},$$

$$\rho_0 = \frac{10^4 g p_0}{RT}, \quad T_c = \frac{2}{k+1} T, \quad \Delta V = -\sqrt{\frac{2(k+1)}{k}} \sqrt{RT} \ln \mu, \quad V = V_0 + \Delta V. \quad (6.3)$$

where $k = 1.4$, $R = 287$ for air and $k = 1.2$, $R = 325$ for rocket gas, V_0 is the initial speed [m/s]. Substituting $k = 1.4$, $R = 287$ for air into the above expressions, we obtain the following equations:

$$\Delta V = -31.68\sqrt{T} \ln \mu, \quad w_c = 18.13(T)^{0.5}, \quad (w_c + P/\beta) = 31.68(T)^{0.5}, \quad (6.4)$$

$$\rho_c = 0.634\rho_0, \quad p_c = 0.565p_0, \quad T_c = 0.833T.$$

If we substitute $k = 1.2$, $R = 325$ for rocket gas:

$$\Delta V = -34.5\sqrt{T} \ln \mu. \quad (6.5)$$

The conditional temperature T in the combustion chamber without molecular dissociation and with a constant coefficient of heat capacity at constant pressure C_p , may be calculated by the equation (for kerosene):

$$\Delta T = \frac{Q}{C_p} = \frac{2.95 \times 10^3 \left(\frac{n}{21} \right)}{1.115 \left[1 + 0.067 \left(\frac{n}{21} \right) \right]}, \quad T = 288^\circ + \Delta T, \quad (6.6)$$

where n is the percentage of oxygen in the air ($n = 21\text{--}100\%$); $Q = 0.067\varepsilon = 2.95 \times 10^3$ is the amount of heat [J] when 0.067 kg kerosene is fully combusted in 1 kg of air containing 21% oxygen; $\varepsilon = 44 \times 10^6$ [J/kg] is the heat capacity of kerosene; and $1.115 = C_p$ is the heat capacity of gas at a constant pressure.

The computation gives $n = 21\%$ (conventional atmosphere air); $T = 2768\text{ K}$; $n = 40\%$, $T = 4750\text{ K}$; $n = 60\%$, $T = 6600\text{ K}$; $n = 100\%$, $T \approx 9850\text{ K}$.

In this linear model the top temperatures are higher than the temperatures of molecular dissociation; however, the high pressure retards this dissociation. For example, the dissociation of water vapor at atmospheric pressure starts at temperature of 2500 K and finishes at 4500 K . If the pressure is 100 atm , the water vapor dissociation begins at 3500 K and finishes at 6500 K . We use the pressure from 300 to 1200 atm (and more) where dissociation is not so much. We can also use this because in the rocket nozzle,

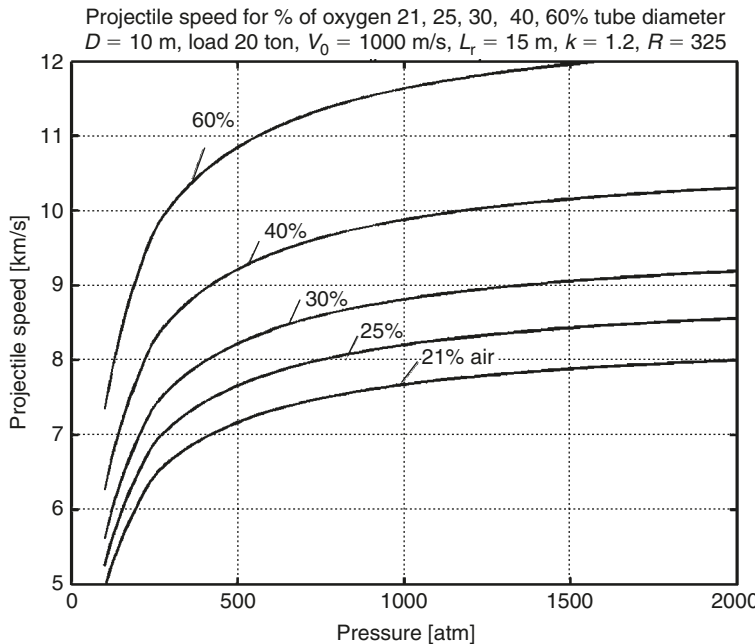


Fig. 6.2. Projectile speed for a load of 20 ton, tube diameter 10 m, rocket air column 15 m and percentage oxygen in air 21–60%.

when the gas expands and the temperature decreases, the molecules recombine and the energy of the dissociation returns (comes back) to the gas. We have the same situation in conventional internal combustion engines, rocket engines, and guns.

The initial velocity of the tube rocket is taken as 1 km/s. It requires approximately one-third additional length of the compressed air rocket column $L_r = 30 \text{ m}$.

Figure 6.2 shows an estimate of the hypersonic velocity V via a given initial (under piston) pressure p_0 and ratio n of oxygen in the air (equation (6.5)), with a cargo (piston plus payload) weight of $M_k = 20 \text{ ton}$ (44,000 lb), a tube diameter of 10 m (15 ft) ($S = 78.5 \text{ m}^2$) and rocket air column length $L_r = 15 \text{ m}$. As one can see, the speed of the projectile reaches 7.2 km/s when $P = 500 \text{ atm}$ for conventional air (oxygen 21%) and reaches 8.2 km/s for 30% gaseous oxygen. For $P = 800 \text{ atm}$ the speed is $V = 7.5$ and 8.8 km/s, respectively. In a conventional tank gun the pressure reaches up to 4500 atm and the temperature up to 4500°C.

The high speed of the projectile is not a surprise because we can get a very high mass ratio $M_0/M_k = 1/\mu$ in this launcher. For example, this ratio reaches 30 for $P = 500 \text{ atm}$, while it only equals maximum 8–10 for a one-stage conventional rocket. The specific impulse is 181 s for air and 280 s for 60% oxygen. Increasing the diameter and the rocket air column increase the charge and projectile speed. Decreasing the air column from 15 to 10 m decreases the projectile speed from 7.2 to 6.5 km/s (Fig. 6.3).

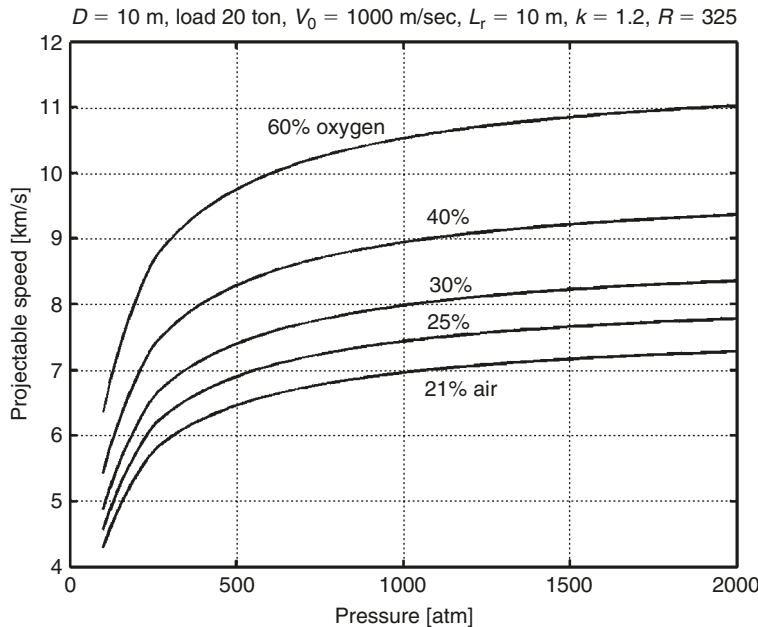


Fig. 6.3. Projectile speed for a load of 20 ton, tube diameter 10 m, rocket air column 10 m and percentage oxygen in air 21–60%.

The rocket nozzle reduces the required fuel (increases efficiency), but this nozzle requires more tube length. Unfortunately, the brevity of this chapter does not allow the presentation of the many computations (see the note at the end of this chapter).

6.3.2 Estimation of tube length

Calculating acceleration requires two assessments: acceleration of the load together with the rocket air column from 0 to speed $V_0 = 1 \text{ km/s}$ (the tube is used as a gun) and the rocket acceleration of the load from V_0 to exit V by the rocket air column 7.

- (a) Length for the initial acceleration from 0 through $V_0 = 1 \text{ km/s}$ (tube is used as a gun) (unmarked equations show the process of arriving at the estimation):

$$\begin{aligned}
 L_1 &= V_0^2 / 2a, \quad t_1 = V_0 / a, \quad a = F / M_0, \quad F = 10^4 g p_0 S, \quad M_0 = M_k + M_f + M_a, \\
 M_a &= 1.225 S p_0 L_r / q, \quad M_f = 0.067 \frac{n}{21} M_a, \\
 q &= \begin{cases} 1 & \text{if } p < 250 \text{ atm} \\ 1 + 0.001332(p - 250) & \text{if } p > 250 \end{cases}, \quad t_1 = \frac{V_0 M_0}{10^4 g p_0 S}, \quad L_1 = \frac{V_0 t_1}{2}, \quad (6.7)
 \end{aligned}$$

where p_0 is the pressure of gas in the tube [kg/cm^2]; L_r is the length of the rocket air column [m]; a is the acceleration [m/s^2]; F is the moving force [N]; M_a is the mass of the air column [kg]; $1.225 \text{ [kg/m}^3\text{]}$ is the air density in a pressure of 1 atm; M_f is the mass of fuel [kg]; M_k is mass of the load (piston + payload) [kg], M_0 is the full mass

of the rocket [kg]; q is the correction of air compressibility for $P_0 > 250$ atm (for $P_0 < 250$ atm $q = 1$); and t_1 is the acceleration time [s] for distance L_1 [m] when the installation works as a gun.

- (b) The length of acceleration as a rocket after substituting equation (6.3) in (6.4) and with the numerical data (k, R for air) is:

$$\begin{aligned} L_2 &= \int_0^{t_2} V dt, \quad L_2 = \int_0^{t_2} \left[V_0 - \left(w + \frac{P}{\beta} \right) \ln \left(1 - \frac{\beta t}{M_0} \right) \right] dt \\ &= V_0 t_2 + \left(w + \frac{P}{\beta} \right) \left(\frac{M_0}{\beta} \right) [\mu(\ln \mu - 1) + 1], \end{aligned} \quad (6.8)$$

where

$$\begin{aligned} t_2 &= (M_a + M_f)/\beta; \quad \beta = \rho_c w S; \quad \mu = M_k/M_0; \\ w + \frac{P}{\beta} &= \sqrt{\frac{2(k+1)RT}{k}}, \\ \rho_c &= \frac{10^4 g p_0}{RT} \left(\frac{2}{k+1} \right)^{\frac{1}{k-1}}. \end{aligned}$$

Here t_2 is the time of acceleration for the distance L_2 ; ρ_c is the gas density in the nozzle; $M_0 = M_k + M_a + M_f$ is the initial mass of rocket; M_k is the mass of shot [load (projectile or payload) + piston]; $M_k = 20,000$ kg; M_a is the mass of air in the rocket; M_f is the mass of fuel in the rocket (see equation (6.7)).

- (c) The full length of the launch tube and the acceleration times are:

$$L = L_1 + L_2 + L_3, \quad t = t_1 + t_2, \quad (6.9)$$

where $L_3 = 1.3L_r$ is the length of air column plus air column for initial acceleration (30% from L_r).

Figure 6.4 represents the barrel length required for the speeds in Fig. 6.2. At a pressure of 500 atm, the tube length equals $L = 650$ m for conventional atmosphere air ($V = 7.2$ km/s) and $L = 1400$ m for 39% additional oxygen (total oxygen is 60%) ($V = 10.9$ km/s). This is no surprise, because we use the same pressure in the shot for air and oxygen. If the tube length is less than the required length for a given air pressure, the use of oxygen (for a given program and the same pressure) does not give an increase in speed but only increases the load (two or more times). The oxygen allows the combustion time to increase (length of tube) and the exit projectile speed to increase. For a pressure of $P_0 = 1000$ atm using 40% gaseous oxygen we can reach a shot velocity of about 10 km/s for a tube length of 700 m (Fig. 6.4). This length is acceptable if we place the tube in water. We can considerably decrease the tube length if we decrease the rocket air column, but the projectile speed is then also decreased. For example, if at 500 atm we decrease the air column from 15 to 10 m, the tube length decreases from 650 to 430 m (Fig. 6.5), and speed from 7.2 to 6.45 km/s (Fig. 6.3).

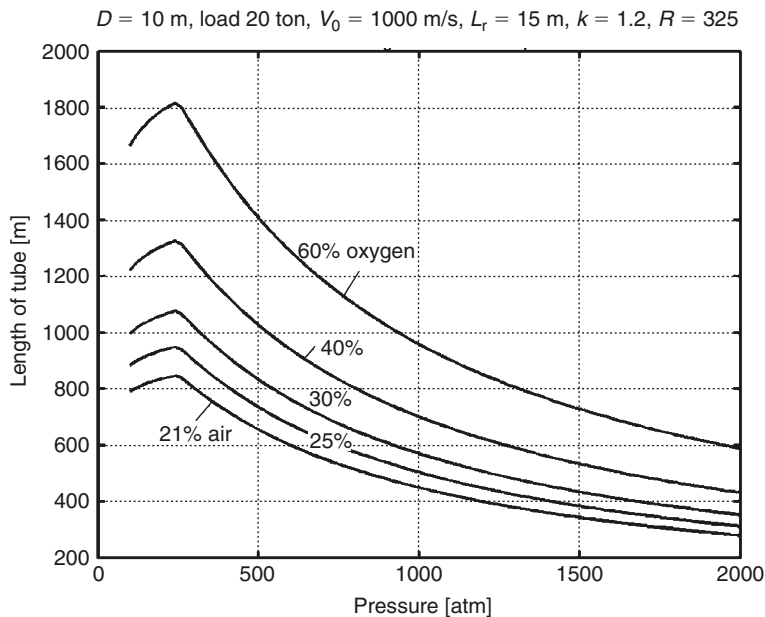


Fig. 6.4. Required tube length for a load of 20 ton, tube diameter 10 m, rocket air column 15 m and percentage oxygen in air 21–60%.

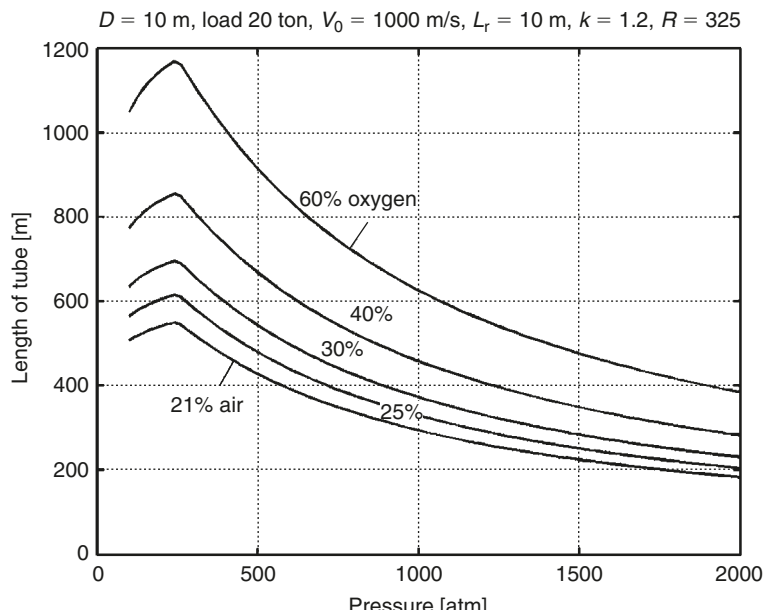


Fig. 6.5. Required tube length for a load of 20 ton, tube diameter 10 m, rocket air column 10 m and percentage oxygen in air 21–60%.

6.3.3 Loss of velocity in the atmosphere

The loss of velocity of the projectile in air is small if the projectile is properly shaped and its trajectory is more than 15° to the horizon. For an exponential density of the atmosphere, at a constant speed of sound ($a = 300 \text{ m/s}$), we arrive at the following equation as an estimation of the decrement of speed (unmarked equations show the process of computation):

$$\begin{aligned} M_p V_p^2 / 2 &= A, \quad A = \int_0^H \frac{D}{\sin \theta} dh, \quad \rho = \rho_0 \int_0^\infty e^{bh} dh = \frac{\rho_0}{b}, \quad D = 2\alpha^2 \rho_0 a V_p S_p / b, \\ A/M_p &= 2\alpha^2 \rho_0 a V_p S_p / M_p \sin \theta, \quad \Delta V_a = V_p - \sqrt{V_p^2 - \frac{2A}{M_p}}, \end{aligned} \quad (6.10)$$

where V_p is the initial projectile speed after shot [m/s]; S_p is the specific projectile area (m^2); α is the relative thickness (0.1); θ is the angle of trajectory to the horizon; ρ is the $\rho(h)$ density of atmosphere (h – altitude); $\rho_0 = 1.225 \text{ kg/m}^3$ is the atmosphere density at sea level; M_p is the mass of projectile [kg]; A is the work of passing [J]; D is the wave drag of projectile (90% of total drag). The drag of the projectile depends linearly on speed for large Mach numbers.

It is shown that the loss of energy in an exponential Earth atmosphere equals the loss of energy in an atmosphere with constant density $\rho_0 = 1.225 \text{ kg/m}^3$ and altitude $h = 8900 \text{ m}$.

The results of the computation for different M_p/S_p [ton/m²] are shown in Fig. 6.6. The loss does not depend on speed because the more the speed the less the time of braking. It is about 30–100 m/s.

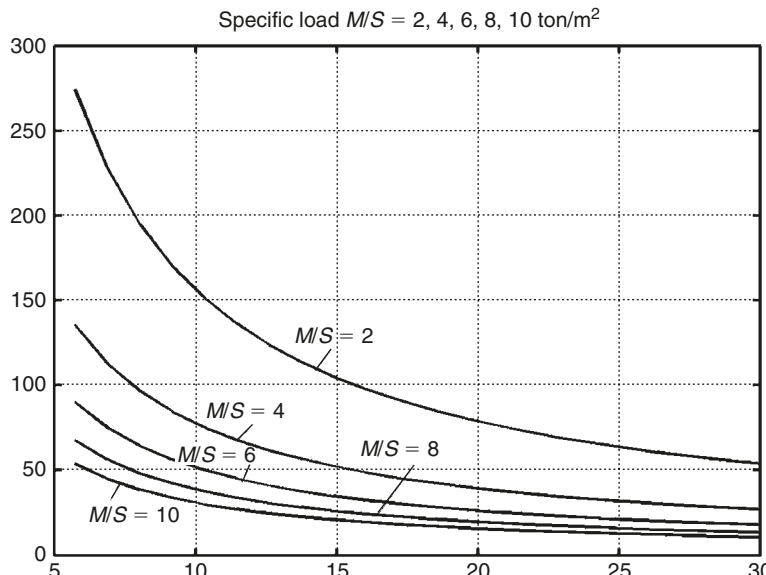


Fig. 6.6. Loss of velocity ΔV_a (m/s) of a projectile via angle θ [°] in the atmosphere versus shot angle for specific load 2, 4, 6, 8 ton/m².

Some people think that passing through the atmosphere makes a projectile heat up consideration. They know that the space “Shuttle” needs a lot of heat protection for re-entry into the Earth’s atmosphere. However, the Shuttle has to decrease its speed from $V_1 = 8$ to $V_2 = 0.3$ km/s. For a mass $m = 20$ ton that equals energy $E = m(V_1^2 - V_2^2)/2 = 6.4 \times 10^{11}$ J. All this energy is converted into a heat. In our case the speed decreases from $V_1 = 8$ to $V_2 = 7.9$ km/s, which for a mass $m = 20$ ton equals energy $E = m(V_1^2 - V_2^2)/2 = 0.16 \times 10^{11}$ J. Hence this is 40 times less.

The same problem exists in electromagnetic launcher. Research mentioned in Ref.¹⁷, p.395 show that a sharp nose 5-ton projectile needs only 0.9 kg of lithium refrigerant for protection projectile head when crossing the atmosphere at an angle of 15°.

6.3.4 Load delivered to orbit

The load delivered to orbit can be computed by the following equations:

$$\begin{aligned} \vartheta &= \frac{V^2}{V_c^2}, \quad V_c = \frac{19.976 \times 10^6}{\sqrt{R_0}}, \quad p = \vartheta r \cos^2 \theta, \quad e = \sqrt{1 - \vartheta(2 - \vartheta) \cos^2 \theta}, \\ r_a &= \frac{p}{1 - e}, \quad r_a = R_0 + H, \quad V_a = \frac{Vr \cos \theta}{r_a}, \quad V_d = V_{c,H} - V_a, \\ \frac{M_k}{M_0} &= \exp\left(-\frac{V_d}{w}\right), \quad R_0 = 6378 \text{ km}, \end{aligned} \quad (6.11)$$

where ϑ is the ratio of speed V to circular speed V_c at a given point [m/s]; R_0 is the Earth radius [m]; p is the parameter of elliptical orbit; e is the eccentricity of elliptical orbit; r_a is the radius apogee [m]; H is the altitude [m]; V_a is the speed at apogee [m/s]; θ is the trajectory angle to horizon; V_d is the required additional speed at apogee [m/s]; $V_{c,H}$ is the required circular speed [m/s]; M_k/M_0 is the ratio of final (useful) mass to initial mass; w is the speed of rocket exhaust gas [m/s].

Results of computation for a rocket engine with impulse $w = 2000$ m/s are presented in Figs. 6.7 and 6.8.

6.3.4.1 Example of use

If we have a tube diameter of 10 m², a load of 20 ton and tube pressure of 500 atm, from Fig. 6.2 and air we find that for air the shot speed is 7.2 km/s, and from Fig. 6.4 the required tube length is 650 m. From Fig. 6.6 the loss of velocity in the atmosphere for a shot angle of 18° and $M/A = 4$ ton/m² is 45 m/s. From Fig. 6.7 we find the apogee of orbit altitude is $H = 1000$ km for the shot angle of 18° and speed 7155 m/s.

Assume that in 20 ton of load a piston weight equals 5 ton and 15 ton is the orbit load. From Fig. 6.8 for $V = 7.155$ km/s and the shot angle of 18° we find that the useful part of the orbit load is 47% or about 7 ton. The 8th ton is rocket fuel for increasing the apogee speed to circular speed at a given altitude.

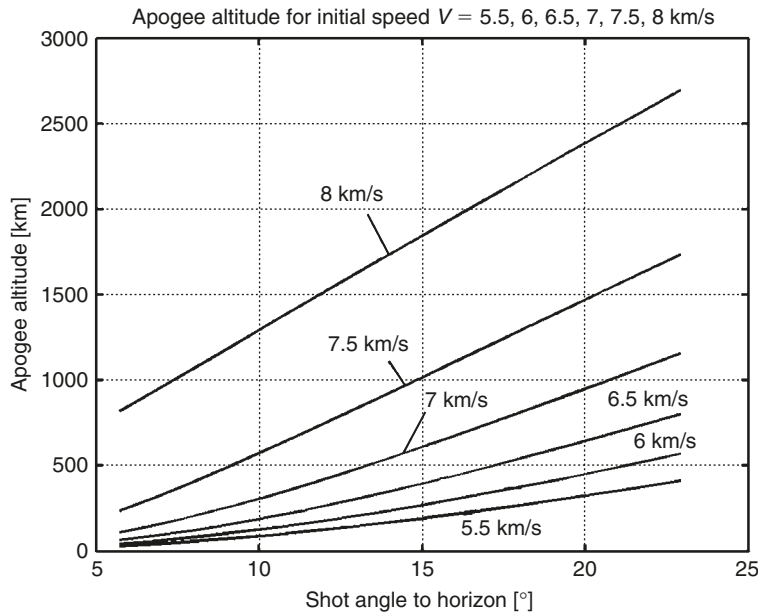


Fig. 6.7. Apogee altitude versus shot angle for initial projectile speed.

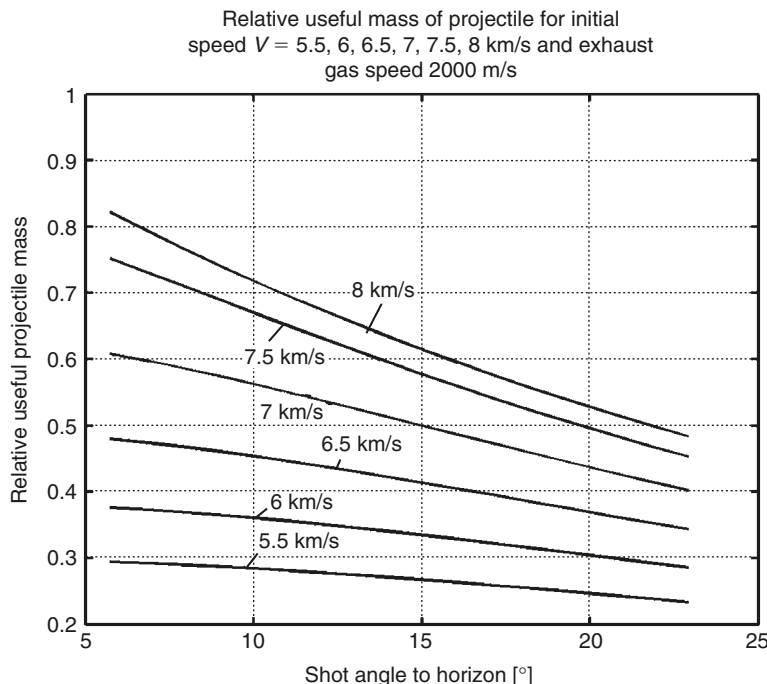


Fig. 6.8. Relative useful mass of projectile for initial speed $5.5\text{--}8 \text{ km/s}$ and specific impulse 2000 m/s .

6.4 Production cost of delivery

The production cost of delivery is the most important feature of the suggested launcher. In "Hypersonic Launcher"¹² Fig. 18 shows computations of delivery cost versus annual payload in thousand ton and an initial cost of the installation. The following data were used: lifetime of the installation 20 years, cost of fuel (kerosene) \$0.25/l, requested time for preparing of a shot 0.5 h, 10 people working with average salary of \$20/h, payload of one launch 5 ton (11,000 lb) (25% from 20 ton of piston-projectile system). The load (20 ton) is: payload – 5 ton, a solid engine for generating additional speed of 3 km/s at apogee – 10 ton; piston – 5 ton. Maximum capability is 86,400 ton/year. The resulting computations are presented in Fig. 6.9.

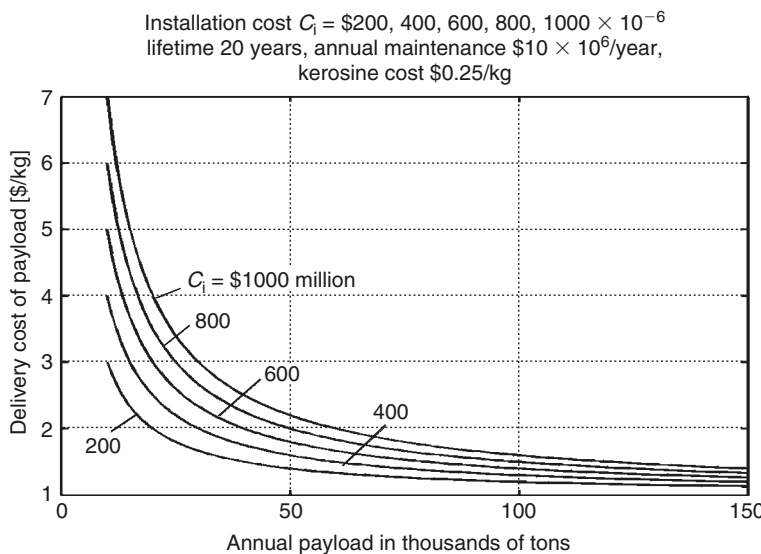


Fig. 6.9. Delivery cost of payload versus annual payload for installation cost \$200–1000 million, lifetime 20 years, annual maintenance \$10 million/year, kerosene cost \$0.25/kg.

As one can see, the production delivery cost may be about \$1–2/kg if the payload is approximately 50–80,000 ton/year. About 70% of this cost is fuel (kerosene or gasoline).

6.4.1 Excess of energy

The hypersonic launcher uses a very high compression ratio, which means that its efficiency coefficient is very high at about 85–95%. Such efficiency is higher than other head engines. Part of this energy is used in load acceleration, and part is lost in non-useful gas expansion. However, the hypersonic launcher has a huge excess of shot energy over gas compression energy. If the launcher has a top valve, this energy can be used for the production of compressed air, electricity, oxygen, etc.

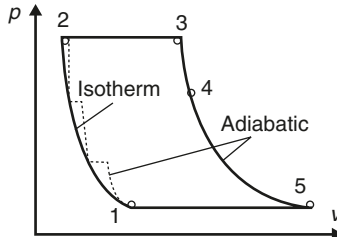


Fig. 6.10. Thermodynamic diagram of launcher. Notations: (1) point of atmospheric pressure; (2) point of common air columns volume and tube pressure; (3) point after fuel combustion; (4) point of tube volume; and (5) point after gas exhaust.

Let us estimate this energy. After the shot is fired the valve closes the tube. The pressure in the tube and the possible work of 1 kg of gas can be computed as follows (Fig. 6.10):

$$\begin{aligned}
 T_3 &= T_2 + \Delta T, \quad L_3 = 1.3L_f \frac{T_3}{T_1}, \quad T_4 = T_3 \left(\frac{L_3}{L} \right)^{k-1}, \quad P_4 = P_3 \left(\frac{L_3}{L} \right)^k, \\
 T_5 &= \frac{T_3}{P_3^{\frac{k-1}{k}}}, \quad T_2 = T_1, \quad W_{4-5} = \frac{RT_5}{k-1} \left[1 - \left(\frac{P_4}{P_5} \right)^{\frac{k-1}{k}} \right], \quad W_{T,1-2} RT_1 \ln \frac{P_2}{P_1}, \\
 W_{A,1-2} &= NRT_1 \frac{k}{k-1} \left(1 - \varepsilon^{\frac{k-1}{k}} \right), \quad \varepsilon = \sqrt[k]{P_2}. \tag{6.12}
 \end{aligned}$$

where T is temperature at marked points [K], $T_1 = 288\text{ K}$; ΔT is increase in temperature from fuel: it equals 2480°C for air, 4660°C for adding 20% oxygen, 6614°C for adding 40% oxygen; P is pressure at marked (sup index) points [atm]; W is work at marked lengths [J]; W_T is isothermal work; W_A is adiabatic work; $R = 287$ is the thermodynamic coefficient; $k = 1.4$ is the thermodynamic coefficient; L is tube length [m]; L_3 is tube length where the pressure can be constant [m]; and N is the number of cooling radiators in the compression process.

The results of computation are presented in Fig. 6.11. A 1 kg of gas for $N = 4$, $p = 500\text{ atm}$ has an excess of energy of about 2535 kJ . Our launcher for $p = 500\text{ atm}$ has about $M = \rho V/q = 1.225 \times 500 \times 78.5 \times 20/1.72 = 559\text{ ton}$ of compressed air, which means after the shot and compressing the air for next shot we have $E_a = 2535 \times 559 = 1,417,065\text{ MJ} = 1.4 \times 10^{12}\text{ J}$ of excess energy.

The required fuel for a shot is $M_f = 0.067 \times 559 = 37.45\text{ ton}$. This has an energy $E = M_f \varepsilon = 37.45 \times 10^3 \times 44.10^6 = 1.65 \times 10^{12}\text{ J}$. The energy of the projectile is $E_p = mV^2/2 = 20,000 \times 7200^2/2 = 0.144 \times 10^{12}\text{ J}$. The excess energy (which can be used) is $E_a = 1.4 \times 10^{12}\text{ J}$. The total efficiency (without loss of compressed gas to the atmosphere) is $(E_p + E_a)/E = (1.4 + 0.144)/1.65 = 0.93$. This is more than any current heat machine because we use a very high compression ratio of $p = 500\text{ atm}$. The exhaust gas has a temperature $T = 980\text{ K}$ ($p = 500\text{ atm}$). Utilization of this high level of heat can give additional energy.

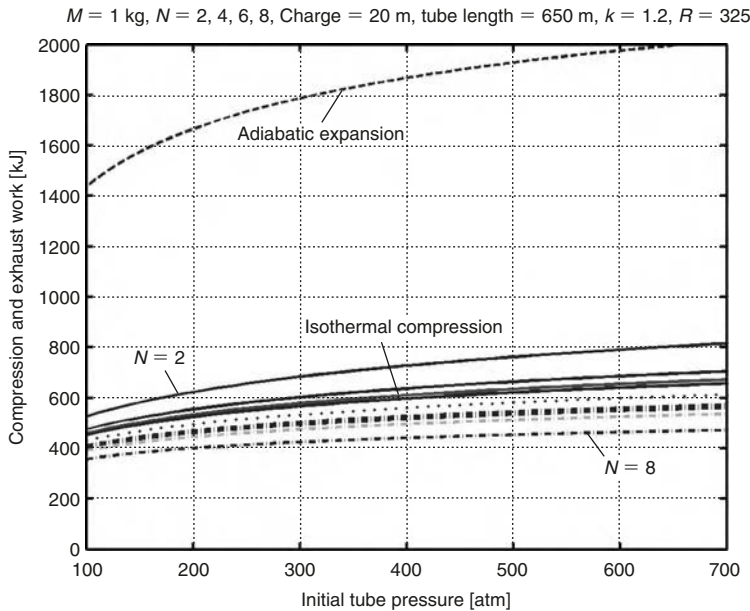


Fig. 6.11. Adiabatic expansion (after shot) and compression work of 1-kg gas for cooling radiators $N = 2\text{--}8$, charge length 20 m, and tube length 650 m.

6.4.2 Launcher as an accumulator of energy

There is a big problem in the electric energy industry. Power stations have high efficiency when they work in a constant regime. This means that they produce excess energy at night and lack energy during the day. To balance their energy the electricity industry builds special hydro-accumulator stations. These stations pump water into a compensation (balancing) reservoir when they generate excess energy and produce additional energy when it is insufficient.

We have a gigantic reservoir for highly compressed air. When the launcher does not have work to do, it can be used as an accumulator of energy. The launcher draws energy from electricity stations, and pumps compressed air into the tube. When there is lack of energy, the launcher produces energy from the compressed air and send it to customers. If it uses seawater for cooling the air during compression and heating the air during expansion, the efficiency of this method may be high (80–90%), especially if we use cool deep-sea ($T_1 = 7^\circ\text{C}$) water for cooling and warm ($T_2 = 20\text{--}25^\circ\text{C}$) surface water for heating. The equation for heating is:

$$\begin{aligned}
 W_1 &= RT_1 N \frac{k}{k-1} \left(1 - \varepsilon^{\frac{k-1}{k}} \right), & \varepsilon &= \sqrt[k]{p_2} \\
 W_2 &= RT_2 N \frac{k}{k-1} \left(1 - \frac{1}{\varepsilon^{\frac{k-1}{k}}} \right), & \eta &= 1 - \frac{W_1 - W_2}{R \frac{T_1 + T_2}{2} \ln \frac{p_2}{p_1}}, \quad (6.13)
 \end{aligned}$$

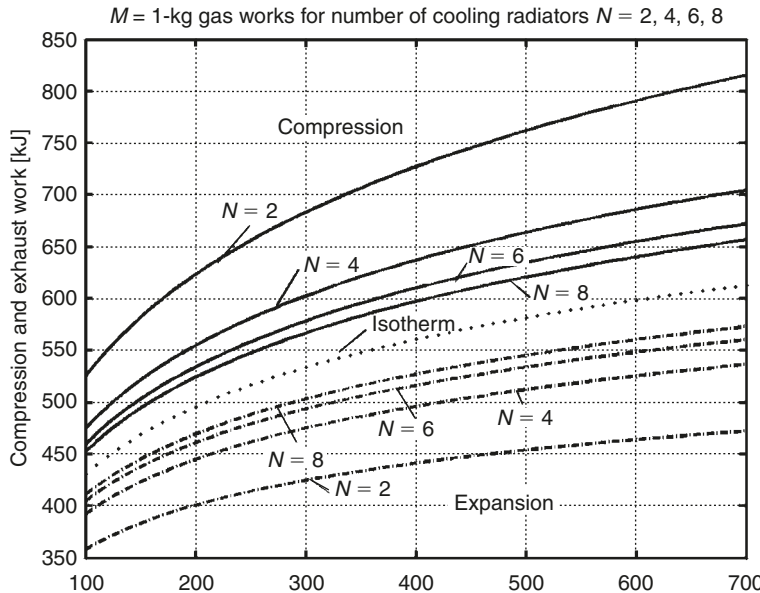


Fig. 6.12. Compression and expansion work versus gas pressure (atm) of 1-kg gas for cooling radiators $N = 2\text{--}8$.

where W_1 is the work in compression; W_2 is the work expansion; p_2 is the tube pressure; η is the efficiency coefficient; and N is the number of cooling radiators.

Results of computation are presented in Fig. 6.12. At 500 atm 1 kg air gives 580 kJ when it is isotherm expending. In the tube $V = SL = 78.5 \times 650 = 51,025 \text{ m}^3$ under pressure $p = 500 \text{ atm}$ we have $M = \rho pV = 1.225 \times 500 \times 5.1 \times 10^4/q = 0.6 \times 10^6 \text{ kg}$ compressed air. This contains $E = 580 \times 30.6 \times 10^6 = 17.748 \times 10^9 \text{ kJ}$ of energy. The installation can work as a 100-MW electric power station in during $17.748 \times 10^9 / 3600 / 10^5 = 49.3 \text{ h}$ and $\eta = 0.88$ if $N = 8$, $T_1 = T_2$.

6.4.3 Gun recoil

The recoil of the launcher can be computed by the theoretical mechanics equation:

$$m_1 V_1 = m_2 V_2, \quad (6.14)$$

where m_1 , m_2 are mass and V_1 , V_2 are speed of the projectile and installation, respectively.

For example, if the projectile mass equals 20 ton and its speed is 8 km/s; the water inside the installation frame $15 \times 15 \times 650 \text{ m}^3$ is $14.6 \times 10^4 \text{ ton}$, the installation speed after the shot will be $V_2 = 20 \times 8000 / 14.6 \times 10^4 = 1.1 \text{ m/s}$.

6.4.4 Tube curvature

Tube straightness is checked using a laser beam and the tube supported by engines located along it. The maximum force from the tube curvature can be calculated using the equation:

$$n = \frac{V^2}{gR}, \quad R = \frac{L^2}{8h}, \quad n = \frac{8hV^2}{gL^2}, \quad (6.15)$$

where n is centrifugal overload [g]; V is projectile speed [m/s]; $g = 9.81 \text{ m/s}^2$ is Earth's gravity; R is the radius of curvature [m]; L is length of the tube [m]; h is deviation of the tube from a straight line [m].

For example, if the middle of the tube has a deviation of 0.1 m, its length is 1000 m and the projectile speed in the middle of the tube is $V = 5000 \text{ m/s}$, the centrifugal overload will be $n = 2 \text{ g}$. This is a very small force in comparison with acceleration along tube which equals about 1000 g.

6.4.5 Wall thickness

The tube wall thickness can be estimated in the following way. Take the tube length $L = 1 \text{ cm}$. The tensile force equals $F = PDL$, where P is pressure, atm [kg/cm^2]; D is a tube internal diameter [cm]; and F is tensile force [kg]. The cross-section area [cm^2] of the tube walls is $s = F/\sigma$, where σ is safe tensile stress [kg/cm^2]. The wall thickness is $s/2$.

For example, if the pressure is $P = 500 \text{ atm}$, the tube diameter is $D = 10 \text{ m} = 1000 \text{ cm}$, $L = 1 \text{ cm}$, then the force is $F = PDL = 500 \text{ ton}$. If the tube is made from a composite material with maximum $\sigma = 500 \text{ kg/mm}^2$, margin of safety 5, and safe tensile stress $\sigma = 100 \text{ kg/mm}^2$, then the wall thickness will be 25 cm.

If the tube is made from steel with maximum $\sigma = 250 \text{ kg/mm}^2$, margin of safety 5, and admissible (safe) tensile stress $\sigma = 50 \text{ kg/mm}^2$, then the wall thickness will be 50 cm for a tube diameter of 10 m.

6.4.6 Gas friction

Let us estimate gas friction around the wall. We use the method described in Ref. [5].

Below, the equation from Anderson for computation of local air friction for a plate is given:

$$\begin{aligned} \frac{T^*}{T} &= 1 + 0.032M^2 + 0.58\left(\frac{T_w}{T} - 1\right), \quad M = \frac{V}{a}, \quad \mu^* = 1.458 \times 10^6 \frac{T^{*1.5}}{T^* + 110.4}, \\ \rho^* &= \frac{\rho T}{T^*}, \quad Re^* = \frac{\rho^* V x}{T^*}, \quad C_{f,l} = \frac{0.664}{(Re^*)^{0.5}}, \quad C_{f,t} = \frac{0.0592}{(Re^*)^{0.2}}, \\ D_L &= 0.5C_{f,l}\rho^*V^2S, \quad D_T = 0.5C_{f,t}\rho^*V^2S, \quad x \approx L_r/3, \end{aligned} \quad (6.16)$$

where T^* , Re^* , ρ^* , μ^* are reference (evaluated) temperature, Reynolds number, air density, and air viscosity respectively. M is Mach number; V is speed; x is the length of plate (distance from the beginning of the cable); T is flow temperature; T_w is body temperature; $C_{f,l}$ is a local skin friction coefficient for laminar flow; $C_{f,t}$ is a local skin friction coefficient for turbulent flow; S is the area of skin [m^2] of both plate sides, which means for the cable we must take $0.5S$; and D is air drag (friction) [N]. Our gas column is moved with acceleration which means (from aerodynamics) and that we have the laminar layer.

The results of computation of laminar friction are presented in Fig. 6.13. The average friction is about $0.4 \text{ ton}/\text{m}^2$. The friction area decreases with increasing speed. If the average area is $S = \pi D L_r / 2 = 3.14 \times 10 \times 15 / 2 = 235.5 \text{ m}^2$, the average wall drag is 94 ton . This is a small value in comparison with the drive force of $20 \times 10^4 \times 0.5 = 10^5 \text{ ton}$.

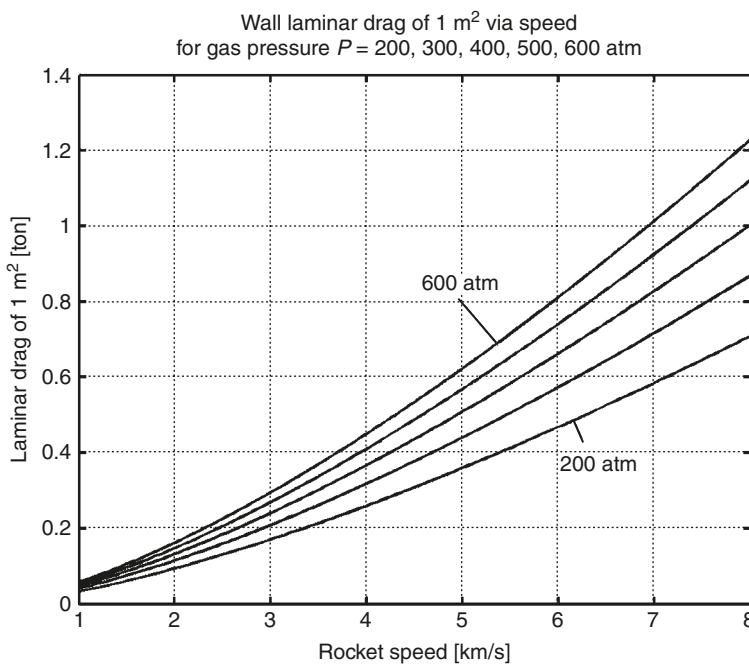


Fig. 6.13. Wall laminar drag of 1 m^2 versus speed for gas pressure 200–600 atm.

6.5 Advantages of the proposed space launcher

One advantage of this launch system over existing fixed “gun” systems is that of placing the launch system in water. The installation becomes mobile and can be aimed (by adjusting the azimuth) at any point in space or on Earth. The launch tube may be integrated into a watertight enclosed frame (Fig. 6.1(c)). Water can then be forced into and out of the frame to control the position of the launch tube like a submarine. Electric motors may be attached to the frame for maneuverability and to maintain the frame in a desired location. The launch tube is fixed inside the frame by control cables. The azimuth of the launch tube, hence the “aim,” is obtained by sinking one end of the

launch tube/frame. The launch tube is brought into a horizontal position to transport the system to another location or to conduct maintenance on the system.

Additional advantages, each of which is an important innovation, that this launch system has over a conventional fixed “gun” system are listed as follows:

1. In a conventional “gun” system, powdered fuel is ignited all at once to move the projectile. The velocity of the projectile cannot exceed the velocity of the combustion gases, which is usually the speed of sound (at most 1–2 km/s). In the proposed launch system, the mass of gas in the launch tube is pushed along with the payload/piston, which later works as a rocket engine. This “rocket engine” is different from conventional rocket engines since the proposed “engine”:
 - does not have to move heavy tanks of compressed oxidizers;
 - is not limited by the speed of sound;
 - is allowed to reach a very high ratio of fuel mass (compressed air + fuel) to payload mass (up to 30 and more);
 - allows the payload to reach hypersonic speeds (up to 7–10 km/s).
2. The vacuum (<0.01 atm) above the payload/piston eliminates a significant amount of air resistance, which could prevent the payload from reaching high velocities when the launch tube is very long.
3. The launch tube can be long (0.4–2 km), which is not conducive in ordinary “gun” systems. In addition, by placing the launch system in water, the payload can be aimed at any point in space or on the Earth. A fixed conventional “gun” system cannot be moved or aimed. The use of water also allows the launch system to be hidden below the surface and in the event of an accident, the high pressures under the water can help contain the explosive materials and avoid injuring people.
4. Conventional fuels and oxidizers (such as air or gaseous oxygen) can be used with the proposed launch system. In regular rockets, for example, gaseous oxygen cannot be used since the fuel tank weights would be too high and liquid oxygen requires special equipment for storage and transportation.

The main advantage of the proposed launch system is a very low cost for payload delivery into space and over long distances. Expensive fuels, complex control system, expensive rockets, computers, and complex devices are not required. The cost of payload delivery to space would drop by a factor of a thousand. In addition, large payloads could be launched into space (in the order of thousands of ton a year) using a single launch system. This launch system is simple and does not require high-technology equipment. The launch system could easily be developed by any non-industrialized country and the cost of this launch system is 10 times lower than that of contemporary rocket systems.

Computations show that if the launch tube is designed to a diameter of 2–7 m, a length of 1–4 km, and gas pressure of 200–800 atm, then 3–20 ton of payload per launch could be delivered into Earth orbit. If the launch frequency is every 30 min, then 15–45,000 ton of payloads could be delivered to space per year at production costs of \$2–10/kg.

During peace time, this launch system can be also used for the delivery of mail or express parcels over long distances (for example, from one continent to another) and give a profit of \$5–10 million/day. The installation can also be used for energy storage. However, during war, this launch system could deliver munitions to targets thousands to tens of thousands of kilometers away. It is known that 90% of loads delivered into orbit are items that can endure high acceleration.

In this chapter I wanted to show the feasibility of the suggested method. The parameters of the launcher are not optimized. Selection of the tube diameter, rocket nozzle, and length of the rocket air column could possibly increase the projectile speed and weight, and decrease the tube length and fuel consumption. The hot gas after the shot may be used for electricity production or as an energy accumulator.

The author has more detailed research on this concept and innovations which solve problems that could appear in development and design of the suggested launcher. The author is prepared to submit his research and to discuss the problems with serious organizations wanting to research and develop this project.

6.6 Discussion

The computations in this chapter are not exact but only estimations to show that the suggested simple gas tube rocket can reach a hypersonic speed of 4–8 km/s. Hypersonic speeds depend only on the right gas tube rocket design and the right fuel injection program. The estimates are made with the conventional technical accuracy of 5–10%, except perhaps temperatures (and projectile speed) with a high level of oxygen (more than 40%) when the temperature exceeds the conventional combustion chamber temperature of 4000 K and the gas dissociation decreases the temperature. However, the velocity of 5.5–7 km/s (Fig. 6.2), which is reached before this temperature, is hypersonic. A more exact computation is complex and would need financial support. There are some factors which allow the increase in temperature in the combustion chamber and the utilization of it in the tube nozzle: (1) the heat is not spent on evaporation and heating of the liquid oxygen from 90 to 288 (we use gaseous oxygen); (2) we use very high pressure, which decreases the temperature dissociation by approximately 500 K per every 100 atm; (3) with the tube nozzle the recombination time is fast enough (0.5–1 s). In a conventional short rocket nozzle the gas flows out into the vacuum space and recombination time is not long enough (0.001 s). Also, ionization for the given temperature is small.

There are also good margins for increasing the efficiency of the gas tube rocket. Some metals (Be, Li, B, Mg, Al, Si) have a heat capability 1.5–2 times more than kerosene. However, their application is limited because in the high expansion nozzle used in a conventional rocket these metals condense from gas to liquid and decrease the efficiency of a nozzle. In our case we have a nozzle that has a small expansion (or use the rocket without a nozzle, as in this chapter). This means we can use a liquid fuel with a high concentration of the metal powder and achieve the high efficiency (projectile speed).

The author has many detailed computations for different gas tube rocket designs and programs for fuel injection. Organizations interested in these projects can contact to

the author (<http://Bolonkin.narod.ru>). Patent applications: 09/013,008 of 01/216/98; 09/344,235; 10/051,013.

References

1. Ed. L. Stiefel, *Gun Propulsion Technology*, AIAA, 1998, Washington, DC, USA.
2. *Development of High-Speed Vehicle Propulsion Systems*, AIAA, 1996.
3. *12th Symposium Propulsion System*, AIAA, 1995.
4. Space Technology and Application International Forum (STAIF), 1996–1997, Albuquerque, MN, Parts 1–3.
5. J.D. Anderson, *Hypersonic and High Temperature Gas Dynamics*, McGraw-Hill Book Co., NY, 1989.
6. B.W. Henderson, “Livermore Proposes Light Gas Gun for Launch of Small Payloads”, *Aviation Week and Space Technology*, July 23, 1990, pp. 98–99.
7. B.W. Henderson, “World’s Largest Light Gas Gun”, *Aviation Week and Space Technology*, August 10, 1992, pp. 57–59.
8. R. Wolkomir, “Shooting Right for the Stars with One Gargantuan Gas Gun”. *Smithsonian*, Vol. 6, No. 10, January, 1996, pp. 84–91.
9. V.M. Tuler, “Gun barrel launching”, *Space/Aeronautics*, February 1959, pp. 52–54.
10. A.E. Seigel, “Theory of High-Muzzle-Velocity Guns”, AIAA, 1978, p. 40.
11. G.V. Bull and C.H. Murphy, Paris Kanoneu – The Paris Guns and Project HARP, 1988.
12. A.A. Bolonkin, “Hypersonic Space Launcher”, *Actual Problem of Aviation and Aerospace*, KAI, No. 1, 2003, pp. 45–69.
13. P.G. Baer, The Traveling Charge Gun as a Hypervelocity Launching Device, Ballistic Research Laboratories, Maryland, 1960.
14. D.C. Vest, “An Experimental Traveling Charge Gun”, Ballistic Research Laboratory, Report No. 773, 1951.
15. A.A. Bolonkin, “Hypersonic Gas-Rocket Launcher of High Capacity”, *Journal of the British Interplanetary Society*, Vol. 57, No. 5/6, 2003, pp. 162–172.
16. A.A. Bolonkin, “Hypersonic Launch System of Capacity up 500 ton per day and delivery cost \$1 per lb”, IAC-02-S.P.15, 53rd International Astronautical Congress, The World Space Congress, 2002, 10–19 October 2002, Houston, TX, USA.
17. M.R. Palmer and A.E. Dabiri, “Electromagnetic Space Launch”, *IEEE Transactions on Magnetics*, No. 1, January 1989, pp. 393–399.

CHAPTER 7

Earth–Moon Cable Transport System*

Summary

This chapter proposes a new transportation system for travel between the Earth and the Moon. This transportation system uses mechanical energy transfer and requires only minimal energy, using an engine located on Earth. A cable directly connects a pole of the Earth through a drive station to the lunar surface. The equation for an optimal equal stress cable for the complex gravitational field of the Earth–Moon has been derived that allows significantly lower cable masses. The required strength could be provided by cables constructed of carbon nanotubes or carbon whiskers. Some of the constraints on such a system are discussed.

7.1 Introduction

The author offers a revolutionary new transportation system for delivering payloads and people from the Earth to the Moon.^{1–4} This method uses mechanical energy transfer, with an engine located on the Earth and energy recovery by simultaneously moving one cabin upward and another cabin downward. The author has not found an analog for this space mechanical energy transfer (transmission to space) or similar facilities for transporting a payload into space in the technical literature or patents. The offered system may also be used as a space elevator between Earth and a geosynchronous station, as a satellite launcher, for traveling to Mars, and for launching or modifying the speed or direction of a space vehicle.

7.2 Brief history

There are many articles that develop tether methods for trajectory change of space vehicles⁵ and concepts exist for a space elevator.³ In the tether method two artificial bodies are

*This chapter is based on the paper B0.3-F3.3-0032-02 that was presented to *34th COSPAR Scientific Assembly, The World Space Congress 2002*, 10–19 October 2002, Houston, TX, USA. This is only part of the original manuscript (one version of the system) presented to the WSC. This part of WSC manuscript was published in as “Non-rocket Earth–Moon Transport System”, *Advanced Space Research*, Vol. 31, No. 11, 2003, pp. 2485–2490.

connected by cable and the system is rotated in space around their common gravitational system center. For example, a two-tether system for Moon travel is described in the current literature⁶ (p. 69) and works as follows. The first tether is located near the Earth, and the second is located near the Moon. High-speed aircraft (which do not exist at the present time) deliver loads to an altitude of 80–100 km. Here the first tether system connects to the load, increases its speed (how?), and sends it in the Moon's direction. After its flight through space, the second (Moon) tether system must catch this load, decrease its speed, and drop it onto Moon's surface. The main problem with this method is that it requires energy for increasing the rotation of the tether system (motorized tether). The problems are how to rotate it with a flexible cable and what to do with momentum after launch if the tether system is to be used again. If this system is used only one time, it is worse than conventional rockets as it loses the second body and requires a large space source of energy.

In the space elevator concept, a cable is connected between a geosynchronous space station and the Earth's equator.³ This cable is used to deliver a payload to the station. The main problems are the very large cable weight and delivery of the energy to move the load container (climber).

The proposed system differs from a conventional tether system, as it connects two natural bodies, the Earth and the Moon. It may be compared with an aerial ropeway in the mountains. It is different also from a space elevator, in that it is connected to the Earth's pole, whereas a space elevator must be connected to the Earth's equator.

The proposed system differs from previous concepts in that it has a relatively simple mechanical system for transferring energy from a mechanical engine located on Earth to a load cabin located in space through a series of cable links. Also now it is the idea of separating the transport cable into sub-sections, which dramatically decreases the total system weight.

7.3 Brief description, theory, and computation of innovations

The objectives of the proposed system are to provide an inexpensive means of travel between the Earth and the Moon, to simplify space transportation technology, and to eliminate complex hardware. The proposed Earth–Moon cable transport system is shown in Fig. 7.1. The system consists of three cables: a main (central) cable, which supports the weight of the entire system, and two closed-loop transport cables, which include a set (5–10) of cable chain links connected sequentially to one another by rollers^{3,4} (see Fig. 1.3a). The system is connected at the Earth's pole and to any position on the Moon's surface that continually faces the Earth. An engine located on a planet (e.g. the Earth, but it could also be the Moon) drives the cable transport system. On the Earth, the cable is supported in the atmosphere by a winged device, which also counteracts the rotation of the Earth. The transfer cable system transfers energy between load cabins moved up and down, which requires the engine moving the cable system to overcome only frictional forces.

An optimal (minimum mass, equal stress) variable diameter cable is defined for the main tether. The main cable has a relatively large but variable cross-section area (diameter), as

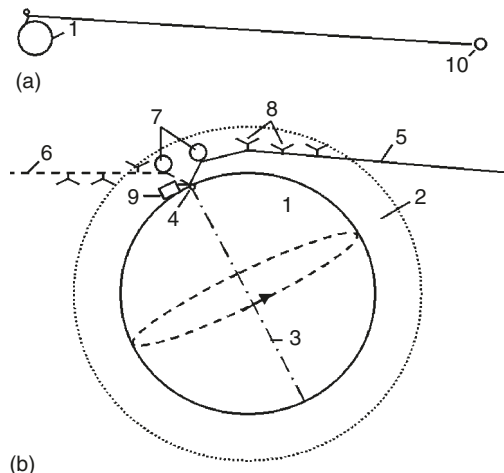


Fig. 7.1. A conceptual Earth–Moon transportation system. One end is connected to the Earth’s pole and the second end is connected to the Moon. *Notations:* (1) the Earth; (2) Earth’s atmosphere; (3) axis of Earth rotation; (4) Earth pole; (5) Earth–Moon cable transport system in right position (one extreme of the Moon’s position); (6) Earth–Moon system in left position; (7) air balloons; (8) support wings; (9) drive station; and (10) Moon.

it has to support the total system weight, which is several hundred times the load weight. In an optimal main cable the cross-section area increases (for $K = 2$, about 20 times) in the altitude range 0–150,000 km, is approximately constant in the range 150,000–380,000 km, and decreases near the Moon’s surface from 20,000 km to the surface.

The mass of the main cable is minimized as its diameter is variable along the distance (see the next section for calculation of the main cable cross-section areas and mass). The transport cables pull (move) the load cabins (one up, the other down) along the main cable. As these are moveable parts, they must have constant diameter. If they had to carry a load to the full distance to the Moon, their mass would be very large. My concept separates the full distance into sub-distances (5–10), with closed-loop links for every sub-distance connected by rollers. These rollers transfer the transport cable movement from one link to another. In this case, the mass of the transport cables is minimized because at every local length (sub-distance) the cable diameter is determined by the local force. Total mass of the transport cable should be close to double the mass of the main cable.

The load containers are connected to the transport cable. When containers come up to the rollers, they pass the rollers, connect to the next link, and continue their motion along the main cable. The load (cabin) has special clamps to allow this transfer between the different diameter cables in each link.¹ Most space payloads, like tourists, must be returned to Earth. When one container is moved up, another container is moved down. The work of lifting equals the work of descent, except for a small friction loss in the rollers. The transport system may be driven by a conventional motor located at the Earth drive station, on a space station, or on the Moon. When payloads are not being delivered into space, the system may be used to transfer mechanical energy to the Moon. For example, the Earth drive station can rotate an electric generator on the Moon.

The cable is supported in the Earth's atmosphere by air balloons (around the pole) and winged devices (far from the pole). The maximum speed of the system in the atmosphere is about 190 m/s at the maximum distance of 2700 km in the right-hand position of Fig. 7.1. When the cable is located in the left-hand position, some wings may be out of the atmosphere and not so effective.

The Moon's orbit has eccentricity. Every 29 days the Moon's distance from Earth changes by about 50,000 km. Devices shown in Fig. 5.4 (in Chapter 5) must be used to change the length (or link length) of the transport cables as the Earth–Moon distance changes. They may be located at the Earth drive station, on a space station, in space, and/or on the Moon. The average speed of a cable length change is about 40 m/s. As the Moon pulls the transport system, it may be used to produce mechanical energy. If the cables can support 9 ton, the power can reach 1.8 million watts (10^6 W). The cables rotate the electric generator and negligibly brake the Moon's movement.

7.4 Theory of optimal cable from earth to moon

1. *Equations for an optimal cable from the Earth to the Moon.* The gravitation of the Earth, the Moon and the cable mass acts on every element of the cable. These forces create stress in the cable material. The cable mass will be minimum if the stress is constant along the cable. The stress equals the force divided by the cross-section area of cable.

The force active in the cable is given by:

$$F = \sigma A = F_0 + \int_{R_0}^R dG = F_0 + \int_{R_0}^R \gamma A dR \quad (7.1)$$

where

$$\gamma = \gamma_0 g_0 \left[\left(\frac{R_0}{R} \right)^2 - \frac{g_m}{g_0} \left(\frac{R_m}{D-R} \right)^2 - \frac{\omega_m^2 R}{g_0} \right] \quad (7.2)$$

where F is force in a given cross-section area [N]; F_0 is force at Earth surface [cabin (load) weight at Earth surface] [N]; dG is weight of a cable element; A is cross-section area of cable [m^2]; σ is tensile strength in the cable [N/m^2]; R is distance from Earth's center [m]; R_0 is radius of Earth [m] ($R_0 = 6378$ km); R_m is radius of Moon = 1737 km; γ is specific weight of cable [kg/m^3] at radius R ; γ_0 is specific weight of the cable [kg/m^3] at the Earth's surface; g_0 is gravitation at R_0 [m/s^2], for Earth, $9.81 \text{ m}/\text{s}^2$; g_m is gravitation on Moon surface [m/s^2], $1.62 \text{ m}/\text{s}^2$; D is distance from Earth to Moon [m], $D_{\min} = 356,400$ km, $D_{\max} = 406,700$ km; ω_m is orbital angle speed of the Moon around Earth [rad/s] $2.662 \cdot 10^{-6}$ rad/s.

Let us substitute equation (7.2) in (7.1) and differentiate to obtain:

$$dA/A = \frac{\gamma_0 g_0}{\sigma} \left[\frac{R_0}{R} - \frac{g_m}{g_0} \left(\frac{R_m}{D-R} \right)^2 - \frac{\omega_m^2 R}{g_0} \right] dR \quad (7.3)$$

The solution of equation (7.3) is

$$a_m(R) = \frac{A}{A_0} = \exp\left[\frac{g_0 B(R)}{k}\right]; \quad (7.4)$$

where

$$B(R) = R_0 - \frac{R_0^2}{R} - \frac{g_m R_m^2}{g_0} \left[\frac{1}{D-R} - \frac{1}{D-R_0} \right] - \frac{\omega_m^2}{2g_0} (R^2 - R_0^2), \quad (7.5)$$

where a_m is the relative cross-section area of Earth–Moon cable; A_0 is the cable's cross-section area at the Earth's surface [m^2]; $k = \sigma/\gamma_0$, is the ratio of cable tensile stress σ to cable density γ_0 [Nm/kg]; and $K = k/10^7$ is the stress coefficient.

2. The mass, W [kg], of the cable is:

$$W = \frac{F_0}{k} \int_{R_0}^R a_m \, dR; \quad (7.6)$$

3. The volume, V [m^3], of the cable is:

$$V = \frac{F_0}{\sigma} \int_{R_0}^R a_m \, dR; \quad (7.7)$$

Figs. 7.2a and 7.3a represent computations of cable cross-section area and mass of a single cable for the maximum distance (400,000 km) from Earth to the Moon and for different stress coefficients K . Figs. 7.2 and 7.3 are computed for the stress coefficient $K = 2$ –4.5. These figures show, if $K = 2$, the maximum cross-section cable area is more than 21 times the cross-section area at Earth ($A_0 = 1$). The cable area equals $19A_0$ at the Moon. The cable weight for a force of 3 ton is 11,200 ton. If $K = 4.5$ the maximum cross-section area is 4 times more than the cross-section area near Earth and the cable weight for the force (load) of 3 ton is decreased to 1000 ton. Figs. 7.2 and 7.3 are computed for some very strong material available in the future. These figures show if, for example, the stress coefficient equals 15, the required cable mass for a load of 3 ton is decreased to 120 ton. For the three-cable system (main + two transport cables) this means that the system mass is 360 ton. Increasing or decreasing the load changes the cable mass proportionally. Moon delivery work of 1-kg load is presented in Fig. 7.4.

7.5 Technical parameters of projects

The following are some data for estimating the characteristics of the cable system. The system has three cables: one main and two transport cables. Each transport cable can

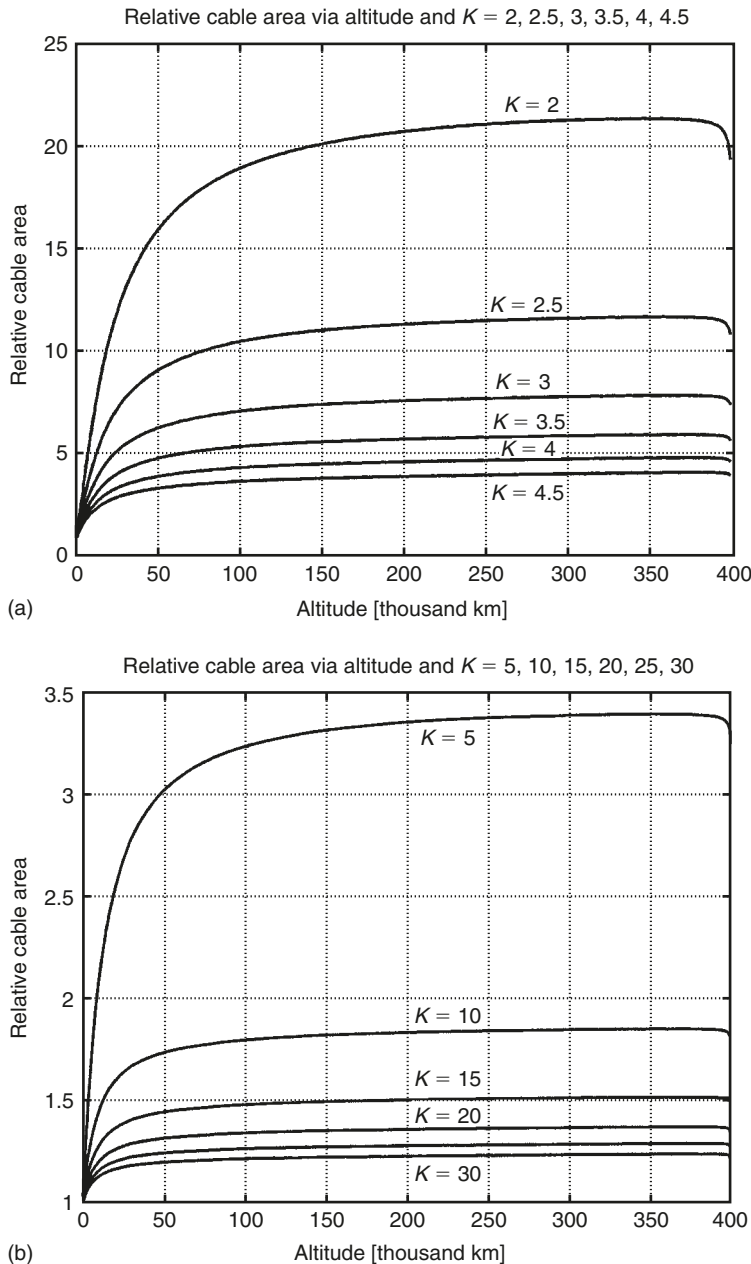


Fig. 7.2 Relative area for a cable from Earth to Moon (up to 400,000 km) for stress coefficient (a) $K = 2\text{--}4.5$, and (b) $K = 5\text{--}30$.

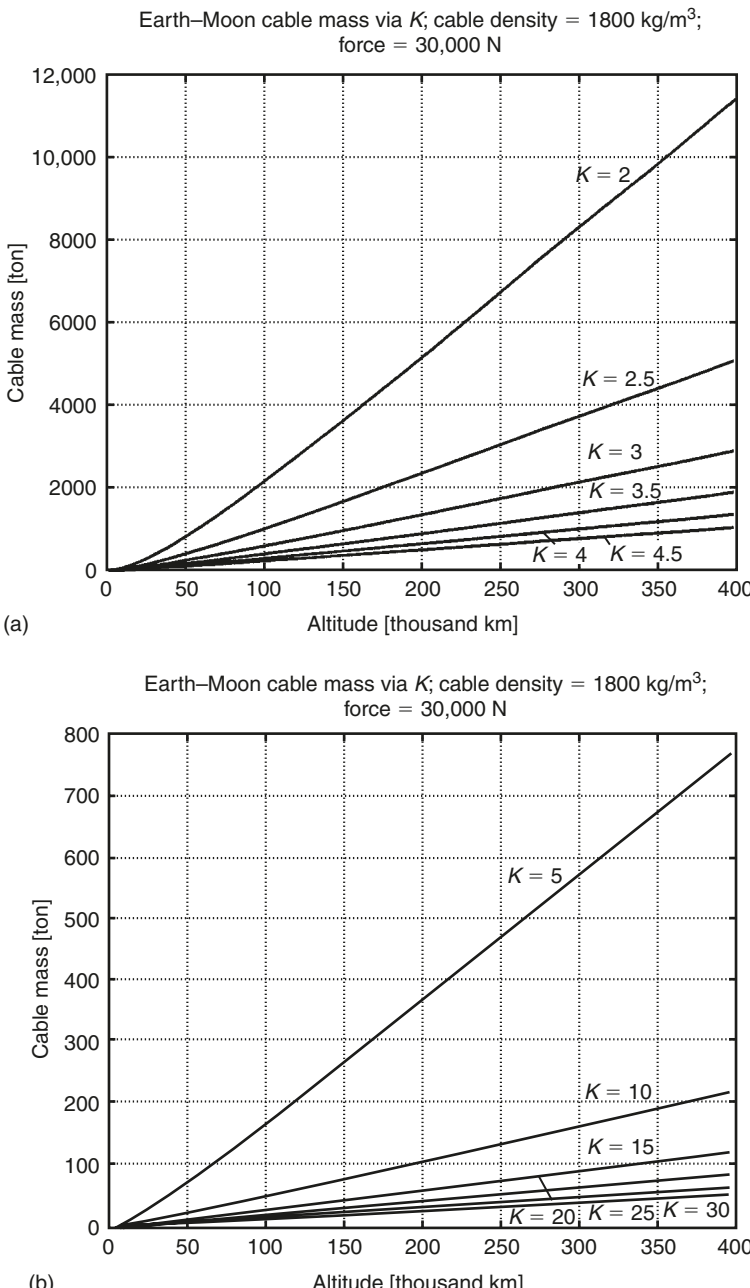


Fig. 7.3 The Earth–Moon cable mass versus altitude [thousand km] for cable density 1800 kg/m^3 , delivery mass of 3 ton, (a) $K = 2\text{--}4.5$, and (b) $K = 5\text{--}30$.

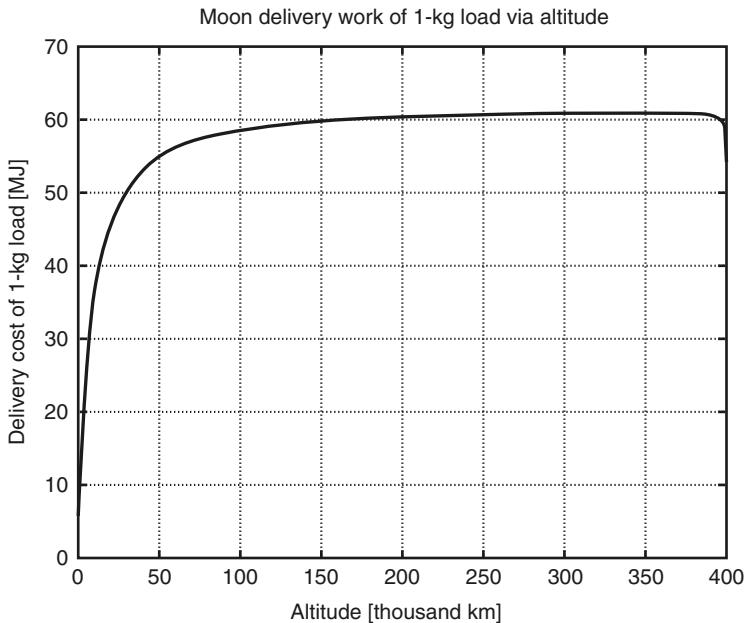


Fig. 7.4. Moon delivery work [MJ] of 1-kg load versus altitude [thousand km].

maintain a force (load) of 3 ton. This means that the cable can support two 3-ton loads, one going up and one going down. The material of the cable is assumed to have $K = 4$. The main cable has the optimal cross-section area for an equal stress cable. The transport cables are approximately optimal for 10 links. The main cable has a minimum cross-section area A_0 of 0.42 mm^2 (diameter $d = 0.73 \text{ mm}$) and maximum cross-section area A_m of 1.9 mm^2 ($d = 1.56 \text{ mm}$). The mass of the main cable would be 1300 ton. The total mass of the main cable plus the two transport cables (for delivering a mass of 3000 kg) is about 3950 ton for the transport system shown in Fig. 7.1. If the cable can be made from nanotubes with $K = 10$, the total mass will be 665 ton, and if the cable has $K = 15$, the total cable mass would be 360 ton. The cabins that ride on the cable transport system are assumed to have a mass of 3 ton. Each would be capable of carrying a payload of either people or cargo. With suitable development, transfer speeds of 6 km/s might be reached. This could allow a single cable system to transfer about 1000 ton of cargo per year to and from the Moon. The cabin speed is controlled by an engine located at the Earth pole drive station. If one cable is damaged, the other two cables can be used to rescue people and to repair the injured cable.

7.6 Conclusion

There are a lot of problems that must be solved before the proposed Earth–Moon transport system can be built. The chief of these is producing a cheap strong cable and composite materials of appropriate strength for the rollers and transmission which can operate at high speed. Another problem is the design of connectors that would allow

the payload to pass the rollers without stopping. The purpose of this work is to draw attention to the possibilities of further studies of this system, which has a great promise for future applications.

New materials could make the suggested transportation system realistic for trips between the Earth and the Moon with little expenditure of energy. The author is prepared to discuss the project details with serious organizations that have similar research and development goals. The same ideas were offered by author in patent applications 09/789,959 of 2/23/01, 09/873,985 of 06/01/01, 09/974,670 of 10/11/01, and the US patent 6,494,143 of 12/17/02.

References

1. A.A. Bolonkin, “Non-rocket Earth–Moon Transport System”, Paper B0.3-F3.3-0032-02 presented to *34th COSPAR Scientific Assembly, The World Space Congress 2002*, 10–19 October 2002, Houston, TX, USA.
2. A.A. Bolonkin, “Non-rocket Earth–Moon Transport System”, *Advanced Space Research*, Vol. 31, No. 11, 2003, pp. 2485–2490.
3. A.A. Bolonkin, “Non-rocket Transport System for Space Travel”, *Journal of British Interplanetary Society*, Vol. 56, No. 7/8, 2003, pp. 237–249.
4. A.A. Bolonkin, “Bolonkin’s Method Movement of Vehicles and Installation for It”, US Patent 6,494,143 B1, 2002.
5. M.L. Cosmo and E.C. Lorenzini (eds.), *Tethers in Space Handbook*, 3rd edition, Smithsonian Astrophysical Observatory, December, 1997.
6. D.V. Smitherman Jr., *Space Elevators*, NASA/CP-2000-210429, US National Aeronautics and Space Administration, Washington, DC, 2000.
7. F.S. Galasso, *Advanced Fibers and Composites*, Gordon and Branch Science Publisher, New York, 1989, p. 158.
8. *Carbon and High Perform Fibers Directory and Data Book*, 6th edition, London, Chapman & Hall, New York, 1995.
9. M.S. Dresselhous, *Carbon Nanotubes*, Springer, New York, 2001.

This page intentionally left blank

CHAPTER 8

Earth–Mars Cable Transport System*

Summary

The author offers and computes a new permanent cable transport system (CTS) that links a pole of the Earth with the Mars' orbit. This system connects Earth and Mars for 1–1.5 months for every 1.7–2 years when they are located at the nearest distance, and allows the transfer of people and loads to Mars and back. The system has many advantages, as it uses a transport engine located on Earth, but it also requires the high-strength cable made from nanotubes. This chapter contains theory of an optimal equal stress cable that connects the Earth and the Mars' orbit, as well as computed parameters of the suggested system.

8.1 Introduction

The author has proposed a new transport system for delivering payloads and people to Mars. The author has not found an analog of similar facilities for transporting a payload into space in the literature^{1–3} and patents.

The present method does not require rockets. The installation has a CTS and uses kinetic energy from the Earth's orbit. The suggested transport system is driven by an engine located on the Earth's surface.

In the proposed method, a CTS is permanently connected from the Earth's pole to the Mars' orbit. This way, a space ship moved to Mars obtains its energy from the Earth's orbit (not Earth's rotation). When the ship returns to the Earth, it obtains its energy from an onboard engine or from an engine located on Earth.

This chapter contains the theory of an optimal equal stress cable for the complex Earth–Sun–Mars gravitational field and results of computations of the project.

*Presented as paper BO.4-C3.4-0036-02 to *The World Space Congress – 2002, 10–19 October 2002*, Houston, TX, USA. Detailed material was published in *Actual Problems of Aviation and Aerospace Systems*, Vol. 8, No. 2 (16), 2003.

The project uses artificial materials like nanotubes and whiskers that have a ratio of tensile strength to density equals 20 million meters or greater.⁴⁻⁶ Theory predicts nanotubes with specific tensile stress of 100 million meters that will significantly improve the parameters of the suggested project.

The author's other non-rocket closed methods are presented in Refs.^{7,8} and in other chapters of this book.

8.2 Brief description

This chapter contains the theory and results of computation for a special project. This project uses three cables (one main cable and two for driving loads) mass from artificial material: whiskers, nanotubes, with the specific tensile strength (ratio of tensile stress to density) $k = \sigma/\gamma = 20 \times 10^7$ ($K = 20$) or more. Nanotubes with the same or better parameters are available in scientific laboratories. The theoretical limit of nanotubes of single-walled nanotube (SWNT) type is about $k = 100 \times 10^7$ ($K = 100$).

A proposed centrifugal Mars' CTS is shown in Figs. 8.1 and 8.2. The system includes the optimal equal stress cable which has a length approximately equal to the minimum distance of the Earth to the Mars' orbit. The installation has a transport system with chains connected by rollers and two transport cables.

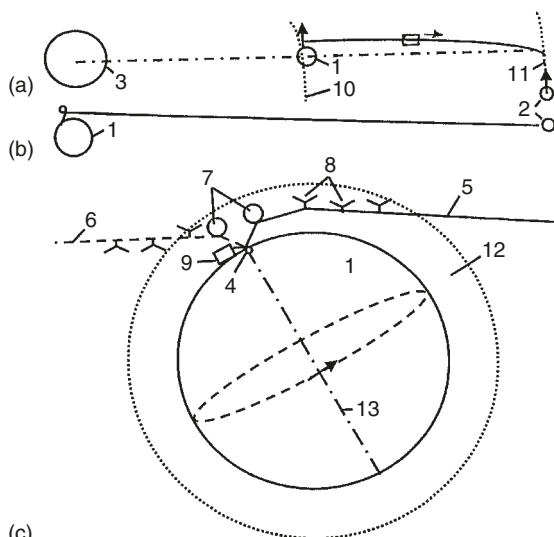


Fig. 8.1. The offered Earth–Mars’ orbit transport system. (a) Sun–Earth–Mars; (b) Earth–Mars; (c) Connection to Earth pole. *Notations:* (1) Earth; (2) Mars; (3) Sun; (4) Earth pole; (5) Earth–Mars cable transport system in right position; (6) Earth–Mars cable transport system in left position; (7) air balloon; (8) support wing; (9) drive station; (10) Earth’s orbit; (11) Mars’ orbit; (12) Earth’s atmosphere; and (13) axis of Earth rotation.

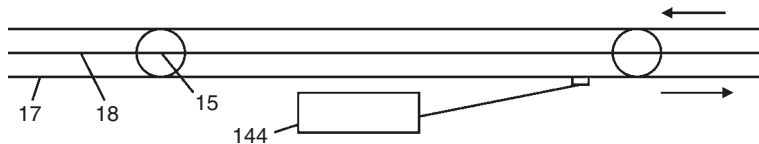


Fig. 8.2. CTS. Notations: (144) Space ship; (15) rollers; (17) transport cable; and (18) main cable.

The upper ends of the cables are located near the Mars' orbit and the lower ends of the cables are connected to the Earth's pole. They are supported in the Earth's atmosphere by air balloons (near the pole) and winged devices at a maximum distance of up to 2800 km. The rotary speed of the cables changes from 0 (at the pole) to 190 m/s (at the end of the maximum distance in the atmosphere). These winged devices can support cables when they are located within the lower atmosphere.

The installation would have a device that allows the length of the cables to be changed. The device would consist of a spool, motor, brake, transmission, and controller. The facility could have mechanisms for delivering people and payloads to Mars and back using the suggested transport system.

The delivery devices include: containers (passenger cabins, space ships, etc.), cables, motors, brakes, and controllers.

The space cabin can temporarily land on the surface of the Mars for loading and performing research. The space cabin has a small rocket engine for maneuvering and landing on the surface of Mars.

Every 2 years Mars comes within a minimum distance from Earth. For about 1–1.5 months the CTS can be used to deliver people and loads to Mars. The space ship moves in advance to the upper end of the CTS, then when Mars arrives, the vehicles land on its surface and the people work on for Mars 1–1.5 months; afterwards the space ships return to Earth. While living on Mars, the people can fly from one place to another with speeds of about 230 m/s (including Mars' round trip at low altitude) in their space cabin (ship). Exploring using the CTS would not require rocket fuel.

8.3 Theory of Earth–Mars equal stress cable

- Writing the equation of equilibrium for a small element of the Earth–Mars cable:

$$\begin{aligned} \sigma dA &= -g_0 \gamma_0 \left(\frac{R_0}{R - R_e} \right)^2 A dR \\ &+ \gamma_0 g_m \left(\frac{R_{m_o}}{R_m - R} \right)^2 A dR + R \omega^2 \gamma_0 A dR - \gamma_0 g_s \left(\frac{R_s}{R} \right)^2 A dR \quad (8.1) \end{aligned}$$

Dividing the left and right sides of equation (8.1) by $\gamma_0 A$ and taking the integral from $(R_m - R_{m_o})$ to R , the equation of the optimal equal stress cable from Earth to Mars may be written and solved as given below:

$$a = \frac{A}{A_0} \\ = \exp \left\{ -\frac{1}{k} \left[g_m R_{m_o}^2 \left(\frac{1}{R_m - R} - \frac{1}{R_{m_o}} \right) + g_o R_o^2 \left(\frac{1}{R - R_e} - \frac{1}{R_m - R_{m_o} - R_e} \right) \right] \right\} \\ + g_s R_s^2 \left(\frac{1}{R} - \frac{1}{R_m - R_{m_o}} \right) + \frac{\omega^2}{2} \left(R^2 - (R_m - R_{m_o})^2 \right) \quad (8.2)$$

2. The mass of cable is:

$$W = \frac{F_0}{k} \int_{R_0}^R a dR. \quad (8.3)$$

3. The volume of cable is:

$$v = \frac{F_0}{\sigma} \int_{R_0}^R a dR. \quad (8.4)$$

Here a is the relative cross-section area of cable; A is the cross-section area of cable [m^2]; A_0 is the near Mars' orbit cross-section area of cable [m^2]; g_0 is gravitation at the planet surface R_0 [m/s^2], for Earth $g_0 = 9.81 \text{ m/s}^2$; $g_m = 3.72 \text{ m/s}^2$ is the gravitation on Mars' surface; $g_s = 274 \text{ m/s}^2$ is gravitation on Sun's surface; F_0 is the force [N] (ship mass); $k = \sigma/\gamma$ is ratio of cable tensile stress to density [Nm/kg]; $K = k/10^7$ is the stress coefficient [millionmeters]; R is the radius from Sun's center to given cross-section of cable [m]; $R_0 = 6.378 \times 10^6$ is the radius of Earth [m]; $R_e = 14.95 \times 10^{10}$ is the Sun-Earth distance [m]; $R_{m_o} = 3.39 \times 10^6$ is the radius of Mars [m]; $R_m = 22.8 \times 10^{10}$ is the radius of Mars' orbit [m]; $R_s = 696 \times 10^6$ is the radius of Sun [m]; v is the volume of the cable [m^3]; W is the mass of the cable [kg]; σ is the cable tensile strength [N/m^2]; $\omega = 2 \times 10^{-7}$ is the angular speed of Earth's orbit [rad/s]; γ is the density of cable [kg/m^3].

Figs. 8.3–8.5 represent the computation for the shortest distance (78 million kilometers) from Earth to Mars.

Readers can find the performances of current cables and a discussion of cable problem in Refs.^{4–8}

8.4 Project

8.4.1 Earth–Mars non-rocket transport system

The following are some data estimations of the Mars' transport system, which provides an inexpensive payload transfer between the Earth and the Mars. The system has three

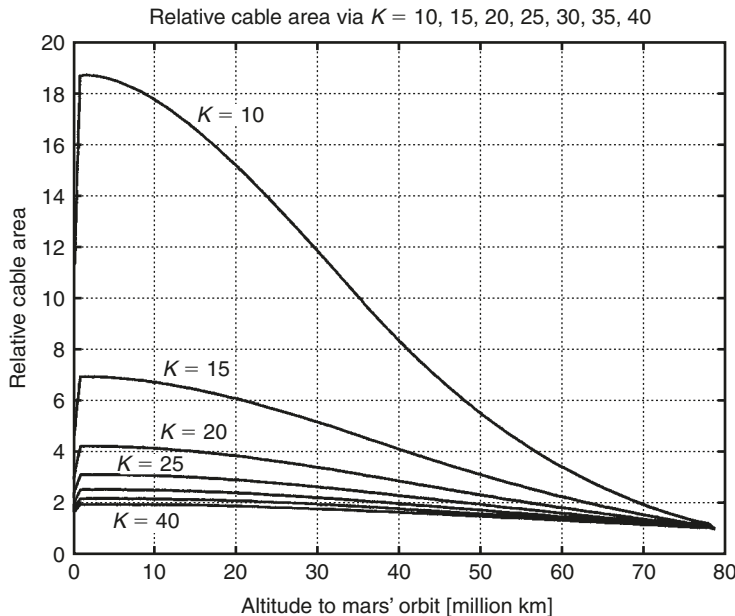


Fig. 8.3. Relative cable area of Earth–Mars transport system via distance to Mars’ orbit [million km].

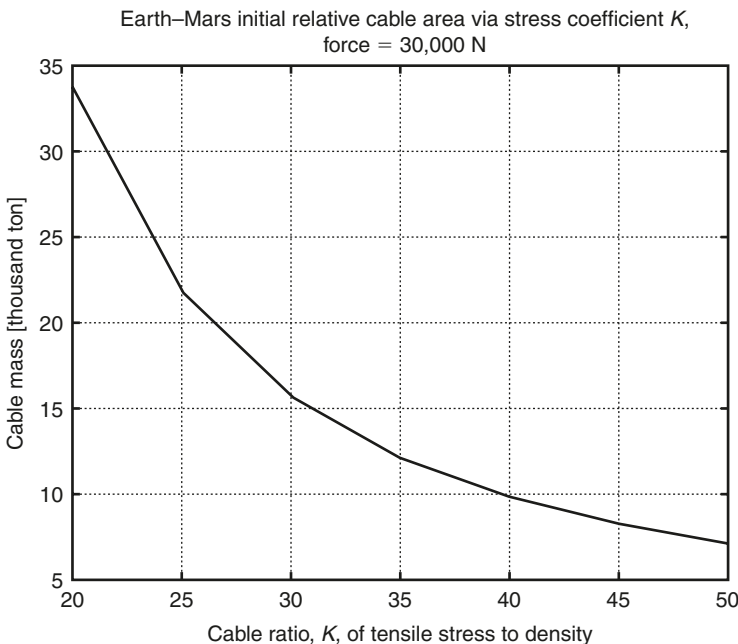


Fig. 8.4. Earth–Mars cable mass via stress coefficient K .

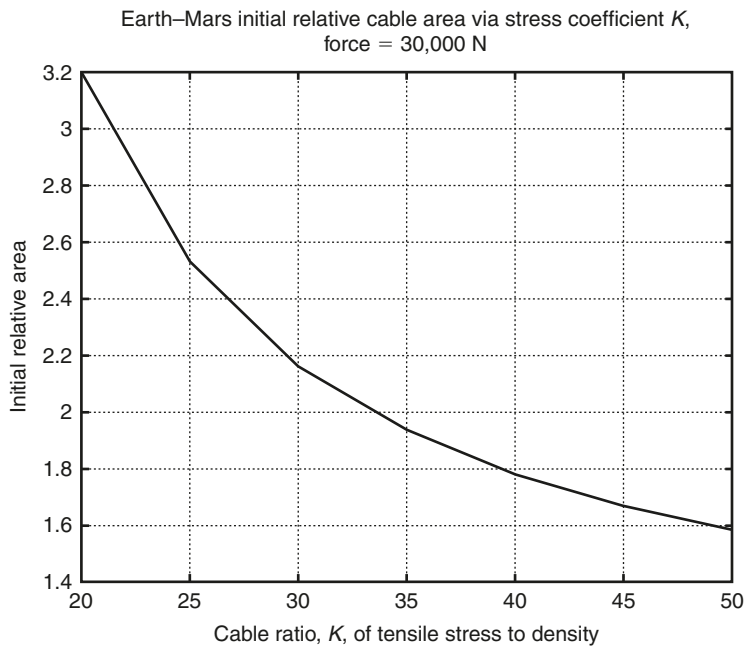


Fig. 8.5. Earth–Mars initial (near Earth) relative cable area via the stress coefficient K .

cables. Each cable can hold a force of 3 ton. All cables have optimal cross-section areas of equal stress.

Results of computation for $K = 20\text{--}50$ are presented in Figs. 8.3–8.5. If material of the cable has specific strength $k = 20 \times 10^7$ ($K = 20$), the ratio of the maximum cross-section area (near Earth) to the minimum cross-section area of the cable (near Mars' orbit) is 4.4 (Fig. 8.3), at the Earth's surface this ratio equals 3.15 (Fig. 8.5). If the space cabin has a mass of 3 ton, the mass of the main cable is 34,000 ton (Fig. 8.4). The total mass of the main cable plus the two container cables (for delivering a mass of 3000 kg) equals about 110,000 ton. If one cable is damaged, two others will be used for assuring people's safety as well as for repairing the original cable.

Patent applications are 09/789,959 of 2/23/01, 09/873,985 of 06/01/01, 09/974,670 of 10/11/01, US patent 6,494,143 of 12/17/02.

8.5 Conclusion

The offered transport system is not a well-known tether system because it does not have the main attributes of a standard tether system: free rotation in space and connecting two *artificial* bodies. Our system does not rotate and it is only temporarily connected to a second *natural* body. It may be compared with an aerial ropeway in mountains. However it is as different from an aerial ropeway as a current airplane is different from a children's paper airplane.

The offered transport system is not a conventional space elevator. The conventional space elevator connects the Earth's equator to a space station located on the geosynchronous Earth's orbit. The offered system is connected to a *pole* of the Earth. It is impossible for space elevator, as it will not work if it is connected to the Earth's pole. The space elevator must rotate a space station using the Earth's energy. It means the Earth end of the space elevator *must* be connected to the Earth's *equator*. Our system is rotated using movement of the Earth along the Earth's orbit around the Sun.

The offered system has a new simple mechanical *transfer* system for transferring energy from the Earth's mechanical engine (located on Earth) to a load cabin, located in space. The system has a new idea – separating the cable transmission into sub-sections, which dramatically decreases the cable weight. This transport system may be applied to the space elevator and it can solve the main problem of the space elevator: how to transfer energy for movement of the load carbine. This idea can also be applied to building space towers, for cable space launchers and for transferring mechanical energy over long distances on Earth.

New materials could make the suggested transportation system realistic for trips between the Earth and the Moon in the future with little expenditure of energy. The author is prepared to discuss the project details with serious organizations that have similar research and development goals.

References

1. M.L. Cosmo and E.C. Lorenzini (eds.), *Tethers in Space Handbook*, 3rd edition, Smithsonian Astronomic Observatory, December, 1997.
2. S.W. Ziegler and M.P. Cartmell, "Using Motorized Tethers for Payload Orbital Transfer", *Journal of Spacecraft and Rockets*, Vol. 38, No. 6, 2001.
3. D.V. Smitherman Jr., *Space Elevators*, NASA/CP-2000-210429.
4. F.S. Galasso, *Advanced Fibers and Composite*, Gordon and Branch Science Publisher, 1989.
5. *Carbon and High Performance Fibers Directory and Data Book*, 1995, London, Chapman & Hall, New York.
6. M.S. Dresselhous, *Carbon Nanotubes*, Springer-Pergamon, New York, 1996–2000.
7. A.A. Bolonkin, "Cable Earth–Mars Transport System", Presented as paper BO.4-C3.4-0036-02 to *The World Space Congress – 2002*, 10–19 October 2002, Houston, TX, USA.
8. A.A. Bolonkin, "Cable Earth–Mars Transport System", *Actual Problems of Aviation and Aerospace Systems*, Vol. 8, No. 2 (16), 2003.

This page intentionally left blank

CHAPTER 9

Kinetic Anti-gravitator*

Summary

This chapter describes a method and devices that provides a repulsive (repel, push, opposed to gravitation) force between given bodies. The basic concept is that a strong, heavy cable is projected upwards using a motorized wheel on the ground. The upward momentum of the cable is transferred to the apparatus by means of a pulley/roller mechanism, which sends the cable back down to the motor. The momentum transferred from the cable to the apparatus produces a push force which can suspend the apparatus in the air or lift it. There is an equal and opposite force on the motorized wheel on the ground. The push force can be great (up to tens of tons) and operate over long distances (up to hundreds of kilometers). This force produces great accelerations and velocities of given bodies (vehicles). This device is called a kinetic (mechanical) anti-gravitator (kinetic repulsator or repellor) because gravitation attracts any two bodies, whereas the offered device repels any two bodies.

The offered method can be applied to: vertical takeoff and landing (VTOL) aircraft, non-rocket space apparatus, flying, walking, and jumping (pogo-stick) superman (vehicles), long-arm (long-hand), high-altitude crane, high tower (up to 200 km), and for construction of space elevator without rockets.

Nomenclature

b	atmospheric experimental coefficient (for example, an altitude H in the interval 0–10 km, $b \approx 1/9218$)
D	average air drag [N]
D_L	laminar air drag [N]
D_T	turbulent air drag [N]

* The main idea of this chapter was presented as IAC-02-IAA.1.3.03, 53rd International Astronautical Congress, The World Space Congress – 2002, 10–19 October 2002, Houston, TX, USA, and the full manuscript accepted as AIAA-2005-4504, 41st Propulsion Conference, 10–12 July 2005, Tucson, AZ, USA.

d	cable diameter [m or mm]
F	repulsive (lift) force [N]
g	gravity, $g_0 = 9.81 \text{ m/s}^2$ is gravity on the Earth's surface
H	the height of the kinetic device (top end of the cable) [m]
$k = \sigma/\gamma$	relative cable stress [m^2/s^2], $K = k/10^7$
L	cable length between an Earth support and the object (load) [m]
$L_s = L^{0.8}s$	cable surface parameter
m, m_c	the cable mass [kg]
m_1	mass of apparatus [kg]
m_2	mass of a repulsive engine [kg]
n	number of the installation cables ($n = 2, 4, 8, \text{etc.}$)
P	engine power [W]
P_T	power of turbulent drag [W]
P_L	power of laminar drag [W]
R	circle radius [m]
V	cable speed [m/s]
V_s	ship speed [m/s]
V_1	apparatus speed [m/s]
v	objective speed [m/s]
$R_0 = 6378 \text{ km}$	Earth radius
S	cable cross-section areas (one branch or all branches) [m^2]
s	perimeter of all cable cross-section areas [m]
α	angle of circle part [rad]
σ	cable tensile stress [N/m^2]
γ	cable density [kg/m^3]
μ	air viscosity [kg/s m]
ρ	air density at altitude H (for example, at $H = 0 \text{ km}$, $\rho_0 = 1.225 \text{ kg/m}^3$, $\mu = 1.7894 \times 10^{-5}$)

9.1 Introduction

At present, we know some methods of flight on Earth and in space. Earth atmospheric devices (aircraft, helicopters) push down the air; space apparatus pushes away a rocket gas. These methods have many disadvantages. For example, we need an atmosphere of sufficient density or rocket fuel. We cannot be immobile and suspended for an extended period of time at a given point over the surface of a planet that has gravity but no atmosphere.

The winged and liquid rocket methods of flight have reached the peak of their development. In the last 30 years there has been no increase in the air speed, no wide application of VTOL aircraft, no significant decrease in space delivery cost, no common space tourism, and no non-vehicle individual flights to the atmosphere. Space launches are very expensive.

The aviation, space, and energy industries need revolutionary ideas which will significantly improve the capability of air and space vehicles.

Other than rockets, one method for reaching space is the space elevator. It is very complex, expensive and technologically impossible at the present time.

Below is a new method.¹⁻³ This method produces a push (repulsive, repel, opposed to gravitation) force between given bodies, for example, between the ground and a flying vehicle. The basic concept is that a strong, heavy cable is projected upwards using a motorized wheel on the ground. The upward momentum of the cable is transferred to the vehicle by means of a pulley/roller mechanism. This mechanism creates a push force and that also sends the cable back down to the motor. The momentum (push force) transferred from the cable to the vehicle can suspend it in the air or lift it. This force is equal and opposite to the force on the motorized wheel on the ground. The push (mechanical) force opposes the gravitational force between these bodies (for example, the ground and a flying vehicle). This force is created by a linear thin cable moved between the given bodies. If there is no roller and air friction and the distance between the given bodies is not changed, the suggested pusher does not require energy (except for the initial start and wheel friction). When the distance is increased, the energy is spent, when the distance is decreased, we gain energy. For some people this push force may be surprising because the bodies are connected only by the flexible thin long cable. But there are no violations of the laws of physics – we transfer a momentum between the bodies through the moving cable. When this momentum in a unit of time (force) is more than the gravity force, the bodies will move away from one other; when the momentum is less than the gravity force, the bodies will be drawn together.

The offered method makes it easy to achieve a large push (repulsive, repel) force over long distances, to accelerate a vehicle in flight or keep it at a given distance and to equalize the gravity force. This chapter contains some applications of this method.

The suggested method is different from a 2000-km space launcher (cable into tube) at an altitude of 80 km offered by K. Lofstrom, published in 2002.⁴ These differences are described in Section 9.6.

9.2 Brief description of the installation

Some variants of the installation are shown in Figs. 9.1–9.5. The installation includes (see notations in Fig. 9.1 and others): a linear closed-loop cable, top and bottom rollers, any conventional engine, and a load. Details of the top roller are shown in Fig. 9.2, the bottom (lower) driver roller is shown in Fig. 9.3. The small rollers (Fig. 9.3) press on the cable and together with the large roller and engine move the cable. The possible cable cross-section areas are shown in Fig. 9.3(c). Fig. 9.4 shows the anti-gravitator in a slope position.

The spool mechanisms are shown in Fig. 9.5(a) and (b). They allow reeling and unreeling of the left and right cable branches or different speeds as well as changing the length of the closed-loop cable without stopping of the installation. The spool may be one of two variants: a mobile spool (Fig. 9.5(a)) or a motionless spool (Fig. 9.5(b)).

The installation works in the following way: the engine rotates the lower driver roller and continuously sends the closed-loop cable upwards at high speed. The cable reaches

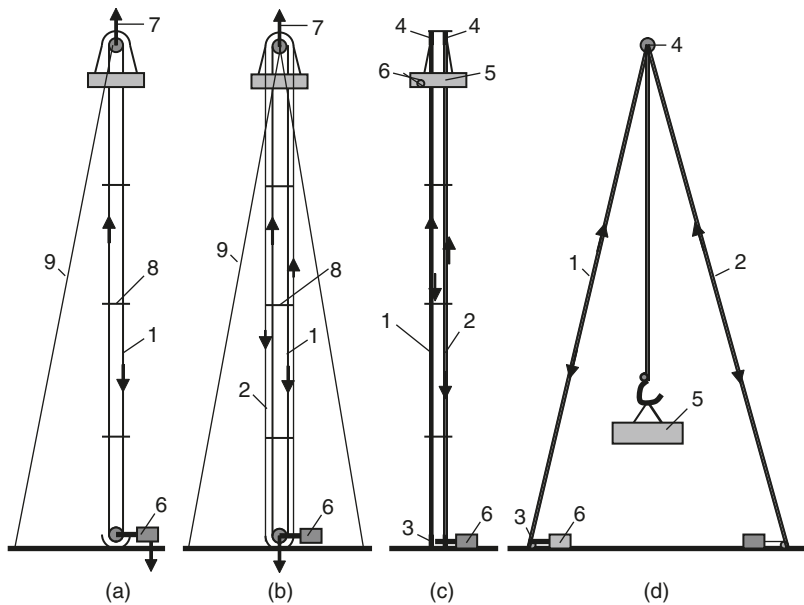


Fig. 9.1. Push devices (kinetic anti-gravitators) with closed-loop cables: (a) single cable with brace; (b) double cables are moved in opposite directions and located in one plane; (c) installation with four closed-loop cables in different planes and without braces; and (d) load crank with a minimum three cables. *Notations:* (1) One closed-loop cable; (2) the second closed-loop cable; (3) lower rollers; (4) top rollers; (5) suspended object; (6) engine; (7) push (lift) force; (8) spreader; and (9) braces.

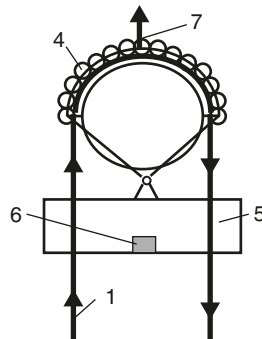


Fig. 9.2. Top roller of kinetic anti-gravitator (*Notation:* Same as in Fig. 9.1).

a top roller (which may be at high altitude), turns back and moves to the lower driver roller. When the cable turns back, it creates a push (repulsive, repel, reflective, centrifugal, momentum) force. This repulsive force can easily be calculated using centrifugal theory (see Section 9.3).

The push force can also be calculated against the mobile cable mass using momentum or reflection theories (see Section 9.3).

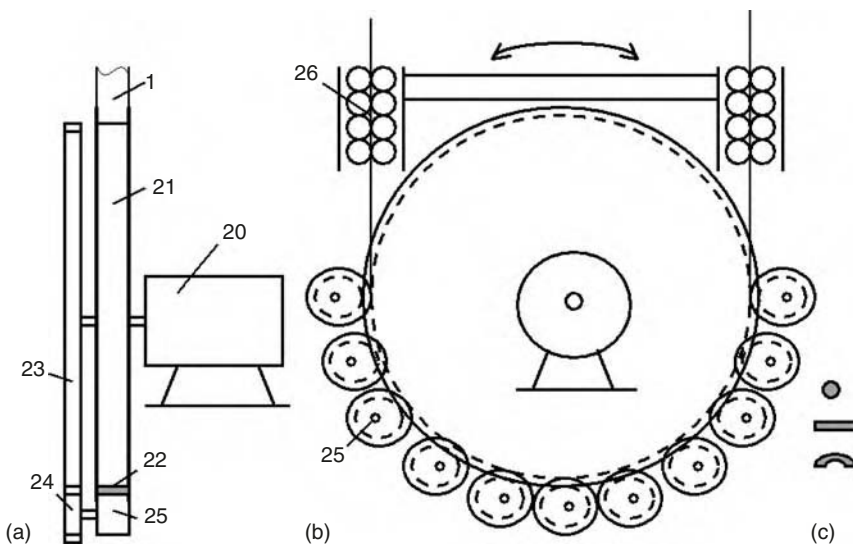


Fig. 9.3. Drive roller of kinetic anti-gravitator. *Notations:* (20) Engine; (21) drive roller; (22) (1) flexible cable; (23) large gear wheel; (24) small gear wheels; and (25, 26) directive rollers. (a) side view; (b) front view; and (c) cable cross-section.

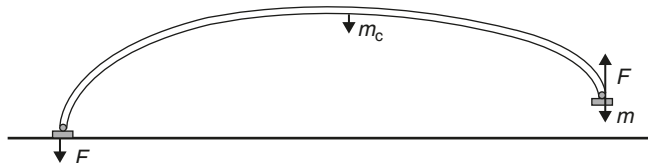


Fig. 9.4. Kinetic anti-gravitator in slope position.

The cable turns 180° around pulleys. That turn produces a centrifugal force which supports or moves the load. However, Newton's law say that for every action there is an equal and opposite reaction. In this case, the action comes from the wheel as this is what is pushing the cable and producing the net negative gravity field direction force on the cable. To do that, the wheel moves (is pressed) by the cable producing the reaction, which adds up to (similar to how the cable loads) an equal load in the positive gravity direction. This means the cable will push the wheel back toward the source of the gravity (in this case to the ground).

The repulsive force points in a vertical direction and it must be more than the gravitational force of the cable and load. This anti-gravity force keeps the load or space station suspended on the top roller; and the load cable (or special elevator) allows the delivery of a load to the space station. The rollers and cable may have high speed and stress. They must be made from a strong (for example, composite) material. In this case, the rollers have the same permitted stress (and permitted rotary speed) as the cable. The permitted (safety assurance) speed (of the cable or roller) is the speed permitted (admitted, safety) by the maximum material strength divided by an assurance factor.

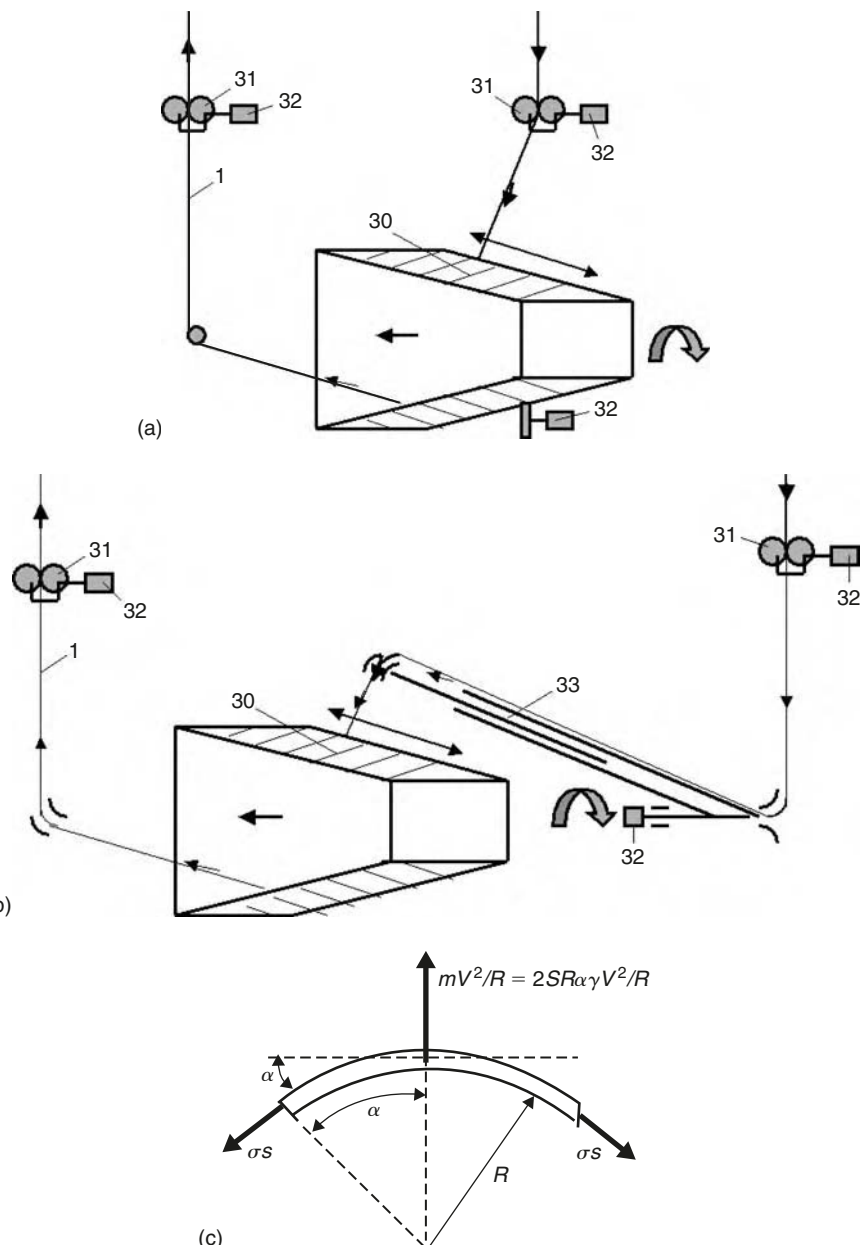


Fig. 9.5. (a) Revolving spool. *Notations:* (30) Cable spool; (31) directive rollers; and (32) spool engine. The left and right cables can have different speeds. (b) Motionless spool (the lever rotates around the spool). *Notations:* (30) Cable spool; (31) directive rollers; (32) motor; and (33) revolving lever. The left and right cables can have different linear speeds. (c) Forces of the rotary circle cable.

The moment of friction in the top roller can be compensated by guy lines as in Fig. 9.1(a), or by the second closed-loop cable rotating in an opposed direction to the first cable (Fig. 9.1(b)–(d)) and located in one plane (Fig. 9.1(a)).

A low-altitude (up to 10 km) pusher may have its cable made from conventional steel wire (or steel fiber). This cable has a smaller permitted maximum speed and air drag. It requires less power for rotation than a light cable made from artificial fibers (see Section 9.5).

As shown in the theoretical section, the current widely produced artificial fibers allow reaching altitudes of up to 100 km (see also Projects 1 and 2 in “Kinetic Space Towers and Launchers”³). If more altitude is required a multi-stage tower must be used (Fig. 2 and Project 3³), and very high altitude is needed (geosynchronous orbit or more), a very strong cable made from nanotubes must be used (Project 4³).

The closed-loop cable can be of variable length. This allows starting from zero altitude, increasing the load (station) altitude to a required value, and spooling the cable for repair. If we change the length of the cable (for example, using the spool) the cable will lift the load to high altitude or into space.

The devices for this action are shown in Fig. 9.5. The offered spools allow reeling and unreeling the left and right branches of the cable with different speeds to change the length of the cable.

The advantages of the proposed method are the same as for the centrifugal launcher.⁵ The suggested design has approximately half the construction cost of the semi-circle launcher⁵ because it uses vertical cables (not circle cables⁵). It also has approximately half the production delivery cost (up to \$2–4 per kg), because it has half the air drag and fuel consumption (the straight line is 3.14 times shorter than the circle).

Experiments requested by author and came out by Mr. Gregory Lishanski in 2002–2003 show the revolving straight closed-loop cable is stable in the vertical and horizontal positions.

9.3 Theory of the kinetic anti-gravitator

9.3.1 Push force for immobile object³

9.3.1.1 Repulsive (repel, push) force in space without gravitation

We can find the push force of the kinetic anti-gravitator from centrifugal theory (Fig. 9.5(c)).

We first take a small part of the rotary circle cable and write the equilibrium rotation for centrifugal force and tensile stress:

$$\frac{2SR\alpha\gamma V^2}{R} = 2S\sigma \sin \alpha, \quad (9.1)$$

where α = angle of the circle part [rad]. When $\alpha \rightarrow 0$ the relationship between maximum rotary speed V and tensile strength σ of a closed-loop (curved) cable is:

$$V = \sqrt{\frac{\sigma}{\gamma}} = \sqrt{k}, \quad (9.2)$$

$$F = 2\sigma S, \quad (9.3)$$

where F is the repulsive (lift) force [N], $k = \sigma/\gamma$ is the relative cable stress [m^2/s^2], S is the area of one branch of the cable cross-section [m^2]. The more convenient value of $K = 10^{-7}k$ is used for graphs. Equation (9.2) is found in the Ref.⁵ for a circle centrifugal cable launcher (Chapter 3). The computation of V versus k for intervals of 0–4 K ($K = k/10^7$) is presented in the same publication (Chapter 3, Fig. 3.10). For example, the cable has the cross-section area $S = 1 \text{ mm}^2$, stress $\sigma = 100 \text{ kg/mm}^2$. Two cables can keep a load of 200 kg at altitude.

We can find the lift force using reflection theory (see textbooks on theoretical mechanics). Writing the momentum of the reflected mass in 1 s gives:

$$F = mV - (-mV) = 2mV, \quad m = \gamma SV, \quad \text{or} \quad F = 2\gamma SV^2. \quad (9.4)$$

Here m is the cable mass reflected in 1 s [kg/s]. If equation (9.2) is substituted in equation (9.4), the expression for the repulsive (lift) force $F = 2\sigma S$ will be same.

9.3.1.2 Repulsive force in constant gravity field

In constant gravity field without air drag, the repulsive force of the offered device equals the centrifugal force F minus the cable weight W :

$$F_g = F - W = F - 2\gamma g SH = 2\gamma S(V^2 - gH) = 2S(\sigma - \gamma gH) = 2S\gamma(k - gH), \quad (9.5)$$

where H is the height of the kinetic device (top end of the cable) [m].

9.3.1.3 Repulsive force in variable gravity field and rotary Earth

Below it is shown a way of finding the final equation for the force F :

$$\begin{aligned} dP &= \left(g - \frac{V^2}{R} \right) dm, \quad g = g_0 \left(\frac{R_0}{R} \right)^2, \quad \frac{V^2}{R} = \omega^2 R, \quad dm = \gamma S dR, \quad R = R_0 + H, \\ P &= \int_{R_0}^R \left[g_0 \left(\frac{R_0}{R} \right)^2 - \omega^2 R \right] \gamma S dR = g_0 \left(R_0 - \frac{R_0^2}{R} \right) - \frac{\omega^2}{2} (R^2 - R_0^2), \quad \text{or} \\ F &= 2\sigma S - 2P = 2\gamma Sk - 2P = 2\gamma S \left[k - g_0 \left(R_0 - \frac{R_0^2}{R} \right) + \frac{\omega^2}{2} (R^2 - R_0^2) \right], \\ k &= \frac{\sigma}{\gamma} = V^2. \end{aligned} \quad (9.6)$$

The minimum cable stress or a minimum cable speed of a revolving planet is:

$$k_{\min} = V_{\min}^2 = g_0 \left(R_0 - \frac{R_0^2}{R} \right) - \frac{\omega^2}{2} (R^2 - R_0^2). \quad (9.7)$$

If $K > 5$ the height of the kinetic tower may be more than the Earth's geosynchronous orbit. For Mars $K > 1$, for Moon $K > 0.3$. Fig. 5.10 (Chapter 5) shows that the offered device with a height of 145,000 km can keep its position without cable rotation (movement), and if the device height is more than 145,000 km, the device has a useful lift force. That allows the lifting of a payload using a non-moving cable. We can stop the cable rotation and create the space elevator.

9.3.2 Repulsive force for a mobile object

For a mobile object the repulsive force is:

$$F = 2\gamma S(V \pm v)^2, \quad (9.8)$$

where v is the objective speed [m/s]. The minus “−” is taken when the cable length is increased, the plus “+” is taken when the cable length is decreased. From equation (9.8) it follows that the maximum object speed obtained from the cable cannot exceed the cable speed. Equation (9.8) is used for launching and landing of flight apparatus.

9.3.3 Restore force

When the cable is deviated from a vertical position in the gravity field, the restore force is:

$$F_r = F - \frac{gm_c}{2}. \quad (9.9)$$

9.3.4 Air drag of the cable

The computation of cable drag is not developed. No experimental data are available for the air drag of a very long cable.

9.3.4.1 The air drag of a double subsonic cable

The air drag of a double **subsonic** cable can be estimated using the drag equations for plates (the Reynolds number (Re) is included):

$$D_L = 0.5 \times 0.664 \rho^{0.5} \mu^{0.5} V^{1.5} L^{0.8} s, \quad D_T = 0.5 \times 0.0592 \rho^{0.8} \mu^{0.2} V^{1.8} L^{0.8} s, \quad (9.10)$$

$$D = 0.5(D_L + D_T).$$

The cable has only one side, as opposed to a plate which has two sides, that way the multiplier 0.5 is inserted (Fig. 9.10).

The power P of cable air drag D is:

$$P = DV = 0.5(D_T V + D_L V) = 0.5(P_T + P_L), \quad V = \sqrt{\sigma/\gamma}. \quad (9.11)$$

The power of turbulent drag P_T and of laminar drag P_L , respectively is:

$$P_L = 0.5 \times 0.664 \rho^{0.5} \mu^{0.5} \left(\frac{\sigma}{\gamma} \right)^{1.25} L^{0.8} s, \quad P_T = 0.5 \times 0.0592 \rho^{0.8} \mu^{0.2} \left(\frac{\sigma}{\gamma} \right)^{1.4} L^{0.8} s, \quad (9.12)$$

where the total cable perimeter s of the round cables is:

$$s = 2 \sqrt{\frac{\pi n F}{\sigma - \gamma g H}}. \quad (9.13)$$

Most of the engine power (80–90%) takes the turbulent cable drag. In space there is no air, thus no air drag and we can use a very long cable. If the altitude H is small (up to 5–6 km), we can ignore the factor $\gamma g H$. In this case, the cable depends on the relation $(\sigma^{0.9}/\gamma^{1.4})$. As you see, a cable with low tensile stress σ and high density γ (for example, conventional steel cable) requires less power because the safe maximum cable speed is small ($V \approx 250$ –350 m/s). However, the required cable weight increases 10–15 times. The round and single closed-loop cable ($n = 2$) requires minimum power. The plate and semi-circle cables require more power, but they may be more suitable for a drive mechanism.

9.3.4.2 Air drag of supersonic and hypersonic double cable

Below, the equation from Anderson⁶ for the computation of local air friction for a two-sided plate is given:

$$\begin{aligned} \frac{T^*}{T} &= 1 + 0.032 M^2 + 0.58 \left(\frac{T_w}{T} - 1 \right), \quad M = \frac{V}{a}, \quad \mu^* = 1.458 \times 10^6 \frac{T^{*1.5}}{T^* + 110.4}, \\ \rho^* &= \frac{\rho T}{T^*}, \quad Re^* = \frac{\rho^* V x}{T^*}, \quad C_{f,L} = \frac{0.664}{(Re^*)^{0.5}}, \quad C_{f,T} = \frac{0.0592}{(Re^*)^{0.2}}, \\ D_L &= 0.5 C_{f,L} \rho^* V^2 S, \quad D_T = 0.5 C_{f,T} \rho^* V^2 S, \quad D = 0.5 D_T + 0.5 D_L, \end{aligned} \quad (9.14)$$

where⁶ T^* , Re^* , ρ^* , μ^* are the reference (evaluated) temperature, Re , air density, and air viscosity, respectively. $M = V/a$ is the Mach number, a is the speed of sound [m/s], V is cable speed [m/s], x is the length of the plate (distance from the beginning of the cable)[m], T is flow temperature [K], T_w is body temperature [K], $C_{f,L}$ is a local skin friction coefficient for laminar flow, $C_{f,T}$ is a local skin friction coefficient for turbulent flow. As S is the area of skin [m^2] of both plate sides, it means for the cable we must take $0.5S$; D is the general air drag (friction) [N]. It may be shown that the general air drag for the cable is $D = 0.5D_T + 0.5D_L$, where D_T is the turbulent drag and D_L is the laminar drag.

For a **horizontal** cable, the friction drag can be computed using equation (9.10) where $\rho = \rho^*$, $\mu = \mu^*$.

From equation (9.14) we can derive the following equations for turbulent and laminar boundary flows of a **vertical** cable:

$$\begin{aligned}
 D_T &= \frac{0.0592s}{4} \rho_0^{0.8} \left(\frac{T}{T^*} \right)^{0.8} \mu^{0.2} V^{1.8} \int_{H_0}^H h^{-0.2} e^{0.8bh} dh \\
 &= 0.0547d \left(\frac{T}{T^*} \right)^{0.8} \mu^{0.2} V^{1.8} \int_{H_0}^H h^{-0.2} e^{0.8bh} dh, \\
 D_L &= \frac{0.664s}{4} \rho_0^{0.5} \left(\frac{T}{T^*} \right)^{0.5} \mu^{0.5} V^{1.5} \int_{H_0}^H h^{-0.5} e^{0.5bh} dh \\
 &= 0.5766d \left(\frac{T}{T^*} \right)^{0.5} \mu^{0.5} V^{1.5} \int_{H_0}^H h^{-0.5} e^{0.5bh} dh,
 \end{aligned} \tag{9.15}$$

where s is the cable perimeter. The laminar drag for high speed is 50–300 times less than the turbulent drag and we can ignore it.

Engine power and additional cable stress can be computed using conventional equations:

$$P = 2DV, \quad \sigma = \pm \frac{D}{S} = \pm \frac{4D}{\pi d}, \tag{9.16}$$

The factor 2 is needed because we have two branches of the cable: one moves up and the other moves down. The drag does not decrease the repulsive (lift) force because in the different branches the drag is in the opposite directions.

9.3.5 Computations

Computations of equation (9.8) are presented in Figs. 9.6–9.8 for low cable speeds and in Figs. 9.9 and 9.10 for high cable speeds for different value $L_s = L^{0.8}s$.

9.3.6 Calculations

For space apparatus that starts from a planet with no atmosphere (asteroid), which has a mass much greater than the apparatus mass, speed is calculated using equation:

$$V_1 = V \frac{m_1 + 0.5m_2}{m_1 + m_2}. \tag{9.17}$$

If the space ship uses asteroid rubble (or ships garbage) to create thrust via a repulsive engine, the ship speed is (in an immovable coordinate system with the origin located in the system's center of gravity):

$$V_s = V_3 \frac{m_3}{m_1 + m_2}. \tag{9.18}$$

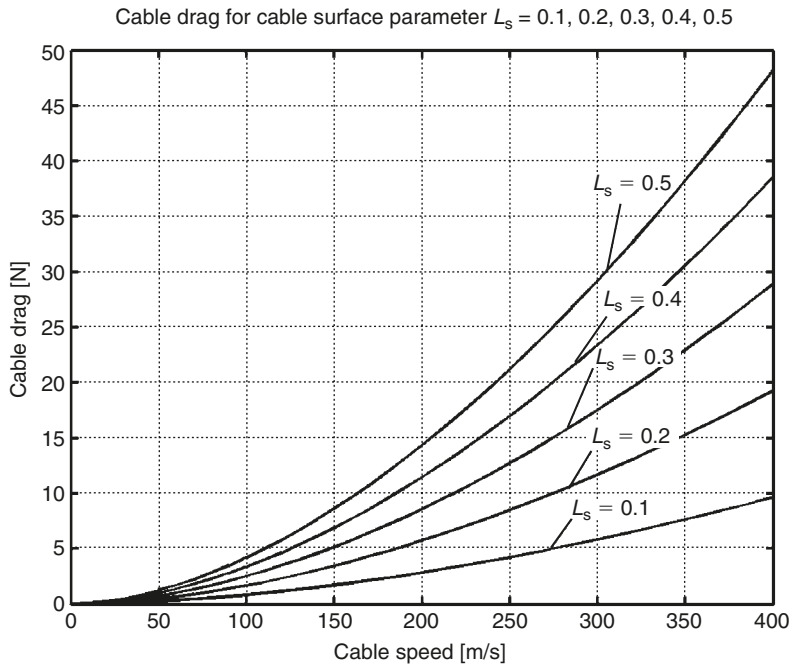


Fig. 9.6. Air cable drag versus cable speed for the cable surface parameter $L_s = L^{0.8}s = 0.1\text{--}0.5$.

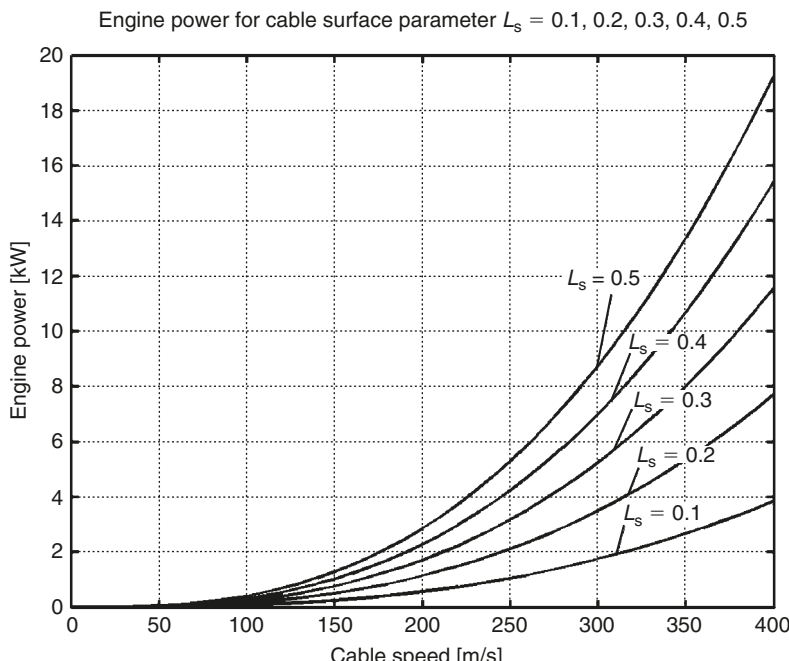


Fig. 9.7. Engine power versus cable speed for the cable surface parameter $L_s = L^{0.8}s = 0.1\text{--}0.5$.

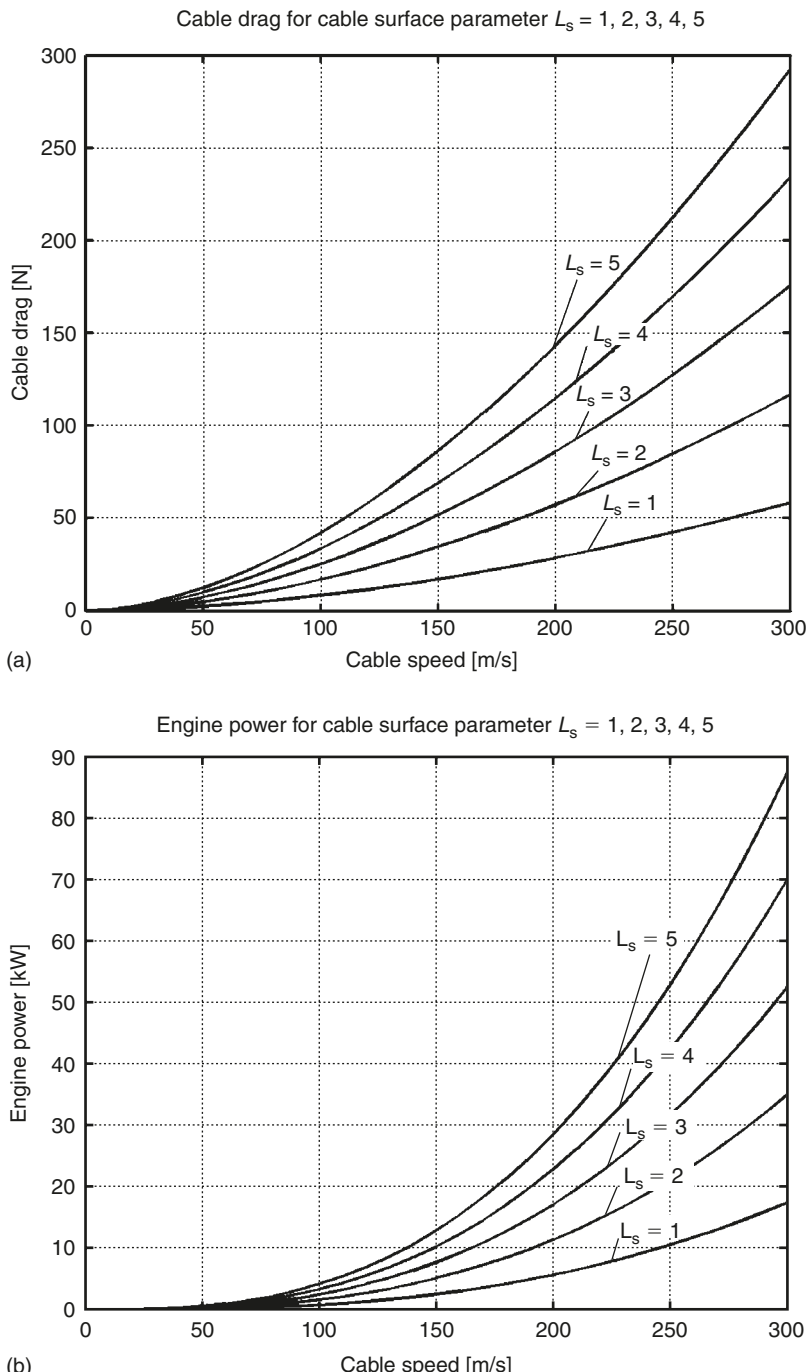


Fig. 9.8. (a) Cable drag versus cable speed for the cable surface parameter $L_s = L^{0.8}s = 1-5$.
 (b) Engine power versus cable speed for the cable surface parameter $L_s = L^{0.8}s = 1-5$.

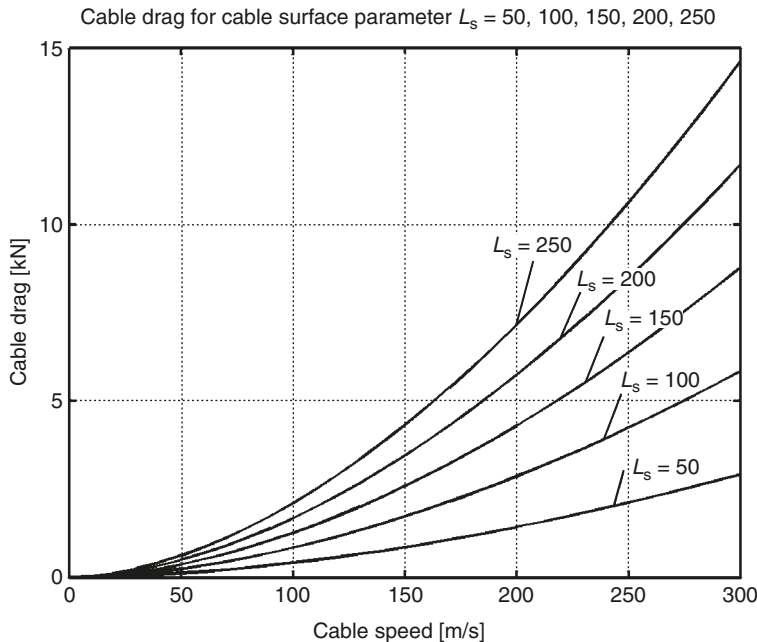


Fig. 9.9. Air cable drag versus cable speed for the cable surface parameter $L_s = L^{0.8}s = 50\text{--}200$.

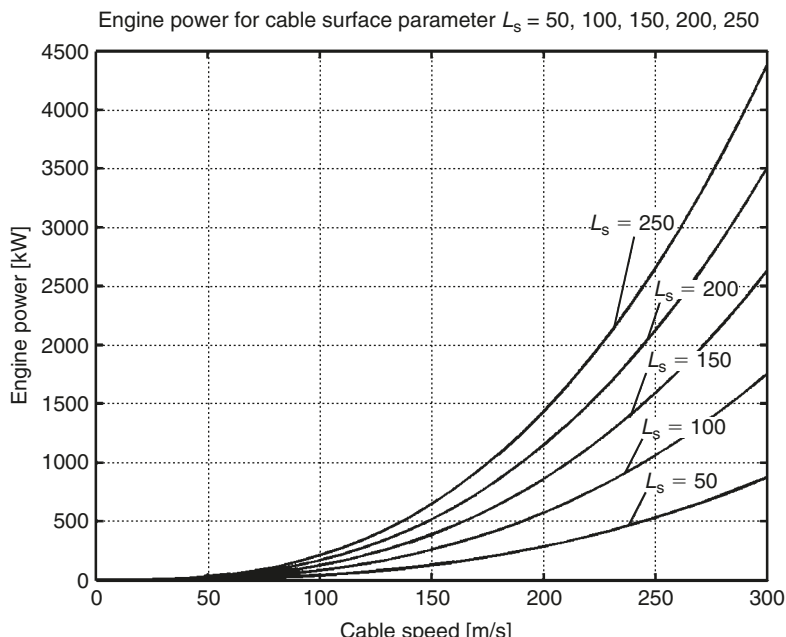


Fig. 9.10. Engine power versus cable speed for the cable surface parameter $L_s = L^{0.8}s = 50\text{--}200$.

9.4 Advantages of offered method

The advantages of the proposed method are tremendous. We can fly out of the atmosphere without aircraft, helicopters, dirigibles, and rockets. The installation is very simple (only an engine and a thin cable) and very light, especially when the cable is made from the artificial fiber, a fortiori, from nanotubes. When the cable is located outside the atmosphere, it does not require power for rotation, except for a small amount of power to compensate for the friction in the rollers. We can create a big force (up to tens or hundreds of tons) and operate at long distances (tens of kilometers in the Earth's atmosphere and hundreds of kilometers in space).

The kinetic anti-gravitator may have applications in many fields of civilian and military life: flights on Earth, in space, to planets and asteroids, launching space ships, lifting loads at high altitude, problems of communication, observation, searching, and rescues. The same idea may be used to transfer mechanical energy over long distances,⁷ for moving aircraft in the air⁸ or ground vehicles using an engine located at a large distance, for building simple air bridges over straits, canals, and mountains instead of tunnels or conventional bridges,⁹ and so on. Some of these problems are considered below.

9.5 Applications

Conventional steel cable has a maximum tensile stress of $\sigma = 300 \text{ kg/mm}^2$ and density of $\gamma = 7900 \text{ kg/m}^3$, and fiber steel cable has a tensile strength of about $\sigma = 2000 \text{ kg/mm}^2$. At present, industry widely produces cheap artificial fibers with a maximum tensile stress of $\sigma = 500\text{--}620 \text{ kg/mm}^2$ and density^{10,11} $\gamma = 800\text{--}1800 \text{ kg/m}^3$. Whiskers have $\sigma = 2000\text{--}8000 \text{ kg/mm}^2$ and density¹⁰ $\gamma = 2000\text{--}4000 \text{ kg/m}^3$, and nanotubes, created in scientific laboratories, have $\sigma = 20,000 \text{ kg/mm}^2 = 2 \times 10^{11} \text{ N/m}^2$ and density $\gamma = 800\text{--}1800 \text{ kg/m}^3$. Theory¹¹ predicts that nanotubes can have $\sigma = 100,000 \text{ kg/mm}^2$ and density $\gamma = 800\text{--}1800 \text{ kg/m}^3$. We will consider a double closed-loop cable in projects below. We will also use the conventional steel cable that has confirmed (safety, permitted) tensile stress of $\sigma = 50\text{--}100 \text{ kg/mm}^2$ or the conventional fibers with a maximum confirmed strength of $\sigma = 200 \text{ kg/mm}^2$ and density $\gamma = 1800 \text{ kg/m}^3$. This means the safety factor is 3–6 or 2.5–3.1. The use of whiskers or nanotubes dramatically improves the parameters of the kinetic anti-gravitator for long distances.

9.5.1 VTOL conventional aircraft (Fig. 9.11)

Let us estimate the parameters of the kinetic anti-gravitator for conventional aircraft. Assume the mass of the aircraft is $M = 20 \text{ ton}$, the takeoff speed is less than or equal to $V_m = 80 \text{ m/s}$ (most aircraft have takeoff speeds of 50–70 m/s), safety stress of the artificial fiber cable is $\sigma = 200 \text{ kg/mm}^2$ and density is $\gamma = 1800 \text{ kg/m}^3$, and the start and landing acceleration is $a = 3g \approx 30 \text{ m/s}^2$. This acceleration is acceptable for the general population (with training, people can withstand 8g permanently and 16g for a short time). The required cable length is $L = V_m^2 / 2a = 80^2 / 60 = 107 \text{ m}$. The total cross-section area of all artificial cable is $S = Ma/(g\sigma) = 20,000 \times 30 / (10 \times 200) = 300 \text{ mm}^2$, and one branch of the four-cable system has a diameter of $d = 10 \text{ mm}$. Cable mass is

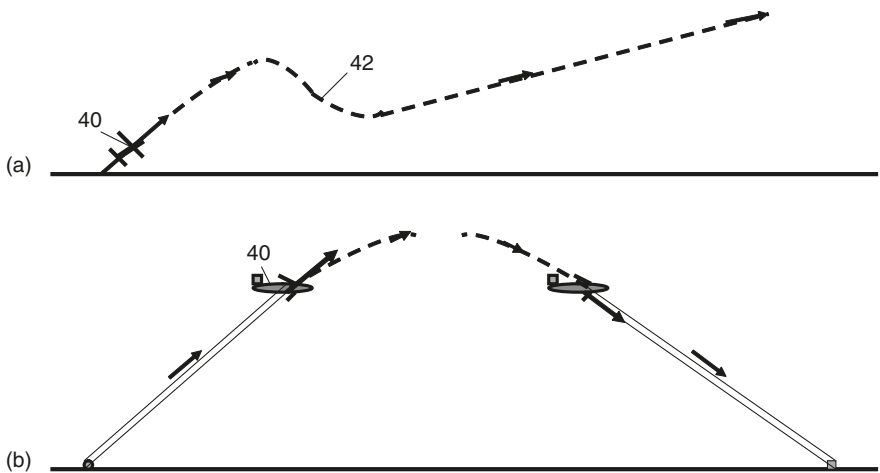


Fig. 9.11. Slope takeoff (a) and landing (b) of conventional aircraft using the kinetic anti-gravitator.
Notations: (40) aircraft and (42) aircraft start trajectory.

$m = SL\gamma = 300 \times 10^{-6} \times 107 \times 1800 = 58$ kg. The cable speed is $V_c = (200 \times 10^7 / 1800)^{0.5} = 1054$ m/s (see equation (9.2)). If the roller is made from the same composite material as the cable, they will maintain this speed. Time of acceleration is $t = V/a = 80/30 = 2.7$ s. The engine power equals the kinetic energy divided by time $P = MV^2/2t = 20,000 \times 80^2/(2 \times 2.7) = 23,704$ kW. This value is 2–3 times more than the power of a typical aircraft engine. However, the start engine may be located on the ground and can have any power. If we want to use an aircraft engine (for cable drive), we must decrease the start acceleration by 2–3 times or use a flywheel. In landing, this energy will return to the flywheel because the distance between the ground and the apparatus is reduced (see the description of innovation).

9.5.2 Non-rocket space apparatus

The same results will apply for a space ship starting from an asteroid or planet without atmosphere. However, if the final speed is high, we must use equation (9.8).

9.5.3 Flying “superman” (Fig. 9.12(a))

Taking on altitude $H = 100$ m, the maximum load is $M = 200$ kg (this is enough for superman, his girl-friend, an engine, and a parachute for safety). The steel cable has tensile stress $\sigma = 100$ kg/mm² and density $\gamma = 7900$ kg/m³. The required total cross-section area of all cables is $S = Mg/\sigma = 2$ mm², cable diameter is $d = 1.6$ mm, the perimeter of the four cables is $s = 10$ mm. The cable mass is $m = SL\gamma = 2 \times 10^{-6} \times 100 \times 7800 = 1.56$ kg, and cable speed is $V = \sqrt{\sigma/\gamma} = \sqrt{10^9/7900} = 356$ m/s. Area parameter is $L_s = L^{0.8}s = 100^{0.8} \times 0.01 = 0.4$. The cable drag is $D = 31$ N (Fig. 9.6 or equations (9.11)–(9.12)), and the required engine power is $P = 11$ kW (Fig. 9.7). The cable can be made from transparent fibers and in any case it will be invisible from a long distance.

9.5.4 Walking “superman” or vehicle (Fig. 9.12(b))

The lower rollers can be made separately and have separate controls. This allows the supermen to walk, run, and move with high speed. For example, if the previous “flying superman” described above takes one step (length 100 m) in 2 s, he will have a speed of 180 km/h.

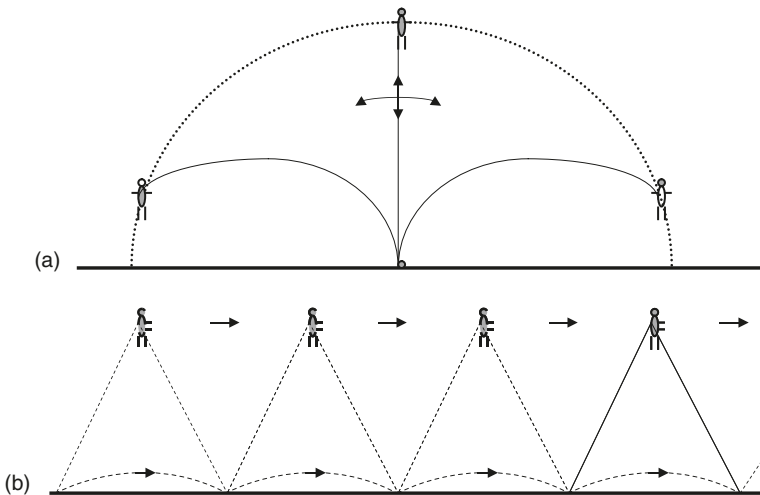


Fig. 9.12. (a) Flying superman using the kinetic anti-gravitator. (b) Legged (walking) superman using two kinetic anti-gravitators.

9.5.5 Jumping (pogo-stick) “superman” (Fig. 9.13(a))

Assume the short kinetic anti-gravitator gives a man of mass $M = 100\text{ kg}$ the speed $V = 70\text{ m/s}$ with acceleration $a = 3g = 30\text{ m/s}^2$. The cable length is $L = V^2/2a = 70^2/(2 \times 30) = 82\text{ m}$. The time of acceleration $t = V/a = 70/30 = 2.33\text{ s}$. The total cross-section areas of all cables is $S = Ma/\sigma = 100 \times 30/(200 \times 10^7) = 1.5\text{ mm}^2$, and the cable mass is $m = SL\gamma = 1.5 \times 10^{-6} \times 82 \times 1800 = 230\text{ g}$. The jump distance at an angle $\alpha = 45^\circ$ without air drag (it is small at this speed) is $J = V^2/g = 70^2/10 = 490\text{ m}$, the altitude is $H = V^2 \sin \alpha / 2g = 70^2 \sin 45^\circ / 20 = 173\text{ m}$, jump time is about 10 s. The required starting thrust is 300 kg, and the start (jump) power is about $P = E/t = mV^2/2t = 100 \times 70^2/(2 \times 2.33) = 105\text{ kW}$, but the start energy will be restored in landing except for the air drag loss of 10–20%. If we have an energy accumulator, a permanent power of 5–10 kW will be enough for this device.

9.5.6 Jumping vehicle

Assume the kinetic anti-gravitator gives a vehicle of mass $M = 1000\text{ kg}$ the speed of $V = 200\text{ m/s}$ with acceleration $a = 8g = 80\text{ m/s}^2$ (which is acceptable for military soldiers).

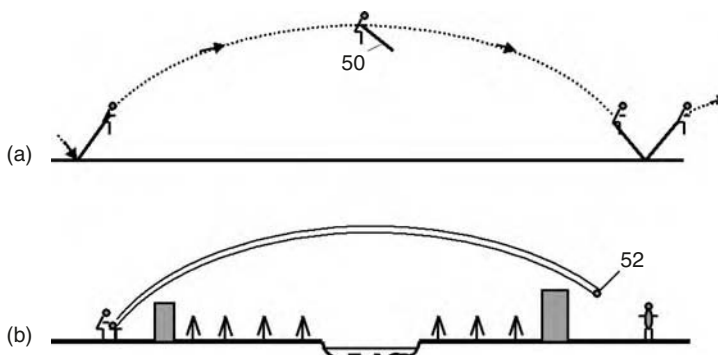


Fig. 9.13. (a) “Superman” using the jump kinetic anti-gravitator (50). (b) The super-hand (52), which allows operation at long distances of 1–10 km.

The cable length is $L = V^2/2a = 200^2/2/80 = 250$ m. The time of acceleration $t = V/a = 2.5$ s. The jump distance at an angle of 45° without air drag (it is not very much for a streamlined body) is about 4 km, the altitude is 1.4 km, and the jump time is about 20 s. The cross-section area of all the cables is $S = Ma/\sigma = 1000 \times 80/200/10^7 = 40$ mm 2 . Cable mass is $m = SL\gamma = 40 \times 10^{-6} \times 250 \times 1800 = 18$ kg. The required start thrust is 8 ton, and the jump power is about $P = 8000$ kW, but the start energy will be restored in landing except for the air drag loss of 10–20%. If we have an energy accumulator, an engine with 500–800 kW power will be enough for this device. The vehicle can have a small wing (area 2 m 2) and glide from an altitude of 1.4 km for a the distance of 14–17 km to the selected place for the next jump.

9.5.7 Long arm (long hand) (Fig. 9.13(b))

The proposed method allows us to create a “long arm” which suspends a video camera or weapon aloft. Assume the load mass of the long hand is $M = 2$ kg and the hand has a length of 1 km. The hand uses a steel cable with $\sigma = 100$ kg/mm 2 and $\gamma = 7.9$ g/cm 3 . Maximum speed is:

$$V = \sqrt{\sigma/\gamma} = \sqrt{10^9/7900} = 356 \text{ m/s.}$$

The cross-section area is $S = M/\sigma = 2/100 = 0.02$ mm 2 , $d = 0.08$, $s = 1$ mm, and the cable mass is $m = SL\gamma = 0.02 \times 10^{-6} \times 1000 \times 7900 = 158$ g. The cross-section area parameter is $L_s = L^{0.8}s = 1000^{0.8} \times 0.001 = 0.25$. The cable drag is $D = 20$ N (Fig. 9.6 or equations (9.11)–(9.12)), and the required engine power $P = 6.8$ kW (Fig. 9.7). The operator (for example, a soldier) can observe regions within a 1-km radius and immediately apply the weapon if necessary. The radius may be increased up to 10 km. If using a more powerful kinetic anti-gravitator that can hold a load of 200 kg with a net and catcher installed at the end of the cable, the operator can catch the soldier and deliver him or her to another place. This may be very useful for rescue and anti-terrorist operations.

9.5.8 High-altitude crane

The construction of skyscrapers needs high cranes. Consider the design of a crane of $L = H = 500\text{-m}$ height using the offered method. Take the useful load as 1 ton and the steel cable as having safe tensile stress of $\sigma = 50\text{ kg/mm}^2$ and cable density of $\gamma = 7.9\text{ g/cm}^3$. The total cross-section cable area is (equation (9.4)) $S = F/(\sigma - \gamma gH) = 22\text{ mm}^2$. The cable mass is $m = SyH = 2 \times 10^{-6} \times 500 \times 7900 = 87\text{ kg}$, and safe cable speed is $V = (\sigma/\gamma)^{0.5} = 250\text{ m/s}$. If the installation has four cables of diameter $d = 2.6\text{ mm}$ each, the total perimeter of the four cable is $s = 4\pi d = 33.2\text{ mm}$, the parameter $L_s = L^{0.8}s = 500^{0.8} \times 0.0332 = 4.8$, the cable air drag is $D = 200\text{ N}$ (Fig. 9.6, equation (9.10)), and the required power to support cable rotation is $P = 50\text{ kW}$ (Fig. 9.7, equation (9.12)). This is the highest (500 m) and the lightest (87 kg) crane in the world having a load capability of 1 ton.

9.5.9 High tower

Consider the design of a high tower of $L = H = 4\text{ km}$ using the offered method. Take the useful load as 30 ton and the steel cable as having a safe tensile stress of $\sigma = 50\text{ kg/mm}^2$ and cable density of $\gamma = 7.9\text{ g/cm}^3$. The total cross-section (all branches) of the cable area is (equation (9.4)) $S = F/(\sigma - \gamma gH) = 1630\text{ mm}^2$. Cable mass is $m = SyH = 51.5\text{ ton}$, and safe cable speed is $V = (\sigma/\gamma)^{0.5} = 250\text{ m/s}$. If the installation has four cables, the diameter of one cable is $d = 23\text{ mm}$, the total perimeter of the four cable is $s = 4\pi d = 0.289\text{ m}$, the parameter $L_s = L^{0.8}s = 4000^{0.8} \times 0.289 = 220$, the cable air drag is $D = 9500\text{ N}$, and the required power to support cable rotation is $P = 2.3\text{ MW}$. This is highest (4 km) and the lightest (52 ton) tower in the world, which has a load capability of 30 ton at the top.

Note: The computation for the same tower in “Kinetic Space Towers and Launchers”³ with an artificial fiber cable, having a safe tensile stress of $\sigma = 200\text{ kg/mm}^2$ and density of $\gamma = 1800\text{ kg/m}^3$, gives the required speed of $V = 1000\text{ m/s}$ and power $P = 11\text{ MW}$. We have changes only in the cable material (from artificial fiber to steel). As a result, the required support power decreases by approximately 5 times, and the total production cost for delivery of one tourist decreases from \$3.35 to \$1.4. This happens because the required speed decreases from 1000 to 250 m/s, decreasing the required power and fuel consumption. The power depends on the third order ($V^{2.8}$, see equation (9.12)) of speed.

This shows that the parameters of the considered example are very far from optimal. On the other hand, the cable mass increases from 1.13 to 51.5 ton.

9.5.10 The construction of the Artsutanov space elevator without rockets

The space elevator, first proposed by Y. Artsutanov in 1959, may be a promising breakthrough in space. However, the space elevator needs an equalizer weighing hundreds of tons, and thousands of tons of cable. Also, delivery using rockets into geosynchronous orbit is very expensive. When nanotubes become cheaper the offered kinetic anti-gravitator will allow the construction of the space elevator without rockets. The author shows in “Kinetic Space Towers and Launchings”³ that if $K = \sigma/\gamma/10^7 > 5$ the cable

space tower (cable mast) can be up to 150,000 km high or more. This is enough to reach geosynchronous orbit (37,000 km).

9.6 Discussion

In 2002 Loftstrom⁴ published a description of a space launcher. The offered device has the following technical and physical differences from the Loftstrom installation.

The Loftstrom installation has a 2000-km long launch path located at an altitude of 80 km, which accelerates the space vehicle to space speed. The Loftstrom space launcher is *non-connected plates* of complex path enclosed in an immobile tube. The *plates are* made from rubber–iron material and is moved using an electromagnetic linear engine. The *plates are* turned by electromagnets.

The idea offered in this chapter is the kinetic device which creates a push (repulsive, repel) force between two given bodies (for example, between a planet and the apparatus). This force supports a body at a given altitude. The body is connected to the cable by rollers that slide along the cable. The cable can be made of artificial fiber and moved by the rollers and any engine. The kinetic anti-gravitator supports any body at altitude (for example, towers) and may also be used to launch vehicles. The Loftstrom device is

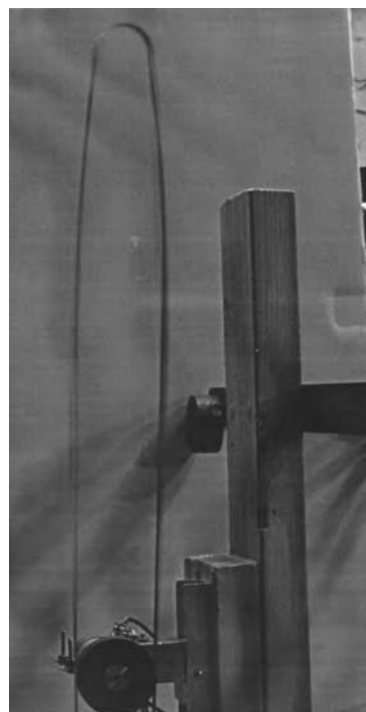


Fig. 9.14. Experiment: Rotated closed-loop cable in vertical position. Experiments show that the high speed closed-loop straight-line cable is stable in any direction including the horizontal position.

only a space launcher and cannot permanently support a body at altitude or towers (he did not write anything about this).

The kinetic anti-gravitator creates a permanent controlled force. If the distance between bodies does not change, the kinetic anti-gravitator requires only a small amount of energy to compensate for the friction in the rollers and air.¹²

9.7 Conclusion

The offered method, the kinetic anti-gravitator, may be applied in many fields and may have a big future. The method does not need special technology. Current cheap and widely produced materials such as steel or artificial fiber can be used to operate up to an altitude of 75–225 km. The kinetic anti-gravitator is simple and does not need complex equipment. If the installation is designed correctly, Lishanski's experiments show that the high-speed closed-loop straight line cable is stable in any direction including the horizontal positions, Fig. 9.14.

References

1. A.A. Bolonkin, “Theory of Flight Vehicles with Control Radial Force”, *Collection Researches of Flight Dynamics*, Mashinostroenie Publishers, Moscow, 1965, pp. 79–118 (in Russian).
2. A.A. Bolonkin, “Transport System for Delivery of Tourists at Altitude 140 km”, IAC-02-IAA.1.3.03, *53rd International Astronautical Congress. The World Space Congress – 2002*, 10–19 October 2002, Houston, TX, USA.
3. A.A. Bolonkin, “Kinetic Space Towers and Launchers”, *Journal of British Interplanetary Society*, Vol. 57, No. 1/2, 2004, pp. 33–39.
4. K.H. Lofstrom, “The Launch Loop: A Low Cost Earth-to-High-Orbit Launch System”, 2002, <http://www.Launchloop.com/launchloop.pdf>
5. A.A. Bolonkin, “Centrifugal Keeper for Space Stations and Satellites”, *Journal of the British Interplanetary Society*, Vol. 56, No. 9/10, 2003, pp. 314–327.
6. J.D. Anderson, *Hypersonic and High Temperature Gas Dynamics*, McGraw-Hill Book Co., New York, 1989.
7. A.A. Bolonkin, “High Efficiency Transfer of Mechanical Energy”, AIAA-2004-5660, *International Energy Conversion Engineering Conference*, Rhode Island, 16–19 August 2004.
8. A.A. Bolonkin, “Air Cable Transport”, *Journal of Aircraft*, Vol. 40, No. 4, July–August 2003.
9. A.A. Bolonkin, “Air Cable Transport and Bridges”, TN 7567, *International Air and Space Symposium – The Next 100 Years*, 14–17 July 2003, Dayton, OH, USA.
10. *Carbon and High Performance Fibers*, Directory, Chapman & Hall, New York, 1995.
11. M.S. Dresselhous, *Carbon Nanotubes*, Springer, New York, 2000.
12. A.A. Bolonkin, “Kinetic Anti-gravitator”, AIAA-2005-4505, *41st Propulsion Conference*, 10–12 July 2005, Tucson, AZ, USA.

This page intentionally left blank

CHAPTER 10

Centrifugal Space Launchers*

Summary

The purpose of this chapter is to draw attention to the idea of sling rotary launchers. This idea allows the building of inexpensive new space launcher systems, to launch missiles, projectiles, and space apparatus (s.a.), and to use many types of energy. This chapter describes the possibilities of this method and the conditions which influence its efficiency. Included are four projects: a non-rocket sling projectile launcher, a space sling launcher, a space ship for launching using conventional supersonic, and a space ship using subsonic aircraft. The last two only require low-cost cable made from artificial fiber, using whiskers that are produced in industry now or increasingly perfected nanotubes that are being created in a scientific laboratories.

Nomenclature

A	general work [J]
A_1	acceleration work for space apparatus (s.a.)
A_2	sling acceleration work
A_3	s.a. air drag work
A_4	sling air drag work
A_5	acceleration and air drag work of lever (disk). Value A_5 equals 0 for the aircraft launcher and it may be estimated for the lever using conventional calculations
a	the speed of sound [m/s]
c	the relative thickness of the sling ($c = 0.07\text{--}0.1$)
c_L	the lift coefficient of the s.a. ($c_L = 0\text{--}1$)
D	the vehicle drag [N]
D_c	air drag of the sling
$g = 9.81 \text{ m/s}^2$	the Earth's gravity
H	the altitude [m]

* The detailed work was presented as AIAA-2005-4035 at the *41st Propulsion Conference*, 10–12 July 2005, Tucson, AZ, USA.

ΔH	the change in altitude [m]
Δh	the additional altitude of the s.a. [m]
k	the strength coefficient [m^2/s^2]
k_1	the aerodynamic efficiency of the s.a.
L	the vehicle range [m]
L_c	the sling lift force [N]
M	the flywheel's mass [kg]
m	mass of space apparatus [kg]
n	centrifugal overload [g]
n_1	the vertical overload of the s.a. [g]
P	the engine power [W]
R	radius of the s.a. trajectory [m]
R_0	lever radius [m]
R_b	the range of ballistic trajectory [m]
S	cross-section sling area [m^2]
S_0	the sling cross-section area near the lever [m^2]
\bar{S}_0	the relative cross-section area near the lever [m^2]
S_c	the sling wing area [m^2]
S_s	the sling cross-section area at the sling center of gravity [m^2]
S_w	the required area of the s.a. wing [m^2]
T	the thrust of the lead aircraft or force on the lever [N]
t	the acceleration time [s]
t_p	the time between launches [s]
Δt	the elapsed time [s]
V	the speed of the s.a. [m/s]
V_0	speed of the lever end [m/s]
V_c	the average sling speed or speed of the center of gravity of the sling [m/s]
V_a	the average speed of the s.a. [m/s]
ΔV	the change in s.a. speed [m/s]
α_c	the sling attack angle [rad]
σ	sling stress [N/m^2]
σ_f	the safe stress on the flywheel [N/m^2]
γ	the density of the sling [kg/m^3]
γ_f	the density of the flywheel [kg/m^3]
ρ	the air density [kg/m^3]
θ	the trajectory angle [rad]
$\Delta \theta$	the change in the trajectory angle [rad]
θ_a	the average trajectory angle [rad]

The subscript “b” means the initial value of the ballistic trajectory.

10.1 Introduction

At present, rockets are used to carry people and payloads into space.¹ Other than rockets, one method of reaching space is the space elevator.² This is very complex, expensive, and technologically impossible at the present time. Once industry produces low-cost

nanotubes, the author has shown that the space elevator may be easily built without rockets (Project 4).³ Also offered is a transport system for the space elevator.⁴ The author has also proposed a centrifugal keeper and launcher for space stations and satellites,⁵ a hypersonic tube air rocket of high capacity,^{6,9} optimally inflated space towers of 3–100-km height,⁷ using asteroids as a propulsion system for space ships,⁸ a multi-reflection beam launcher,¹⁰ a new method of flight – a kinetic anti-gravitator,¹¹ and has researched optimal trajectories and space cable launcher.^{12,13} Many of them are in this book.

The space elevator requires very strong nanotubes, as well as a rocket and the high technology needed for the initial development. The tube air rocket and non-rocket systems require more detailed research. The electromagnetic transport system, suggested by Minovich,¹⁴ is not realistic at the present time. This requires a vacuum underground tunnel 1530-km long located at a depth of 40 km. The project requires a power cooling system (because the temperature is very high at this depth), a complex electromagnetic power system, and a huge impulse of energy that is greater than the power of all of the electricity generator stations on Earth. The beam propulsion system¹⁵ needs very powerful lasers and magnetic sails¹⁶ have many problems. The author is suggesting a very simple and inexpensive method and installation for launching payloads into space.

The presented work is a new space launcher system for achieving high supersonic speeds. The main difference from a conventional centrifugal launcher is the light, strong sling that dramatically increases the apparatus speed. The sling launcher can produce supersonic vehicle speed in the Earth's atmosphere and space vehicle speed in a vacuum. This method uses a strong sling (cable), a power (drive) station, conventional engines (mechanical, electrical, gas turbines), and flywheels (for energy storage) located on the ground.

A conventional high-speed aircraft may also be used in this manner to launch projectiles and space ballistic space ships.

10.2 Description of innovative launcher

10.2.1 Ground sling launcher

The installation includes (see notations in Fig. 10.1): a tower, a lever (or disk), a sling (cable), and conventional engines and flywheels (drive station). Optimally, the installation is located on a mountain (high altitude) to reduce air drag on the sling and apparatus, and for a lower slope of initial trajectory angle. A winged s.a. (space ship, missile, probe, projectile, etc.) is connected to the end of the sling.

The installation works in the following way (Fig. 10.1). The engine rotates the flywheels. When the flywheels accumulate sufficient energy, they rotate as a lever. The lever accelerates the s.a. The apparatus may be located on the lever and the sling is increased after the start. The apparatus speed increases. It is greater than the lever speed in the ratio R/R_0 , where R is the radius of the apparatus trajectory circle, R_0 is the radius of the lever (or disk). When the apparatus reaches its chosen speed, the winged apparatus is disconnected from the sling at the desired point of the circle. While the winged apparatus is flying in the atmosphere, it can increase its slope and correct its trajectory. If the apparatus has a hypersonic (supersonic) form, the speed loss is small.¹³

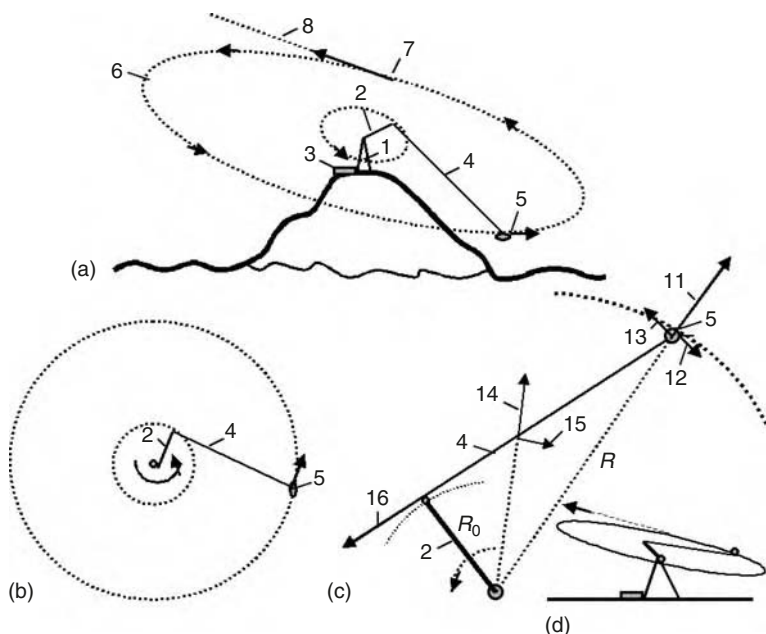


Fig. 10.1. Sling rotary launcher. (a) Launcher located on mountain, (b) top view of installation, (c) acting forces, (d) side view. *Notations:* (1) Tower; (2) lever or disk; (3) engine; (4) sling; (5) s.a.; (6) circular launch trajectory; (7) point of disconnection; (8) direction of launch; (11) centrifugal force of s.a.; (12) drag of s.a.; (13) speed of s.a.; (14) centrifugal force of sling; (15) drag of sling; and (16) lever force.

The offered launcher is different from conventional centrifugal catapults, which have a projectile in a lever. This launcher has a long sling and the projectile is in the sling. The sling increases the lever speed many times and decreases the mass of the lever. Conventional catapults made from nanotubes have a huge mass and require gigantic energy to work. This sling is also made from nanotubes (for space speed), but its mass is small.

If the circle is parallel to the Earth's surface, the winged apparatus disconnects from the cable, converts the linear and centrifugal acceleration into vertical acceleration (while it is flying in the atmosphere) and leaves the Earth's atmosphere.

The power station houses the engine. It can be any engine, for example, a gas turbine, or an electrical or mechanical motor. The power drive station also has an energy storage system (flywheel accumulator of energy), a transmission drive train, and a clutch mechanism.

The installation can be set on a slope, and launch a projectile at an angle to the horizon (Fig. 10.1).

The attained speed may be up to or more than 8 km/s (see Project 2 below). If the planet does not have an atmosphere, a small installation (with a small lever) can give the projectile a very high speed, limited only by the power of the engine and the strength of the sling.

On the Earth's surface the launcher can be located under a special cover (or in a tube) in a vacuum.

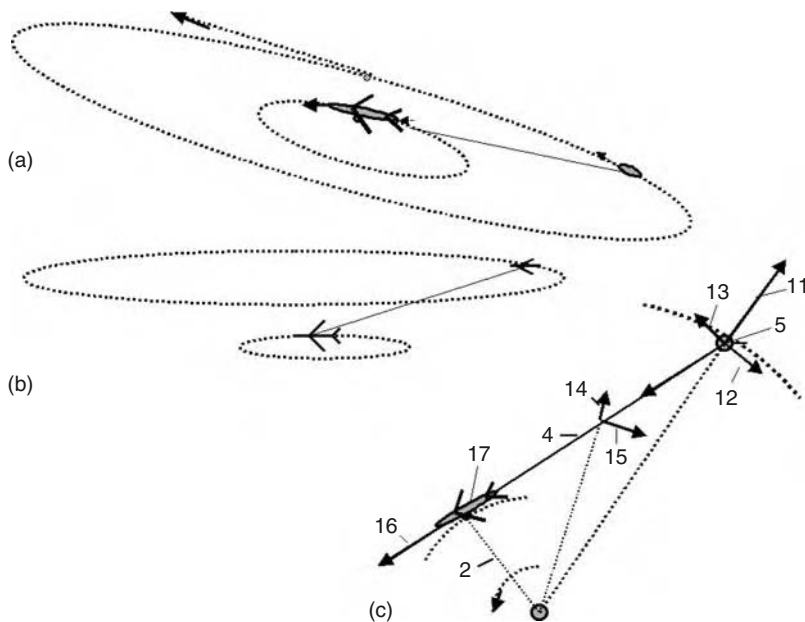


Fig. 10.2. Launching a space ship using aircraft. (a) Slinging slope start; (b) upper start; and (c) installation forces.

10.2.2 Aircraft sling launcher

Another design of this sling launcher is presented in Figs. 10.2–10.4. A small spacecraft (1–2 ton) is connected to a large, high-speed aircraft. The aircraft flies in a circle, increasing the sling length, and accelerating the ship to high speed. The attained speed depends largely on the specific strength of the sling, the maximum aircraft speed, and the thrust of the aircraft. For large existing aircraft operating in the atmosphere, the launch speed may reach up to 2 km/s. This is enough for the X-prize flight, reaching an altitude of up to 100 km and sufficient for a space ship for tourists (see Projects 3 and 4 below).

10.2.3 Advantages

The suggested launch cable system has advantages compared to the current rocket systems, as follows:

1. The sling launcher is many times less expensive than modern rocket-launch systems. No expensive rockets are needed. Only motor and cable are required.
2. The sling launcher reduces the delivery cost by several thousand times (to as low as \$5–10/lb). (No rocket, cheaper fuel.)
3. The sling launcher could be constructed within 1–2 years. The aircraft sling launcher requires only a cable and a space ship. Modern rocket-launch systems require many years for research and development (R&D) and construction.

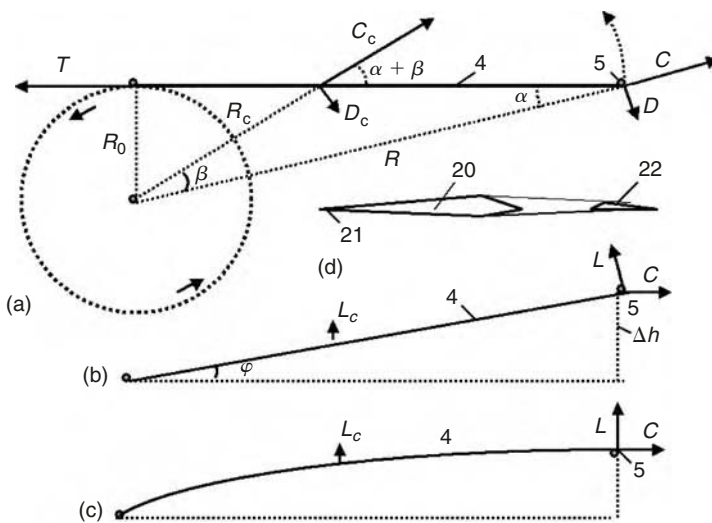


Fig. 10.3. Forces acting on the sling launcher. (a) Top view, (b) cone launching when lift force of sling equals sling weight (side view), (c) cone launching when sling lift force is more than sling weight (side view), (d) cross-section of the sling. Notations: (20) Sharp thin sling; (21) head protection, and (22) stabilizer of sling.

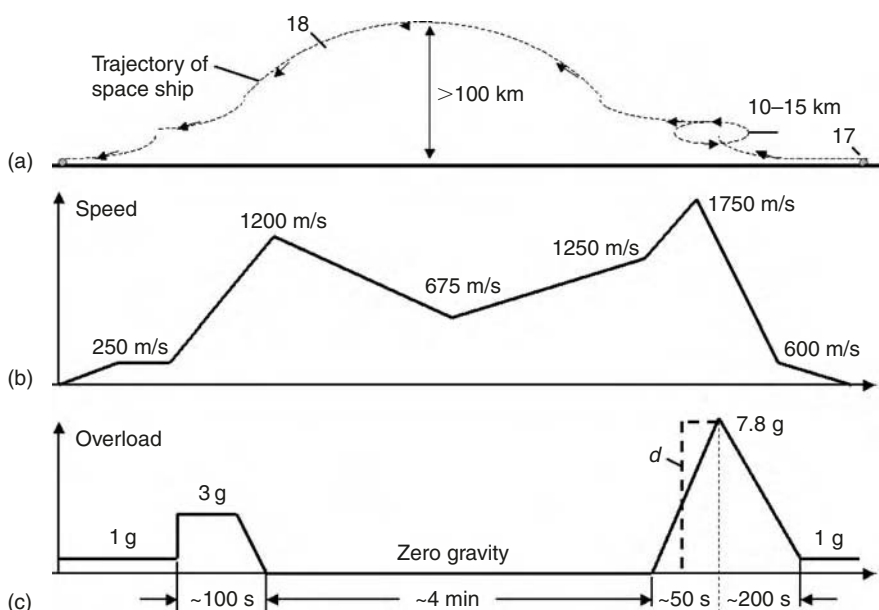


Fig. 10.4. (a) Space flight trajectory. Notations: (17) Aircraft; and (18) trajectory of space ship; (b) Graph of ship speed (Project 3); (c) Graph of ship overload (Project 3); (d) Change of overload graph in Project 4.

4. The sling launcher does not require high technology and can be made by any non-industrial country.
5. Rocket fuel is expensive. The ground sling launcher can use the cheapest sources of energy, such as wind, water, or nuclear power, or the cheapest fuels such as gas, coal, peat, etc., because the engine is located on the Earth's surface. Flywheels may be used as an accumulator of energy.
6. It is not necessary to have highly qualified personnel, such as rocket specialists with high salaries.
7. The fare for space tourists would be small.
8. There is no pollution of the atmosphere from toxic rocket gas.
9. Thousands of tons of useful payloads can be launched annually.

Shortcomings of sling space launchers:

1. The need for a very strong sling (cable), made from carbon whiskers or still-to-be manufactured long nanotubes.
2. The Earth ground sling launcher may be used only for robust loads because high centrifugal acceleration is imposed on the payload. Such payloads normally account for 70–80% of space payloads.

10.2.4 Cable (sling) discussion

The experimental and industrial fibers, whiskers, and nanotubes are considered in Chapters 1 and 2.

The reader can find a more complete cable discussion of cable and cable characteristics in the Refs. [3–13,17–20].

10.3 Theory of the sling launcher

10.3.1 Formulas for estimation and computation (in metric system)

10.3.1.1 Centrifugal force

Centrifugal force, C , cross-section area of the sling at the s.a., S , and the speed of the s.a., V , are calculated using conventional equations:

$$C = \frac{V^2}{R}, \quad n = \frac{C}{g}, \quad S = \frac{mC}{\sigma}, \quad \frac{R}{R_0} = \frac{V}{V_0}. \quad (10.1)$$

10.3.1.2 Optimal relative sling cross-section area

Optimal relative sling cross-section area, \bar{S} , along radius, r , and at $r = 0$, \bar{S}_0 , are:

$$\bar{S} = \exp \left\{ \frac{V^2}{2k} \left[1 - \left(\frac{r}{R} \right)^2 \right] \right\}, \quad \bar{S}_0 = \exp \left\{ \frac{V^2}{2k} \right\}, \quad \text{where } k = \frac{\sigma}{\gamma}, \quad (10.2)$$

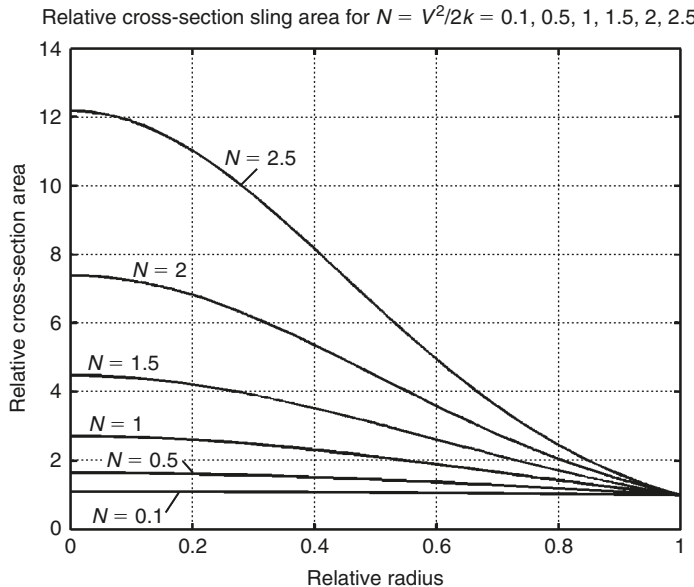


Fig. 10.5. Relative cross-section area of sling for different ratio is $N = V^2/2k$ in equation (10.2).

The results of computation (equation (10.2)) are presented in Figs. 10.5 and 10.6. For low k the relative area, \bar{S} , is very large. For example, a conventional fiber with $k = 2 \times 10^6$ requires this parameter to be 2.72 for a speed of $V = 1410 \text{ m/s}$.

10.3.1.3 Air drag

Air drag (Fig. 10.7) of s.a., D , and air drag of the sling, D_c , are approximated as follows:

$$D = \frac{mn_1 g}{k_1}, \quad D_c = 4c^2 \rho a V_c S_c / 2, \quad S_c = R \sqrt{\frac{S_s}{c}}, \quad L_c = 2\alpha_c \rho a V_c S_c. \quad (10.3)$$

Additional drag forces arising from the sling lift force are small, and are ignored in this analysis.

The sling has a variable speed of from 0 to V , and a variable wing area. To simplify, we assume the average value as near the sling's center of gravity. In an effort to decrease air drag, the sling has a sharp form and is stabilized by a stabilizing tail (Fig. 10.3(d)). The s.a. and sling also have a thin ceramic cover for protection against the short periods of launch heating. More exactly, the sling drag may be calculated by integration.

10.3.1.4 Flight angle of cone

To decrease the sling drag, the wing apparatus and the sling have an attack angle and lift force. They climb at high altitude where the air has low density (Fig. 10.3(b)). The sling moves along a cone surface. The sling lift force may be more than the sling weight and then the sling will be curved at the top, as shown in Fig. 10.3(c). In this case, the

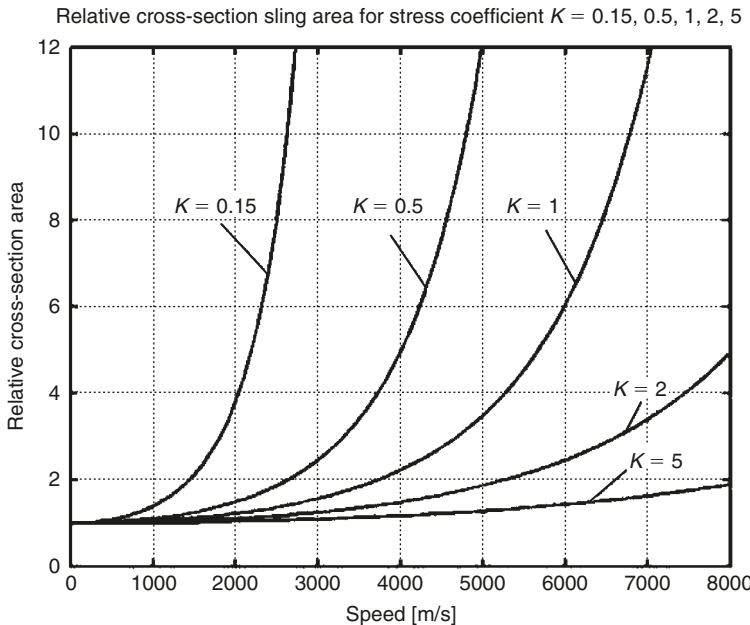


Fig. 10.6. Relative cross-section area of sling with \bar{S}_0 in $r = 0$ via sling end speed and a stress coefficient $K = 10^{-7}k$ (equation (10.2)).

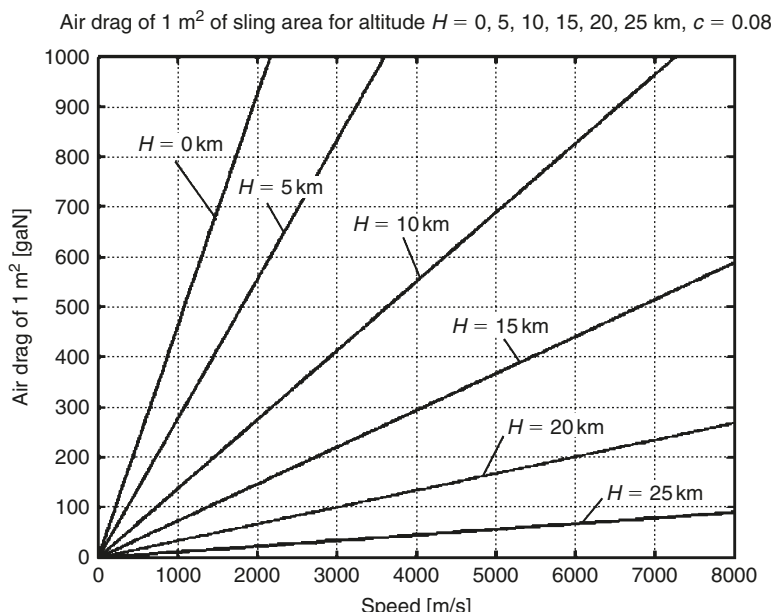


Fig. 10.7. Air drag of 1 m^2 of wing sling (with relative profile thickness $c = 0.08$) based on speed and altitude (equation (10.3)).

fastest part of the cable will be in the low-density upper atmosphere. The additional sling drag from the lift force is small and we ignore it here.

The additional altitude, Δh , of the s.a. may be found from the equation:

$$\sin \varphi \approx \varphi = \frac{\Delta h}{R} = \frac{n_1 - 1}{n} \quad (10.4)$$

10.3.1.5 Vacuum

In a vacuum, the ratio R/R_0 may be large. However, when the sling moves in the atmosphere, the common projection of all forces perpendicular to the sling must be greater than zero. Only in this case may the system be accelerated. This gives rise to two inequalities (the necessary *acceleration inequalities*).

$$\begin{aligned} C \sin \alpha &> (g/k_1) \cos \alpha, & mC \sin \alpha + m_c C_c \sin(\alpha + \beta) &> D \cos \alpha + D_c \cos(\alpha + \beta) \\ C_c &= V_c^2/R_c, & \sin \alpha &= R_0/R, & \sin \beta &= R_0/R_c, \\ C_c &= V_c^2/R_c, & m_c &= \gamma S_s L_s, \end{aligned} \quad (10.5)$$

where C_c is the average centrifugal acceleration of the sling [m/s^2]; m_c is the sling mass [kg]; and L_s is the sling length [m].

10.3.1.6 Engine power

Engine power and the necessary mass of the flywheel may be estimated by the following equations:

$$\begin{aligned} A &= A_1 + A_2 + A_3 + A_4 + A_5, & A_1 &= \frac{mV^2}{2}, \\ A_2 &= \frac{m_c V_c^2}{2}, & A_3 &= \frac{mg}{k_1} t, & A_4 &= \frac{D_c V_c}{4} t, \\ M &= \frac{2\gamma_f A}{\sigma_f}, & P &= \frac{A}{t_p}, & T &= \sigma S_0 = nm g \bar{S}_0, \\ S_w &= \frac{2n_1 mg}{c_L \rho a V}, & L &= \frac{k_1 V^2}{2g}. \end{aligned} \quad (10.6)$$

The value of A_5 equals 0 for the aircraft launcher and may be estimated for the lever using conventional calculations.

10.3.1.7 Estimation of tourist trajectory

Estimation of tourist trajectory of the space vehicle.

(a) *The vertically accelerated part of the trajectory.* The purpose of this part of the trajectory is to increase the trajectory slope, θ , relative to the horizon. The trajectory may be computed by the following differential equations:

$$\dot{H} = V \sin \theta, \quad \dot{V} = -\frac{D}{m} - g \sin \theta, \quad \dot{\theta} = \frac{L}{mV} - \frac{g}{V} \cos \theta. \quad (10.7)$$

Changes in the trajectories parameter may be estimated using equations obtained from conventional aircraft equations (10.7)

$$\Delta t = \frac{\Delta H}{V_a \sin \theta_a}, \quad \Delta V = -g \left(\frac{n_1}{k_1} + \sin \theta_a \right) \Delta t, \quad \Delta \theta = \frac{g}{V_a} (n_1 - \cos \theta_a) \Delta t, \quad (10.8)$$

where n_1 is the vertical overload of the s.a. [g].

(b) *The ballistic part* of the space vehicle (apparatus) trajectory may be calculated by conventional equations as follows:

$$\Delta H_b = \frac{V_b^2 \sin^2 \theta_b}{2g}, \quad R_b = \frac{V_b^2 \sin 2\theta_b}{g}, \quad t_b = \frac{R_b}{V_b \cos \theta_b}, \quad (10.9)$$

where the subscript “b” means the initial value of the ballistic trajectory and R_b is the range of the ballistic trajectory.

10.4 Projects

Described below are details and estimates of four projects:

1. Projectile launcher for long distances, using a sling made from currently available artificial fibers.
2. Space projectile launcher, with a sling made from whiskers.
3. Tourist flights using supersonic aircraft with a sling made from nanotubes.
4. Tourist flights using subsonic aircraft with a sling made from whiskers.

These projects are not optimized. They only illustrate the method and rough estimations for installations for different purposes. We sometimes indicate thrust (forces) in kilograms or tons, and stress in kilogram per square millimeter. For reader reference, $1 \text{ kg} = 9.81 \text{ N} \approx 10 \text{ N}$ (newton), $1 \text{ ton} \approx 10^4 \text{ N}$, and $1 \text{ kg/mm}^2 \cong 10^7 \text{ N/m}^2$.

10.4.1 Project 1

Projectile launcher for long distances, using a sling made from existing artificial fiber (Fig. 10.1).

Assume the mass of the projectile (load) is $m = 100 \text{ kg} = 0.1 \text{ ton}$, the required final projectile speed is $V = 2500 \text{ m/s}$, the length of the lever (or disk radius) is $R_0 = 10 \text{ m}$, the maximum lever speed is $V_0 = 800 \text{ m/s}$, the safe sling stress is $\sigma = 180 \text{ kg/mm}^2$, and the sling density is $\gamma = 1800 \text{ kg/m}^3$. The coefficient $k = \sigma/\gamma = 0.1 \times 10^7$. If aerodynamic efficiency is $k_1 = 6.5$, a speed of 2500 m/s is sufficient for a projectile range of 2000 km (equation (10.6)).

The radius of the circle is $R = R_0 V/V_0 = 10 \times 2500/800 = 31.25$ m. Conventional gas turbines have a blade tip speed of up to 600–800 m/s in a high-temperature gas flow.²¹ Our lever (or disk) made from current composite material can maintain a speed of 800 m/s, because the lever radius is larger and is not exposed to high temperature. These parameters are not optimal. Our purpose is only to show that the offered launcher is possible using current technology. Industry widely produces cheap artificial fiber with $\sigma = 500\text{--}620 \text{ kg/mm}^2$. The safety coefficient is $n = 620/180 = 3.44$.

10.4.1.1 Computations

The maximum centrifugal overload of the projectile is $C = V^2/R = 6 \times 25 \times 10^6/31.25 = 2 \times 10^5 \text{ m/s}^2 = 2 \times 10^4 \text{ g}$. This overload and acceleration are the same as these of a conventional cannon. Maximum centrifugal force exerted on the projectile is $F = m \times C = 10^2 \times 2 \times 10^5 = 2 \times 10^7 \text{ N} = 2000 \text{ ton}$. The sling cross-section area near the projectile is $S = F/\sigma = 2000/0.18 = 11,111 \text{ mm}^2 = 111 \text{ cm}^2$. The sling cross-section area near the lever is $\bar{S} = 23$, $S_0 = \bar{S} \times S = 0.255 \text{ m}^2$, (equation (10.2)). The average cross-section area is $S_a = 0.5 \times (0.0111 + 0.255) = 0.133 \text{ m}$. If the relative sling thickness is $c = 0.1$, the average sling width is $b = (S_a/c)^{0.5} = 1.15 \text{ m}$. The wing sling area is $S_k = b \times R = 1.15 \times 30 = 34.5 \text{ m}^2$, (equation (10.3)). Assume the sling center of gravity is at $R_c = 0.35R = 12.5 \text{ m}$, $V_c = 0.35V = 875 \text{ m/s}$. Sling mass is $m_c = \gamma S_a R = 1800 \times 0.133 \times 30 = 7182 \text{ kg} = 7.2 \text{ ton}$. The sling centrifugal acceleration is $C_c = V_c^2/R_c = 875^2/11 = 69.6 \times 10^3 \text{ m/s}^2$, the sling centrifugal force is $F_c = m_c C_c = 7182 \times 69.6 \times 10^3 = 5 \times 10^8 \text{ N} = 50,000 \text{ ton}$. For $\rho = 1.225$, $a = 330 \text{ m/s}$, $k_1 = 5$, the sling air drag is $D_c = 24.5 \text{ ton}$ (equation (10.3)), and the projectile air drag is only $D = m/k_1 = 100/5 = 20 \text{ kg}$.

The angle $\alpha \approx R_0/R = 10/31.25 = 0.32 \text{ rad}$, and the angle $\beta \approx R_0/R_c = 10/11 = 0.91$ (Fig. 10.3(a)).

The acceleration inequality (10.5) is $46,140 > 24$. This is acceptable.

Assuming an acceleration time of $t = 25 \text{ s}$, the work of acceleration and air drag of the installation are follows: projectile acceleration work $A_1 = 0.312 \times 10^9 \text{ J}$, sling acceleration work $A_2 = 2.75 \times 10^9 \text{ J}$, a 30-ton disk (lever) acceleration work $A_3 = 0.2 \times 10^9 \text{ J}$, sling drag work $A_4 = 1.34 \times 10^9 \text{ J}$ (equation (10.3)). We neglect projectile and disk drag. The total launch energy is $A = 4.6 \times 10^9 \text{ J}$. The flywheel mass is $M = 9.2 \text{ ton}$. If the time between launches is $t_p = 30 \text{ min} = 1800 \text{ s}$, the required engine power is $P = A/t_p = 4.6 \times 10^9/1800 = 2.56 \text{ MW}$. This is the power of a conventional aviation turbo engine.

Without energy recuperation, the launchers efficiency (conversion of mechanical energy into projectile speed) is 7%. With energy recuperation (kinetic energy of the sling and disk is used for flywheels support), the launcher efficiency reaches 36%.

10.4.1.2 Discussion of Project 1

Compare the offered sling launcher with the big cannon (Project HARP²²) built and tested after World War II. The cannon barrel had a diameter of 42.4 cm, and a length of up to 86–126 calibers (58 m). Weight of the gunpowder was 342 kg, projectile weight was 174 kg, and the projectile speed was 1840 m/s. The range was 183 km and the altitude 50 km for a 50°angle of sight. A speed of 3200 m/s was reached for a projectile weight of 20 kg and a length of 126 calibers. Maximum pressure was 340 MPa. The cannon cost about \$10 million (1946).

The offered sling launcher installation can launch a winged projectile and has a range of up to $L = k_1 \times V^2/2g = 6.5 \times 2500^2/20 = 2031$ km.¹² Improved sling material will permit this capability. The end of the sling has a speed of about 7.6 M (Mach) for a short time (some few seconds) and may be protected by conventional methods such as the Shuttle coating (ceramic cover or other heat-resistant material).

10.4.2 Project 2

10.4.2.1 Space projectile launcher with a sling made from whiskers (Fig. 10.1)

Using a space sling launcher with a sling made from whiskers that has a tensile strength rating of $\sigma = 3500$ kg/mm² and a sling density of $\gamma = 1800$ kg/m³, the stress coefficient will be $k = s/g = 3.9 \times 10^7$. Assuming the mass of the projectile (load) is $m = 1000$ kg = 1ton, the required final projectile speed is $V = 8$ km/s, the length of the lever is $R_0 = 50$ m, the maximum lever speed is $V_0 = 800$ m/s, then the maximum radius $R = R_0 V/V_0 = 50 \times 8000/800 = 500$ m. Conventional gas turbines have a turbine blade tip speed of up to 600–800 m/s in high-temperature gas. Our lever, made from current composite material, can withstand a speed of more than 800 m/s, because the lever (or disk) radius is larger and it is protected from high temperature. The sling material attains a speed of $V_0 = \sqrt{\sigma/\gamma} = 6.24$ km/s.^{3–13} The parameters used below are not optimal. Our purpose is only to estimate the offered launcher properties.

10.4.2.2 Computation

The maximal centrifugal overload of the projectile is $C = V^2/R = 64 \times 10^6/500 = 128 \times 10^3$ m/s² = 12.8×10^3 g. This acceleration is less than that achieved by a conventional cannon. Maximal centrifugal force around the projectile is $F = mC = 10^3 \times 128 \times 10^3 = 28 \times 10^6$ N = 12,800 ton. The sling cross-section area near the projectile is $S = F/\sigma = 12,800/3.5 = 3660$ mm² = 36.6 cm². The sling cross-section area near the lever is $\bar{S} = 5$, $S_0 = 181$ cm² (equation (10.2)). We assume the sling's center of gravity is at $R_c = 0.5R$, $V_c = 0.5V$, and $S_s \approx (S + S_0)/2 = 109$ cm². The sling mass is $m_c = \gamma S_c R = 1800 \times 0.0109 \times 500 = 9.81$ ton. Sling centrifugal acceleration is $C_c = V_c^2/R_c = 4000^2/250 = 64 \times 10^3$ m/s², sling centrifugal force is $F_c = m_c C_c = 9810 \times 64 \times 10^3 = 628 \times 10^6$ N = 62,800 ton. For a sling of relative thickness $c = 0.1$, $b = 33$ cm, the sling wing area is $S_s = 165$ m² (equation (10.3)). For $\rho = 1.225$ and $a = 330$ m/s, the sling air drag is $D_c = 54.4$ ton, for $k_1 = 5$ the projectile air drag is only $D = m/k_1 = 1000/5 = 200$ kg. The angle $\alpha \approx R_0/R = 50/500 = 0.1$ rad, the angle $\beta \approx R_0/R_c = 50/250 = 0.2$ (Fig. 10.3(a)).

The acceleration inequality (10.5) is $13,880 > 53.4$ which is acceptable.

Assuming an acceleration time of $t = 25$ s, then the work of acceleration and air drag of the installation are: projectile acceleration work $A_1 = 32 \times 10^9$ J, sling acceleration work $A_2 = 78.5 \times 10^9$, 100 ton disk (lever) acceleration work $A_3 = 10 \times 10^9$ J, sling drag work $A_4 = 133.5 \times 10^9$ J, disk drag work $A_4 = 40 \times 10^9$ J (equation (10.6)). Ignoring projectile drag, the common launch energy is $A = 300 \times 10^9$ J. The flywheel mass is $M = 30$ ton for material similar to the sling. If the time between launches is $t_p = 3$ h = 10,800 s, the required engine power is $P = A/t_p = 300 \times 10^9/10,800 = 27.8$ MW. This is the power of two or three large aviation turbo engines.

Without energy recuperation, the launcher's efficiency (transfer of mechanical energy into projectile speed) is 10%, and with energy recuperation (kinetic energy of the sling

and disk is used for flywheel support), the launcher efficiency reaches 30%. Launch capability is 8 ton of payload, every day.

10.4.2.3 Economic efficiency

Assume a cost of \$100 million for the installation,²³ a useful life of 20 years, and an annual maintenance cost of \$2 million. If each launch has a payload of 1 ton, and there are eight launches per day for 300 days a year, then the annual payload capacity is 2400 ton. The launch cost for each kilogram of payload is $7 \times 10^6 / 2.4 \times 10^6 = \$2.9/\text{kg}$ plus fuel cost. If 10,000 l of fuel are used every day and the fuel price is \$0.25/l, then the fuel cost is \$2500/day, resulting in a launch capability of 8000 kg/day or \$0.31/kg. This results in a total cost of \$3.2/kg of payload. If the revenue generated is based on sales of \$23.2/kg of payload in space, then the operating profit would be about \$48 million/year.

The reader may calculate using other assumptions. In every reasonable case, the cost of delivery would be hundreds of times less expensive than delivery by existing rockets. It is emphasized that the primary efforts of this chapter are not economical estimations, but a new concept in space launch capability.

10.4.2.4 Discussion

Currently, there are whiskers that have parameters close to those required for this project. Industrial production of nanotubes will soon allow the design of a better space sling launcher. The heating problem of the sling end may be solved by head protection, given that the heat will be imposed for only a few of seconds. The heating of the projectile and the problem of speed loss in the atmosphere are considered elsewhere.^{6,13} It is shown that the speed loss is small, about 100–250 m/s. There is also a speed “reserve” of 460 m/s provided by the Earth’s rotation if the launch is made near the equator.

10.4.3 Project 3

10.4.3.1 The launcher for space tourists with a sling made from nanotubes (Fig. 10.2)

Let us consider a ship which flies to an altitude of 100 km, carrying three people. The following is an estimation of a sling launcher installation which achieves these objectives. We will use the method depicted in Fig. 10.2, where ship acceleration is provided using a sling and a supersonic aircraft.

It is known that the average person can withstand centrifugal forces of 3–4g. A trained (or in good health) person can withstand up to 7–8g, and for short periods up to 16g. With the proposed sling launcher, we assume centrifugal forces of $n = 7.8g$, a permissible overload for trained people.

We assume that the mass of the space ship is $m = 1500 \text{ kg} = 1.5 \text{ ton}$. The vehicle has only a small engine and fuel for maneuverability during landing and half of its total weight is payload (10 people). It may be shown that the necessary ship speed for reaching an altitude of 100 km is $V = 1600\text{--}1750 \text{ m/s}$. Assuming the speed $V = 1750 \text{ m/s}$, $n = 7.8g$.

10.4.3.2 Computation

The required radius of the circle is $R = V^2/g \times n = 1750^2/78 \approx 40 \text{ km}$. Assume a sling length of $L = 35 \text{ km}$. If speed of the supersonic aircraft is $V_0 = 600 \text{ m/s}$, the flight radius is $R_0 = RV_0/V = 13.8 \text{ km}$. Constructing the sling from carbon nanotubes with the

permitted stress of $\sigma = 9000 \text{ kg/mm}^2$, the sling density is $\sigma = 1800 \text{ kg/m}^3$. The coefficient $k = \sigma/\gamma = 10 \times 10^7$, $\bar{S} = 1.06 \cong 1$, aircraft thrust $T = F = 7.8 \times 1.5 = 11.7 \text{ ton}$. The required sling cross-section area is $S = F/\sigma = 11.7/9 = 1.3 \text{ mm}^2 \approx S_0$. Mass of the sling is $m_c = \gamma SL = 800 \times 1.3 \times 10^{-6} \times 3000 = 82 \text{ kg}$.

Take $c = 0.08$. Then $b = (S/c)^{0.5} = 4 \text{ mm}$, $S_s \approx b \times L = 0.004 \times 35,000 = 140 \text{ m}^2$. Assume the sling has the lift force and form (shown in Fig. 10.2(b)), with convexity toward the top. The supersonic aircraft has an altitude of 15 km, the average altitude of the sling's center of gravity is $H = 25 \text{ km}$ (air density $\rho = 0.041 \text{ kg/m}^3$) and the space ship has an altitude of 30 km (air density $\rho = 0.018 \text{ kg/m}^3$). Speed of the sling's center of gravity is $V_c = 1181 \text{ m/s}$, the speed of sound at this altitude is $a = 295 \text{ m/s}$. The sling drag is (equation (10.3)) $D_c = 4 \times 0.08^2 \times 0.41 \times 295 \times 1181 \times 140/2 = 2.56 \text{ ton}$. $R_c = R_0 + 0.5 \times (R - R_0) = 27 \text{ km}$, $C_c = 51.6 \text{ m/s}^2$ [equation (10.5)]. Calculating angles, $\sin \alpha = R_0/R = 13.8/40 = 0.345$, $\sin \beta \approx R_0/2R = 0.69$. Calculating the acceleration inequality (10.6), this figure is $4.2 > 2.04$. This is acceptable. Assume we increase the sling length with speed 150 m/s. Then the time of untwisting will be $t = 35,000/150 = 233 \text{ s} \approx 4 \text{ min}$. The maximum overload of 7.8 g is imposed on the passengers for only a few seconds.

On disconnection, the winged space ship has an average vertical acceleration of $n \approx 4g$. The integration of equation (10.8) during $t = 50 \text{ s}$ for average $k_1 = 6.5$ indicates that the angle of trajectory increases from 0° to 57.3° , the altitude increases up to 59 km, and the speed decreases to 1250 m/s. An alternate way is to compute using equation (10.9), as a ballistic trajectory out of the atmosphere. The result is an altitude of 115 km, a range of 145 km, and a time of 215 s. After the ballistic part of the trajectory, the vehicle enters the atmosphere again, increases its vertical acceleration up to $3g$ and its trajectory angle to near 0° , flying into the atmosphere and landing. The graphs of trajectory, flight acceleration, and flight time are shown in Fig. 10.4(a)–(c). The total time out of the Earth's gravitational field is about 4 min and the maximum altitude is 115 km (Fig. 10.4(a)).

10.4.3.3 Discussion

Acceptable aircraft. Data for large existent and old supersonic aircraft are shown in Table 10.1.

Conventional aircraft have the following characteristics: their empty weight is 30–40% of their total weight (or takeoff weight), the fuel for long range is 30–40%, and the payload is 30–40%.

Table 10.1. Data for large existent and old supersonic aircraft.

Name	Maximum weight [ton]	Maximum speed [m/s]	Maximum altitude [km]	Engine thrust [tons]
TU-144	195	694	18	51
Concorde	185	603	16	48
TU-160	275	600	15	68
XB-70	244	900	21	61
SR-71A	77	935	24	29
F-111A	41	738	16	11

Source: Jane's.

A safe vertical overload for passengers and large military aircraft (bombers) is 2.5–2.6 g; the aerodynamic efficiency in supersonic speed is 6–7.5, the maximum thrust is about 25% of the maximum weight for an aircraft with a maximum speed of 2 M (Mach number) and 35% for aircraft with a maximum speed of 3 M.

For our purposes, we consider a supersonic aircraft without a payload and with only a small amount of fuel, resulting in a net weight of about half the takeoff weight. In flights with speed $V = 600 \text{ m/s}$ and radius $R = 13.8 \text{ km}$, the overload equals $V^2/gR = 2.6 \text{ g}$. If the aircraft weight is 50% of its takeoff weight, this means that the true aircraft overload is only $n_1 = 0.5 \times 2.6 = 1.3 \text{ g}$.

The required additional thrust for our space vehicle increases from zero to maximum $T_{\max} = ngW\bar{S} = 7.8 \times 9.81 \times 1500 \times 1.06 \text{ N} = 12.2 \text{ ton}$. The required aircraft thrust for aerodynamic efficiency $k_1 = 6.8$ and aircraft weight $W_a = 195 \text{ ton}$ is $T = n_1 \times W_a/k_1 = 1.3 \times 195/6.8 = 37.3 \text{ ton}$ when the engine is in its cruise regime. The additional thrust necessary is only required for 40–50 s. This may be provided by a brief boost of the engine performance (takeoff regime, plus injection of fuel through a jet engine nozzle). This is done at high aircraft speed. The thrust may be temporarily increased by up to 50–80%. In our case, in the cruise regime, the engines provide thrust of $195/6.8 = 28.7 \text{ ton}$. In boost regime, they provide $1.8 \times 28.7 = 51.7 \text{ ton}$. The difference is $51.7 - 37.3 = 14.4 > 12.2 \text{ ton}$. This is enough. If the boost thrust provided is less, then the required thrust may be obtained by the installation of an additional outboard-suspended air or rocket engine.

The end of the sling has a high speed (5.9 M) for a short period and may be protected by a ceramic skin. The main technical problem is producing the necessary high-strength sling. There is as yet no commercial production of cheap, long nanotubes. A low-strength sling cannot be used, because people cannot tolerate the overload (minimal radius is 40 km, for the initial speed of 1750 m/s and the overload 7.8 g), which has a large air drag and so the acceleration inequality (10.5) is unsatisfied.

However, our parameters are not optimal and the offered space launch needs further R&D. For example, the slope circle trajectory (Fig. 10.2) improves all flight parameters.

10.4.4 Project 4

10.4.4.1 The launch of space tourists accelerated by subsonic aircraft with a sling made from whiskers (see Fig. 10.2)

The previous project design has its drawbacks: it requires a sling made of nanotubes and a supersonic aircraft. Let us consider the project which uses a sling made from whiskers and a commercial subsonic aircraft. This may be realized at the present time. To reduce the sling length, we install a small rocket engine in the space ship.

To estimate a sling installation which satisfies these conditions, we use the method depicted in Fig. 10.2, where the rocket ship acceleration is provided by the sling along with a current subsonic aircraft. Assume the weight of the space ship is $m = 2 \text{ ton}$, where 450 kg of this is a rocket fuel and 1550 kg is space body and payload. The number of passengers is 10, including a pilot. The safe overload is $n = 7.8 \text{ g}$.

The ship has a rocket engine and a small amount of fuel to increase the speed after separating from the sling and to increase the trajectory angle by 1 rad (57.3°). Assume the speed after the sling acceleration is $V = 1000$ m/s.

10.4.4.2 Computation

The required radius is $R = V^2/g \times n = 1000^2/78 \approx 12.8 \approx 13$ km. Assume the sling length $L = 11$ km. If the speed of the supersonic aircraft is $V_0 = 265$ m/s ($V = 0.89$ M), the flight radius is $R_0 = RV_0/V = 3.4$ km. The aircraft overload in this flight radius is $n_1 = V^2/gR_0 = 2.1$. Using a sling made from C_D whiskers with a maximum stress of $\sigma = 8000$ kg/mm², the density is $\gamma = 3500$ kg/m³ (see Ref. [17], p. 158). Assume safe stress is $\sigma = 2000$ kg/mm². The coefficient $k = \sigma/\gamma = 0.572 \times 10^7$, $\bar{S} = 1.09$, maximum aircraft thrust $T = F_0 = 2 \times 7.8 \times 1.09 = 17$ ton. The centrifugal force from the aircraft is $F = m \times n \times g = 15.3$ ton. The required sling cross-section areas are $S = mn/\sigma = 2.7 \times 8/2 = 7.8$ mm², $S_0 = 1.09 \times 7.8 = 8.5$ mm², and $S_a = 8.15$ mm². The mass of the sling is $m_c = \gamma S_a \times L = 3500 \times 8.15 \times 10^{-6} \times 11,000 = 385$ kg.

Assuming $c = 0.08$, that $b = (S_a/c)^{0.5} = 10$ mm, $S_s \approx bL = 0.01 \times 11,000 = 110$ m². Assume the sling has a lift force and form as in Fig. 10.2(b) with convexity to the top. The subsonic aircraft has an altitude of 12 km, the average altitude of the sling's center of gravity is $H = 15$ km (air density $\rho = 0.191$ kg/m³) and the space ship has an altitude of 17 km (air density $\rho = 0.142$ kg/m³). Speed of sling's center of gravity is $V_c = 618$ m/s, and the speed of sound at this altitude is $a = 295$ m/s. The sling drag is (equation (10.3)) $D_c = 4 \times 0.08^2 \times 0.191 \times 295 \times 618 \times 110/2 = 4.9$ ton. $R_c = R_0 + 0.5(R - R_0) = 8.1$ km, $C_c = 1.85$ m/s² (equation (10.5)). Calculating the angles, $\sin \alpha = R_0/R = 3.4/12.8 = 0.27$ rad, $\sin \beta \approx R_0/2R = 0.54$. The inequality (10.6) is $5.2 > 4.2$, which is acceptable. Assume we increase the sling length with a speed of 100 m/s. Then the time of untwisting will be $t = 11,000/100 = 110$ s ≈ 2 min. The maximum overload 7.8 g will be imposed on the passengers for only a few seconds (Fig. 10.4).

After space ship's disconnection the average vertical acceleration is $n \approx 7.8g$. The integration of equation (10.7) during $t = 14$ s for an average $k_1 = 6.5$ shows that the angle of trajectory increases from 0° to 57.3° (1 rad), the altitude increases up to 19.1 km, and the speed decreases to $V_2 = 890$ m/s. During the next part of the flight, the rocket engine turns on and accelerates the space vehicle with a constant overload of 7.8 g and with a constant slope of trajectory. The changes in the trajectory parameters may be estimated by the following equations:

$$\Delta t = \frac{V_e}{ng} \ln \frac{m_e}{m}, \quad \Delta V = g \left(n - \frac{1}{k_1} - \sin \theta \right) \Delta t, \quad \Delta H = V_a \Delta t, \quad V_a = V_2 + \frac{\Delta V}{2}, \quad (10.10)$$

where $m_e = 1550$ kg is the final mass of the space vehicle; k_1 is the aerodynamic efficiency of the ship; and θ is the angle of trajectory.

The result of computation are $\Delta t = 9.33$ s, $\Delta V = 623$ m/s, and $\Delta H = 11.2$ km. At the end of the acceleration part of the trajectory, we will have $V = 890 + 623 = 1513$ m/s, altitude $H = 15 + 4 + 11.2 = 30.2$ km, and the trajectory angle $\theta = 1$ rad $= 57.3^\circ$.

The ballistic part of the trajectory gives (equation (10.9)) additional altitude $H_b = 82.4 \text{ km}$, ballistic distance $R_b = 212 \text{ km}$, gravity zero time $t_b = 260 \text{ s} = 4.3 \text{ min}$. The total altitude is $H = 30.2 + 82.4 = 112.6 \text{ km}$. The total time of flight with overload 7.8 g is $14 + 9.3 = 23.3 \text{ s}$.

After the ballistic part of the trajectory, the vehicle re-enters the atmosphere, increasing vertical acceleration up to $3g$ or less and angle trajectory from -57° up to near 0° , flying into the atmosphere and landing. The graph of flight acceleration is shown in Fig. 10.4(d). The amount of time out of gravitation is about 4 min. The maximum altitude is 115 km.

10.4.4.3 Discussion

Required aircraft: Data on some large existing commercial subsonic aircraft are given in Table 10.2.

Conventional subsonic aircraft have the following characteristics: their empty weight is 30–40% of the total maximum weight (or takeoff weight), fuel for a long-range flight is 30–40%, and the payload is 30–40%. An safe vertical overload for passenger aircraft is 2.5 g. The aerodynamic efficiency at supersonic speed is 10–14, the maximum thrust is 25% of the maximum weight for an aircraft than has a maximum speed of 0.92 M. The takeoff regime of the engine gives a thrust of about 50% more than the cruising regime.

For our purposes, we consider a subsonic aircraft, without a payload and only a small amount of fuel, resulting in a net weight equal to about half that of normal takeoff weight. When an aircraft has a speed of $V = 265 \text{ m/s}$ and trajectory radius of $R_0 = 3.4 \text{ km}$, the overload is $V^2/g \times R_0 = 2.1 \text{ g}$. If the aircraft weight is 50% of its takeoff weight, this means that the true aircraft overload is only $n_1 = 0.5 \times 2.1 = 1.05 \text{ g}$.

The required additional thrust for our space vehicle increases from zero to maximum $T_{\max} = ngm\bar{S} = 7.8 \times 9.81 \times 2000 \times 1.09 \text{ N} = 17 \text{ ton}$. The required aircraft with thrust for aerodynamic of efficiency $k_1 = 12$ and an aircraft weight of $W_a = 397 \text{ ton}$, results in $T = n_1 \times W_a/k_1 = 1.05 \times 397/12 = 34.7 \text{ ton}$ in cruise regime. If the engine works in takeoff regime, the additional thrust will be $0.5 \times 34.7 = 17.35 \text{ ton}$, which is sufficient for the sling launcher. The additional thrust is necessary only for 80–110 s. If we use a middle-sized aircraft, this thrust may also be obtained from a brief engine boost (takeoff engine regime, plus additional force generated by the injection of fuel by the jet engine nozzle applied in combat aircraft), or the installation of an additional outboard-suspended air or rocket engine.

The end of the sling has a speed of 3.4 M for a short time, and may be made of or protected by heat-resistant material.

These parameters are not optimal, and the offered space launch needs further research.

Table 10.2. Data on large existing commercial subsonic aircraft.

Name	Maximum weight [ton]	Maximum speed [m/s]	Maximum altitude [km]	Engine thrust [ton]
Boeing 747	397	265	14	98
Airbus	230	265	14	58

Source: Jane's.

10.4.4.4 Economic efficiency

Our projects presented here are intended for large-scale commercial implementation, with eight to nine tourists per flight and can be reused up to 1000 times.

Let us estimate the cost of a space ticket per passenger, if the space ship takes eight passengers.

A fully loaded long-distance Boeing 747 carries 400 passengers, for an average passenger ticket cost of \$200, and a flight from New York to London takes about 8 h. This translates to a cost of about \$15,000/h of flight. Our flight will be about 1.5 h, costing about \$22,500. Assuming the space ship costs \$3 million to build and is designed for 1000 flights, the average depreciation cost per flight is \$3000. Assuming the maintenance cost for one flight is \$4500, the total cost of one flight would be \$30,000. The net actual cost per passenger is $\$30,000/8 = \3850 . At the present time with existing rocket technology, it costs \$20 million. With the proposed successful X-prize projects, the projected cost per passenger is \$0.7–2 million.

10.5 General discussion

Project 1 describes the suggested method for delivering projectiles to a distance of up to 2000 km, using current technology and inexpensive, currently available materials. The space launcher (Project 2) requires whiskers, and it may be used for non-human space payloads. The X-prize space flights (Project 3) requires a sling made of nanotubes or whiskers (Project 4) and, in all probability, the installation of an additional outboard air or rocket engine on a currently existing subsonic or supersonic aircraft.

Industry now produces whiskers, and science laboratories can make nanotubes that have high tensile strength.²⁰ Theory indicates that these values are only 10% of the potential strength. We need to develop the means to manufacture a long, thin cable, such as the strings or threads produced from cotton or wool, from whiskers and nanotubes.

The fiber industry at the present time produces fibers which are theoretically employed in the author's concept projects. However, whiskers, and especially nanotubes, strongly improve the possibilities of this method. They increase the potential speed and decrease the cable mass and drag (rotation energy). These projects are unusual for specialists and others now, but there are advantages, and it is believed that they have good commercial potential.

A reviewer drew the author's attention to the Slingaton Launcher described by D.A. Tidman.²⁴ This launcher is very different from the sling launcher in this chapter. Tidman's launcher is a vacuum circle tube bulb-like form with a circle diameter up to 1 km. The rocket and space ship are located inside this tube. The tube has big mass and makes oscillation like a conventional hula-hoop. This oscillation helps to move the inside apparatus. The weaknesses of this design are its large installation mass, large required power, very big friction (huge centrifugal force presses the vehicle to the wall of the tube), problems with exit of the vehicle into atmosphere from the vacuum tube, etc.

By contrast, the sling launcher described here is very simple. It has only the lever, motor and sling, and it is all located in the atmosphere.

Many people ask about heating problems when a vehicle returns into the atmosphere. They recall the heating tile defects of the “Space Shuttle” and think that this problem is very troublesome for the suggested vehicles. However, there is a big difference between a re-entry space vehicle and a launch space vehicle. The re-entry vehicle has high speed and enormous kinetic energy, which must be dispersed. It has a bulbous fuselage and wing edges, and slides along the Earth’s atmosphere for a long time. The offered projectiles save energy (speed) during flight. They have sharp edges, fly in the atmosphere for a short time, and have a small projected area.²⁵

References

1. Space Technology and Application International Forum (STAIF), 1996–1997, Albuquerque, MN, USA.
2. D.V. Smitherman Jr., “Space Elevators”, NASA/CP-2000-210429, National Aeronautics and Space Administration, Washington, DC, 2000.
3. A.A. Bolonkin, “Kinetic Space Towers and Launchers”, *Journal of the British Interplanetary Society*, Vol. 57, No. 1/2, 2004, pp. 33–39.
4. A.A. Bolonkin, “Non-rocket Transport System for Space Travel”, *Journal of the British Interplanetary Society*, Vol. 56, No. 7/8, 2003, pp. 232–254.
5. A.A. Bolonkin, “Centrifugal Keeper for Space Stations and Satellites”, *Journal of the British Interplanetary Society*, Vol. 56, No. 9/10, pp. 314–327.
6. A.A. Bolonkin, “Hypersonic Gas-Rocket Launcher of High Capacity”, *Journal of the British Interplanetary Society*, Vol. 57, No. 5/6, pp. 162–172.
7. A.A. Bolonkin, “Optimal Inflatable Space Towers with 3–100 km Height”, *Journal of the British Interplanetary Society*, Vol. 56, No. 3/4, pp. 87–97.
8. A.A. Bolonkin, “Asteroids as Propulsion Systems of Space Ships”, *Journal of the British Interplanetary Society*, Vol. 56, No. 9/10, 2003, pp. 98–107.
9. A.A. Bolonkin, “Hypersonic Gas-Rocket Launch System”, AIAA-2002-3927, 38th AIAA/ASME/ SAE/ASEE Joint Propulsion Conference and Exhibition, 7–10 July 2002, Indianapolis, IN, USA.
10. A.A. Bolonkin, “Multi-reflex Propulsion Systems for Space and Air Vehicles and Energy Transfer for Long Distance”, *Journal of the British Interplanetary Society*, Vol. 57, No. 11/12, 2004, pp. 379–390.
11. A.A. Bolonkin, “Kinetic Anti-gravitator”, AIAA-2005-4504, 41st Propulsion Conference, 10–12 July 2005, Tucson, AZ, USA.
12. A.A. Bolonkin, “Optimal Trajectories of Air and Space Vehicles”, *Aircraft Engineering and Aerospace Technology*, Vol. 76, No. 2, 2004, pp. 193–214.
13. A.A. Bolonkin, “Space Cable Launchers”, Paper No. 8057 presented at the Symposium “The Next 100 years”, Dayton, OH, USA, 14–17 July 2003.
14. M. Minovich, “Electromagnetic Transportation System for Manned Space Travel”, US Patent #4,795,113, 3 January 1989.

15. “Beamed Energy Propulsion”, *First International Symposium on Beamed Energy Propulsion*, American Institute of Physics, Melville, New York, 2003.
16. R.M. Zubrin, “The Use of Magnetic Sails to Escape from Low Earth Orbit”, *Journal of the British Interplanetary Society*, Vol. 46, No. 1, 1993, pp. 3–10.
17. F.S. Galasso, *Advanced Fibers and Composites*, Gordon and Breach Scientific Publisher, New York, 1989.
18. *Carbon and High Performance Fibers*, Directory, Chapman & Hall, New York, 1995.
19. *Concise Encyclopedia of Polymer Science and Engineering*, Ed. J.I. Kroschwitz, New York, 1990.
20. M.S. Dresselhous, *Carbon Nanotubes*, Springer, New York, 2000.
21. J.D. Anderson, *Hypersonic and High Temperature Gas Dynamics*. McGraw-Hill Book Co., New York, 1989.
22. G.V. Bill and C.H. Murphy, Paris Kanoneu – The Paris Guns and Project HARP, JFF91-1277, 1988.
23. D.E. Koell, *Handbook of Cost Engineering*, TCS, Germany, 2000.
24. D.A. Tidman, “Constant – Frequency Hypervelocity Slings”, *Journal Propulsion and Power*, Vol. 19, No. 4, 2003, 0748-4658, pp. 581–587.
25. A.A. Bolonkin, “Sling Rotary Space Launcher”, AIAA-2005-4035, *41st Propulsion Conference*, 10–12 July 2005, Tucson, AZ, USA.

This page intentionally left blank

CHAPTER 11

Asteroids as Propulsion System of Space Ships*

Summary

Currently, rockets are used to change the trajectory of space ships and probes. Sometimes space probes use the gravity field of a planet. However, there are only nine planets in the solar system, all separated by great distances. There are tens of millions of asteroids in outer space. This chapter offers a revolutionary method for changing the trajectory of space probes. This method uses the kinetic or rotary energy of asteroids, comet nuclei, meteorites, or other space bodies (small planets, natural planet satellites, space debris, etc.) to increase (or to decrease) ship (probe) speed up to 1000 m/s (or more) and to achieve any new direction in outer space. The flight possibilities of space ships and probes are increased by a factor of millions.

11.1 Introduction

At the present time, rockets are used to carry people and payloads into space.¹ Other than rockets, methods used to reach space speed include the space elevator,² tethers,^{3,4} the electromagnetic system,⁵ and the tube rocket.^{9,10} The space elevator is not technically feasible at the present time; it would require substantial costs for development. In particular, the space elevator concept requires extremely strong nanotubes. Tethers are very complex and would require two artificial bodies. Electromagnetic systems are also complex and expensive. The author has previously discussed several other non-rocket launch methods (see other author proposals and articles) that are potentially low cost, but which require much additional research^{6–17}. These include cable launchers,^{6–10} circle launchers,¹¹ and inflatable towers.¹²

There are many small solid objects in the solar system called asteroids. The vast majority are found in a swarm called the asteroid belt, located between the orbits of Mars and Jupiter at an average distance of 2.1–3.3 astronomic units (AU) from the Sun. Scientists

*Detailed description is in *Journal of the British Interplanetary Society*, Vol. 56, No. 3/4, 2003, pp. 98–107.

know of approximately 6000 large asteroids of a diameter of 1 km or more, and of millions of small asteroids with a diameter of 3 m or more. Ceres, Pallas, and Vesta are the three largest asteroids, with diameters of 785, 110, and 450 km (621, 378, and 336 miles), respectively. Others range all the way down to meteorite size. In 1991 the Galileo probe provided the first closeup view of the asteroid Caspra; although the Martian moons (already seen closeup) may also be asteroids, captured by Mars. There are many small asteroids, meteorites, and comets outside the asteroid belt. For example, scientists know of 1000 asteroids of diameter larger than 1 km located near the Earth. Every day 1-ton meteorites with mass of over 8 kg fall on the Earth. The orbits of big asteroids are well known. The small asteroids (from 1 kg) may also be located and their trajectory can be determined by radio and optical devices at a distance of hundreds of kilometers.

Radar observations enable to discern of asteroids by measuring the distribution of echo power in time delay (range) and Doppler frequency. They allow a determination of the asteroid trajectory and spin, and the creation of an asteroid image.

Most planets, such as Mars, Jupiter, Saturn, Uranus, and Neptune have many small moons that can be used for the proposed space transportation method.

There are also the asteroids located at the stable Lagrange points of the Earth–Moon system. These bodies orbit with the same speed as Jupiter, and might be very useful for propelling spacecraft further out into the solar system. Comets may also be useful for propulsion once a substantial spacecraft speed is obtained. It seems likely that the kinetic and rotational energy of both comets and asteroids will eventually find application in space flight.

Most asteroids consist of carbon-rich minerals, while most meteorites are composed of stony-iron.

The present idea^{6–8} is to utilize the kinetic energy of asteroids, comets, meteorites, and space debris to change the trajectory and speed of space ships (probes). Any space bodies more than 10% of a ship's mass may be used, but here mainly bodies with a diameter of 2 m (6 ft) or larger are considered. In this case the mass (20–100 ton) of the space body (asteroid) is some 10 times more than the mass of probe (1 ton, 2000 lb) and the probe mass can be disregarded.

11.2 Connection method

The *method* includes the following main steps:

- (a) Finding an asteroid using a locator or telescope (or looking in catalog), and determining its main parameters (location, mass, speed, direction, rotation); selecting the appropriate asteroid; and computing the required position of the ship with respect to the asteroid.
- (b) Correcting the ship's trajectory to obtain the required position; convergence of the ship with the asteroid.

- (c) Connecting the space apparatus (ship, station, and probe) to the space body (planet, asteroid, moon, satellite, meteorite, etc.) by a net, anchor, and a light strong rope (cable), when the ship is at the minimum distance from the asteroid.
- (d) Obtaining the necessary position for the apparatus by moving around the space body and changing the length of the connection rope.
- (e) Disconnecting the space apparatus from the space body and spooling the cable.

The equipment required to change a probe (spacecraft) trajectory includes:

- (a) a light strong cable (rope);
- (b) a device to measure the trajectory of the spacecraft with relative to the space body;
- (c) a device for spacecraft guidance and control;
- (d) a device for the connection, delivery, control, and disconnection and spooling of the rope.

11.2.1 Description of utilization

The following describes the general facilities and process for a natural space body (asteroid, comet, meteorite, or small planet) with a small gravitational force to change the trajectory and speed of a space apparatus.

Fig. 11.1(a–c) shows the preparations for using a natural body to change the trajectory of the space apparatus; for example, the natural space body, 2, which is moving in the same direction as the apparatus (perpendicular to the sketch, Fig. 11.1(a)). The ship

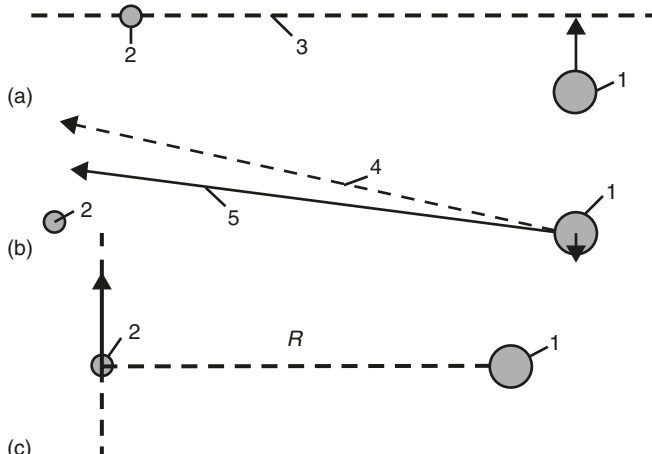


Fig. 11.1. Preparing for employment of the asteroid. *Notations:* (1) Space ship; (2) asteroid; (3) plane of maneuver; (4) old ship direction; and (5) corrected ship direction. (a) Reaching the plane of maneuver. (b) Correcting the flight direction and reaching the required radius. (c) Connection to asteroid.

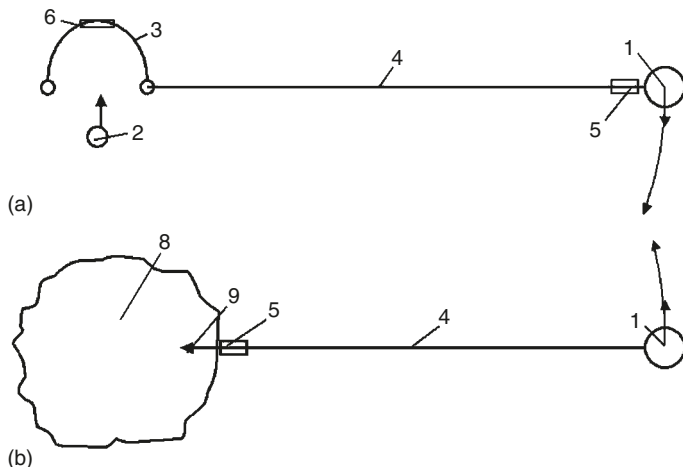


Fig. 11.2. (a) Catching a small asteroid using net. (b) Connection to a big asteroid using an anchor and cable. *Notations:* (1) Ship; (2 and 8) asteroid; (3) net with inflatable ring; (4) cable (rope); (5) load cabin; (6) value in net; and (9) anchor.

wants to make a maneuver (change direction or speed) in plane 3 (perpendicular to the sketch), and the position of the apparatus is corrected and moved into plane 3. It is assumed that the space body has more mass than the apparatus.

When the apparatus is at the shortest distance R from the space body, it connects to the space body means of the net (Fig. 11.2(a)) or by the anchor (Fig. 11.2(b)) and rope. The apparatus rotates around the common center of gravity at the angle ϕ with angular speed ω and linear speed ΔV (Fig. 11.4). The cardioids of additional speed and direction of the apparatus are shown in Fig. 11.4 (right side). The maximum additional velocity is $\Delta V = 2V_a$, where V_a is the relative asteroid velocity when the coordinate center is located in the apparatus.

Fig. 11.4(b) shows the case where the space body moves in the opposite direction to the apparatus with velocity ΔV .

Fig. 11.2(a) shows how a net can be used to catch a small asteroid or meteorite. The net is positioned in the trajectory of the meteorite or small asteroid, supported in an open position by the inflatable ring and connected to the space apparatus by the rope. The net catches the asteroid and transfers its kinetic energy to the space apparatus. The space apparatus changes its trajectory and speed, and then disconnects from the asteroid and spools the cable. If the asteroid is large, the astronaut team can use the asteroid anchor (Figs. 11.2(b) and 11.3).

The astronauts use the launcher (a gun or a rocket engine) to fire the anchor (harpoon fork) into the asteroid. The anchor is connected to the rope and spool. The anchor is implanted into the asteroid and connects the space apparatus to the asteroid. The anchor contains the rope spool and a disconnect mechanism (Fig. 11.3). The space apparatus

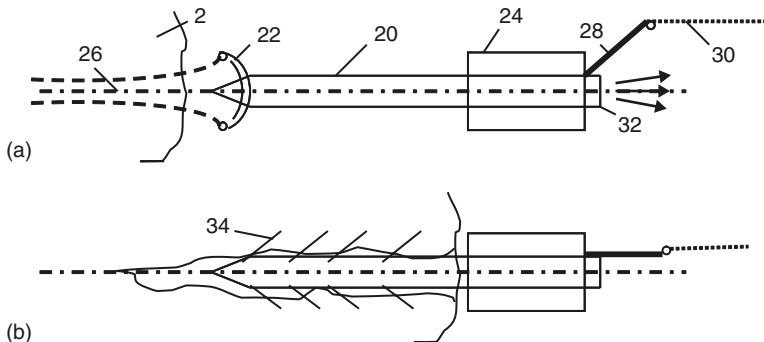


Fig. 11.3. (a) Anchor (harpoon fork). *Notations:* (2) Asteroid; (20) anchor; (22) cumulative charge (shaped charge); (24) rope spool; (26) cannel made by shaped charge; (28) rope keeper; (30) rope; and (32) rocket impulse engine, which implants the anchor into the asteroid. (b) Anchor connected to the asteroid. *Notation:* (34) Anchor catchers.

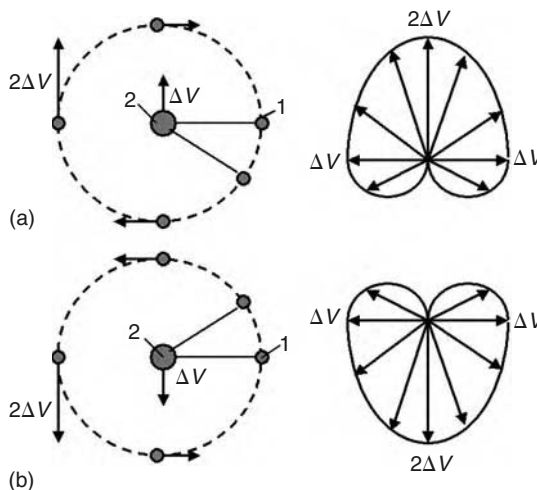


Fig. 11.4. Using the kinetic energy of an asteroid, to change the space ship trajectory (speed and direction). On the right are cardioids of the additional velocity and its direction. The ship can get this velocity from the asteroid. *Notations:* (1) Space ship; (2) asteroid; and ΔV is the difference between velocities of space ship and asteroid. (a) Case when the asteroid has to same direction as the ship. (b) Case when the asteroid has the opposite direction to the ship.

contains a spool for the rope, motor, gear transmission, brake, and controller. The apparatus may also have a container for delivering a load to the asteroid and back (Fig. 11.2(b)). One possible design of the space anchor is shown in Fig. 11.3. The anchor has a body, a rope, a cumulative charge (shared charge), the rocket impulse (explosive) engine, the rope spool, and the rope keeper. When the anchor strikes the asteroid surface the cumulative charge burns a deep hole in the asteroid and the rocket impulse engine hammers the anchor body into the asteroid. The anchor body pegs the catchers

into the walls of the hole and the anchor's strength keeps it attached to the asteroid. When the apparatus is to be disconnected from the asteroid, a signal is given to the disconnect mechanism.

If the asteroid is rotated with angular speed ω (Fig. 11.5), its rotational energy can be used for increasing the velocity and changing the trajectory of the space apparatus. The rotary asteroid spools the rope on its body. The length of the rope is decreased, but the apparatus speed is increased (see momentum theory in physics).

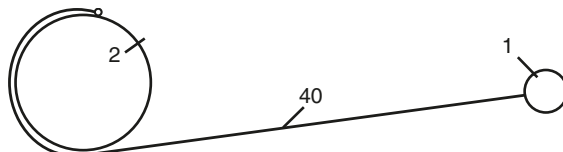


Fig. 11.5. Using the rotary energy of a rotating asteroid. Notation: (40) Connection cable.

The ship can change the length of the cable. When the radius decreases, the linear speed of the apparatus increases; conversely, when the radius increases the apparatus speed decreases. The apparatus can obtain energy from the asteroid by increasing the length of the rope.

The computations and estimations show the possibility of making this method a reality in a short period of time (see Projects, Section 11.5).

An abandoned space vehicle or large piece of space debris in Earth's orbit can also be used to increase the speed of the new vehicle and to remove the abandoned vehicle or debris from orbit.

11.2.2 Theory and computation

1. The differential equation can be found from the equilibrium of a small cable part under centrifugal force. This equation for optimal (equal stress from centrifugal force) cable is:

$$\frac{da}{A} = (\omega^2 \gamma / \sigma) R dR.$$

Its solution is the cable equal stress:

$$a(R) = A/A_0 = \exp(V^2/2k) = \exp(\omega^2 R^2/2k), \quad (11.1)$$

where a is the relative cross-section area of cable; A is the cross-section area of cable [m^2]; A_0 is the initial (near probe) cross-section area of cable [m^2]; V is the speed of probe or space ship about asteroid [m/s]; $k = \sigma/\gamma$ is the ratio of cable tensile stress to density [Nm/kg]; $K = k/10^7$ is the coefficient; R is the radius from the common gravity

center: asteroid + probe [m]; ω is the angular speed of a probe around asteroid [rad/s]; σ is the tensile strength [N/m^2]; and γ is the density of cable [kg/m^3].

2. Mass W [kg] of cable is:

$$W = A_0 \gamma \int_0^R a(r) dr = \frac{F_0}{k} \int_0^R e^{\omega^2 r^2 / 2k} dr, \quad (11.2)$$

where r is the variable [m] and F_0 is the force from the probe [N].

3. Relative cable mass $W_r = W/W_s$ is:

$$W_r = B(1 + B), \quad B = \frac{n}{k} \int_0^{v^2/ng} \exp \left[\left(\frac{ng}{V} \right)^2 \frac{r^2}{2k} \right] dr, \quad (11.3)$$

where the integration interval is $[0, V^2/ng]$, $n = F_0/g$ is the overload; V is the circle apparatus speed around the common center of gravity; W_s is the ship (probe) mass; and g is the Earth's gravitation [m/s^2], $g = 9.81 \text{ m/s}^2$.

4. Circular velocity of ship around asteroid:

$$R = V^2/gn, \quad V = (gnR)^{0.5}. \quad (11.4)$$

Computations are represented in Figs. 11.6–11.8.

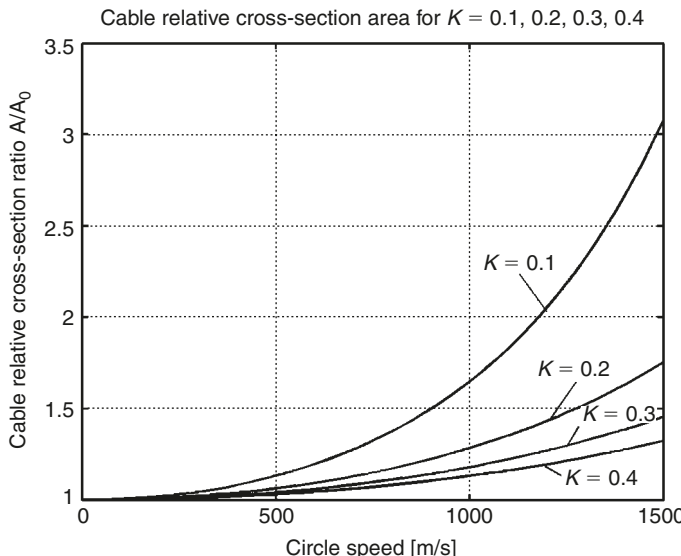


Fig. 11.6. Asteroid cable relative ratio via circle speed [m/s] and coefficient $K = 0.1–0.4$.

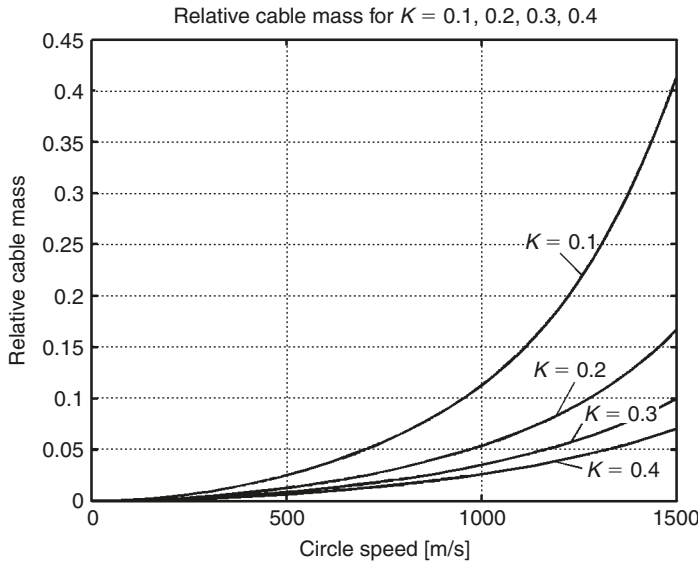


Fig. 11.7. Relative cable asteroid mass via circle speed [m/s] and coefficient $K = 0.1\text{--}0.4$.

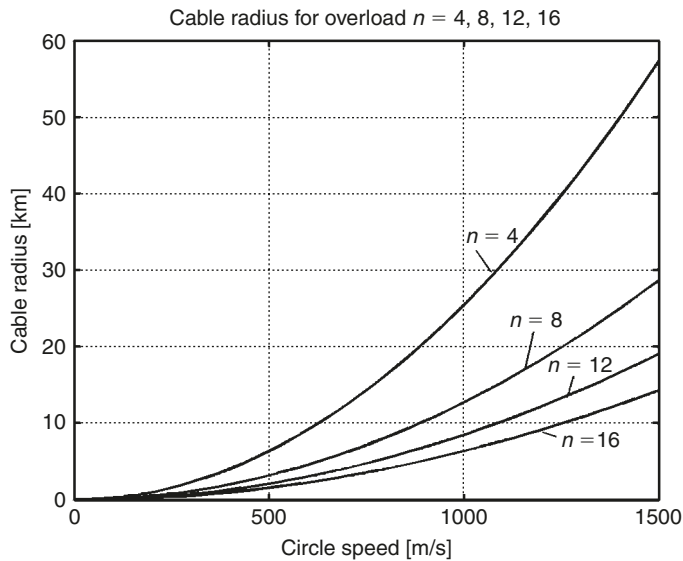


Fig. 11.8. Cable radius [km] via circle speed [m/s] and overload $n = 4\text{--}16$.

5. Relative mass of cable with constant cross-section area for small speed:

$$W_r = W/W_s = \gamma V^2/\sigma g = V^2/kg. \quad (11.5)$$

6. Finding the additional velocity the space vehicle has received from the asteroid.

Let us take the coordinate axis along the positive direction of the asteroid speed and write the momentum and energy laws of the asteroid-apparatus system for this axis:

$$m_1 V_1 + m_2 V_2 = m_1 u_1 + m_2 u_2, \quad (11.6)$$

$$0.5m_1 V_1^2 + 0.5m_2 V_2^2 = 0.5m_1 u_1^2 + 0.5m_2 u_2^2 + A, \quad (11.7)$$

where m_1, V_1 are the mass and speed of the asteroid, respectively, before connection to apparatus; m_2, V_2 are the mass and speed of the apparatus, respectively, before connection to asteroid; u_1 is speed of the asteroid after disconnection from the apparatus; u_2 is speed of the apparatus after disconnection from the asteroid; and A is energy (work) applied by the apparatus to change the length of the connection cable.

Let us locate beginning of the axis of the apparatus (this means $V_2 = 0$) and apply the variable $V = V_1$ is the asteroid speed around apparatus; $u = u_2$ is the additional apparatus speed; and $m = m_2/m_1$ is the relative apparatus mass.

Substitute u_1 from equation (11.6) into (11.7), we receive the quadratic equation about u :

$$(m + 1)u^2 - 2Vu + 2A/m_1 m = 0. \quad (11.8)$$

Solution of this equation is:

$$u = \{V \pm [V^2 + 2A(m + 1)/mm_1]^{0.5}\}/(m + 1). \quad (11.9)$$

Investigating this equation, if $A = 0$ (the apparatus does not change the length of the connection cable) and the asteroid mass is large ($m \approx 0$), the maximum additional speed of the apparatus is $u = 2V$ in the asteroid direction and $V = 0$ in the opposite direction. If $A \neq 0$, then maximum work (energy) apparatus can receive from the asteroid by increasing the connection cable length is less than:

$$A \leq mm_1 V^2 / 2(m + 1). \quad (11.10)$$

If the apparatus expends internal energy (decreases the length of the connection cable), the additional apparatus speed is limited only by the safe cable strength and apparatus overload. The apparatus does not lose mass to increase its speed.

If apparatus is disconnected in a direction with an angle of φ to the asteroid speed direction, the additional apparatus speed is:

$$\Delta V = V(1 + \cos \varphi), \quad (11.11)$$

where V is initial speed of the asteroid around the space ship [m/s] (coordinate center is located at the space apparatus); ΔV is additional speed received by the ship from the

asteroid [m/s]; and φ is the angle between the old velocity vector of the asteroid and the new velocity vector of the apparatus.

The additional kinetic energy of the apparatus is then:

$$E_k = 0.5m_2(\Delta V)^2. \quad (11.12)$$

7. The known formulas below may be useful:

$$\begin{aligned} V &= \omega R, \quad V_3 R_3 = V_2 R_2, \quad V_1 = R_0 \left(\frac{g_0}{R} \right)^{0.5}, \\ V_2 &= \sqrt{2}V_1, \quad R_g = \left(\frac{g_0 R_0^2}{\omega^2} \right)^{1/3}, \end{aligned} \quad (11.13)$$

where V_1 is the circular speed around the Earth; V_2 is the escape speed; R_0 is the Earth's radius; and R_g is the radius of Earth's geosynchronous orbit.

11.3 Project

The capability to change the trajectory and speed of a space vehicle using an asteroid is shown in Fig. 11.4. The space ship could obtain a maximum additional speed equal to twice the speed difference between the space vehicle and the asteroid (speed of the asteroid around the space ship). If the length of the connection cable is changed, the speed of the space ship could change by more than double the speed difference. If the asteroid is rotating, the space ship can also obtain an additional speed increase from the rotation. The additional speed from one asteroid is also limited (for a manned ship) by the mass of the cable. For an additional speed of 1000 m/s and $K = 0.2$, the mass of cable would equal 5% of the mass of the space apparatus. For an additional speed of 2000 m/s, the mass of cable would equal 23% of the mass of the space apparatus. To travel to an asteroid, a connection device may be mounted onto the transport cable. The cable may be used many times.

The results of computation for different cases are shown in Figs. 11.6–11.11.

11.4 Discussion

If the change in the ship's speed is less than 1000 m/s, the conventional widely produced fiber (safe $K = 0.1$) can be used¹⁸. The cable mass is about 8% of the ship's mass. After disconnection the cable will be spooled and can be used again. The reader can make estimations for other cases. Radio or optical devices can locate asteroids at distance of thousands of kilometers. Their speed, direction of flight, and mass can be computed. The ship (probe) can make small corrections to its own trajectory to obtain the required position relative to the asteroid. All big asteroids with a diameter of more than 1 km are

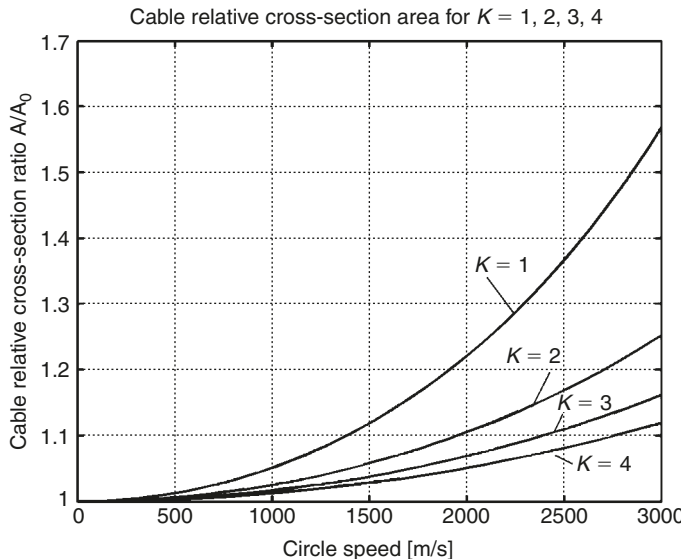


Fig. 11.9. Asteroid cable relative ratio via a circle speed [m/s] and coefficient $K = 1\text{--}4$.

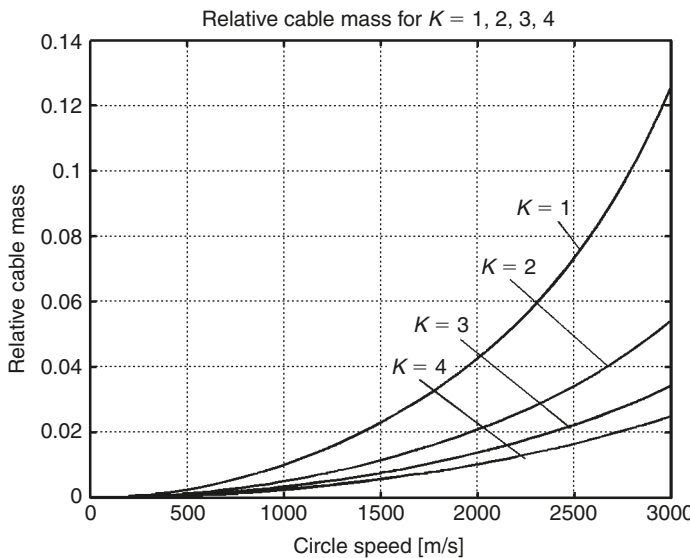


Fig. 11.10. Relative cable asteroid mass via circle speed [m/s] and coefficient $K = 1\text{--}4$.

listed in astronauic catalogs and their trajectories are well known. One thousand of them are located near the Earth. For those, we can compute in advance the intercept parameters. At the present time, long-range space apparatus uses the gravity of a planet to change its trajectory. However, the solar system has only nine planets, and they are

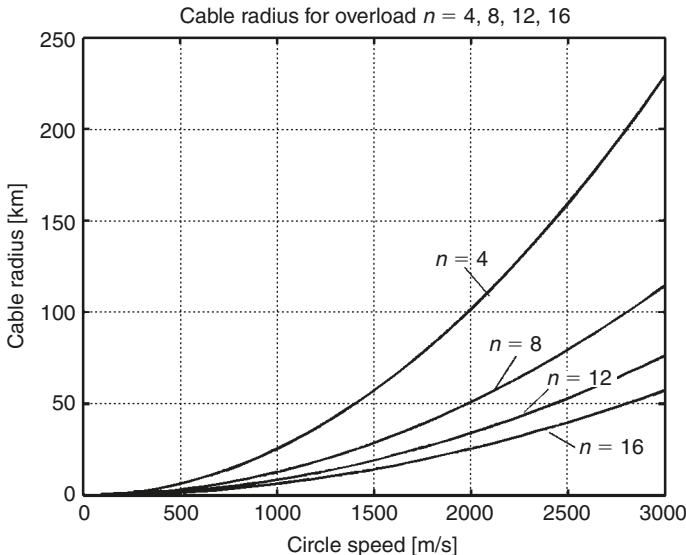


Fig. 11.11. Cable radius [km] via circle speed [m/s] and overload n .

located very far from one another. The employment of asteroids increases this possibility a million times over.

11.4.1 Estimation of the probability of meeting a small asteroid

It is known that every day about a ton of meteorites with a mass greater than 8 kg fall into the Earth's atmosphere. The Earth's surface area is about 512 million square kilometer. If the average mass of meteorites is 10 kg, then the Earth encounters 100 meteorites/day or one meteorite a day for every 5 million square kilometer. If a space probe has a mass around 100 kg, a 10 kg meteorite has enough mass for it to be employed to change the direction and speed of the space probe. Ground locators can detect a 1 kg space mass at distances up to thousands of kilometer. If the space ship can detect over a range of 1000 km, it means it can see a space body with an area of 1 million square kilometer, or about one meteorite in every 5 days. If one meteorite in ten is suitable for employment, it means every 50 days the space apparatus will meet an eligible meteorite near the Earth. The likelihood is 10 times greater in the asteroid belt between Mars and Jupiter. For 6000 big asteroids, we can compute the intercept parameters now. This number is expected to increase as more small asteroids are registered.

There are about 8000 fragments of old rockets and space equipment near the Earth. The trajectories of these are known. They also can be used to accelerate space apparatus. In this case we will have a double benefit: to accelerate the current space apparatus and remove space garbage into the Earth's atmosphere (or into outer space). This space garbage is dangerous for current ships and the problem increases every year.

Note that the kinetic energy of space bodies may be used if the space body has a different speed or direction. It is difficult to use a tether system (for example, the last stage of a rocket and the Shuttle ship) because they have the same speed and direction.

11.4.2 Cable

If the required change of speed is less than 1000 m/s, then cable from current artificial fibers can be used. In Chapter 1 the reader will find a brief overview of the research information regarding the proposed experimental test fibers.^{19–22}

11.5 Conclusion

The availability of both current and new materials makes the suggested propulsion system and projects more realistic for a long trip to outer space with a minimum expenditure of energy.²³

References

1. Space technology and Application. International Forum, 1996–1997, Albuquerque, MN, Parts 1–3.
2. D.V. Smitherman Jr., *Space Elevators*, NASA/CP-2000-210429, US National Aeronautics and Space Administration, Washington, DC, 2000.
3. M.L. Cosmo and E.C. Lorenzini (eds.), *Tethers in Space Handbook*, 3rd edition, Smithsonian Astronomic Observatory (USA), December, 1997.
4. S.E. Ziegler and M.P. Cartmell, “Using Motorized Tethers for Payload Orbital Transfer”, *Journal of Space and Rockets*, Vol. 38, No. 6, 2001.
5. M.R. Palmer, “A Revolution in Access to Space Through Spinoff of SDI Technology”, *IEEE Transactions on Magnetic*, Vol. 27, No. 1, January 1991, pp. 11–20.
6. A.A. Bolonkin, “Theory of Flight Apparatus with Control Radial Force”, *Collection Researches of Flight Dynamic*, Ed. I.V. Ostoslavsky, Mashinostroenie Publication, Moscow, 1965, pp. 79–118 (in Russian).
7. “Asteroids as Engine of Space Ships” (Suggestions of American scientist Alexander Bolonkin), *Weekly News*, 28 April 1998, Israel (in Russian).
8. A.A. Bolonkin, “Employment of Asteroids for Movement of Space Ship and Probes”, IAC-02-S.6.04, 53rd International Astronautical Congress, *The World Space Congress – 2002*, 10–19 October 2002, Houston, TX, USA.
9. A.A. Bolonkin, “Hypersonic Gas-Rocket Launch System”, AIAA-2002-3927, 38th AIAA/ASME/SAE/ASEE Joint Propulsion Conference and Exhibition, 7–10 July 2002, Indianapolis, IN, USA.
10. A.A. Bolonkin, “Hypersonic Launch System of Capability up 500 tons per day and Delivery Cost \$1 per lb”, IAC-02-S.P.15, 53rd International Astronautical Congress, *The World Space Congress – 2002*, 10–19 October 2002, Houston, TX, USA.

11. A.A. Bolonkin, "Inexpensive Cable Space Launcher of High Capability", IAC-02-V.P.07, *53rd International Astronautical Congress, The World Space Congress – 2002*, 10–19 October 2002, Houston, TX, USA.
12. A.A. Bolonkin, "Non-rocket Missile Rope Launcher", IAC-02-IAA.S.P.14, *53rd International Astronautical Congress, The World Space Congress – 2002*, 10–19 October 2002, Houston, TX, USA.
13. Bolonkin, "Non-rocket Space Rope Launcher for People", IAC-02-V.P.06, *53rd International Astronautical Congress, The World Space Congress – 2002*, 10–19 October 2002, Houston, TX, USA.
14. Bolonkin, "Non-rocket Earth–Moon Transport System", COSPAR 02-A-02226, *34th Scientific Assembly of the Committee on Space Research (COSPAR), The World Space Congress – 2002*, 10–19 October 2002/Houston, TX, USA.
15. A.A. Bolonkin, "Non-rocket Earth–Mars Transport System", COSPAR 02-A-02224, *34th Scientific Assembly of the Committee on Space Research (COSPAR), The World Space Congress – 2002*, 10–19 October 2002, Houston, TX, USA.
16. A.A. Bolonkin, "Transport System for Delivery Tourists at Altitude 140 km", IAC-02-IAA.1.3.03, *53rd International Astronautical Congress, The World Space Congress – 2002*, 10–19 October 2002, Houston, TX, USA.
17. A.A. Bolonkin, "Optimal Inflatable Space Towers of High Height", COSPAR 02-A-02228, *34th Scientific Assembly of the Committee on Space Research (COSPAR), The World Space Congress – 2002*, 10–19 October 2002, Houston, TX, USA.
18. F.S. Galasso, *Advanced Fibers and Composite*, Gordon and Branch Scientific Publisher, New York, 1989.
19. *Carbon and High Performance Fibers*, 6th edition, Chapman & Hall, Directory, New York, 1995.
20. M.S. Dresselhous, *Carbon Nanotubes*, Springer, New York, 2000.
21. *Concise Encyclopedia of Polymer Science and Engineering*. Ed. J.I. Kroschwitz, New York, 1990.
22. Newsletter Chim.& Rng., 8 October, New York, 2001.
23. A.A. Bolonkin, "Asteroids as Propulsion Systems of Space Ships", *Journal of the British Interplanetary Society*, Vol. 56, No. 3/4, 2003, pp. 98–107.

The reader can find the information about asteroids in the following publications:

A.R. Dobrovolskis, *Icarus*, Vol. 88, No. 24, 1990; J.V. Scotti and H.J. Melosh, *Nature*, Vol. 365, No. 733, 1993; P. Weissman, *Nature*, Vol. 320, No. 242, 1986; S.J. Weidenschilling, *Nature*, Vol. 368, No. 721, 1994; D. Sekanina and D.K. Yeomans, *Astronomical Journal*, Vol. 90, No. 2335, 1985; D. Sekanina, *Science*, Vol. 262, No. 382, 1993; R. Hudson and S. Ostro, *Science*, Vol. 263, No. 940, 1994; S. Ostro, *Reviews of Modern Physics*, Vol. 65, No. 1235, 1995; S. Ostro, *et al.*, *Nature*, Vol. 375, No. 474, 1995; J. Hills and P. Leonard, *Astrophysical Journal*, Vol. 109, No. 401, 1995; and J. Solem and J. Hills, *Astrophysical Journal*, Vol. 111, No. 1382, 1996.

CHAPTER 12

Multi-reflex Propulsion Systems for Space and Air Vehicles and Energy Transfer for Long Distance*

Summary

The purpose of this chapter is to draw attention to the revolutionary idea of light multi-reflection. This idea allows the design of new engines, space and air propulsion systems, storage systems (for a beam or solar energy), transmission of energy (over millions of kilometers), creation of new weapons, etc. This method and the main innovations were offered by the author in 1983 in the former USSR. Now the author shows the immense possibilities of this idea in many fields of engineering – aeronautics, aviation, energy, optics, direct conversion of light (laser beam) energy to mechanical energy (light engine), to name a few. This chapter considers the multi-reflex propulsion systems for space and air vehicles, and energy transmission over long distances in space.

12.1 Introduction

12.1.1 Short history

The relatively conventional way to send a spacecraft on an interstellar journey is to use the solar sail¹ or a laser sail.² This method is not effective because the light intensity is very low, with only one reflection. There has been a lot of research in this area and into solar sails in general.

A. Kantrowitz offered the conventional method for using a laser beam for space propulsion.³ He transferred energy using laser beam to a space vehicle, converted light energy into heat and evaporated a material, then obtained thrust from the gas pressure of this evaporated material. There is much research on this method.⁴ However, it is

* A detailed manuscript was published by A.A. Bolonkin, *Journal of British Interplanetary Society*, Vol. 57, No. 11/12, 2004, pp. 379–390.

complex, has low efficiency, has limited range (divergence of the laser beam), requires special materials located onboard the space ship, and requires a very powerful laser.

In 1983 the author offered another method: that of using light beam energy, then the direct conversion of light energy into mechanical pressure (for an engine), or thrust (for launchers and propulsion systems) by multiple reflections.⁵

The author found only one work related to this topic, published in 2001.⁶ However, our work is very different from this. Our suggested system has several innovations which make the proposed method possible to improve its parameters millions of times. The difference between our suggested system and the previous system⁶ is analyzed in Section 12.4.

The reflection of light is the most efficient method to use for a propulsion system. It gives the maximum possible specific impulse (light speed is 3×10^8 m/s). The system does not expend mass. However, the light intensity in full reflection is very small, about 0.6×10^{-6} kg/kW. In 1983, the author suggested the idea of increasing the light intensity by a multi-reflex method (multiple reflection of the light beam), and he offered some innovations to dramatically decrease the losses in mirror reflection (including a cell mirror and reflection by a superconducting material). This allows the system to make some millions of reflections and to gain some newtons of thrust per kW of beam power. This allows for the design of many important devices (in particular, beam engines⁷), which convert light directly into mechanical energy and solve many problems in aviation, space, energy, and energy transmission.

In the past years, achievements in optic materials and lasers have decreased the losses from reflection. The author returned to this topic and made it his primary area of research. He solved the main problems: the design of a highly efficient reflector (cell mirror); a light lock; focusing prismatic lightweight mirrors and lenses; a laser ring; and a beam transfer over very long distances (millions of kilometers) with only very small beam divergence, light storage, a beam amplifier, a modulator of light frequency, balloon suspension of mirrors, and so on.

12.1.2 Brief information about light and light devices

A short description of electromagnetic radiation can be found in the publication.⁷ A conventional mirror can reflect a maximum of 98–99% of the incident light energy of some bands of light waves. This gives a maximum of 200–300 reflections which is not enough for propulsion systems and engines. As the light pressure is so low (about 0.6×10^{-6} kg/kW), we need at least a million reflections.

There is a well-known method for increasing mirror reflection. The layers of a quarter-wave optical thickness of high and low refractive-index materials increase the reflectance. After more than 12 layers, the reflective efficiency of a dielectric mirror approaches 100%, with virtually no absorption or scattering. Maximum reflectance occurs only in a region around the design wavelength. The size of the region depends on the design of the stack of multiple dielectric coatings. Outside this region the reflectance is reduced.

For example, at one-half the design wavelength, it falls to the level of the uncoated substrate. The dielectric mirror is also designed for use at a specific angle of incident radiation. At other angles, the performance is reduced, and the wavelength of maximum reflectance is shifted.

Unfortunately, this dielectric mirror method is not suitable for mirrors moving relative to each other as the reflected frequency is shifted slightly, and this frequency shift accumulates over multiple reflections. Also conventional mirrors tend to reflect the beam off in some other direction if the mirrors are not kept in perfect alignment to the beam. The author's proposed cell mirror reflects the beam in the same direction which is very important for decreasing the beam divergence. The small cells provide high reflectance and small absorption.

A narrow laser beam is the most suitable for a light engine and light propulsion. There are many different types of lasers with different powers (peak power up to 10^{12} W), wavelength (0.2–700 μm), efficiency (1% up to about 95%), and pulse rate (up to some thousands of impulses per second) or continuous operations. In publications in the References the reader will find a brief description of the laser⁷ or more detail.⁸

At the present time we are seeing significant advances in high-power weapons-class lasers.⁷ The laser power reaches 1 million watts.

For our computation the beam divergence is very important. The laser beam divergence (see [Ref.⁸, p. 4]) is:

$$\theta = \frac{2}{\sqrt{\pi}} \frac{\lambda}{D} = 1.13 \frac{\lambda}{D}, \quad (12.1)$$

where θ is the angle of divergence [rad], λ is the wavelength [m], and D is an aperture diameter [m]. In particular, the diameter of the laser beam may be increased by an optical lens for reducing the beam divergence. The aperture diameter may be also increased by offered *laser ring* (Fig. 12.1). The reflex capacity may be improved by using a superconductive material⁵ (this idea needs additional research).

For more detailed information see Refs.^{7–9}

12.2 Description of innovation

12.2.1 Multi-reflex launch installation of a space vehicle

In a multiple reflection propulsion system a set of tasks appear: how to increase a mirror's reflectivity; how to decrease the light dispersion (from mirror imperfections and non-parallel surfaces); how to decrease the beam divergence; how to inject the beam between the mirrors (while keeping the light between the mirrors for as long as possible); how to decrease the attenuation (a mirror, prism material, etc.); how to increase the beam range; and how much force the system has.

To solve these problems, the author proposes:⁵ a special *cell mirror* which is very reflective and reflects light in the same direction from which it came; a *laser ring* which

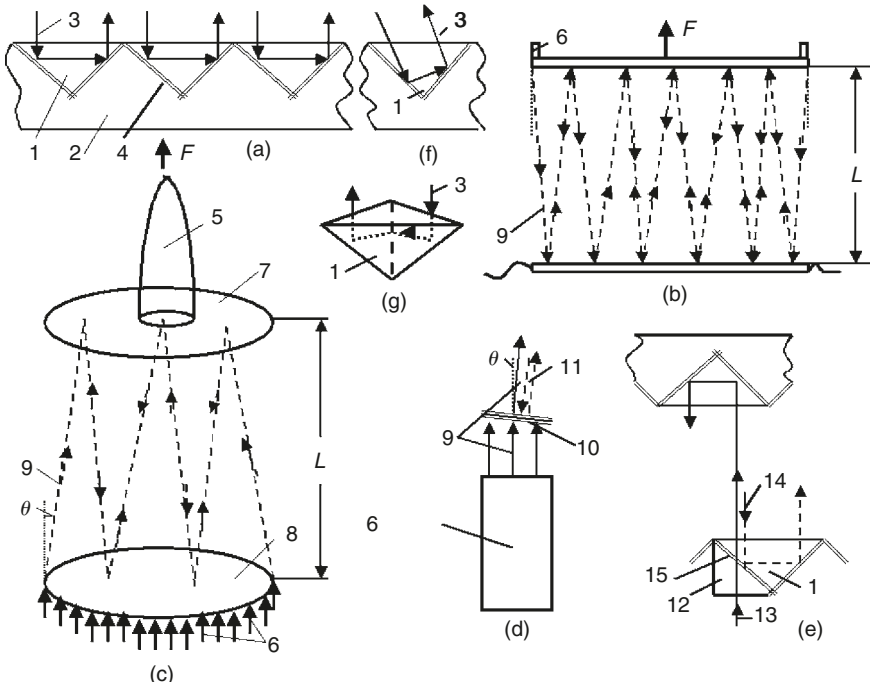


Fig. 12.1. Space launcher. *Notations:* (1) Prism; (2) mirror base; (3) laser beam; (4) mirror after chink (optional); (5) space vehicle; (6) lasers (ring set of lasers); (7) vehicle (ship) mirror; (8) planet mirror; (9) laser beam; (10) multi-layer dielectric mirror; (11) laser beam after multi-reflection (wavelength $\lambda_{11} > \lambda_9$); (12) additional prism; (13) entry beam; (14) return beam; and (15) variable chink between main and additional prisms. (a) Prism (cell, corner cube) reflector; (b) beam multi-reflection; (c) launching by multi-reflection; (d) the first design of the light lock; (e) the second design of the light lock; (f) reflection in the same direction when the beam is not perpendicular to mirror surface; and (g) mirror cell (retroreflector cell or cube corner cell). A light ray incident on it is returned parallel to itself after three reflections.

decreases the beam divergence; *light locks* which allows the light beam to enter but keeps it from exiting; and a *beam transfer* – a focusing prismatic thin lens, prisms, a set of lenses, and mirrors located in space (asteroids, moons, satellites, and so on).

12.2.1.1 Cell mirrors

To achieve the maximum reflectance, reduce light absorption, and preserve beam direction the author uses special *cell mirrors* which have millions of small 45° prisms (1 in Fig. 12.1(a) and (g)). Cell mirrors are retroreflector cells or cube corner cells. A light ray incident on a cell is returned parallel to itself after three reflections (Fig. 12.1(g)). In the mirror, provided the refractive index of the prism is greater than $\sqrt{2}$ (≈ 1.414), the light will be reflected by total internal reflection. The small losses may be only from prism (medium) attenuation, scattering, or due to small surface imperfections and Fresnel reflections at the entrance and exit faces. Fresnel reflections do not result losses when the beam is perpendicular to the entry surface. No entry losses occur where the beam is polarized in parallel of the entry surface or the entry surface has an anti-reflection coating

with reflective index $n_1 = \sqrt{n_0 n_2}$, where n_0 and n_2 are reflective indexes of the vacuum and prism, respectively. These cell mirrors turn a beam (light) exactly back at 180° if the beam deviation is less than $5\text{--}10^\circ$ from a perpendicular to the mirror surface. For incident angles greater than $\sin^{-1}(n_1/n_2)$, no light is transmitted, an effect called total internal reflection. Here n is the refractive index of the medium and the lens ($n \approx 1\text{--}4$). Total internal reflection is used for our reflector, which contains two plates (mirrors) with a set of small corner cube prisms reflecting the beam from one side (mirror) to the other side (mirror) (Fig. 12.1(b), (c), and (f)). Each plate can contain millions of small ($30\text{--}100\ \mu\text{m}$) prisms from highly efficient optic material used in optical cables.⁹ For this purpose a superconductivity mirror⁵ may also be used.

12.2.1.2 Laser ring

The small lasers are located in a round ring (Fig. 12.1(c)). A round set of lasers allows us to increase the aperture, resulting in a smaller divergence angle θ . The entering round beam (9 in Fig. 12.1(a)) has slip θ (or $\theta/2$) to the vertical. The beam is reflected millions of times as is shown in Fig. 12.1(b) and (c), and creates a repulsive force, F . This force may be very high, tens of N/kW (see Section 12.3.7) for motionless plates. In a vacuum it is limited only by the absorption (dB) of the prism material (see below) and beam divergence. For the mobile mirror (as for a launch vehicle) the wavelength increases and beam energy decreases as the mirrors move apart.

This system⁵ can be applied to a space vehicle launch on a planet that has no atmosphere and small gravity (for example, the Moon; high gravity requires high beam power).

12.2.1.3 Light lock

The first design of *light lock* allows the laser beam to enter, but closes the exit of a returned ray. The beam (9 in Fig. 12.1(d)) of continuous laser passes through a multi-layer dielectric mirror (10 in Fig. 12.1(d)). The entering beam runs the full length between mirrors (Fig. 12.1(b) and (c)), reflects a million times, and enters from the other side (11 in Fig. 12.1(d)). For moving (separating) mirrors the wavelength is changed because the beam gives up energy to the moving mirrors (see Section 12.3.7). As a result the wavelength increases ($\lambda_{11} > \lambda_9$) when the distance increases, and the wavelength decreases ($\lambda_{11} < \lambda_9$) when the distance decreases. The mirror (10 in Fig. 12.1(d)), is designed to pass the laser beam (9 in Fig. 12.1(d)) and to reflect back the *used* ray (11 in Fig. 12.1(d)). If the beam is not reflected by the mirror (10 in Fig. 12.1(d)), it enters into the laser and will be reflected back by the laser's internal mirror.

The second design of the *light lock* is shown in Fig. 12.1(e). This contains an additional prism (12) and an impulse laser. When laser beam (13) enters the system, the additional prism (12) is pushed into the main prism (1). While the beam runs between the mirrors, the additional prism is disconnected from the main prism and the return beam (14) cannot go back in. It travels inside the reflected mirrors with a lot of reflections if the mirrors have the right focuses. The chink (15) between the additional and main prisms may be very small, about a light wavelength ($1\ \mu\text{m}$). A piezoelectric plate can be used to move the additional prism.

A continuous or pulse laser may be used for the first light lock and a pulse laser may be used for the second lock. We compute average laser power.

The details of attenuation of light propagating through an optical material are considered in physics textbooks. To increase the number of reflections, we use a set of very small prisms and a highly efficient optical material ($\text{dB} = 0.1\text{--}0.5$).

12.2.2 Space beam transfer

Space *beam transfer* is shown in Fig. 12.2(a). The first lens has a large aperture for the laser beam and focuses the beam which decreases the divergence angle θ . The other Fresnel's lens then continues to focus the beam (Fig. 12.2(a)).

Non-focused beam is losing intensity through diffracted rays but *beam transfer* has a special focusing lens. If the focus is located at a distance $S_1 = D/2\theta$, the beam does not have losses through up to a diffracted rays in this distance S , but after the distance S the divergence angle becomes 2θ (Fig. 12.2(b)). If we need to transmit energy a distance $L < S$ (for example, in launching), this method is fine since the distance between the mirrors $L \ll S$ and the beam is reflected many times without loss. If we want to transfer the energy over very long distance, the method shown in Fig. 12.2(c) may be better. In this method the beam is focused on point at a distance $S_2 = D/\theta$. The beam has small amounts of diffraction everywhere, but the losses are smaller after a distance $1.5S_1$ than

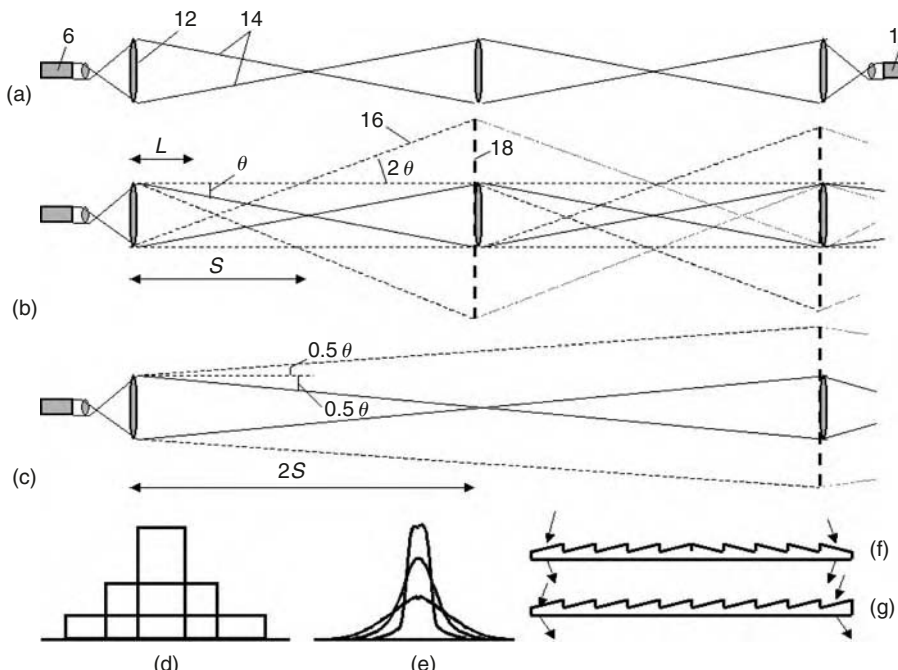


Fig. 12.2. Laser beam long-distance transfer. Notations: (12) Lens; (14) bounds of laser rays; (15) light receiver; and (16) divergence ray. (a) Focused beam; (b) focused beam with angle θ which has part S without divergence; (c) focused beam with angle 0.5θ which has minimum divergence at a long distance; (d) beam with a plate wave front; (e) Gaussian beam with normal distribution of beam front; (f) Fresnel's (prism) lens; and (g) lens for changing the beam direction.

in the case of Fig. 12.2(b). If an intermediate lens with a much larger diameter than the initial lens (Fig. 12.2(b) and (c)) is added midway, it is possible to decrease the beam diffraction energy losses to a very small value.

The distribution of energy in a cross-section area of the beam is also important for divergence and diffraction losses. The plate front (Fig. 12.2(a)) of the wave, and plate distribution of energy and divergence (Fig. 12.2(d)) are worst and give the maximum of energy losses. A normal distribution of beam energy and a Gaussian beam is better because the losses of beam energy through diffraction are reduced at the edges (Fig. 12.2(e)).

Energy transfer is done in the following way. First the Fresnel's lenses (collimators) (Fig. 12.2(f)), Fresnel's prisms (Fig. 12.2(g)), and mirrors are (permanently) located in space (Fig. 12.3(a)). Their trajectories and the receiving space vehicle's trajectory in space are known. Through commands from Earth, a space ship, or the vehicle's computer, the mirrors, and lenses are turned to the required angles (angular position). A small pilot ray may be used for aiming and focusing. The required angular changes are small (for focusing and small corrections in direction) and may be made by piezoelectric controlled plates. After the pilot ray reaches the space vehicle as required, the full power beam is transmitted to the space vehicle. This beam may be used to launch vehicles from an asteroid or small mass planetary satellites (Fig. 12.1(c)), to change the vehicle's trajectory (Fig. 12.3(b)), or to increase the acceleration of the space vehicle near an asteroid (Fig. 12.3(c)) using the multi-reflex method (Fig. 12.3(a–c)). This beam energy may also be used by the space vehicle for its rocket engine and internal power requirements. The distance between lenses may reach tens of millions of kilometers (see Section 12.3.7, Fig. 12.13). The average distances of the nearest planets from the Sun

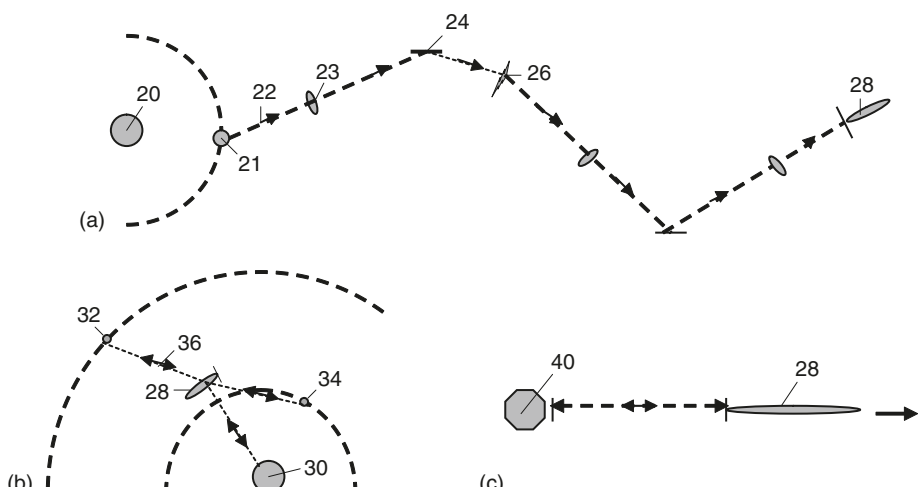


Fig. 12.3. Space energy transfer over long distance. Notations: (20) Sun; (21) Earth; (22) laser beam; (23) Fresnel's lens; (24) mirror; (26) Fresnel's prism; (28) space vehicle; (30) planet; (32 and 34) planet satellite; (36) multi-reflection; and (40) asteroid. (a) Transferring thrust from Earth to space ship by laser beam; (b) using of satellites (or Moons) to change the vehicle's trajectory; and (c) using of asteroid for launching of ship.

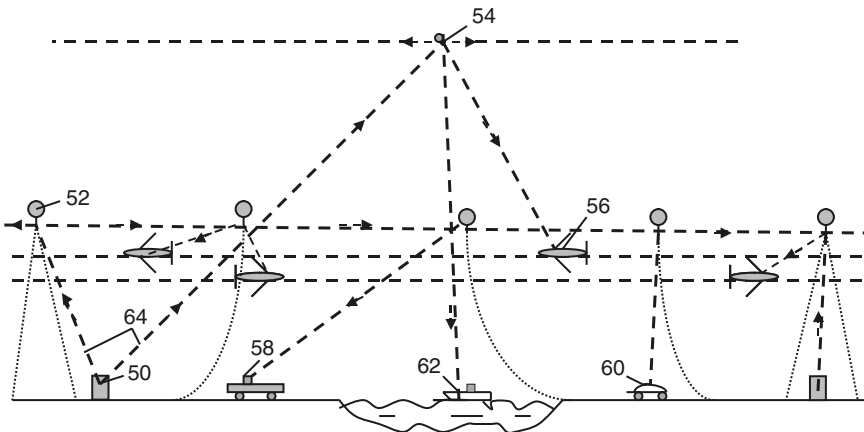


Fig. 12.4. Beam energy transfer to air, land, and sea vehicles. *Notations:* (50) Beam energy station; (52) control mirror suspended from a tethered air balloon; (54) mirror suspended from planet satellite; (56) aircraft; (58) ground track; (60) car; (62) sea (ocean) ship; and (64) beams.

are: Venus 108×10^6 km, Earth 150×10^6 km, and Mars 228×10^6 km. Transfer efficiency of system may be about 0.7–0.9 (see Section 12.3.7).

12.2.3 Aviation and energy air transfer

This method may be used for the transfer of energy to air, land, sea, and ocean vehicles (Fig. 12.4). The transfer beam passes through the atmosphere only once and loses little energy. The vehicle may use light (multi-reflex) engines.^{5,7} A multi-reflex engine transfers (converges) the beam (light) energy directly into mechanical energy (rotates the propeller) with high efficiency.

The system should include beam energy station(s), control mirrors suspended from air balloons at an altitude of 12–18 km (or on satellites), and a control system. The energy station sends the beam to the nearest mirror. The mirror reflects it to other mirrors (or lenses, or prisms). These mirrors distribute the beam to the system's customers (aircraft, ground vehicles, river or sea ships, and so on). These customers may have light (multi-reflex) engines^{5,7} and directly convert the light (electromagnetic radiation) into mechanical work. The control system guides the energy distribution. In a clear atmosphere, the efficiency of this energy delivery system is high. It is important that the air is clean and clear at the initial, mainly vertical distance (from the energy station to the first mirror). At times of rain or smoke (from fires, etc.), a backup method should be in place, perhaps using orbiting satellite mirrors. At altitudes over 12 km the atmosphere is generally clear. This method allows us to deliver energy over some thousands of kilometers (see Section 12.3.7, Fig. 12.14). In wartime the beam may be focused and used against the enemy.

12.3 Theory (estimation) of multi-reflex launching and beam transfer

Special theory, methods, and computation for this case are developed below.

12.3.1 Attenuation of beam

The attenuation of light-pass propagating through an optical material is caused either by absorption or by scattering. In both absorption and scattering, the power is lost over a distance (z) from the power $N(z)$, propagating at that point. So we expect an exponential decay:

$$N(z) = N(0)\exp(-yz). \quad (12.2)$$

The attenuation coefficient (y) is normally expressed in dB/km, with 1 dB/km being the equivalent of $2.3 \times 10^{-4}/\text{m}$. Absorption is a material property in which the optical energy is normally converted into heat. In scattering processes, some of the optical power in the guided modes is radiated out of the material.

Attenuation in some current and some potential very low loss materials that have been created for fiber communication has a dB value of up to $a = 0.0001^7$ (Fig. 12.3 or Fig. A3.3 in this book). However, some of these materials are highly reactive chemically and are mechanically unsuitable for drawing into a fiber. Some are used as infrared light guides, none are presently used for optical communication, but may be useful for our purposes. Our mechanical property and wavelength requirements are less stringent than for optical communications. We use in our computation $a = 0.1\text{--}0.4 \text{ dB/km}$. The conventional optical material widely produced by industry for optical cable has an attenuation coefficient of 2 dB/km.

12.3.2 Change in beam power

The beam power will be reduced if one (or both) reflector is moved, as the wavelength changes. The total relative loss of the beam energy in one double cycle (when the light ray is moved to the reflector and back) is:

$$q = (1 - 2\gamma)(1 - 2\xi)(1 \pm 2v)\varsigma, \quad (12.3)$$

where $v = V/c$, V is the relative speed of the mirrors [m/s], and $c = 3 \times 10^8 \text{ m/s}$ is the speed of light. We take the “+” when the distance is reduced (braking) and take “−” when the distance is increased (as in launching, a useful work for light); γ is the light loss through prism attenuation; ξ is the loss (attenuation) in the medium (air) (in clean air $\xi = 0.333 \times 10^{-6}/\text{m}$); v is the loss (useful work) through relative mirror (lens) movement; and ς is the loss through divergence and diffraction.

12.3.3 Multi-reflex light pressure

The light pressure, T , of two opposed high reflectors after a series of reflections, n , to one another is:

$$T_0 = \frac{2N_0}{c}, \quad T_1 = \frac{2N_0}{c}q, \quad T_2 = \frac{2N_0}{c}q^2, \quad T_3 = \frac{2N_0}{c}q^3, \quad \dots, \quad T_{n-1} = \frac{2N_0}{c}q^n. \quad (12.4)$$

When q is a constant, then it is a geometric series. The sum of n members of the geometric series is:

$$T = \frac{2N_0}{c} \frac{q^n - 1}{q - 1}. \quad \text{If } n = \infty, \quad \text{then} \quad T_\infty = \frac{2N_0}{c} \frac{1}{1 - q}, \quad q < 1. \quad (12.5)$$

12.3.4 Limitation of reflection number

If the reflector is moved away, the maximum number of reflections, n , is limited by cell size, l , because the wavelength, λ , is increased and that cannot be more than the cell size. This limit is:

$$n \leq \frac{\ln(l/\lambda_0)}{2v}, \quad (12.6)$$

where l is the cell width [m] and λ_0 is the initial wavelength [m].

If the reflector is moved forward to another position the wavelength is reduced, but it cannot be less than the wavelength of X-rays because the material transmits the X-rays (the material lessens the reflective capability).

This limit is about $\lambda_{\min} = 10 \text{ nm}$. The maximum number of brake reflections is:

$$n \leq \frac{\ln(\lambda_0/\lambda_{\min})}{2v}. \quad (12.7)$$

12.3.5 Coefficient of efficiency

The efficiency coefficient, η , may be computed using the equation:

$$\eta = TV/N_0. \quad (12.8)$$

12.3.6 Focusing the beam

If the lens used in focused at a range S_1 , the distance, S , without ray divergence is (Fig. 12.2(b)):

$$S = \frac{D}{2\theta}, \quad \theta = \frac{2}{\sqrt{\pi}} \frac{\lambda}{D}, \quad S = \frac{\sqrt{\pi}}{4} \frac{D^2}{\lambda} = 0.443 \frac{D^2}{\lambda}, \quad (12.9)$$

where D is the diameter of the lens or mirror [m]. This distance is equal to the lens focus distance for the case in Fig. 12.2(b) ($S_1 = S$). In the case Fig. 12.2(c) (transfer over very long distance), the optimal focus distance is $S_2 = 2S_1$.

12.3.7 Some computations

The computation of equation (12.9) is presented in Figs. 12.5 and 12.6. As you will see, the necessary focus distance may be high.

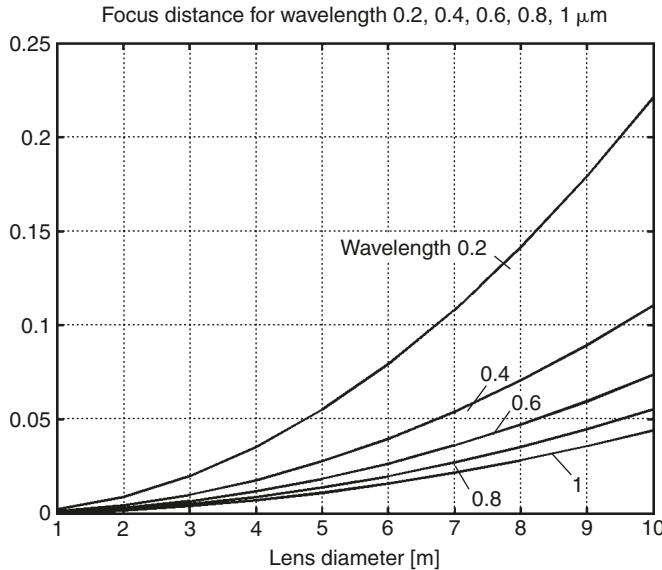


Fig. 12.5. Focus distances [10^6 km, million kilometers] versus lens diameters 1–10 m and wavelength $\lambda = 0.2\text{--}1 \mu\text{m}$.

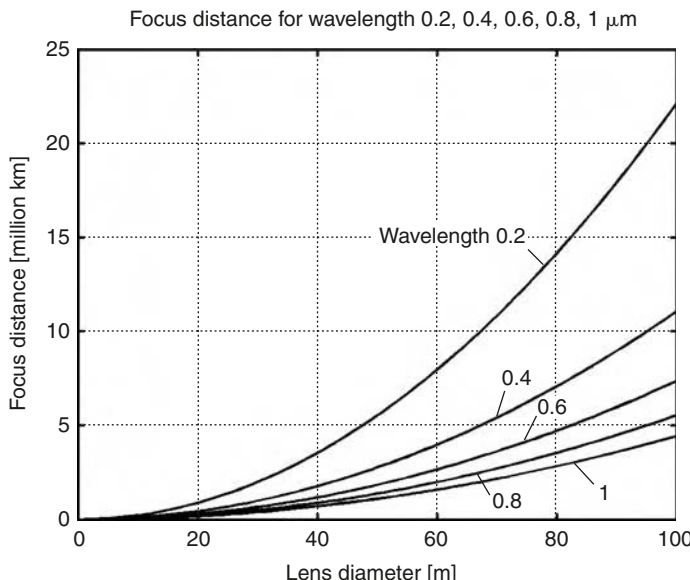


Fig. 12.6. Focus distances versus lens diameters $D = 1\text{--}100$ m and wavelength $\lambda = 0.2\text{--}1 \mu\text{m}$.

The values in equation (12.3) can be computed as:

$$\gamma = yz = 0.00023al, \quad l = m\lambda, \quad m \geq 1, \quad \xi = 0.333 \times 10^{-6} L, \quad (12.10)$$

where a is the attenuation coefficient in dB [km⁻¹]⁷ (Fig. 12.3) and m is initial value of the wavelength which can be located in cell size l [m].

The loss through divergence, s , for the case in Fig. 12.2(b) and (d) is:

$$\begin{aligned} &= \frac{\pi(D/2)^2}{\pi(D/2 + 2\gamma(L - S))^2}, \quad 2\gamma(L - S) = \frac{4k}{\sqrt{\pi}} \frac{\lambda(L - S)}{D}, \\ &= 1/\left(1 + \frac{8k\lambda(L - S)}{\sqrt{\pi}D^2}\right)^2 \quad \text{for } L > S, \end{aligned} \quad (12.11)$$

where L is the distance between the mirrors (lenses) [m] and k is the focus coefficient. In case in Fig. 12.2(b) (where the focus distance is $D/2\theta$) $k = 0$ when $L < S$ (for transfer) or $n < S/L$ (for reflection), and $k = 2$ when $L > S$, or $n > S/L$; in the case in Fig. 12.2(c) (S is absent, $S = 0$) $k = 0.5$ if the focus distance is D/θ ; $k = 1$ if focus distance is infinity (no focusing).

The relative beam power along its trajectory for plate power distribution as in Fig. 12.2(d) is:

$$\bar{N} = N/N_0 = 1 \quad \text{when} \quad L \leq S_1 \quad \text{and} \quad \bar{N} = s \quad \text{when} \quad L > S_1 = D/2\theta. \quad (12.12)$$

The force coefficient, A , shows how many times the initial light pressure is increased. For $L < S_1$ it is:

$$A = \frac{q^n - 1}{q - 1}. \quad (12.13)$$

The multi-reflex launch of a space vehicle from a small planet with low gravity, are without an atmosphere (the Moon or an asteroid) may be computed using the following equations (for focusing Fig. 12.2(b) and beam distributions Fig. 12.2(d)):

$$\begin{aligned} T &= \frac{2N_0}{c} \frac{q^{n_1} - 1}{q - 1} + \frac{2N_0}{c} q^{n_1} \frac{q_1^{n_2} - 1}{q_1 - 1}, \quad n_1 = \frac{S_1}{L}, \quad n_2 = n_1 - n_3, \quad n_3 = \frac{\ln m}{2\nu}, \\ q &= (1 - 2\gamma)(1 - 2\nu), \quad q_1 = qs, \quad \Delta V = \left(\frac{T}{M} - g\right)\Delta t, \quad V_{i+1} = V_i + \Delta V, \\ \Delta L &= V_i \Delta t. \quad L_{i+1} = L_i + \Delta L, \quad t_{i+1} = t_i + \Delta t. \end{aligned} \quad (12.14)$$

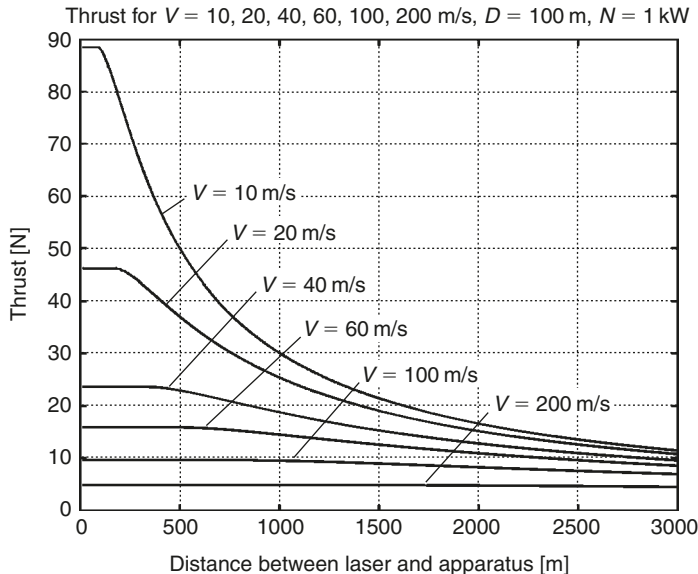


Fig. 12.7. Thrust (N) versus distance [m] for vehicle speed $V = 10\text{--}200 \text{ m/s}$, attenuation coefficient $a = 0.5 \text{ dB}$, cell size $m = 30$, mirror diameter $D = 100 \text{ m}$, and beam power $N = 1 \text{ kW}$.

Here the first element in T is the thrust when the beam runs the distance S_1 without divergence.

The second element in T is the thrust when the beam runs the distance with divergence. M is space vehicle mass [kg], and g is the planet's gravity [m/s^2]. When $n_3 < n_1$, we take $n = n_3$ and compute T using equation (12.5). If $n_3 > n_1$, we compute T using equation (12.14).

Computation of thrust, T (the first part of equation (12.14)), and the efficiency coefficient, η , equation (12.8) are presented in Figs. 12.7 and 12.8.

The thrust and the efficiency coefficient decrease when the distance is above a some critical value, then a portion of the energy beam leaves the space between the mirrors through diffraction.

The computation for a vertical (the worst case) launch, equation (12.14), of a space vehicle from the Earth's Moon (the Moon has gravity, $g = 1.62 \text{ m/s}^2$) is presented in Figs. 12.9–12.12 ($\lambda = 1 \mu\text{m}$).

The power required to launch from the Earth's Moon is quite high because, as the vehicle's speed increases, the energy transfer efficiency is reduced. In the initial launch state that efficiency starts at $\eta = 0.97$. After acceleration (limit is $16g$, $g = 9.81 \text{ m/s}$) for a distance of $L = 2\text{--}10 \text{ km}$ the efficiency decreases (Fig. 12.10). The accelerating is high for only $0.1\text{--}2 \text{ s}$ ($16g$ is acceptable for trained cosmonauts). The mission designers could limit the maximum acceleration to $8g$ without significantly losing speed.

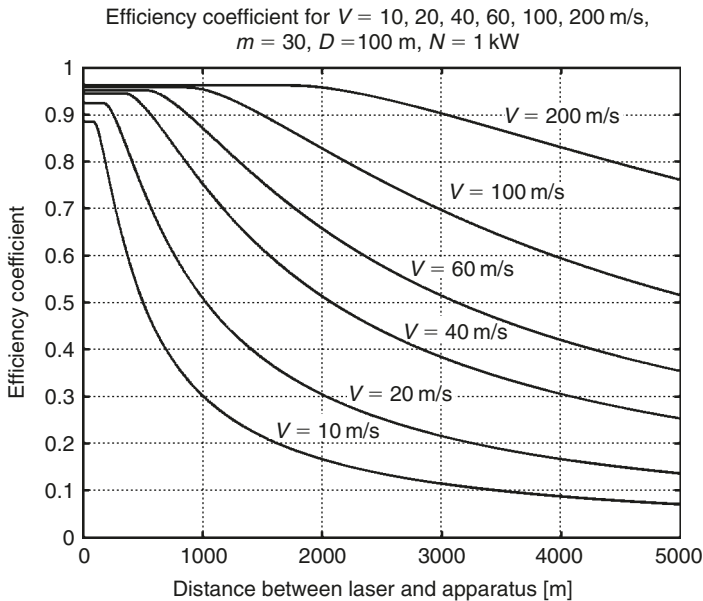


Fig. 12.8. Efficiency coefficient versus distance [m] for vehicle speed $V = 10\text{--}200 \text{ m/s}$, attenuation coefficient $a = 0.5 \text{ dB}$, cell size $m = 30$, mirror diameter $D = 100 \text{ m}$, and beam power $N = 1 \text{ kW}$.

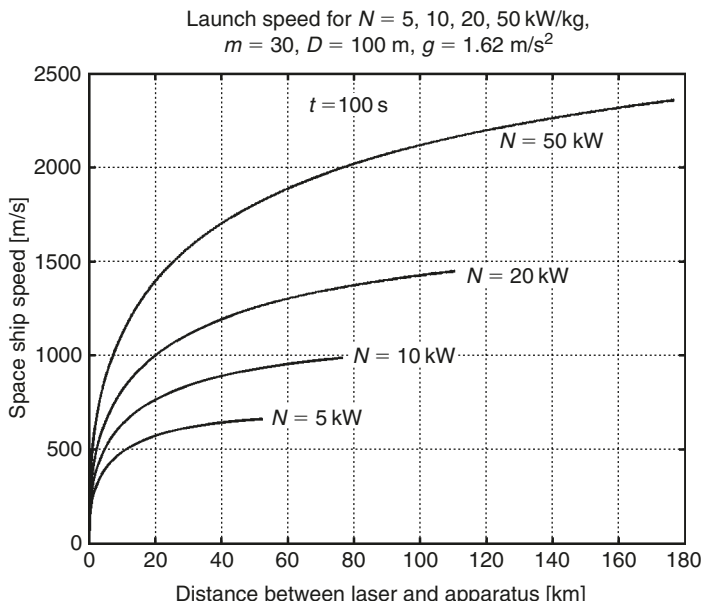


Fig. 12.9. Vertical launch of a space vehicle from the Earth's Moon (Moon gravity, $g = 1.62 \text{ m/s}^2$). Space ship speed (m/s) versus distance (km) is computed for relative beam power $N = 5\text{--}50 \text{ kW/kg}$, attenuation coefficient $a = 0.5 \text{ dB}$, cell size $m = 30$, and mirror diameter $D = 100 \text{ m}$. Acceleration is limited to $16g$ ($g = 9.81 \text{ m/s}^2$).

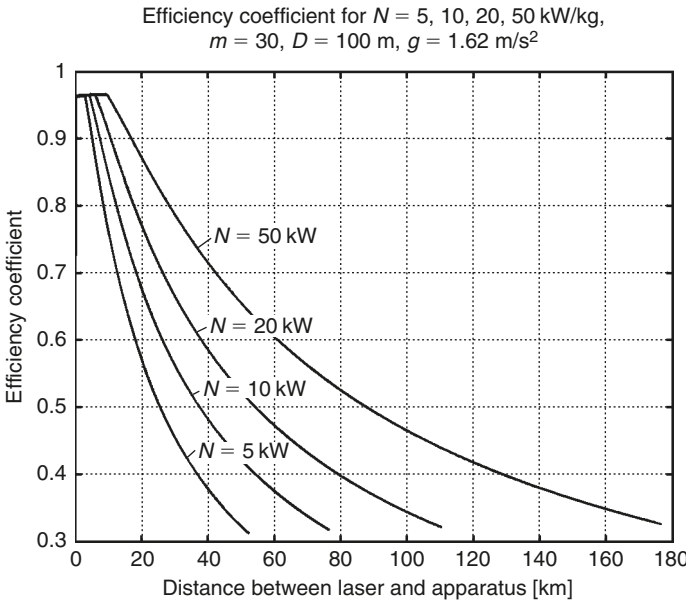


Fig. 12.10. Vertical launch of a space vehicle from the Earth's Moon (Moon gravity is $g = 1.62 \text{ m/s}^2$). Efficiency coefficient versus distance is computed for relative beam power $N = 5\text{--}50 \text{ kW/kg}$, attenuation coefficient $a = 0.5 \text{ dB}$, cell size $m = 30$, and mirror diameter $D = 100 \text{ m}$.

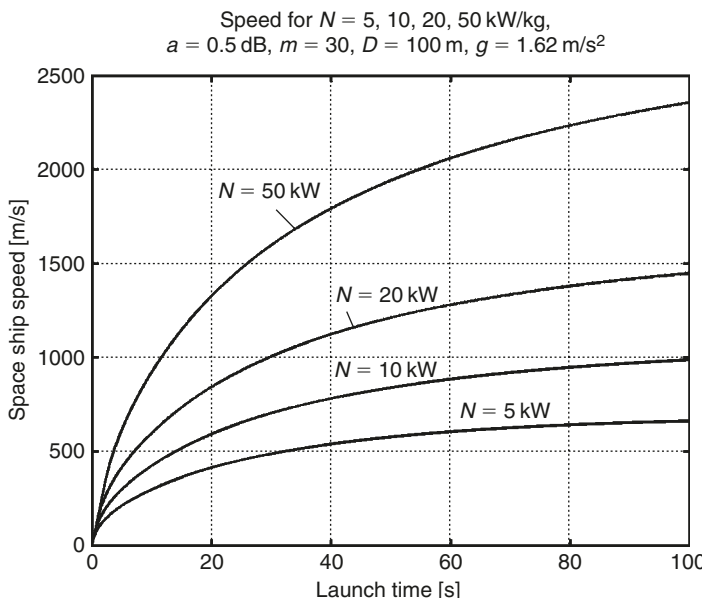


Fig. 12.11. Vertical launch of a space vehicle from the Earth's Moon (Moon gravity is $g = 1.62 \text{ m/s}^2$). Space ship speed (m/s) versus time (s) is computed for relative beam power $N = 5\text{--}50 \text{ kW/kg}$, attenuation coefficient $a = 0.5 \text{ dB}$, cell size $m = 30$, mirror diameter $D = 100 \text{ m}$, and $\lambda = 1 \mu\text{m}$.

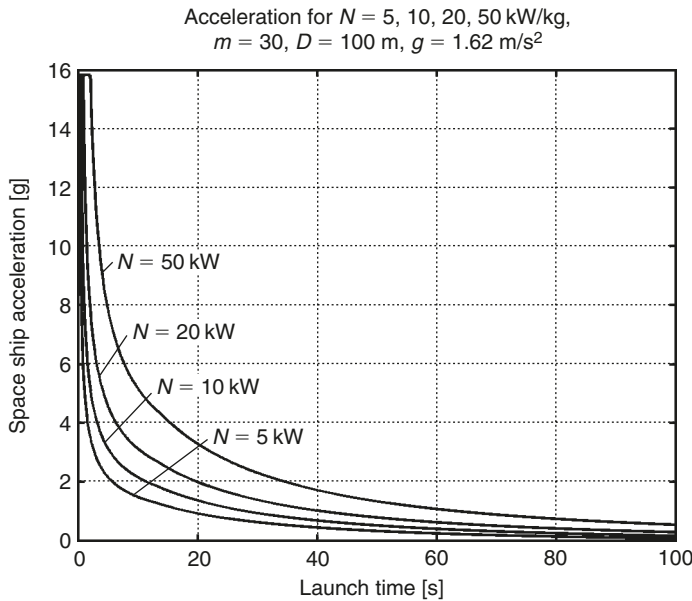


Fig. 12.12. Vertical launch of a space vehicle from the Earth's Moon (Moon gravity is $g = 1.62 \text{ m/s}^2$). Limited ($<16g = 16 \times 9.81 = 157 \text{ m/s}^2$) acceleration is computed for relative beam power $N = 5-50 \text{ kW/kg}$, attenuation coefficient $a = 0.5 \text{ dB}$, cell size $m = 30$, mirror diameter $D = 100 \text{ m}$, and $\lambda = 1 \mu\text{m}$.

The mirror diameter is large because small mirror diameters decrease the attainable speed. Starting from an asteroid or a planet's moon, that has low gravity, improves the attainable speed. Unfortunately, the multi-reflex launch from planets with an atmosphere does not work well because the multi-reflected rays travel long distances in a gas medium and lose a lot of energy.

Below is the equation for computing the beam power from the divergence and distance when the Gaussian beam has normal distribution (Fig. 12.2(f)). For case 1 (the focus is into point $2S_1$, Fig. 12.2(c)):

$$\bar{N}_1 = 2\psi \left[s \left(\frac{D}{D + \theta L} \right)^2 \right], \quad \theta = \frac{2}{\sqrt{\pi}} \frac{\lambda}{D}, \quad S = 0. \quad (12.15)$$

Here ψ is the probability function of normal distribution.

For case 2 (the focus is located at point S , Fig. 12.2(b)):

$$\text{When } L \leq S_1, \quad \bar{N}_2 = 1. \quad \text{When } L > S_1, \quad \bar{N}_2 = 2\psi \left[s \left(\frac{D}{D + 4\theta(L - S_1)} \right)^2 \right]. \quad (12.16)$$

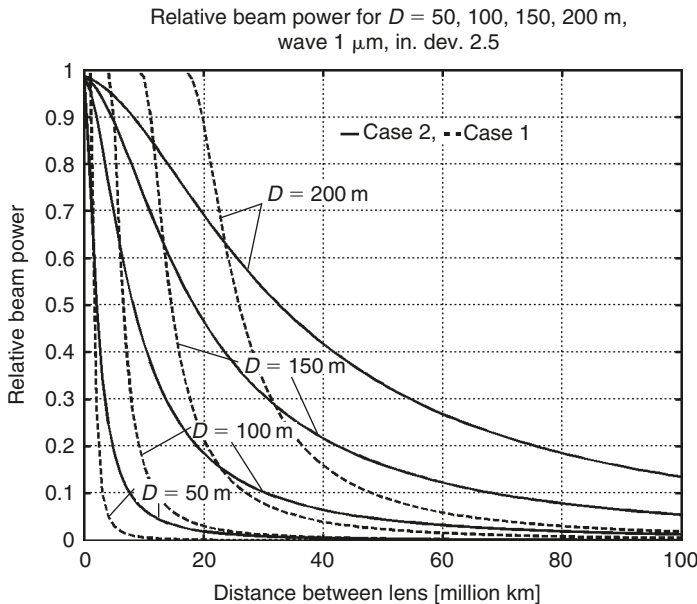


Fig. 12.13. Relative beam power of the normal (Gaussian) distribution ($s = \sigma = 2.5$) (Fig. 12.2(f)) in a vacuum versus distance in million kilometers between lenses for focusing at $D/2\theta$ (-, case 1) and D/θ (-, case 2).

Here s is a relative distribution value. The results of computations for space (vacuum) are presented in Fig. 12.13. It is shown that the focused beam travels without major losses if the distance between the mirrors (for mirror diameter $D = 100\text{--}200\text{ m}$) is $10\text{--}18$ million kilometers, and may travel up to 100 million kilometers with an efficiency of about 0.2. This means the focused beam can permanently transfer (without losses) energy from the Earth to the Moon or back (a distance of $0.4 \times 10^6\text{ km}$), and for 2–3 months (with efficiency 0.2) every 2 years, to Mars at a distance of $60\text{--}150 \times 10^6\text{ km}$.

For computation of the relative beam power in air at altitude H , we may use equations (12.15) and (12.16) corrected for air attenuation. That is:

$$\bar{N}_{a1} = \bar{N}_1(1 - b), \quad \bar{N}_{a2} = \bar{N}_2(1 - b), \quad \text{where} \quad b = 0.334 \times 10^{-6} \frac{\rho_H}{\rho_0} L, \quad (12.17)$$

where ρ_H and ρ_0 are the air density at altitudes H and $H = 0$, respectively.

The computation for an atmospheric balloon lens located at $H = 15\text{ km}$ ($\rho_H/\rho_0 = 0.159$) is presented in Fig. 12.14. As can be seen, the beam energy may be transferred by mirrors located on an air balloon to distances 4000 km out, with an efficiency of 0.8. If the energy is transferred through a satellite the range is not limited and the efficiency may reach to 0.98. Any smog, mist, haze, rain, or clouds (in the region of the power station) decreases the efficiency. However, these aerosols are absent at altitudes above 12 km. We must therefore have power stations in different locations to circumvent weather phenomena.

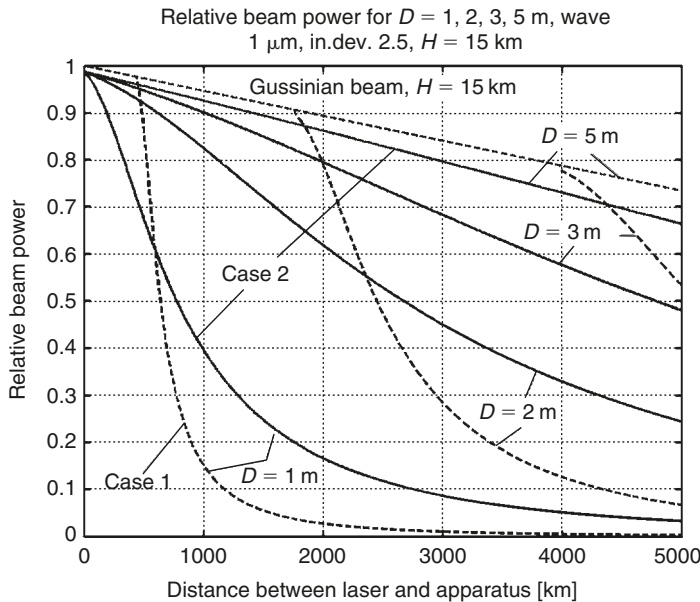


Fig. 12.14. Relative beam power of the normal (Gaussian) distribution ($s = \sigma = 2.5$) (Fig. 12.2(f)) in air (altitude $H = 15$ km) versus distance in kilometers between lenses for focusing at $D/2\theta$ (—) and at D/θ (---).

The computed parameters are not optimal. Our purpose is to demonstrate the method of computation.

Computations (Figs. 12.7 and 12.8) are made for a beam power $N_0 = 1$ kW. For beam power $N_0 = 10, 100, 1000$ kW we must multiply the force in Figs. 12.7 and 12.8 by 10, 100, and 1000, respectively.

12.4 Discussion

Comparing the *Multi-bounce laser-based sail system*⁶ with the proposed method – the *Multi-reflex propulsion system*:

1. The *Multi-bounce sail* uses the well-known multi-layer mirror, which has high reflectance only in a region around the design wavelength. Outside this region the reflectance is reduced. For example, at one-half the design wavelength, it falls to that of the uncoated substrate. As shown in this work, the wavelength changes by a small amount at each reflection in the mobile mirror. This means that after enough reflections the multi-layer mirror has lost its high reflectivity. It is impossible to use the multi-layer mirror for a multi-bounce space sail that is moving. The author has proposed the innovative new cell mirror for which the reflectivity does not depend on wavelength for wavelengths that are less than a cell length.
2. The multi-layer mirror⁶ is extremely large (1 km), with extremely small thickness (1600 nm), density (10 g/m²), and weight (7850 kg). A very small angle of deviation

at the multi-layer mirror surface (one-thousandth of a degree) under beam pressure, leads to complete defocusing at a distance of some millions of kilometers. This means the mirror⁶ will make only one reflection. The average mirror angle will also be changed permanently for a moving space ship.

It is impossible to control (turn) exactly the orientation of this gigantic and very thin sail.

The new cell mirror reflects the laser beam back in exactly the same direction if the surface and sail deviation are less than 5–10°. This means the mirror directoral control is not necessary on the spacecraft. Also, there may be imperfections in the surface film and the mirror control is not necessary.

3. The maximum reflection at multi-layer mirror is 99.95 (see Ref.⁶). The reflection of the cell mirror is $((1-0.4) \times 10^{-9})$ or 10^8 times better than the multi-layer mirror. The maximum reflection value of the multi-layer mirror is only 1000 (see Ref.⁶). Value for reflections of the cell mirror are in the millions.
4. The diameter of the multi-layer mirror is 1 km, the size of our cell mirror is 100 m.
5. The gigantic multi-layer mirror gives an acceleration of only 0.33 m/s^2 . This is not enough to launch itself from Earth (Earth's gravity is 9.8 m/s^2), Mars (3.72 m/s^2), or the Moon (1.62 m/s^2). The author's cell mirror gives an acceleration of 20 m/s^2 , and its size is 100 times smaller. If we were to make cell mirror 1 km in diameter, the capability of a space ship would be fantastic.

The author shows here only some of the advantages of one innovation (changing from the well-known multi-layer mirror to the new *cell mirror*). There are many deficiencies of the previous system⁶ which make its application virtually impossible. For example, with the multi-layer mirror the laser is located on the Earth's surface and its beam moves (from the laser to the ship and back to the laser) through the Earth's atmosphere a lot of times. The computation shows that the beam's energy will quickly be lost due to absorption and scattering by the Earth's (or Mars) atmosphere when it travels a long distance through it. In our system the beam moves through the atmosphere only one time and reflects between the Moon mirror and the space ship of all other times. This is insured by the innovation of the *light lock*.

Another deficiency of the laser-based sail system is that when the space ship is close to Earth, the sail will reflect the beam back to the laser. If the efficiency of the propulsion system were sufficient, the laser might be damaged or destroyed. This problem is absent in the author system because it uses a *light lock*, which closes the return path of laser beam.

The suggested *laser ring* (a set of small lasers located in a circle), *beam transfer*, *self-focused mirror*, and *Fresnel's lens* decrease the beam divergence and increase the beam transfer distance. It is possible to install the cell mirror on the Moon or on the Mars and transfer a laser beam to them, and then to make a space ship decelerate.

The other system⁶ requires a nuclear electric power station (of several gigawatts power) to be built and to deliver it, and a super powerful laser on Mars.

I do not mean to criticize other small mistakes in the work⁶ as, for example, the computation of multiple reflection acceleration (thrust) is not correct. The beam energy after every reflection will be decreased and the ship acceleration also will be decreased. For a large number of reflections this decrease is quite large (see the equations in this chapter).

The idea of a multiple reflection engine and cell, and superconductivity mirrors was probably offered first by author in 1983.⁵ But as I know, this work⁶ (2001) was the first research on this topic which is important.

12.4.1 General discussion

The offered multi-reflex light launcher, space and air focused energy transfer system is very simple (needing only special mirrors, lenses, and prisms), and it has a high efficiency. One can directly transfer the light beam into space acceleration and mechanical energy. A distant propulsion system can obtain its energy from the Earth. However, we need very powerful lasers. Sooner or later the industry will create these powerful lasers (and cell mirrors) and the ideas presented here will become possible. The research on these problems should be started now.

Multi-reflex engines⁷ may be used in aviation as the energy can be transferred from the power stations on the ground to the aircraft using laser beams. The aircraft would no longer carry fuel and the engine would be lighter in weight so its load capability would double. The industry produces a 1-MW (1000-kW) laser now. This is the right size for mid-weight aircraft (10–12 ton).

The linear light engine does not have a limit to its speed and may be used to launch space equipment and space ships in non-rockets method described in^{10–29}. This method is certain also to have many military applications.

References

1. R.L. Garwin, “Solar Sailing – A Practical Method of Propulsion within the Solar System”, *Jet Propulsion*, Vol. 28, March 1958, pp. 188–190.
2. R.L. Forward, “Pluto – The Gateway to the Stars”, *Missiles and Rockets*, Vol. 10, April 1962, pp. 70–75.
3. A. Kantrowitz, “Propulsion to Orbit by Ground-Based Lasers”, *Astronautics and Aeronautics*, Vol. 10, May 1972, pp. 74–76.
4. Beamed Energy Propulsion. *First International Symposium on Beamed Energy Propulsion*, American Institute of Physics, Melville, New York, 2003.
5. A.A. Bolonkin, “Light Pressure Engine”, Patent (Author Certificate) #1183421, USSR (priority on 5 January, 1983), 1985.
6. R.A. Metzger and G. Landis, “Multi-Bounce Laser-Based Sails”. *Proceedings of the Shape Technology and Application, Forum 2001*, Albuquerque, NM, 2001, *AIP Conference Proceedings*, Vol. 552, p. 397 [File: STAIF 2001 B].

7. A.A. Bolonkin, "Light Multreflex Engine", *Journal of British Interplanetary Society*, Vol. 57, No. 9/10, 2004, pp. 353–359.
8. P.W. Milonni and J.H. Eberly, *Lasers*, John Wiley & Sons, New York, 1988.
9. R.G. Driggers (ed.), *Encyclopedia of Optical Engineering*, Marcel Dekker Inc., New York, 2003.
10. A.A. Bolonkin, "Earth Accelerator for Space Ships and Missiles", *Journal of British Interplanetary Society*, Vol. 56, No. 11/12, 2003, pp. 394–404.
11. A.A. Bolonkin, "Kinetic Space Towers and Launchers", *Journal of British Interplanetary Society*, Vol. 57, No. 1/2, 2004, pp. 33–39.
12. A.A. Bolonkin, "Bolonkin Anti-gravitator", AIAA-2005-4504, *41st Propulsion Conference*, 10–12 July 2005, Tucson, AZ, USA.
13. A.A. Bolonkin, "Air Cable Transport", *Journal of Aircraft*, Vol. 40, No. 2, March–April 2003. US Patent 6,494,143 B1.
14. A.A. Bolonkin, "Non-Rocket Space Rope Launcher for People", IAC-02-V.P.06, *53rd International Astronautical Congress, The World Space Congress – 2002*, 10–19 October 2002, Houston, TX, USA.
15. A.A. Bolonkin, "Non-Rocket Missile Rope Launcher", IAC-02-IAA.S.P.14, *53rd International Astronautical Congress, The World Space Congress – 2002*, 10–19 October 2002, Houston, TX, USA.
16. A.A. Bolonkin, "Optimal Trajectory of Air Vehicles", *Aircraft Engineering and Aerospace Technology*, Vol. 76, No. 2, 2004, pp. 193–215.{AQ7}
17. A.A. Bolonkin, "Inexpensive Cable Space Launcher of High Capability", IAC-02-V.P.07, *53rd International Astronautical Congress, The World Space Congress – 2002*, 10–19 October 2002, Houston, TX, USA.
18. A.A. Bolonkin, "Employment Asteroids for Movement of Space Ship and Probes", IAC-02-S.6.04, *53rd International Astronautical Congress, The World Space Congress – 2002*, 10–19 October 2002, Houston, TX, USA.
19. A.A. Bolonkin, "Non-Rocket Earth–Moon Transport System", COSPAR-02 B0.3-F3.3-0032-02, 02-A-02226, *34th Scientific Assembly of the Committee on Space Research (COSPAR), The World Space Congress – 2002*, 10–19 October 2002, Houston, TX, USA.
20. A.A. Bolonkin, "Non-Rocket Earth–Mars Transport System", COSPAR-02 B0.4-C3.4-0036-02, *34th Scientific Assembly of the Committee on Space Research (COSPAR), The World Space Congress – 2002*, 10–19 October 2002, Houston, TX, USA.
21. A.A. Bolonkin, "Transport System for Delivery Tourists at Altitude 140 km", IAC-02-IAA.1.3.03, *53rd International Astronautical Congress, The World Space Congress – 2002*, 10–19 October 2002, Houston, TX, USA.
22. A.A. Bolonkin, "Asteroids as Propulsion Systems of Space Ships", *Journal of British Interplanetary Society*, Vol. 58, No. 3/4, 2003, pp. 97–107.
23. A.A. Bolonkin, "Non-Rocket Transportation System for Space Travel", *Journal of British Interplanetary Society*, Vol. 56, No. 7/8, 2003, pp. 231–249.
24. A.A. Bolonkin, "Centrifugal Keeper for Space Stations and Satellites", *Journal of British Interplanetary Society*, Vol. 56, No. 9/10, 2003, pp. 314–327.
25. A.A. Bolonkin, "Non-Rocket Earth–Moon Transport System", *Advances in Space Research*, Vol. 31/11, 2003, pp. 2485–2490, Elsevier.

26. A.A. Bolonkin, “Earth Accelerator for Space Ships and Missiles”, *Journal of British Interplanetary Society*, Vol. 56, No. 11/12, 2003, pp. 394–404.
27. A.A. Bolonkin, “High Speed Catapult Aviation”, AIAA Conference “Atmospheric Flight Mechanics”, August, 2005, USA, Paper AIAA-2005-6221.
28. A.A. Bolonkin, “Long Distance Transfer of Mechanical Energy”, International Energy Conversion Engineering Conference at Providence Rhode Island (USA), 16–19 August, 2004. Paper AIAA-2004-5660.
29. A.A. Bolonkin, “Non-Rocket Transport System Earth–Mars”, *Actual problems of Aviation and Aerospace Systems*, Kazan, Russia, Vol. 8, No. 2(16), 2003.
30. A.A. Bolonkin, “Multi-Reflex Propulsion Systems for Space and Air Vehicles and Energy Transfer for Long Distance”, *Journal of British Interplanetary Society*, Vol. 57, No. 11/12, 2004, pp. 379–390.

CHAPTER 13

Electrostatic Solar Wind Propulsion*

Summary

A revolutionary method for space flights in outer space is suggested by the author. Research is present to show that an open high-charged (100 MV/m) ball of small diameter (4–10 m) made from thin film collects solar wind (protons) from a large area (hundreds of square kilometers). The proposed propulsion system creates many newtons of thrust, and accelerates a 100-kg space probe up to 60–100 km/s for 100–800 days. The 100-kg space apparatus offers flights into Mars orbit of about 70 days, to Jupiter about 150 days, to Saturn about 250 days, to Uranus about 450 days, to Neptune about 650 days, and to Pluto about 850 days.

The author has computed the amount thrust (drag), to mass of the charged ball, and the energy needed for initial charging of the ball and discusses the ball discharging in the space environment. He also reviews apparent errors found in other articles on these topics. Computations are made for space probes with a useful mass of 100 kg.

13.1 Introduction

13.1.1 General

At present, we use only one main method of launch for extraplanetary flight, that is liquid- or solid-fuel rockets. This method is very complex, expensive, and dangerous.

The current method of flight has reached the peak of its development. In the last 30 years it has not allowed cheap delivery of loads to space, or made tourist trips to the cosmos affordable, much less individual flights to the upper atmosphere. Space flights are very expensive and not conceivable for average people. The main method used for

* The work was presented as AIAA-2005-3857 at the *41st Propulsion Conference*, 10–13 July 2005, Tucson, AZ, USA.

electric energy separation is photomontage cells. Such solar cells are expensive and have a low-energy storage capacity.

The aviation, space, and energy industries need revolutionary ideas which will significantly improve the capability of future air and space vehicles. The author has offered a series of new ideas^{1–47} particularly in manuscripts presented to the World Space Congress (WSC) – 1992, 1994 and to WSC – 2002, 10–19 October 2002, Houston, TX, USA^{4–5,7–13} and in his articles, patent applications.^{1–47,53–59}

In this chapter a revolutionary method and installations for future space flights are proposed. The method uses an open high-charged ball made from thin film which collects solar wind from a large area. The offered propulsion system creates many newtons of thrust, and accelerates a 100-kg space apparatus to high speeds. This allows it, in an acceptable time of 100–800 days, to reach speeds of up to tens of km/s (50–100 km/s). A flight to Mars would take only 70 days, to Jupiter about 150 days, to Saturn about 250 days, to Uranus about 450 days, to Neptune about 650 days, and to the farthest planet Pluto about 850 days.

13.1.2 History

During 1982–1983 in series of patent applications^{29–41} the author offered some methods and installations for space propulsions and electric generators using solar wind. In 1987 these ideas were published in Report ESTI.⁴² In 1990 the author published brief information about this topic⁴³ (see pp. 67–80) and in 1992–1994 he reported on further researches at the WSC – 1992, 1994, 2002.^{44–47} In 2003, N. Omidi and H. Karimabadi published an article on a similar topic.⁴⁸ Differences between the ideas and results in this chapter and their work⁴⁸ are raised in Section 13.4.

13.1.3 Brief information about solar wind

The Sun emits plasma which is a continuous outward flow (solar wind) of ionized solar gas throughout our solar system. The solar wind contains about 90% protons and electrons, and some quantities of ionized α -particles and gases. It attains speeds in the range of 300–750 km/s and has a flow density of 5×10^7 to 5×10^8 protons/electrons/cm²s. The observed speed rises systematically from low values of 300–400 km/s to high values of 650–700 km/s in 1 or 2 days and then returns to low values during the next 3–5 days (Fig. 13.1). Each of these high-speed streams tends to appear at approximately 27-day intervals or to recur with the rotation period of the Sun. On days of high Sun activity the solar wind speed reaches 1000 (and more) km/s and its flow density 10^9 – 10^{10} protons/electrons/cm²s, 8–70 particles in cm³. The Sun has high activity periods, some days each year.

The pressure of the solar wind is very small. For full braking it is in the interval $2.5 \times 10^{-10} \div 6.3 \times 10^{-9}$ N/m². This value is double when the particles have full reflection. The interstellar medium also has high-energy particles. Their density is about 1 particle/cm³.

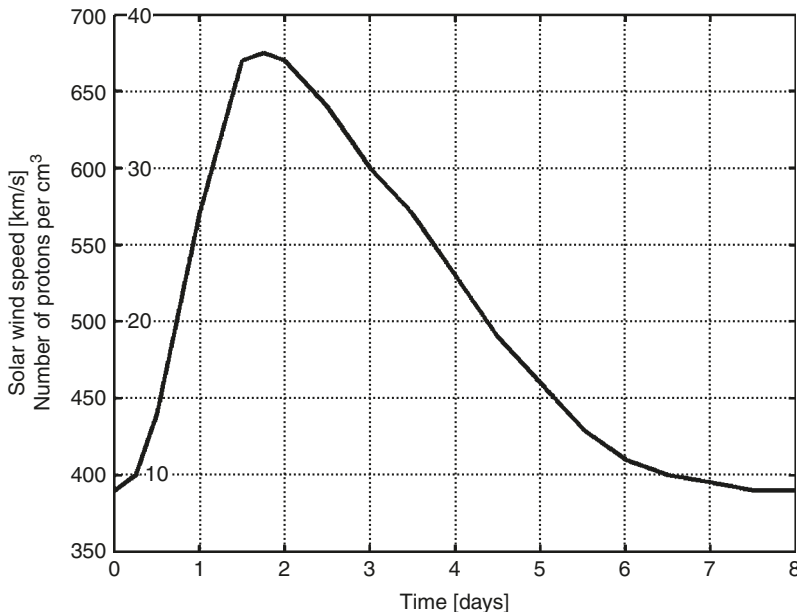


Fig. 13.1. Speed and density variations in solar wind. The speed is in km/s, and the density is in protons/cm³.

13.2 Brief description of the propulsion system

13.2.1 Space propulsion system

The suggested propulsion system is very simple. It includes a hollow ball made up of a thin, strong, film – covered conductive layer or a ball of thin net. The ball is charged by high-voltage static electricity which creates a powerful electrostatic field around it. Charged particles of solar wind of like charges repel and particles with the unlike charges attract. A small proportion of them run through the ball, a larger proportion flow round the ball in hyperbolic trajectory into the opposite direction, and another proportion are deviates from their initial direction in hyperbolic curves. As a result the charged ball has drag when the ball speed is different from solar speed (Figs. 13.2 and 13.3). The drag also occurs when the particles and the ball have the same electrical charge. In this case the particles are repelled from the charged ball (Fig. 13.3) and brake it. This solar wind drag provides thrust in our proposed propulsion system. The pressure of solar wind is very small, but the offered system (a charged ball of radius 6–10 m) collects particles (protons or electrons) from a large area (an area of tens of kilometers radius for protons and hundreds of kilometers for electrons), creates a thrust of some newtons and a 100-kg space ship reaches speeds of tens of km/s in 50–300 days (see Theory and computation below and Refs.^{29,42–47}).

13.2.2 Steerability

Steerability of the system and control of thrust. The magnitude of thrust is determined by the controlled ball charge value, and the deviation of this thrust from the direction

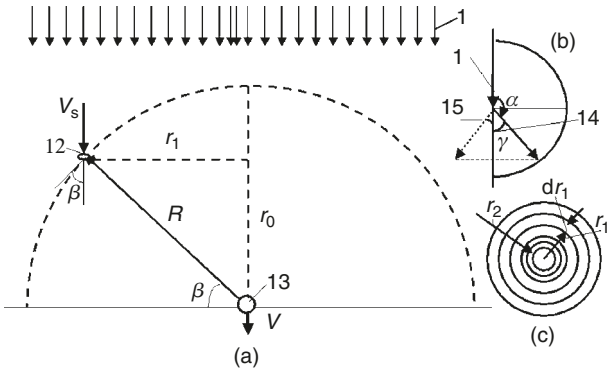


Fig. 13.2. (a) Interaction between solar wind and the electrostatic field of a charged ball. Notations: (1) Solar wind (protons/electrons); (12) charged particles (protons/electrons); (13) electrically charged ball (balloon); (14) line of turn of angle γ of a particle that is attracted (attracted force of unlike charges); (15) line of turn of angle of a particle that is repelled (repulsive force of like charges); R is the radius of interaction or neutral radius; r_1 is the radius of integration; V_s is the wind speed; and V is the ship speed. (b) Change of particle direction caused by electric ball field. (c) Collection area (top view).

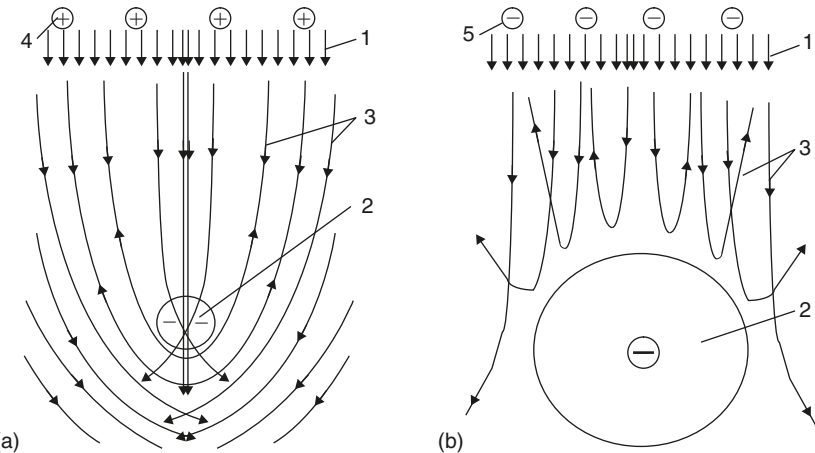


Fig. 13.3. (a) Hyperbolic trajectory of protons around static negative charge (or electrons around positive charge) (unlike charges). Notations: (1) Solar wind (charged particles); (2) hollow negatively charged ball of thin film; (3) hyperbolic trajectory of charged particles; and (4) positively charged particles (protons). (b) Trajectory of particles having the same charge as the ball. Notation: (5) Negatively charged particles.

of the Sun is controlled using one of the two methods shown in Fig. 13.4. In the first method the inclination of a plane formed by balls in a triangle is changed by adjusting the cable length (8) and the thrust T is deviated from the direction of the Sun (Fig. 13.4(a)). In the second method the propulsion system has a cylindrical capacitor (20) (Fig. 13.4(b) and (c)), which accelerates the particles on one side and brakes or turns back the

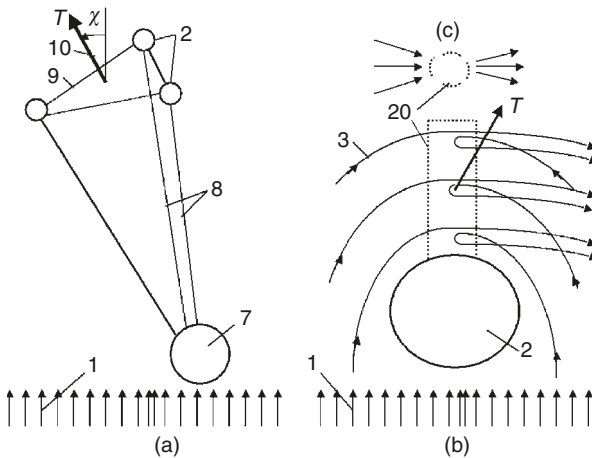


Fig. 13.4. Two methods of controlling the thrust direction. (a) Control using three balls. *Notations:* (7) Space ship (probe); (8) links (cables) connected to the space ship and the electrostatic balls; (9) cable connection of balls; and (10) T is the thrust of the propulsion system. (b) Control of thrust direction by capacitor (electrostatic mirror). (c) Top view of capacitor. The other notations are presented in Fig. 13.3.

particles on the opposite side (for the opposite side the capacitor works as an electrostatic mirror, Fig. 13.4(c)). As a result the thrust deviates from the direction of the Sun. A collection of three balls enables the thrust to be deviated by up to 10° (Fig. 13.4(a)), and an additional net capacitor enables deviation of up to $20\text{--}30^\circ$ (Fig. 13.4(b)).

13.2.3 Ball discharge

The solar wind has high speed at a large distance from the ball. This means the particles have a trajectory close to a hyperbolic curve in the ball's area of influence and most of them will fly again into infinity. Only a proportion of them will travel through the ball. These particles decrease its speed and can discharge the ball. However, their speed and kinetic energy are very large because they are accelerated by the high voltage of the ball's electric field (some tens or hundreds of MV). The necessary ball film is very thin (only of microns). The particles pierce through the ball. If their loss of speed is less than the solar wind speed, their trajectory will be close to a hyperbolic curve and they will fly into space. If their loss of a speed is more than the solar wind speed, their trajectory will be close to an ellipse, so they will return to the ball and after many revolutions they can discharge it if their perigee is less than the ball's radius. This discharge may be compensated using special methods.

There are some possible methods for decreasing this discharge (Fig. 13.5(a)-(c)): (a) A ball made of net; (b) a charged cylindrical capacitor located in front of the ball to deflect the particles from the ball; and (c) a capacitor located behind ball to increase the speed of the particles to hyperbolic speed (this is a particle accelerator) and to reflect the returning particles.

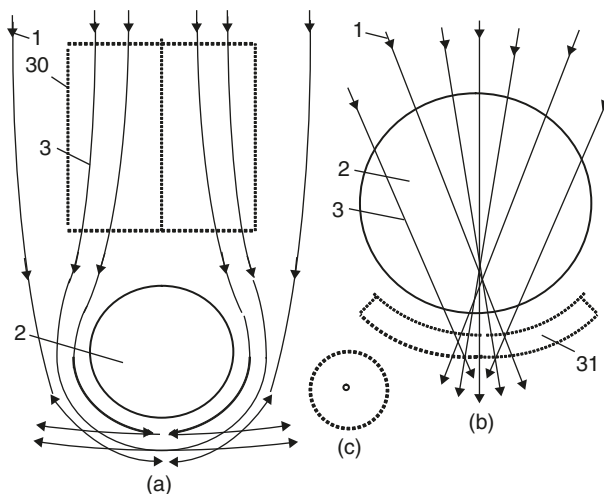


Fig. 13.5. Two methods of decreasing the ball discharge. (a) A charged cylindrical capacitor located in front of the ball deflects particles from the ball. (b) A capacitor located behind the ball adds speed to the particles and reflect the returned particles. (c) Top view of capacitor. Notations: (30) Cylindrical capacitor and (31) back capacitor (particles accelerator and electrostatic mirror).

13.2.4 Blockading of the ball charge

Blockading of the charge on the ball by unlike particles is the main problem with this method. The charge on the ball attracts unlike particles and repels like particles. The opposite-charge particles accumulate near the ball and block its charge. As a result only the area near the ball deflects and reflects the particles. The area is many times less than the area of interaction of the ball are the particles when there is no blockading. The forces are thus greatly reduced. Omidi and Karimabadi⁴⁸ apparently had not seen this and all their results seem to be wrong. There are other apparent errors in their text which affect all their other results (see Section 13.4).

The author of this work proposed two models for estimation of the efficient charge area (diameter of neutral working charge). In the first model the radius of the efficient area is computed as the area where particles of like charge to the ball are absent and the density of opposite-charge (unlike) particles is the same as the solar wind. This model gives the lower limit of the efficient area. In the second model the radius of the efficient area is computed as the area where the density of unlike particles is less than the solar wind density because the unlike particles inside the efficient area have generally higher velocity than those outside this area. The neutral area (neutral sphere) in Model 2 is larger than in Model 1. Model 2 is better, but this problem needs more detailed research.

The proposed system could be used as a thermonuclear propulsion system and a thermonuclear electric generator. The suggested idea may be useful in the design of thermonuclear propulsion systems and electric generators. The solar wind particles approach the ball with very high energy (hundreds of MV). Their density near the ball axis and

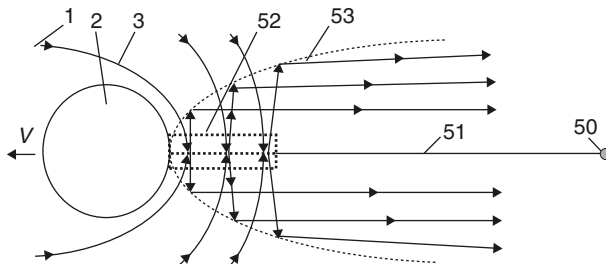


Fig. 13.6. Nuclear propulsion system using solar wind (or interstellar particles). *Notations:* (50) Space apparatus; (51) cable connecting the space apparatus and the ball; (52) collector particles and thermonuclear reactor; and (53) reflector of reaction products or light photons. Other notations are the same as previous figures.

behind the ball may also be high. An energy of 5–15 MV is enough for a nuclear reaction. This may be a proton–proton reaction or protons with any other matter (central electrode). In last case the cylindrical capacitor (Fig. 13.6) is located behind the ball. This capacitor changes the particle speed (energy) to the required value. The capacitor has a central electrode made of matter which gives a nuclear reaction (product). The products of the reaction are reflected by a parabolic electrostatic mirror in one direction that forms the thermonuclear propulsion system. The products of nuclear reaction may be photons and the mirror may be a light reflector, in which case we have a photon propulsion system. The electrostatic mirror is made from a thin net and the light reflector is made from a thin film with a reflective layer. They do not influence the particle flow to the central electrodes because the particles have very high speed and energy. The energy of the charged particles can be converted to electrical energy by braking of the electrostatic field as the author has proposed.^{31–47} These tasks need more detailed research.

13.2.5 Interstellar propulsion system

The previously proposed (no-nuclear) propulsion system does not allow speeds to be reached more than the maximum speed of the solar wind – 1000 km/s. This is not enough for an interstellar trip. For an interstellar voyage the speed must be about 100,000 km/s. The thermonuclear wind propulsion system does increase propulsion capability. The space speed can be greater than the wind speed and the space ship can therefore move against the solar wind.

The interstellar medium also contains high-energy particles (cosmos rays) a density of about 1 particle/cm³. These particles can be collected from a large area by the electrostatic ball and used by the thermonuclear propulsion system. The author calls on all nuclear scientists to research these possibilities. The thermonuclear propulsion system and power thermonuclear electric generator may be easier to design for space than for the Earth because we have a natural high vacuum and a multitude of natural particles in space, and the suggested method and installation solve a major problem of thermonuclear reaction – obtaining high-energy particles and collecting them in a small volume with high density.

13.3 Basic theories of the solar wind installation and main estimations and computations

13.3.1 Note on general theory

Interplanetary space has a magnetic field. The motion of the charged particles in the magnetic and ball electric field is described by the Lorenz force law:

$$m dV/dt = q(E + V \times B), \quad (13.1)$$

where m is the mass of particles [kg]; V is the speed of particles [m/s] (vector); t is the time [s]; q is the charge [C]; E is the electric intensity of charged ball field [V/m or N/C] (vector); and B is the interplanetary magnetic field [T] (vector).

For a charged ball the electric intensity is $E = kQ/r^2$, where the coefficient $k \approx 9 \times 10^9$ [Nm²/C²]; Q is the ball charge [C]; and r is the distance from the ball center [m].

The first element on the right-hand side of equation (13.1) is electrostatic (Coulomb's) force and the second element is Lorenz force.

The interplanetary magnetic field, B , at 1 AU (AU is the astronomical unit, 150×10^6 km, radius of Earth orbit) is typically very small at 10 nT and makes an angle of 45° with the Sun–Earth line (that is the radial direction). For a typical wind speed, V_s , the second element is small (~ 4 mV/m). In a full vacuum (without space plasma) the electric intensity from 1 C of the ball at a distance of 1000 km is $\sim 10^{-22}$ V/m. Moreover, the Lorenz force does not increase the radial speed. It only deflects the particle's trajectory from the radial line. Because of that, we can ignore the Lorenz force.

The charged ball repels the like charged particles. In particular, a negatively charged ball repels the space plasma's electrons.

It is possible to find the minimum distance which solar wind electrons can approach a negatively charged ball. The full energy of a charged particle (or body) is the sum of the kinetic and potential electric energy. Any change of energy equals zero:

$$\frac{mV^2}{2} + E_p = 0, \quad E_p = \int_{\infty}^r F dr, \quad F = k \frac{qQ}{r^2},$$

$$E_p = kqQ \left(\frac{1}{\infty} - \frac{1}{r} \right) = -\frac{kqQ}{r}, \quad \frac{mV^2}{2} - \frac{kqQ}{r} = 0, \quad (13.2)$$

where m is the mass of a particle [kg] (mass of a proton is $m_p = 1.67 \times 10^{-27}$ kg, mass of an electron is $m_e = 9.11 \times 10^{-31}$ kg); V is the speed of particles ($V \ll c$, where c is light speed) [m/s] (for solar wind $V_s = 300$ –1000 km/s); E_p is the potential energy of a charged particle in the electric field [J]; F is the electric force, [N]; q is the electrical charge of a particle [C] ($q = 1.6 \times 10^{-19}$ C for electrons and protons); $k = 9 \times 10^9$ is a coefficient; r is the distance from a particle to the center of the ball [m]; and Q is the ball charge [C].

From equation (13.2) the minimum distance for a solar wind electron is ($m = m_e, V = V_s$):

$$r_{\min} = \frac{2kqQ}{mV^2} = \frac{2K}{V_s^2} = \frac{2a^2Eq}{m_e V_s^2}, \quad K = \frac{kqQ}{m}, \quad Q = \frac{a^2E}{k}, \quad K = \frac{a^2Eq}{m}, \quad (13.3)$$

where K is a coefficient; m_e is the electron mass; V_s is the solar wind speed [m/s]; a is the radius of ball [m]; and E is electrical intensity at the ball surface [V/m]. The maximum electrical intensity of negative charge is about 10^8 – 2×10^8 V/m in a vacuum.

For $a = 6$ m, $E = 10^8$ V/m, $V_s = 4 \times 10^5$ m/s we have $r_{\min} \approx 8 \times 10^6$ km. Other values are presented in Figs. 13.7(a) and (b).

13.3.2 Minimum neutral sphere around a charged ball

13.3.2.1 Model 1: Constant particle density

The charge density of the unlike space plasma particles inside a neutral sphere is equal to the density of solar wind. The minimum radius of the neutral sphere is:

$$Q = \frac{4}{3} \pi R_n^3 d, \quad R_n = \sqrt[3]{\frac{3Q}{4\pi d}} = \sqrt[3]{\frac{3a^2 E}{4\pi k d}}, \quad d = 10^6 N q, \quad (13.4)$$

where d is the density of solar wind [C/m^3]; R_n is the minimum radius of the neutral sphere [m]; and N is the number of particles in cm^3 . The solar wind charge density may be taken by linear interpolation from Table 13.1 for a distance from the Sun equals to 1 AU = 150 million kilometers.

Computation of the minimum radius of the neutral sphere is presented in Fig. 13.8.

13.3.2.2 Model 2: Variable particle density

Density of the unlike particles inside the neutral sphere will be less than the density of solar wind particles because the particles are strongly accelerated by the ball charge to speed approximately the speed of light. The new density and new corrected radius can be computed in the following way:

1. The speed of protons along a ball radius is:

$$V_r^2(r) = V_0^2 + 2K \left(\frac{1}{r} - \frac{1}{r_0} \right), \quad (13.5)$$

where $V_0 = V_s$ is the proton speed at an initial radius of $R \gg R_n$ and R_n is the radius of the neutral sphere:

2. Particle charge density, d_p , along a ball radius is:

$$d_p = d_{po} \frac{V_0}{V_r(r)}, \quad d_{po} = 10^6 N q / s^2, \quad s = \frac{S}{S_0}, \quad (13.6)$$

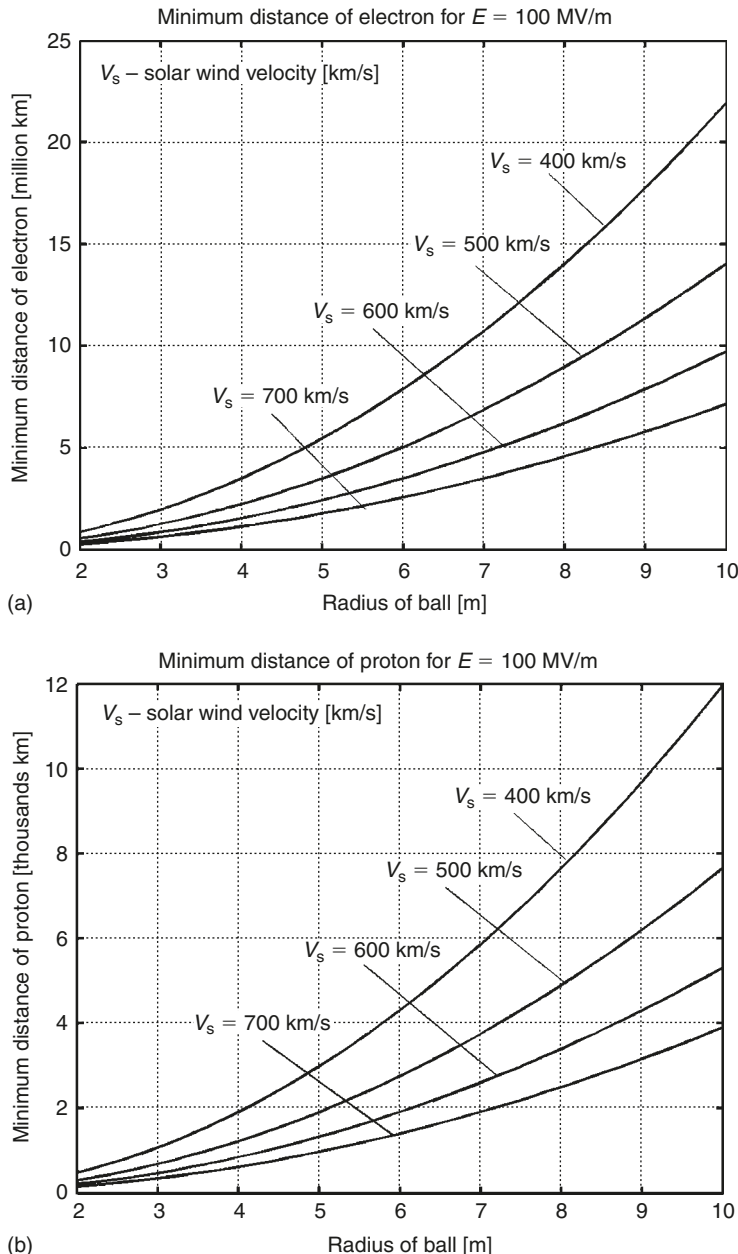
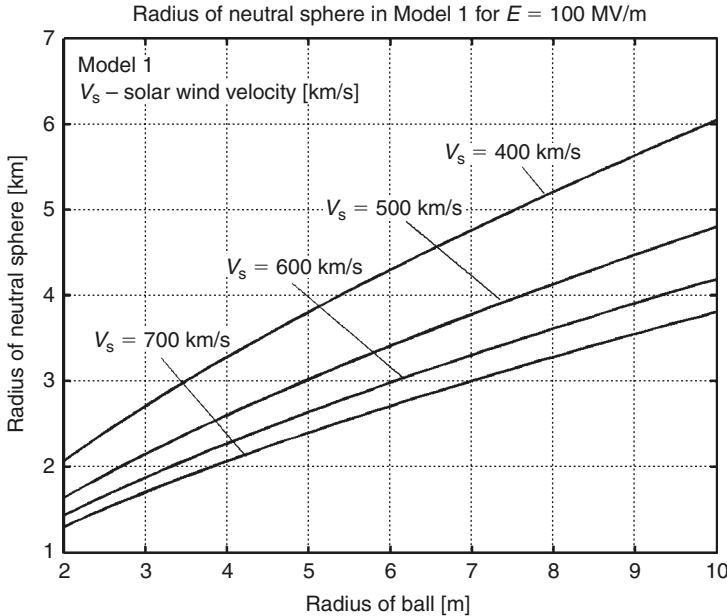


Fig. 13.7. (a) Minimum distance of a single electron from a negatively charged ball with electric intensity of $E = 100 \text{ MV/m}$. (b) Minimum distance of a single proton from positively charged ball with electric intensity of $E = 100 \text{ MV}$.

Table 13.1. Distance from Sun is 1 AU.

V_s [m/s]	0	4×10^5	10^6
N [cm ³]	0	10	70

**Fig. 13.8.** Radius of the neutral sphere in Model 1, when particle density in the sphere equals space plasma density.

where S is the distance from the Sun in AU; $S_0 = 1\text{AU}$; s is the relative distance from the Sun; and d_{po} is the density at 1AU.

3. Charge of the neutral sphere along a sphere radius is:

$$Q_r = Q - 4\pi d_{po} V_0 \int_a^R \frac{r^2}{V_r(r)} dr. \quad (13.7)$$

4. The radius of the neutral sphere can be found from the condition $Q_r = 0$. For our estimation we will find it using the stronger condition $Q_r = 0.5Q$, and call it the efficiency radius R_e of charge q .

Results of computation are presented in Fig. 13.9.

As you can see the efficiency radius in Model 2 is significantly more than in Model 1.

13.3.3 Electrostatic sail drag

All protons in the neutral sphere change the direction of their trajectories from 0° to 180° .

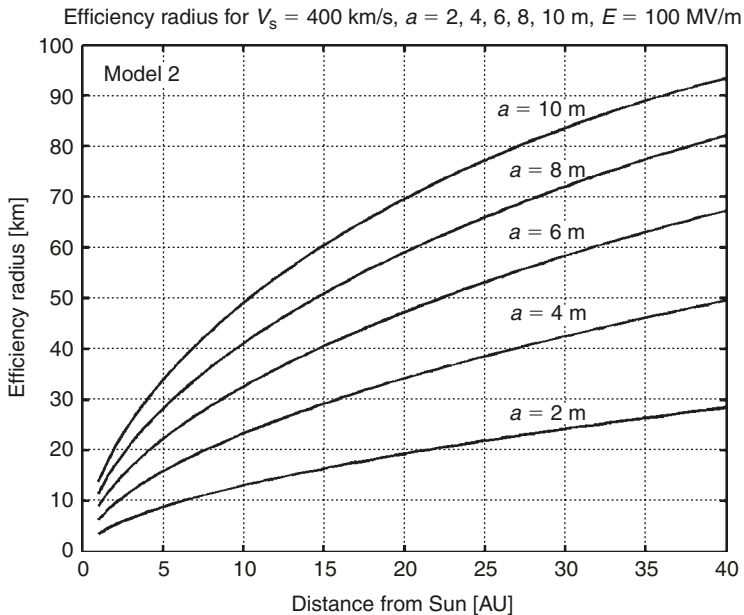


Fig. 13.9. Radius of the neutral sphere in Model 2 via distance from the Sun, when particle density is variable with radius in the neutral sphere and depends on the variable speed of accelerated particles.

The drag (thrust), D , of the electrostatic sail can be estimated by the equation:

$$D = C_D 10^6 N m_p V_p^2 \pi R_e^2 / s^2, \quad V_p = V_s - V, \quad (13.8)$$

where V_p is the relative speed of the probe [m/s]; and C_D is the drag coefficient. If not all particles change their direction, $C_D = 0$; if all particles turn to 90° , $C_D = 1$; if all particles turn to 180° , $C_D = 2$. We take $C_D = 1.5$ for our computation. V is the probe speed [m/s]. When $V \ll V_s$, the relative speed is $V_p \approx V_s$.

Results of computation of the sail drag for $V_p \approx V_s$ using equation (13.8) are presented in Figs. 13.10 and 13.11.

13.3.4 The ball stress, cover thickness, and ball mass

The ball has tensile stress from the like electric charge. We need to find the ball stress and the required thickness of the ball cover. If the ball is in a vacuum and the ball charge, Q , is constant, its ball internal force is:

$$\begin{aligned} f &= \frac{\partial W}{\partial a}, \quad W = \frac{Q^2}{2C}, \quad C = \frac{a}{k}, \quad k = \frac{1}{4\pi\epsilon_0} = 9 \times 10^9, \quad W = \frac{kQ^2}{2a}, \\ f &= -\frac{kQ^2}{2a^2}, \quad Q = \frac{a^2 E}{k}, \quad f = -\frac{(aE)^2}{2k}, \end{aligned} \quad (13.9)$$

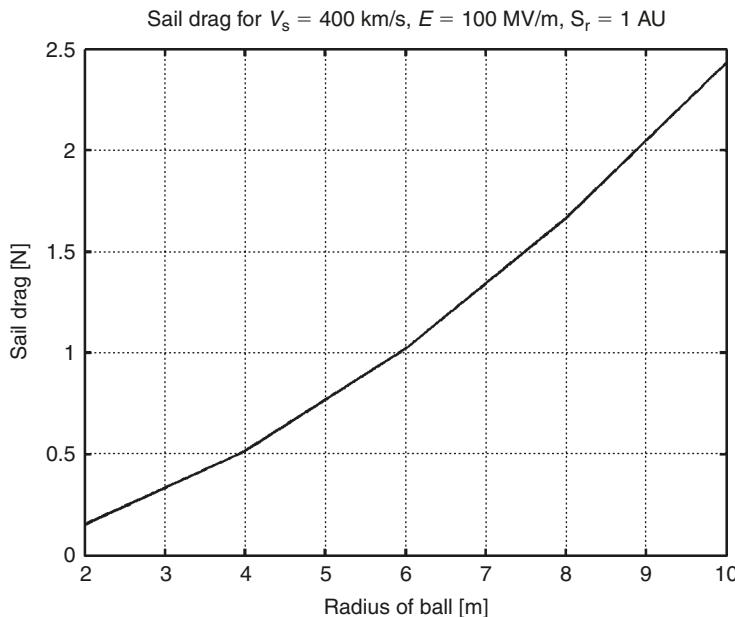


Fig. 13.10. Drag of the electrostatic sail versus ball radius at the Earth's orbit (at 1 AU) for the solar wind speed 400 km/s and electrical intensity $E = 100 \text{ MV/m}$.

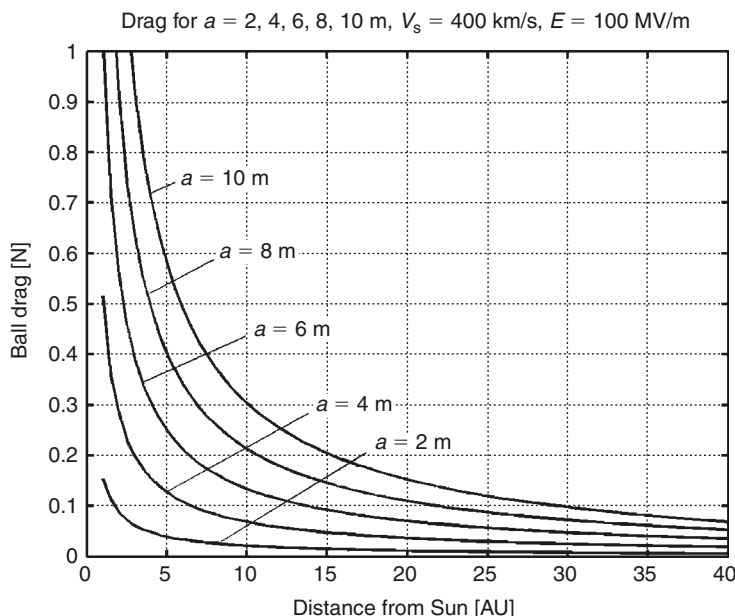


Fig. 13.11. Drag of the electrostatic sail versus distance from the Sun (in AU) for ball radius $a = 2\text{--}10 \text{ m}$, solar wind speed 400 km/s, and electrical intensity $E = 100 \text{ MV/m}$.

where f is the tensile force inside the ball [N]; W is the charge energy [J]; C is the capacity of the ball as a sphere capacitor [F]; and E is the electrical intensity [V/m].

The internal ball pressure is:

$$p = \frac{f}{S}, \quad S = 4\pi a^2, \quad p = \frac{E^2}{8\pi k}, \quad (13.10)$$

where p is the internal pressure [N/m²] and S is the ball surface area [m²].

The thickness of the ball cover, δ , is:

$$\pi a^2 p = 2\pi a \delta \sigma, \quad \delta = \frac{ap}{2\sigma}, \quad \delta = \frac{aE^2}{16\pi k \sigma}, \quad (13.11)$$

where δ is cover thickness [m] and σ is safe cover stress [N/m²].

The ball mass is:

$$M_s = S \delta \gamma, \quad S = 4\pi a^2, \quad M_s = \frac{a^3 E^2 \gamma}{4k\sigma}, \quad (13.12)$$

where M_s is the ball (sail) mass [kg] and γ is the ball cover density [kg/m³]; and σ is the safe stress of the ball cover [N/m²].

Computation of the ball thickness and ball mass are presented in Figs. 13.12 and 13.13.

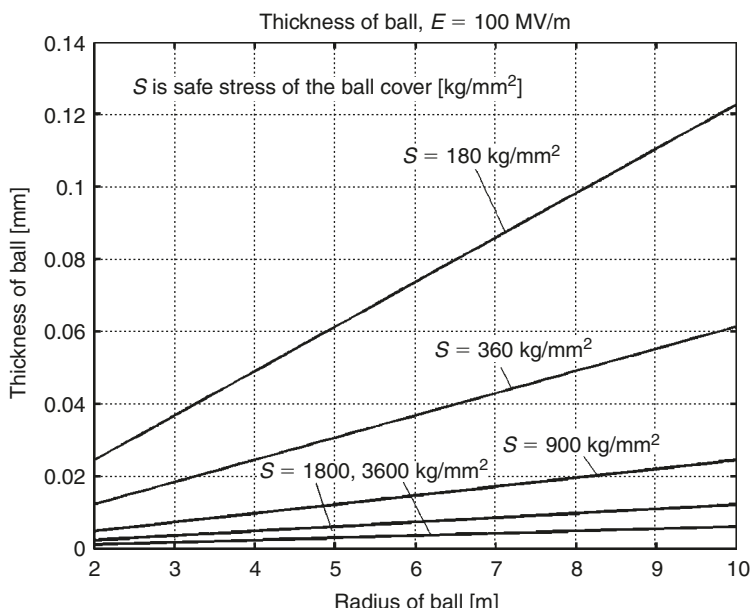


Fig. 13.12. Thickness of ball cover versus ball diameter for different safe cover stress value, electrical intensity $E = 100 \text{ MV/m}$.

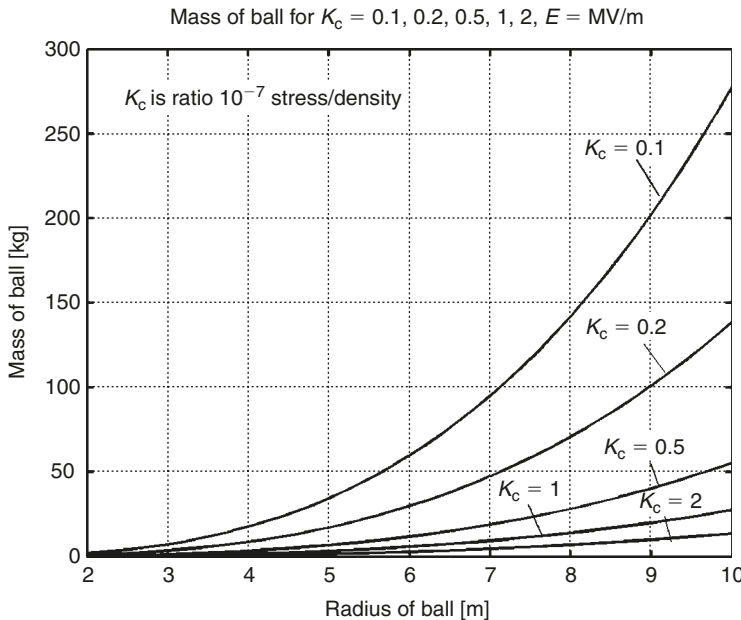


Fig. 13.13. Mass of ball cover versus ball diameter for different safe ratio's of stress/cover density and electric intensity $E = 100 \text{ MV/m}$.

13.3.5 Probe acceleration, speed, and flight time

We estimate these values only for a probe moving along the Sun's radius. The equations are:

$$A_c = \frac{D(R_e)}{M + M_s}, \quad dV = \frac{D(R_e)}{(M + M_s)V} ds, \quad dt = \frac{1}{V} ds, \quad (13.13)$$

where A_c is the probe acceleration [m/s]; D is the probe drag [N]; M is the probe mass [kg]; M_s is the sail (ball) mass [kg] (Fig. 13.13); V is the radial probe speed [m/s]; t is the flight time [s]; and s is the distance from Sun [m].

The result of computation for $a = 6 \text{ m}$, $E = 10^8 \text{ V/m}$, $M = 100 \text{ kg}$, $\sigma = 180 \text{ kg/mm}^2$, $\gamma = 1800 \text{ kg/m}^3$, and $s = 1\text{--}40 \text{ AU}$ are presented in Figs. 13.14–13.17.

The ball (sail) weight increases as a cubic value and the total acceleration reaches a maximum. Fig. 13.14 shows optimal ball radius for current materials.

The proposed probe can reach Mars orbit in about 70 days (and reaches a speed of 50 km/s), Jupiter in about 150 days, Saturn in about 250 days, Uranus in about 450 days, Neptune in about 650 days, and the farthest planet Pluto (5800 million kilometers) in about 850 days.

Probe acceleration for $M = 100 \text{ kg}$, $E = 100 \text{ MV/m}$, $S_r = 1 \text{ AU}$

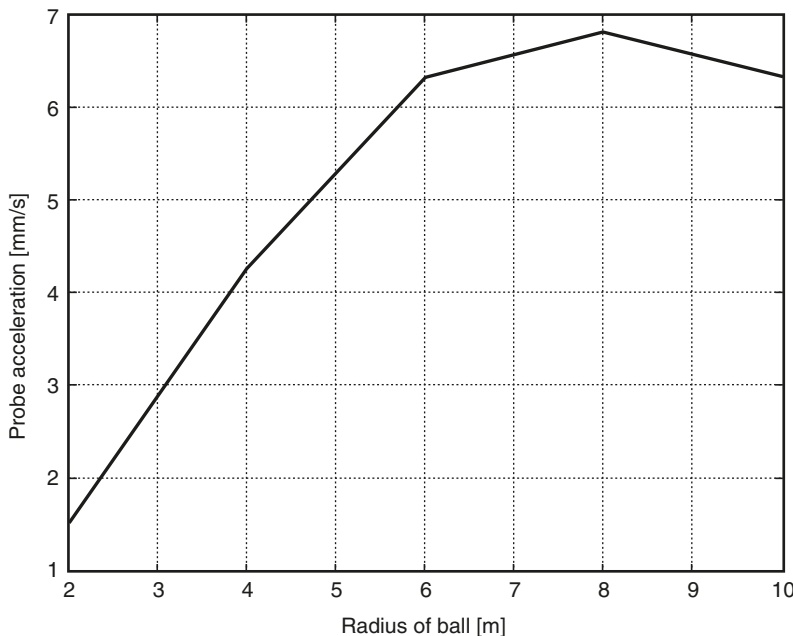


Fig. 13.14. Probe acceleration versus distance from Sun for useful probe mass $M = 100 \text{ kg}$, and the sail weight computed for safe cover stress $\sigma = 180 \text{ kg/mm}^2$, cover density $\gamma = 1800 \text{ kg/m}^3$, electric intensity $E = 100 \text{ MV/m}$, at a distance from the Sun of 1 AU (Earth orbit).

Acceleration for $M = 100 \text{ kg}$, $a = 2, 4, 6, 8, 10 \text{ m}$, $E = 100 \text{ MV/m}$

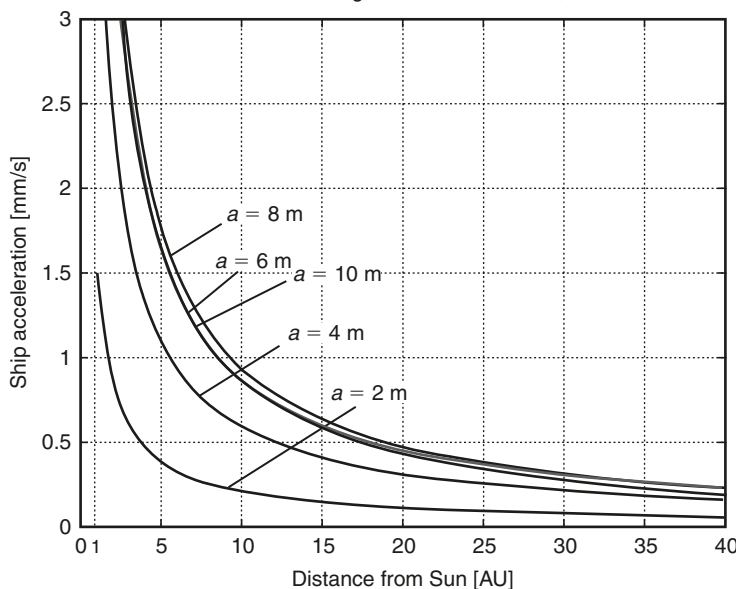


Fig. 13.15. Probe acceleration versus ball radius for useful probe mass $M = 100 \text{ kg}$, and sail weight computed for safe cover stress $\sigma = 180 \text{ kg/mm}^2$, cover density $\gamma = 1800 \text{ kg/m}^3$, electric intensity $E = 100 \text{ MV/m}$, at a distance from the Sun of 1–40 AU.

Distance for $M = 100 \text{ kg}$, $E = 100 \text{ MV/m}$,
 $S = 0.2 \text{ ton/mm}^2$, $W = 1800 \text{ kg/m}^3$

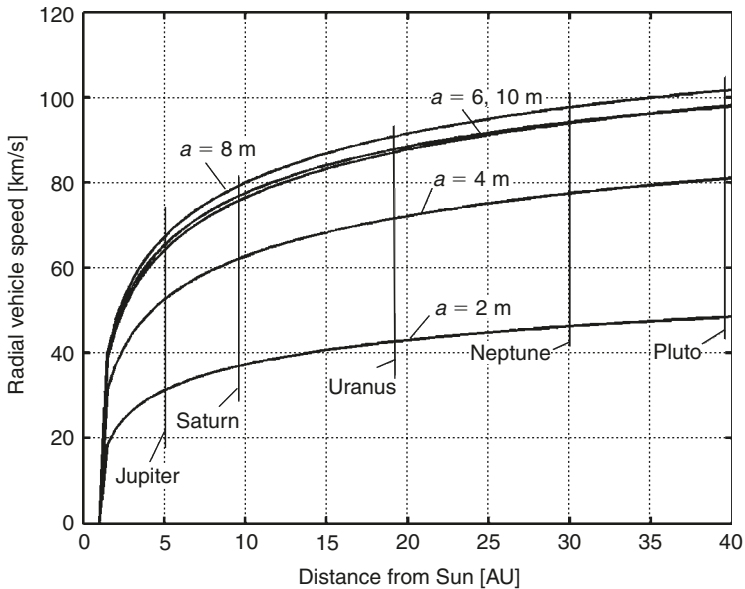


Fig. 13.16. Probe velocity versus distance from Sun and the ball radius for useful probe mass $M = 100 \text{ kg}$, and sail weight computed for safe cover stress $\sigma = S = 180 \text{ kg/mm}^2$, cover density $\gamma = 1800 \text{ kg/m}^3$, electrical intensity $E = 100 \text{ MV/m}$, at a distance from Sun 1–40 AU, $V_p \approx V_s$.

Trip time for $M = 100 \text{ kg}$, $a = 2, 4, 6, 8, 10 \text{ m}$,
 $E = 100 \text{ MV/m}$, $S = 200 \text{ kg/mm}^2$

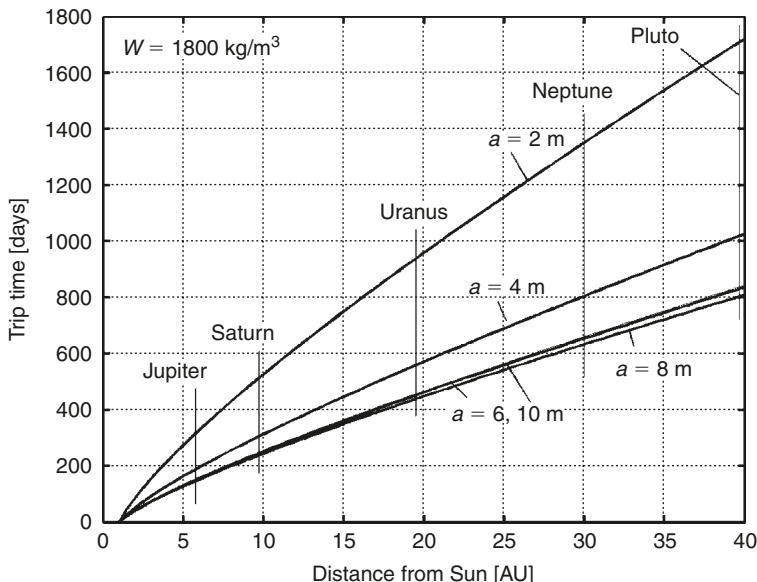


Fig. 13.17. Probe trip time versus distance from the Sun and the ball radius for useful probe mass $M = 100 \text{ kg}$, and sail weight computed for safe cover stress $\sigma = S = 180 \text{ kg/mm}^2$, cover density $\gamma = 1800 \text{ kg/m}^3$, electrical intensity $E = 100 \text{ MV/m}$, at a distance from the Sun of 1–40 AU, $V_p \approx V_s$.

The final (interstellar) speed is about 100 km/s.

The parameters of the probe (space ship) are not optimal, but may be improved.

13.3.6 Absorption of particles by ball cover

The particle (proton) track in the matter can be computed in following way (p. 953, Table 44.1⁵⁰):

$$l = R_t / \gamma \quad (13.14)$$

where l is the track distance of the particles [cm]; $R_t = R_t(U)$ is the magnitude (from table) [g/cm^2]; and γ is the matter density [g/cm^3]. The magnitude of R_t depends on the kinetic energy (voltage) of the particles. For protons the values of R_t are presented in Table 13.2.

The proton energy is $U = aE$. For magnitudes $a = 6 \text{ m}$, $E = 10^8 \text{ V/m}$, proton energy $U = 600 \times 10^6 \text{ V}$, and ball cover density $\gamma = 1.8 \text{ g/cm}^3$ the proton track is $l = 197 / 1.8 = 109 \text{ cm}$. The required ball cover thickness is only $230 \mu\text{m}$ (see Fig. 13.12). All protons will run across the ball cover. However, if the losses of speed in the ball cover are less $V_s = 400 \text{ km/s}$, the protons will leave a neutral sphere. In other cases they can rotate in a neutral sphere, cross the cover thousands of times, lose their energy, and discharge the ball's charge.

The safe ball cover thickness may be estimated using the following method. The solar wind proton energy is:

$$E_d = \frac{m_p V_s^2}{2}. \quad (13.15)$$

For $V_s = 400 \times 10^3 \text{ m/s}$ the proton energy is $E_d = 13.4 \times 10^{-17} \text{ J} = 13.4 \times 10^{-17} \times 0.625 \times 10^{19} \text{ eV} = 840 \text{ eV}$.

If the loss of proton energy is proportional to the cover thickness, the maximum safe cover thickness (which will not discharge the ball) will be:

$$E_d = U \frac{\delta_{\max}}{l}, \quad \text{or} \quad \delta_{\max} = \frac{Ed(V_s)l}{U}, \quad U = aE. \quad (13.16)$$

For $a = 6 \text{ m}$, $E = 10^8 \text{ V/m}$ the required ball cover thickness is $\delta_{\max} = 1.53 \mu\text{m}$. For $a = 4, 10 \text{ m}$, $\delta_{\max} = 1.22, 1.73 \mu\text{m}$, respectively.

This magnitude is less than the ball thickness required for the charge stress (see Fig. 13.12) for current cover matter. Methods of decreasing the cover discharge are offered in the description section.

Table 13.2. Magnitude of R_t as a function of accelerated voltage $U = aE$ [V].

U [MV]	100	200	300	400	500	600	700	1000	2000	3000	5000
R_t [g/cm^2]	10	33.3	65.8	105	149	197	248	370	910	1463	2543

For electrons the thickness of half absorption may be calculated using equation (p. 958⁵⁰):

$$R_r = 0.095 \frac{Z}{A} (aE)^{3/2} [\text{g/cm}^2], \quad d_{0.5} = \frac{R_r}{\gamma} [\text{cm}]. \quad (13.17)$$

Here Z is the nuclear charge of the ball matter; and A is the mass number of the ball matter.

13.3.7 Initial expenditure of electrical energy needed to charge the ball

The ball must be charged with electrical energy of high voltage (millions of volts). Let us estimate the minimum energy when the charged device has 100% efficiency. This energy equals the work of moving of the ball charge to infinity, which may be computed using equation:

$$W = \int_a^\infty F dr = \int_a^\infty k \frac{Q_1 Q_2}{r^2} dr = k \frac{Q_1 Q_2}{a}, \quad W = \frac{Q^2}{C}, \quad Q = \frac{a^2 E}{k}, \quad C = \frac{a}{k}, \quad W = \frac{a^3 E^2}{k}, \quad (13.18)$$

where W is the ball charge energy [J]; C is the ball capacitance [F]; and Q is the ball charge [C]. The result of this computation is presented in Fig. 13.18. As can be seen this

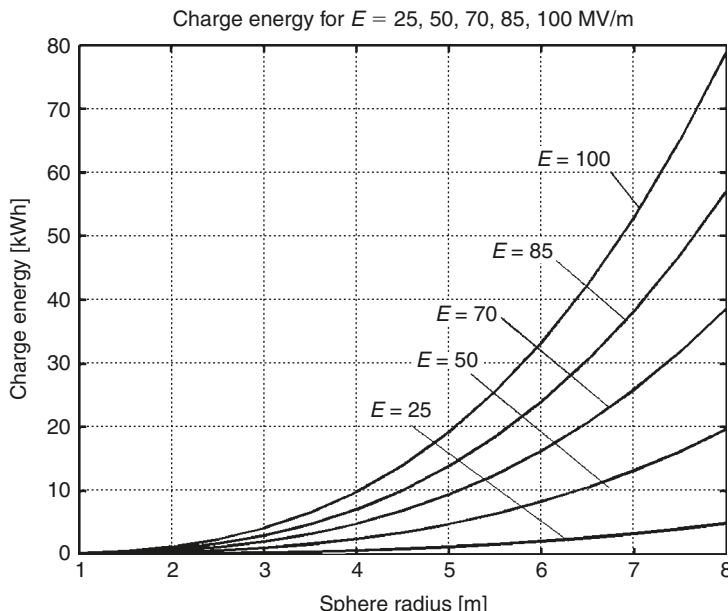


Fig. 13.18. Initial expenditure of electrical energy needed to charge the space apparatus, $a = 1-8$ m, electrical intensity is 25–100 MV/m and coefficient of efficiency 1.

energy not great as it is about 1–20 kWh for a ball radius of $a = 5\text{ m}$ and the electrical intensity is 25–100 MV/m. This energy may be restored through ball discharge by emitting the charge into space using a sharp edge.

13.3.8 Notes about thermonuclear propulsion from solar wind

When particles are moved toward the ball, they gain a huge amount of energy equal to the voltage (aE) of the charged ball in infinite space $U = aE$ (100–1000 MeV), approaching the speed of light. The particle reactions have the greatest efficiency when the particles move in opposite directions. Their energy is more than the energy of most common thermonuclear reactions (5–20 MeV). The electric field of the brake capacitor can decrease this energy to the required value. The particles may be used for a proton–proton reaction (as inside the Sun), or proton–electrode, or electron–electrode thermonuclear reaction, where the central electrode is made from a suitable matter. The solar wind also contains α -particles and ions of other elements (up to 10%). These are accelerated to high energy and can take part in the thermonuclear reaction.

The thermonuclear reaction also needs a certain concentration of the free particles. These are concentrated in the area of the central electrode. This concentration, Q_x , can be computed. The angle of deviation of the initial (in infinity) solar wind particles is small (about 1–2°) and the diameter of the central area (maximum concentration near the electrode) is small (possibly <1 mm), meaning the thermonuclear cross-section is large. The Lawson criterion is executed because the collision time is infinity. We have continuous particle flow and do not use internal apparatus energy. I call on nuclear experts to research the possibility of thermonuclear reactions in the proposed engine (and generator). This thermonuclear engine is impossible on Earth where the solar wind is blocked by the atmosphere and the Earth's magnetic field, but it is possible in extraplanetary space, in a high vacuum. It may be a way of achieving not only interplanetary trips, but also interstellar apparatus where a spacecraft is accelerated to a relativistic velocity.

13.3.9 Charging the ball

The main innovation in the proposed idea is the open electric charge of one sign and high intensity. To obtain this open charge, it is necessary to send an opposite charge into infinite space. This is possible if we accelerate the opposed particles (protons, electrons, and ions) with energy of more than $aE = 100\text{--}10^3\text{ MV}$ (a is the ball diameter [m], and E is the electrical intensity [MV/m]). It can be carried using simple electrostatic accelerators or linear accelerators (electric guns). Their design for use in space is easier than for Earth because outer space has a high vacuum and a high allowable electrical intensity. For example, the allowable electrical intensity is only 3 MV/m on the ground belongs to the Earth's atmosphere and >100 MV/m in a space vacuum. A Van de Graaff accelerator on the ground needs a special high-pressure camera and special vacuum camera, but in space they are not needed. Data of some ground accelerators of protons (p) and electrons (e) are given below.

Electrostatic accelerators (Tandem Van de Graaff, Tandem pelletron, Vivitron) accelerate particles (p, d, α, e) up to 20–35 MV, linear accelerators (p) up to 50–800 MeV,

electron linear accelerators (e) up to 100 GeV, and alter-gradient synchrotron (p, e) up to 900 GeV (p) (v. 13, p. 130⁵¹).

These data show there is no significant problem in designing a high-efficiency space charging gun which will move charges to infinity and create the open charged ball. The energy for this charging is not high (see Fig. 13.18).

These and other possible problems are discussed in the next section.

13.4 Discussion

13.4.1 Possible limitations

The above computations suggest a range of possibilities for acceleration using solar wind. The pressure of solar wind is very small but charged particles may be collected by the open charged ball from a big region. They will give enough thrust for mobile space apparatus. They can accelerate the directable apparatus to speed of about 100 km/s and offer flights to far planets of the Solar system in a short time. If the thermonuclear engine (and the electric generator) are possible, thermonuclear wind propulsion will permit us to realize interstellar trips. This is a revolutionary breakthrough in interstellar space.

What restrictions may appear in detailed researches to limit these possibilities? The author sees the following problems:

- (a) Discharging of the ball. The author offers some methods (Fig. 13.5) for reducing the discharging. Detailed computation is needed.
- (b) Design of an acceptable charging gun. This is a technical problem which can be solved by current technology.
- (c) Source of energy.
- (d) Research and development into the offered space thermonuclear propulsion system and power generator.

13.4.2 Comparison with other works

The author suggested a series of solar wind propulsion systems and generators in 1982–1983 and later.^{29–47} These works included also the nuclear propulsion system and electric generators, and particle and solar wind electrostatic mirrors. In American scientific literature the author found only work published in 2003.⁴⁸ The proposed methods, installation, and results have the following differences:

- (a) The offered propulsion installation design is very different from work.⁴⁸ They use magnetic field, I use only electric field. They use a conventional spherical capacitor with two skin (layers) and polarity (unlike) charges (see Fig. 6⁴⁸). These

authors wrote (p. 6): “So, from the point of EPS power consumption, it is highly desirable to keep the charge separation distance as small as possible while achieving acceleration.”

In my opinion this design cannot work efficiently because the main part of the electric field is inside the capacitor. The authors⁴⁸ understood that when they wrote (p. 6): “one charge layer is exposed to the solar wind electric field the other is exposed to a considerably reduced electric field.”

My proposed propulsion design has a single-skin ball, one type of charge (the opposite charge is expelled in infinity), and an open electric field effective over long distance. The intensity of this field is decreased as $1/r^2$. If the charges in the other system⁴⁸ are dipolar their intensity will be small and decrease as $1/r^3$. This means, the author’s electric field should be stronger by thousands of times over long distance.

- (b) The work⁴⁸ contains only common speculation. It does not contain theory, initial data, and detailed numerical results. The authors give only some pictures of solar wind disturbances. In Fig. 3 (p. 4), the apparatus speed is twice the wind speed (?). No explanation is given for this strange result.

Omidi and Karimabad⁴⁸ use the very high-specific charges of up to 300–500 C (0.1–1 (and more) C/kg for full spacecraft mass). This requires a very large spherical capacitor and very high electrical intensity which is impossible in physics. They wrote: “this technology would initially be applied to the propulsion of micro spacecraft where charge levels of a low C would be sufficient.”

My results are very different from these.⁴⁸ The authors do not show their calculation’s, but say their apparatus with its propulsion can reach a speed of 64 km/s at a distance 33 AU of 5 years. This means the acceleration is 0.0004 m/s and the thrust is very small.

There are also many articles about magnetic sails using solar wind drag into a magnetic field of a gigantic superconductive ring (diameter 60–150 km). Unfortunately, no theory currently exists to allow computation of magsail drag. It is beyond the capability of current technology. The reader can find information about the space magsail in Refs. [52].

13.5 Conclusion

The proposed new propulsion mechanism differs from previous concepts in very important respects; including the coupling to the protons of the solar wind using an open single-charge ball. The opposite charge is expelled into infinite space. This innovation increases the area of influence by up to hundreds of kilometers for protons and allows the acquisition of significant vehicle thrust. This thrust is enough to accelerate a heavy spacecraft to very high speed and permits very short flight times to far planets.

The offered revolutionary propulsion system has a simple design, which can give useful acceleration to various types of spacecraft. The offered propulsion system creates many newtons of thrust, and can accelerate a 100-kg space probe up to 60–100 km/s in 100–800 days.

In the offered wind propulsion system the particles run away from the ball, brake, and return in infinity for initial speed. These premises must be examined using more complex theories to account for the full intersection between the suggested installation and solar wind (including thermonuclear reactions). This would be a revolutionary breakthrough in interplanetary space exploration.

The author has developed the initial theory and the initial computations to show the possibility of the offered concept. He calls on scientists, engineers, space organizations, and companies to research and develop the offered perspective concepts.

References

1. A.A. Bolonkin, "Theory of Flight Vehicles with Control Radial Force", *Collection Researches of Flight Dynamics*, Public house "Mashinostroenie", Moscow, 1965, pp. 79–118 (in Russian).
2. A.A. Bolonkin, "Air Cable Transport and Bridges", TN 7567, *International Air and Space Symposium – The Next 100 Years*, 14–17 July 2003, Dayton, OH, USA.
3. A.A. Bolonkin, "Kinetic Space Towers and Launchers", *Journal of British Interplanetary Society*, Vol. 57, No. 1/2, 2004, pp. 33–39.
4. A.A. Bolonkin, "Non-rocket Space Rope Launcher for People", IAC-02-V.P.06, *53rd International Astronautical Congress, The World Space Congress – 2002*, 10–19 October 2002, Houston, TX, USA.
5. A.A. Bolonkin, "Non-rocket Missile Rope Launcher", IAC-02-IAA.S.P.14, *53rd International Astronautical Congress, The World Space Congress – 2002*, 10–19 October 2002, Houston, TX, USA.
6. A.A. Bolonkin, "Optimal Trajectory of Air Vehicles", *Aircraft Engineering and Aerospace Technology*, Vol. 76, No. 2, 2004, pp. 193–214.
7. A.A. Bolonkin, "Inexpensive Cable Space Launcher of High Capability", IAC-02-V.P.07, *53rd International Astronautical Congress, The World Space Congress – 2002*, 10–19 October 2002, Houston, TX, USA.
8. A.A. Bolonkin, "Hypersonic Launch System of Capability Up 500 Tons per Day and Delivery Cost \$1 per lb", IAC-02-S.P.15, *53rd International Astronautical Congress, The World Space Congress – 2002*, 10–19 October 2002, Houston, TX, USA.
9. A.A. Bolonkin, "Employment Asteroids for Movement of Space Ship and Probes", IAC-02-S.6.04, *53rd International Astronautical Congress, The World Space Congress – 2002*, 10–19 October 2002, Houston, TX, USA.
10. A.A. Bolonkin, "Optimal Inflatable Space Towers of High Height", COSPAR-02 C1.1-0035-02, *34th Scientific Assembly of the Committee on Space Research (COSPAR)*, *The World Space Congress – 2002*, 10–19 October 2002, Houston, TX, USA.
11. A.A. Bolonkin, "Non-rocket Earth–Moon Transport System", COSPAR-02 B0.3-F3.3-0032-02, 02-A-02226, *34th Scientific Assembly of the Committee on Space Research (COSPAR)*, *The World Space Congress – 2002*, 10–19 October 2002, Houston, TX, USA.
12. A.A. Bolonkin, "Non-rocket Earth–Mars Transport System", COSPAR-02 B0.4-C3.4-0036-02, *34th Scientific Assembly of the Committee on Space Research (COSPAR)*, *The World Space Congress – 2002*, 10–19 October 2002, Houston, TX, USA.

13. A.A. Bolonkin, "Transport System for Delivery Tourists at Altitude 140 km", IAC-02-IAA.1.3.03, *53rd International Astronautical Congress, The World Space Congress – 2002*, 10–19 October 2002, Houston, TX, USA.
14. A.A. Bolonkin, "Optimal Inflatable Space Towers with 3–100 km Height", *Journal of British Interplanetary Society*, Vol. 56, 2003, pp. 87–97.
15. A.A. Bolonkin, "Asteroids as Propulsion Systems of Space Ships", *Journal of British Interplanetary Society*, Vol. 58, 2003, pp. 97–107.
16. A.A. Bolonkin, "Hypersonic Gas-Rocket Launch System", AIAA-2002-3927, *38th AIAA/ASME/SAE/ASEE Joint Propulsion Conference and Exhibit*, 7–10 July 2002, Indianapolis, IN, USA.
17. A.A. Bolonkin, "Non-rocket Transportation System for Space Travel", *Journal of British Interplanetary Society*, Vol. 56, No. 7/8, 2003, pp. 231–249.
18. A.A. Bolonkin, "Hypersonic Space Launcher of High Capability", *Actual Problems of Aviation and Aerospace Systems, Kazan*, Vol. 8, No. 1(15), 2003, pp. 45–58.
19. A.A. Bolonkin, "Centrifugal Keeper for Space Stations and Satellites", *Journal of British Interplanetary Society*, Vol. 56, 2003, pp. 314–327.
20. A.A. Bolonkin, "Non-rocket Earth–Moon Transport System", *Advances in Space Research*, Vol. 31/11, 2003, pp. 2485–2490.
21. A.A. Bolonkin, "Earth Accelerator for Space Ships and Missiles", *Journal of British Interplanetary Society*, Vol. 56, 2003, pp. 394–404.
22. A.A. Bolonkin, "Air Cable Transport", *Journal of Aircraft*, Vol. 40, No. 4, July–August 2003.
23. A.A. Bolonkin, "High Speed Catapult Aviation", AIAA-2005-6221, *AIAA Atmospheric Flight Mechanic Conference*, 15–18 August 2005, USA.
24. A.A. Bolonkin, "High Efficiency Transfer of Mechanical Energy", AIAA-2004-5660, *International Energy Conversion Engineering Conference*, 16–19 August 2004, RI, USA.
25. A.A. Bolonkin, "Light Multi-reflex Engine", *Journal of British Interplanetary Society*, Vol. 57, No. 9/10, 2004, pp. 353–359.
26. A.A. Bolonkin, Multi-reflex Propulsion System, *Journal of British Interplanetary Society*, Vol. 57, No. 11/12, 2004, pp. 370–390.
27. A.A. Bolonkin, "Sling Rotary Space Launchers", AIAA-2005-4035, *41st Propulsion Conference*, 10–13 July 2005, Tucson, AZ, USA.
28. A.A. Bolonkin, "Kinetic Anti-gravitator", AIAA-2005-4504, *41st Propulsion Conference*, 10–13 July 2005, Tucson, AZ, USA.
29. A.A. Bolonkin, "Space Propulsion Using Solar Wing and Installation for It", Russian Patent Application #3635955/23 126453, 19 August 1983 (in Russian), Russian PTO.
30. A.A. Bolonkin, "Installation for Open Electrostatic Field", Russian Patent Application #3467270/21 116676, 9 July 1982 (in Russian), Russian PTO.
31. A.A. Bolonkin, "Getting of Electric Energy from Space and Installation for It", Russian Patent Application #3638699/25 126303, 19 August 1983 (in Russian), Russian PTO.
32. A.A. Bolonkin, "Protection from Charged Particles in Space and Installation for It", Russian Patent Application #3644168 136270, 23 September 1983 (in Russian), Russian PTO.

33. A.A. Bolonkin, "Method of Transformation of Plasma Energy in Electric Current and Installation for It", Russian Patent Application #3647344 136681, 27 July 1983 (in Russian), Russian PTO.
34. A.A. Bolonkin, "Method of Propulsion using Radioisotope Energy and Installation for It", Russian Patent Application #3601164/25 086973, 6 June 1983 (in Russian), Russian PTO.
35. A.A. Bolonkin, "Transformation of Energy of Rarefaction Plasma in Electric Current and Installation for It", Russian Patent Application #3663911/25 159775, 23 November 1983 (in Russian), Russian PTO.
36. A.A. Bolonkin, "Method of a Keeping of a Neutral Plasma and Installation for It", Russian Patent Application #3600272/25 086993, 6 June 1983 (in Russian), Russian PTO.
37. A.A. Bolonkin, "Radioisotope Propulsion", Russian Patent Application #3467762/25 116952, 9 July 1982 (in Russian), Russian PTO.
38. A.A. Bolonkin, "Radioisotope Electric Generator", Russian Patent Application #3469511/25 116927, 9 July 1982 (in Russian), Russian PTO.
39. A.A. Bolonkin, "Radioisotope Electric Generator", Russian Patent Application #3620051/25 108943, 13 July 1983 (in Russian), Russian PTO.
40. A.A. Bolonkin, "Method of Energy Transformation of Radioisotope Matter in Electricity and Installation for It", Russian Patent Application #3647343/25 136692, 27 July 1983 (in Russian), Russian PTO.
41. A.A. Bolonkin, "Method of Stretching of Thin Film", Russian Patent Application #3646689/10 138085, 28 September 1983 (in Russian), Russian PTO.
42. A.A. Bolonkin, "New Way of Thrust and Generation of Electrical Energy in Space", Report ESTI, 1987, p. 109 (Soviet Classified Project).
43. A.A. Bolonkin, "Aviation, Motor and Space Designs", *Emerging Technology in the Soviet Union*, 1990, Falls Church, VA, USA, Delphic Ass., Inc., pp. 32–80 (in English).
44. A.A. Bolonkin, "A Space Motor Using Solar Wind Energy", IAF-0615, *The World Space Congress*, 28 August–5 September 1992, Washington, DC, USA.
45. A.A. Bolonkin, "The Simplest Space Electric Generator and Motor with Control Energy and Thrust", IAF-94-R.1.368, *45th International Astronautical Congress*, 9–4 October 1994, Jerusalem, Israel.
46. A.A. Bolonkin, "Space Electric Generator, Run by Solar Wing", IAF-92-0604, *The World Space Congress*, 28 August–5 September 1992, Washington, DC, USA.
47. A.A. Bolonkin, "Simple Space Nuclear Reactor Motors and Electric Generators Running on Radioactive Substances", IAF-92-0573, *The World Space Congress*, 28 August–5 September 1992, Washington, DC, USA.
48. N. Omidi and H. Karimabadi, "Electrostatic Plasma Sail", AIAA 2003-5227, 2003 *39th AIAA/ASME/SAE/ASEE Joint Propulsion Conference and Exhibit*, 20–23 July 2003, Huntsville, AL, USA. See also this work in NIAC site <http://niac.usra.edu>, Omidi final report where director NIAC Mr. Cassanova awarded this work \$75000.
49. V.I. Feodosev, *Base of Rocket Flight Techniques*, Science, Moscow, 1981 (in Russian).
50. I.K. Kikoin (ed.), *Tables of Physical Values Directory*, Atomisdat, Moscow, 1976 (in Russian).

51. *McGraw-Hill Encyclopedia of Science & Technology*, New York, Vol. 1–20, 2002.
52. L. Funaki, *et al.*, “Trust Production Mechanism of Magnetoplasma Sail”, AIAA 2003-4292, 34th AIAA Plasmadynamics and Lasers Conference, Orlando, Florida, June 23–26, 2003.
53. A.A. Bolonkin, “Electrostatic Solar Wind Propulsion System”, AIAA-2005-3653, *41st Propulsion Conference*, 10–12 July 2005, Tucson, AZ, USA.
54. A.A. Bolonkin, “Electrostatic Utilization of Asteroids for Space Flight”, AIAA-2005-4032, *41st Propulsion Conference*, 10–12 July 2005, Tucson, AZ, USA.
55. A.A. Bolonkin, “Radioisotope Space Sail and Electric Generator”, AIAA-2005-4225, *41st Propulsion Conference*, 10–12 July 2005, Tucson, AZ, USA.
56. A.A. Bolonkin, “Guided Solar Sail and Electric Generator”, AIAA-2005-3857, *41st Propulsion Conference*, 10–12 July 2005, Tucson, AZ, USA.
57. A.A. Bolonkin, “Problems of Electrostatic Levitation and Artificial Gravity”, AIAA-2005-4465, *41st Propulsion Conference*, 10–12 July 2005, Tucson, AZ, USA.
58. A.A. Bolonkin, “Guided Solar Sail and Electric Generator”, AIAA-2005-3857, *41st Propulsion Conference*, 10–12 July 2005, Tucson, AZ, USA.
59. A.A. Bolonkin, “Problems of Electrostatic Levitation and Artificial Gravity”, AIAA-2005-4465, *41st Propulsion Conference*, 10–12 July 2005, Tucson, AZ, USA.

CHAPTER 14

Electrostatic Utilization of Asteroids for Space Flight*

Summary

This chapter offers a electrostatic method for changing the trajectory of space probes. The method uses electrostatic force and the kinetic or rotary energy of asteroids, comet nuclei, meteorites or other space bodies (small planets, natural planet satellites such as moons, space debris, etc.) to increase or decrease ship/probe speed by 1000 m/s or more and to achieve any new direction in outer space. The flight possibilities of space ships and probes are thereby increased by a factor of millions.

14.1 Introduction

The method includes the following main steps (Fig. 14.1):

- (a) Finding an asteroid using a locator or telescope (or looking in a catalog) an asteroid and determining its main parameters (location, mass, speed, direction, rotation); selecting the appropriate asteroid; computing the required position of the ship with respect to the asteroid.
- (b) Correcting the ship's trajectory to obtain the required position; convergence of the ship with the asteroid.
- (c) Charging the asteroid and space apparatus ball using a charge gun.
- (d) Obtaining the necessary apparatus position and speed for the apparatus by flying it around the space body and changing the charge of the apparatus and space body (asteroids).
- (e) Discharging the space apparatus and the space body.

*The full text was presented by the author as Paper AIAA-2005-4032 at the *41st Propulsion Conference*, 10–12 July 2005, Tucson, AZ, USA.

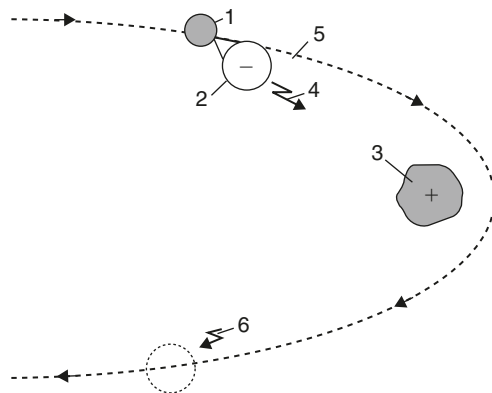


Fig. 14.1. Method of electrostatic maneuvers of the space apparatus. Notations: (1) Space apparatus; (2) charged ball; (3) asteroid; (4) charged gun; (5) new apparatus trajectory; and (6) discharging the apparatus and asteroid.

The equipment required for changing a probe (spacecraft) trajectory includes:

- (a) A charging gun.
- (b) Devices for finding and measuring the asteroids (space bodies), and computing the trajectory of the spacecraft relative of the space body.
- (c) Devices for spacecraft guidance and control.
- (d) A device for discharging of the apparatus and asteroids (space body) (see Fig. 14.1).

14.2 Description of utilization

The following describes the general facilities and process for a natural space body (asteroid, comet, meteorite, and small planet), or other space ship with a small gravitational force to change the trajectory and speed of a space probe.

Fig. 14.2(a-d) shows the preparations for using a natural body for changing the trajectory of the space apparatus, for example the natural space body 2, which moves near the space apparatus. The ship needs to make a maneuver (change direction or speed) in plane 3 (perpendicular to the sketch), and the position of the apparatus is corrected and it is moved into the required plane 3 using small rocket impulses. It is assumed that the natural elected object has more mass than the artificial apparatus, and the space body speed is close to that of the apparatus (the difference can be as much as 1000 m/s).

In the early computed point of the trajectory the space apparatus sends the asteroid a charge which takes root on asteroid surface, electrifying it. The apparatus also is charged (with unlike or like charges). If the apparatus and asteroid have unlike charges, they will be attracted one to another (Fig. 14.2(c)). If they have like charges, they will repel such other (Fig. 14.2(d)). The electrostatic force changes the apparatus trajectory and speed. The trajectory gains a new direction with a new velocity. When the trajectory has the selected direction and speed, the apparatus is then discharged and leaves the asteroid.

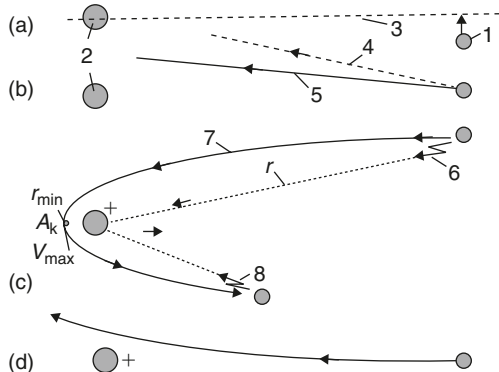


Fig. 14.2. Maneuvers of electrostatic space apparatus. (a) Preparing for maneuver, correcting the plane of maneuver. (b) Correcting the apparatus trajectory in the maneuver plane. (c) Charging the apparatus and asteroids, changing apparatus trajectory and velocity, discharging apparatus and asteroid. (d) The case of like charges (which repel). *Notations:* (1) Space apparatus (ball); (2) asteroid; (3) plane of maneuver; (4) initial apparatus trajectory; (5) primary correction of the trajectory in the maneuver plane; (6) charge impulse from apparatus to asteroid using charge gun; (7) new apparatus trajectory; and (8) discharge impulse from apparatus (return part of charge energy) using sharp edge.

The charge energy returns to the apparatus. If efficiency equals 1, this energy will be less when the new apparatus speed is more than before, equal when the speeds are same, and more when the apparatus speed is less than the previous speed.

Charging is done using a special charge gun, which accelerates charged particles (electrons or ions) to the required speed, and discharging is done using the edge of a pike. The return energy is an electric current through the pike's edge. The apparatus can also utilize the asteroid's speed and asteroid kinetic energy by mechanical connection as described herein.^{1–6}

An abandoned space vehicle or large piece of space debris in the Earth's orbit can also be used to increase the speed of the new vehicle and to remove the abandoned vehicle or debris from orbit (see Section 14.3.5).

The charging equipment may be used to land the apparatus on an asteroid (small planet) surface and to launch the apparatus from an asteroid (see Section 14.3.5). The apparatus ball is usually charged with negative charges because negative charges (electrons) are emitted from an open surface which does not have a high-resistance electric cover, when the electrical intensity (in a vacuum) is over 100 MV/m.

14.3 Theory and computation (in metric system)

14.3.1 The electrostatic force

The electrostatic force between charged bodies is:

$$F = k \frac{Q_1 Q_2}{r^2}, \quad \text{if } Q = Q_1 = Q_2, \quad F = k \frac{Q^2}{r^2}, \quad Q = \frac{a^2 E}{k}, \quad (14.1)$$

where F is the force [N]; k is a coefficient, $k = 9 \times 10^9$; Q is the charge [constant]; r is the distance between the center of charges [m]; a is radius of the charged ball apparatus [m]; and E is the electrical intensity at the ball's surface [V/m] (it may be up 100–200 MV/m in the vacuum and negative charge, and is more for positive charge).

14.3.2 Computation of space apparatus trajectories

Assume the asteroid mass is many times greater than the apparatus mass and start the origin of the coordinate system at the asteroid's center of gravity. The initial apparatus position is shown in Fig. 14.3.

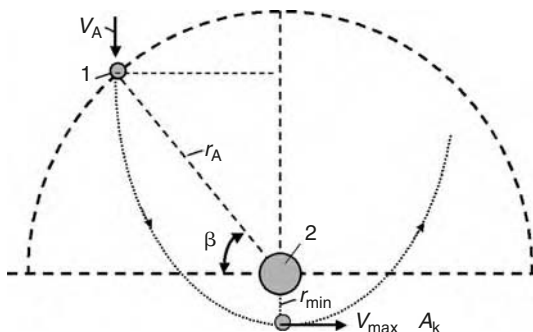


Fig. 14.3. Interaction between the charged ball apparatus and the charged asteroid. *Notations:* (1) Space apparatus and electrically charged ball (balloon) and (2) asteroid; r_A is the initial radius, V_A is the initial apparatus speed.

We assume the charging happens instantly and the charges are constant up to point of discharge.

The equations for computation of the hyperbolic ($e > 1$) apparatus trajectory are (asteroid mass \gg apparatus mass):

$$\begin{aligned}
 K &= \frac{kqQ}{m}, \quad H = V_A^2 \mp \frac{2K}{r_A}, \quad c = r_A V_A \cos \beta, \quad e = \frac{c}{K} \sqrt{H + \frac{K^2}{c^2}}, \\
 \alpha &= 2 \arctan \sqrt{e^2 - 1}, \quad e > 1, \quad \gamma = \pi - \alpha, \quad V = \sqrt{H + \frac{2K}{r}}, \\
 p &= \frac{c^2}{K}, \quad r = \frac{p}{1 + e \cos \varphi}, \quad T = \frac{2\pi}{\sqrt{K}} \left(\frac{p}{1 - e^2} \right)^{3/2}, \quad r_{\min} = \frac{p}{1 + e}, \\
 V_{\max} &= \sqrt{H + \frac{2K}{r_{\min}}}, \quad A_k = \frac{V_{\max}^2}{p},
 \end{aligned} \tag{14.2}$$

where K is the coefficient [constant]; m is the apparatus mass [kg]; q is the electrical charge of the space apparatus [constant]; Q is the electrical charge of the asteroid [constant], which is conventionally $q = Q$; H is the coefficient of apparatus energy (kinetic and electric potential) around the asteroid; V_A is the relative speed of the asteroid about

space ship [m/s] at the initial radius r_A (moment of charge impulse); $V(r)$ is the space ship speed [m/s]; c is the momentum constant; e is the eccentricity of the apparatus trajectory ($e > 1$ for a hyperbolic trajectory, $e = 1$ for parabolic trajectory, $0 < e < 1$ for an elliptical trajectory, $e = 0$ for a circle); β is the angle between V_A and perpendicular to r_A at the moment of charging (see Fig. 14.2); α is the angle between the asymptotes of the hyperbolic trajectory; γ is the final deviation of the hyperbolic trajectory from the initial direction [rad]; p is the parameter of the hyperbolic trajectory [m]; r is the variable radius-vector at the trajectory point [m]; r_{\min} is the minimum distance of the charge apparatus center from the asteroid [m]; V_{\max} is the maximum apparatus speed relative to the asteroid [m/s]; and A_k is the maximum centrifugal acceleration of apparatus [m/s²].

The constant (H) may be found from the initial position (r_A) and initial speed of the apparatus (V_A) (see the second formula in equation (14.2)). Sign “−” is used for attraction, sign “+” is used for repelling charges.

Note that the trajectory may be circular or elliptical and the apparatus can orbit for a long time around the asteroid.

Readers can find initial formulas for gravity fields in space mechanics and physics textbooks and modify them for electrical charged bodies (electric fields). Formulas in equation (14.2) are used for deviation of the charged apparatus by the electrically charged asteroid.

Computations of a typical parameter of trajectory versus parameter r_A for space apparatus of mass 100 kg are presented in Figs. 14.4–14.7.

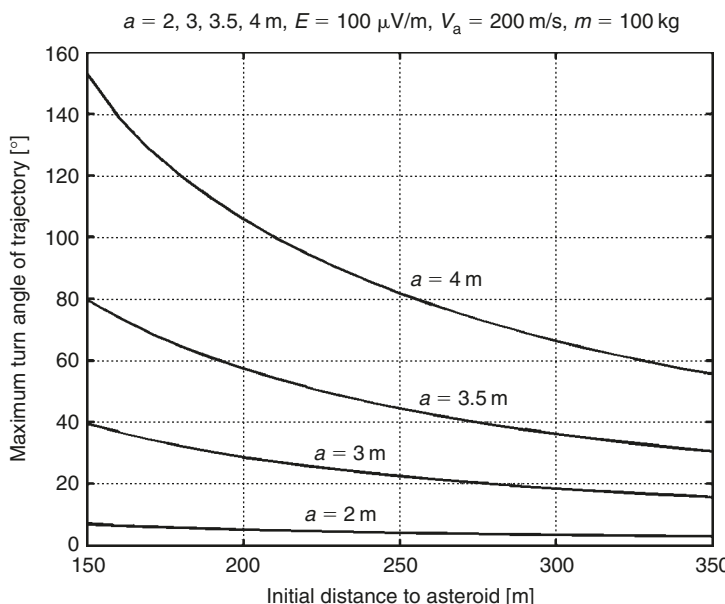


Fig. 14.4. Maximum turn angle of trajectory, γ , versus the initial charge distance to asteroid and radius of the charged ball for electrical intensity of 100 MV/m, initial apparatus speed 200 m/s, and apparatus mass 100 kg, $\beta = \pi/4$.

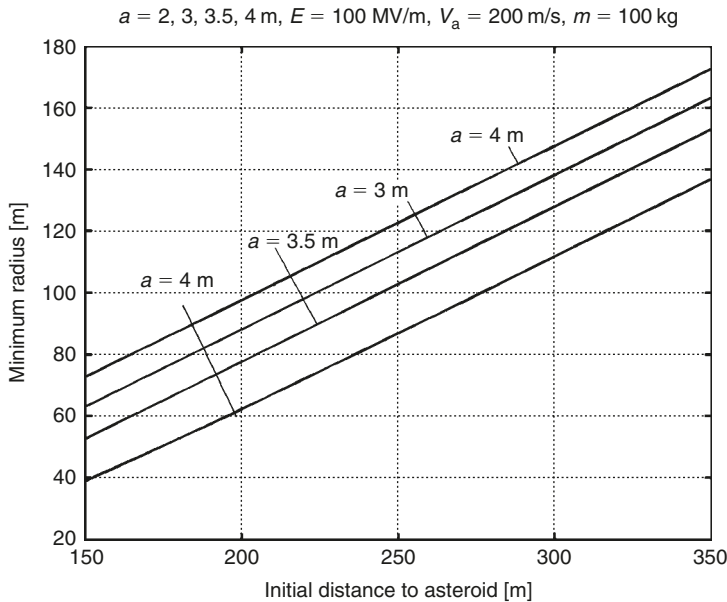


Fig. 14.5. Minimum radius of trajectory versus the initial charge distance to the asteroid and radius of the charged ball for electrical intensity 100 MV/m , initial apparatus speed 200 m/s , and apparatus mass 100 kg , $\beta = \pi/4$.

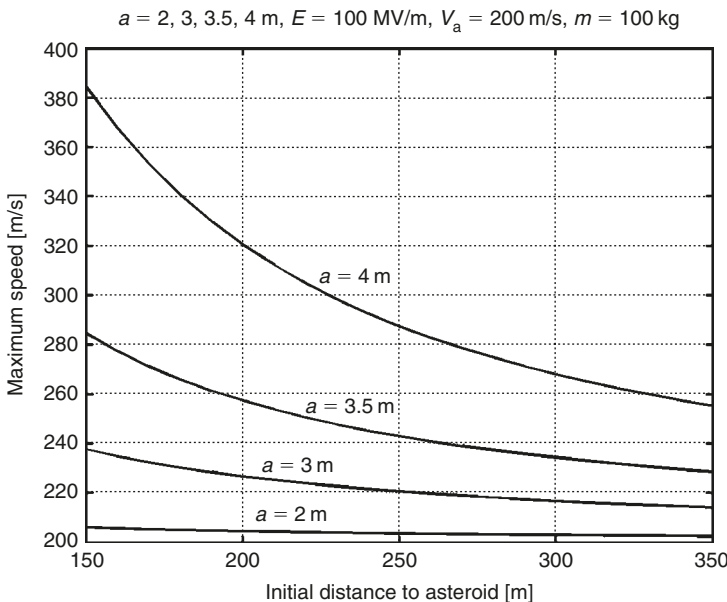


Fig. 14.6. Maximum speed of the space apparatus versus the initial charge distance to the asteroid and radius of the charged ball for electrical intensity 100 MV/m , initial apparatus speed 200 m/s , and apparatus mass 100 kg , $\beta = \pi/4$.

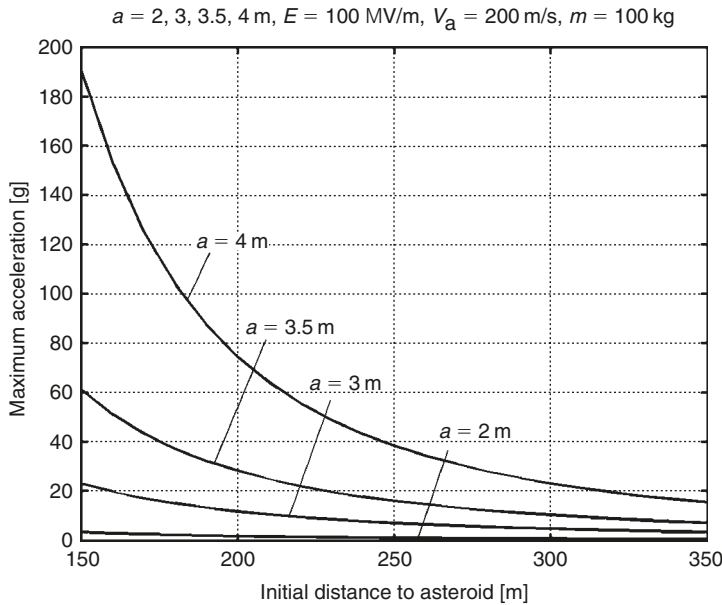


Fig. 14.7. Maximum acceleration (g) of space apparatus versus the initial charge distance to the asteroid and radius of the charged ball for electrical intensity 100 MV/m, initial apparatus speed 200 m/s, and apparatus mass 100 kg, $\beta = \pi/4$.

14.3.3 Initial expenditure of electrical energy needed to charge of the ball

The ball must be charged with electrical energy of high voltage (millions of volts). Let us estimate the minimum energy, when charged the device has 100% efficiency. This energy is equal to the work of moving of the ball charge to infinity. This may be computed using the equation:

$$W = \frac{Q^2}{2C}, \quad Q = \frac{a^2 E}{k}, \quad C = \frac{a}{k}, \quad W = \frac{a^3 E^2}{2k}, \quad (14.3)$$

where W is ball charge energy [J]; C is ball capacitance [F]; and Q is ball charge [constant].

The result of this computation is presented (same) in Fig. 13.18. As you can see this energy is not enormous – it is about 1–10 kWh for a ball radius of $a = 2\text{--}4$ m and electrical intensity of 25–100 MV/m. This energy (equal, or less, or more) may be returned when the ball is discharged by emitting of the charge into space using a sharp edge.

The energy (work) requirement for the separation of unlike charges (apparatus – asteroid, $q = Q$) can be computed by the following equations (for efficiency equal to 1):

$$\begin{aligned} W &= \int_a^{r_A} k \frac{Q^2}{r^2} dr = kQ^2 \left(\frac{1}{a} - \frac{1}{r_A} \right), \quad \Delta W = \frac{mV_A^2}{2} - \frac{mV_f^2}{2}, \\ \Delta W &= kQ^2 \left(\frac{1}{r_A} - \frac{1}{r_f} \right), \end{aligned} \quad (14.4)$$

where ΔW is increment in energy [J]; V_f is apparatus speed on the moment of discharge [m/s]; and r_f is the distance to the asteroid at the moment of discharge [m]. Charging the asteroid requires less energy because it is located at a limited distance from the space apparatus. The increment ΔW may be either positive, zero, or negative.

14.3.4 The ball stress, cover thickness, and ball mass

The ball has tensile stress from the like electric charges. The equations are same as equations (13.9)–(13.12) of Chapter 13.

The computations of the ball thickness and ball mass are presented in Figs. 13.12 and 13.13.

14.3.5 Landing on and launching the space apparatus from asteroids and small planets

If the apparatus and the asteroid have like charges, they will repel each other. This can be used to brake the apparatus for landing on the asteroid or for launching the apparatus from the asteroid surface. The change in apparatus speed can be computed using the following equations:

$$Q = \frac{a^2 E}{k}, \quad \frac{mV^2}{2} = k \frac{Q^2}{a} = \frac{a^3 E^2}{k}, \quad V = \sqrt{\frac{2a^3 E^2}{km}}, \quad (14.5)$$

where V is the initial (for braking) or final (for launching) speed of the apparatus [m/s]. Computations of braking (landing) and launch speed are presented in Fig. 14.8. The launch speed can be quite high, at up to 1600 m/s or more.

14.4 Project

As a project we can take the space apparatus of the mass 100 kg. All its parameters and maneuver capabilities can be estimated from the figures.

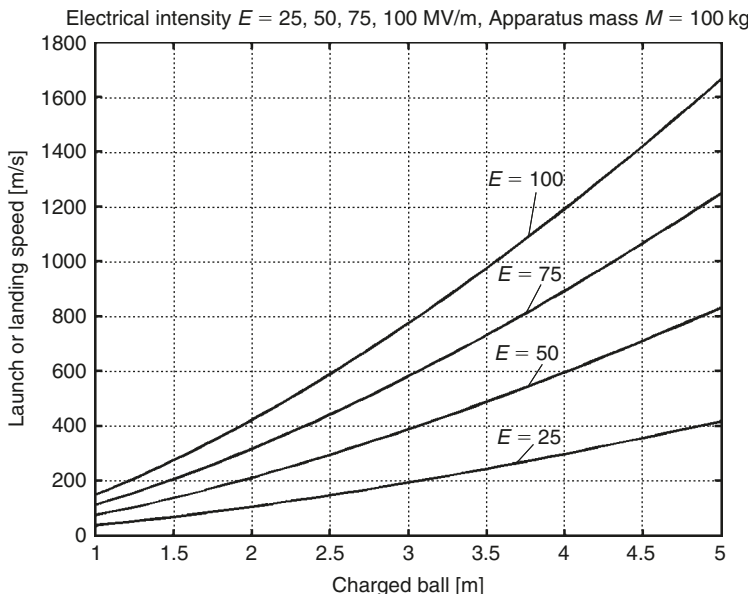


Fig. 14.8. Launch and landing (braking) speed of apparatus versus the charged ball radius and the electrical intensity (MV/m).

14.5 Discussion

14.5.1 Estimation of probability of meeting a small asteroid

This problem was considered in Chapter 11. Note that the kinetic energy of space bodies may be used through mechanical connections⁴ if the space body has a different speed or direction. However, electrostatic apparatus can use space body that has the same direction and speed for its acceleration if the apparatus has electrical energy (through charging and discharging the space body).

14.5.2 Charging the ball

This problem was considered in Section 13.3.9.

14.5.3 Blockading of the ball charge

Blockading of the charge on the ball and the asteroid by unlike solar wind particles may be a problem with this method. The charge on the ball attracts unlike particles and repels like particles and opposite-charge particles accumulate near the ball and block its charge. As the result the efficient area near the ball is less than electrostatic theory predicts. The area has a radius of about 7–25 km in Earth orbit. The electrostatic forces can be reduced. The method of computation for a neutral (efficient) area is offered by author

elsewhere (see also Chapter 13).⁵ This problem is not important for suggested method by following reasons:

1. The apparatus trajectory is usually located inside the neutral sphere.
2. The maneuvers are usually made far from the Sun where the solar wind intensity (density of space plasma) is very small.
3. The maneuvers are made quickly.

Possible drawbacks of the method may include the mass of the charge gun, electrical energy storage, and the mass of ball because the apparatus has big centrifugal acceleration.

References

1. A.A. Bolonkin, “Theory of Flight Apparatus with Control Radial Force”, *Collection Researches of Flight Dynamic*, ed. I.V. Ostoslavsky, Mashinostroenie, Moscow, 1965, pp. 79–118 (in Russian).
2. M. Krinker, “Asteroids as Engine of Space Ships” (Suggestion of American Scientist Alexander Bolonkin), *Weekly News*, 28 April 1998, Israel (in Russian).
3. A.A. Bolonkin, “Employment of Asteroids for Movement of Space Ship and Probes”, IA C-02-S.6.04, *53rd International Astronautical Congress, The World Space Congress – 2002*, 10–19 October 2002, Houston, TX, USA.
4. A.A. Bolonkin, “Asteroids as Propulsion Systems of Space Ship”, *Journal of British Interplanetary Society*, Vol. 56, No. 3/4, 2003, pp. 98–107.
5. A.A. Bolonkin, “Electrostatic Solar Wind Propulsion System”, AIAA-2005-3653, *41st Propulsion Conference*, Tucson, AZ, USA, July 10–13, 2005.
6. A.A. Bolonkin, “Electrostatic Utilization of Asteroids”, AIAA-2005-4032, *41st Propulsion Conference*, Tucson, AZ, USA.

CHAPTER 15

Electrostatic Levitation on the Earth and Artificial Gravity for Space Ships and Asteroids*

Summary

The author offers and researches the conditions which allow people and vehicles to levitate on the Earth using the electrostatic repulsive force. He shows that by using small electrically charged balls, people and cars can take flight in the atmosphere. Also, a levitated train can attain high speeds. He has computed some projects and discusses the problems which can appear in the practical development of this method. It is also shown how this method may be used for creating artificial gravity (attraction force) into and out of space ships, space hotels, asteroids, and small planets which have little gravity.

15.1 Introduction

People have dreamed about a flying freely in the air without any apparatus for many centuries. In ancient books we can find pictures of flying angels or God sitting on clouds or in heaven. At the present time you can see the same pictures on walls in many churches.

Physicist know only two methods for creating repulsive force: magnetism and electrostatics. Magnetism is well studied and the use of superconductive magnets for levitating a train has been widely discussed in scientific journals, but repulsive magnets have only a short-range force. They work well for ground trains but are bad for air flight. Electrostatic flight needs powerful electric fields and powerful electric charges. The Earth's electric field is very weak and cannot be used for levitation. The main innovations presented in this chapter are methods for creating powerful static electrical fields in the atmosphere and powerful, stable electrical charges of small size which allow levitation (flight) of people, cars, and vehicles in the air. The author also shows how this method can be utilized into and out of a space ship (space hotel) or on an asteroid surface for creating artificial gravity. The author believes this method has applications in many fields of technology.

* Presented as paper AIAA-2005-4465, *41st Propulsion Conference*, 10–13 July 2005, Tucson, AZ, USA.

Magnetic levitation has been widely discussed in the literature for a long time. However, there are few scientific works related to electrostatic levitation. Electrostatic charges have a high voltage and can create corona discharges, breakthrough, and relaxation. The Earth's electrostatic field is very weak and useless for flight. That is why many innovators think that electrostatic forces cannot be useful for levitation.

The author's first innovations in this field which changed this situation were offered in (1982),¹ and some practical applications were given in (1983).² The idea was published in 1990 (see Ref.³ [p. 79]). In the following presented work, these ideas and innovations are researched in more detail. Some projects are also presented to allow estimation of the parameters of the offered flight systems.

15.2 Brief description of innovation

It is known that like electric charges repel, and unlike electric charges attract (Fig. 15.1(a–c)). A large electric charge (for example, positive) located at altitude induces the opposite (negative) electric charge at the Earth's surface (Figs. 15.1(d–g)) because the Earth is an electrical conductor. Between the upper and lower charges there is an electric field. If a small negative electric charge is placed in this electric field, this charge will be repelled from the like charges (on the Earth's surface) and attracted to the upper charge (Fig. 15.1(d)). That is the electrostatic lift force. The majority of the lift force is determined by the Earth's charges because the small charges are conventionally located near the Earth's surface. As shown below, these small charges can be connected to a man or a car and have enough force to lift and supports them in the air.

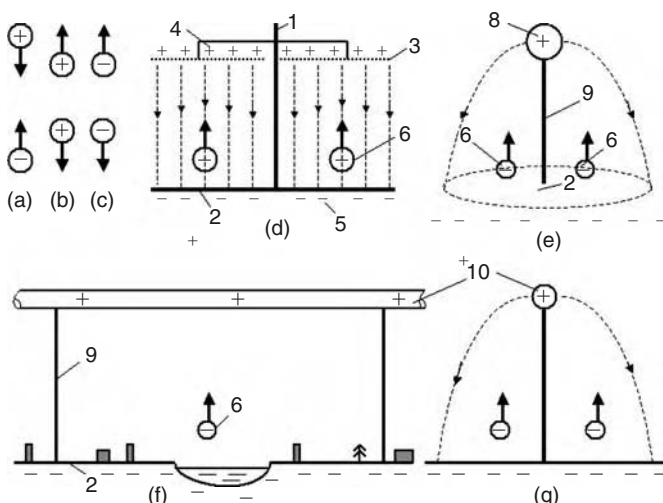


Fig. 15.1. Explanation of electrostatic levitation: (a) Attraction of unlike charges; (b and c) repulsion of like charges; (d) creation of the homogeneous electric field (highway); (e) electrical field from a large spherical charge ; (f and g) electrical field from a tube (highway) (side and front views). *Notations:* (1 and 9) Column; (2) Earth's (or other) surface charged by induction; (3) net; (4) upper charges; (5) lower charges; (6) levitation apparatus; (8) charged air balloon; and (10) charged tube.

The upper charge may be located on a column as shown in Fig. 15.1(d–g), or a tethered air balloon (if we want to create levitation in a small town) (Fig. 15.1(e)), or air tube (if we want to build a big highway), or a tube suspended on columns (Fig. 15.1(f) and (g)). In particular, the charges may be at two identically charged plates, used for a non-contact train (Fig. 15.3(a)).

A lifting charge may use charged balls. If a thin film ball with maximum electrical intensity of below $3 \times 10^6 \text{ V/m}$ is used, the ball will have a radius of about 1 m (the man mass is 100 kg). For a 1-ton car, the ball will have a radius of about 3 m (see the Section 15.3 and Fig. 15.2(g–i)). If a higher electric intensity is used, the balls can be small and located underneath clothes (see below and Fig. 15.2(a–c)).

The offered method has big advantages in comparison to conventional vehicles (Figs. 15.1 and 15.2):

1. Not very expensive highways are necessary. Rivers, lakes, forests, and buildings are not obstacles for this method.
2. In given regions (Figs. 15.1 and 15.2) people (and cars) can move at high speeds (man up 70 km/h and cars up to 200–400 km/h) in any direction using simple

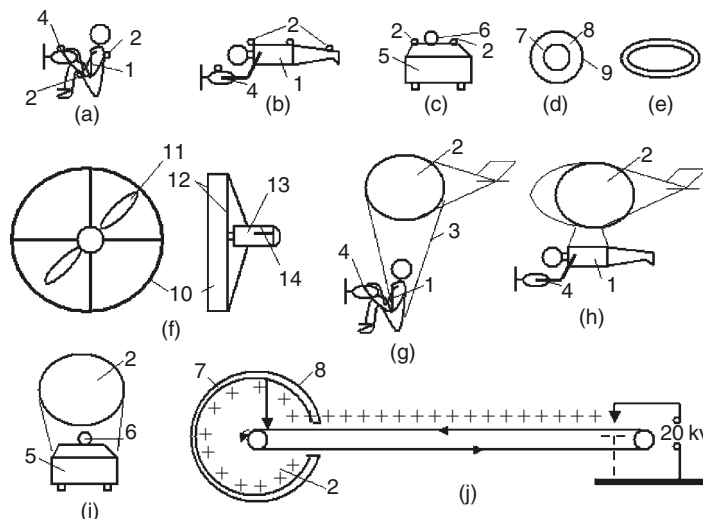


Fig. 15.2. Levitation apparatus: (a and b) Single levitated man (mass up to 100 kg) using small highly charged balls 2. (a) Sitting position; (b) reclining position; (c) small charged ball for levitating car; (d) small highly charged ball; (e) small highly charged cylindrical belt; (f) small air engine (forward and side views); (g) single levitated man (mass up to 100 kg) using a big non-highly charged ball which does not have an ionized zone (sitting position); (h) the same man in a reclining position; (i) large charged ball to levitate a car which does not have an ionized zone; and (j) installation for charging a ball using a Van de Graaff electrostatic generator (double generator potentially reaches 12 MV) in horizontal position. *Notations:* (1) Man; (2) charged lifting ball; (4) handheld air engine; (5) car; (6) engine (turbo-rocket or other); (7) conducting layer; (8) insulator (dielectric); (9) strong cover from artificial fibers or whiskers; (10) lagging; (11) air propeller; (12) preventive nets; (13) engine; and (14) control knobs.

equipment (small balls under their clothing and small engines (Fig. 15.2(a–c)). They can perform vertical takeoffs and landings.

3. People can reduce their weight and move at high speed, jump a long distance, and lift heavy weights.
4. Building high altitude homes will be easier.

This method can be also used for a levitated train and artificial gravity in space ships, hotels, and asteroids (Fig. 15.3(a) and (b)).

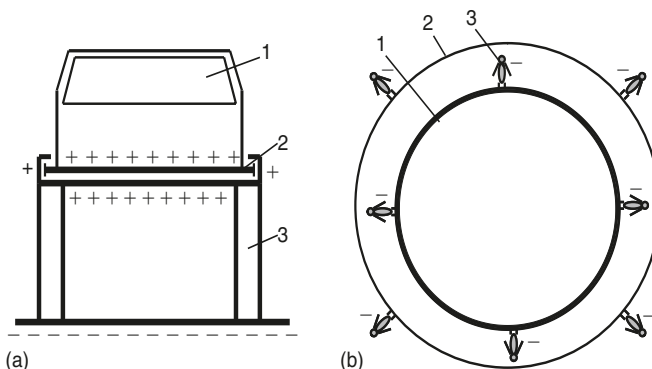


Fig. 15.3. Levitated train on Earth's and artificial gravity into and on space ships and asteroids.
 (a) Levitated train. *Notations:* (1) Train; (2) charged plates; (3) insulated column. (b) Artificial gravity on a space ship. *Notations:* (1) Charged space body; (2) space ship; and (3) man.

A space ship (hotel) definitely needs artificial gravity. Any slight carelessness in space can result in the cosmonaut, instruments, or devices drifting away from the space ship. Presently, they are connected to the space ship by cables, but this is not comfortable for working. Science knows only two methods of producing artificial gravity and attractive forces: rotation of space ship and magnetism. Both methods are bad. The rotation creates artificial gravity only inside the space ship (hotel). Observation of space from a rotating ship is very difficult. The magnetic force is only effective over a very short distance. The magnets stick together and a person has to expend a large effort to move (it is the same as when you are moving on a floor smeared with glue).

If there is a charge inside the space ship and small unlike charges attached to objects elsewhere, they will fall back to the ship if they are dropped.

The same situation occurs for cosmonauts on asteroids or small planets which have very little gravity. If you charge the asteroid and cosmonauts with unlike electric charges, the cosmonauts will return to the asteroid during any walking and jumping.

The author acknowledges that this method has problems. For example, we need a high electrical intensity if we want to use small charged balls. This problem (and others) is discussed below.

15.3 Theory of an electrostatic lift force and results of computations (in metric system)

15.3.1 Brief information about electric charges, electrical fields, and electric corona

Electric charge creates an electrical field. Every point this field has a vector of magnitude called electrical intensity, E , measured in volts per meter. If the unlike charges (or non-insulated electrodes under voltage) are located in an air atmosphere with a surface atmospheric pressure and the electrical intensity is less than $E_c = (3-4) \times 10^6 \text{ V/m}$, the discharge current will be very small. If $E > E_c = 3 \times 10^6 \text{ V/m}$ and we have a closed-loop high-voltage circuit (*for non-insulated electrodes*), electric current appears. The current increases following an exponential law when the voltage is increased. In a homogeneous electric field (as between plates), the increasing voltage makes a spark (flashover, breakthrough, lightning). A non-homogeneous electric field (as between a sphere and plate, or an open sphere) makes an electric *corona*. Electrons break away from the metal-*negative* electrode and ionize the air. Positive ions hit the non-insulated positive electrode and knockout electrons. These unlike ions can cause a particle blockade (discharge) of the main charge. The efficiency of ionization by positive ions is much less than for electrons of the same energy. Most ionization occurs as a result of secondary electrons released at the negative electrode by positive ion bombardment. These electrons produce ionization as they move from the strong field at the electrode out into the weak field. This, however, leaves a positive-ion space charge, which slows down the incoming ions. That has the effect of diminishing the secondary electron yield. As the positive ion mobility is low, there is a time lag before the high field conditions can be restored. For this reason the discharge is somewhat unstable.

The air contains a small amount of free electrons. These electrons can also create an electric corona around the *positive non-insulated electrode*, but under higher voltage than the negative electrode. The effect here is to enable the free electrons to ionize by collision in the high field surrounding this electrode. One electron can produce an avalanche in such a field, because each ionization event releases an additional electron, which can then do further ionization. To sustain the discharge, it is necessary to collect the positive ions and to produce the primary electrons far enough from the positive electrode to permit the avalanche to develop. The positive ions are collected at the negative electrode, and it is their low mobility that limits the current in the discharge. The primary electrons are thought to be produced by photo-ionization.

The particular characteristics of the discharge are determined by the shape of the electrodes, the polarity, the size of gap (ball), and the gas or gas mixture and its pressure. In high voltage electric lines the corona discharge that surrounds a high-potential power transmission line represents power loss and limits the maximum potential which can be used.

The offered method is very different from the conventional cases described in textbooks. The charges are *isolated* using an insulator (dielectric). They cannot emit electrons in the air. There is not a closed circuit. This method is nearer to single polarity electrets, when like charges are inserted into an insulator.⁵ Electrets have typical surface charges of about $\sigma = 10^{-8} \text{ C/cm}^2$, polyethylene terephthalate (PETP) up to $1.4 \times 10^{-7} \text{ C/cm}^2$ (see Ref.⁵[p. 17]), and thermally stimulated depolarization (TSD) with plasticized

polyvinyl butyral (PVB) up to $1.5 \times 10^{-5} \text{ C/cm}^2$ (see Ref.⁵ [p. 253]). This means the electrical intensity near their surface reaches ($E = 2\pi k\sigma$, $k = 9 \times 10^9$) $6 \times 10^6 \text{ V/m}$, $80 \times 10^6 \text{ V/m}$, and $8500 \times 10^6 \text{ V/m}$, respectively. The charges are not blockaded and the discharge (half-life time) continues from 100 days up to several years. In humid air the electrets lose part of their properties, but in dry air they regain them.

Natural Earth's radioactivity and cosmic rays create about 1.5–10.4 ions into 1 cm³ every second (see Ref.⁷ [p. 1004]). These ions gradually recombine back into conventional molecules.

In a vacuum the discharge mechanism is different. In non-insulated negative metal electrodes, the electrons may be extracted from the conducting electrode by the strong electric field. The critical surface electric intensity, E_0 , is about $100 \times 10^6 \text{ V/m}$ at the non-insulated negative electrode. This intensity is about 1000 times more at the positive electrode because the ions are very difficult to tear away from the solid material. Conducting sharp edges increase the electric intensity. That is why it is better to charge the planet or asteroid surface with positive charges. A very sharp spike allows the electrical energy of the charged ball to be regained.

15.3.2 Size of corona (ionized sphere) and safety of a ball of electric intensity

The size of the corona may be found as a spherical area where the electrical intensity is more than safe air intensity:

$$\begin{aligned} E &\geq E_c, \quad \frac{kq}{R_c^2} \geq E_c, \quad q = \frac{E_a a^2}{k}, \quad R_c \leq \sqrt{\frac{kE_a a^2}{kE_c}}, \\ \bar{R}_c &= \frac{R_c}{a} \leq \sqrt{\frac{E_a}{E_c}}, \end{aligned} \quad (15.1)$$

where E is the electrical intensity of the charge [V/m]; E_c , the electrical intensity at the beginning of the corona [V/m], $E_c \approx 3 \times 10^6$; E_a , the electrical intensity at the ball surface [V/m]; a , the ball radius [m]; R_c , the radius of corona [m]; and $k = 9 \times 10^9$.

To find the safe electrical intensity, E_a , for a negatively charged ball in an insulated cover from the point of rupture (spark) into a neutral environment, the following equation can be used:

$$\begin{aligned} U < U_i, \quad U &= \frac{kq}{\varepsilon} \left(\frac{1}{a} - \frac{1}{a + \delta} \right), \quad U_i = \varepsilon E_i \delta, \quad \frac{kq}{\varepsilon} \left(\frac{1}{a} - \frac{1}{a + \delta} \right) < \varepsilon E_i \delta, \\ q &= \frac{a^2 E_a}{k}, \quad \bar{\delta} = \frac{\delta}{a} > \frac{E_a}{\varepsilon E_i} - 1, \quad \text{for } \bar{\delta} = 0, \quad E_a < \varepsilon E_i, \end{aligned} \quad (15.2)$$

where U is the ball voltage [V]; U_i , the safe voltage of ball insulator [V]; E_i , the safe electrical intensity of ball insulator [V/m]; δ , the thickness of the ball cover [m]; and ε , the dielectric constant.

In equations (15.1) and (15.2) the last formulas are the final result.

Table 15.1. Properties of various good insulators (recalculated in metric system).

Insulator	Resistivity [ohm-m]	Dielectric strength [MV/m], E_i	Dielectric constant, ϵ	Tensile strength [kg/mm ²], $\sigma \times 10^7$ N/m ²
Lexan	10^{17} – 10^{19}	320–640	3	5.5
Kapton H	10^{19} – 10^{20}	120–320	3	15.2
Kel-F	10^{17} – 10^{19}	80–240	2–3	3.45
Mylar	10^{15} – 10^{16}	160–640	3	13.8
Parylene	10^{17} – 10^{20}	240–400	2–3	6.9
Polyethylene	10^{18} – 5×10^{18}	40–680*	2	2.8–4.1
Poly(tetra-fluoroethylene)	10^{15} – 5×10^{19}	40–280**	2	2.8–3.5
Air (1 atm, 1 mm gap)	–	4	1	0
Vacuum (1.3 × 10 ⁻³ Pa, 1 mm gap)	–	80–120	1	0

* For room temperature 500–700 MV/m.

** 400–500 MV/m.

Source: Encyclopedia of Science and Technology⁹ (Vol. 6, pp. 104, 229, 231) and Kikoin⁶, p. 321.*Note:* dielectric constant ϵ can reach 4.5–7.5 for mica (E is up 200 MV/m), 6–10 for glasses ($E = 40$ MV/m), and 900–3000 for special ceramics (marks are CM-1, T-900)⁶, p. 321, ($E = 13$ – 28 MV/m). Dielectric strength appreciably depends from surface roughness, thickness, purity, temperature and other conditions of materials. It is necessary to find good insulate materials and to research conditions which increase the dielectric strength.

Example: The ball is covered by Mylar with $E_i = 160$ MV/m, $\epsilon = 3$ (see Table 15.1). Then $E_a = 3 \times 160 = 480$ MV/m, and the relative radius of the ionized sphere [equation (15.1)] is $(480/3)^{0.5} = 12.6$. If $a = 0.05$ m, the real radius is $R_c = 12.6 \times 0.05 = 0.63$ m.

15.3.3 For a cylindrical cable or belt

The radius of the corona (ionized cylinder) can be found using the same method:

$$E \geq E_c, \quad E = \frac{2k\tau}{R_c}, \quad \tau = \frac{aE_a}{2k}, \quad \frac{aE_a}{R_c} \geq E_c, \quad R_c \leq a \frac{E_a}{E_c},$$

$$\bar{R}_c = \frac{R_c}{a} \leq \frac{E_a}{E_c}, \tag{15.3}$$

where τ is the linear charge [C/m].

To find using the same method [equation (15.2)] the safe intensity, E_a , for a negatively charged cable (belt, tube) in an insulated cover from point of rupture into a neutral environment the following equation can be used:

$$U < U_i, \quad U = 2k\tau \ln \left(\frac{a + \delta}{a} \right), \quad U_i = \epsilon E_i \delta, \quad 2k\tau \ln \left(\frac{a + \delta}{a} \right) < \epsilon E_i d,$$

$$\tau < \frac{\epsilon E_i a \delta / a}{2k \ln(1 + \delta / a)}, \quad \text{for } \frac{d}{a} \rightarrow 0, \quad \bar{\tau} = \frac{\tau}{a} < \frac{\epsilon E_i}{2k}, \quad E_a = k \frac{2\tau}{a},$$

$$\frac{\tau}{a} = \frac{E_a}{2k}, \quad \frac{E_a}{2k} < \frac{\epsilon E_i}{2k}, \quad E_a < \epsilon E_i. \tag{15.4}$$

15.3.4 Discharging by corona

Below, the author makes computations to show how the milliards ($10^9 \times 1 \text{ m}^3$) of charged particles influence the main charge.

If 1 m^3 of air contains d like-charged (electrons or ions) particles and the charge density is constant, the charge, q , of a sphere with radius, r , is:

$$q = \frac{4}{3} \pi r^3 ed, \quad (15.5)$$

where $e = 1.6 \times 10^{-19}$; charge of one particle, q , is C (electron or single charged ion); and d , the particle density.

On the other side, the main charge, q_0 , will be partially blockaded until the intensity at radius, r , becomes E_c . As a result the equation is:

$$q_0 - q = \frac{E_c}{k} r^2, \quad \frac{4}{3} \pi edr^3 + \frac{E_c}{k} r^2 - q_0 = 0, \quad (15.6)$$

where $k = 9 \times 10^9$. The equation (15.6) has only one real root. The results of this computation are presented in Figs. 15.4 and 15.5, which show that a large density only

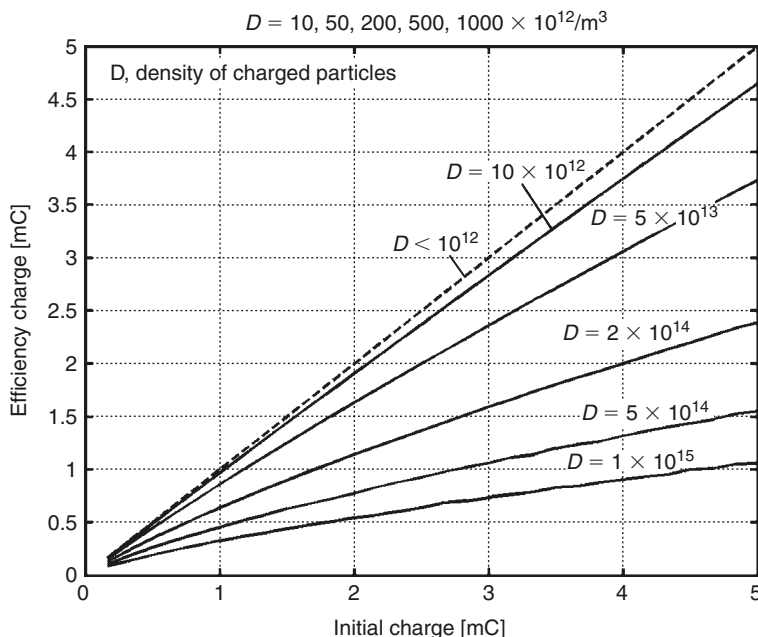


Fig. 15.4. Efficiency charge versus the main charge and density of charged particles in the environment (ionized zone).

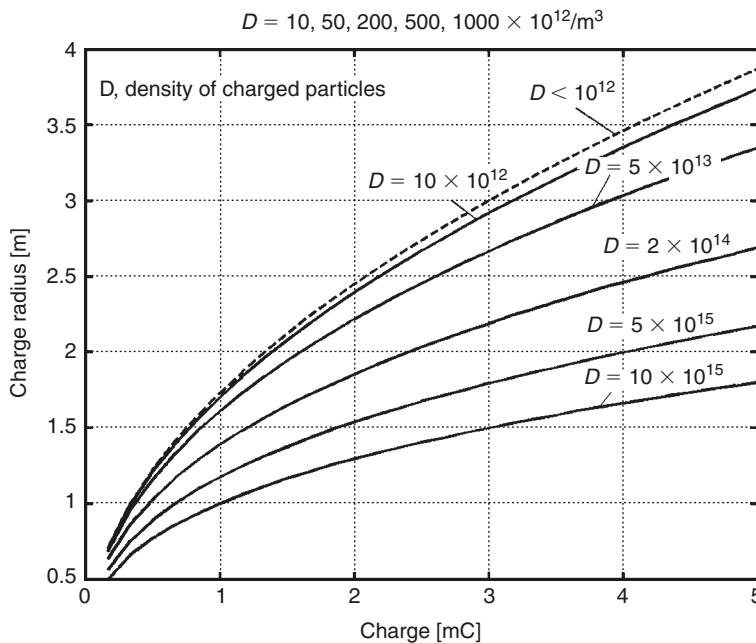


Fig. 15.5. Critical radius of main charge versus the main charge and density of charged particles in the environment (ionized zone).

decreases the main charge. But only experiments can show what causes this discharge to take place.

15.3.5 Some data about the ball material

The properties of electrical insulation vary depending on the impurities in the material, temperature, thickness, etc. and different for the same material with a different dielectric. For example, the resistivity of fused quartz is $10^{15} \text{ ohm}\cdot\text{cm}$ for $T = 20^\circ\text{C}$, the resistivity of the quartz fused (from crystal) reaches about $10^{24} \text{ ohm}\cdot\text{cm}$ for $T \approx 20^\circ\text{C}$ (see Ref.⁶ [pp. 231, 329] and Fig. 20.2 in publication).

Below are properties of some materials recalculated in the metric system (Table 15.1).

For small balls, the tensile stress is important for reducing the weight (because like charges tear the ball). The author believes that an artificial fiber having a maximum tensile stress at $500\text{--}620 \text{ kg/mm}^2$ (fiber) or whiskers up to 2000 kg/mm^2 is better. These fibers can also be used to strengthen balls insulated by a dielectric (for example, as an additional cover, Fig. 15.2(d)).

15.3.6 The half-life of the charge

15.3.6.1 Spherical ball

Let us take a very complex condition; where the unlike charges are separated *only* by an insulator (charged spherical condenser):

$$\begin{aligned} Ri - U = 0, \quad U = \delta E, \quad E = \frac{kq}{\delta^2}, \quad R = \rho \frac{\delta}{4\pi a^2}, \quad U = \frac{q}{C}, \quad R \frac{dq}{dt} + \frac{a}{C} = 0, \\ \frac{dq}{q} = \frac{dt}{RC}, \quad C = \frac{a\epsilon}{k}, \quad q = q_0 \exp\left(-\frac{4\pi\epsilon a k}{\rho\delta} t\right), \quad \frac{q}{q_0} = \frac{1}{2}, \\ -\frac{4\pi\epsilon a k}{\rho\delta} t_h = \ln \frac{1}{2} = -0.693 \approx -0.7, \quad t_h = 0.693 \frac{\rho\delta}{4\pi\epsilon a k}, \end{aligned} \quad (15.7)$$

where t_h is the half-life time [s]; R , the insulator resistance [ohm]; i , the current [A]; U , the voltage [V]; δ , the thickness of insulator [m]; E , the electrical intensity [V/m]; q , the charge [C]; t , the time [s]; ρ , the specific resistance of insulator [ohm-m, Ω m]; a , the internal radius of the ball [m]; and C , the capacity of the ball [C]; and $k = 9 \times 10^9$.

Example: Let us take typical data: $\rho = 10^{19} \Omega\text{m}$, $k = 9 \times 10^9$, $\delta/a = 0.2$, then $t_h = 1.24 \times 10^7 \text{ s} = 144 \text{ days}$.

15.3.6.2 Half-life of cylindrical tube

The computation is same as for tubes (1 m charged cylindrical condenser):

$$\begin{aligned} q = q_0 \exp\left(-\frac{1}{RC} t\right), \quad C = \frac{\epsilon}{k \ln(1 + \delta/a)}, \quad R = \frac{\rho\delta}{2\pi a}, \quad -0.693 = -\frac{1}{RC} t_h, \\ t_h = \frac{0.693\rho\delta\epsilon}{2\pi ka \ln(1 + \delta/a)}, \quad \text{for } \frac{\delta}{a} \rightarrow 0, \quad t_h \approx 0.7 \frac{\rho\epsilon}{2\pi k}. \end{aligned} \quad (15.8)$$

15.3.7 Rupture (breakthrough) of insulator

The breakthrough of a ball can only occur when the charge contacts an unlike charge or conducting material. The voltage between the charges must be less than $U = \delta E_i$, where E_i is the breakthrough intensity for a given insulator and δ , the thickness of the insulator. For a good insulator (very clean, without mixture) this is up to $E_i \approx 700 \text{ MV/m}$, (for example, quartz) for thin mica (muscovite) it as up to $E_i = 1000 \text{ MV/m}$.

15.3.8 Levitation between flat net and ground surface (Fig. 15.1(d))

This is the simplest for both utilization and computation. The top of the column contains the insulated metallic net with a high voltage (it may be a direct current electricity line). This induces the opposite charge in the Earth and powers the static electric field. The man (car) has charged balls or a balloon with like charges to the Earth's charge. These balls repel from the Earth's surface (charges) and support the man (car) in the air.

The lifting force, L , and radius, a , of a small lifting balloon with charge, q , can be computed by the equations:

$$L = qE_0, \quad E_a = k \frac{q}{a^2}, \quad a = \sqrt{k \frac{q}{E_a}} = \sqrt{\frac{kMg}{E_a E_0}}, \quad U = E_0 h, \quad (15.9)$$

where E_0 is the electrical intensity between the net and the Earth's surface [V/m]; E_a , the electrical intensity at the ball's (balloon) surface from the internal ball (balloon) charge [V/m]; a , the internal radius of ball (balloon) [m]; M , the mass of the flight vehicle (man, car); $g = 9.81 \text{ m/s}^2$, the Earth's gravity; U , the voltage between the net and Earth [V]; and h , the altitude of the net [m].

Examples: Assume $E_0 = E_a = 2.9 \times 10^6 \text{ V/m}$, the man's mass is $M = 100 \text{ kg}$, and the car's mass is 1000 kg . The radius of a single support balloon will be $a \approx 1.1 \text{ m}$ for the man and $a \approx 3.3 \text{ m}$ for the car, respectively. Note that this voltage is lower than the discharge voltage for a non-insulated conductor and the ionized zone is absent. We can change the single balloon to some small highly charged balls or a belt with an ionized zone.

The flying vehicles can be protected from contact with the top net by a dielectric (insulator) safety net located below the top net (7 in Fig. 15.1(d)).

15.3.9 Electrostatic levitation of a train (Fig. 15.3(a))

Two identically charged closed plates of area, S , have a repelling force, L :

$$L = 2\pi k\sigma_c^2 S, \quad (15.10)$$

where σ_c is surface charge density [C/m^2].

For example, two 1 m^2 plates with identical charge $\sigma_c = 2 \times 10^{-4} \text{ C/m}^2$ will have a specific lift force of $L = 2260 \text{ N/m}^2 = 226 \text{ kgf/m}^2$. Conventional electrets have $\sigma_c = 10^{-4}$ to $1.4 \times 10^{-3} \text{ C/m}^2$ charge and can be used for a non-contact train.

15.3.10 Top tube highway

The parameters of a tube highway can be calculated by the following equations:

$$\begin{aligned} \tau &= \frac{aE_a}{2k}, \quad E_0 = \frac{4k\tau}{h}, \quad \frac{E_0}{E_a} = \frac{a}{h}, \quad C_1 \approx \frac{1}{2k \ln(2h/a)}, \quad U = \frac{\tau}{C_1}, \quad W = \frac{\tau^2}{2C_1}, \\ \text{for } \tau &= \text{constant} \quad F_h = \frac{\partial W}{\partial h} = \frac{2k\tau^2}{h}, \quad F_a = \frac{\partial W}{\partial a} = -\frac{2k\tau^2}{a}, \end{aligned} \quad (15.11)$$

where τ is the linear charge of 1 m of tube [C/m]; a , the radius of tube cross-section [m]; E_a , the electric intensity at tube surface [V/m]; E_0 , the electrical intensity at the Earth's surface at a point under the tube [V/m], for other points $E = E_0 \cos^3 \alpha$ where α is the

angle between a vertical line from the tube center and a line to a given point (electric lines are perpendicular to the Earth's surface, there is no lateral acceleration); h , the altitude [m]; $k = 9 \times 10^9$, the coefficient [Nm^2/C^2]; C_1 , the capacity of 1 m of tube [C/m] (see Ref.⁸ [p. 64]); U , the voltage [V]; W , the electrical energy of 1 m of tube [J/m]; F_h , the electric force of 1 m of tube between the tube and the Earth's surface [N/m]; and F_a , the radial tensile force of 1 m of tube [N/m].

The thickness and mass of the top tube (with a thin cover) are given by:

$$F_a = -2\sigma\delta, \quad \delta = \frac{k\tau^2}{a\sigma}, \quad M_1 = 2\pi\gamma a\delta, \quad (15.12)$$

where σ is the safe tensile stress of tube cover [N/m²]; δ , the thickness of the tube cover [m]; M_1 , the mass of 1 m of tube cover [kg/m]; and γ , the density of tube cover [kg/m³].

The lift force of the tube as an air balloon filled by helium can be computed by the equation:

$$F_L = (\rho - \rho_g)\pi a^2 \bar{\rho}(h)g, \quad (15.13)$$

where $\rho = 1.225 \text{ kg/m}^3$ is the air density; ρ_g , the filling gas density (for helium $\rho_g = 0.1785 \text{ kg/m}^3$); a , the radius of tube [m]; $\bar{\rho}(h)$, the relative air density at altitude, for $h = 0 \text{ km}$ the $\bar{\rho}(h) = 1$, for 1 km $\bar{\rho}(h) = 0.908$. Note that E_c decreases in proportional to the atmospheric density. Unfortunately, the attractive electric force F_h in many cases is more than the air lift force F_L .

See the example computation in Section 15.4.2.

15.3.11 Spherical main ball on mast and air balloon

The parameters of charges of the main ball and spherical balloon can be calculated using the following equations:

$$\begin{aligned} E_a &= k \frac{q}{a^2}, & E_0 &= k \frac{2q}{h^2}, & \frac{E_0}{E_a} &= 2 \left(\frac{a}{h} \right)^2, & C &= \left[k \left(\frac{1}{a} - \frac{1}{2h-a} \right) \right]^{-1} \approx \frac{a}{2k}, \\ U &\approx \frac{kq}{a}, & W &= \frac{q^2}{2C}, & \text{for } q &= \text{constant}, & F_h &= \frac{\partial W}{\partial h} = -\frac{kq^2}{4h^2}, \end{aligned} \quad (15.14)$$

where q is the charge of air balloon (sphere) [C]; a , the radius of air balloon [m]; E_a , the electrical intensity at the balloon's surface [V/m]; E_0 , the electrical intensity at the Earth's surface at a point under the balloon [V/m], for other points $E = E_0 \cos^2 \alpha$ where α is the angle between a vertical line from the balloon center and a line to a given point (electric lines are perpendicular to the Earth's surface, there is no lateral acceleration); h , the altitude [m]; $k = 9 \times 10^9$, the coefficient [Nm^2/C^2]; C , the capacity of balloon [C]; U , the voltage [V]; W , the electrical energy of the balloon [J]; F_h , the electrical force between the balloon and the Earth's surface [N].

The thickness and mass of the top atmospheric air balloon as a spherical capacitor 1 m (with a thin cover) are:

$$\begin{aligned}
 F_a &= \frac{\partial W}{\partial a}, \quad W = \frac{q^2}{2C}, \quad c = \frac{a}{k}, \\
 \text{for } q &= \frac{a^2 E_a}{k} = \text{constant}, \quad F_a = -\frac{kq^2}{2a^2} = -\frac{(aE_a)^2}{2k}, \\
 p &= -\frac{F_a}{4\pi a^2} = \frac{E_a^2}{8\pi k}, \quad \pi a^2 p = 2\pi a \delta \sigma, \\
 \delta &= \frac{ap}{2\sigma} = \frac{aE_a^2}{8\pi k}, \quad M_b = 4\pi a^2 \gamma \delta = \frac{a^3 E_a^2 \delta}{4k\sigma}, \tag{15.15}
 \end{aligned}$$

where σ is the safe tensile stress of the balloon cover [N/m^2]; δ , the thickness of the balloon cover [m]; M_b , the mass of the balloon cover [kg]; γ , the density of the balloon cover [kg/m^3]; p , the internal pressure under like charges [N/m^2].

The lift force of the air balloon filled by helium can be computed using the equation:

$$F_L = \frac{4}{3}(\rho - \rho_g)\pi a^3 \bar{\rho}(h)g, \tag{15.16}$$

where $\rho = 1.225 \text{ kg/m}^3$ is the air density; ρ_g , the filling gas density (for helium $\rho_g = 0.1785 \text{ kg/m}^3$); a , the radius of balloon [m]; $\bar{\rho}(h)$, the relative air density at altitude, for $h = 0 \text{ km}$ $\bar{\rho}(h) = 1$, for 1 km $\bar{\rho}(h) = 0.908$. In many cases the attracted electric force F_h is more than the air lift force F_L .

See the computation in Section 15.4.3.

15.3.12 Small spherical lifting balls

Assume the electrical intensity of the main top charge is significantly more than the lifting charges. The parameters of large spherical balls with thin covers can be computed using the equations above. The parameters of small balls with thick covers can be computed using the following equations:

$$L = nqE_0, \quad q = CU, \quad C = \frac{r}{k}, \quad U = aE_a, \quad q = \frac{a^2 E_a}{k}, \quad L = n \frac{a^2 E_a E_0}{k}, \tag{15.17}$$

where L is the total lift force [N]; n , the number of balls; E_a , the electrical intensity at the ball surface from electrical charge of the ball q [C]; and a , the internal radius of the ball [m].

The thickness and mass of the ball (with a thick cover) are:

$$\begin{aligned}
 p_b &= \frac{E_a^2}{8\pi k}, \quad \sigma = \frac{p_b}{(R/a)^2 - 1} = \frac{E_a^2}{8\pi k [(R/a)^2 - 1]}, \quad (R/a)^2 - 1 = \frac{E_a^2}{8\pi k \sigma}, \\
 M_b &= \frac{4}{3}\pi \gamma a^3 \left(\frac{R^3}{a^3} - 1 \right), \tag{15.18}
 \end{aligned}$$

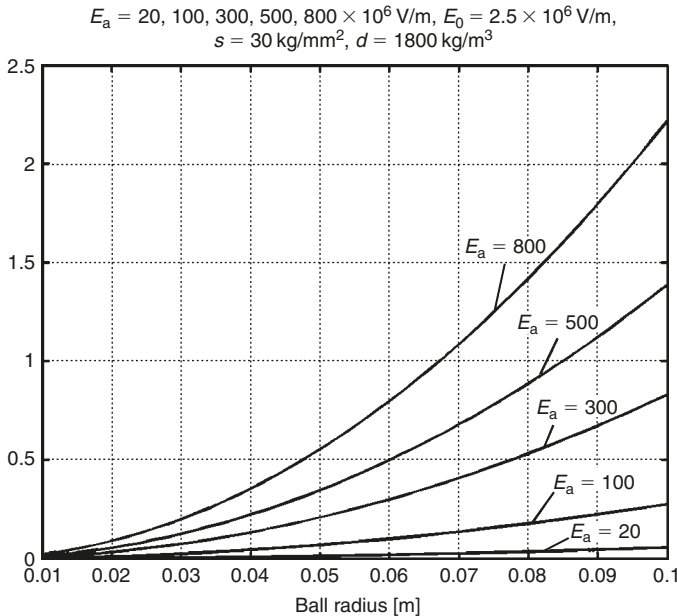


Fig. 15.6. Electrostatic lift force (kN) of small lifting ball versus radius of ball for the electrical intensity of the ball's surface $E_a = (20-800) \times 10^6 \text{ V/m}$, general electrical intensity $E_0 = 2.5 \times 10^6 \text{ V/m}$, safe tensile stress of the ball cover 30 kg/mm^2 , specific density of the ball cover 1800 kg/m^3 .

where $R = a + \delta$ is the external radius of ball [m]; σ , the safe tensile stress of the ball material [N/m^2]; δ , the thickness of the ball cover [m]; M_b , the mass of the ball cover [kg]; γ , the density of the ball cover [kg/m^3].

Results of this computation are in Figs. 15.6–15.9. Notice that the lifting balls have a large ratio of lift force/ball mass, about 10,000–20,000.

15.3.13 Long ($a \ll l$) cylindrical lifting belt

The maximum charge and mass of a 1-m-long cylindrical lifting belt may be computed using the following equations (from (15.11)):

$$\begin{aligned} L &= E_0 \tau l, \quad 2\sigma\delta = F_a, \quad F_a = \frac{2k\tau^2}{a}, \quad \tau = \sqrt{\frac{a\delta\sigma}{k}}, \\ q &= \tau l, \quad M_1 = 2\pi\gamma a\delta, \quad M = M_1 l, \quad E_a = k \frac{2\tau}{a}, \end{aligned} \quad (15.19)$$

where τ is the charge of 1 m [C/m]; a , the internal radius of the belt cross-section area [m]; δ , the thickness of the belt [m]; σ , the safe tensile stress of the belt cover [N/m^2]; q , the charge of the belt [C]; l , the length of the belt [m]; M , the mass of the belt [kg]; E_a ,

$$E_a = 20, 100, 300, 500, 800 \times 10^6 \text{ V/m}, E_0 = 2.5 \times 10^6 \text{ V/m}, \\ s = 30 \text{ kg/mm}^2, d = 1800 \text{ kg/m}^3$$

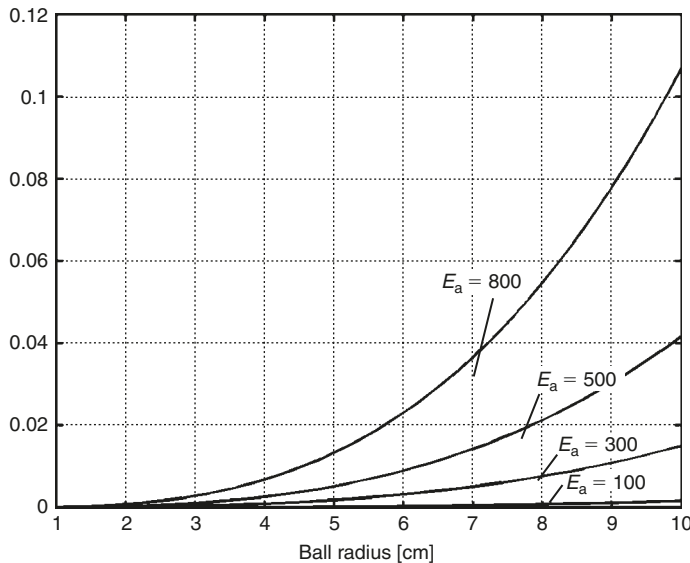


Fig. 15.7. Mass (kg) of small lifting ball versus radius of ball for the electrical intensity of the ball's surface $E_a = (100-800) \times 10^6 \text{ V/m}$, general electrical intensity $E_0 = 2.5 \times 10^6 \text{ V/m}$, safe tensile stress of the ball cover 30 kg/mm^2 , specific density of the ball cover 1800 kg/m^3 .

$$E_a = 3, 50, 100, 200, 300 \times 10^6 \text{ V/m}, E_0 = 2.5 \times 10^6 \text{ V/m}, \\ s = 100 \text{ kg/mm}^2, d = 1800 \text{ kg/m}^3$$

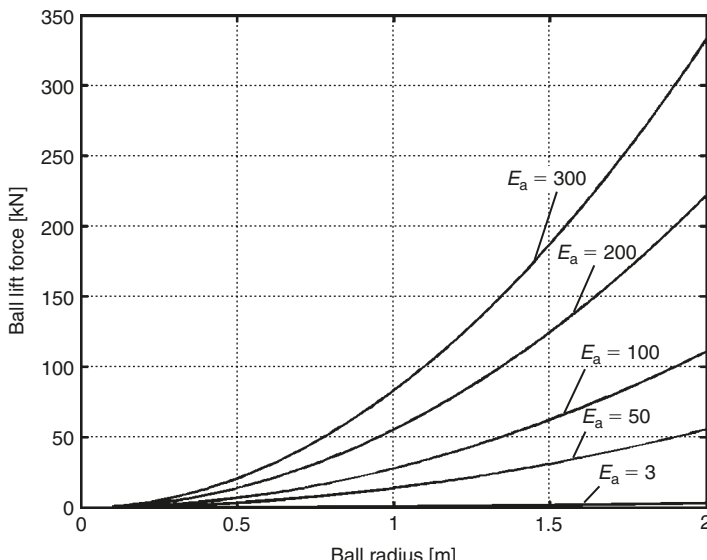


Fig. 15.8. Electrostatic lift force (kN) of the lifting ball versus radius of ball for the electrical intensity of the ball's surface $E_a = (3-300) \times 10^6 \text{ V/m}$, general electrical intensity $E_0 = 2.5 \times 10^6 \text{ V/m}$, safe tensile stress of the ball cover 100 kg/mm^2 , specific density of the ball cover 1800 kg/m^3 .

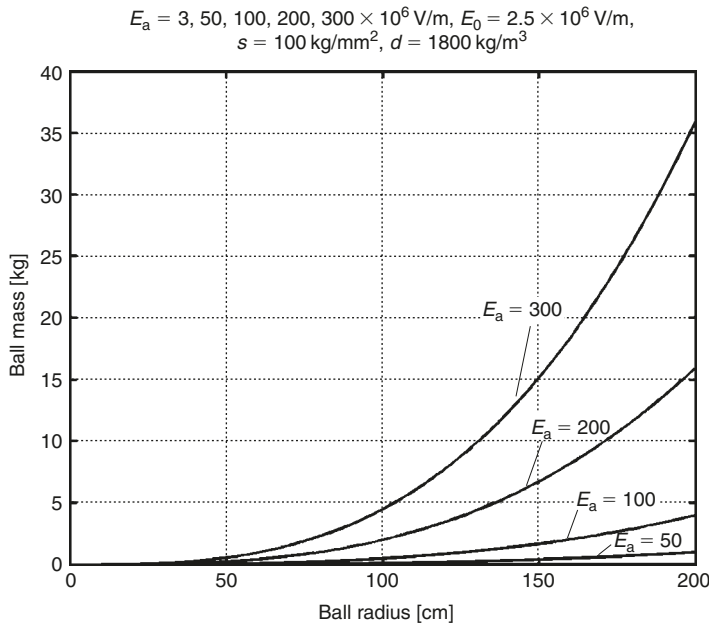


Fig. 15.9. Mass (kg) of the lifting ball versus radius of ball for the electrical intensity of the ball's surface $E_a = (3-300) \times 10^6 \text{ V/m}$, general electrical intensity $E_0 = 2.5 \times 10^6 \text{ V/m}$, safe tensile stress of the ball cover 100 kg/mm^2 , specific density of the ball cover 1800 kg/m^3 .

the electrical intensity of the belt surface [V/m]; F_a , the electrostatic force in the tube [N] [see equation (15.11)]; γ , the density of belt cover [kg/m^3]. Computations are presented in Figs. 15.10 and 15.11. See also example computation in Section 15.4.3.

15.3.14 Aerodynamics of the levitated vehicles

The drag [D] (required thrust, T) and required power of the levitated person, car, and vehicles can be computed by the following equations:

$$T = D = C_D \frac{\rho V^2}{2} S, \quad W = \frac{VD}{\eta}, \quad a = \frac{T}{M}, \quad (15.20)$$

where C_D is the aerodynamic drag coefficient, for a sitting person $C_D \approx 0.5$, for a lying man $C_D \approx 0.3$, for a car $C_D \approx 0.25$, for a sphere $C_D \approx 0.1-0.2$ (depending on the size and speed), and for a dirigible $C_D \approx 0.06-0.1$; $\rho = 1.225 \text{ kg/m}^3$, the standard air density; V , the speed [m/s]; S , the vehicle cross-section area [m^2]; W , the required power [W]; and η , the propeller coefficient of efficiency, $\eta = 0.7-0.8$.

For example, a flying person ($S = 0.3 \text{ m}^2$) has $D = 5.5 \text{ N}$ for speed $V = 10 \text{ m/s}$ (36 km/h). He only needs a small motor, $W = 0.073 \text{ kW}$.

$$s = 10, 20, 50, 100, 200 \text{ kg/mm}^2, E_0 = 2.5 \text{ MV/m}, \\ d = 1800 \text{ kg/m}^3, b = 0.01$$

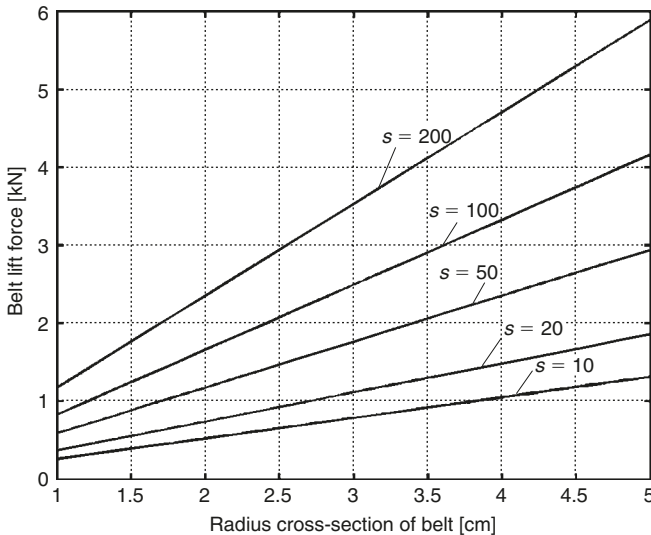


Fig. 15.10. Electrostatic lift force (kN) of a 1 m small lifting belt via radius of ball cross-section area for general electrical intensity $E_0 = 2.5 \times 10^6 \text{ V/m}$, safe tensile stress of the ball cover 10–200 kg/mm², $\sigma = (10\text{--}200) \times 10^7 \text{ N/m}^2$, density of ball cover $\gamma = 1800 \text{ kg/m}^3$.

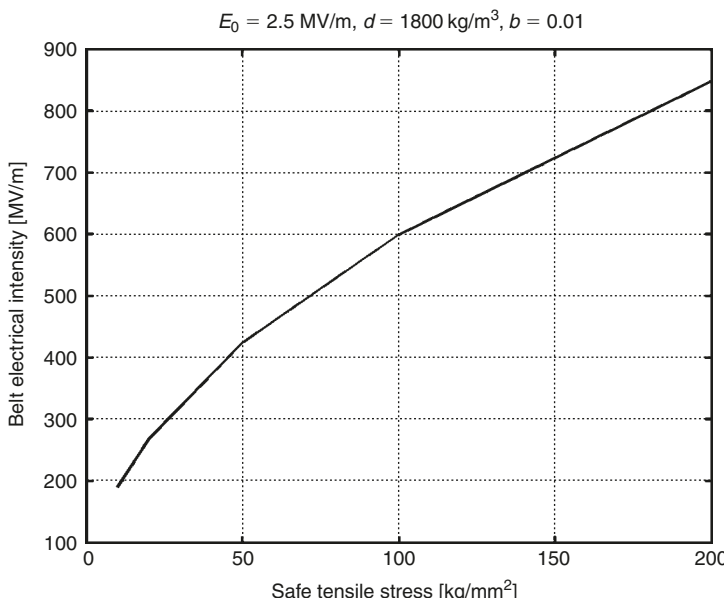


Fig. 15.11. Belt electrical intensity via safe tensile stress for general electrical intensity $E_0 = 2.5 \times 10^6 \text{ V/m}$, safe tensile stress of the ball cover 10–200 kg/mm², $\sigma = (10\text{--}200)(10^7 \text{ N/m}^2)$, γ – specific density of ball cover 1800 kg/m³, relative thickness of belt cover, $\delta = 0.01 \times a$.

15.3.15 Control and stability

Control is accomplished using the direction (and magnitude) of motor thrust (and variable torque), and the charging and discharging of lifting charges. The levitated vehicle will be stable in a vertical position if its center of gravity is lower than the center of levitation (lift) force. The dipole moment of the particular vehicle's design can give additional stability. Note that electric lines are vertical at the Earth's surface (Fig. 15.1(d–g)), which means that the lift force is vertical.

15.3.16 Flight in thunderstorms

Thunderstorms produce an electric field of about 300,000–1,000,000 V/m. This field can be used for levitation.

15.3.17 Charging

In the author's opinion, the easiest method of charging and maintaining the charge is by using a Van de Graaff electrostatic generator (Fig. 15.2(j)). Any other high voltage generation devices can also be used.

15.3.18 Safety

It is not known exactly how static fields of electrical intensity affect a human body. People in an electric field of about 300,000–1,000,000 V/m during a thunderstorm or under high voltage electrical lines feel normal. The inside space of a conventional car with a metal body (or conductive paint) does not have an electric field. The Museum of the Massachusetts Institute of Technology (MIT) shows people inside metal shells, under high voltage, and surrounded by lightning. People can wear clothes armored by conductive filaments as a defense against the electric field.

15.3.19 Charged ball as an accumulator of energy

The energy required to charge a ball (accumulate in the ball) can be calculated by the following equations:

$$W = \frac{1}{2} \frac{q^2}{C}, \quad C = \frac{a}{R}, \quad E_a = k \frac{q}{a^2}, \quad q = \frac{a^2 E_a}{k}, \quad W = \frac{1}{2} \frac{a^3 E_a^2}{k}, \quad (15.21)$$

where W is energy [J].

The ball mass at safe stress levels with repelling charges can be calculated using equation (15.17):

$$\left[\left(\frac{R}{a} \right)^2 - 1 \right] = \frac{E_a^2}{8\pi k \sigma}, \quad \left(\frac{R}{a} \right) = \sqrt{\frac{E_a^2}{8\pi k \sigma} + 1}, \quad M = \frac{4\pi \gamma a^3}{3} \left[\left(\frac{R}{a} \right)^3 - 1 \right],$$

$$\frac{W}{M} = \frac{3E_a^2}{8\pi \gamma k [(R/a)^3 - 1]}, \quad (15.22)$$

where M is the mass [kg]; σ , the safe tensile stress of the ball cover [N/m^2]; γ , the specific density of the ball cover [kg/m^3]; and $R = a + \delta$, the external radius of the ball [m].

The accumulated relative energy for $\sigma = 200 \text{ kg/mm}^2$ may be close to conventional powder and last a lot larger than electrical energy in a typical condenser. This electrical energy can be reclaimed (by using a sharp spike) or used for launching or accelerating space vehicles if we take two like charges (balls) and allow them to repel each other. This method of transforming electrical energy into thrust may be more useful than the thrust from a conventional electric space engine because one can create a big thrust by utilizing space masses (asteroids).

15.4 Projects

Let us estimate the main parameters for some offered applications. Most people understand the magnitudes and properties of applications better than theoretical reasoning and equations. The suggested application parameters are not optimal, but our purpose is to show the method can be utilized by current technology.

15.4.1 Levitation highway (Fig. 15.1(d))

The height of the top net is 20 m. The electrical intensity is $E_0 = 2.5 \times 10^6 \text{ V} < E_c = (3-4) \times 10^6 \text{ V}$. The voltage between the top net and the ground is $U = 50 \times 10^6 \text{ V}$. The width of each side of the road is 20 m. We first find the size of the lifting ball for the man (100 kg), car (1000 kg), or track (10,000 kg). Here R_c is the radius of the ionized zone [m]:

1. Flying man (mass $M = 100 \text{ kg}$, $\varepsilon = 3$, $E_i = 200 \times 10^6 \text{ V/m}$, and $g \approx 10 \text{ m/s}^2$):

$$E_a \leq \varepsilon E_i = 3 \times 200 \times 10^6, a = \sqrt{\frac{kMg}{E_0 E_a}} = \sqrt{\frac{9 \times 10^9 \times 100 \times 10}{2.5 \times 10^6 \times 6 \times 10^8}} \approx 0.08 \text{ m},$$

$$R_c = \sqrt{\frac{E_a}{E_c}} \approx 1 \text{ m}.$$

Notice that the radius of a single ball supporting the man is only 8 cm, or the man can use two balls $a = 5-6 \text{ cm}$, $R_c = 0.75 \text{ m}$ (or even more smaller balls). If the man uses a 1 m cylindrical belt, the radius of the belt cross-section area is 1.1 cm, $\sigma = 100 \text{ kg/mm}^2$, $E_a = 600 \times 10^6 \text{ V/m}$ (Figs. 15.10 and 15.11). The belt may be more comfortable for some people.

2. With the same calculation you can find that a car of mass $M = 1000 \text{ kg}$ will be levitated using a single charged ball $a = 23 \text{ cm}$, $R_c = 3.2 \text{ m}$ (or two balls with $a = 16 \text{ cm}$, $R_c = 2.3 \text{ m}$).
3. A truck of mass $M = 10,000 \text{ kg}$ will be levitated using a single charged ball $a = 70 \text{ cm}$, $R_c = 10 \text{ m}$ (or two balls with $a = 0.5 \text{ m}$, $R_c = 7 \text{ m}$).

15.4.2 Levitating tube highway

Assume the levitation highway has the design of Fig.15.1(f) and (g) where the top net is changed to a tube.

Take the data $E_0 = 2.5 \times 10^6 \text{ V} < E_c = (3-4) \times 10^6 \text{ V}$, $E_a = 2 \times 10^8 \text{ V/m}$, and $h = 20 \text{ m}$. This means the electrical intensity, E_0 , at ground level is the same as in the previous case. The required radius, a , of the top tube is:

$$\frac{a}{h} = \frac{E_0}{2E_a} = 0.00625, \quad a = 0.00624 h = 0.125 \text{ m}, \quad R_c = a \frac{E_a}{E_0} = 10 \text{ m}.$$

The diameter of the top tube is 0.25 m, the top ionized zone has a radius of 10 m.

15.4.3 Charged ball located on a high mast or tower

Assume there is a mast (tower) 500 m high with a ball of radius $a = 32 \text{ m}$ at its top charged up to $E_a = 3 \times 10^8 \text{ V/m}$. The charge is:

$$q = \frac{a^2 E_a}{k} = 34 \text{ C}, \quad E_0 = k \frac{2q}{h^2} = 2.45 \times 10^6 \text{ V/m}.$$

This electrical intensity at ground level means that within a radius of approximately 1 km, people, cars, and other loads can levitate.

15.4.4 Levitation in low cumulonimbus and thunderstorm clouds

In these clouds the electrical intensity at ground level is about $E_0 = 3 \times 10^5 - 10^6 \text{ V/m}$. A person can take more (or more highly charged) balls and levitate.

15.4.5 Artificial gravity on space ship's or asteroids

Assume the space ship is a sphere with an inner radius at $a = 10 \text{ m}$ and external radius of 13 m. We can create the electrical intensity $E_0 = 2.5 \times 10^6 \text{ V/m}$ without an ionized zone. The electrical charge is $q = a^2 E_0 / k = 2.8 \times 10^{-2} \text{ C}$. For a man weighing 100 kg ($g = 10 \text{ m/s}^2$, force $F = 1000 \text{ N}$), it is sufficient to have a charge of $q = F/E_0 = 4 \times 10^{-4} \text{ C}$ and small ball with $a = 0.1 \text{ m}$ and $E_a = qk/a^2 = 3.6 \times 10^8 \text{ V/m}$. In outer space at the ship's surface, the artificial gravity will be $(10/13)^2 = 0.6 = 60\%^{10}$ of g .

15.4.6 Charged ball as an accumulator of energy and rocket engine

The computations show the relative W/M energy calculated from safe tensile stress does not depend on E_a . A ball cover with a tensile stress of $\sigma = 200 \text{ kg/mm}^2$ reaches 2.2 MJ/kg. This is close to the energy of conventional powder (3 MJ/kg). If whiskers or nanotubes are used the relative electrical storage energy will be close to than of liquid rocket fuel.

Two like charged balls repel one another and can give significant acceleration for a space vehicle, VTOL aircraft, or weapon.

15.5 Discussion

Electrostatic levitation could create a revolution in transportation, building, entertainment, aviation, space flights, and the energy industry.

The offered method needs development and testing. The experimental procedure it is not expensive. We just need a ball with a thin internal conducting layer, a dielectric cover, and high voltage charging equipment. This experiment can be carried out in any high voltage electric laboratory. The proposed levitation theory is based on proven electrostatic theory. There may be problems may be with discharging, blockage of the charge by the ionized zone, breakdown, and half-life of the discharge, but careful choice of suitable electrical materials and electric intensity may be also to solve them. Most of these problems do not occur in a vacuum.

Another problem is the affects of the strong electrostatic field on a living organism. Only experiments using animals can solve this. In any case, there are protection methods – conducting clothes or vehicle is (from metal or conducting paint) which offer a defense against the electric field.

Other related ideas from the author are shown in Refs.¹⁰⁻¹³

References

1. A.A. Bolonkin, Installation for creating open electrostatic field, Patent Applications #3467270/21 116676, 9 July 1982, USSR Patent Office.
2. A.A. Bolonkin, Electrostatic method for tensing of films. Patent Application #3646689/10 138085, 28 September 1983, USSR Patent Office.
3. A.A. Bolonkin, “Aviation, Motor, and Space Design”, Collection *Emerging Technology in the Soviet Union*, Delphic Association, Falls Church, USA, 1990, pp. 32–80.
4. G. Shortley and D. Williams, *Elements of Physics*, 5th edition, Prentice-Hall Inc., NJ, USA, 1971.
5. V.N. Kestelman, L.S. Pinchuk and V.A. Goldale, *Electrets in Engineering, Fundamentals and Applications*. Kluwer Academic Publisher, New York, 2000.
6. I.K. Kikoin (ed.), *Tables of Physical Values, Directory*, Atomisdat, Moscow, 1976 (in Russian).
7. N.I. Koshkin and M.G. Shirkevich, *Directory of Elementary Physics*, Nauka, Moscow, 1982 (in Russian).
8. C.K. Kalashnikov, *Electricity*, Nauka, Moscow, 1985 (in Russian).
9. McGraw-Hill, *Encyclopedia of Science and Technology*.

10. A.A. Bolonkin, "Electrostatic Utilization of Asteroids for Space Flight", AIAA-2005-4032, *41st Joint Propulsion Conferences*, 10–13 July 2005, Tucson, AZ, USA.
11. A.A. Bolonkin, "Electrostatic Solar Wind Propulsion System", AIAA-2005-4225, *41st Joint Propulsion Conferences*, 10–13 July 2005, Tucson, AZ, USA.
12. A.A. Bolonkin, "Kinetic Anti-Gravitator", AIAA-2005-4505, *41st Joint Propulsion Conferences*, 10–13 July 2005, Tucson, AZ, USA.
13. A.A. Bolonkin, "Sling Rotary Space Launcher", AIAA-2005-4035, *41st Joint Propulsion Conferences*, 10–13 July 2005, Tucson, AZ, USA.

CHAPTER 16

Guided Solar Sail and Energy Generator*

Summary

A solar sail is a large thin film mirror that uses solar energy for propulsion. The author proposed innovations and a new design of solar sail in 1985.¹ This innovation allows (main advantages only): (1) an easily controlled amount and direction of thrust without turning a gigantic sail; (2) utilization of the solar sail as a power generator (for example, electricity generator); (3) use of the solar sail for long-distance communication systems.

16.1 Description of method and innovations

16.1.1 Introduction

Solar sails are composed of large flat smooth sheets of very thin film, supported by ultra-lightweight structures. The side of the film which faces the Sun is coated with a highly reflective material so that the resulting product is a huge mirror, typically about the size of a football field (see Fig. 16.1). The force generated by the Sun shining on this surface

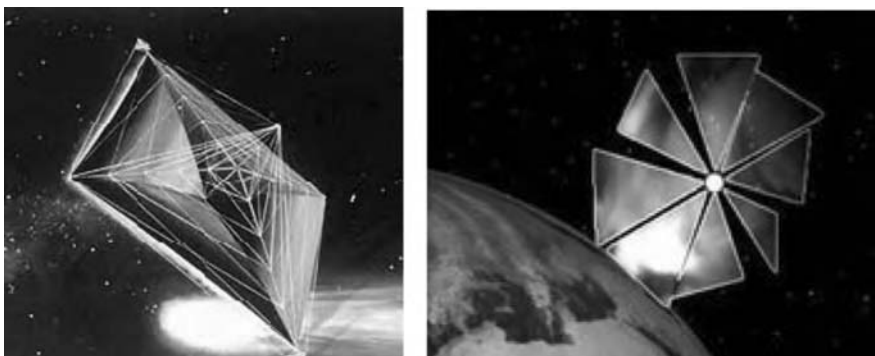


Fig. 16.1. Artist's conception of a solar sail.

* The detail manuscript was presented as AIAA-2005-3857 on the *41st Propulsion Conference*, 10–12 July 2005, Tucson, AZ, USA.

is about equal to the weight of a letter sent via first-class mail. Even though this is a very tiny force, it is perpetual, and over days, weeks, and months, this snail-paced acceleration results in the achievement of velocities large enough to overtake and pass the voyagers and pioneers that are now speeding away through the outer reaches of our solar system.

NASA has a program in place to develop solar sail technology to a point where it can be used to implement important space exploration missions. There are a number of missions on the NASA strategic roadmap that require this type of propellantless propulsion to achieve their objectives. There are other classes of missions that are greatly enhanced by solar sails because these vehicles are inexpensive to construct and can deliver such high-performance propulsion.

There are important applications for solar sails beyond the science missions that NASA has planned. The National Oceanic and Atmospheric Administration (NOAA) needs this technology to create a new class of space and Earth weather monitoring stations that can provide greater coverage of the Earth and provide better advance warning of the solar storms that sometimes plague communications and electrical power grids. There are also a number of military missions in Earth orbit that can be enabled by low-cost sailcraft.

Solar sailing is a method of converting light energy from the Sun into a source of propulsion for spacecraft. In essence, a solar sail is a giant mirror that reflects sunlight in order to transfer the momentum from light particles (photons) to the object one that is interested in propelling. Since the phrase “solar sails” is often confused with “solar cells”, which is a technology for converting solar light into electrical energy, we will use the term “light sail” for the purpose of this discussion:

$$\text{Solar radiation pressure} = 9.12 \mu\text{N/m}^2.$$

The light sail material must be as thin and lightweight as possible. Conventional light sail film has comprised 5- μm thick aluminized mylar or kapton with a thin film aluminum layer (approximately 100-nm thick) deposited on one side to form a mirror surface with 90% reflectivity.

For 5- μm thick mylar, which has an areal density of 7 g/ m^2 , the acceleration would be 1.2 mm/ s^2 . This acceleration results in a daily velocity increase of about 100 m/s, a velocity which is useful for maneuvering around the solar system. Although mylar is inexpensive and readily available in 0.5- μm thickness, it is not ideal sail film material because it is easily degraded by the Sun’s ultraviolet radiation. The other key contender, kapton, can withstand ultraviolet radiation but is not available in layers much thinner than 8 μm , with a resulting area density of 12 g/ m^2 .

A solar sail is a spacecraft with a large, lightweight mirror attached to it that moves by being pushed by light reflecting off the mirror instead of using rockets. The light to push a sail can come from the Sun or large lasers we could build. Satellites in orbit around the Earth can survive for many years without any maintenance while using only a small amount of rocket propellant to hold their positions. Solar sails can be made to survive in space for many years as well. But, because solar sails use sunlight that never runs out

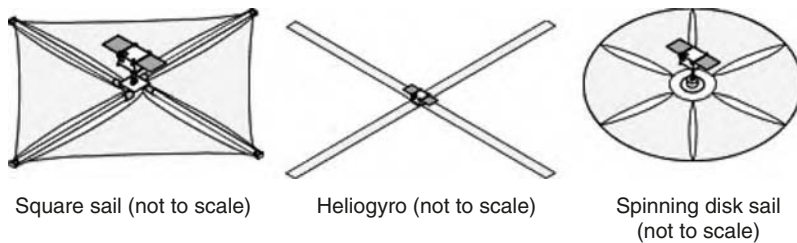


Fig. 16.2. Design of light sail.

like rocket propellant, during those years the sail can move around as much as you want it to, such as from the Earth to Mars and back, possibly several times if the sail remains in good condition. A similarly equipped rocket would either be ridiculously huge because it has to carry the fuel for each trip, or would need to be refueled regularly.

Sunlight exerts a very gentle force. The power of sunlight in space at the Earth's distance from the Sun is between 1.3 and 1.4 kW/m^2 . When you divide 1.4 kW by the speed of light, about 300 million meters per second, the result is very small. A square mirror of side 1 km would only receive about 9 N.

Light pressure is $P = E/c$ if the light is absorbed (black surface) and $P = 2E/c$ if the light is reflected (mirror). Here E is light energy, $c = 3 \times 10^8 \text{ m/s}$ is light speed.

There are three major designs used for light sail construction (Fig. 16.2):

1. Three axes stabilized sails which require booms to support the sail material.
2. Heliogyro sails, which are bladed like a helicopter and must be rotated for stability.
3. Disk sails which must be controlled by moving the center of mass relative to the center of pressure.

A practical sail places great demands on our physical construction capabilities. The sail must be as large as possible so that it can collect enough light to gain a useful thrust. At the same time it must be as lightweight as possible. This implies an extremely thin sail film with minimal mass. Finally, it must be durable enough to withstand a wide range of temperature changes, charged particles, and micrometeoroid hazards. A laser beam may be used for moving the solar sail.³⁻¹¹

16.2 Description of innovation and their advantages

The proposed innovation of a solar sail¹ is presented in Fig. 16.3. Theory developed in author publication² may be useful for flight analysis. The solar sail contains: (1) a space ship; (2) a spherical reflector; (5) a mirror; and additional devices to support spherical reflector, control the thrust direction, and convert the light energy into electricity and additional thrust.

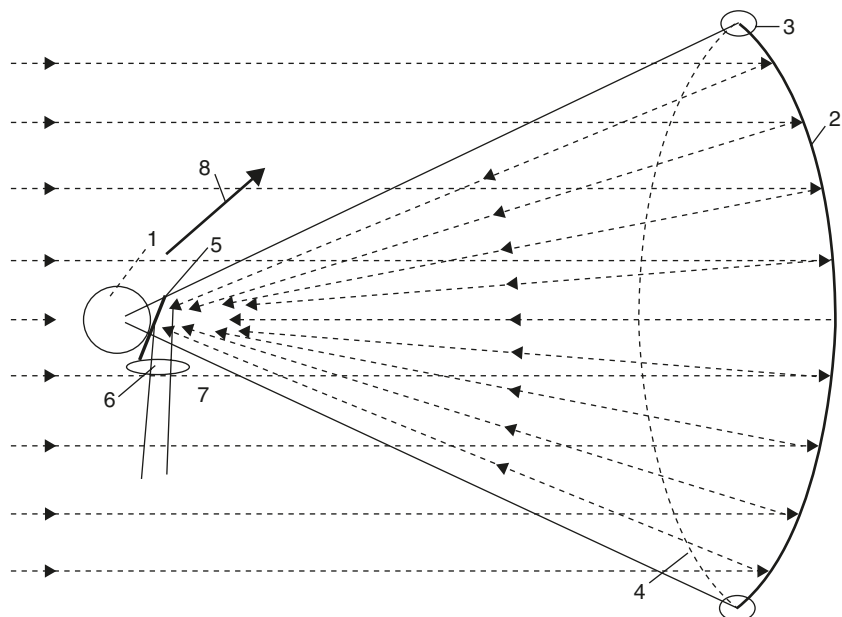


Fig. 16.3. Proposed guided solar sail and electricity generator. *Notations:* (1) Space ship; (2) thin film reflector; (3) inflatable (or electrically charged) toroid which support the reflector in an open (unfolded) position; (4) transparent thin film or light charged net which support the spherical form of the reflector; (5) control mirror, which guides thrust direction; (6) lens or trap for communication; (7) reflected beam (located at the center of the ship's mass); and (8) direction of thrust.

The suggested propulsion system works in the following way. The reflector (2) focuses the sunlight into the control ship mirror (5) located at the space ship's center of mass. We are able to change the position of this mirror, send the focused beam in the right direction and achieve the necessary thrust direction without turning the space sail because the space sail is large, turning it is very complex problem, but this problem is avoided in the suggested design.

If we direct the solar beam into the ship, we can convert the huge solar energy into any other sort of energy, for example, into electricity using a conventional method (solar cell or heat machine). A reflector of $100 \times 100 \text{ m}^2$ produces 14,000 kW energy at 1 AU. The developed ion thrusters are very efficient and have a high specific impulse, but they need a great amount of energy. We have this energy in the proposed sail and can increase the thrust over time.

The offered system can be also used for long-distance communication by sending a focused beam to the Earth and transmitting the necessary information.

The author has also proposed a method using surface tension of a solar sail and a solar mirror.¹⁰

The suggested revolutionary propulsion system uses current technology and may be produced in the near future but needs detailed research and computation.

16.3 Further development

Initial attempts to improve sail acceleration failed to take future development into account because they focused only on developing the lowest-density film material possible. For example, researchers anticipate a 25 times improvement over the baseline mylar design described above by removing the plastic substrate and leaving the 100-nm aluminum layer. Reducing the aluminum thickness from 100 to 4 or 5 nm would yield another factor of 12, resulting in a net 300 times increase in sail acceleration. The trade off, of course, is that the reflectivity goes down for such a thin metal film thereby driving one to use longer wavelengths such as microwaves. Perforating the aluminum metal sail pushes this number somewhere between 500 and 5000 times. More recently, nanotubes, a meshwork of interlocking carbon fibers which can provide stiff, but extremely lightweight support for the sail coating, are being explored. Since carbon is relatively impervious to solar radiation damage and has a higher melting point than aluminum, nanotubes are thought to have high potential for providing a significant breakthrough for light sail development, potentially yielding factors of 10,000 to 100,000 in Earth orbit acceleration. One concept, gray sails, tries to turn the tables on the heating problem by moving to within 3 solar radii to heat the sail up to 2000°C. The radiating heat would then act as a propellant as the space-craft passes through the perihelion and arcs away from the Sun.

References

1. A.A. Bolonkin, "Solar Sail Engine for Spaceships", Patent (Author certificate #1262870), priority since 10 January 1985, USSR Patent Office.
2. A.A. Bolonkin, "Theory of Flight Vehicles with Control Radial Force", *Collection Researches of Flight Dynamics*, Mashinostroenie, Moscow, 1965, pp. 79–118 (in Russian).
3. K.E. Tsiolkovskiy, *Extensions of Man into Outer Space*, 1921, See also K.E. Tsiolkovskiy, *Symposium on Jet Propulsion*, No. 2, United Scientific and Technical Presses (NIT), 1936 (in Russian).
4. R.L. Forward, "Roundtrip Interstellar Travel Using Laser-Pushed Lightsails", *Journal of Spacecraft*, Vol. 21, 1984, pp. 187–195.
5. A. Marx, "Interstellar Vehicle Propelled by Terrestrial Laser Beam", *Nature*, July 1966, pp. 22–23.
6. D. Spieth and R. Zubrin, *Ultra-Thin Solar Sails for Interstellar Travel: Phase I Final Report*, Pioneer Astronautics, Inc., Lakewood, CA., published December 1999.
7. K. Tsander, "From a Scientific Heritage", NASA TTF-541, 1967 (quoting a 1924 report by the author).
8. B. Mallove and G. Matloff, *The Starflight Handbook: A Pioneer's Guide to Interstellar Travel*, John Wiley & Sons, Inc, New York, 1989.
9. L. Funaki, *et al.*, "Thrust Production Mechanism of Magnetoplasma Sail", AIAA 2003-4292.
10. A.A. Bolonkin, "Method of Stretching of Thin Film", Russian Patent Application #3646689/10 138085, 28 September 1983 (in Russian), Russian PTO.
11. A.A. Bolonkin, "Guided Solar Sail and Electric Generator", AIAA-2005-3857, *41st Propulsion Conference*, 10–12 July 2005, Tucson, AZ, USA.

This page intentionally left blank

CHAPTER 17

Radioisotope Space Sail and Electro-Generator*

Summary

Radioisotope sail is a thin film of an alpha-particle-emitting radioisotope deposited on the back of a plastic sail that can provide useful quantities of both propulsion and electrical power to a deep space vehicle. The momentum kick of the emitted alpha particles provides radioisotope sail thrust levels per square meter comparable to that of a solar sail at 1 astronauitic unit (AU). The electrical power generated per 1 m² is comparable to that obtained from solar cells at 1 AU. Radioisotope sail systems will maintain these propulsion and power levels at distances from the Sun where solar powered systems are ineffective.

The propulsion and power levels available from this simple and reliable high-energy-density system would be useful for supplying propulsion and electrical power to a robotic deep space mission to the Oort Cloud or beyond, or to a robotic interstellar flyby or rendezvous probe after its arrival at the target star.

17.1 Description of method and innovations

17.1.1 Brief history of innovation

The idea of using a radioisotope recoil propulsion as it is shown in Fig.17.1(a) is very old.¹⁵

The author has proposed many innovations in method is using radioisotope space sail and electric generators in patent applications^{1–13} in 1983 and in paper IAF 92-0573 presented to the *World Space Congress* in 1992.¹⁴ The work¹⁶ written in 1995 summarized the knowledge for the conventional case in Fig. 17.1(a). Bolonkin innovations decrease the weight of traditional radioisotope sail (RadSail, RS, IsoSail) by 2–4 times; increase the thrust by 2–3 times, and the electric power by 2 times and allows control of thrust and thrust direction without needing to turn the large RadSail.¹⁸

* Detailed work was presented by the author as AIAA-2005-4225 at the *41st Propulsion Conference*, 10–12 July 2005, Tucson, AZ, USA.

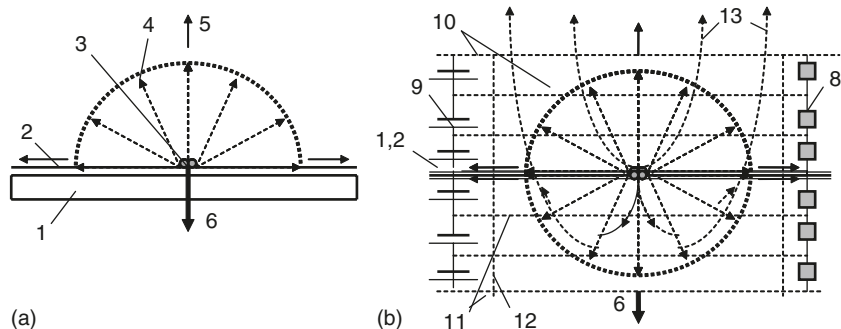


Fig. 17.1. (a) Conventional radioisotope sail and (b) suggested (innovated) radioisotope sail. *Notations:* (1) Substrate (base of sail); (2) isotope layer; (3) isotope atom; (4) alpha particles; (5) direction of 1/6 particle flow; (6) thrust; (8) electric loading; (9) initial charging; (10–12) condenser nets; and (13) particle trajectory.

Our innovation allows us to reach a probe speed of more than 2000 km/s, so the design may be used for interstellar probes.

This method allows nuclear waste and unnecessary nuclear bombs to be used for producing the radioisotope material.

The offered method is realistic at the present time, has a high possibility of being successful, and is much cheaper for deep missions than other currently proposed methods.

17.2 General information about the isotope sail

There are a number of radioactive elements that emit particles at a high velocity. It is conceptually possible to utilize these high-velocity particles to provide rocket thrust for a space vehicle. Usually, the concepts involve placing a thin layer of the radioactive material on the back of a metal or plastic film substrate, producing a radioisotope sail. The particles emitted in the forward direction would be absorbed by the substrate, while the particles emitted in the backward direction would produce thrust on the vehicle.

Since the emitted particles also carry electric charge, they generate a current flow as they leave, which can be harnessed to provide electric power to the vehicle.

A short list of isotopes with a decay lifetime and alpha-particle energy of interest for deep space propulsion and power is given in Table 17.1.

Charged particles such as alpha particles have a finite stopping range in materials, which depend upon the charge, mass, and energy of the alpha particle, the density of the stopping material, and, to a slight degree, on the mass number A of the stopping material. The range of all the alpha particles is within a few percent of the average. As a result, for a conventional radioisotope sail (see Fig. 17.1(a)), a substrate of stopping material with thickness, a little greater than the average alpha-particle range will stop

Table 17.1.¹⁷ Some alpha particle radioisotopes.

Element	Mass number <i>A</i>	Atomic number <i>Z</i>	Lifetime half-life	(year) <i>1/e</i>	α energy (MeV)	Specific density
Polonium	208	84	2.9	4.2	5.12	9.4
Polonium	209	84	103	149	4.88	9.4
Thorium	228	90	1.9	2.8	5.42	11.7
Uranium	232	92	72	104	5.32	19.1
Plutonium	236	94	2.8	4.1	5.77	19.1
Plutonium	238	94	86	124	5.50	19.8

all alpha particles. The range for 5-MeV alpha particles in hydrogen-containing materials like water and plastic is $50 \mu\text{m}$. In heavy metals, the range is $200 \mu\text{m}/\rho$, where ρ is the specific density. For polonium, with $\rho = 9.4$, the range is $20 \mu\text{m}$. For plutonium, with $\rho = 19.8$, the range is $10 \mu\text{m}$.

For propulsion, the radioisotope should be deposited as a thin metal film on the back of a space sail substrate made of plastic. If made $50\text{-}\mu\text{m}$ thick, the plastic substrate will stop all the alpha particles going in the forward direction. Then, if the radioisotope film is made thin, most of the alpha particles emitted in the backward direction will exit the thin metal film and produce a reaction thrust on the sail. For example, if the film of polonium is made $10\text{-}\mu\text{m}$ thick, then a large percentage of the rearward-emitted alpha particles will emerge from the surface of the film with most of their energy. A square meter of such a sail would consist of 50 gm/m^2 of plastic substrate with 94 gm/m^2 of polonium deposited on it.

The conventional IsoSail allows (theoretically) reaching a velocity of 200 km/s . Our innovation allows us to reach more than 1000 km/s . This design may be used for interstellar probes.

17.3 Description of new method, installation, and innovation

The old RadSail has a substrate layer (base about $50\text{-}\mu\text{m}$ thick) and a thin $10\text{-}\mu\text{m}$ film of a 5-MeV alpha-particle-emitting radioisotope (Fig. 17.1(a)). The substrate layer (sail base) absorbs the high-energy particles.

The innovations and their advantages are follows (Fig. 17.1(b)):

1. The sail base, 1, is thin, and particles pass across it. Both sides of the base contain horizontal condenser nets, 10 and 11, and vertical nets, 12. These nets create the electric fields. The lower electric field turns the lower particles back (to an upward), and this doubles (at least) the sail thrust. The top electric field also turns the side particles to an upward direction and accelerates them. As a result, the efficiency coefficient increases from the theoretical level (up to 25%) for conventional isotope sails by a minimum of 2–3 times and can potentially reach 90%.
2. We can control the amount of thrust and the thrust direction. By changing the electric tension (voltage) of our fields (horizontal nets), we can change the thrust

up to zero. By changing the electric tension of the vertical nets, we can change the thrust direction without turning the sail. This is the important innovation because the large size of the isotope sail makes turning it a very complex problem.

3. The suggested isotope sail may work as an electricity generator (as well as a propulsion system). By decreasing the electrical tension of the electric field, a proportion of the charged particles will be adsorbed by the net and produce electricity.
4. The sail base (base film) has a thickness of 2–10 μm (not 50–100 μm as conventional isotope sail). The net is made of wire of 2–10 μm and has cells 5–10 cm or a film thickness of 1–2 μm (for an electricity generator). That means the weight of the proposed sail will be 2–5 times less than the conventional isotope sail.

17.4 Improvements to the radioisotope sail

The way to improve the performance of the IsoSail is to choose an initial radioisotope, that has a decay chain with a large number of alpha particles 1–14. For example, $^{232}\text{U}^{92}$ emits in turn a 5.32 MeV ${}^4\alpha^2$ with a $1/e$ lifetime of 104 years to become $^{228}\text{Th}^{90}$, and that emits a 5.42 MeV ${}^4\alpha^2$ after a $1/e$ lifetime of 2.8 years to become $^{224}\text{Ra}^{66}$, which emits a 5.68 MeV ${}^4\alpha^2$ after 5 days to become $^{220}\text{Rn}^{86}$. This radon emits a 6.78 MeV ${}^4\alpha^2$ after 80 s and becomes $^{212}\text{Pb}^{82}$. The $^{212}\text{Pb}^{82}$ then emits a 0.34-MeV electron after 15 h and changes to $^{212}\text{Pb}^{83}$, which emits a 2.25-MeV electron after 85 min to become $^{212}\text{Pb}^{84}$, then this emits a 8.78 MeV ${}^4\alpha^2$ after 0.4 μs to become $^{212}\text{Pb}^{82}$, which is finally stable. Thus $^{232}\text{U}^{92}$ would be a good choice for a mission with a lifetime much longer than 2.8 years but less than 104 years. This cascade is shown below:



The total increment in velocity in the old design after six cascades reaches 210 km/s. In my new design, the final speed is 10 times more. This is large enough to be useful for exploration of comet bodies and brown dwarfs outside the solar system, to divert the propulsion of an interstellar flyby probe to allow it to maneuver close to a planet observed on the way into the target system, and for propulsion within an extra-solar planetary system after completing a rendezvous mission at the target star using some other method to stop, such as a magnetic sail drag brake.

17.5 Possibility of electric power

The emission of charged particles from a radioisotope sail produces a current flow outward from the vehicle. In conventional designs, the current per unit area is carried by the escaping half of the alpha particles (each with charge $2e = 3.2 \times 10^{-19} \text{ C}$) emitted by a sail. The maximum power of $^{208}\text{Po}^{84}$ per unit area available from a power source sail, given the full potential of 5 MV, is 1600 W/m^2 . For comparison, a solar cell array with an efficiency of 14% would provide 200 W/m^2 of electric power at 1 AU. If no propulsion, only electric power, is desired from the radioisotope sail, the electric power generated can be increased by a factor of two by decreasing the thickness of the plastic substrate and radioisotope film so that nearly all the alpha particles can escape from both sides of the sail. That case is our design.

17.5.1 Heating

An area of concern is the waste heat generated by the radioisotope material. If we assume that half of the alpha particles deposit their energy in the sail (conventional design), the thermal power deposited per unit area by a 10- μm layer of polonium is 850 W/m². This is less than from the Sun (1400 W/m²), so heating should not be a significant problem once the sail is unfurled.

Our design of IsoSail has twice as much efficiency and does not have this problem.

17.6 Equation for computation of conventional IsoSail

The mass M of a given amount of radioactive isotope decays exponentially with time according to the well-known relation from the physics of isotopes:

$$M(t) = M_0 e^{-t/\tau}, \quad (17.1)$$

where M_0 is the mass of the initial quantity of radioisotope and τ is the 1/e lifetime, t is time. The “half-life” is the time t_h when $\exp(-t_h/\tau) = 1/2$. The half-life t_h is $\ln(2) = 0.693$ of the 1/e lifetime τ .

$$t_h = 0.693\tau.$$

Conventionally scientists chose as a typical example the radioisotope $^{208}\text{Po}^{84}$ with a 1/e lifetime of 4.2 years and specific density of 9.4. The number per second dn/dt of alpha particles emitted from a given mass M is given by the equation:

$$\frac{dn}{dt} = \frac{N_A M}{A\tau}, \quad [\text{alphas/kg s}] \quad (17.2)$$

where n is the number of alpha particles, $N_A = 6.02 \times 10^{26}$ [atoms/kg-mol] is Avogadro’s number. For the radioisotope matter with a mass number of $A = 208$ kg/kg-mol and an 1/e lifetime of $\tau = 4.2$ this magnitude is $dn/dt = 2.2 \times 10^{16} M$ [alphas/kg s].

The velocity V of an alpha particle is:

$$v = \left(\frac{2E}{m} \right)^{1/2}. \quad (17.3)$$

For a mass of $m = 4$, a unit of atom mass (amu) = 6.64×10^{-27} kg emitted at an energy of $E = 5.12$ MeV = 8.2×10^{-13} J, this value is: $v = 16,000$ km/s = 16 Mm/s = $0.05c$, where $c = 300$ Mm/s is the speed of light. The speed of particles is equivalent specific impulse of $I_{sp} = 1,600,000$ s.

The thrust T per unit area B of a conventional IsoSail is estimated by the equation:

$$\frac{T}{B} = \frac{1}{4B} \frac{dn}{dt} mV, \text{ for polonium } \frac{T}{B} = 5.7 \times 10^{-4} \frac{M}{B} [\text{N/kg}] \text{ or}$$

$$T/B = 5.3 \times 10^{-5} [\text{N/m}^2], \quad (17.4)$$

where the coefficient 1/4 shows that only one-fourth of full thrust used in conventional IsoSail.

For the proposed IsoSail this coefficient is about 1/2 or more.

For comparison the solar light pressure thrust at 1 AU for full reflection is:

$$\frac{T}{B} = 2 \frac{S}{c} \approx 9.3 \times 10^{-6} [\text{N/m}^2], \quad (17.5)$$

where $S = 1400 \text{ W/m}^2$ is the solar light flux at 1 AU. This shows that the IsoSail has thrust in 5.7 times greater than the solar sail. Unfortunately, the mass of the conventional IsoSail is also much greater than the solar sail at distance from the Sun equals 1 AU. However, the IsoSail produces useful thrust at great distances from the Sun.

The maximum sail velocity of a conventional IsoSail is estimated using the momentum equation:

$$V = \frac{vm}{M - m}. \quad (17.6)$$

For example, if $M = 208 \text{ amu}$, $m = 4 \text{ amu}$, $v = 16,000 \text{ km/s}$, this velocity is about 300 km/s. In reality the conventional IsoSail can reach only one-fourth of this velocity or less. The maximum is up 30 km/s.

The net impulse given by the cascade is approximately estimated by equation (from (17.1), (17.2), and (17.4)):

$$I_t = \int_0^t T dt = \frac{m V_t N_A M_0}{4A} (1 - e^{-t/\tau}), \quad (17.7)$$

where V_t is the average particle velocity. If the sail mass makes up most of the space vehicle, the conventional sail consists of a 50-μm thick layer of plastic sail with a mass of 50 g/m², and a 5-μm thick layer of ²³²U⁹² with a density of 19.8 g/cm³ and a mass of 100 g/m², then the velocity increment after a 1/e lifetime of $\tau = 104$ years is $\Delta V = 210 \text{ km/s}$.

For proposed IsoSail ΔV is about 3–5 times more (thrust is double, weight is less).

17.6.1 Electric power of conventional IsoSail

The current I per unit area carried by particles (each with a charge of $2e = 3.2 \times 10^{-19} \text{ C}$) emitted by a conventional IsoSail with area B and mass M is:

$$\frac{I}{B} = \frac{1}{2B} (2e) \frac{dn}{dt}. \quad (17.8)$$

For isotope $^{208}\text{Po}^{84}$ this magnitude is $3.5 M/B \text{ mA/kg} = 0.33 \text{ mA/m}^2$.

The maximum power, P , per unit area available from a power source conventional sail power source with area B and radioisotope mass M is:

$$\frac{P}{B} = \frac{IE}{B}. \quad (17.9)$$

For $E = 5 \text{ MV}$, this value is $P/B = 17,500 M/B \text{ W/m}^2 = 1600 \text{ W/m}^2$. For comparison, a solar cell array with an efficiency of 14% would provide 200 W/m^2 of electrical power at 1 AU.

In reality that value is arrived at because the conventional IsoSail has very low coefficient of efficiency (10–15%). For the proposed IsoSail this power is increased by a factor of two. The efficiency of the offered device can reach 70–85% for a multilayer IsoSail, which has some condenser nets.

17.6.2 Heating a conventional Isosail

In a conventional IsoSail half of the alpha particles deposit their energy in the sail and the thermal power P_t deposited per unit area B is:

$$\frac{P_t}{B} = \frac{1}{2} \frac{dn}{dt} \frac{E}{B}. \quad (17.10)$$

For a 10- μm layer of polonium $P_t/B = 9M/B \text{ kW/kg} = 850 \text{ W/m}^2$. That is less than from the Sun (1400 W/m^2), so heating should not be a significant problem. This problem does not apply to the proposed IsoSail because its efficiency is high and the amount of heating is small.

17.7 Conclusion

The IsoSail concept can potentially provide useful amounts of propulsion and electrical power in robotic deep space and interstellar missions. Whether the actual performance ultimately achievable would justify the immense problems of coping with the technical difficulties of fabricating, deploying, and using this new technology with its extremely hazardous material that is “hot” in both the thermal and nuclear sense, is a question to be answered by further studies. The IsoSail (especially the offered IsoSail) needs in more detailed research and development.

This method allows nuclear waste and unnecessary nuclear bombs to be used to produce the radioisotope material.

References

1. A.A. Bolonkin, “Radioisotope Propulsion”, Russian Patent Application #3467762/25 116952, 9 July 1982 (in Russian), Russian PTO.

2. A.A. Bolonkin, “Radioisotope Electric Generator”, Russian Patent Application #3469511/25 116927, 9 July 1982 (in Russian). Russian PTO.
3. A.A. Bolonkin, “Radioisotope Electric Generator”, Russian Patent Application #3620051/25 108943, 13 July 1983 (in Russian), Russian PTO.
4. A.A. Bolonkin, “Method of Propulsion using Radioisotope Energy and Installation for It”, Russian Patent Application #3601164/25 086973, 6 June 1983 (in Russian), Russian PTO.
5. A.A. Bolonkin, “Method of Energy Transformation of Radioisotope Matter in Electricity and Installation for It”, Russian Patent Application #3647343/25 136692, 27 July 1983 (in Russian), Russian PTO.
6. A.A. Bolonkin, “Space Propulsion Using Solar Wind and Installation for It”, Russian Patent Application #3635955/23 126453, 19 August 1983 (in Russian), Russian PTO.
7. A.A. Bolonkin, “Installation for Open Electrostatic Field”. Russian Patent Application #3467270/21 116676, 9 July 1982 (in Russian), Russian PTO.
8. A.A. Bolonkin, “Getting of Electric Energy from Space and Installation for It”, Russian Patent Application #3638699/25 126303, 19 August 1983 (in Russian), Russian PTO.
9. A.A. Bolonkin, “Protection from Charged Particles in Space and Installation for It”, Russian Patent Application #3644168 136270, 23 September 1983, (in Russian), Russian PTO.
10. A.A. Bolonkin, “Method of Transformation of Plasma Energy in Electric Current and Installation for It”, Russian Patent Application #3647344 136681, 27 July 1983 (in Russian), Russian PTO.
11. A.A. Bolonkin, “Transformation of Energy of Rarefaction Plasma in Electric Current and Installation for it”, Russian Patent Application #3663911/25 159775, 23 November 1983 (in Russian), Russian PTO.
12. A.A. Bolonkin, “Method of a Keeping of a Neutral Plasma and Installation for It”, Russian Patent Application #3600272/25 086993, 6 June 1983 (in Russian), Russian PTO.
13. A.A. Bolonkin, “Method of Stretching of Thin Film”, Russian Patent Application #3646689/10 138085, 28 September 1983 (in Russian), Russian PTO.
14. A.A. Bolonkin, “Simple Space Nuclear Reactive Motors and Electric Generators Running on Radioactive Substances”, *The World Space Congress – Jerusalem, 1992*, IAF Preprint 92-0573.
15. A. Berman, *Physical Principles of Aeronautics*, New York, 1961, pp. 252–254.
16. R.L. Forward, “Radioisotope Sails for Deep Space Propulsion and Electric Power”, AIAA 95-2596.
17. D.E. Gray, *American Institute of Physics Handbook*, McGraw-Hill, New York, 1972.
18. A.A. Bolonkin, “Radioisotope Space Sail and Electric Generator”, AIAA-2005-4225, *41st Propulsion Conference*, 10–12 July 2005, Tucson, AZ, USA.

CHAPTER 18

Electrostatic Solar Sail

Summary

The solar sail has become well known after much discussion in the scientific literature as a thin continuous plastic film, covered by sunlight-reflecting appliquéd aluminum. Earlier, there were attempts to launch and operate solar sails in near-Earth space and there are experimental projects planned for long powered space voyages. However, as currently envisioned, the solar sail has essential disadvantages. Solar light pressure in space is very low and consequently the solar sail has to be very large in area. Also it is difficult to unfold and unfurl the solar sail in space. In addition it is necessary to have a rigid framework to support the thin material. Such frameworks usually have great mass and, therefore, the spacecraft's acceleration is small.

Here, the author proposes to discard standard solar sail technology (continuous plastic aluminum-coated film) with the intention instead of using millions of small, very thin aluminum-charged plates and to release these plates from a spacecraft, instigated by an electrostatic field. Using this new technology, the solar sail composed of millions of plates can be made to gigantic area but have very low mass. The acceleration of this new kind of solar sail may be as much as 300 times that achieves by an ordinary solar sail. The electrostatic solar sail can even reach a speed of about 300 km/s (in a special maneuver up to 600–800 km/s). The electrostatic solar sail may be used to move a large space ship or to act as an artificial Moon illuminating a huge region of the Earth's surface.

18.1 Introduction

The description of solar sail is described in Chapter 16. Solar radiation pressure equals $9.12 \mu\text{N/m}^2$ at distance 1 astronautic unit (AU) from the Sun.

No solar sails have been successfully deployed as primary propulsion systems, but research into this technology is continuing. On 9 August 2004, the Japanese ISAS successfully deployed two prototype solar sails in low Earth orbit. A clover-shaped sail was deployed at 122 km altitude and a fan-shaped-type sail at 169 km. Both sails used 7.5- μm -thick film.

A joint private project between the Planetary Society, Cosmos Studios, and the Russian Academy of Science launched *Cosmos 1*, the first solar sail space ship, on 21 June 2005. The rocket was supposed to push the 124-kg spacecraft into 800-km orbit where it was intended to unfurl the 15-m sails (with a total area of 600 m^2). Unfortunately, the launch was unsuccessful. A suborbital prototype test by the group also did not succeed in 2001 because of rocket failure.

18.2 Brief description of the innovations

A conventional solar sail is a dielectric thin film (thickness $5 \mu\text{m} = 5000 \text{ nm}$) with an aluminum layer of 100 nm thickness, and it has 90% reflectivity. The weight of 1 m^2 is $5-7 \text{ g/m}^2$. If it accelerates by itself the maximum acceleration is about 1 mm/s^2 . However, the gigantic thin film needs a rigid structure to support the very thin film in an unfolded position and to enable it to be controlled. This rigid structure has a large weight, so it is very difficult to launch and to unfurl the structure in space. All attempts to do this (for example, to unfurl the inflatable radio-antennas in space) have failed.

The author proposes to use small thin charged aluminum plates (petals) supported by a central electrostatic ball and rotated around the ball (Fig. 18.1). They rotate also around their own axis and maintain a direction perpendicular to the solar rays. The diameter of the plate-petals is small, about 1 mm or less, and it is not a necessity to use the dielectric film. The aluminum film may be very thin because the individual petal size is small.

The electrostatic sail can be controlled by changing charge on the ball (diameter of the mirror) and by the positioning of an additional charged ball (9 in Fig. 18.2), which turns the mirror.

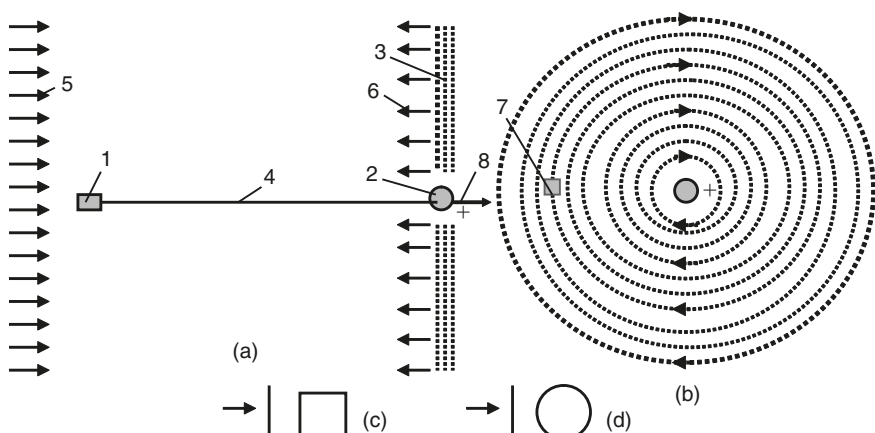


Fig. 18.1. The proposed electrostatic solar sail: (a) side view; (b) front view; (c) side and front views of square petal; (d) side and front views of round petal. *Notations:* (1) Space ship; (2) charged ball; (3) charged plate-petals; (4) cable connecting the ship and the ball; (5) solar rays; (6) reflected rays; (7) charged petals; and (8) thrust (drag).

The unfurling of the sail may be done using a rotated charged head (10 in Fig. 18.3). The head is detached from the apparatus in the radius of sail, and is rotated around its axis (parallel to the solar rays) and around the ball. The head emits the negatively charged petals. The speed of the petals may be controlled by the head charge (voltage). The same charge stretches the petals³ and repels them from the others. The sail can be collected back by the head, through the head changing the opposite charge.

The proposed solar sail has many unique advantages in comparison with the conventional solar sail or a space mirror:

1. The proposed sail (made only of film) is easier to use (has less mass) in 50–100 times because of the absence of a support substrate (dielectric film of 5000-nm

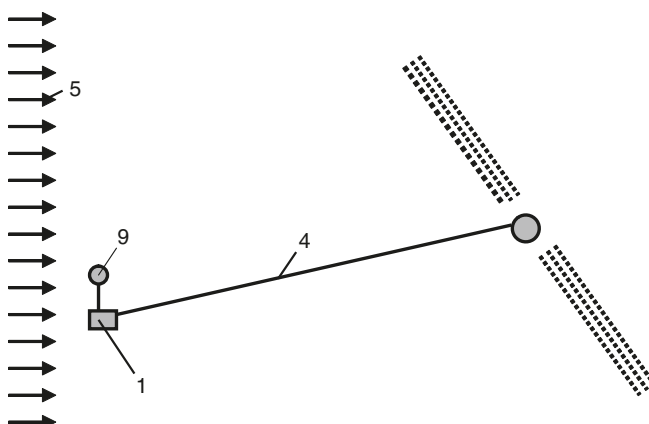


Fig. 18.2. Guidance and control of the electrostatic solar sail. Notation: (9) charged ball for control. All other notations are the same as in Fig. 18.1.

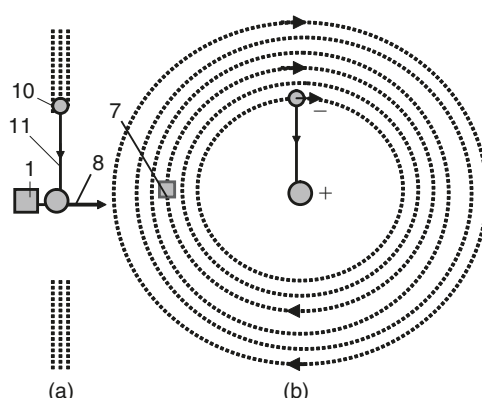


Fig. 18.3. Unfurling of the electrostatic solar sail. Notations: (10) rotating mobile charged head connected by a variable cable to the central ball and (11) variable cable connecting the head and the ball. All other notations are the same as in Fig. 18.1.

thickness) and the aluminum film used can be of minimum thickness (6–15 nm, not 100 nm).

2. A rigid support structure giving a large additional mass is unnecessary.
3. The size of the reflected mirror is not limited and may be more than 1 km. This means the proposed sail can accelerate a large space ship with a mass of 1 ton or more.
4. There are no big problems with the unfurling and collection of the sail.
5. The electrostatic sail may be collected (furled) to the head.

18.3 Theory of estimation and computation

18.3.1 The sail

The spectrum of solar radiation is presented in Fig. 18.4.¹ If we want to use the most energy, the sail must reflect or absorb all waves having the wavelength less than $\lambda = 1\text{--}2 \mu\text{m}$.

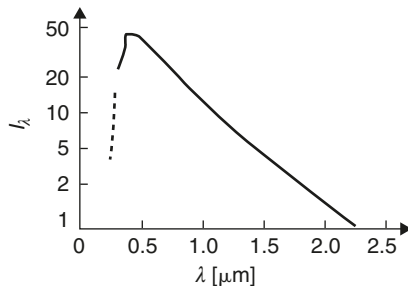


Fig. 18.4. Spectrum of solar radiation. λ is the wavelength [0–2.5 μm], I_λ is the energy density.

The amount of light that can pass capability through metal depends on its thickness:²

$$I = I_0 \exp(-4\pi nkd/\lambda), \quad d = -\frac{\lambda \ln(I/I_0)}{4\pi nk}, \quad (18.1)$$

where I is the light intensity after passing through metal film; I_0 is the initial light intensity; I/I_0 is the coefficient of clarity; n is the refraction coefficient; k is the absorption coefficient; d is the metal thickness [m], and λ is the wavelength [m].

The refraction and absorption coefficients of aluminum are equal (see Ref.², p. 639):

for $\lambda = 0.5 \mu\text{m}$, coefficient $n = 0.5$, $k = 9.18$, $nk = 4.59$; $\lambda/nk = 0.109 \times 10^{-6}$;

for $\lambda = 5 \mu\text{m}$, coefficient $n = 6.7$, $k = 5.61$, $nk = 37.59$; $\lambda/nk = 0.133 \times 10^{-6}$.

For other values the product nk can be found using linear interpolation: $\lambda = 1 \mu\text{m}$, $nk = 8.26$; $\lambda = 2 \mu\text{m}$, $nk = 15.59$.

The computation of the metal film thickness versus the coefficient of clarity I/I_0 is presented in Fig. 18.5.

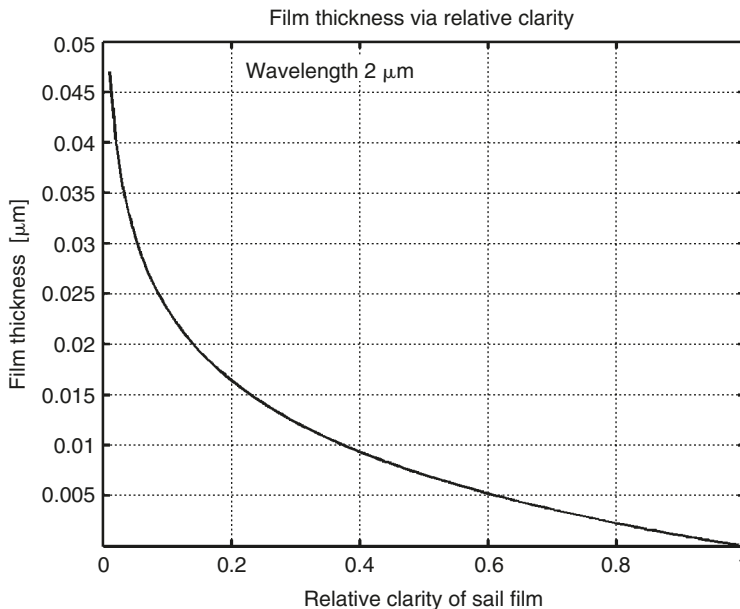


Fig. 18.5. The sail film thickness via clarity coefficient I/I_0 for the wavelength $\lambda = 2 \mu\text{m}$.

The weight of the sail is computed using the equation:

$$W = \rho S d, \quad (18.2)$$

where W is the sail weight (mass) [kg]; $\rho = 2700 \text{ kg/m}^3$ is the density of aluminum; S is the sail area [m^2]; and d is the sail (aluminum) thickness [m].

The mass of a 1 m^2 sail of thickness $d = 10 \text{ nm}$ is $W = 2700 \times 10^{-8} = 0.027 \text{ g/m}^2$. Compared with $5\text{--}7 \text{ g/m}^2$ for the conventional sail this is 185–260 times less. Clarity correction makes this value 110–150 times less.

The acceleration, a , of a space ship with a sail can be computed using the equation:

$$a = \frac{P_0 S (1 - I/I_0)}{M - W} = \frac{P_0 S (1 - I/I_0)}{M} = \frac{\lambda \rho S \ln(I/I_0)}{4\pi n k}, \quad (18.3)$$

where P_0 is the light pressure [N] and M is the useful mass (of the ship without sail) [kg]. If we take solar radiation pressure for 88% reflection at 1 AU, it is about $P_0 = 8 \times 10^{-6} \text{ N/m}^2$. This works out at 8 N for a sail with a radius of 564 m (area 10^6 m^2).

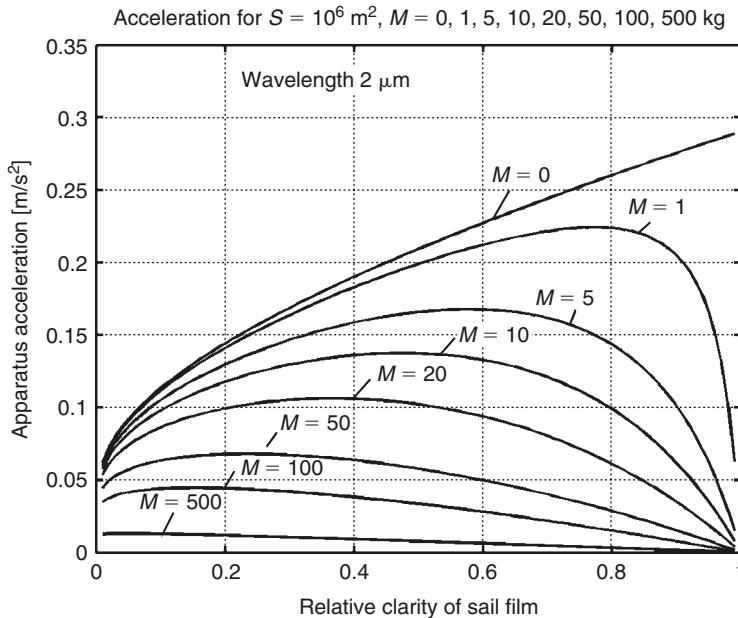


Fig. 18.6. Apparatus acceleration via relative clarity of sail film and additional apparatus mass.

The mass of our sail is 27 kg, the mass of a conventional sail (without the support structures) is 5 ton. However, the unbiased comparison is of sail acceleration for $M = 0$.

The result of computation for equation (18.3) is presented in Fig. 18.6. As you can see, the acceleration of the proposed sail reaches as much as $a \approx 0.3 \text{ m/s}^2 = 300 \text{ mm/s}^2$. In comparison, acceleration of the conventional solar sail without a useful load is 1 mm/s^2 . If our sail spacecraft has an additional useful mass (the ship, the ball, and other devices) of 100 kg, the acceleration is 45 mm/s^2 ; for a useful mass of 500 kg, the acceleration is 13 mm/s^2 .

The maximum speed of a solar-sail spacecraft can be estimated using the equation:

$$\begin{aligned} dV &= a dt, \quad dt = \frac{s}{V}, \quad a = a_0 \left(\frac{s_0}{s} \right)^2, \\ V dV &= a_0 \left(\frac{s_0}{s} \right)^2 ds, \quad V^2 = 2a_0 s_0^2 \left(\frac{1}{s_0} - \frac{1}{s} \right), \end{aligned} \tag{18.4}$$

where V is the apparatus speed [m/s]; a is the acceleration [m/s²]; t is the time [s]; a_0 is the acceleration at distance 1 AU (for Earth's orbit of radius $s_0 = 15 \times 10^{10} \text{ m}$); and s is the distance from the Sun [m].

If $s \gg s_0$, the maximum apparatus speed is:

$$V_{\max} = \sqrt{2a_0 s_0}. \quad (18.5)$$

The proposed solar sail without a load reaches a maximum speed of 295 km/s \approx 300 km/s, whereas the conventional sail without a load reaches only 55 km/s. With a load of 100 kg the new sail reaches a speed of 116 km/s. If the apparatus makes a maneuver and starts at $s_0 = 30$ million kilometers from the Sun ($a = 25a_0$) the maximum speed reaches 660 km/s.

We can find the tangent speed of the petals (aluminum plates) around the charged ball from the following equations:

$$F = k \frac{qQ}{r^2} = \frac{mv^2}{r}, \quad q = \frac{Q}{N}, \quad m = \frac{\rho Sd}{N}, \quad v = Q \sqrt{\frac{k}{\rho Srd}}, \quad (18.6)$$

where F is the electrostatic force between the central ball and the petal [N]; $k = 9 \times 10^9$ is the electrostatic coefficient; q is the charge of a petal [C]; Q is the charge of the ball [C]; r is the distance between the petal and the center of ball [m]; m is the mass of a petal [kg]; v is the tangent speed of a petal (around the ball) [m/s]; and N is the number of petals.

If $\rho = 2700 \text{ kg/m}^3$ (for aluminum), $S = 10^6 \text{ m}^2$, $r = 600 \text{ m}$, $d = 10^{-8} \text{ m}$, then $v = 745Q$. For $Q = 0.01 \text{ C}$ the speed $v = 7.45 \text{ m/s}$.

18.3.2 Initial expenditure of electrical energy to charge of the ball

The ball has to be charged with electrical energy of high voltage (millions of volts). Let us estimate the minimum energy, when the charged device has 100% efficiency. This energy equals the work done to move of the ball charge to infinity. It can be computed using the equation:

$$W_b = \frac{Q^2}{2C}, \quad Q = \frac{a^2 E}{k}, \quad C = \frac{a}{k}, \quad W_b = \frac{a^3 E^2}{2k}, \quad (18.7)$$

where W_b is the ball charge energy [J]; C is the ball capacitance [F]; Q is the ball charge [C]; a is the radius of ball [m]; and E is the electric intensity [V/m].

For our charge $Q = 0.01 \text{ C}$ and electrical intensity (safe for a vacuum) $E = 10^8 \text{ V/m}$, the required ball radius is $a = 0.95 \text{ m} \approx 1 \text{ m}$ (equation (18.7)), and the required charge energy is $W_b = 0.154 \text{ kW-h}$ (equation (18.7)). This energy is not great, and it may be returned when the ball discharged by emitting the charge into space using a sharp edge.

18.3.3 The ball stress, cover thickness, and ball mass

The ball has tensile stress from the like electric charge. We can find the ball stress and the necessary thickness of the ball cover. If the ball is in a vacuum and the ball charge, Q , is constant, the internal force within the ball is:

$$f = \frac{\partial W_b}{\partial a}, \quad W_b = \frac{Q^2}{2C}, \quad C = \frac{a}{k}, \quad k = \frac{1}{4\pi\epsilon_0} = 9 \times 10^9, \quad W_b = \frac{kQ^2}{2a}, \quad (18.8)$$

$$f = -\frac{kQ^2}{2a^2}, \quad Q = \frac{a^2 E}{k}, \quad f = -\frac{(aE)^2}{2k}, \quad (18.9)$$

where f is the ball's internal tensile force [N]; W_b is the charge energy [J]; C is the capacity of the ball as a spherical capacitor [F]; and E is the electric intensity [V/m].

The internal pressure of the ball is then:

$$p = \frac{f}{S_b}, \quad S_b = 4\pi a^2, \quad p = \frac{E^2}{8\pi k}, \quad (18.10)$$

where p is the internal pressure [N/m^2] and S_b is the ball surface area [m^2].

The thickness of a ball cover is:

$$\pi a^2 p = 2\pi a \delta \sigma, \quad \delta = \frac{ap}{2\sigma}, \quad \delta = \frac{aE^2}{16\pi k \sigma}, \quad (18.11)$$

where δ is the cover thickness [m] and σ is the safe cover stress [N/m^2].

The ball mass is then:

$$M_s = S_b \delta \gamma, \quad S_b = 4\pi a^2, \quad M_s = \frac{a^3 E^2 \gamma}{4k\sigma}, \quad (18.12)$$

where M_s is the ball (sail) mass [kg]; γ is the ball cover density [kg/m^3]; and σ is the safe stress level of the ball cover [N/m^2].

For our case where $a = 1 \text{ m}$, $E = 10^8 \text{ V/m}$, $\gamma = 1800 \text{ kg/m}^3$, $\sigma = 10^9 \text{ N/m}^2$, the mass of the ball is $M_s = 0.5 \text{ kg}$ (equation (18.12)).

18.3.4 Technology

The thin plate-petals can be produced by electrolytic or vapor precipitation.

18.3.5 Artificial Moon

The proposed idea may be used to construct an artificial Moon when the light pressure equals the Earth's gravity and a gigantic electrostatic mirror illuminates the Earth's surface.

Other electrostatic applications are offered in Refs.⁴⁻⁹

References

1. "Dispersion of Light", *Big Soviet Encyclopedia*, Moscow (in Russian).
2. I.K. Kikoin, *Tables of Physical Values*, Directory, Moscow, 1975 (in Russian).
3. A.A. Bolonkin, Method of Stretching of Thin Film. Russian Patent Application #3646689/10 138085, 28 September 1983 (in Russian), Russian PTO.
4. A.A. Bolonkin, "Electrostatic Utilization of Asteroids for Space Flight", AIAA-2005-3857, *41st Propulsion Conference*, 10-12 July 2005, Tucson, AZ, USA.
5. A.A. Bolonkin, "Electrostatic Solar Wind Propulsion", AIAA-2005-3653, *41st Propulsion Conference*, 10-12 July 2005, Tucson, AZ, USA.
6. A.A. Bolonkin, "Guided Solar Sail and Electric Generator", AIAA-2005-3857, *41st Propulsion Conference*, 10-12 July 2005, Tucson, AZ, USA.
7. A.A. Bolonkin, "Electrostatic Levitation and Artificial Gravity", AIAA-2005-3365, *41st Propulsion Conference*, 10-12 July 2005, Tucson, AZ, USA.
8. A.A. Bolonkin, "Radioisotope Space Sail and Electric Generator", AIAA-2005-3653, *41st Propulsion Conference*, 10-12 July 2005, Tucson, AZ, USA.

This page intentionally left blank

CHAPTER 19

Utilization of Space

Summary

This chapter describes some new ideas^{1–23} which may be useful for utilization in space: (1) recombination propulsion, (2) a space mirror, (3) electronic sail, (4) astronauts in space without space suits, and (5) an electrostatic space radiator.

19.1 Recombination space jet propulsion engine

19.1.1 Summary

There are four known ionized layers in the Earth's atmosphere, located at an altitude of 85–400 km. Here the concentration of ions reaches millions of particles in 1 cm³. In the interplanetary medium the concentration of ion reaches 10–10³ particles in 1 cm³ and in interstellar space it is about 1–10 in 1 cm³. As a result there is interaction between solar radiation in the Earth's atmosphere, solar wind, and galactic radiation.

About 90% of these particles are protons and electrons. The particle density is low and they can exist for a long time before they come into collision with each other. However, if we increase the density of the particles in an engine, they collide with one another, recombine, warm up, leave the propulsion system with high speed, and create thrust.

The energy of recombination is significantly more than the heat capability of conventional fuel and the specific impulse of the propulsion system is high.

The author proposes collecting and concentrating charged particles from a large area using a magnetic field. Space ships, space apparatus, and satellites would then not need fuel and could be accelerated or fly to infinity. This may be a revolution in aerospace.

19.1.2 Description of method and innovation

19.1.2.1 Introduction

The Earth's atmosphere

The present atmosphere of the Earth is probably not its original form. Our current atmosphere is what chemists would call an *oxidizing atmosphere*, while the original atmosphere

was what chemists would call a *reducing atmosphere*. In particular, it probably did not contain oxygen.

Composition of the atmosphere The original atmosphere may have been similar to the composition of the solar nebula and close to the present composition of the gas giant planets, though this depends on the details of how the planets condensed from the solar nebula. That atmosphere was lost into space, and replaced by compounds given out as gases from the crust or (in some more recent theories) much of the atmosphere may have come instead from the impacts of comets and other planets similarly rich in volatile materials.

The oxygen so characteristic of our atmosphere was almost all produced by plants (cyanobacteria or, more colloquially, blue-green algae). Thus, the present composition of the atmosphere is 79% nitrogen, 20% oxygen, and 1% other gases.

Layers of the atmosphere The atmosphere of the Earth may be divided into several distinct layers, as the Fig.19.1 indicates. The *troposphere* is where all the weather takes place; it is the region of rising and falling packets of air. The air pressure at the top of the troposphere is only 10% of that at sea level (0.1 atmospheres). There is a thin buffer zone between the troposphere and the next layer called the *tropopause*.

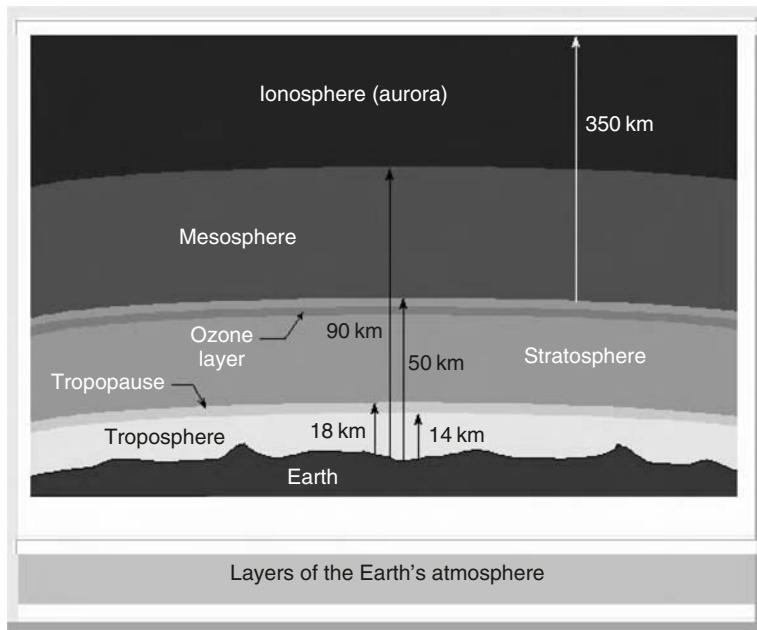


Fig. 19.1. Layers of the Earth's atmosphere.

Above the troposphere is the *stratosphere*, where air flow is mostly horizontal.

Above the stratosphere is the *mesosphere* and above that is the *ionosphere* (or *thermosphere*), where many atoms are ionized (gain or lose electrons so they have a net electrical charge). The ionosphere is very thin, but it is where aurora takes place, and it is also

responsible for absorbing the most energetic photons from the Sun, and for reflecting radio waves, thereby making long-distance radio communication possible.

The structure of the ionosphere is strongly influenced by the charged particle wind from the Sun (solar wind), which is in turn governed by the level of solar activity. One measure of the structure of the ionosphere is the free electron density, which is an indicator of the degree of ionization. There are electron density contour maps of the ionosphere available for months in 1957 to the present. As an example, comparison of the simulations of the monthly variation of the ionosphere for the year 1990 shows this was a period of high solar activity with many sunspots, and that 1996 was a period of low solar activity with few sunspots.

The ionosphere can be further broken down into the D, E, and F regions. This breakdown is based on what wavelength of solar radiation is absorbed in that region most frequently, or on what level of radiation is needed to photodissociate the molecules found in these individual regions.

The D region is the lowest in altitude, although it absorbs the most energetic radiation, hard X-rays. The D region has not have a definite starting and stopping point, but includes the ionization that occurs below about 90 km (or ionization that occurs below the E region).

The E region peaks at about 105 km. It absorbs soft X-rays.

The F region starts around 105 km and reaches a maximum at about 600 km. It is the highest of all of the regions. Extreme ultra-violet radiation (EUV) is absorbed there.

On a more practical note, the D and E regions (the lower parts of the ionosphere), reflect standard AM radio waves back to Earth. Radio waves with shorter lengths are reflected by the higher F region. Visible light, radar, TV, and FM wavelengths are all too short to be reflected by the ionosphere, so these types of global communication are made possible by satellite transmissions.

19.1.2.2 Description of innovation

In the recombination propulsion engine contains a tube with an intake and a nozzle, and a solenoid (Fig. 19.2).

The solenoid may be conventional or superconductive. It produces a powerful magnetic field, which collects charged particles. If the density of the charged particles is sufficient (the distance the particles travel is less than the tube length) the particles came into contact with each other and recombine.

The energy of recombination (ionization and dissociation atoms and molecules) is:

Atom	Symbol	Level from 1 to top (eV)
<i>Ionization:</i>		
Proton	H	13.6
Nitrogen	N	14.54–666.83
Oxygen	O	13.6–871.12
<i>Dissociation:</i>		
Hydrogen	$H + H = H_2$	4.48

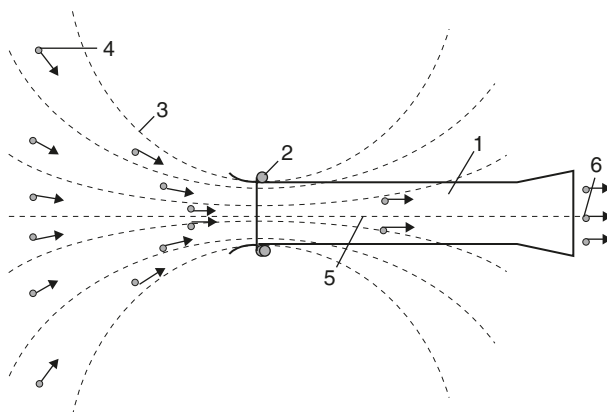


Fig. 19.2. Recombination space jet propulsion engine (actuator of magnetic field). *Notations:* (1) Engine; (2) solenoid; (3) magnetic lines; (4) charged particles; (5) recombination zone; and (6) exit.

This minimum energy is more than the energy of the most efficient chemical reaction, $H_2 + O = H_2O$, by hundreds of times. This means the specific impulse of the recombination engine will be very high. The heating of engine walls will be small, however, because the density of the particle gas is low. Using this proposed method, we do not need to expend fuel and can achieve a large acceleration of a space vehicle, or support the satellite at altitude for an infinite amount of time.

Idea's are needed in research and development of this method.

19.2 Utilization of high-altitude mirror for lighting in local Earth areas

19.2.1 Summary

A space mirror is a large thin film space reflector. It may be used for lifting, heating of local Earth areas, and controlling weather on Earth. The author proposes a innovation and new design of space mirror, which allows the mirror to be located on the Moon or in high-altitude orbits. The main advantages of these innovations are: (1) the Moon moves slowly around the Earth (its period is 29 days) and mirror control is easy, (2) the Moon is located outside Earth's shadow and the mirror can illuminate any town on Earth in full night in any area, for example, a region where there has been a disaster such as a tsunami, earthquake, etc., (3) the proposed mirror can be used to heat polar towns and control the weather, (4) the mirror is easy to maintain and repair, especially if we have an astronaut station on the Moon, (5) controlling the angle and focus of the proposed mirror is easy, and (6) and the mirror may be used to support solar sail propulsion systems for space apparatus.

This innovation of a revolutionary solar mirror needs future research and computations.

19.2.2 Description of method and innovations

19.2.2.1 Introduction

Short history

The space mirror that reflects the Sun's rays onto the nightside of our planet is one of the impressive space projects. In 1993, the space ship "Progress M-15" placed into orbit a 20-m film mirror (the project "Znamya 2"). The mirror unfurled and produced a light spot that was equal in strength approximately to one full Moon. A huge plash of sun-light glanced over a cloud-covered Europe to be seen only by astronomers on the top of the Alps.

The project "Znamya 2.5" stood head and shoulders above its predecessor. The mirror was expected to be perceived on the Earth as 5–10 full Moons and it formed a trace of about 7 km in diameter which could be controlled by fixing it on one spot for a long time. The space mirror was a slightly concave membrane of 25 m in diameter made of thin film with a mirror surface, which was attached around the periphery of the station. The membrane was expected to unfold and to be held unfolded by centrifugal forces (Fig. 19.3). However, the project was a failure. Soon after deployment started, the membrane caught on the antenna. The space ship Progress M-40 was taken out of orbit and buried in the ocean.

The Russian Space Agency announced a plan to launching in the spring 2005 a space mirror of tennis-court size. It was to be made from 2- μm film and weigh 2 kg. Its solar beam (trace) would have a diameter of 5 km (RIA "News" of 13 January 2005).

Current design of space mirror

A space mirror is composed of large flat smooth sheets of very thin film, supported by ultra-lightweight structures. The side of the film which faces the Sun is coated with a highly reflective material so that the resulting product is a huge mirror, typically about the size of a football field. The solar mirror is a method of using light energy from the Sun to illuminate the Earth at night. There are also a number of military missions in Earth orbit. The light mirror material must be as thin and lightweight as possible. Conventional light sail film has comprised 5- μm thick aluminized mylar or kapton with a thin film aluminum layer (approximately 100 nm thick) deposited on one side to form a mirror surface with 90% reflectivity.

For 5- μm thick mylar, the area density is 7 g/m^2 . Although mylar is inexpensive and readily available in 0.5- μm thickness, it is not the ideal mirror film material because it is easily degraded by the Sun's ultraviolet radiation. The other key contender, kapton, can withstand ultra-violet radiation but is not available in layers much thinner than 8 μm , with a resulting a real density of 12 g/m^2 .

A *solar mirror* is a satellite with a large, lightweight reflector attached to it. Satellites in orbit around the Earth can survive for many years without any maintenance while using only a small amount of rocket propellant to hold their positions. Solar mirrors can be made to survive in space for many years as well.

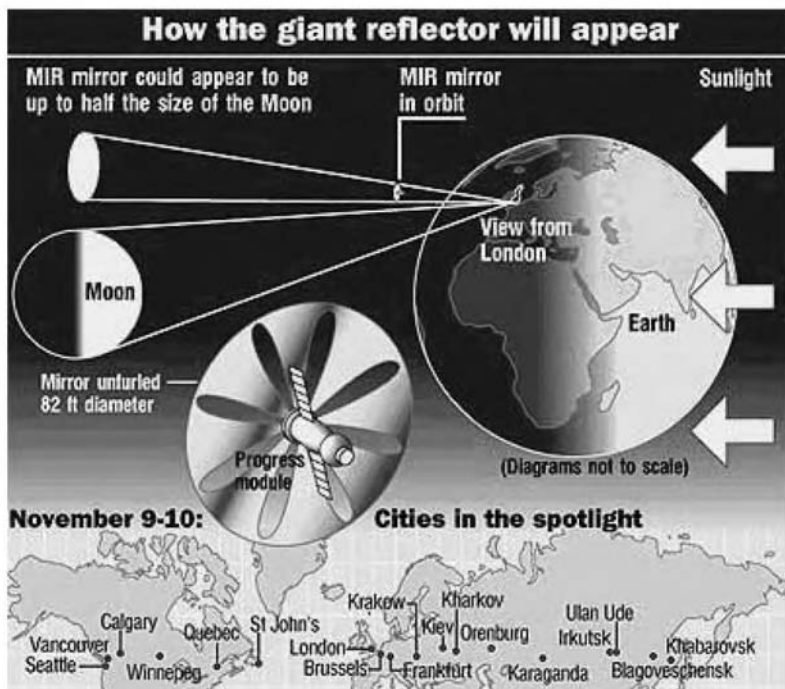
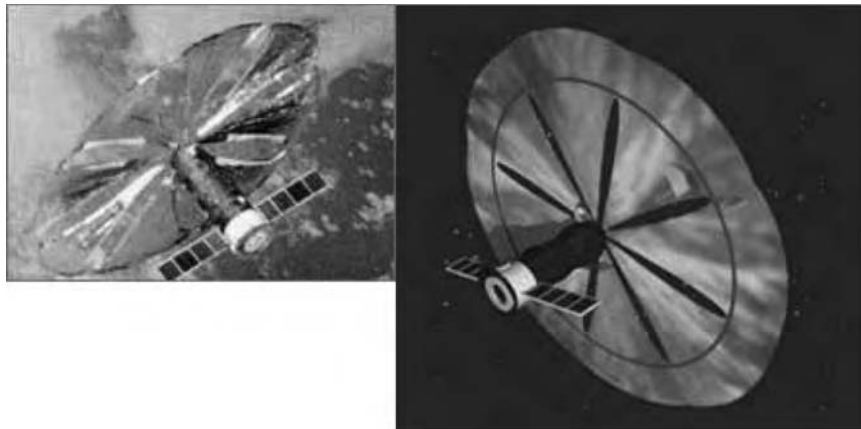


Fig. 19.3. Images of project “Znamya 2.5”.

Standard lighting (luxs):

1. Sun in cloudless noon at a middle latitude	100,000
2. Cloudy day	1000
3. Necessary for reading	30–50
4. Full Moon	0.2
5. Starlight on a moonless night	0.0003

The last above table shows a sunbeam at 1×1 km can illuminate an area of 2000–3300 km 2 at night with sufficient light for reading. The Sun mirror of 100×100 m can illuminate 22–33 km 2 . The average area of a small town is $2 \times 2 = 4$ km 2 , a medium size town is $3 \times 3 = 9$ km 2 and a city $10 \times 10 = 100$ km 2 . Two 100×100 m mirror are enough to illuminate a city 5×5 km as much as on a cloudy day. The power of a 1 km 2 solar beam is about 1.4 million kilowatt, which is enough to heat a small polar town covered by thin film. We could thus save vast amounts energy in illumination and heating. By concentrating sunbeams from several mirrors or focusing a beam from one large mirror on a given point (the center of a hurricane or tornado), we could influence the Earth's weather.

Unfortunately, the conventional (altitude up to 1000 km) space mirror has a lot of imperfections which limit its application (see Fig. 19.4):

1. A satellite has a high speed (8 km/s) and is located for only a short time over a given Earth area (a few minutes).
2. Satellites observe only a narrow Earth zone.
3. The satellite's high speed means a quick turn of the mirror is required to illuminate a given point (town). This is very difficult because the mirror has a large size and very thin structures, and does not allow a large angle of acceleration. It also requires a very complex control devices and a lot of fuel.
4. The satellite has orbit located in the ecliptic (equator) plane. This means it is difficult to light the polar zones, which are more in need of indirect lighting at night or additional solar heating.

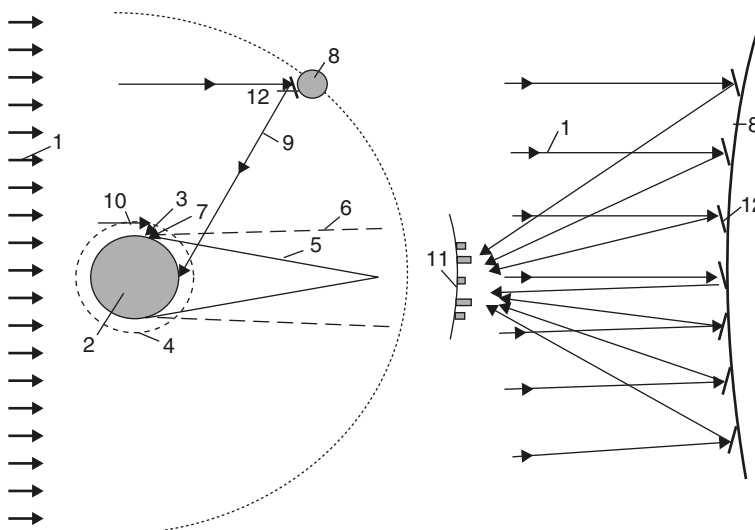


Fig. 19.4. Solar mirror located in conventional orbit. *Notations:* (1) Solar light; (2) Earth; (3) conventional mirror satellite; (4) conventional mirror orbit (altitude about 200 km); (5) Earth shadow; (6) Earth semi-shadow; (7) small Earth region which can be illuminated; (8) satellite; (9) reflected solar beam; (10) solar beam of conventional mirror; (11) Earth town; and (12) mirror in the high altitude.

These imperfections are absent from the proposed new space mirror system. It can illuminate a given point for a long time and it is easy to operate. Some of these innovations are described below.

19.2.2.2 Description of innovations and their advantages

The proposed space system for lighting, heating, and weather control is presented in Fig. 19.4. The detailed design is presented in Fig. 19.5. The mirror is made from a double thin film and installed on inflatable controlled columns made from thin film. The mirror has controls for this a film tension, mirror focus, and angle (all are inventions). The system includes a set of controlled mirrors.

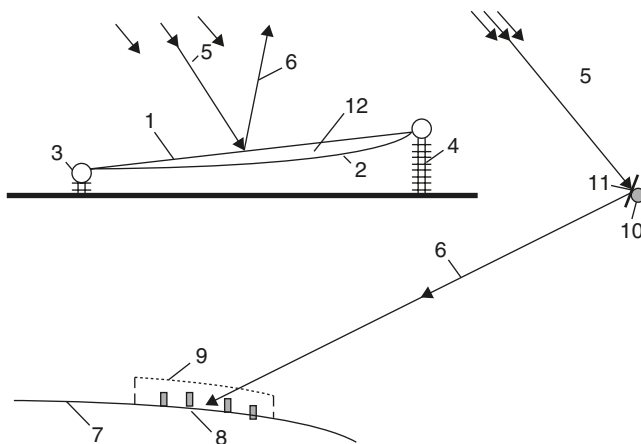


Fig. 19.5. Guided mirror on the Moon and heating a town at night. *Notations:* (1,2) Double thin film mirror; (3) toroid ring to support and the mirror surface tension; (4) inflatable column for controlling the mirror angle; (5) solar beam; (6) reflected beam; (7) Earth; (8) town; (9) thin transparent film protecting the town from cold air; (10) satellite; and (11) mirror; (12) gas for control of mirror focus.

If we send the solar beam into a special Earth station, we can convert the huge amount of solar energy into any other form of energy, for example, into electricity using a conventional method (solar cell or heat machine). The $100 \times 100 \text{ m}^2$ reflector produces 12,000 kW energy at the Earth's surface. The proposed system can be also used for long-distance communication. The focused beam is directed at far distant space apparatus and can transmit information.

The set of focused mirrors may be used as an outer propulsion system for solar sail apparatus.

The suggested revolutionary system is achievable using current technology and could be produced in the near future but needs in detailed research and computation.

19.3 Electronic sail

19.3.1 Summary

A solar sail reflects solar light and can be used as a propulsion system, as described in Chapter 16. It needs thin film of a very large area. This section proposes a new way of

creating a reflecting surface of large area using an electronic method. This method needs research and development but it may be easier and more efficient than the film method.

19.3.2 Brief description of innovation

The proposed electronic sail has a positive charge, 1 (see Fig. 19.6). The free electrons, 2, are injected into space around the positive charge so they rotate around the center of the charge and form a thin disk in a plane perpendicular to the direction of the sunlight. If the concentration of electrons is sufficient, they will reflect the solar light like a mirror and produce thrust.

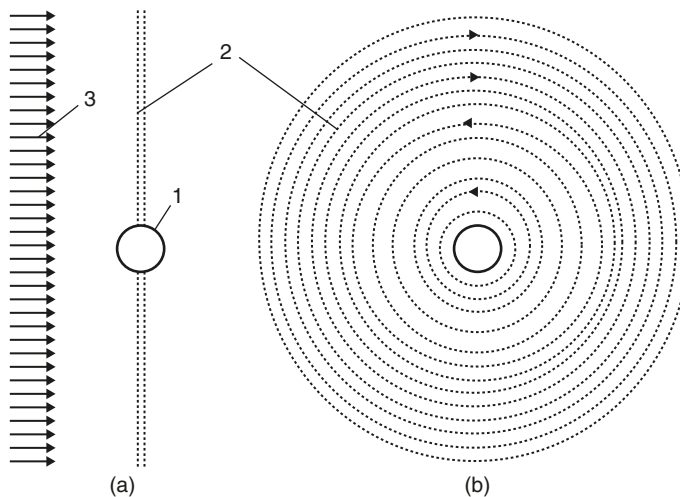


Fig. 19.6. Electronic solar sail. (a) side view; (b) front view. Notations: (1) Positive charge; (2) electronic disk; and (3) solar light.

This electronic sail may be an electrostatic solar wind sail, as described in Chapter 13, if the central charge is positive. The solar wind electrons became concentrated around it and the mass of electrons reflects the solar light. Thrust from the solar wind is small because the electron mass is about 2000 times less than the proton mass, but the solar light pressure is thousands of times greater than solar wind (protons) pressure. The offered installation may also be used as a space mirror to illuminate the Earth's surface. This idea needs further research.

19.4 In outer space without a space suit?

19.4.1 Summary

The proposed system would enable a person to be in outer space without a space suit.

19.4.2 Brief description of innovation

A space suit is a very complex and expensive device (Fig. 19.7). Its function is to support the person's life, but it makes an astronaut immobile and slow, prevents him or her

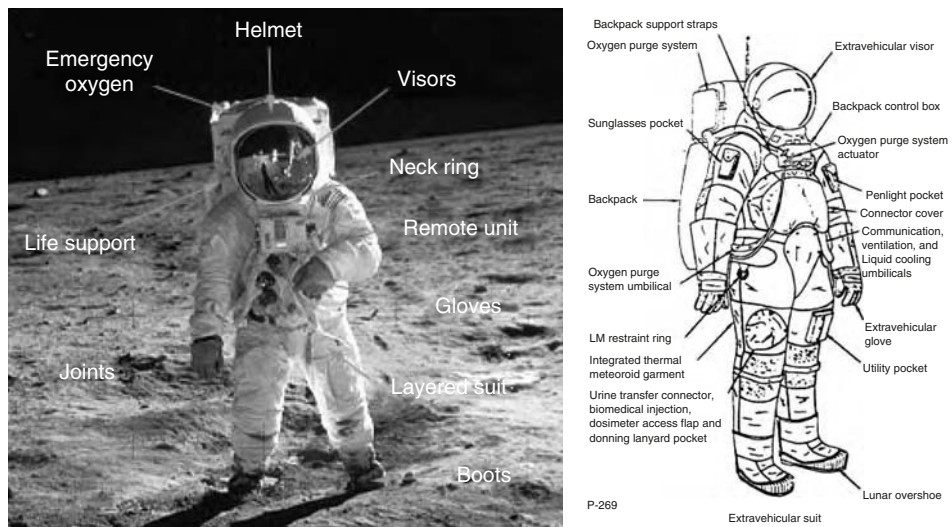


Fig. 19.7. (a) Astronaut in a space suit. (b) Diagram showing component parts of a space suit.

working, creates discomfort, does not allow eating in space, has a toilet, etc. Astronaut need a space ship or special space home located not far from away where they can undress for eating, toilet, and rest.

Why do we need a special space suit in outer space? There is only one reason – we need an oxygen atmosphere for breathing, respiration. Human evolution created lungs which aerates the blood with oxygen and remove carbon dioxide. However we can also do that using artificial apparatus. For example, doctors, performing surgery on someone's heart or lungs connect the patient to a heart-lung machine that acts in place of the patient's lungs or heart.

We can design a small device which will aerate the blood with oxygen and remove the carbon dioxide. If a tube from the main lung arteries could be connected to this device, we could turn on (off) the artificial breathing at any time and enable the person to breathe in a vacuum (on an asteroid or planet without atmosphere) in a bad or poisonous atmosphere, or under water, for a long time. In space we can use a conventional Earth suit to protect us against solar light. This idea may be investigated animals on Earth.

19.5 Electrostatic space radiator

A large space ship needs a vast amount of energy. For example, we can travel to far planets in a space ship with a nuclear reactor. However, its powerful electricity generator or engine requires a very large radiator to remove the surplus heat. The coefficient of efficiency of any heat machine is about 30–60%. This means that about a half the heat gained from the reactor has to be removed through radiation. Computation shows the heat radiator needs to have a size and weight many times greater than the space ship.

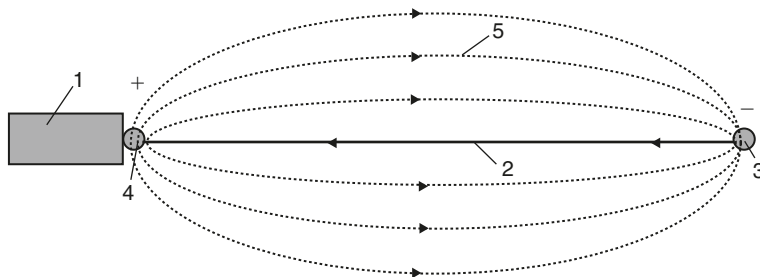


Fig. 19.8. Electrostatic radiator. Notations: (1) Space ship; (2) tube; (3, 4) electrode; and (5) trajectory of drops.

The author proposes an electrostatic radiator which has small weight and can cool a refrigerant very quickly. This is shown in Fig. 19.8.

The radiator works in the following way. The refrigerant is charged and sprays from one electrode and retracts from the opposite electrode. The small drops of refrigerant have a very large surface area and emit (radiate) heat very quickly.

These and others ideas are in Refs.¹⁻²³

References

1. A.A. Bolonkin, "Solar Sail Engine for Spaceships", Patent (Author Certificate #1262870), priority since 10 January 1985, USSR Patent Office.
2. A.A. Bolonkin, "Space Propulsion Using Solar Wing and Installation for It", Russian Patent Application #3635955/23 126453, 19 August 1983 (in Russian), Russian PTO.
3. A.A. Bolonkin, "Installation for Open Electrostatic Field", Russian Patent Application #3467270/21 116676, 9 July 1982 (in Russian), Russian PTO.
4. A.A. Bolonkin, "Getting Electric Energy from Space and Installation for It", Russian Patent Application #3638699/25 126303, 19 August 1983 (in Russian), Russian PTO.
5. A.A. Bolonkin, "Protection from Charged Particles in Space and Installation for It", Russian Patent Application #3644168 136270, 23 September 1983 (in Russian), Russian PTO.
6. A.A. Bolonkin, "Method of Transformation of Plasma Energy in Electric Current and Installation for It", Russian Patent Application #3647344 136681, 27 July 1983 (in Russian), Russian PTO.
7. A.A. Bolonkin, "Method of Propulsion Using Radioisotope Energy and Installation for It", Russian Patent Application #3601164/25 086973, 6 June 1983 (in Russian), Russian PTO.
8. A.A. Bolonkin, "Transformation of Energy of Rarefaction Plasma in Electric Current and Installation for it", Russian Patent Application #3663911/25 159775, 23 November 1983 (in Russian), Russian PTO.
9. A.A. Bolonkin, "Method of a Keeping of a Neutral Plasma and Installation for It", Russian Patent Application #3600272/25 086993, 6 June 1983 (in Russian), Russian PTO.

10. A.A. Bolonkin, "Radioisotope Propulsion", Russian Patent Application #3467762/25 116952, 9 July 1982 (in Russian), Russian PTO.
11. A.A. Bolonkin, "Radioisotope Electric Generator", Russian Patent Application #3469511/25 116927, 9 July 1982 (in Russian), Russian PTO.
12. A.A. Bolonkin, "Radioisotope Electric Generator", Russian Patent Application #3620051/25 108943, 13 July 1983 (in Russian), Russian PTO.
13. A.A. Bolonkin, "Method of Energy Transformation of Radioisotope Matter in Electricity and Installation for It", Russian Patent Application #3647343/25 136692, 27 July 1983 (in Russian), Russian PTO.
14. A.A. Bolonkin, "Method of stretching of Thin Film", Russian Patent Application #3646689/10 138085, 28 September 1983 (in Russian), Russian PTO.
15. A.A. Bolonkin, "New Way of Thrust and Generation of Electrical Energy in Space", Report ESTI, 1987, (Soviet Classified Project).
16. A.A. Bolonkin, "Aviation, Motor and Space Designs", *Collection Emerging Technology in the Soviet Union*, Delphic Ass., Inc., USA, 1990, pp. 32–80.
17. A.A. Bolonkin, "A Space Motor Using Solar Wind Energy", IAF-0615, *The World Space Congress*, 28 August–5 September, 1992, Washington, DC, USA.
18. A.A. Bolonkin, "The Simplest Space Electric Generator and Motor with Control Energy and Thrust", IAF-94-R.1.368, *45th International Astronautical Congress*, 9–14 October, 1994, Jerusalem, Israel.
19. A.A. Bolonkin, "Space Electric Generator, Run by Solar Wing", IAF-92-0604, *The World Space Congress*, 28 August–5 September 1992, Washington, DC, USA.
20. A.A. Bolonkin, "A Simple Space Nuclear Reactor Motors and Electric Generators Running on Radioactive Substances", IAF-92-0573, *The World Space Congress*, 28 August–5 September 1992, Washington, DC, USA.
21. A.A. Bolonkin, "Theory of Flight Vehicles with Control Radial Force", *Collection Researches of Flight Dynamics*, Mashinostroenie Publisher, Moscow, 1965, pp. 79–118 (in Russian).
22. Internet site: <http://Bolonkin.narod.ru>
23. Internet site: <http://NASA-NIAC.narod.ru>

Attachments: Non-conventional and non-rocket flight on Earth

This page intentionally left blank

ATTACHMENT 1

Air Cable Transport and Bridges*

Summary

Currently aircraft are used to move payloads and passengers from one place to other. This method is expensive, because aircraft use expensive fuel and have high capital costs. The author proposes a new method for less expensive delivery of payloads and people from one city to another (similar to airlines), or across streams, rivers, canyons, and mountains. This method uses a closed-loop cable path with a propulsion system located on the ground. The system can utilize any inexpensive energy source and air vehicles or cheaper winged containers without expensive electronic equipment. This method is particularly effective for providing an air bridge across straits, or mountains, or for gas lines. It is cheaper by hundreds of times than conventional long bridges, tunnels, and gas lines.

The author develops the theory and provides computations for two projects: airline travel from New York to Washington and New York to Paris, and air bridges such as across the Straits of Gibraltar, the English Channel, Bering Straits (Russia–America), Sakhalin–Asia, Russia–Japan, etc. Calculations are also provided for one gas line project. The proposed systems can also transfer large amounts of mechanical energy from one place to another (about 3–10 MW) with high efficiency.

A1.1 Introduction

Currently, aircraft, cars, trucks, trains, and ships are used to move payloads from one place to another. This method is expensive and requires good highway systems and expensive vehicles, which limits the feasibility of delivering many types of freight. Aircraft use expensive fuel and have high capital costs. The author offers a new, revolutionary method and installations for cheaper delivery of payloads and people (1) from one place to another, (2) across streams, rivers, canyons, etc., (3) accelerating vehicles to

* Detailed work was published by the author as “Air Cable Transport System”, *Journal of Aircraft*, Vol. 40, No. 2, March–April, 2003, pp. 265–269. “Air Cable Transport and Bridges”, TN 7567, *International Air & Space Symposium – The Next 100 Years*, Dayton, Ohio, USA, 14–17 July 2002. “Bolonkin’s Method Movement of Vehicles and Installation for It”, US Patent 6,494,143 B1, Priority is on 28 June 2001.^{1–3}

a desired velocity, and (4) cheaper vehicles which do not require their own engine. The method uses a closed-loop cable path with the propulsion system located on the ground; the concept includes airlines. The proposed system is unique with no references found for similar systems in the literature or patents.

At the present time, all vehicles (cars, trucks, buses, trains, aircraft, airships, dirigibles, sea ships) use engines located on the vehicle. Their engines require expensive fuel (for example, gasoline). The vehicle must carry both the engine and the fuel, which reduces the payload capacity. For example, for aircraft flying long distances the fuel weight may reach 30–40% of the takeoff weight, and the engine weight is about 10% of the full weight of the vehicle. As a result the payload is decreased to only 10–20% of the vehicle takeoff weight.

The proposed method maximizes the payload (no engine, no fuel in the vehicle), allows use of the cheapest form of energy (such as liquid fuel, natural gas, wind, or hydro-power stations) and cheaper vehicles.

The basic idea is simple (see Fig. A1.1): to connect the vehicle to an engine located on the ground using a strong light cable. Loss of flexibility is not a large problem, because

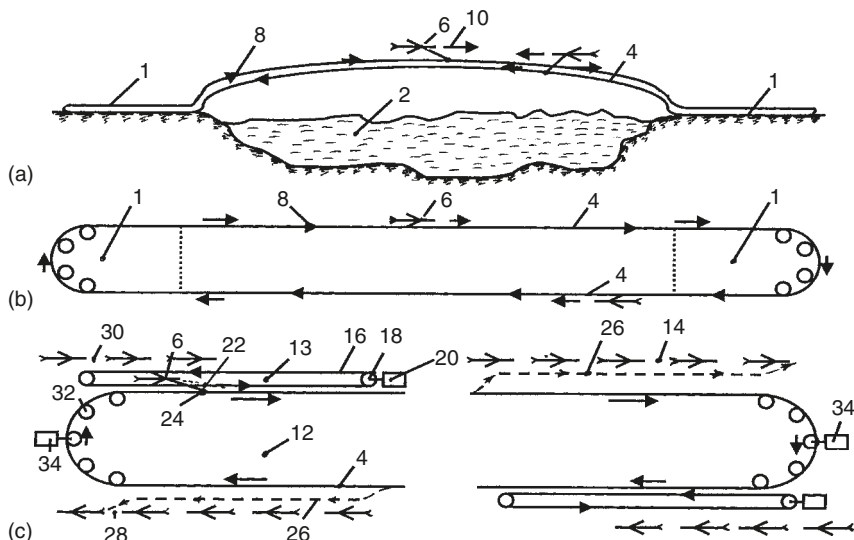


Fig. A1.1. (a) Airline or bridge (side view). *Notations:* (1) Terminal; (2) Earth's surface, strait, river, mountain, canyon, etc.; (4) main closed-loop cable (loop, rope, chain) of the transport system; (6) winged container (cabin); (8) support devices (support wings); and (10) direction of a winged container motion. (b) Air line or bridge (top view). (c) Terminals. *Notations:* (12) Departure (starting) port (terminal); (13) acceleration station; (14) braking station of an arrival port; (16) closed-loop cable (loop, rope) of acceleration station; (18) rollers; (20) drive system (station); (22) connection–disconnection device to an acceleration cable; (24) connection–disconnection device to the main transport cable; (26) landing (braking) runway for the winged container; (28) delivery (arrival) (unloading) port; (30) departure (loading) port; (32) rollers of the main cable; and (34) engines of the main cable.

heavily traveled routes for civilian airlines are fixed. The problems appear when we want to cover a long distance (from one mile up to hundreds or thousands of miles) across a stream, river, sea, ocean, or heavily congested area, especially when suspending the cable in the air at high altitudes (5–11 km). For highways, the connection and disconnection of the vehicle (auto, car, truck, bus) at required locations along the route of a permanently moving cable is also a problem. For city transport systems (large numbers of routes and stops), the changing of lines and directions, and the organization of the delivery of a huge flow of different vehicles to many points also must be addressed.

These main problems are solved in the proposed innovation.^{1–3}

The important feature of this invention is the possibility of using existing aircraft and autos (trucks, or buses) for the suggested system after connection–disconnection devices are added to them.

Computations show a strong and light cable (rope) for long-distance movement (delivery, transportation) system (some hundreds or thousands of miles) is required. Currently, industry is producing cheap fibers which have the required properties. We also have fibers, whiskers, and experimental nanotubes, that have the required properties for application to the proposed ideas.

For distances of over 100 km the light, strong, cable (rope) requires a ratio of tensile strength/specific weight, of more than 200 km.

The objective of this innovation is to provide cheap delivery of payloads and people from one place to another. This may include airlines from one city to another, bridge delivery over a stream, river (flying bridge), ferry-boats, a ground highway, a city transportation system or gas line.

Moreover the suggested transportation system can transfer large amounts of mechanical energy from one place to another on Earth (about 3–10 MW) with high efficiency.

Other applications that use these ideas are presented in the References.^{4–12}

A1.2 Short description of installation

An example of an installation is shown in Fig. A1.1(a) (side view). This is an airline, an air bridge over a sea strait, stream, or channel, for example, the Straits of Gibraltar (16 km). The installation includes the terminals (departure and arrival), a light, strong closed-loop (main) cable (rope, chain) over the surface, strait, mountain, or water (in both directions), winged containers (winged cabins) for payloads and people, a wing support devices (suspension, support system). The Fig. A1.1(b) shows the upper (top) view of this installation.

Fig. A1.1(c) shows the terminals (departure and arrival ports). The departure terminal (port) has a starting (acceleration) station (system), a takeoff runway, on arrival (braking) station (system), a starting (acceleration) closed-loop cable (rope), starting rollers,

starting engine (engine of the starting system), starting connection-disconnection sliding device (connected to a starting cable and to the winged container), main connection-disconnection sliding devices (connected to the main cable and to the winged container), landing runway, platform for arriving winged containers (unloading station), platform for departing winged containers (loading station). The terminals also have rollers for the main cable and an engine (drive) station for the main cable. The engine (drive) station includes engines, storage of energy (energy storage system, for example, inertial flywheel), transmission, clutches, brake, control system, and an energy transfer system.

This installation works in the following way (Fig. A1.1(c)). The acceleration engine moves the closed-loop starting cable (rope, chain) and the main engine moves the primary closed-loop main cable. When payload (cars, trucks) and people arrive at the port, they are loaded onto the platform and rolled to the winged containers. The winged container is connected to the starting cable via the connection device and the starting engine system accelerates the container to a velocity on which the wing can keep the container in the air. At the end of the takeoff segment of the flight, the container is disconnected from the starting cable and transferred on to the main cable. The container flies over the surface (strait, water) and lands at the arrival port. Here it is disconnected from the main cable, and brakes on the landing runway. It moves to the arrival platform, where it is unloaded, and moved to the departure platform for the next loading and flight. Delivery in the opposite direction is the same.

Fig. A1.2 shows the support wings at the main transport cable. Fig. A1.3(a) and (b) shows the support system using columns or air balloons.

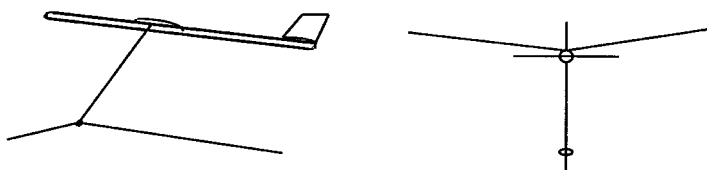


Fig. A1.2. Support wings of main transport cable.

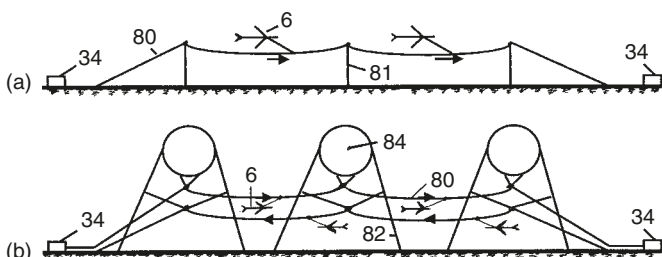


Fig. A1.3. (a) Column support system of the main transport cable. Notations: (80) Main transport cable and (81) column. (b) Air balloon support system. Notations: (82) Balloon cable tether and (84) balloon.

In a ground (highway) system, then the cars and trucks can connect to the moving cable and travel without using fuel or polluting the environment.

A1.3 Advantages

The suggested movement system has large advantages in comparison with the current systems of airlines, bridges, underground tunnels, and delivery by conventional cars and trucks.

A1.3.1 Airlines

1. Aircraft are very expensive. The suggested Airlines system does not use conventional aircraft. It uses a cheap winged container or cabin, without engines and expensive electronic equipment for navigation and communication.
2. Aviation fuel is expensive. The proposed airline system can use any sort of energy such as wind, water, or nuclear power or fuels such as natural gas, coal, peat, etc., because the engine is located on the Earth's surface. The cheapest energy can be used. The old airplanes (without their engines and electronic equipment) may be used as winged containers.
3. It is not necessary to have highly qualified personnel such as pilots with their high salaries.
4. The fare for the flight will be much lower.
5. Terrorists cannot use this system to damage important structures.

A1.3.2 Bridge or underground tunnel

1. The suggested air bridge is cheaper than a conventional long bridge, or especially an underground (underwater) tunnel, by hundreds of times (for long bridges, by thousands of times). The cost decreases from some billions of dollars to some tens of millions of dollars.
2. An air bridge can be made in a few months, whereas a conventional bridge or tunnel requires years for construction.
3. The cost of an air bridge does not increase as its length increases (only the length of the cable increases). The cost of a conventional bridge or tunnel increases more quickly as its length increases.
4. The air bridge can be built in places where it is impossible to build a bridge or tunnel by modern technology (for example, across the Bering Straits between the continents of Asia and North America (between Russia and the USA)).
5. The transit time (time of delivery) is reduced significantly.
6. The toll fee for using an air bridge will be lower and/or decrease more rapidly due to lower overall construction costs.

A1.3.3 Surface transport (movement) system

1. Very simple and cheap vehicles can be used for passenger and payload transportation by the suggested transportation system. It may be a simple (no engine) box or platform with wheels, a roller board or roller skates. It can also be a conventional car, bus, or truck. The vehicle only need to have (or be equipped with) the sliding connection device.
2. The system does not pollute the environment on highways nor, especially, in large cities.
3. The system does not use expensive liquid fuels (gasoline or diesel). It may use wind, water or any cheap form of energy.
4. Delivery can be made without a conventional vehicle (for example, people on roller skates).
5. It can use as vehicles cars, buses, trucks, trains, and ships, and can utilize old vehicles, with their engines turned off to prolong the life of the old vehicle, whose engines may be outdated.
6. It reduces traffic accidents because the vehicles move sequentially and cannot pass one another.

A1.3.4 Air gas line

1. The suggested air gas line is cheaper than a conventional ground gas pipeline by hundreds of times. The cost falls from some billions of dollars to some tens of millions of dollars.
2. An air gas line can be made in a few months whereas a conventional ground pipeline requires several years for building.
3. There is no damage to the environment.
4. It has very high load capability. The line can delivery gaseous, liquid, and solid payloads.
5. It has impossible to steal the gas when the pipeline runs across the territory of a third country.
6. It is easy to change the direction (the route) of the line, for example when a conflict arises with a country whose territory is used (crossed) by the gas line.

A1.4 Formulas for estimation and computation (in metric system)

The following formulas have been developed or used by the author. They allow you to calculate different variants.

1. The cross-section area and weight of a starting (acceleration) cable of constant cross-section area can be found from equation (balance, equilibrium) inertia

force to cable stress:

$$S = mng/(\delta - ngyL), \quad W = SL\gamma, \quad (\text{A1.1})$$

where S is the cross-section area of cable area [m^2]; m is the mass of apparatus [kg]; n is the overload; δ is the tensile stress [N/m^2]; γ is the specific density [kg/m^3]; L is the distance between power stations [m]; W is the cable weight [kg]; $g = 9.81 \text{ m/s}^2$.

2. Cross-section area S_o and weight W_o of a transportation cable supported by wings are:

$$S_o = (D + m/K_1)/(\sigma - \gamma L/K_2), \quad (\text{A1.2})$$

$$W_o = S_o \gamma L, \quad (\text{A1.3})$$

where K_1 is the ratio of lift force to drag force of the winged container ($K_1 = 10 - 17$), K_2 is the ratio of lift force to drag force of the support cable wing, D is the drag of cable. The cable drag is small. Results of computation for $D = 0$ presented in Figs. A1.4 and A1.5.

Equation (A1.2) gives a maximum cable distance L supported by wings

$$L = KK_2, \quad (\text{A1.4})$$

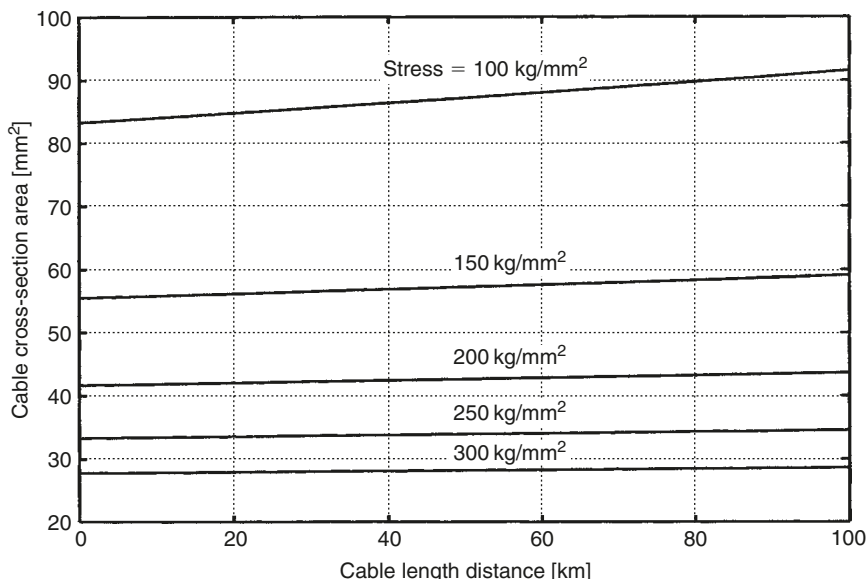


Fig. A1.4. Cable cross-section area versus distance 0–100 km for safe tensile stress 100–300 kg/mm^2 . Airplane mass is 100 ton. Cable specific density is 1800 kg/m^3 . Airplane ratio of lift/drag is 12. Support wing ratio of lift/drag is 20. Cable drag is 0.

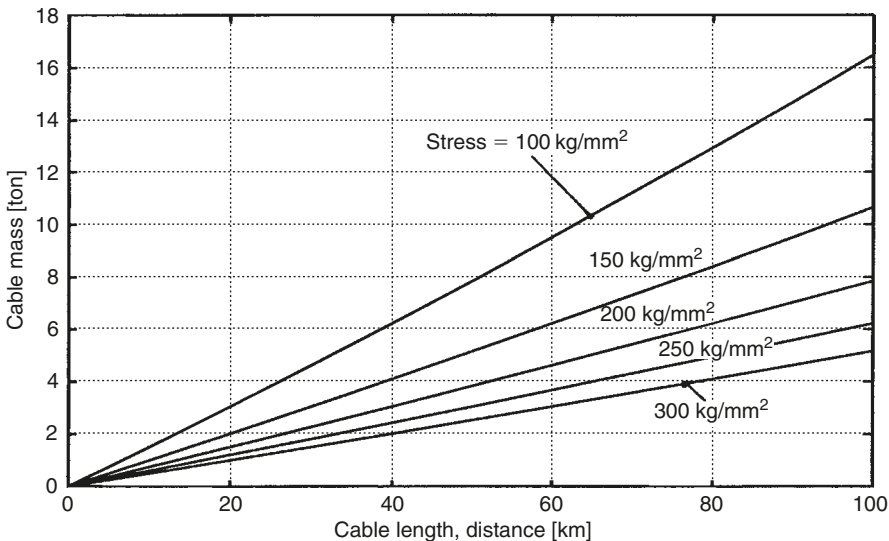


Fig. A1.5. Cable mass versus distance 0–100 km for safe cable tensile stress 100–300 kg/mm². Airplane mass is 100 ton. Cable specific density is 1800 kg/m³. Airplane ratio of lift/drag is 12. Support wing ratio of lift/drag is 20. Cable drag is 0.

where $K = 10^{-7} \sigma/\gamma$ is the stress coefficient. Results of the computation are presented in Fig. A1.6. The other methods of cable support (balloons or columns) do not have this restriction. They may be computed using equations (A1.2)–(A1.3) if $K_2 = \infty$.

3. Energy, E , stored by the rotary flywheel per 1 kg cable [joules/kg] can be found from the known equation of the kinetic energy:

$$E = 2\delta/\gamma. \quad (\text{A1.5})$$

4. Estimation of cable friction due to air. This estimation is difficult because there are no experimental data for air friction of an infinitely thin cable. Let us use the well-known equation for air friction (drag) of a flat plate. This friction (drag) may be turbulent or laminar. Their values are different. The plate has two sides, which means for the cable, the drag value must be halved. For subsonic speed and a flat plate the equations for turbulent and laminar drags are:

$$D_T = 0.0573\rho^{0.8}\mu^{0.2} V^{1.8} L^{0.8} d, \quad (\text{A1.6})$$

$$D_L = 1.04\rho^{0.5}\mu^{0.5} V^{1.5} L^{0.5} d, \quad (\text{A1.7})$$

where D_T is turbulent drag, D_L is laminar drag; ρ , μ are air density and air viscosity respectively; $\rho = 1.225 \text{ kg/m}^3$, $\mu = 1.79/10^5 \text{ kg/m}^2$ at altitude 0 km

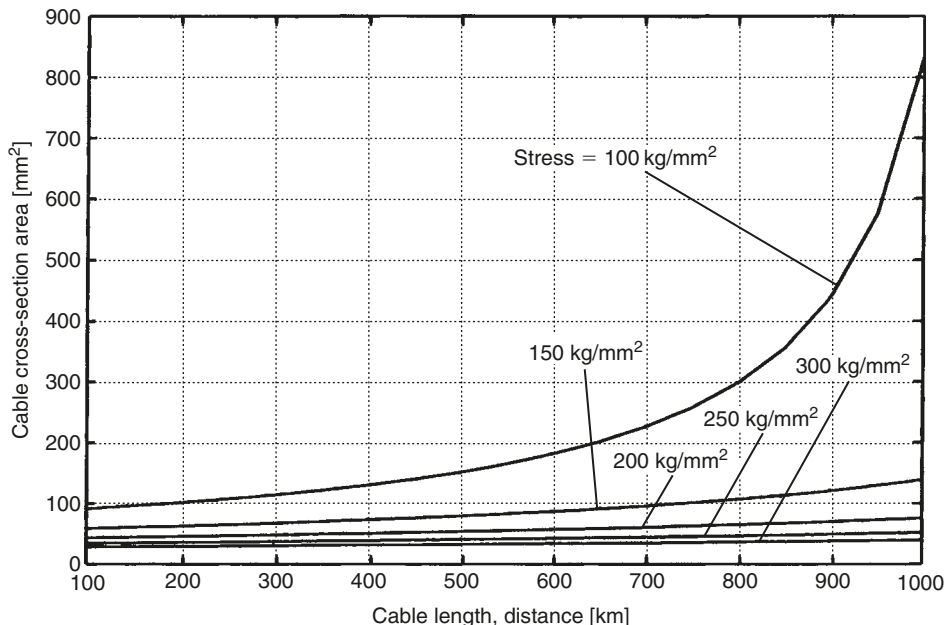


Fig. A1.6. Cable cross-section area versus distance 100–1000 km for safe tensile stress 100–300 kg/mm². Airplane mass is 100 ton. Cable specific density is 1800 kg/m³. Airplane ratio of lift/drag is 12. Support wing ratio of lift/drag is 20. Cable drag is 0.

and $\rho = 0.5258 \text{ kg/m}^3$, $\mu = 1.527/10^5 \text{ kg/m}^2$ at altitude 8 km; V is speed [m/s], L is length of plate (distance between drive station) [m], d is diameter of the cable [m]. It is postulated that the cable surface has a half-laminar boundary layer because a small side wind will blow away the turbulent layer and restore the laminar flow.

$$D = 0.5(D_T + D_L), \quad (\text{A1.8})$$

where D is air drag (friction) [N].

Results of these computations are given in Figs. A1.7–A1.10.

A1.5 Cable problems

The cable problem were discussed in Chapter 1. They are same for all projects in other chapters.

Below, the author provides a brief overview of recent research information regarding the proposed experimental (tested) fibers.

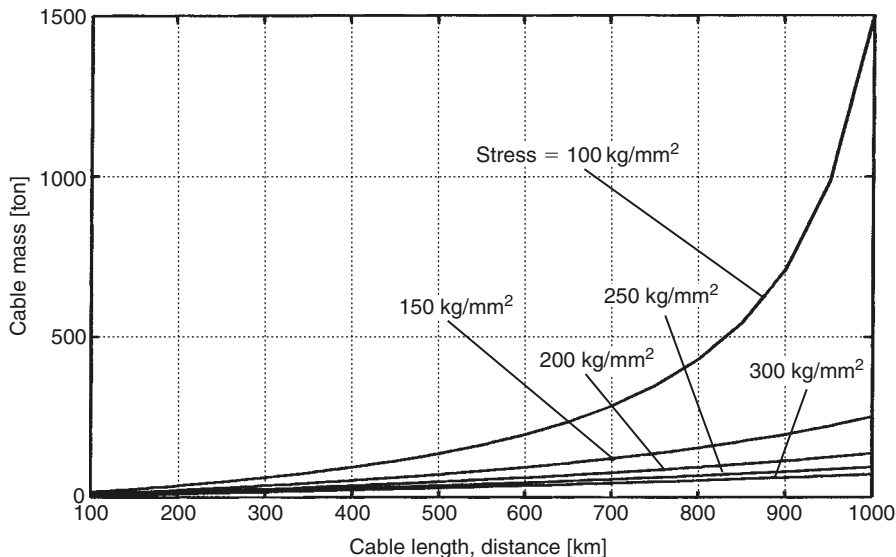


Fig. A1.7. Cable mass versus distance 100–1000 km for safe cable tensile stress 100–300 kg/mm². Airplane mass is 100 ton. Cable specific density is 1800 kg/m³. Airplane ratio of lift/drag is 12. Support wing ratio of lift/drag is 20. Cable drag is 0.

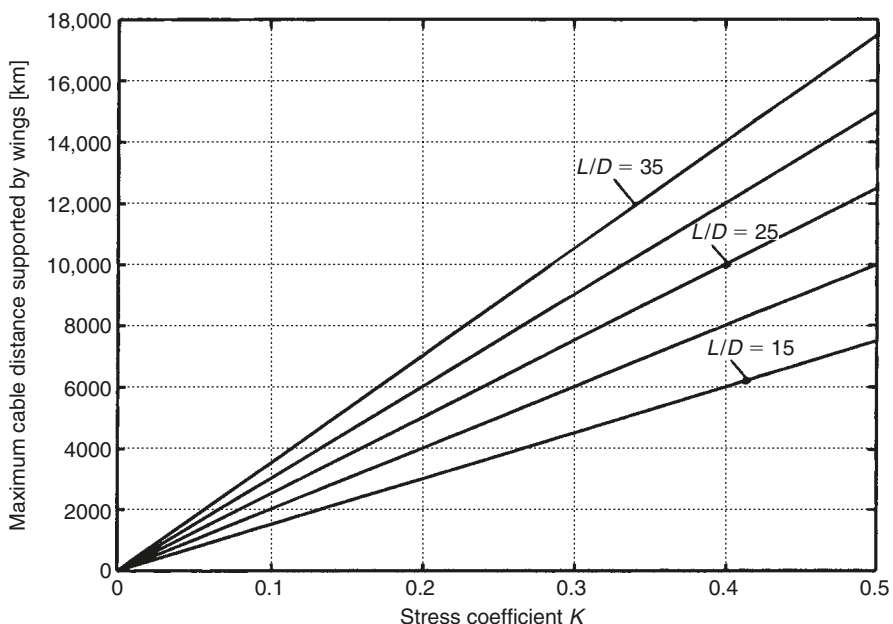


Fig. A1.8. Maximum cable distance supported by wings versus stress coefficient for lift/drag ratio 15, 20, 25, 30, 35.

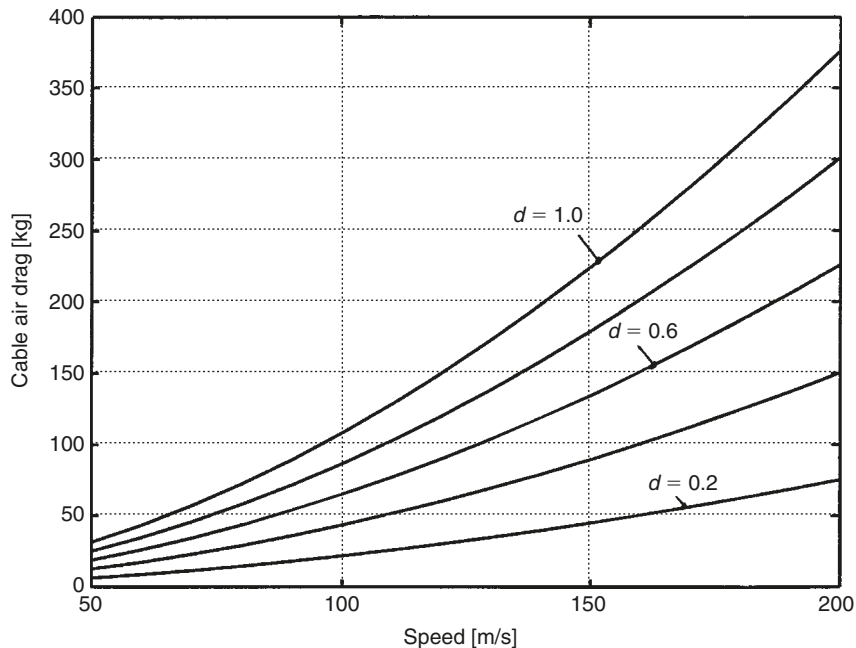


Fig. A1.9. Cable air drag versus speed for cable diameter 0.2, 0.4, 0.6, 0.8, 1.0 cm. Cable length is 100 km. Altitude is 4 km.

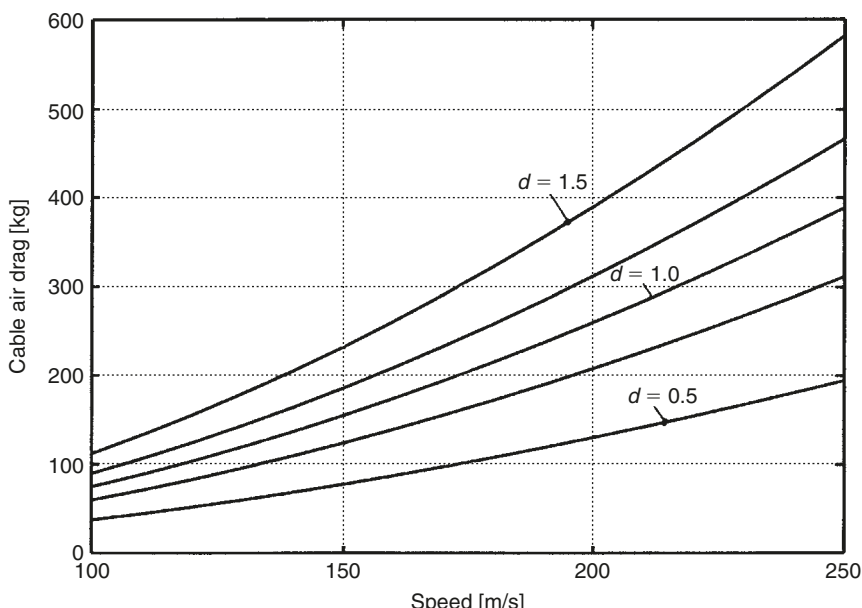


Fig. A1.10. Cable air drag versus speed for cable diameter 0.5, 0.8, 1.0, 1.2, 1.5 cm. Cable length is 100 km. Altitude is 8 km.

A1.6 Data which can be used for computation

Let us consider the following experimental and industrial fibers, whiskers, and tubes (see Chapters 1 and 2):

1. Experimental nanotube carbon nanotube (CNT) has a tensile strength of 200 GPa ($20,000 \text{ kg/mm}^2$), Young's modulus is over 1 TPa, specific density $\gamma = 1800 \text{ kg/m}^3$ (1.8 g/cm^3) (year 2000).

For a safety margin $n = 2.4$, $\sigma = 8300 \text{ kg/mm}^2 = 8.3 \times 10^{10} \text{ N/m}^2$, and $\gamma = 1800 \text{ kg/m}^3$, $(\sigma/\gamma) = 46 \times 10^6$. Single-walled nanotubes (SWNTs) have a density of 0.8 g/cm^3 , multi-walled nanotubes (MWNTs) have a density of 1.8 g/cm^3 . Unfortunately, nanotubes are very expensive at the present time (2002).

2. C_D whiskers have $\sigma = 8000 \text{ kg/mm}^2$ and $\gamma = 3500 \text{ kg/m}^3$ (1989). The computations assume $\sigma = 7000 \text{ kg/mm}^2$, $\gamma = 3500 \text{ kg/m}^3$, and $\sigma/\gamma = 20 \times 10^6$.
3. Industrial fibers have $\sigma = 500\text{--}620 \text{ kg/mm}^2$, $\gamma = 1800 \text{ kg/m}^3$, and $\sigma/\gamma = (0.278\text{--}0.344) \times 10^6$.

A1.7 Projects

Below readers could find some examples of projects which utilize the suggest ideas.

A1.7.1 Project 1: Air line from New York to Washington (340 km)

Let us take one winged cabin (container) with a weight of 100 ton. The payload is 2/3 of the full weight ($66 \text{ ton} \approx 660 \text{ passengers}$). The flight time at a speed of 200 m/s is $28.3 \text{ min} \approx 30 \text{ min}$, or about 100 flights/day (in both directions). The total (maximum) number of passengers is 66,000 or 6600 ton of payload per day. Assuming an aerodynamic efficiency of 16 (ratio of lift/drag), the required thrust is $100/16 = 6.2 \text{ ton}$. We assume a thrust of 10 ton for one direction (including cable drag and drag of the support devices). For safe cable tensile strength $\sigma = 250 \text{ kg/mm}^2$, the required cable cross-section area is 40 mm^2 , the cable diameter is 7.2 mm, and the cable weight is 24.5 ton for a cable density of 1.8 g/cm^3 . The air drag of a cable at an altitude of 7 km is 1.08 ton.

Estimation of drag for the support flight devices assumes the aerodynamic efficiency equals 25. Then the support device drag will be $24.5/25 = 1 \text{ ton}$. The total drag is $6.2 + 1.08 + 1 = 8.28 \text{ ton}$, which is less than the 10 ton of thrust available. The required power is $VT = 200 \times 10,000 \times 10 = 20 \text{ MW}$ or 40 MW for both directions. This equals the power of four 10,000 kW turbo-jet engines.

The winged container has a wing area of 170 m^2 and a wingspan of 42 m.

A1.7.1.1 Production cost of one passenger delivered

Assume the cost of the installation is \$20 million and it has a service life of 20 years. The system requires 40 employees with an average salary of \$50 K/year, the fuel cost is \$0.25/l. The depreciation is \$2750/day, the salary is \$5500/day, and the fuel cost is

\$64,750/day. Assuming 66,000 passengers daily, we find that the delivery production cost is less than \$1/passenger ($64,750/66,000$). If this cost is divided by a loading coefficient of 0.75, the delivery cost is \$1.3/passenger. This is less than a subway fare in New York (\$2, 2005). If a flight fare of \$4.99 is charged, the profit is \$173 K/day or \$63 million/year. You can live in New York and work in Washington, DC. The flight takes about 30 min, which is less than the average transit time of the NY subway.

A1.7.2 Project 2: Airline from New York to Paris (6200 km)

Assume a flight speed of $V = 250 \text{ m/s}$, an altitude of $H = 11 \text{ km}$, and a cable is supported by winged devices. The New York to Paris flight time is $(6,200,000/250) \approx 7 \text{ h}$.

Let us take three winged cabins (containers) for one route, which move simultaneously in one direction. Each cabin has a weight of 100 ton (the payload is 66 ton) and has an aerodynamic efficiency of 16 (ratio of lift/drag). The required cable thrust is about $6.2 \times 3 = 18.6 \approx 20 \text{ ton}$ for one direction or 40 ton for both directions. There are 10 flights/day in one direction and 10 flights in the return direction. The total load capability is $(6600 \times 2) 13,200 \text{ passengers in both direction per day or } 1320 \text{ ton of payload}$.

Assume the cable is manufactured from whiskers, C_D , with a tensile strength $\sigma = 8000 \text{ kg/mm}^2$ and density of 3.5 g/cm^3 . Using a typical safety coefficient (safe margin) of 2.4, the safe tensile strength $\sigma = 3300 \text{ kg/mm}^2$, the cable cross-section area of 12.1 mm^2 , and cable diameter is 4 mm for a thrust of 40 ton in one direction. The cable weight is 262.6 ton (for 6200 km), and the cable drag is 3.3 ton (half the boundary layer is turbulent and half is laminar). If the aerodynamic efficiency of the support devices is 25, their additional drag is $(262.6/25) 10.5 \text{ ton}$. The total drag is $(18.6 + 3.3 + 10.5) 32.4 \text{ ton}$, which is less than the assumed thrust of 40 ton.

The winged cabin is the same as the New York–Washington, DC project. If the support device supports 10 km of cable (424 kg), the required wing area equals 0.743 m^2 , with a wing span of 3.3 m.

The required power is $P = 4,000,000 \times 250 = 100 \text{ MW}$ for one end; that is 10 turbo-jet engines with 10,000 kW of power each.

A1.7.2.1 Economical estimation

The system installation cost is \$30 million with a service lifetime of 10 years. Employee costs assume 100 men with an average salary of \$50 K/year, and fuel cost is \$0.25/l.

Assuming a depreciation of \$8.24 K/day, salaries of \$13.74 K/day, and fuel costs of \$324 K/day; if the average load equals 75% of the maximum load, the number of passengers is 9150/day. The operational cost of the delivery of one passenger is \$38/person or \$0.38/kg. If the fare is \$120, the profit is $80 \times 9150 = \$732 \text{ K/day} = \$266.5 \text{ million/year}$.

More than 90% of this cost is fuel; if aviation fuel is not required, a lower cost fuel (for example natural gas) can reduce operational costs in proportion to the reduced cost of the fuel.

A1.7.3 Project 3: Air bridge

There are a lot of islands in the world, located close to one another or located close to a continent, which have large transportation flows. For example:

1. Straits of Gibraltar (16 km); connects Europe with Africa.
2. English Channel (40 km); connects England with Europe.
3. Sicily and Italy (5 km).
4. The Dardanelles (2 to 5 km).
5. Various Japanese Islands.
6. Taiwan with mainland China (25 km).
7. Bering Straits (100 km) (Russia and America).
8. Sakhalin–Asia (20 km) (Russia).

An estimation of the main parameters for a Gibraltar air bridge (16 km) are presented, this estimation is similar for the English Channel or the other bridges listed above.

The main parameters are computed for the following daily load flow (same in both directions):

1. 1000 cars, the weight of each is 1 ton, total is 1000 ton.
2. 1000 trucks, the weight of each is 10 ton, total is 10,000 ton.
3. 10,000 people, the weight of each is 100 kg, the total is 1000 ton.

The total daily load flow in one direction is 12,000 ton, for a total load flow of 24,000 ton.

Let us assume the average payload of a winged container is 2/3 of its maximum payload capability. The total payload capability of the winged container is 300 ton, thus the average payload is 200 ton for one container. Then we will need $(12,000/200) = 60$ flights/day in each direction.

Let us assume a flight (cable) speed of 100 m/s (speeds up 250 m/s can be used). The flight takes $(16,000/100) 160$ s (about 3 min) in one direction; the English Channel transit time (40 km) will be 7 min with a speed of 100 m/s and 3 min with a speed of 250 m/s.

If the loading of the winged container takes 25 min, one wing container can make 50 flights/day. For 120 flights we will need 3 winged containers.

Estimates for the cables assume they are manufactured from fibers which have a tensile strength $\sigma = 620 \text{ kg/mm}^2$ and density of 1.8 g/cm^3 (for example, QC-8805). Let us use a safety coefficient of 2.4, then the safe $\sigma = 250 \text{ kg/mm}^2$. Let us use an aerodynamic efficiency (ratio of lift/drag) of 12 (current airplanes are up to 17, and gliders up to 40). Then the drag of the container is $(300/12) 25$ ton. This is increased to 30 ton (we assume

about 2–3% cable air drag plus 1–2% drag from the flight support devices). The cross-section area of the cable is $(30,000/250) 120 \text{ mm}^2$, and the cable diameter $d = 12.4 \text{ mm}$. The weight of two cable branches (32 km) is $6912 \text{ kg} \approx 7 \text{ ton}$. If the aerodynamic efficiency of the flight support devices equals 20–30 the additional drag will be $7000/20 = 350 \text{ kg}$ or $350/30,000 = 0.012 = 1.2\%$ of the total thrust.

The required energy impulse $N = 300,000 \text{ N} \times 100 \text{ m/s} = 30 \text{ MW}$ over a 160 s period. If we use an inertial accumulator of energy and the flight frequency is 12 min, we will need an engine with a steady state power output of $N = 30 \times 160/12 \times 60 = 6670 \text{ kW}$; this is equivalent to one turbo engine. The weight of the inertial accumulator of energy (constructed from fibers) is $30 \times 160/0.75 = 6400 \text{ kg} = 6.4 \text{ ton}$.

Estimations of acceleration system requirements assume an acceleration for takeoff and landing of $a = 0.5g = 5 \text{ m/s}^2$. Takeoff and landing distance $L = V^2/2a = 10,000/10 = 1000 \text{ m} = 1 \text{ km}$. The thrust required for acceleration is $T = Wa/g = 300 \times 5/10 = 150 \text{ ton}$. The cable has a cross-section area of $(150,000/250) 600 \text{ mm}^2$, a diameter of 28 mm^2 , and a weight of 4320 kg .

Estimation of the support flight devices assumes that one device supports 1 km of cable. The weight of 1 km of cable with a cross-section area of 120 mm^2 is 216 kg . If the lift coefficient is 1, the necessary wing area is 0.42 m^2 , resulting in a wing size of $2 \times 0.2 \text{ m}$.

Data on the flight container assume the wing area is 480 m^2 , the wing span is 80 m ($80 \times 6 \text{ m}$), the size of the container is $10 \times 5 \times 86 \text{ m}$, the useful area of the floor is 500 m^2 , and the useful volume is 2500 m^3 .

For the suggested bridge we need only 11.4 ton of cable, 3 winged containers, a 6700 kW engine, an inertial accumulator of energy with a disk weight of 6.4 ton, and two simple ports with 1 km of runway length. The bridge system would cost \$10–30 million and require 6 months for construction. The English Channel tunnel costs some billions of dollars, construction took many years, and delivery transit time is more than 0.5 h. If the tunnel is damaged, the repair will be very expensive and take a long time.

A1.7.3.1 Economic estimation

Let us assume the cost of the air bridge is \$15 million (winged containers, engines, fly-wheels, and departure and arrival stations) and has a service life of 15 years (depreciation is \$1 million/year). Employee costs assume 80 people with an average salary of \$50 K/year (maintenance is \$5 million/year, \$14 K/day), and fuel costs of \$0.25/l (\$10,850/day). The total load flow is 24,000 ton/day. The direct operating costs will be less than \$2/ton (\$2/car). If the toll charge for using the bridge is \$5 from 1 car (1 ton), the profit will be \$13 million/year.

A1.7.4 Project 4: Ground vehicles (for example, auto highway)

Assume a closed-loop ground cable section with a length of 100 km in one direction. The cable is made of fibers with a safe tensile strength $\sigma = 250 \text{ kg/mm}^2$ and a density of 1.8 g/cm^3 . Also assume 1000 cars, weighing 1 ton each, connected to the line in one

direction. Using an average friction coefficient of 0.05 requires a cable thrust of (1000×0.05) 50 ton. The cable cross-section area is $(50,000/250)$ 200 mm^2 , the cable diameter is 16 mm, and the cable weight (200 km) is 72 ton.

It may be shown that roller friction (ball bearing), and air friction (speed 30 m/s) will account for less than 3% of the total thrust.

The energy required to move 1000 ton at a speed of 30 m/s (108 km/h or about 70 miles/h) is $(500,000 \times 30)$ 15 MW at each end of the section (the total is 30 MW) (three turbo engines of 10,000 kW each are required for the two ends). This system may be used for highways or as an internal city system.

A1.7.5 Project 5: Gas line of the 2000 km (1250 miles) and capability of carrying 20 billion cubic meters/year

There is a big demand for gas pipelines, for example, in the connection of Alaska to the USA or Russia to Europe. A ground-based gas (oil) pipeline is very expensive, requires years for building, and damages the environment. Often they cross the territory of other country, which may steal gas or oil or to capture the pipeline.

A1.7.5.1 Technical data

Assume that a gas balloon (airship, dirigible) has a volume of 10^4 m^3 (diameter 11.3 m, length 115 m) (the balloon can have wings). The line has length 2000 km, speed 35 m/s, and balloons are connected every 500 m. The delivery time is 19 h (delivery time by pipeline is 3–5 times more, oil line is 30–50 times more).

It is then easy to calculate than the transit capability of this gas line is about 20 billion cubic meters/year.

The line contains 4000 balloons and one middle drive station. The cable has a safe tensile strength of 200 kg/mm^2 , the cross-section area of the cable is 150 mm^2 , its diameter is 14 mm, and the cable weight is 1080 ton.

The total balloon drag is 60 ton, the total cable drag is 1.3 ton. The total power of 3 engines is 18,000 kW (which is the power of three aviation gas turbines). The density of natural gas is 0.72 kg/m^3 , the density of air is 1.225 kg/m^3 , and the payload lift force of each balloon is about 3–4 ton.

A1.7.5.2 Economical estimation

The balloon area is 3140 m^2 , and its weight is 500 kg. Assume 1 m² a balloon film (cover) costs \$0.15, then balloons will cost is about \$2000 each. The total cost of 4000 balloons is then \$8 million. If 1 kg cable costs \$1, the cable cost is about \$1 million. Let us include two engines (gas turbines) and departure and arrival ports. The total installation cost is \$15 million and its lifetime is 15 years. The depreciation is \$1 million/year.

Taking a maintenance cost \$2 million/year, and gasoline cost of \$0.25/l, the fuel cost is \$30 K/day or \$10 million/year. The total annual expense is \$13 million/year. Some 77% of this expense is the cost of the fuel (gasoline for driving).

The production delivery cost of 1000 m^3 of gas is $\$0.7/1000\text{ m}^3$ for a distance of up to 2000 km (1250 miles). If the fee for the delivery of 1000 m^3 gas is $\$1$, the profit is $\$18.6$ million/year. We can reduce the production delivery cost if we use the wind energy.

A1.7.5.3 Additional possibility

Every balloon can lift 2–3 ton of useful loads. This means we can deliver about 15,000 ton of payload (for example, oil) per day in one direction.

A1.8 Conclusion

The proposed method and installation for transportation are significantly cheaper than the current methods of flying traditional airlines, are constructing bridges, tunnels, and gas pipelines. This system would dramatically reduce the price of flights on conventional airlines; the cost and time of construction of long bridges, or tunnels; and put into practice huge projects such as connections between Europe and Africa across Gibraltar, Russia and America across the Bering Straits, Russia–Japan across Sakhalin, Taiwan with mainland China, and so on. It would reduce the cost and construction time of gas pipelines too, and save the environment.

The author has detailed solutions for many problems which seem difficult using current technology. He is prepared to discuss the project details with serious organizations that have similar research and development goals.

US Patent 6,494,143 B1. Patent applications are 09/974,670; 09/873,985; 09/789,959; 09/978,507 (2001). The closed ideas are in Refs.^{4–12}

References

1. A.A. Bolonkin, “Air Cable Transport”, *Journal of Aircraft*, Vol. 40, No. 2, July–August 2003, pp. 265–269.
2. A.A. Bolonkin, “Bolonkin’s Method Movement of Vehicles and Installation for It”, US Patent 6,494,143 B1, Priority is on 28 June 2001.
3. A.A. Bolonkin, “Air Cable Transport and Bridges”, TN 7567, *International Air & Space Symposium – The Next 100 Years*, 14–17 July 2002, Dayton, OH, USA.
4. A.A. Bolonkin, “Non-Rocket Missile Rope Launcher”, IAC-02-IAA.S.P.14, *53rd International Astronautical Congress, The World Space Congress – 2002*, 10–19 October 2002, Houston, TX, USA.
5. A.A. Bolonkin, “Inexpensive Cable Space Launcher of High Capability”, IAC-02-V.P.07, *53rd International Astronautical Congress, The World Space Congress – 2002*, 10–19 October 2002, Houston, TX, USA.
6. A.A. Bolonkin, “Employment Asteroids for Movement of Space Ship and Probes”, IAC-02-S.6.04, *53rd International Astronautical Congress, The World Space Congress – 2002*, 10–19 October 2002, Houston, TX, USA.

7. A.A. Bolonkin, "Non-Rocket Space Rope Launcher for People", IAC-02-V.P.06, *53rd International Astronautical Congress, The World Space Congress – 2002*, 10–19 October 2002, Houston, TX, USA.
8. A.A. Bolonkin, "Non-Rocket Earth–Moon Transport System", COSPAR-02 B0.3-F3.3-0032-02, 02-A-02226, *34th Scientific Assembly of the Committee on Space Research (COSPAR), The World Space Congress – 2002*, 10–19 October 2002, Houston, TX, USA.
9. A.A. Bolonkin, "Non-Rocket Earth–Mars Transport System", COSPAR-02 B0.4-C3.4-0036-02, *34th Scientific Assembly of the Committee on Space Research (COSPAR), The World Space Congress – 2002*, 10–19 October 2002, Houston, TX, USA.
10. A.A. Bolonkin, "Transport System for delivery Tourists at Altitude 140 km", IAC-02-IAA.1.3.03, *53rd International Astronautical Congress, The World Space Congress – 2002*, 10–19 October 2002, Houston, TX, USA.
11. A.A. Bolonkin, "Asteroids as Propulsion Systems of Space Ships", *Journal of British Interplanetary Society*, Vol. 58, 2003, pp. 97–107.
12. A.A. Bolonkin, "Kinetic Anti-Gravitator", AIAA-2005-4505, *41st Propulsion Conference*, 10–12 July 2005, Tucson, AZ, USA.

ATTACHMENT 2

High-Speed Catapult Aviation*

Summary

The current passenger-transport aviation systems have reached the peak of their development. In the last 30 years there has been no increase in speed or reductions in trip costs. The aviation industry needs a revolutionary idea, which allows jumps in speed and delivery capability, and dramatic drops in trip price. The author offers a new idea in aviation in which flight time practically does not depend on distance (it is the same for lines from New York to Washington as from New York to Paris), and vehicle load capability doubles and which has a drive engine that is located on the ground and can use any cheap source of energy.

A2.1 Introduction

Current takeoff mass of a long-distance aircraft is made up of approximately 1/3 aircraft body, 1/3 fuel, and 1/3 payload. The aircraft engine needs expensive aviation fuel. The passenger-transport aircraft cannot exceed the speed of sound. The “Concorde” history shows that the conventional passenger supersonic aircraft is unprofitable. The hypersonic aircraft, which is under development by the USA, will be more unprofitable as a passenger long-distance aircraft because it will use very expensive hydrogen fuel, it is very complex, and it has a high production cost. The hypersonic engine problems have not been solved in spite of spending tens of million dollars in research and testing. Aviation needs new ideas which increase speed, load capability, and reduce a delivery cost. Some of these ideas have been published by the current author.¹⁻⁷

The author's idea is the acceleration of a flight vehicle (non-engine aircraft) to high speed using a cable engine located on the ground. The vehicle will then use its kinetic energy for flight. The computation shows that a kinetic aircraft accelerated to subsonic speed of 270–300 m/s can fly 60–80 km until its speed decreases to a landing speed of 50–60 m/s. This is far enough for suburban transport or for air bridges across the Straits of Gibraltar,

* See detailed manuscript AIAA-2005-6221, *Atmospheric Flight Mechanic Conference – 2005*, 15–18 August, USA.

English Channel, Bering Straits (Russia–America), Sakhalin–Asia, Russia–Japan, etc. For acceleration to this speed at a rate this is acceptable to passengers ($3g$) the runway length must be 1.5 km (current runways for large aircraft are 1.5–3-km long). For the long-distance flight (6000–8000 km), the air vehicle must be accelerated to a speed of 4–4.5 km/s. For acceleration of no more than $3g$ the required runway length would then be 290–340 km. It is constructed using the methods described in Refs.^{5,7} Rather than being a conventional runway, it is an air cable acceleration system^{5–7} for the acceleration of space vehicles and it is located in atmosphere.

A2.2 Brief description of the innovation

This system for kinetic vehicles (KV) includes (Fig. A2.1) a chain made of closed-loop cables and drive stations. A subsonic system (Fig. A2.1(b)) may be located on the surface or underground and a high-speed (up to hypersonic speed) system (Fig. A2.1(a)) is located above ground.^{5–7} The chain is supported in the air by flight devices^{1–7} or by columns with rollers. Drive stations have engines located on the ground and work on any cheap energy.

The system works in the following way. The subsonic aircraft starts from a conventional aerodrome, and is accelerated (with $3g$) up to a speed of 270–300-m/s (Mach number 0.9) by the drive station on the runway which is 1200–1500 m long (Fig. A2.1(b)). The aircraft takes off, flies (50–70 km, Figs. A2.1(c) and A2.2), gradually loses speed and increases its attack angle. When the speed drops so it is close to landing speed, the aircraft lands.

The high-speed aircraft also starts from a conventional aerodrome, lifts off the ground at takeoff and is accelerated up to a speed of 1000–5000 m/s in air by the ground drive stations. The acceleration distance (with $3g$) may be 13–400 km (depending on the final speed, see Figs. A2.4 and A2.5). This is not a problem because acceleration is made in the air (Fig. A2.1(a)).

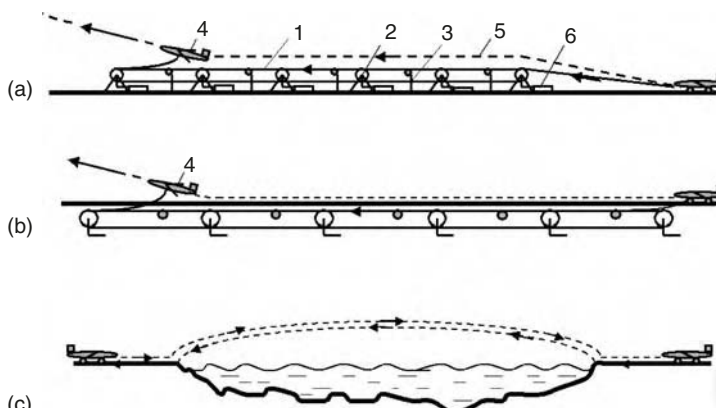


Fig. A2.1. Drive system for acceleration of kinetic aircraft. (a) Hypersonic and supersonic aircrafts. (b) Subsonic aircraft. Notations: (1) Chain of closed-loop cables; (2) drive stations; (3) support column with roller; (4) flight vehicle; (5) trajectory of flight vehicle; and (6) engine of drive station. (c) Kinetic subsonic aircraft as an air bridge across a stream.

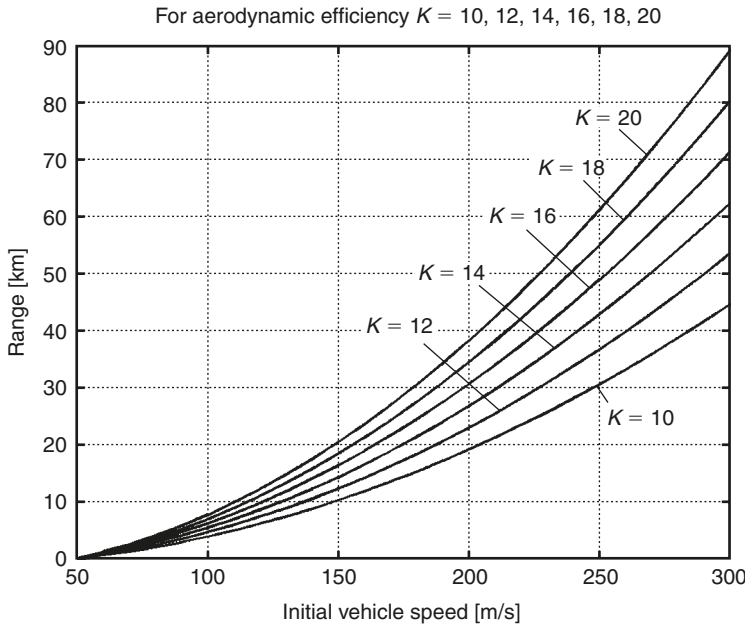


Fig. A2.2. Range of the subsonic kinetic aircraft versus initial speed for different aerodynamic efficiency $K = 10, 12, 14, 16, 18, 20$.

The range of the high-speed aircraft may reach 200–8000 km (see Fig. A2.3). The aircraft can make a full circle and return to its base (see Figs. A2.8 and A2.9). The flight data are significantly improved if the vehicle has variable wing area or variable swept wings.⁵ Other similar ideas and useful points for kinetic aviation are presented in Refs.^{5–7} The flight altitude does not influence its range because the energy spent in climbing will be returned in gliding.

A2.3 Theory of KV and a general estimation of flight data (in metric system)

A2.3.1 Maximum range

The *maximum range*, R , of kinetic air vehicles is obtained from the kinetic energy of theoretical mechanics. It is equals:

$$\begin{aligned} d\left(\frac{mv^2}{2}\right) &= \frac{mg}{K} dR, \quad g = g_0 - \frac{V^2}{R_0}, \\ R &= -\frac{KR_0}{2g_0} \ln \frac{g_0 - V_1^2/R_0}{g_0 - V_0^2/R_0}, \quad R \approx \frac{K}{2g} (V_1^2 - V_0^2), \end{aligned} \quad (\text{A2.1})$$

where R is range [m]; $R_0 = 6378 \times 10^6$ is the Earth's radius [m]; K is the average aerodynamic efficiency ($K = 10$ –20 for subsonic air vehicles and $K = 5$ –8 for supersonic air vehicles. For example: the subsonic Boeing-747 has maximum $K = 16$, the supersonic

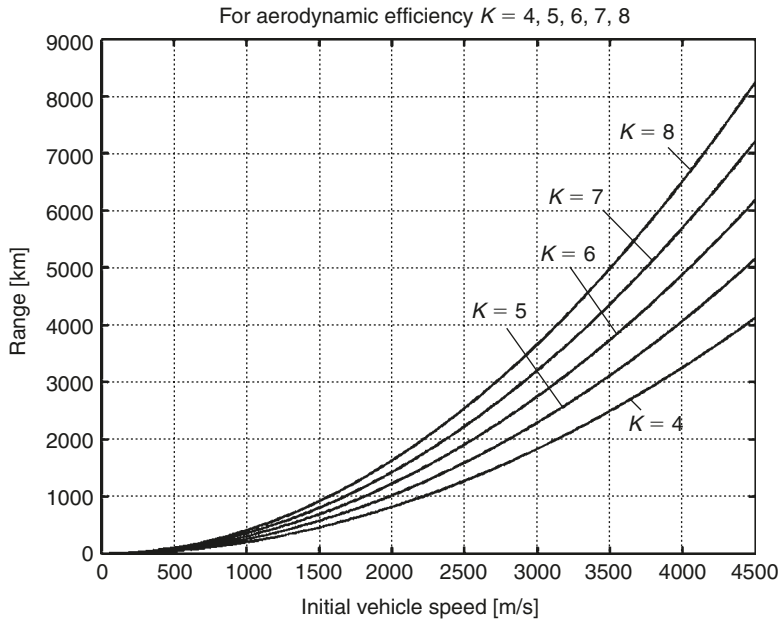


Fig. A2.3. Range of the supersonic kinetic aircraft versus initial speed for different aerodynamic efficiency $K = 4, 5, 6, 7, 8$.

“Concorde” has maximum $K = 7.5$, the supersonic aircraft XB-70 and YF-12 have $K = 7$, and Boeing-2707-300 has $K = 7.8$); $g_0 = 9.81 \text{ m/s}^2$ is gravity; V_1 is initial (after acceleration) speed [m/s]; $V_0 < V_1$ is final (near-landing) speed [m/s] ($V_0 = 50\text{--}60 \text{ m/s}$); and V is variable speed, $V_0 < V < V_1$ [m/s]. For estimation $V = 0.5(V_1 + V_0)$; $mg/K = D$ is air drag [N]; and m is vehicle mass [kg]. For $V < 2000 \text{ m/s}$, variable gravity $g \approx g_0$. Last equation in (A2.1) is obtained from the first equation using integration.

Results of computations for subsonic ($V < 300 \text{ m/s}$; $M < 0.9$, M is Mach number) and supersonic vehicles are presented in Figs. A2.2 and A2.3. The range of a subsonic vehicle is 45–90 km for $V_1 = 300 \text{ m/s}$ and the range of a supersonic vehicle can reach 4000–8200 km for $V_1 = 4500 \text{ m/s}$.

A2.3.2 Maximum acceleration

The *maximum acceleration* distance can be calculated using the equation:

$$S = \frac{V_1^2}{2gn}, \quad (\text{A2.2})$$

where n is overload, g . Results of computations for subsonic and supersonic aircraft are presented in Figs. A2.4 and A2.5.

Acceleration ($3g$) distance is 1500 m for a speed of 300 m/s for the subsonic vehicle and 340 km for a speed of 4.5 km/s for the supersonic vehicle.

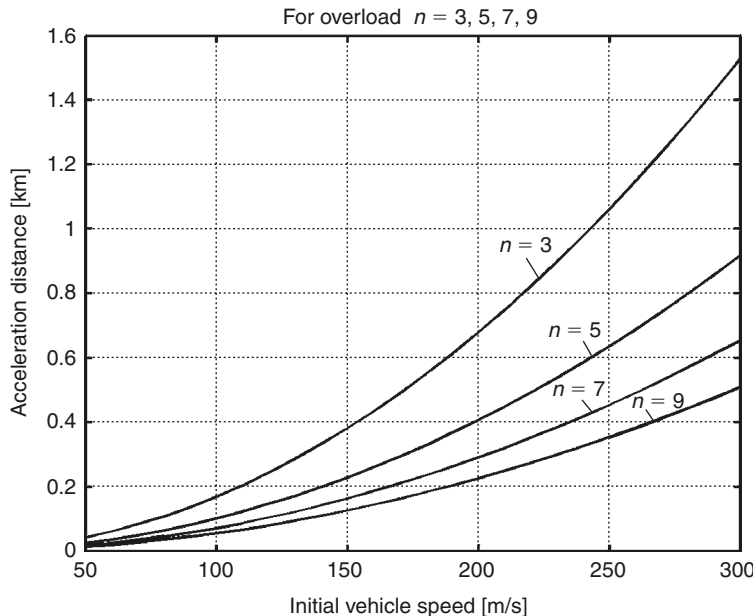


Fig. A2.4. Acceleration distance of subsonic kinetic aircraft versus initial speed and different overloads.

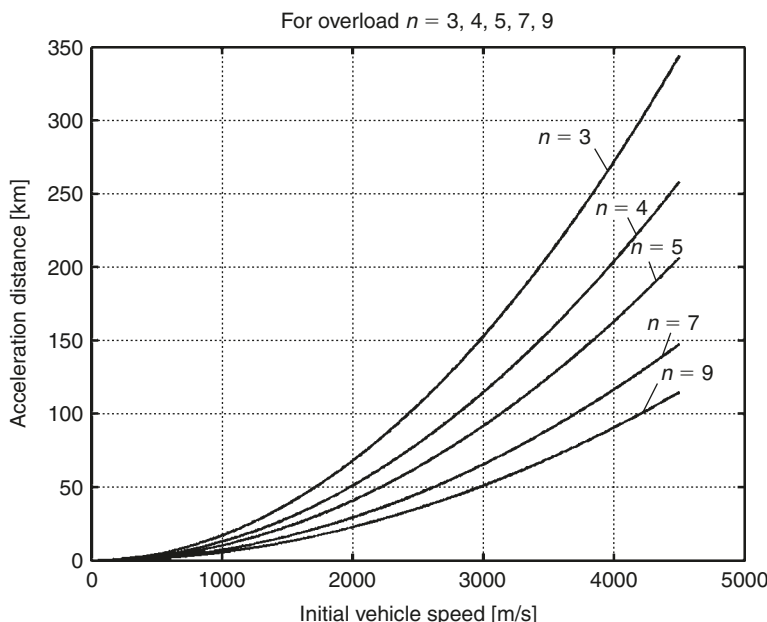


Fig. A2.5. Acceleration distance of supersonic kinetic aircraft versus initial speed and different overloads.

A2.3.3 Average speed

The *average speed* and flight time are:

$$V_a = \frac{V_1 + V_0}{2}, \quad T = \frac{R}{V_a}. \quad (\text{A2.3})$$

The results of computation are presented in Figs. A2.6 and A2.7. The subsonic vehicle has an average speed 1.5 times greater than conventional aircraft (because the KV has high subsonic speed of the beginning), and the average speed of the supersonic (hypersonic) vehicle is more than 6–9 times that of a conventional subsonic vehicle. The flight time is less for both cases.

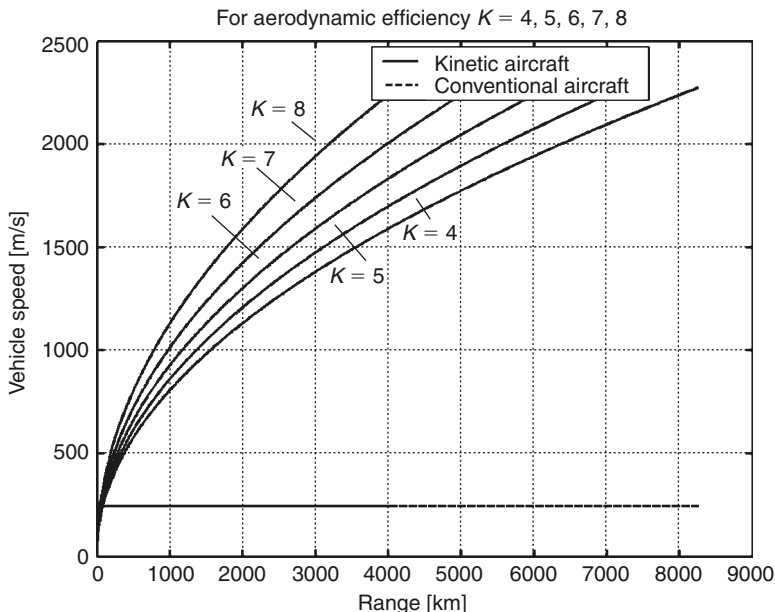


Fig. A2.6. Average speed of the kinetic and conventional aircraft versus range for different aerodynamic efficiency $K = 4, 5, 6, 7, 8$.

A2.3.4 Horizontal turn

The trajectory of *horizontal turn* can be found from the following differential equations:

$$\begin{aligned} \dot{V} &= -\frac{gn}{K}, \quad \dot{\varphi} = \frac{L_1}{mV} = \frac{g\sqrt{n^2 - 1}}{V}, \\ \dot{x} &= V \cos \varphi, \quad \dot{y} = V \sin \varphi, \quad \text{or} \\ V &= V_1 - \frac{gn}{K} t > V_0, \quad \varphi = -\frac{K\sqrt{n^2 - 1}}{n} \ln \left(1 - \frac{gn}{K} t \right), \\ \dot{x} &= V \cos \varphi, \quad \dot{y} = V \sin \varphi, \end{aligned} \quad (\text{A2.4})$$

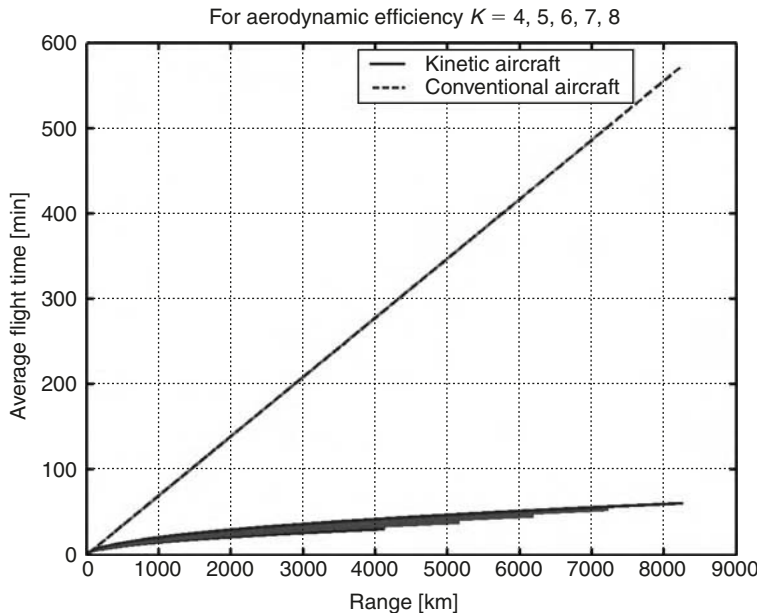


Fig. A2.7. Average flight time of the kinetic and conventional aircraft versus range.

where L_1 is the projection of the vehicle lift force to a horizontal plane (vertical overload: t is time [s] and φ is turn angle [rad]).

Results of computations for different overloads are presented in Figs. A2.8 and A2.9. They show that the vehicle can turn back and return to its original aerodrome (for example a bomber after a flight into enemy territory).

A2.4 Advantages

The offered method has the following advantages:

1. The load capability of kinetic aircraft increases as a factor of 2 (no fuel or engine in the aircraft).
2. The kinetic aircraft is significantly cheaper than conventional aircraft (no aviation engine which is very expensive and has limited resources).
3. The engine located on the ground can work on cheaper fuel (for example natural gas, gasoline, diesel fuel, electricity).
4. The average speed for long-distance travel is increased by 6–9 times (see Fig. A2.6).
5. The maximum flight time is about 55 min for a distance at 8000 km (see Fig. A2.7).
6. The flight production cost is dramatically reduced.

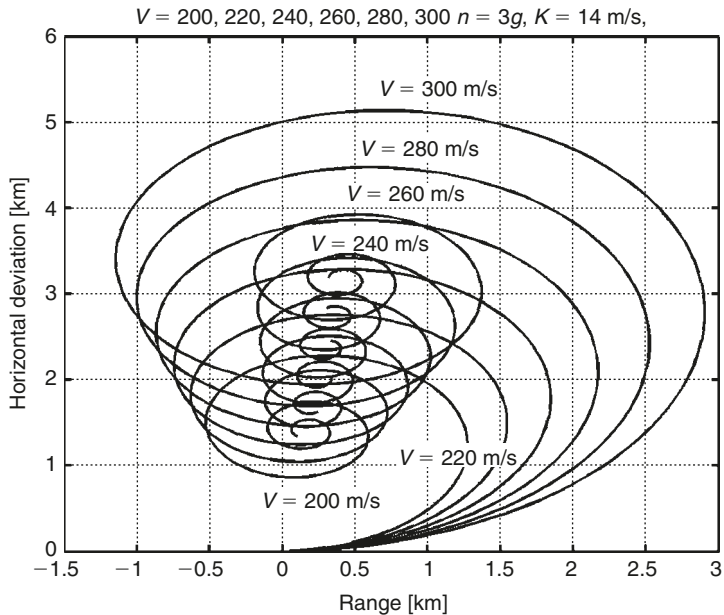


Fig. A2.8. Horizontal deviation versus range of the subsonic KV for initial speed $V = 200, 220, 240, 260, 280, 300$ m/s, horizontal overload $n = 3g$, and aerodynamic efficiency $K = 14$.

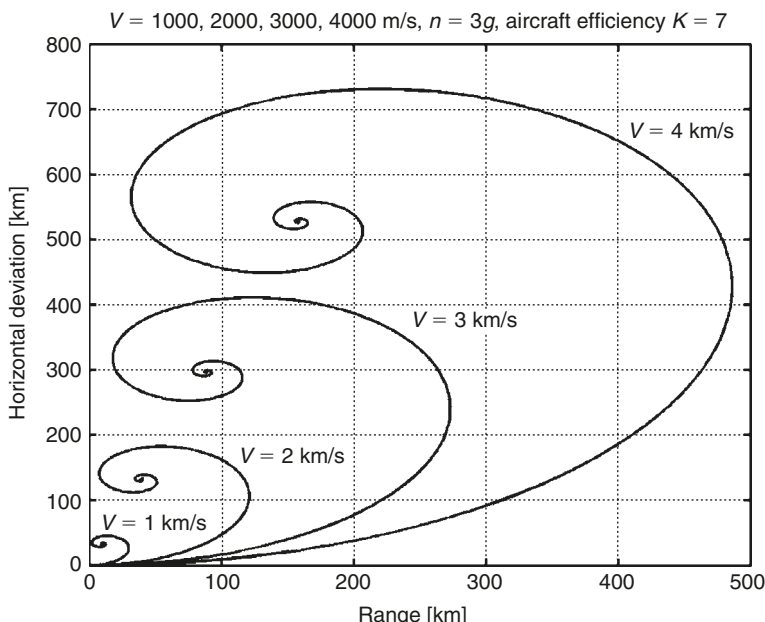


Fig. A2.9. Horizontal deviation versus range of the supersonic KV for $V = 1, 2, 3, 4$ km/s, horizontal overload $n = 3g$, and aerodynamic efficiency $K = 7$.

7. One installation can have a very large capability and can serve many airlines, for example, most airlines from USA to Europe (New York to London, Paris, Berlin, Madrid, Brussels, etc.). The load capability is also increased greatly.
8. The installation can be used to launch of satellites and probes (some projects currently offered use conventional airplanes but they have a maximum speed of only 270 m/s).
9. The installation can be used for space tourism and flights along high-altitude ballistic trajectories.

A2.5 Project

Assume the mass of the space vehicle is $m = 15$ ton (100 passengers and 4 members of crew) and the acceleration is $a = 3g$ (this acceleration is acceptable for conventional people). The range is approximately 7200 km (see Fig. A2.3) or calculate using $R \approx KV^2/2g$ for a final acceleration speed of 4.5 km/s and $K = 7, g = 9.81$ m/s².

The request acceleration distance is $S = 340$ km. The time of horizontal acceleration is $t = (2S/a)^{0.5} = 150$ s = 2.5 min. Assuming it uses the artificial cheap fiber ($\sigma = 600$ kg/mm²) widely produced by current industry, a safe tensile strength of the vehicle cable is $\sigma = 180$ kg/mm² (the safety factor is 600/180 = 3.33), density $\gamma = 1800$ kg/m³ ($K_1 = 180/1800 = 0.1$). Then the cross-section area of the vehicle cable around the vehicle will be $S_1 = 3m/\sigma = 250$ mm², and the cable diameter is $d = 18$ mm. Let us assume that the drive stations are located every 10 km²¹. It therefore needs 34 drive stations. The mass of the cable is $M = 1.5S_1\gamma L_d = 6750$ kg. Here $L_d = 10$ km is the distance between drive stations. A directive cable⁷ and a variable cross-section area of the main cable are included in the coefficient 1.5.

The energy required for acceleration of the aircraft and the cable is $E = (m + M)V^2/2$. This is about 220 GJ (1 GJ = 10^9 J) if $V = 4.5$ km/s. The drag of the aircraft and cable is about $D = 3$ ton, which means $E = DL = 3 \times 10^4 \times 390,000 = 11.7$ GJ. If the launches are made every 0.1 h the engines must have a total power of about $P = E/t = 231.7 \times 10^9/60 = 643,600$ kW distributed between the 34 drive stations (which is 18,900 kW each). If the engine efficiency is $\eta = 0.3$ the fuel consumption will be $F = E/\varepsilon/\eta = 232 \times 10^9/\varepsilon/0.3 = 18.4$ ton/flight. Here $\varepsilon = 42 \times 10^6$ [J/kg] is the energy capability of diesel fuel. This means that 184 kg of fuel is used for each passenger.

If safe tensile strength is $\sigma = 180$ kg/mm² = 1.8×10^9 N/m², $\gamma = 1800$ kg/m³, then the total weight of the flywheels (as storage energy) will be about $M_w = 2E\gamma/\sigma = 2 \times 232 \times 10^9 \times 1800/1.8 \times 10^9 = 835$ ton or $835/34 = 25.6$ ton for each drive station (see more details in Ref.⁷).

A2.5.1 Economical efficiency

Assume a cost of \$500 million for the installation (see Ref.⁸), a lifetime of 20 years, and an annual maintenance cost of \$5 million. If 100 passengers are launched on every flight, there are 10 flights every hour for 350 days a year and the load coefficient is 0.75, then $= 100 \times 10 \times 24 \times 350 \times 0.75 = 6,300,000$ passengers will be launched per year

Table A2.1. Cost of mechanical energy for different fuels.

No.	Fuel	Price [\$/kg]	Energy [J/kg]	Price of 10^6 J [\$]	Conventional coefficient	Cost of mechanical energy [\$/ 10^6 J]
1	Liquid	0.3	43×10^6	0.007	0.3	0.0233
2	Natural gas	0.2	45×10^6	0.0044	0.3	0.0147
3	Coal	0.035	22×10^6	0.0016	0.3	0.0053
4	Electricity	0.06 kWh	–	0.0167	0.95	0.0176

Source: Internet, Cost of fuel, July 2003.

(one installation can serve many lines, for example, New York to London, Paris, Berlin, Rome, etc.). The launch cost per passenger is $\$30,000,000/6,300,000 = \4.76 plus fuel cost. If 184 kg of fuel is used for 1 passenger and the liquid fuel price is \$0.25/kg, then the cost is \$46 for liquid fuel. The total production cost will be about \$53/person for liquid fuel. If the ticket costs \$153, then the profit will be about \$630 million/year. It significantly reduces the fuel cost if the aircraft uses a cheap natural gas as fuel for the drive station engines. The flight from the USA to Europe will be cheaper and take less time than it does now. The efficiency will be improved when the aircraft can take 200 and more passengers. The number of required aircraft decreases by 6–9 times because each hypersonic aircraft has very high speed.

In Table A2.1 the reader will find the approximate costs of the different form of energy converted to mechanical energy.

Fuel prices change with time, but in any case the cost of delivery will be sometimes less than delivery by conventional aircraft. Critics must remember that main content of this article is not economic estimations, but the new idea for aviation and space apparatus.

A2.6 Discussion of problems

1. *Cable problem:* At present the current industry produces cheap artificial fiber with a tensile stress up $\sigma = 500\text{--}620 \text{ kg/mm}^2$ and density $\gamma = 970\text{--}1800 \text{ kg/m}^3$ (see Chapters 1–2). This is enough for the subsonic, supersonic, and even the hypersonic systems (see Refs.^{1–7}). A hypersonic system with this cable requires a drive station every 10 km. When the industry produces cheap whiskers or nanotubes the distance between the drive stations can be increased up to 100 km and the system parameters will be significantly improved.
2. *Vehicle heating:* The proposed hypersonic vehicle will have heating from compressed air. The space ship “Shuttle” and warheads of ballistic rockets have the same problem, and in more difficult form because they have greater maximum speed (about 8 km/s). The heat flow increases by more than a third power of speed as $V^{3.15}$. This problem is successfully solved by a demountable terminal cover on “Shuttle” and on warheads. The same solution may apply in the proposed KV. The other solution is cooling, but that needs additional research. The nose and the leading edges of the wing of supersonic (speed is less than $4M$) KV can be made from heat-resistant material. If the speed is more than $4M$, the hypersonic vehicle may need to have a cooling system. However, this problem is not as difficult for KV as

it is for the space Shuttle. The problems of the “Shuttle” and the KV are different. The “Shuttle” has much greater speed (about 8000 m/s) and kinetic energy, and has to reduce this speed and energy by air drag. For this the “Shuttle” has an obtuse nose and leading edges of the wings. The KV must conserve its speed and energy for the long flight. The KV has a sharp nose and leading edges of the wings. The maximum speed of a hypersonic KV is 2 times less, which means the heat flow will be approximately 5 times less than the “Shuttle”. This problem can be solved by a light knockout ceramic cover (as on the “Shuttle”) or by a cooling system. If it uses water for cooling, the vapor can be used for additional thrust. Lithium as a cooler has 5 times the capability of water, 0.9 kg of lithium is enough to cool a 5-ton projectile launched from the ground at a speed of 8 km/s. However, this method needs more research and computation.

3. *High aerodynamic efficiency*: The KV can be more efficient than a conventional hypersonic aircraft with an engine because it does not have the air intake needed for air-breathing engines. The permanent high aerodynamic efficiency can be preserved by having variable wing area and variable swept wing.⁵ The optimal trajectory is as follows: after acceleration the hypersonic vehicle has a high vertical acceleration (3g), reaches its optimal (high) altitude, and flies along the optimal trajectory (see Attachment 4 of this book). After this the KV glides to the airport. On arrival the KV brakes and lands.
4. *Maneuverability in a landing*: This problem can be solved by conventional methods, air brakes and a small engine.

Some other ideas the reader finds in of the author can be found in Refs.^{5–7}

References

1. A.A. Bolonkin, “High Speed Catapult Aviation”, AIAA-2005-6221, *Atmospheric Flight Mechanic Conference*, 15–18 August 2005, USA.
2. A.A. Bolonkin, “Air Cable Transport”, *Journal of Aircraft*, Vol. 40, No. 2, July–August, 2003, pp. 265–269.
3. A.A. Bolonkin, “Bolonkin’s Method Movement of Vehicles and Installation for It”, US Patent 6,494,143 B1, Priority is on 28 June 2001.
4. A.A. Bolonkin, “Air Cable Transport and Bridges”, TN 7567, *International Air and Space Symposium – The Next 100 Years*, 14–17 July 2002, Dayton, OH, USA.
5. A.A. Bolonkin, “Non-Rocket Missile Rope Launcher”, IAC-02-IAA.S.P.14, 53rd *International Astronautical Congress, The World Space Congress – 2002*, 10–19 October 2002, Houston, TX, USA.
6. A.A. Bolonkin, “Inexpensive Cable Space Launcher of High Capability”, IAC-02-V.P.07, 53rd *International Astronautical Congress, The World Space Congress – 2002*, 10–19 October 2002, Houston, TX, USA.
7. A.A. Bolonkin, “Non-Rocket Space Rope Launcher for People”, IAC-02-V.P.06, 53rd *International Astronautical Congress, The World Space Congress – 2002*, 10–19 October 2002, Houston, TX, USA.
8. D.E. Koell, *Handbook of Cost Engineering*, TCS, Germany, 2000.

This page intentionally left blank

ATTACHMENT 3

Light Multi-reflex Engine*

Summary

The purpose of this attachment is to draw attention to the revolutionary idea of multi-reflection. The method and its main innovations were offered by the author in 1983 in the former USSR. Now the author is showing the huge possibilities of this idea in many fields such as space, aviation, energy, energy transmission, beam amplification, light transformation, and so on. This chapter considers the direct transfer of light beam energy to mechanical energy and back.

A3.1 Introduction

A3.1.1 Short history

In 1972 Kantrowitz draw attention to the use of a laser beam for a space propulsion system.¹ He proposed using the conventional method: to transfer energy by laser beam to space apparatus, to convert light energy into heat and evaporate matter, and to gain thrust from evaporated matter. There is a lot of research on this method.² However, it is complex, not very efficient, has limited range (divergence of the laser beam), requires special matter located on board the space ship, and requires a very powerful laser.

In 1983 the author offered another method of using beam (light) energy: the direct conversion of light energy into mechanical pressure (for engines) or thrust (for launchers and propulsion systems) using multiple reflection.³

The directing away or reflecting of light is the most efficient method for a propulsion system. It gives the maximum possible specific impulse (a speed of 3×10^8 m/s). The system does not expend mass, which is important for space ships, because launching mass into space is very expensive (at the present time it costs about \$20,000–50,000/kg).

*Full text is published by author as “Light Multi-reflex Engine”, *Journal of British Interplanetary Society*, Vol. 57, No. 9/10, 2004, pp. 353–359.

However, light pressure is very low at about 0.3×10^{-6} kg/kW (solar light pressure without reflection is about 0.2×10^{-6} kg/m²). In 1983 the author proposed the idea of increasing the light pressure using multi-reflex method and offered some innovations which dramatically reduce the loss of mirror reflection. This enables the system to make millions of reflections and to gain several newtons of the thrust per kilowatt of beam power. It allows the design of many important devices (in particular, engines) which transfer light directly into mechanical energy and solve many problems in aviation, space, energy, and energy transmission.

The advances in optical materials and lasers in the recent years have reduced the loss from reflection. The author returned to this topic and carried out the primary research. He solved the main problems that arise in research: the design of the very highly efficient reflector, a light lock, self-focusing lightweight mirrors and lenses, a beam transforer for very long distances (millions of kilometers) without beam divergence, light storage, a beam amplifier, etc. As with any new innovation it appears many additional problems will need to be addressed in the research and development. However, the solution of these problems promises a revolution in many technical fields. The author wants to draw the attention of researchers and engineers to these innovative ideas.

A3.1.2 Brief information about light and used light devices

The optical diapason of electromagnetic radiation is approximately from a few nanometers to 1 cm. Visible light is approximately located in the interval 400–700 nm (1 nm is 10^{-9} m). Ultraviolet radiation has a shorter range than visible light while the range of infrared rays is longer than visible light. The diapason of microwave radio waves is a higher than the optical diapason, and X-rays have a smaller optical diapason.

A conventional mirror can reflect a maximum of 98–99% of the light energy of some light waves and can give a maximum of 200–300 reflections. This is not enough, because the light pressure is very small at only about 0.6×10^{-6} kg/kW (for high reflection). For technical applications it is necessary to have a minimum of a million reflections.

This method is not suitable for our purpose (see Chapter 12). The wavelength is considerably changed for a mobile reflector (rotary disk). A conventional mirror reflects the beam in another direction if the mirror plate is not perpendicular to the beam.

A narrow laser beam is the most suitable for a light engine. There are many different types of lasers with different powers (peak power up to 10^{12} W), wavelength (0.2–700 μm), efficiency (from 1% up to about 95%), and impulse (up to some thousands of impulses per second) or continuous operations. A gas laser may be suitable for our purpose. Many molecular gases, such as hydrogen cyanide, carbon monoxide, and carbon dioxide, can provide laser action. Carbon dioxide lasers can be operated at a number of wavelength near 10 μm on various vibrational–rotational spectral lines of the molecule. They can be relatively efficient, up to about 30%, and have been made large enough to give continuous power outputs exceeding tens of thousands of watts.

At the present time we have seen significant advances in high-power weapons-class lasers. The Missile Defense Agency/USAF Airborne Laser (ABL) program is rapidly

developing a six-module chemical oxygen–iodine laser (COIL) to go at the heart of the weapon. Preparations are under way at the System Integration Laboratory for a mothballed 747-200 converted into a ground test platform, for first testing of the megawatt-class COIL flight hardware. The laser mirror is larger than 1.5 m in diameter.

The Air Force Research Laboratory (AFRL) has contracted with Northrop Grumman Space Technologies and Raytheon to develop a high-power solid-state 25-kW laser.

The laser beam divergence is:

$$\theta = \frac{2}{\sqrt{\pi}} \frac{\lambda}{D} = 1.13 \frac{\lambda}{D}, \quad (\text{A3.1})$$

where θ is the angle of divergence [rad]; λ is the wavelength [m]; and D is the aperture diameter [m]. Diffraction theory gives the coefficient in equation (A3.1) as 1.22.

Solar light has a radiation spectrum approximately in the interval $\lambda = 0.4\text{--}2.2\,\mu\text{m}$ and maximum energy when $\lambda = 0.5\,\mu\text{m}$. The divergence of solar light is about 0.005 rad.

More detailed information is given in the Refs.^{1–10,15}

A3.2 Description of innovation

To achieve maximum reflectance, 45° prisms (Fig. A3.1(a)) are used. For incident angles greater than $\sin^{-1}(n_1/n_2)$, no light is transmitted. Here n is the refractive index ($n \approx 1\text{--}4$). Instead the light is totally reflected back into the incident medium. This effect is called total internal reflection. Total internal reflection is used in the proposed reflector. Our reflector contains two plates than have a set of small prisms reflecting a beam from one prism to another prism (Fig. A3.1(b)). Every plate can contain millions of small ($30\text{--}100\,\mu\text{m}$) prisms. (An optical cable has a diameter of $2\text{--}10\,\mu\text{m}$.) The entering beam (3) is reflected millions of times as shown in Fig. A3.1(c) and (d) (see path 2) and creates a repulsive force F . This force may be very high at thousands of N/kW (see computation below) for motionless plates. It is limited only by the absorption (dB) of the prism material (see below).

The prisms and their cells can have a slope (Fig. A3.2(a)) and located on a rotor outer surface and a stator inner surface (Fig. A3.2(b)) or plates (Fig. A3.2(a)). This system can be applied to rotary or linear engines. Two questions arise: how the beam enters this cell (without the possibility of leaving the cell) and how much force the system has. The prism material attenuates the light energy and reduce the beam power (wave amplitude).

To solve the first problem the author offers a *light lock* which allows the light beam to enter but closes the exit (Fig. A3.1(b)). Fig. A3.1 shows three designs of *light locks*.

The first light lock is shown in Fig. A3.1(b). The beam enters through a narrow beam canal (4). The entering beam runs the full path (2) (Fig. A3.1(b-d)), is reflected in millions

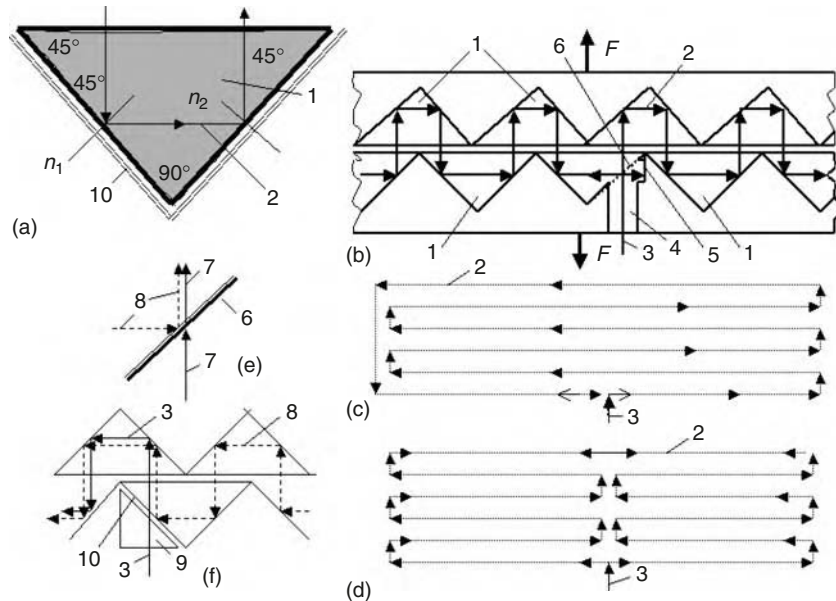


Fig. A3.1. Multi-reflection system (a) Prism with full internal reflection. Notations: (1) Prism; (2) path of a light beam; and (10) gap between the prism and the body of the plate, rotor, stator (it may be filled with a matter (cover) which has $n_1 < n_2$, n – reflective index. (b) Passage of the beam a through series of prisms. Notations: (3) Entering beam; (4) entrance canal; (5) mirror (light lock version 1); and (6) light lock (version 2) (multi-layer mirror), F – repulsive force. (c) The first version of the beam path through the reflected cells. (d) The second version of the beam path through the reflected cells. (e) Light lock (version 2). Notations: (6) Multi-layer mirror; (7) entering beam; and (8) final path of beam ($\lambda_8 \neq \lambda_7$). (f) Light lock (version 3). Notations: (9) Additional prism and (10) variable gap between main prism (1) and additional prism (9).

of cells, and travels up to enter the cell from the other side. Here the beam is partially reflected back into the system by mirror (5), and partially reflected back to way it came in a straight line. With mobile plates part of the beam is reflected back to the laser and the laser mirror returns it into the system. This part of the beam is s_1/s_2 , where s_1 is the width of the beam canal and s_2 is the length of a prism hypotenuse.

The second light lock is shown in Fig. A3.1(e). This has a mirror (6) with a multi-layer coating. This coating lets the entering beam (3, 7) passes but reflects the internal beam (8). This is possible because the wavelengths of beams (7 and 8) are different ($\lambda_8 \neq \lambda_7$) in the mobile plates.

The third light lock is shown in Fig. A3.1(f). It contains an additional prism (9) and is used as an impulse laser. When the laser beam (3) enters into the system, the prism (9) is pressed against the main prism (1). As the beam travels along path (2), the additional prism (9) is disconnected from prism (1) and the beam (3) can only travel inside the reflected system while it expends all its energy. The gap (10) may be very small, about a light wavelength ($1 \mu\text{m}$). A piezoelectric plate can be used for this purpose.

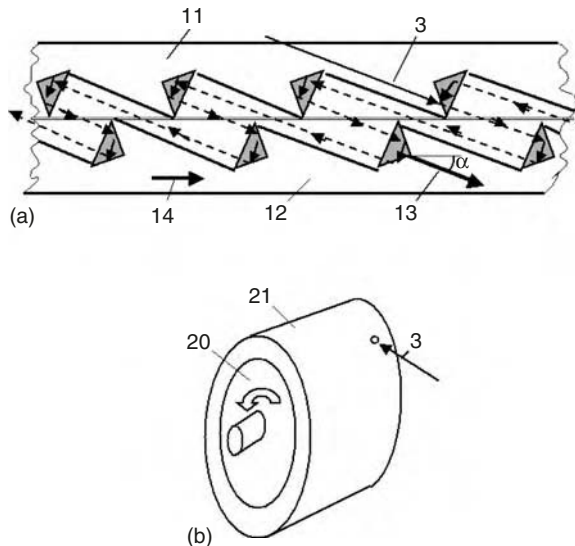


Fig. A3.2. Sloping reflective cells and light engine. (a) *Notations:* (3) Entering laser beam; (11) stator (motionless); (12) mobile rotor; (13) local force (of single cell); and (14) direction of rotor movement. (b) Light engine. *Notations:* (20) Rotor and (21) stator.

The detailed attenuation of light propagating through optical matter is considered in the next section. To increase the number of reflection we use a set of very small prisms and current high-efficiency optical matter.

A pulsed or continuous laser may be used. We compute an average laser power.

A3.3 Theory of the multi-reflex engine

The attenuation of light propagating through optical matter is caused either by absorption or by scattering. In both absorption and scattering, the power lost over a distance, z , and the power $N(z)$, propagating at that point is given by an exponential decay:

$$N(z) = N(0) \exp(-\gamma z). \quad (\text{A3.2})$$

The attenuation coefficient, γ , is normally expressed in dB/km, with 1 dB/km being the equivalent of $2.3 \times 10^{-4}/\text{m}$. Absorption is a material property in which the optical energy is normally converted into heat. In scattering processes, some of the optical power in the guided modes is radiated out of the material.

Attenuation of some current and some potential future very low loss materials created for fiber communication is presented in Fig. A3.3. However, some of these materials are highly reactive chemically and are mechanically unsuitable for drawing into fibers. Some are used as infrared light guides. None is presently used for optical communication but

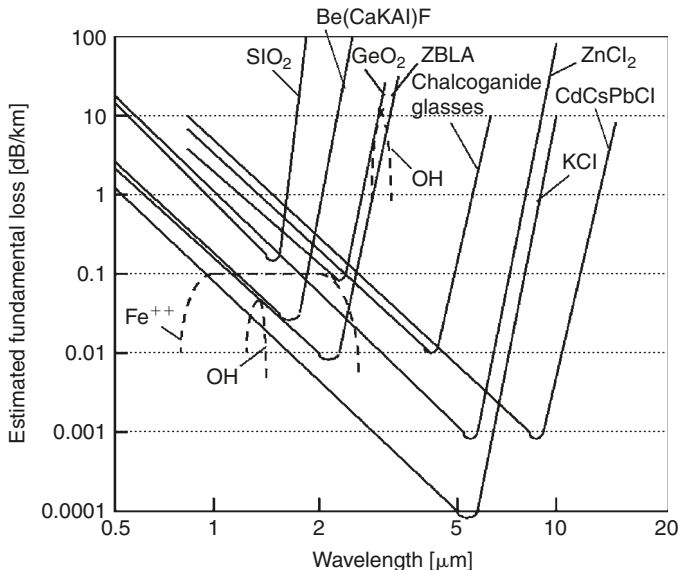


Fig. A3.3. Estimation of basic attenuation of some possible very low loss materials.

may be used for our purposes. Our mechanical property and wavelength requirements are less than in optical communication. However, we use in our computation conventional values of 0.1–0.4 dB. Clean air has $\xi = 0.333 \times 10^{-6}/\text{m}$. The conventional optical matter widely produced currently in industry has an attenuation coefficient equal to 2 dB.

The beam power will be reduced if one (or both) reflector is moved, because the wavelength is increased. The total loss of beam energy in one double cycle (as the light beam is moved to the reflector and back) is:

$$q = (1 - 2\gamma)(1 - 2\xi)(1 \pm 2v), \quad (\text{A3.3})$$

where $v = V/c$; V is relative speed of cells [m/s] and $c = 3 \times 10^8 \text{ m/s}$ is light speed. We take the “+” when the distance is reduced (braking) and take “−” when the distance is increased (useful work by light).

The light pressure, T , of two opposed high reflectors after a series of reflections, n , to one another is:

$$\begin{aligned} T_0 &= \frac{2N_0}{c}, & T_1 &= \frac{2N_0}{c} q, & T_2 &= \frac{2N_0}{c} q^2, \\ T_3 &= \frac{2N_0}{c} q^3, & \dots &, & T_{n-1} &= \frac{2N_0}{c} q^n. \end{aligned} \quad (\text{A3.4})$$

This is a geometric series. The sum of n members of the geometric series is:

$$T = \frac{2N_0}{c} \frac{q^n - 1}{q - 1}. \quad \text{If } n = \infty \text{ then } T_\infty = \frac{2N_0}{c} \frac{1}{1 - q}, \quad q < 1. \quad (\text{A3.5})$$

If the reflector is moved away, the maximum number of reflections, n , is limited by the cell size, l , because the wavelength is increased and that cannot be more than the cell size. This limit is:

$$n \leq \frac{\ln(l/\lambda_0)}{2v}, \quad (\text{A3.6})$$

where l is cell width [m] and λ_0 is the initial wavelength [m].

If the reflector is moved forward to another position, the wavelength is reduced, but it cannot be less than the wavelength of X-rays because the material transmits X-rays (the material lowers the reflective capability).

This limit is about $\lambda_{\min} = 10 \text{ nm}$. The maximum number of brake reflections is:

$$n \leq \frac{\ln(\lambda_0/\lambda_{\min})}{2v}. \quad (\text{A3.7})$$

The force of the engine with slope, α , cells (Fig. A3.2) and engine coefficient efficiency, η , may be computed by the equation:

$$T = \frac{2N_0}{c} \frac{q^n - 1}{q - 1} \cos \alpha, \quad \eta = \frac{TV}{N_0}. \quad (\text{A3.7}')$$

The values in equation (A3.3) can be computed using:

$$\gamma = 0.00023al, \quad l = m\lambda, \quad m \geq 1, \quad \xi = 0.333 \times 10^{-6}l_c, \quad l_c = \frac{l + \delta}{\tan \alpha}, \quad (\text{A3.8})$$

where a is the attenuation coefficient in dB [km] (see Fig. A3.3); m is the initial number of wavelengths which can be located in cell size l ; l_c is the length of a cell [m]; and δ is the gap between engine disks [m].

The engine rotor force coefficient, A , shows how many times the initial light pressure is increased. It is:

$$A = \frac{q^n - 1}{q - 1}. \quad (\text{A3.9})$$

The results of computations are presented in Figs. A3.4–A3.8. The computed parameters are not optimal. Our purpose is to demonstrate the method of computation.

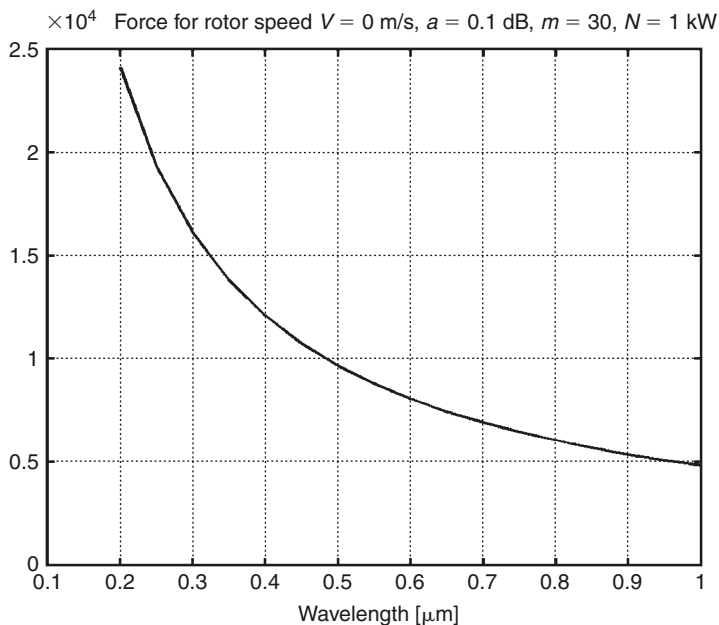


Fig. A3.4. Repulsive force, T [N], of motionless plates ($V = 0$ m/s) for infinite reflections, attenuation coefficient $a = 0.1$ dB, cell size $m = 30$, beam power $N_0 = 1$ kW, and different wavelengths.

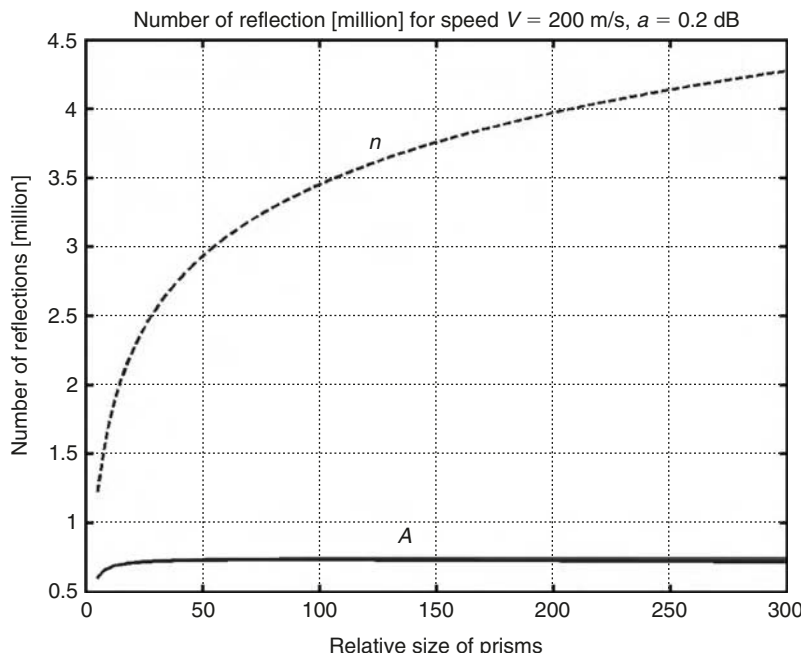


Fig. A3.5. Force coefficient, A (equation (A3.9)) and number of reflections n (equation (A3.6)) for rotor speed $V = 200$ m/s, $a = 0.2$ dB, and relative size of prisms $m = 10-300$.

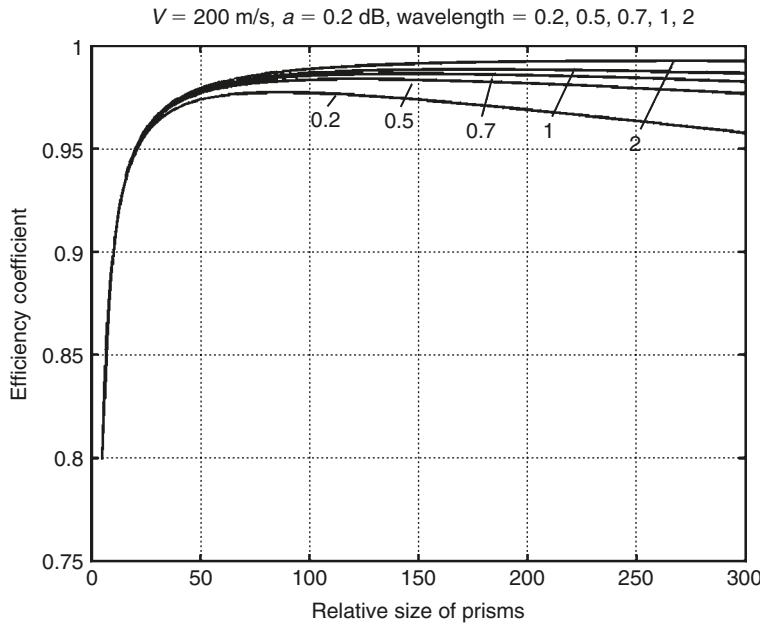


Fig. A3.6. Efficiency coefficient (equation (A3.7)) for rotor speed $V = 200 \text{ m/s}$, $a = 0.2$, wavelength $\lambda = 0.2\text{--}2 \mu\text{m}$, and relative size of prisms $m = 10\text{--}300$.

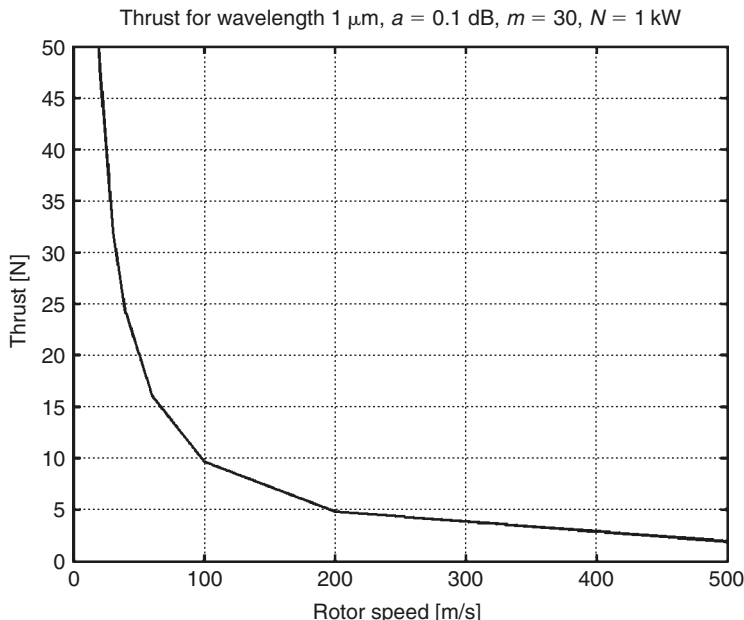


Fig. A3.7. Thrust (force) (equation (A3.7)) versus the rotor speed ($V = 20\text{--}500 \text{ m/s}$) for wavelength $\lambda = 1 \mu\text{m}$, $a = 0.1 \text{ dB}$, $m = 30$, and beam power $N_0 = 1 \text{ kW}$.

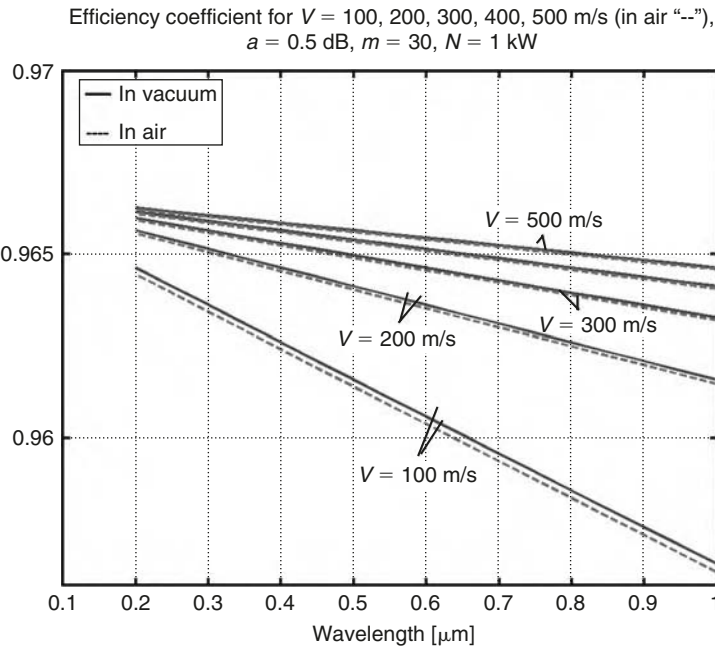


Fig. A3.8. Efficiency coefficient (equation (A3.10)) versus wavelength $\lambda = 0.2\text{--}1 \mu\text{m}$, $a = 0.5 \text{ dB}$, $m = 30$, $N_0 = 1 \text{ kW}$, and rotor speed $V = 100\text{--}500 \text{ m/s}$. The broken lines -- show the computations with air attenuation.

Fig. A3.4 shows the maximum pressure that can be created by a 1 kW beam in the cell design of Fig. A3.1(b) for a motionless disk ($V = 0, a = 0.1 \text{ dB}, m = 30, N_0 = 1 \text{ kW}$, and $\lambda = 0.1\text{--}1 \mu\text{m}$). This pressure reaches a high force of 5000 N for the wavelength of 1 μm . This high pressure may be used, for example, for moving a heavy device a micron distance, for loudspeaker devices, or for frequency modulation of laser beams by mechanical energy, etc.

Fig. A3.5 presents the number of reflections for disk speed $V = 200 \text{ m/s}$, $a = 0.2 \text{ dB}$, and $m = 10\text{--}300$. This number reaches 4-million double reflections (one from each mirror).

Fig. A3.6 presents the transmission efficiency coefficient of light energy, η_t , converted into mechanical energy for $V = 200 \text{ m/s}$; $a = 0.2 \text{ dB}$; $\lambda = 0.2, 0.5, 0.7, 1, 2 \mu\text{m}$; and $m = 10\text{--}300$. The efficiency of the proposed light engine is very high and reaches 98–99% if $m > 50$ (equation (A3.7)).

Fig. A3.7 presents the force on the rotary disk of the light engine for different speeds $V = 20\text{--}500 \text{ m/s}$, $a = 0.1 \text{ dB}$, $m = 30$, $P = 1 \text{ kW}$. This force changes from 50 N through 2 N.

Fig. A3.8 presents the efficiency coefficient for a rotary engine for the data in Fig. A3.7, when the engine works in a vacuum (-) and in air (—). The gap between disks is 0.1 mm. This coefficient reaches more than 0.96 and only considers the transformation loss without mechanical friction. The mechanical friction is conventional for turbines and it is small.

All computations are made for a beam power of $N_0 = 1 \text{ kW}$. For beam powers $N_0 = 10, 100, 1000 \text{ kW}$ we must multiply the forces in Fig. A3.7 by 10, 100, 1000, respectively.

We can ignore the loss from the sides of the cells because this is small if the beam divergence is small and the lateral side of the cells has the full reflection cover (as in the light cable).

A3.4 Discussion

The proposed multi-reflex light engine is very simple (only two disks), has a small size, a very high ratio of power/weight, and is efficient. One can directly convert the beam light into mechanical energy.

This engine may be applied in aviation because the energy can be transferred from an Earth surface station to an aircraft by the laser beam. The aircraft does not need to carry fuel and has a more lightweight engine, so its load capability doubles as a result. Industry can produce a 1 MW (1000 kW) laser now. This is enough for middle-range aircraft with a weight of 10–12 ton.¹⁰

The linear light engine does not have a speed limit and one may be used to launch space equipment and space ships.^{11–13} This method may be also used in the design of new efficient weapons.¹⁴

The intensity of solar light on a clear day is about 1 kW/m^2 . If we can convert this light into mechanical energy, the mechanical energy can be converted into electrical energy. The efficiency of this process may be higher and cheaper than the efficiency of expensive commercial solar cells (10–12% efficient).

This text is published in Refs.^{15,16}

References

1. A. Kantrowitz, “Propulsion to Orbit by Ground-Based Lasers”, *Astronautics and Aeronautics*, Vol. 10, May 1972, pp. 74–76.
2. *Beamed Energy Propulsion. First International Symposium on Beamed Energy Propulsion*, American Institute of Physics, Melville, New York, 2003.
3. A.A. Bolonkin, “Light Pressure Engine”, Patent (Author Certificate) #1183421, 1985, USSR (priority on 5 January 1983).
4. R.G. Driggers (ed.), *Encyclopedia of Optical Engineering*, Marcel Dekker, Inc., New York, 2003.
5. M. Bass (ed.), *Handbook of Optics*, 2nd edition, McGraw-Hill, Inc., New York, 2000.
6. *Military Standardization Handbook. Optical Design*, No. 141, 1962.
7. P.W. Milonni and J.H. Eberly, *Lasers*, John Wiley & Sons, New York, 1988.
8. D.C. O’Shea, *Elements of Modern Optical Design*, John Wiley and Sons, New York, 1985.

9. A.W. Snyder, *Optical Waveguide Theory*, Chapman and Hall, New York–London, 1983.
10. A.A. Bolonkin, “Multi-reflex Propulsion Systems for Space and Air Vehicles and Energy Transfer for Long Distance”, *Journal of British Interplanetary Society*, Vol. 57, No. 11/12, 2004, pp. 379–390.
11. A.A. Bolonkin, “Kinetic Space Towers and Launchers”, *Journal of British Interplanetary Society*, Vol. 57, No. 1/2, 2004, pp. 33–39.
12. A.A. Bolonkin, “Hypersonic Launch System of Capability Up 500 Tons per Day and Delivery Cost \$1 per Lb”, IAC-02-S.P.15, *53rd International Astronautical Congress, The World Space Congress*, 10–19 October 2002, Houston, TX, USA.
13. A.A. Bolonkin, “Earth Accelerator for Space Ships and Missiles”, *Journal of British Interplanetary Society*, Vol. 56, No. 11/12, 2003, pp. 394–404.
14. A.A. Bolonkin, “Air Cable Transport”, *Journal of Aircraft*, Vol. 40, No. 2, March–April 2003.
15. A.A. Bolonkin, “Light Multi-reflex Engine”, *Journal of British Interplanetary Society*, Vol. 57, No. 9/10, 2004, pp. 353–359.
16. A.A. Bolonkin, US Patent 6,494,143 B1, USA.

ATTACHMENT 4

Optimal Trajectories of Air and Space Vehicles*

Summary

The author has developed a theory on optimal trajectories for air vehicles with variable wing areas and with conventional wings. He applied a new theory of singular optimal solutions and obtained in many cases the optimal flight. The wing drag of a variable area wing does not depend on air speed and air density. At first glance the results may seem strange, however, this is the case and this chapter will show how the new theory may be used. The equations that follow enable computations of the optimal control and optimal trajectories of subsonic aircraft with pistons, jets, and rocket engines, supersonic aircraft, winged bombs with and without engines, hypersonic warheads, and missiles with wings.

The main idea of the research is to use the vehicle's kinetic energy to increase the range of missiles and projectiles.

The author shows that the range of a ballistic warhead can be increased 3–4 times if an optimal wing is added to it, especially a wing with variable area. If we do not need increased range, the warhead mass can be increased. The range of large gun shells can also be increased 3–9 times. The range of an aircraft may be improved by 3–15% or more.

The results can be used for the design of aircraft, missiles, flying bombs, and shells for large guns.

Nomenclature (in metric system)

a the speed of sound [m/s]

a_1, b_1, a_2, b_2 coefficients of exponential atmosphere

* This theory was published in author's book *New Method of Optimization and Their Applications*, Moscow, MVTU, 1972 (in Russian), presented to *AIAA/NASA/USAF/SSMO Symposium on Multidisciplinary Analysis and Optimization*, 7–9 September 1994, Panama City, FL, USA.

Full text of this chapter is published in *Aircraft Engineering and Space Technology*, Vol. 76, No. 2, 2004, pp. 193–214.

Author wishes to acknowledge scientist Dr. D. Handwerk for correction English in this article.

C_L	lift coefficient
C_D	drag coefficient
C_{D0}	drag coefficient for $C_L = 0$
C_{DW}	wave wing drag coefficient when $\alpha = 0$
C_{Db}	body drag coefficient
c	relative thickness of a wing
c_b	relative thickness of a body
c_1	relative thickness of a vehicle body
c_s	fuel consumption, kg/s/kg thrust
\bar{D}	drag of vehicle [N]
D	drag of vehicle without α [N]
D_{0W}	wave wing drag when $\alpha = 0$ [N]
D_{0b}	drag of a vehicle body [N]
H	Hamiltonian
h	altitude [m]
$K = C_L/C_D$	the wing efficiency coefficient
k_1, k_2, k_3	vehicle average aerodynamic efficiencies for sub-distances 1, 2, 3, respectively
L	range
$M = V/a$	Mach number
m	mass of vehicle [kg]
$p = m/S$	load on a square meter of wing
$q = \rho V^2/2$	a dynamic air pressure
R	aircraft range or $R = \text{distance from flight vehicle to Earth center}; R = R_o + h$, where $R_o = 6378 \text{ km}$ is Earth radius
t	time
$T = V_e \beta$	thrust [N]
V	vehicle speed [m/s]
V_c	speed of throw back mass (air for propeller engine, jet for jet and rocket engine) [m/s]
S	wing area [m^2]
s	length of trajectory
T	engine thrust [N]
Y	lift force [N]
α	wing attack angle
β	fuel consumption
θ	angle between the vehicle velocity and the horizon
ω	thrust angle between thrust and velocity
ω_E	Earth angle speed
φ_E	lesser angle between the Earth's Polar axis and a perpendicular to a flight plate
ρ	air density [kg/m^3]

A4.1 Introduction

The topic of the optimal flight of air vehicles is very important. There are numerous articles and books about the optimal trajectories of rockets, missiles, and aircraft. The

classical research of this topic is by Miele.¹ Unfortunately, the optimal theory of this problem is very complex. In most cases, the researchers obtained complex equations, that allow one to compute a single optimal trajectory for a given aircraft and for given conditions, but the structure of optimal flight is not clear and simple formulas of optimal control (which depend only on flight conditions) are absent.

The author's new theory of singular optimal solutions, developed earlier,^{2–14} does not contain unknown coefficients or variables as previous theories have. He found that the optimal flight path depends only on the flight conditions and the addition of certain variable wing structures.

In conclusion, the author applies his solution to ballistic missiles, warheads, flying bombs, large gun shells, and subsonic, supersonic, and hypersonic aircraft with rocket, turbo-jet, and propeller engines. He shows that the range of these air vehicles can be increased 3–9 times.

A4.2. General equations

Let us consider the movement of an air vehicle given the following conditions:

1. The vehicle moves in a plane containing the Earth's center.
2. The vehicle design allows the wing area to be changed (this will prove important in the remainder of this chapter).
3. We ignore the centrifugal force from the Earth's rotation (it is less than 1%).
4. Earth has a curvature.

Then the equations for flying vehicle (in a system of coordinates where the center of the system is located at the center of gravity of the flying vehicle, the x -axis is in the direction of flight, the y -axis is perpendicular to the x -axis, Fig. A4.1) are:

$$\begin{aligned}\frac{dL}{dt} &= V \cos \theta, \\ \frac{dh}{dt} &= V \sin \theta,\end{aligned}\tag{A4.1} \tag{A4.2}$$

$$\begin{aligned}\frac{dV}{dt} &= \frac{T(h, V, \beta) \cos \omega - \bar{D}(\alpha, V, h)}{m} - g \sin \theta, \\ \frac{d\theta}{dt} &= \frac{T(h, V, \beta) \sin \omega + Y(\alpha, V, h)}{mV} - \frac{g}{V} \cos \theta + \frac{V \cos \theta}{R} + 2\omega_E \cos \varphi_E, \\ \frac{dm}{dt} &= -\beta.\end{aligned}\tag{A4.3} \tag{A4.5}$$

All values are in the metric system and all angles are taken to be in radians.

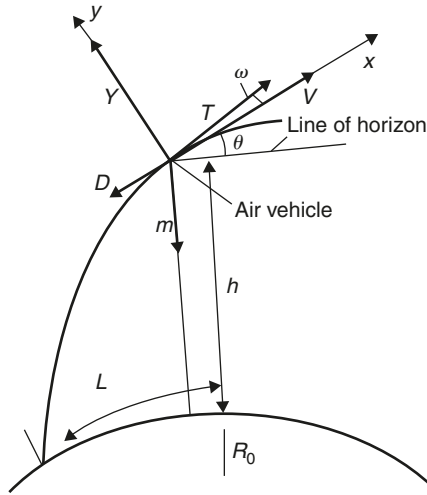


Fig. A4.1. Vehicle forces and coordinate system.

A4.3 Flight with a small change of vehicle mass and flight path angle

Most air vehicles fly at an angle θ in the range $\pm 15^\circ$ ($\theta = \pm 0.2618 \text{ rad}$), with the engine located along the velocity vector. This means:

$$\sin \theta = \theta, \quad \cos \theta = 1, \quad \omega = 0, \quad (\text{A4.6})-(\text{A4.8})$$

because $\sin 15^\circ = 0.25882$, $\cos 15^\circ = 0.9659$.

Let us substitute (A4.6)–(A4.8) into (A4.1)–(A4.5):

$$\frac{dL}{dt} = V, \quad (\text{A4.9})-(\text{A4.10})$$

$$\frac{dh}{dt} = V\theta,$$

$$\frac{dV}{dt} = \frac{T(h, V) - \bar{D}(\alpha, V, h)}{m} - g\theta, \quad (\text{A4.11})-(\text{A4.12})$$

$$\frac{d\theta}{dt} = \frac{Y(\alpha, V, h)}{mV} - \frac{g}{V} + \frac{V}{R} + 2\omega_E \cos \varphi_E,$$

$$\frac{dm}{dt} = -\beta, \quad (\text{A4.13})$$

where

$$|\theta| \leq \theta_{\max}. \quad (\text{A4.14})$$

Many air vehicles fly with a low angular speed of $d\theta/dt$. The change of mass is also low in flight. This means $m = \text{constant}$, $dm/dt \approx 0$:

$$d\theta/dt \approx 0, \quad dm/dt = 0. \quad (\text{A4.15})-(\text{A4.16})$$

Let us take a new independent variable $s = \text{length of trajectory}$:

$$dt = ds/V, \quad (\text{A4.17})$$

and substitute (A4.14)–(A4.17) in (A4.8)–(A4.13). Then system (A4.8)–(A4.13) takes the form:

$$\begin{aligned} \frac{dL}{ds} &= 1, \\ \frac{dh}{ds} &= \theta, \\ \frac{dV}{ds} &= \frac{T(h, V) - \bar{D}(\alpha, V, h)}{mV} - \frac{g}{V} \theta, \\ 0 &= \frac{Y(\alpha, V, h)}{mV} - \frac{g}{V} + \frac{V}{R} + 2\omega_E \cos \varphi_E. \end{aligned} \quad (\text{A4.18})-(\text{A4.21})$$

Let us rewrite equation (A4.21) in the form:

$$Y(\alpha, V, h) - mg + \frac{mV^2}{R} + 2mV\omega_E \cos \varphi_E = 0. \quad (\text{A4.22})$$

If we ignore the last element, equation (A4.22) takes the form:

$$Y(\alpha, V, h) - mg + \frac{mV^2}{R} = 0. \quad (\text{A4.22})'$$

If V is not very large ($V < 3 \text{ km/s}$), the two last elements in equation (A4.21) are small and they may be ignored. Equations (A4.22) and (A4.22)' can be used for deleting α from \bar{D} .

Note the new drag without α is:

$$D = D(h, V). \quad (\text{A4.23})$$

If we substitute α from (A4.22) into equation (A4.20) the equation system take the form:

$$\begin{aligned} \frac{dL}{ds} &= 1, \\ \frac{dh}{ds} &= \theta, \\ \frac{dV}{ds} &= \frac{T(h, V) - D(h, V)}{mV} - \frac{g}{V} \theta. \end{aligned} \quad (\text{A4.24})-(\text{A4.26})$$

Here the variable θ is new control limited by:

$$|\theta| \leq \theta_{\max}. \quad (\text{A4.27})$$

A4.4 Statement of the problem

Consider the problem: finding the maximum range of an air vehicle described by equations (A4.24)–(A4.26) for the limitation (A4.27). This problem may be solved using conventional methods. However, it is a non-linear problem but contains the linear control, which means the problem has a singular solution. To find this singular solution, we will use methods developed previously.^{2,4}

Write the Hamiltonian:

$$H = 1 + \lambda_1 \theta + \lambda_2 \frac{1}{V} \left(\frac{T - D}{m} - g\theta \right), \quad (\text{A4.28})$$

where $\lambda_1(s)$, $\lambda_2(s)$ are unknown multipliers. Application of the conventional method gives:

$$\dot{\lambda}_1 = -\frac{\partial H}{\partial h} = -\lambda_2 \frac{1}{V} \left(\frac{T'_h - D'_h}{m} \right), \quad (\text{A4.29})$$

$$\dot{\lambda}_2 = -\frac{\partial H}{\partial V} = -\lambda_2 \left[-\frac{1}{V^2} \left(\frac{T - D}{m} - g\theta \right) + \frac{1}{V} \left(\frac{T'_V - D'_V}{m} \right) \right], \quad (\text{A4.30})$$

$$\theta = \max_{\theta} H = \theta_{\max} \operatorname{sign} \left[\lambda_1 - \lambda_2 \frac{g}{V} \right]. \quad (\text{A4.31})$$

where D'_h , D'_v , T'_h , T'_v denote the first partial derivatives of D , T by h , V , respectively.

The last equation shows that the control θ can have only two values $\pm\theta_{\max}$. We consider the singular case when:

$$A = \lambda_1 - \lambda_2 \frac{g}{V} \equiv 0. \quad (\text{A4.32})$$

This equation has two unknown variables λ_1 and λ_2 and does not contain information about the control θ .

Let us differentiate equation (A4.32) for the independent variable s . After substitution the equations (A4.26), (A4.29), (A4.30), and (A4.32) into the result of differentiation, we obtain the relation for $\lambda_1 \neq 0, \lambda_2 \neq 0$:

$$V(T'_h - D'_h) = g(T'_v - D'_v). \quad (\text{A4.33})$$

This equation does not contain θ either, but it contains the important relation between the variables V and h on the optimal trajectory.

If we have the formulas (or graphs):

$$D = D(h, V), \quad (\text{A4.34})$$

$$T = T(h, V), \quad (\text{A4.35})$$

we could find the relation:

$$h = h(V). \quad (\text{A4.36})$$

and the optimal trajectory for a given air vehicle.

This also gives important information about the structure of the optimal solution. Investigation of equation (A4.33) shows that the equation has one solution in each of the subsonic, supersonic, and hypersonic fields. The equation can have two solutions for a transonic field.

This means the optimal trajectory in most cases has three parts (see Fig. A4.2):

- (a) When climbing and in flight a vehicle moves from the initial point A with the angle $\pm\theta_{\max}$ up to the optimal curve (A4.36), then continues along the optimal curve (A4.36) and moves with at an angle $\pm\theta_{\max}$ to point B .
- (b) When descending and in flight (Fig. A4.3) a vehicle moves from the initial point A with the angle $\pm\theta_{\max}$ (up or down) to the optimal curve (A4.36), then continues down the optimal curve (A4.36), and moves at an angle $\pm\theta_{\max}$ (up or down) to the point B .

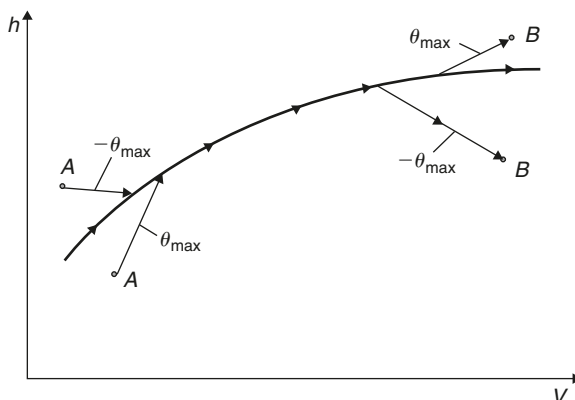


Fig. A4.2. Optimal trajectory for air vehicle climb and flight.

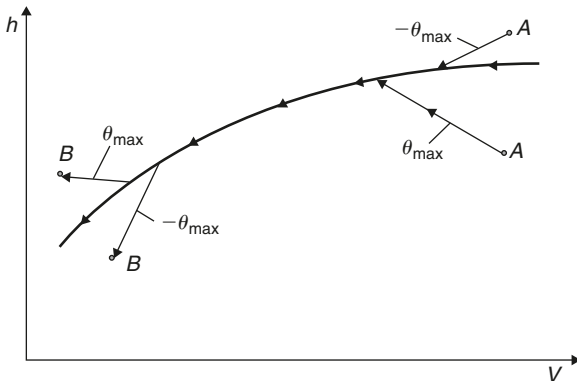


Fig. A4.3. Optimal trajectory for air vehicle descent and flight.

The selection of direction (up or down, with θ_{\max} or $-\theta_{\max}$, respectively) depends only on the position of the initial and end points A and B .

For air vehicles with rocket engines $T = \text{constant}$, equation (A4.33) has a very simple form:

$$VD'_h = gD'_V. \quad (\text{A4.37})$$

The same form (same curve) also applies for a ballistic warhead, which does not have engine thrust (after its short initial burn) ($T = 0$).

If we want to find an equation for the control θ , we continue to differentiate equation (A4.33) with the independent variable s , and substitute into the equations (A4.25), (A4.26), (A4.29), (A4.30), (A4.32), and (A4.33). We obtain the relation for θ if $\lambda_1 \neq 0$, $\lambda_2 \neq 0$:

$$\theta = \frac{B_1(T - D)}{mV \left(B_1 \frac{g}{V} - B_2 \right)}, \quad (\text{A4.38})$$

where

$$\begin{aligned} B_1 &= (T'_h - D'_h) + V(T''_{hv} - D''_{hv}) - g(T''_{vv} - D''_{vv}), \\ B_2 &= V(T''_{hh} - D''_{hh}) - g(T''_{hv} - D''_{hv}). \end{aligned} \quad (\text{A4.39})-(\text{A4.40})$$

Here signs in form D''_{hv} are the second partial derivatives D for h, V .

$$D''_{hv} = \frac{\partial^2 D}{\partial h \partial V}. \quad (\text{A4.41})$$

If the thrust does not depend on h, V ($T = \text{constant}$) or no engine ($T = 0$), the equation for θ becomes simpler:

$$\theta = \frac{[(gD''_{VV} - D'_h) - VD''_{hV}](T - D)}{m[g(gD''_{VV} - D'_h) + V^2 D''_{hh}]} . \quad (\text{A4.42})$$

In accordance with other publications^{2–8} (for example, equation (4.2)⁴) the necessary condition for optimal trajectory is:

$$-(-1)^k \frac{\partial}{\partial \theta} \left[\frac{d^{2k}}{ds^{2k}} \left(\frac{\partial H}{\partial \theta} \right) \right] \geq 0. \quad (\text{A4.43})$$

where $k = 1$.

To obtain results for different forms of the drags and thrusts, we must take formulas (or graphs) for subsonic, transonic, supersonic, or hypersonic speed, and specific formulas for the thrust and substitute them in the equations (A4.33) and (A4.38). Consider two cases: subsonic and hypersonic speeds.

A4.4.1 Subsonic speed ($V < 270 \text{ m/s}$) and different engines

Lift, drag, and derivative equations for subsonic speed are:

$$\begin{aligned} L &= mg = s\alpha \frac{\rho V^2}{2} S, \quad \bar{D} = C_D \frac{\rho V^2}{2} S, \quad C_D = C_{Do} + \varepsilon\alpha^2, \\ D &= \left[C_{Do} + \varepsilon \left(\frac{2mg}{s\rho V^2 S} \right)^2 \right] \frac{\rho V^2}{2} S, \quad \rho = a_1 e^{-h/b_1}, \quad \frac{\partial D}{\partial V} = \left[C_{Do} - \varepsilon \left(\frac{2mg}{s\rho V^2 S} \right)^2 \right] \rho VS, \\ \frac{\partial D}{\partial h} &= -\frac{1}{b_1} \left[C_{Do} - \varepsilon \left(\frac{2mg}{s\rho V^2 S} \right)^2 \right] \frac{\rho V^2}{2} S. \end{aligned} \quad (\text{A4.44})$$

where $s = 6.24\lambda/(\lambda + 2)$, $\varepsilon = s^2/\pi\lambda$, magnitude $\varepsilon \approx \zeta^2/\pi\lambda$ is an induced drag coefficient, $\lambda = l^2/S$, l is a wing span.

It is known in conventional aerodynamics that the coefficient of flight efficiency k is:

$$k = \frac{C_L}{C_D} = \frac{s\alpha}{C_{Do} + \varepsilon\alpha^2}, \quad \text{from } \max_{\alpha} k \text{ we obtain } \alpha_{\text{opt}} = \sqrt{\frac{C_{Do}}{\varepsilon}}, \quad k_{\text{max}} = \frac{s}{2\sqrt{\varepsilon C_{Do}}}. \quad (\text{A4.45})$$

A4.4.1.1 Aircraft with rocket engine

For this aircraft the thrust T is constant or 0. Equation (A4.33) has form (A4.37). Find the partial derivatives:

$$T'_V = 0, \quad T'_h = 0. \quad (\text{A4.46})$$

Substituting (A4.44)–(A4.46) in (A4.37) we obtain the relation between air density ρ , altitude h , and aircraft speed V :

$$\rho = \frac{2gp}{sV^2} \sqrt{\frac{\varepsilon}{C_{\text{Do}}}}, \quad p = \frac{m}{S}, \quad h = b_1 \ln \frac{a_1}{\rho}. \quad (\text{A4.47})$$

where $p = m/S$ is the load on a square meter of wing. For a diapason of $h = 0$ –11 km the coefficients $a_1 = 1.225$, $b_1 = 9086$.

Results of this computation are presented in Fig. A4.4.

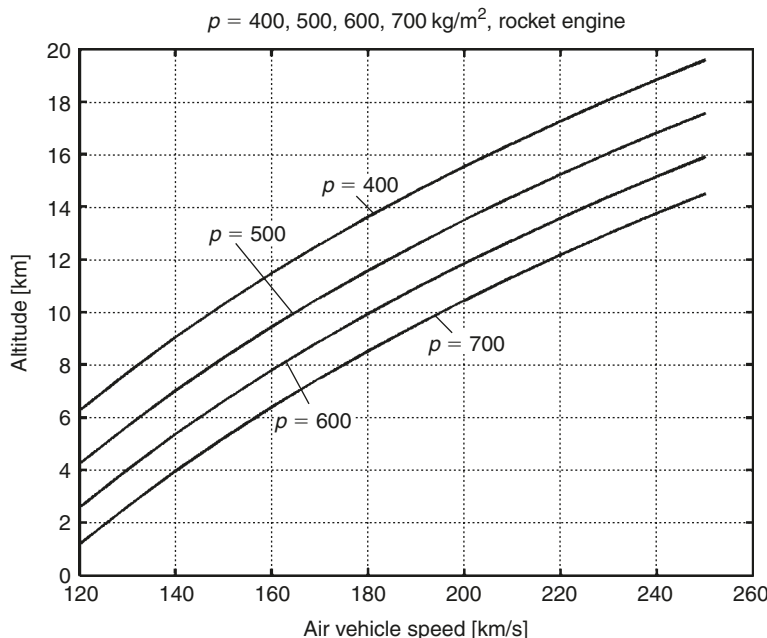


Fig. A4.4. Air vehicle altitude versus speed for wing load $p = 400, 500, 600$, and 700 kg/m^2 and a rocket engine.

A4.4.1.2 Aircraft with turbo-jet engine

The thrust for this engine is:

$$T = T_0 \frac{\rho}{\rho_0}, \quad T'_h = -\frac{T}{b_1}, \quad T'_V = 0. \quad (\text{A4.48})$$

Substitute (A4.48) in (A4.33). We obtain:

$$V \left(-\frac{T}{b_1} - D'_h \right) = -g D'_V \quad \text{or} \quad T = \frac{b_1}{V} (g D'_V - V D'_h), \quad (\text{A4.48})'$$

and substituting (A4.44) and (A4.48) in (A4.33), we obtain:

$$\frac{1}{p} \left(\frac{V^2}{2b_1} + g \right) \left[C_{D_0} - \epsilon \left(\frac{2pg}{s\rho V^2} \right)^2 \right] = \frac{\bar{T}_0}{b_1 \rho_0}, \quad \text{where} \quad \bar{T}_0 = \frac{T_0}{m}. \quad (\text{A4.49})$$

We can then find ρ, h from (A4.49):

$$\rho = \frac{2pg\sqrt{\epsilon}}{sV^2\sqrt{A_2}}, \quad \text{where} \quad A_2 = C_{D_0} - \frac{2p\bar{T}_0}{\rho_0(V^2 + 2b_1g)} \quad \bar{T}_0 = \frac{T_0}{m}, \quad h = b_1 \ln \frac{a_1}{\rho} \quad (\text{A4.50})$$

Results of computation for the different p , $T = 0.8 \text{ N/kg}$, $a_1 = 1.225$, $b_1 = 9086$ are presented in Fig. A4.5.

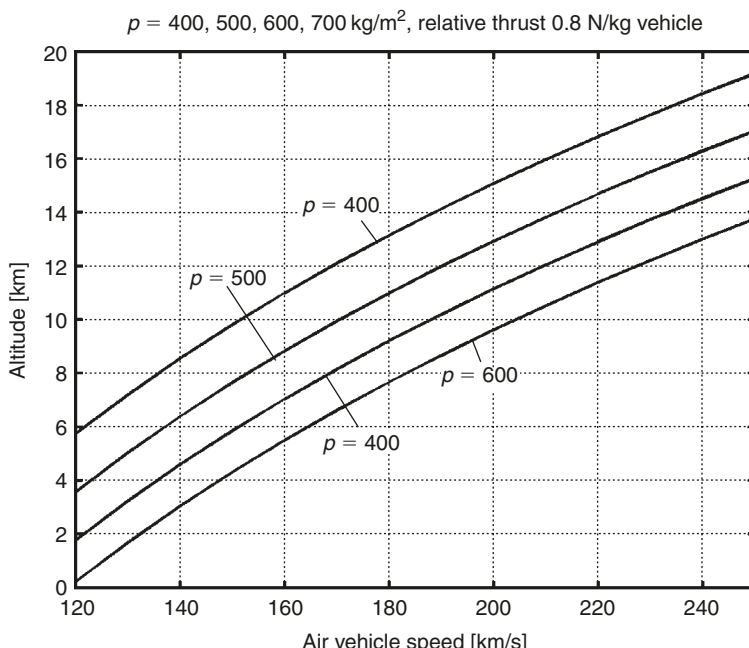


Fig. A4.5. Air vehicle altitude versus speed for wing load $p = 400, 500, 600$, and 700 kg/m^2 , turbo-jet engine, and relative thrust 0.8 N/kg vehicle.

A4.4.1.3 Piston and turbo engines with propeller

All current propeller engines have propellers with variable pitch. The propeller coefficient efficiency, η , approximately is constant. The thrust of this engine is:

$$T = \frac{N_0}{V} \frac{\rho}{\rho_0}, \quad T'_V = -\frac{T}{V}, \quad T'_h = -\frac{T}{b_1}, \quad (\text{A4.51})$$

where $N_0 = N_e \eta$; N_e is engine power at $h = 0$.

Substituting (A4.44) in (A4.33). We obtain the equation for thrust:

$$V \left(\frac{T}{b_1} + D'_h \right) = g \left(\frac{T}{V} + D'_V \right) \quad \text{or} \quad T = \frac{b_1 V (g D'_V - V D'_h)}{V^2 - g b_1}. \quad (\text{A4.51})'$$

Substitute (A4.44) and (A4.51) in (A4.33). We obtain:

$$\frac{V}{p} \left(\frac{V^2}{b_1} - g \right) \left[C_{D0} - \varepsilon \left(\frac{2pg}{\rho V^2} \right)^2 \right] = \frac{\bar{N}_0}{\rho_0} \left(\frac{g}{V^2} - \frac{1}{b_1} \right), \quad \text{where} \quad \bar{N}_0 = \frac{N_0}{m}, \quad p = \frac{m}{S}. \quad (\text{A4.52})$$

We can then find ρ, h from (A4.52):

$$\rho = \frac{2pg\sqrt{\varepsilon}}{sV^2\sqrt{A_3}}, \quad \text{where} \quad A_3 = C_{D0} + \frac{p\bar{N}_0}{\rho_0 V^3}, \quad h = b_1 \ln \frac{a_1}{\rho}. \quad (\text{A4.53})$$

Results of computation for $C_{D0} = 0.025$, $\lambda = 10$, for different values of p, N are presented in Fig. A4.6.

A4.4.2 Hypersonic speed ($1 \text{ km/s} < V < 7 \text{ km/s}$)

The lift and drag forces in hypersonic flight are approximately (see equation (A4.22)):

$$\begin{aligned} L(\alpha, V, h) &= mg - \frac{mV^2}{R} = s\alpha \frac{a\rho V}{2} S, \quad \bar{D} = (C_{DW} + \varepsilon\alpha^2) \frac{a\rho V}{2} S + C_{Db} \frac{a\rho V}{2} S_b, \\ \alpha &= \frac{2p(g - V^2/R)}{s\rho a V}, \quad D = \left[C_{DW} \frac{a\rho V}{2} + \frac{2\varepsilon}{\rho a V} \left(\frac{m(g - V^2/R)}{sS} \right)^2 \right] S \\ &\quad + C_{Db} \frac{a\rho V}{2} S_b, \quad \text{or} \quad \frac{D}{m} = \left[C_{DW} \frac{q}{p} + \frac{\varepsilon p}{q} \left(\frac{g - V^2/R}{s} \right)^2 \right] + C_{Db} \frac{q}{p_b}, \quad q = \frac{\rho a V}{2}. \end{aligned} \quad (\text{A4.54})$$

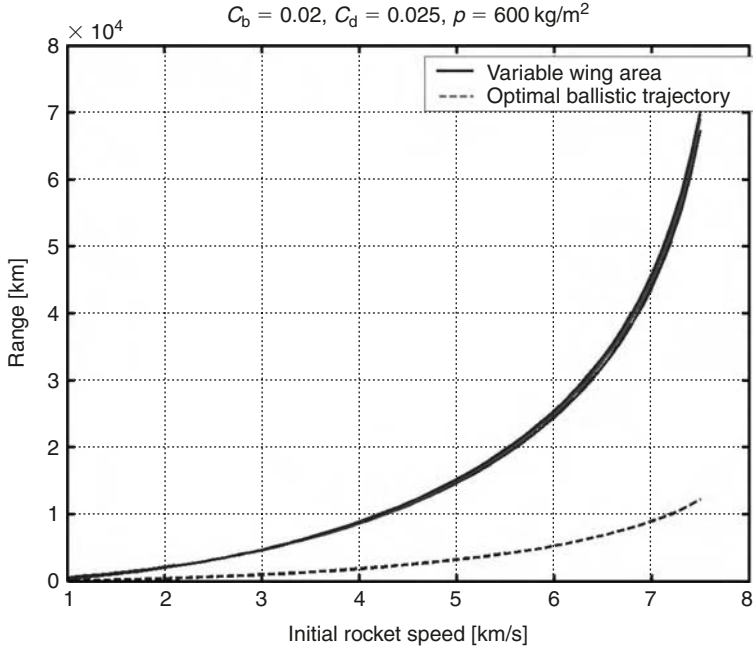


Fig. A4.6. Air vehicle altitude versus speed for wing load $p = 250, 300, 350$, and 400 kg/m^2 , piston (propeller) engine, and relative engine power 100 W/kg vehicle.

Note

$$D_{0W} = C_{DW} \frac{\rho a V}{2} S, \quad D_{0b} = C_{Db} \frac{\rho a V}{2} S_b, \quad C_{DW} = 4c,$$

$$C_{Db} = 2c_b, \quad \rho = a_2 e^{-\frac{h-11,000}{b_2}}. \quad (\text{A4.55})$$

The derivatives of D by V, h are:

$$D'_V = \frac{D_{0W}}{V} + \frac{D_{0b}}{V} - \frac{2\varepsilon mp}{s^2 \rho a} \left(g - \frac{V^2}{R} \right) \left(\frac{3}{R} + \frac{g}{V^2} \right),$$

$$D'_h = D'_\rho \rho'_h = -\frac{1}{b_2} \left(D_{0W} + D_{0b} - \frac{2\varepsilon mp(g - V^2/R)^2}{s^2 \rho a V} \right). \quad (\text{A4.56})$$

A4.4.2.1 Rocket engine or hypersonic glider

The derivatives from $T = \text{constant}$ and $T = 0$ are:

$$T'_V = 0, \quad T'_h = 0. \quad (\text{A4.57})$$

Substituting (A4.55) in (A4.56), and expressions (A4.56) and (A4.57) in (A4.37) to find ρ, h , we obtain for $h > 11,000$ m:

$$\rho = \frac{2p\sqrt{\varepsilon}}{sa} \sqrt{A_4}, \quad A_4 = \frac{\left(g - \frac{V^2}{R}\right) \left[g\left(\frac{3}{R} + \frac{g}{V^2}\right) + \frac{1}{b_2} \left(g - \frac{V^2}{R}\right)\right]}{\left(\frac{V^2}{b_2} + g\right) \left[C_{\text{DW}} + C_{\text{Db}} \left(\frac{S_b}{S}\right)\right]},$$

$$h = 11,000 + b_2 \ln \frac{a_2}{\rho}, \quad (\text{A4.58})$$

where $a_2 = 0.365$; $b_2 = 6997$ are coefficients of the exponent atmosphere for the stratosphere at 11–60 km.

If we ignore the small term $g(3/R + g/V^2)$ for $M > 3$ in (A4.58), the equations take the form:

$$\rho = \frac{2p(g - V^2/R)\sqrt{\varepsilon}}{sa} \sqrt{A_5}, \quad A_5 = \frac{1}{C_{\text{Do}}(V^2 + gb_2)}, \quad \text{where}$$

$$C_{\text{Do}} = C_{0\text{W}} + C_{\text{Db}} \left(\frac{S_b}{S}\right),$$

where $C_{\text{DW}} \approx 4c$. If we ignore the term gb_2 (for $M > 3$), then:

$$\rho = \frac{2p(g - V^2/R)}{saV} \sqrt{\frac{\varepsilon}{C_{\text{Do}}}}. \quad (\text{A4.59})$$

In the limit as $R \rightarrow \infty$ in (2–54), we find:

$$\rho = \frac{2pg}{saV} \sqrt{\frac{\varepsilon}{C_{\text{Do}}}}. \quad (\text{A4.59})'$$

Here $\sqrt{C_{\text{Do}}/\varepsilon} = \alpha_{\text{opt}}$ is an optimal (maximum C_L/C_D) wing attack angle of the horizontal flight.

Results of the computation in (A4.58) are presented in Fig. A4.7.

A4.4.2.2 Ramjet engine

The thrust of the jet engine is approximately ($M < 4$):

$$T = \xi \frac{\rho}{\rho_2} V^2, \quad T'_V = \frac{2T}{V}, \quad T'_h = -\frac{T}{b_2}, \quad (\text{A4.60})$$

where ξ is a numerical coefficient, ρ_2 is the air density at the lower end of the selected atmospheric diapason (in our case 11 km).

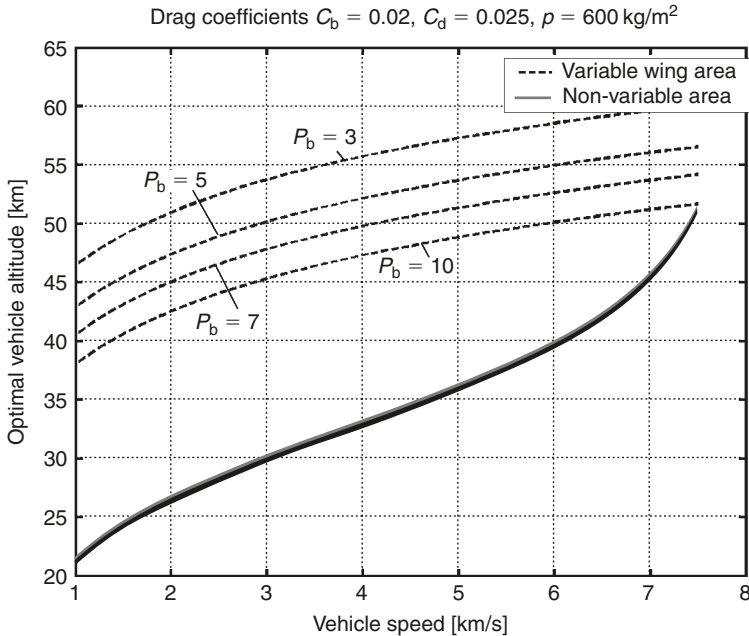


Fig. A4.7. Optimal vehicle altitude versus speed for specific body load $p_b = 3, 5, 7$, and 10 ton/m^2 , body drag coefficient $C_b = 0.02$, wing drag coefficient $C_d = 0.025$, wing load $p = 600 \text{ kg/m}^2$.

Substituting (A4.60) and (A4.56) in our main equation (A4.33), by repeat reasoning we can obtain the equation for the given engine:

$$\rho = \frac{2p\sqrt{\varepsilon}}{sa} \sqrt{A_6}, \quad A_6 = \frac{(g - V^2/g) \left[g \left(\frac{3}{R} + \frac{g}{V^2} \right) + \frac{1}{b_2} (g - V^2/R) \right]}{\left[C_{DW} + C_{Db} \left(\frac{S_b}{S} \right) \right] \left[\left(\frac{V^2}{b_2} + g \right) - \frac{2\bar{T}_0 p}{a\rho_0} \left(\frac{V}{b_2} - \frac{2g}{V} \right) \right]},$$

$$\bar{T} = \frac{T_0}{m}, \quad (\text{A4.61})$$

where T_0 is taken at the lower end of the exponent atmospheric diapason (in our case 11 km). The curve of air density versus altitude h is computed similarly to (A4.58).

A4.5 Optimal wing area

The lift force and drag of any wing may be written as:

$$Y = mg(\alpha, q, S), \quad D = D(\alpha^2, q, S). \quad (\text{A4.62})$$

Substituting (A4.62) in (A4.28) and finding the minimum H versus S , we obtain the equation:

$$D + \bar{D}'_\alpha \alpha'_S S = 0 \quad \text{or} \quad D + D'_S S = 0, \quad (\text{A4.63})$$

where α is the value found from the first equation (A4.62). Equation (A4.63) is the general equation for the optimal wing area and optimal specific load $p = m/S$ on a wing area:

A4.5.1 Subsonic speed

Lift force and drag of the subsonic wing are:

$$\begin{aligned} Y &= mg = s\alpha qS \quad \text{or} \quad \alpha = \frac{mg}{sqS}, \quad \bar{D} = (C_{D0} + \varepsilon\alpha^2)qS, \\ D &= C_{DW}qS + \varepsilon \left(\frac{mg}{s} \right)^2 \frac{1}{qS}, \end{aligned} \quad (\text{A4.62})'$$

where $q = \rho V^2/2$ is a dynamic air pressure for subsonic speed.

Substituting the last equation in (A4.62) into the first equation in (A4.63), we obtain the optimal specific load on the wing area:

$$p_{\text{opt}} = \frac{sq}{g} \sqrt{\frac{C_{DW}}{\varepsilon}}. \quad (\text{A4.63})'$$

Substituting α from (A4.62)' into the last equation in (A4.63)' and dividing both sides by vehicle mass m , we obtain:

$$\frac{D}{m} = \left[C_{DW} \frac{1}{p} + \varepsilon \left(\frac{g}{sq} \right)^2 p \right] q. \quad (\text{A4.64})$$

Here D/m is specific drag (drag per unit weight for the vehicle). Substituting (A4.63)' into (A4.64). We obtain the minimum drag for a variable wing:

$$\min \left(\frac{D}{m} \right) = 2 \frac{g}{s} \sqrt{\varepsilon C_{DW}}, \quad (\text{A4.64})'$$

where the term on the right is wing drag for the lift of one unit of weight for the vehicle. We discover the important fact than the *optimal* wing drag of a variable wing *does not depend* on airspeed, it depends *only* on the geometry of the wing. This may look wrong, but consider the following example. Wing drag is $D = mg/K$, where $K = C_L/C_D$ is the wing efficiency coefficient. The value D/m does not depend on speed.

If the air vehicle has a body, the minimum drag is:

$$\min\left(\frac{D}{m}\right) = 2 \frac{g}{s} \sqrt{\varepsilon C_{DW}} + C_{Db} \frac{q}{p_b}, \quad q = \frac{\rho V^2}{2}. \quad (\text{A4.65})$$

Full vehicle drag depends on speed because the body drag depends on V .

Substituting the (A4.63)' term for α into (A4.62)', we obtain the optimal attack angle:

$$\alpha_{\text{opt}} = \sqrt{\frac{C_{DW}}{\varepsilon}}. \quad (\text{A4.66})$$

This is the angle of optimal efficiency, but C_{DW} is the wing drag coefficient *only* when $\alpha = 0$ (not the full vehicle as in conventional aerodynamics). The coefficient of flight efficiency:

$$k = \frac{g}{D/m} \quad \text{or} \quad k_{\text{max}} = \frac{g}{\min(D/m)}. \quad (\text{A4.67})$$

A4.5.2 Hypersonic speed

The equations of wing lift force and wing air drag for hypersonic speed are as follows:

$$\begin{aligned} Y &= s\alpha q S = m\left(g - \frac{V^2}{R}\right) \quad \text{or} \quad \alpha = \frac{p(g - V^2/R)}{sq}, \\ \bar{D} &= (C_{DW} + \varepsilon\alpha^2)qS, \quad q = \frac{\rho a V}{2}. \end{aligned} \quad (\text{A4.68})$$

Substituting α from (A4.68) into \bar{D} , we obtain:

$$D = \left[C_{DW} + \varepsilon \left(\frac{m(g - V^2/R)}{sqS} \right)^2 \right] qS. \quad (\text{A4.68})'$$

Substituting the wing load $p = m/S$ into (A4.68)', we obtain:

$$\frac{D}{m} = \left[C_{DW} \frac{1}{p} + \varepsilon \left(\frac{g - V^2/R}{\xi q} \right)^2 p \right] q. \quad (\text{A4.69})$$

To find the minimum the air drag D for p , we take the derivatives and set them equal to zero, then we obtain:

$$p_{\text{opt}} = \frac{sq}{(g - V^2/R)} \sqrt{\frac{C_{DW}}{\varepsilon}}. \quad (\text{A4.70})$$

Substituting (A4.70) into (A4.69), we find the minimum wing drag:

$$\min \left(\frac{D}{m} \right)_w = \frac{2}{s} \left(g - \frac{V^2}{R} \right) \sqrt{\varepsilon C_{DW}}.$$

The sum of the minimum vehicle drag plus body drag is:

$$\min \left(\frac{D}{m} \right) = \frac{2}{s} \left(g - \frac{V^2}{R} \right) \sqrt{\varepsilon C_{DW}} + C_{Db} \frac{q}{p_b}, \quad q = \frac{\rho a V}{2}, \quad p_b = \frac{m}{S_b}. \quad (\text{A4.71})$$

Substituting (A4.70) into the term for α in (A4.65), we find the optimal attack angle of a vehicle without a body:

$$\alpha_{\text{opt}} = \sqrt{C_{DW}/\varepsilon}. \quad (\text{A4.72})$$

The coefficient of flight efficiency $k = Y/D$ is:

$$k = \frac{g - V^2/R}{D/m}, \quad k_{\text{max}} = \frac{g - V^2/R}{\min(D/m)}.$$

For hypersonic speed the coefficients are approximately:

$$s = 4, \quad \varepsilon = 2, \quad C_{DW} = 4c^2, \quad C_{Db} = 2c_1^2, \quad C_L = s\alpha, \quad C_{Do} = C_{DW} + C_{Db}. \quad (\text{A4.73})$$

In numerical computation the angle θ can be found from (A4.25) as $\theta = \Delta h/\Delta R_g$.

For the rocket engine or gliding flight we find the following relation: when S is optimum (variable), the partial derivatives from (A4.71) are:

$$D'_V = -\frac{4V}{sR} \sqrt{\varepsilon C_{DW}} + C_{Db} \frac{\rho a}{2p_b}, \quad D'_h = -\frac{C_{Db}\rho a V}{2b_2 p_b}.$$

Substituting these into (A4.37), we find the relationship between speed, altitude, and optimal wing load for a hypersonic vehicle with a rocket engine and *variable* optimal wing:

$$\rho = \frac{8gp_b V \sqrt{\varepsilon C_{DW}}}{saC_{Db} R(g + V^2/b_2)}, \quad h = 11,000 + b_2 \ln \frac{a_2}{\rho}. \quad (\text{A4.74})$$

For $\zeta = 4, \varepsilon = 2$, equation (A4.74) has the form:

$$\rho = \frac{2gp_b V \sqrt{2C_{DW}}}{C_{Db} a R(g + V^2/b_2)}, \quad h = 11,000 + b_2 \ln \frac{a_2}{\rho}. \quad (\text{A4.74})'$$

Results of computation using (A4.74)' for $\zeta = 4, \varepsilon = 2, a_2 = 0.365, b_2 = 6997$ and different p_b are presented in Fig. A4.7 (dashed lines). As you see, the variable area wing saves kinetic energy, because its curve is located over an invariable (fixed) wing. This is advantageous only at orbital speed (7.9 km/s) because no lift force is necessary.

A4.6 Estimation of flight range

A4.6.1 Air and space vehicles without thrust

The aircraft range can be found from equation (A4.26):

$$R_a = \int_{V_1}^{V_2} \frac{mV dV}{T - D - mg\theta}, \quad V_1 > V_2 \quad \text{or} \quad R_a = \int_{V_2}^{V_1} \frac{V dV}{D/m + g\theta}, \quad \text{if } T = 0. \quad (\text{A4.75})$$

Consider a missile with the *optimal variable wing* in a descent trajectory with thrust $T = 0$:

- (a) Make the simplest estimation using equations for kinetic energy from classical mechanics. Separate the flight into two stages: hypersonic and subsonic. If we have the ratio of vehicle efficiency $k_1 = C_L/C_D$, $k_2 = C_L/C_D$, where k_1, k_2 are the ratios of flight efficiency for the hypersonic and subsonic stages respectively, we find the following equations for a range in each region:

$$\frac{m}{2}(V_1^2 - V_2^2) = \frac{m(g - V^2/R)}{k_1} R_1, \quad R_1 = \frac{k_1(V_1^2 - V_2^2)}{2(g - V^2/R)},$$

$$R_2 = k_2 h, \quad R_a = R_1 + R_2.$$

Or more exactly:

$$d\left(\frac{mV^2}{2}\right) = \frac{m(g - V^2/R)}{k_1} dR_1, \quad R_1 = -\frac{k_1 R}{2} \ln\left(\frac{g - V_2^2/R}{g - V_1^2/R}\right). \quad (\text{A4.76})$$

where R_1 is the hypersonic part of the range; R_2 is the subsonic part of the range; V_1 is the initial (maximum) vehicle hypersonic speed; V_2 is a final hypersonic speed; and h is the altitude at the initial stage of the subsonic part of the trajectory.

- (b) To be more precise. Assume in (A4.75) $\rho = \text{constant}$ (taking average air density):

- For the *hypersonic* part of the trajectory: substitute (A4.71) into (A4.76). We then have:

$$R_{1H} = \int_{V_1}^{V_2} \frac{V dV}{aV^2 + bV + c}, \quad \text{or} \quad R_{1H} = \int_{V_1}^{V_2} \frac{V dV}{X}, \quad \text{where} \quad X = aV^2 + bV + c,$$

$$a = \frac{2\sqrt{\varepsilon C_{DW}}}{\xi R}, \quad b = -C_{Db} \frac{\rho a}{2p_b}, \quad c = \frac{T}{m} - \frac{2g}{s} - g\theta, \quad \Delta = 4ac - b^2,$$

$$R_{1H} = \left[\frac{1}{2a} \ln X - \frac{b}{2a} \int \frac{dV}{X} \right]_{V_1}^{V_2}, \quad \int \frac{dV}{X} = \frac{2}{\sqrt{\Delta}} \arctan \frac{2aV + b}{\sqrt{\Delta}} \quad \text{for } \Delta \geq 0,$$

$$\int \frac{dV}{X} = -\frac{2}{\sqrt{-\Delta}} \arctan h \frac{2aV + b}{\sqrt{-\Delta}} = \frac{1}{\sqrt{-\Delta}} \ln \frac{2aV + b - \sqrt{-\Delta}}{2aV + b + \sqrt{-\Delta}} \quad \text{for } \Delta \leq 0. \quad (\text{A4.77})$$

2. For the *subsonic* part of the trajectory: substitute (A4.65) into (A4.75). We then have:

$$R_{1S} = -\frac{1}{2C_2} \ln \left| \frac{C_1 - C_2 V_2^2}{C_1 - C_2 V_1^2} \right|, \quad (\text{A4.78})$$

where the values for C_1, C_2 are:

$$C_1 = \frac{T}{m} - g \left(\frac{2\sqrt{\varepsilon C_{DW}}}{as} + \theta \right), \quad C_2 = C_{Db} \frac{\rho}{2p_b}. \quad (\text{A4.79})$$

The trajectory (without the rocket part of the trajectory) is:

$$R_1 = R_{1H} + R_{1S} \quad \text{or} \quad R_g = R_{1H} + R_{1S} + R_2, \quad (\text{A4.80})$$

where $R_2 = k_2 h$ computed for altitude h at the end of the kinetic part of the subsonic trajectory.

3. The *ballistic* trajectory of a wingless missile without atmosphere drag is:

$$\begin{aligned} h &= \frac{gt^2}{2}, & t &= \sqrt{\frac{2h}{g}}, & R_b &= V_1 t = V_1 \sqrt{\frac{2h}{g}}, & V_i &= \sqrt{V_1^2 + V_y^2}, \\ V_y^2 &= 2h(g - V^2/R), \end{aligned} \quad (\text{A4.81})$$

where h is the initial altitude; V_1 is the initial horizontal speed of the wingless missile at altitude h ; V_y is initial (shot) vertical speed at $h = 0$; V_i is the full initial (shot) speed at $h = 0$.

For the hypersonic interval $5 < V < 7.5$ km/s, we can use the more exact equation:

$$R_b = V_1 \sqrt{\frac{2h}{(g - V_1^2/R)}}, \quad (\text{A4.82})$$

where $R = 6378$ km is the radius of Earth. The full range of a ballistic rocket plus the range of a winged missile is:

$$R_f = R_b + R_a + R_g, \quad (\text{A4.83})$$

where $R_g = kh$ is the vehicles gliding range from the final altitude h_2 (see Fig. A4.11) with aerodynamic efficiency k .

The classical method finding of the optimal shot ballistic range for spherical Earth without atmosphere is:

$$R_b = 2R\beta_{opt}, \quad \tan \beta_{opt} = \frac{\nu_A}{2\sqrt{1 - \nu_A}}, \quad \nu_A = \frac{V_A^2}{V_c^2}, \quad (\text{A4.84})$$

where β_{opt} is the optimal shot angle; V_A is the shot projectile speed; and V_c is an orbital speed for a circular orbit at a given altitude.

4. *Cannon projectile.* We divide the distance into three sub-distances: (1) $1.2M < M$, (2) $0.9M < M < 1.2M$, and (3) $0 < M < 0.9M$. The range of the wing cannon projectile may be estimated using the equation:

$$R = \frac{k_1}{2g} (V_1^2 - V_2^2) + \frac{k_2}{2g} (V_2^2 - V_3^2) + \frac{k_3}{2g} (V_3^2 - V_0^2),$$

where $0 < V_0 < V_3 < V_2 < V_1$, (A4.85)

where k_1 , k_2 , and k_3 are the average aerodynamic efficiencies for sub-distances 1, 2, 3, respectively. Conventionally, these coefficients have the following values: subsonic $k_3 = 8\text{--}15$, near sonic $k_2 = 2\text{--}3$, and supersonic and hypersonic $k_1 = 4\text{--}9$. If $V > 600 \text{ m/s}$, the first term in (A4.85) has the greatest value and we can use the more simple equation for range estimation:

$$R = \frac{k_1}{2g} V_1^2. \quad (\text{A4.84})'$$

At the top of its trajectory, a modern projectile can have an additional impulse from small rocket engines. Their weight is 10–15% of the full mass of the projectile and increases the maximum range by 7–14 km. In this case we must substitute $V = V_1 + dV$ into (A4.84)', where dV is the additional impulse (150–270 m/s).

A4.6.2 Subsonic aircraft with thrust: horizontal flight

The optimal climb and descent of a subsonic aircraft with a constant mass and fixed wing is described by equations (A4.50) and (A4.47). Any given point in a climb curve may be used for horizontal flight (with different efficiency). We consider in more detail the horizontal flight when the aircraft mass decreases because the fuel is spent. This consumption may reach 40% of the initial aircraft mass. The optimal horizontal flight range may be computed in the following way:

$$dR = V dt, \quad dt = \frac{dm}{c_s T} = \frac{g dm}{c_s D}, \quad dR = \frac{gV}{c_s D(m)} dm, \quad R = \frac{gV}{c_s} \int_{m_k}^m \frac{dm}{D(m)}, \quad (\text{A4.86})$$

where m is fuel mass; c_s is fuel consumption, kg/s/kg thrust.

- (a) For a *fixed wing*, we have (from (A4.44)):

$$D = C_{\text{Do}} q S + \frac{\varepsilon}{qS} \left(\frac{g}{s} \right)^2 m^2, \quad \text{where } C_{\text{Do}} = C_{\text{Dw}} + C_{\text{Db}} \left(\frac{S_b}{S} \right), \quad q = \frac{\rho V^2}{2}. \quad (\text{A.87})$$

Substituting (A4.87) into (A4.86), we obtain:

$$R = \frac{gV}{c_s \sqrt{C_1 C_2}} \arg \tan \frac{\sqrt{C_1/C_2}(m - m_k)}{1 + (C_1/C_2)m m_k}, \quad \text{where} \quad C_1 = \frac{\varepsilon}{qS} \left(\frac{g}{s} \right)^2, \\ C_2 = C_{D0} q S. \quad (\text{A4.88})$$

(b) For a *variable wing* we have (from (A4.65)):

$$R = \frac{gV}{c_s C_1} \ln \frac{C_1 m - C_2}{C_1 m_k - C_2}, \quad \text{where} \quad C_1 = 2 \frac{g}{s} \sqrt{\varepsilon C_{DW}}, \\ C_2 = C_{Db} q S_b, \quad \rho = \rho_0 e^{-h/b_1}. \quad (\text{A4.89})$$

Results of the computation are presented in Fig. A4.8. The aircraft have the following parameters: $C_{DW} = 0.02$; $C_{Db} = 0.08$; $b_1 = 9086$; $S = 120 \text{ m}^2$; $m = 100 \text{ ton}$, $m_k = 80 \text{ ton}$, $c_s = 0.00019 \text{ kg/s/kg}$ thrust; wing ratio $\lambda = 10$.

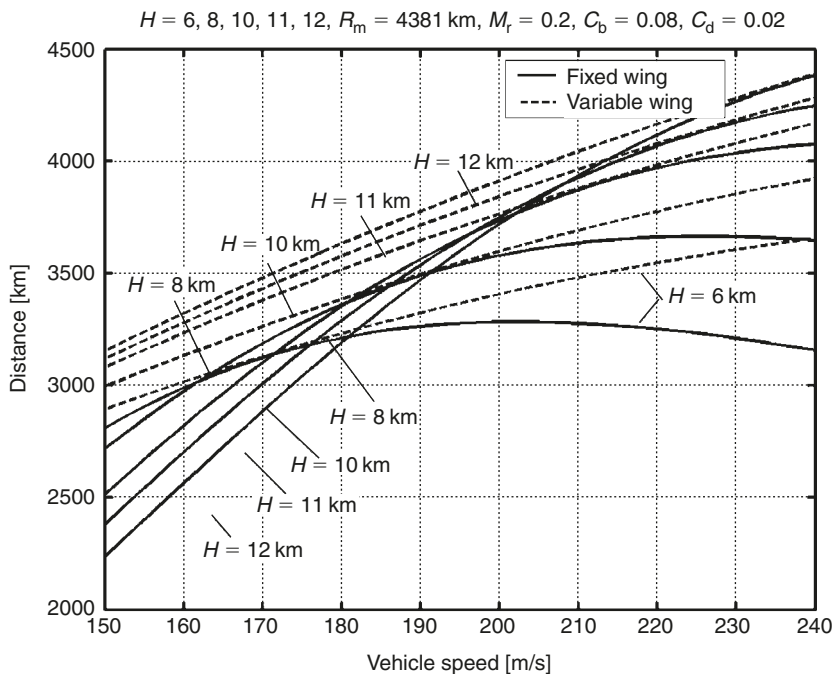


Fig. A4.8. Aircraft range [km] for altitude $H = 6, 8, 10, 11$, and 12 km ; maximum range $R_m = 4381 \text{ km}$; relative fuel mass $M_r = 0.2$; body drag coefficient $C_b = 0.08$; and wing drag coefficient $C_d = 0.02$.

As you see, the specific fuel consumption does not depend on speed and altitude, a good aircraft design reaches the maximum range only at one point, in one flight regime: when the aircraft flies at the maximum speed possible for the critical Mach number, at the maximum altitude possible for that engine. The deviation from this point decreases in the range in 5–10–15% or more. The variable wing increases efficiency of the other regime, which that approximately reduces the losses by a half.

The coefficient of flight efficiency may be computed using equation $k = g/(D/m)$, where the values:

$$\frac{D}{m} = C_{DW} \frac{q}{p} + \frac{\varepsilon p}{q} \left(\frac{g}{s} \right)^2 + C_{Db} \frac{q}{p_b}, \quad \left(\frac{D}{m} \right)_1 = 2 \frac{g}{s} \sqrt{\varepsilon C_{DW}} + C_{Db} \frac{q}{p_b}, \quad (\text{A4.90})$$

apply for fixed and variable wings, respectively. Results of computation are presented in Fig. A4.9. The curve of the variable wing is the round curve of the fixed wing.

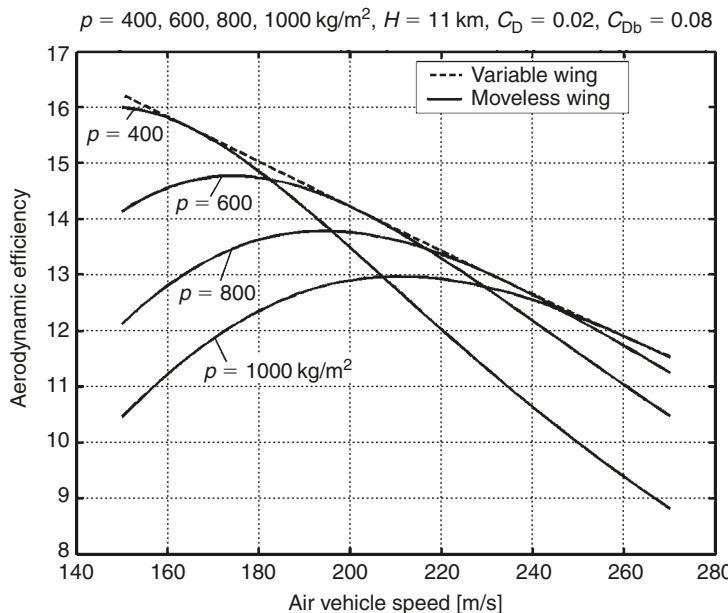


Fig. A4.9. Aerodynamic efficiency of non-variable and variable wings for wing load $p = 400, 600, 800$, and 1000 kg/m^2 ; wing drag $C_D = 0.02$, body drag $C_{Db} = 0.08$, wing ratio 10.

A4.7 Optimal engine control for constant flight pass angle

Let us consider equations (A4.1)–(A4.5) for a constant angle of trajectory, $\theta = \text{constant}$. Substituting $\theta = \text{constant}$, thrust $T = V_e \beta$, and a new independent variable $s = Vt$

(where s is the length of the trajectory) into the equation system (A4.1)–(A4.5). We obtain the following equations:

$$\frac{dL}{ds} = \cos \theta,$$

$$\frac{dh}{ds} = \sin \theta,$$

$$\frac{dV}{ds} = \frac{V_e(h, V)\beta - \bar{D}(\alpha, V, h)}{mV} - \frac{g}{V} \sin \theta,$$

$$\frac{dm}{ds} = -\frac{1}{V} \beta,$$

$$Y(\alpha, V, h) - gm \cos \theta + \frac{mV^2}{R} + 2mV\omega_E \cos \varphi_E = 0,$$

$$0 \leq \beta \leq \beta_{\max}.$$

(A4.91)–(A4.96)

Equation (A4.95) is used to substitute for α in equation (A4.93) and for a change of air drag:

$$\bar{D}(\alpha, V, h) = D(V, h). \quad (\text{A4.97})$$

We find a non-linear system with a linear fuel control β . This means the system can have a singular solution.

A4.8 Solution

Consider the maximum range for vehicles described by equation (A4.91) – (A4.96).

Let us write the Hamiltonian H :

$$H = \cos \theta + \lambda_1 \sin \theta + \lambda_2 \left[\frac{V_e(h, V)\beta - D(V, h)}{mV} - \frac{g}{V} \sin \theta \right] - \lambda_3 \frac{1}{V} \beta, \quad (\text{A4.98})$$

where $\lambda_1(s), \lambda_2(s), \lambda_3(s)$ are unknown multipliers. Application of conventional methods gives:

$$\dot{\lambda}_2 = -\frac{\partial H}{\partial V} = -\lambda_2 \left[\left(-\frac{1}{V^2} \right) \left(\frac{V_e \beta - D(V, h)}{m} - g \sin \theta \right) - \frac{D'_V}{mV} \right] - \lambda_3 \frac{1}{V^2} \beta,$$

$$\dot{\lambda}_3 = -\frac{\partial H}{\partial m} = \lambda_2 \frac{V_e \beta - D}{m^2 V},$$

$$\beta = \max_{\beta} H = \beta_{\max} \operatorname{sign}[\lambda_2 V_e - \lambda_3 m]. \quad (\text{A4.99})–(\text{A4.101})$$

where D'_V is the first partial derivative of D by V .

The last equation shows that the fuel control β can have only two values, $\pm\beta_{\max}$. We consider the singular case when:

$$A = \lambda_2 V_e - \lambda_3 m \equiv 0. \quad (\text{A4.102})$$

This equation has two unknown variables, λ_2 and λ_3 , and does not contain information about fuel control β .

The first two equations (A4.91) and (A4.92) do not depend on variables and can be integrated:

$$L = s \cos \theta, \quad (\text{A4.103})$$

$$H = s \sin \theta. \quad (\text{A4.104})$$

In accordance with the Ref.² let us differentiate equation (A4.102) by the independent variable s . After substitution into equations (A4.93)–(A4.95), (A4.97), (A4.99), (A4.100), (A4.102), and (A4.104) we obtain the relation for $\lambda_2 \neq 0, \lambda_3 \neq 0$:

$$\begin{aligned} \dot{A} &= VD - mVD'_m + V_e(-D - mg \sin \theta + VD'_V) - VV'_{e,V}(D - mg \sin \theta) \\ &\quad + mV^2V'_{e,s} = 0. \end{aligned} \quad (\text{A4.105})$$

This equation also does not contain β , however, it does contain an important relation between variables m, h and V , on an optimal trajectory. This is a 3-dimentional surface. If we know:

$$D = D(h, V), \quad (\text{A4.106})$$

$$V_e = V_e(h, V). \quad (\text{A4.107})$$

The mass of our apparatus m , and its altitude h , we can find the optimal flight speed. This means we can calculate the necessary thrust and the fuel consumption for every point m, h, V (Fig. A4.10).

If we want to find an equation for the fuel control β , we continue to differentiate equation (A4.105) to find the independent variable s and substitute in equations (A4.91)–(A4.104). If we calculate the relation for β , if $\lambda_2 \neq 0, \lambda_3 \neq 0, V_e = \text{constant}$, then:

$$\beta = \frac{\dot{A}'_V(D + mg \sin \theta) - mV\dot{A}'_s}{V_e \dot{A}'_V - m\dot{A}'_m}, \quad (\text{A4.108})$$

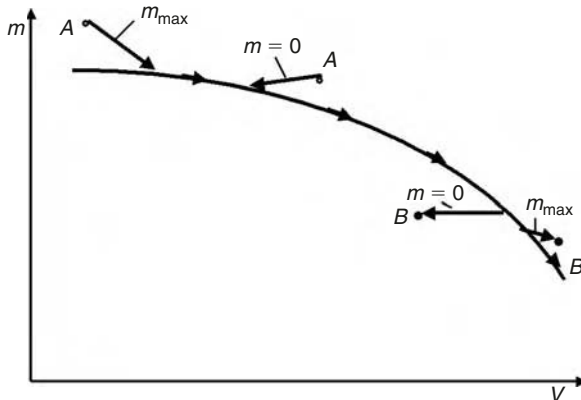


Fig. A4.10. Optimal fuel consumption of flight vehicles.

where

$$\dot{A}'_V = \frac{\partial}{\partial V} \left(\frac{dA}{ds} \right), \quad \dot{A}'_s = \frac{\partial}{\partial s} \left(\frac{dA}{ds} \right). \quad (\text{A4.109})$$

The necessary condition of the optimal trajectory as it is shown in the Refs.²⁻⁸ (see, for example, equation (4.2)⁴) is:

$$-(-1)^k \frac{\partial}{\partial \theta} \left[\frac{d^{2k}}{ds^{2k}} \left(\frac{\partial H}{\partial s} \right) \right] \geq 0. \quad (\text{A4.110})$$

where $k = 1$.

If the flight is horizontal ($\theta = 0$), the expression (A4.108) is very simply:

$$\beta = \frac{D}{V_e}. \quad (\text{A4.111})$$

This means the thrust equals the drag, a fact that is well known in aerodynamic science.

To obtain the specific equations for different forms of drag and thrust, we must take formulas (or graphs) for subsonic, transonic, supersonic and hypersonic speed for thrust and substitute them into the equations (A4.105) and (A4.108).

A4.9 Simultaneous optimization of the path angle and fuel consumption

Consider the case where the path angle and the fuel consumption are simultaneously optimized.

In this case the general equations (A4.1)–(A4.5) have the form:

$$\begin{aligned}\frac{dL}{ds} &= 1, \\ \frac{dh}{ds} &= \theta, \\ \frac{dV}{ds} &= \frac{V_e(h, V)\beta - D(m, V, h)}{mV} - \frac{g}{V}\theta, \\ \frac{dm}{ds} &= -\frac{1}{V}\beta, \\ Y(\alpha, V, h) &= mg + \frac{mV^2}{R} + 2mV\omega_E \cos \varphi_E.\end{aligned}\quad (\text{A4.112})\text{--}(\text{A4.116})$$

Let us write the Hamiltonian:

$$H = 1 + \lambda_1\theta + \lambda_2 \left(\frac{V_e(h, V)\beta - D(m, V, h)}{mV} - \frac{g}{V}\theta \right) - \lambda_3 \frac{1}{V}\beta. \quad (\text{A4.117})$$

The necessary conditions of optima give:

$$\begin{aligned}A &= \frac{\partial H}{\partial \theta} = V\lambda_1 - g\lambda_2 = 0, \\ B &= \frac{\partial H}{\partial \beta} = V_e\lambda_2 - m\lambda_3 = 0.\end{aligned}\quad (\text{A4.118}) \text{ and } (\text{A4.119})$$

The lambda equations are:

$$\begin{aligned}\dot{\lambda}_1 &= -\frac{\partial H}{\partial h} = -\lambda_2 \frac{V'_{e,h}\beta - D'_h}{mV}, \\ \dot{\lambda}_2 &= -\frac{\partial H}{\partial V} = -\lambda_2 \left[\frac{(V'_{e,h}\beta - D'_V)V - (V_e\beta - D)}{mV^2} + \frac{g}{V^2}\theta \right] - \lambda_3 \frac{1}{V^2}\beta, \\ \dot{\lambda}_3 &= -\frac{\partial H}{\partial m} = \lambda_2 \frac{V_e\beta - D + mD'_m}{m^2V}.\end{aligned}\quad (\text{A4.120})\text{--}(\text{A4.122})$$

If we differentiate A (A4.118), from $dA/ds = 0$, we find the optimal fuel consumption:

$$\beta = \frac{gVD'_V - V^2D'_h}{g(V_e + V'_{e,V}V) - V'_{e,h}V^2}. \quad (\text{A4.123})$$

Then we differentiate B (A4.119), from $dB/ds = 0$ we find the optimal path angle:

$$\theta = \frac{V'_{e,V}D - V_eD'_V - V_eD/V - D + mD'_m}{m(g + V'_{e,h}V - V'_{e,V}g)}. \quad (\text{A4.124})$$

We have used the conventional forms for the partial derivatives in (A4.120)–(A4.124) as in the earlier sections of this chapter (see for example (A4.51)).

If we know from analytical formulas or graphic functions V_e, D, Y we can find the optimal trajectory of the air vehicle.

In the general case, this trajectory includes four parts:

1. Moving between limitations θ and β .
2. Moving between one limitation θ or β and one optimal control β or θ .
3. Moving simultaneously with both optimal controls θ and β .
4. Moving at a given point along one limitation and/or both limitations.

A4.10 Application to aircraft, rocket missiles, and cannon projectiles

A4.10.1 Application to rocket vehicles and missiles

Let us apply the previous results to typical current middle- and long-distance rockets with warheads. We will show: if the warhead has wings and uses the optimal trajectory, the range of the warhead (or its useful load) is increased dramatically in most cases. We will compute the optimal trajectories for a rocket-launched warhead at a particular altitude (20–60 km) and speed (1–7.5 km/s). Point B is located on the curve (A4.58) for a fixed wing and on curve (A4.74) for a variable wing (Fig. A4.11). Further, the winged warhead flies (descends) along the optimal trajectory BD (Fig. A4.11) according to equations (A4.58) (fixed wing) or equations (A4.74) (variable wing), respectively. When the speed is reduced by a small amount (for example, 1 km/s) (point D in Fig. A4.11), the winged warhead glides (distance DE in Fig. A4.11).

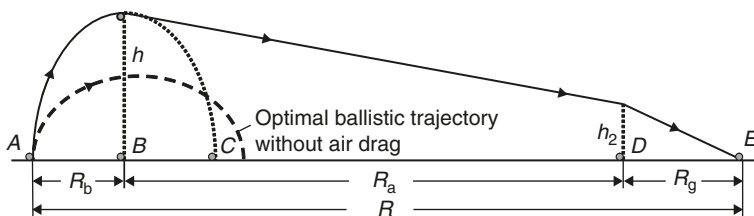


Fig. A4.11. Trajectory of flying vehicles.

The following equations are used for computation.

A4.10.1.1 The optimal trajectory for a fixed wing space vehicle

- (a) Equation (A4.58) is used to calculate $h = h(V)$ to find the optimal trajectory of a warhead with a non-variable fixed wing in the speed interval $1 < V < 7.5 \text{ km/s}$. The result is presented in Fig. A4.7.

(b) Equation (A4.54) gives the magnitude (D/m).

(c) The equation (A4.75) in the form:

$$\begin{aligned}\Delta R_a &= \frac{V\Delta V}{(D/m) + g\theta}, \quad R_a = \sum \Delta R_a, \quad \theta = -\frac{\Delta h}{\Delta R_a}, \\ k &= \frac{g - V_0^2/R}{D/m}, \quad R_g = h_0 k.\end{aligned}\quad (\text{A4.125})$$

is used for computation in the intervals R_a , R_g (Fig. A4.11). Here R_g is the range of a gliding vehicle.

(d) Equation (A4.75) is used to calculate R_b in the launch interval AB (Fig. A4.11).

(e) The full range, R , of a warhead with a fixed wing and the full ballistic warhead range, R_w , are:

$$R = R_b + R_a + R_g, \quad R_w = 2R_b. \quad (\text{A4.126})$$

(f) Equation (A4.84) is used to calculate the optimal *ballistic* trajectory of a shot without air drag (a vehicle *without* wings). The range of this trajectory, as it is known, may be significantly more than the range in the atmosphere.

The results are presented in Fig. A4.12. Computation of the relative range (for different p_b) using the formula:

$$R_r = \frac{R_f}{R_b}, \quad (\text{A4.127})$$

is presented in Fig. A4.13. The optimal range of the winged vehicle is approximately 4.5 times that of the ideal ballistic rocket computed without air drag. In the atmosphere this difference will be significantly more.

A4.10.1.2 Rockets, missiles and space vehicles with variable wings

The computation is the same. For computing ρ , h , D/m we can use equations (A4.74) and (A4.71), respectively. The results for different body loads are presented in Fig. A4.7. The optimal trajectories of vehicles with variable wing areas have less slope. This means the vehicle loses less energy when it moves. It travels above the optimal trajectory of a vehicle with fixed wings, which means it needs a lot more time (10–20) and more wing area than a fixed wing space vehicle (Fig. A4.14). The computation of the optimal variable wing area is presented in Fig. A4.15. The relative range (equation (A4.127)) is presented in Fig. A4.16.

The aerodynamic efficiency of vehicles with fixed (for different p_b bodies) and optimal variable wings computed using equations (A4.125) and (A4.67), respectively is presented in Fig. A4.17. The difference between vehicles with fixed and variable wings reaches 0.2–0.6. The slope of the trajectory to horizontal is small (Fig. A4.18).

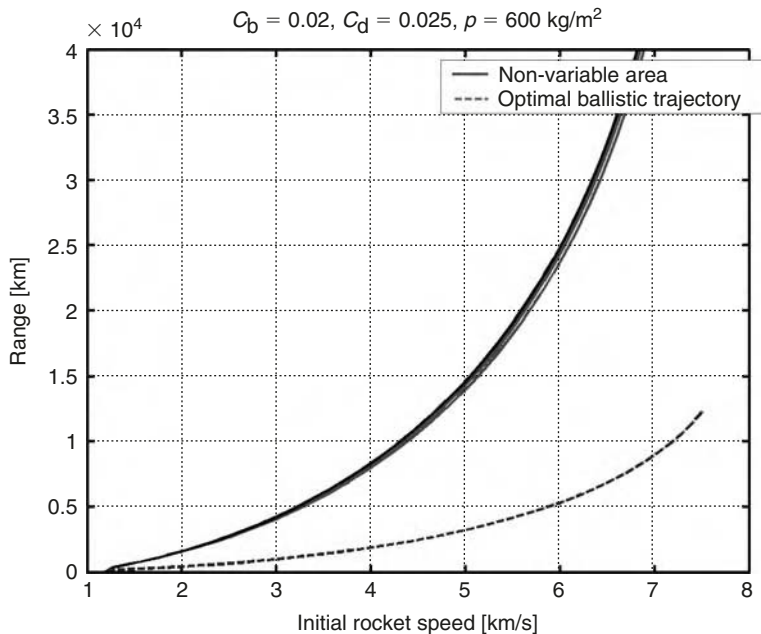


Fig. A4.12. Range of *non-variable* wing vehicle for body drag coefficient $C_b = 0.02$, wing drag coefficient $C_d = 0.025$, and wing load $p = 600 \text{ kg/m}^2$.

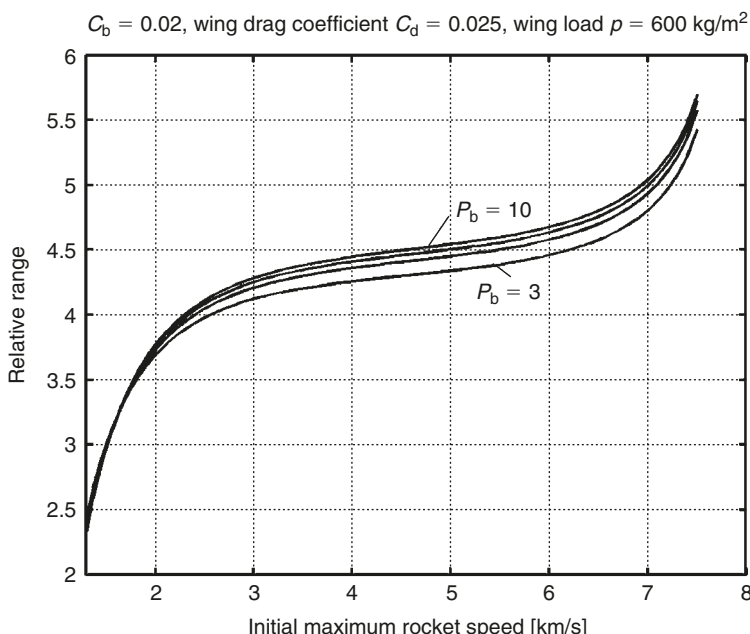


Fig. A4.13. The relative range of a *non-variable* wing vehicle for the body drag coefficient $C_b = 0.02$, wing drag coefficient $C_d = 0.025$, wing load $p = 600 \text{ kg/m}^2$, and body load $P_b = 3\text{--}10 \text{ ton/m}^2$.

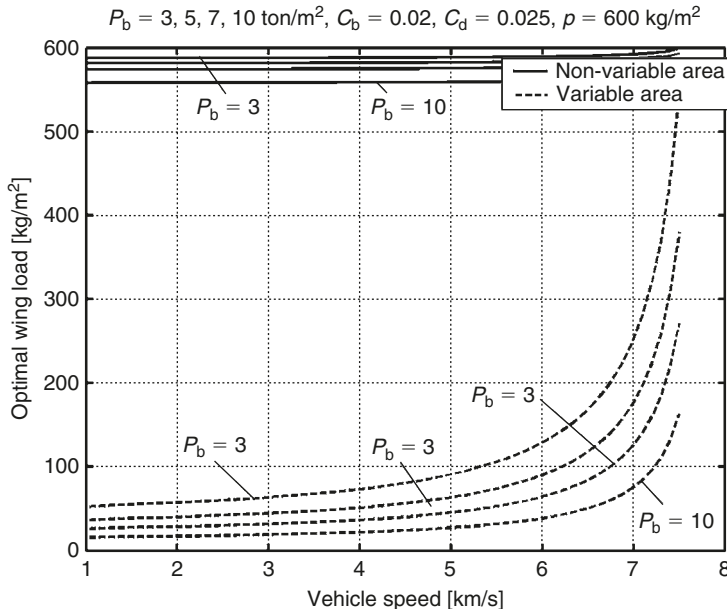


Fig. A4.14. Optimal wing load versus speed for specific body load $P_b = 3, 5, 7$, and 10 ton/m^2 , body drag coefficient $C_b = 0.02$, wing drag coefficient $C_d = 0.025$, and wing load $p = 600 \text{ kg/m}^2$.

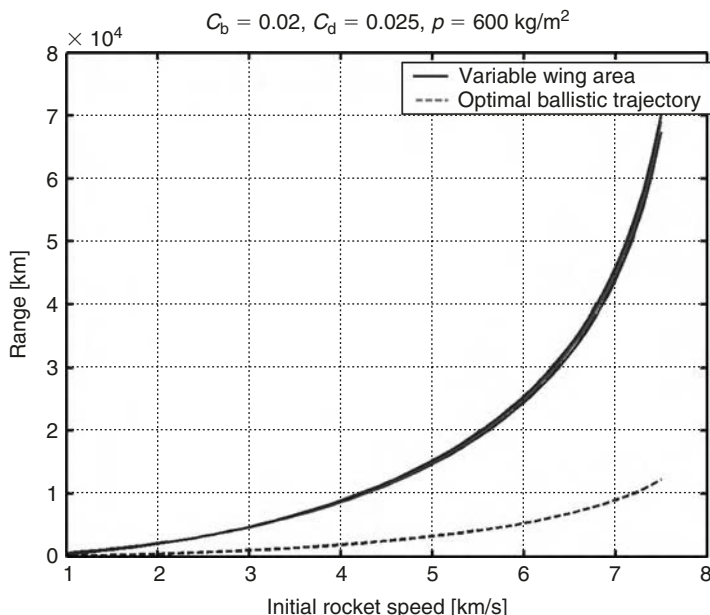


Fig. A4.15. Range of a variable wing vehicle for the body drag coefficient $C_b = 0.02$, the wing drag coefficient $C_d = 0.025$, and the wing load $p = 600 \text{ kg/m}^2$.

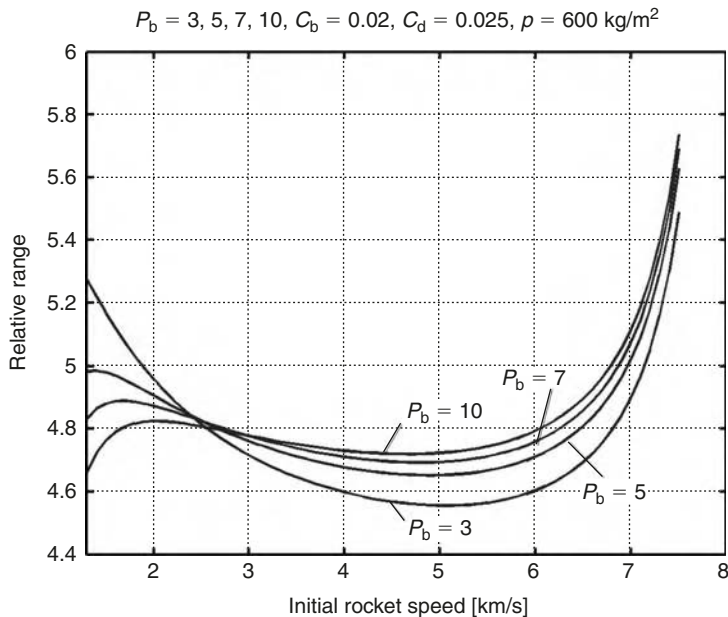


Fig. A4.16. Relative range of variable wing vehicle for the body drag coefficient $C_b = 0.02$, the wing drag coefficient $C_d = 0.025$, the wing load $p = 600 \text{ kg/m}^2$, and the body load $P_b = 3-10 \text{ ton/m}^2$.

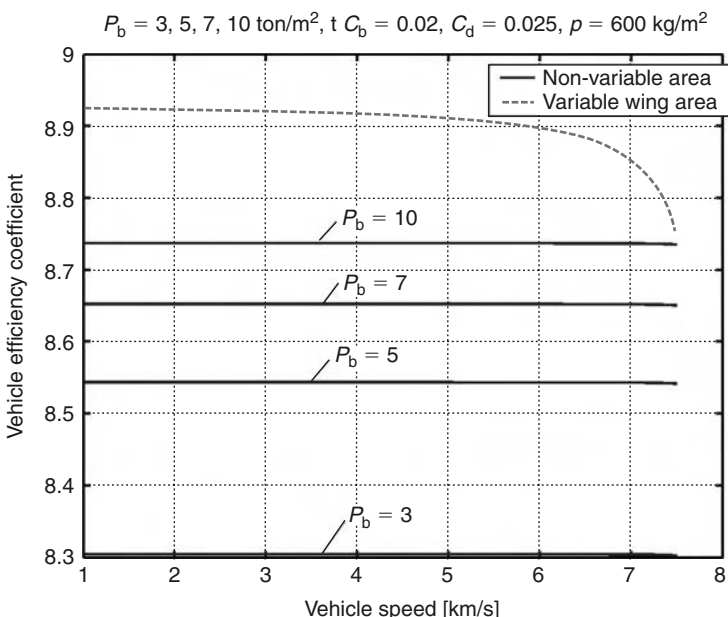


Fig. A4.17. Vehicle efficiency coefficient versus speed for specific body load $P_b = 3, 5, 7$, and 10 ton/m^2 , body drag coefficient $C_b = 0.02$, wing drag coefficient $C_d = 0.025$, and wing load $p = 600 \text{ kg/m}^2$.

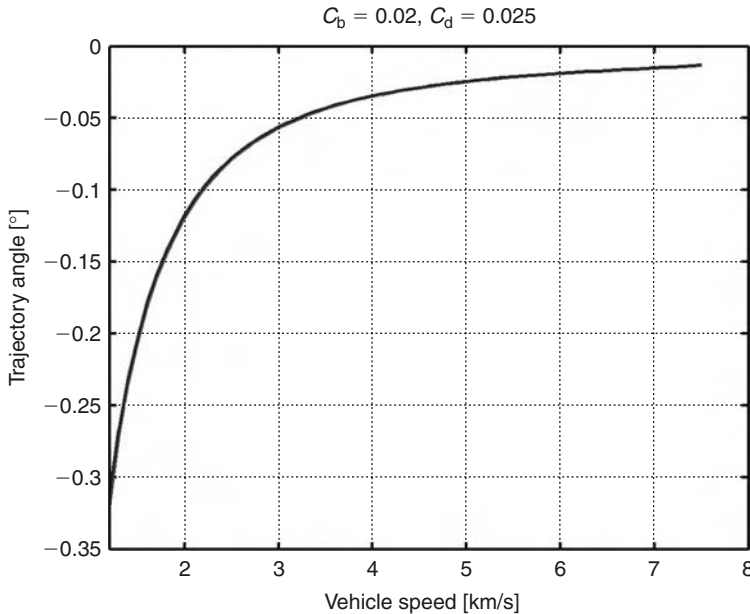


Fig. A4.18. Trajectory angle versus speed for body drag coefficient $C_b = 0.02$ and wing drag coefficient $C_d = 0.025$.

The range of the *fixed* wing vehicle computed using equation (A4.125) is presented in Fig. A4.12. The range of the *variable* wing vehicle computed using equation (A4.126) is presented in Fig. A4.15. The curve is practically the same (see Figs. A4.12 and A4.15).

A4.10.1.3 Increasing the rocket payload for the same range

If we do not need to increase the range, the winged vehicle can be used to increase the payload, or to save rocket fuel. We can change the mass of the fuel or the payload. The additional payload may be estimated by the following equation:

$$\mu = 1 - e^{-\frac{\Delta V}{V_e}}. \quad (\text{A4.128})$$

where $\mu = m/m_b$ is relative mass (the ratio of rocket mass of the winged vehicle to the ballistic rocket), $\Delta V = V_b - V$ is the difference between the optimal ballistic rocket speed (equation (A4.84)) and the rocket with a winged vehicle (equation (A4.126)) for given range (see Fig. A4.12). Results of computation are presented in Fig. A4.19. The mass of the rocket with a winged vehicle may be only 20–35% of the optimal ballistic rocket flown without air drag.

A4.10.1.4 Conclusion

The winged air-space vehicle has a range that is greater by a minimum of 4.5–5 times than an optimal shot ballistic space vehicle. The variable wing improves the aerodynamic efficiency by 3–10% and also improves the range. An optimal variable wing

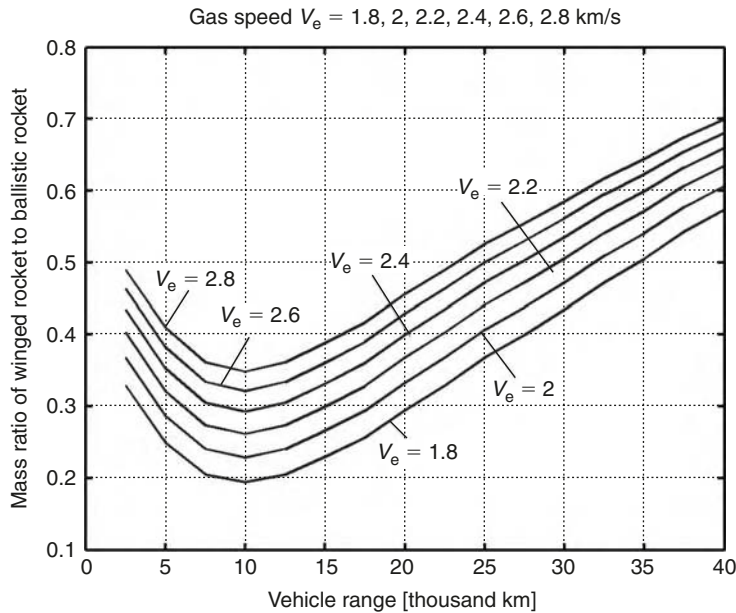


Fig. A4.19. Ratio of mass of winged rocket to ballistic rocket for specific engine run-out gas speed $V_e = 1.8, 2, 2.2, 2.4, 2.6$, and 2.8 km/s .

Table A4.1. Properties of current typical cannons.

Name	Caliber (mm)	Nozzle speed (m/s)	Mass of projectile (kg)	Range (km)	RAP (km)
M107	175	509–912	67	15–33	
SD-203	203	960	110	37.5	
2S19	155	810	43.6	24.7	
2S1	122	690–740	21.6	–	
S-23	180	–	–	30.4	43.8
2A36	152	–	–	17.1	24
D-20	152	600–670	43.5–48.8	20	

Source: Jane's.

requires a large wing area. If you do not need to increase the range, you may instead increase payload.

A4.10.2 Application to cannon wing projectiles

Properties of a typical current cannons are shown in Table A4.1.

The computations using equation (A4.84)' for different k and Rocket Artillery Projectile (RAP) with $dV = 270 \text{ m/s}$ are presented in Figs. A4.20 and A4.21.

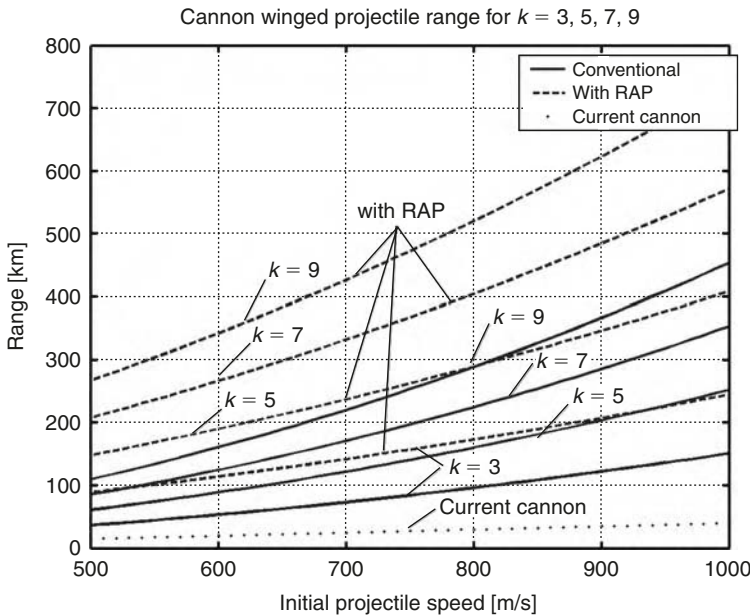


Fig. A4.20. Cannon winged projectile range for average aerodynamic efficiency $k = 3, 5, 7$, and 9.

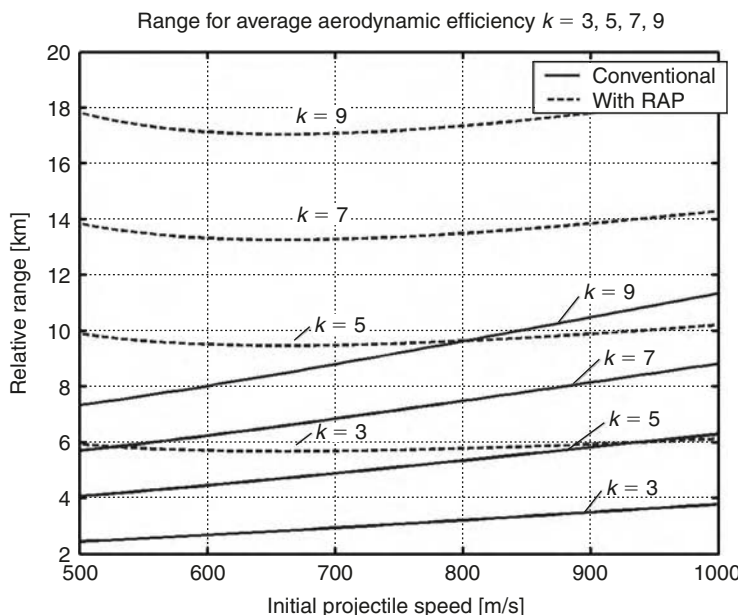


Fig. A4.21. Cannon winged projectile relative range for average aerodynamic efficiency $k = 3, 5, 7$, and 9.

A4.10.2.1 Conclusion

As you see (Figs. A4.20 and A4.21), the winged projectile increase its range 3–9 times (from 35 up to 360 km, $k = 9$). The projectile with RAP increases its range 5–14 (from 40 up to 620 km, $k = 9$). Winged shells have another important advantage: they do not need to rotate. We can use a barrel with a smooth internal channel. This allows for an increase in projectile nozzle speed of up to 2 km/s and in shell range of up to 1000 km ($k = 5$).

A4.10.3 Application to current aircraft

We can use equations (A4.88) and (A4.89) for computations for typical passenger airplanes (Figs. A4.22, A4.23 and A4.8), where all values are divided by the maximum range $R_m = 4381$ km (for a fuel mass that is 20% of vehicle mass) at a speed of $V = 240$ m/s, and altitude $H = 12$ km. The speed is limited by the critical Mach number ($V < M = 0.82$), and the altitude is limited by the engine trust, when engine stability is such that it works in a cruise regime. Fig. A4.22 shows the typical long-range trajectory of aircraft.



Fig. A4.22. Optimal trajectory of aircraft.

A4.10.3.1 Conclusion

The best flight regime for a given air vehicle (closed to Boeing 737) is altitude $H = 12$ km, speed $V = 240$ m/s, specific fuel consumption $C_s = 0.00019$ kg fuel/s/kg thrust. Any deviation from this flight regime significantly reduces the maximum range (by up to 10–50%). The vehicle with a variable wing area loses 50% less range than a vehicle with a fixed wing.

A4.11 General discussion and conclusion

- The current space missiles were designed 30–40 years ago. In the past we did not have navigation satellites that allowed one to locate a missile (warhead) as close as 1 m to a target. Missile designers used inertial navigation systems for ballistic trajectories only. At the present time, we have a satellite navigation system and cheap devices, that enable aircraft, sea ships, cars, vehicles, and people to be located. If we exchange the conventional warhead for a warhead with a simple fixed wing with having a control and navigation system, we can increase the range of our old rockets 4.5–5 times (Fig. A4.13) or significantly increase the useful warhead weight (Fig. A4.19). We can also notably improve the precision of our aiming.
- Current artillery projectiles for big guns and cannons were created many years ago. The designers assumed that the observer could see an aim point and correct the artillery. Now we have a satellite navigation system that allows one to determine the exact coordinates of targets and we have cheap and light navigation

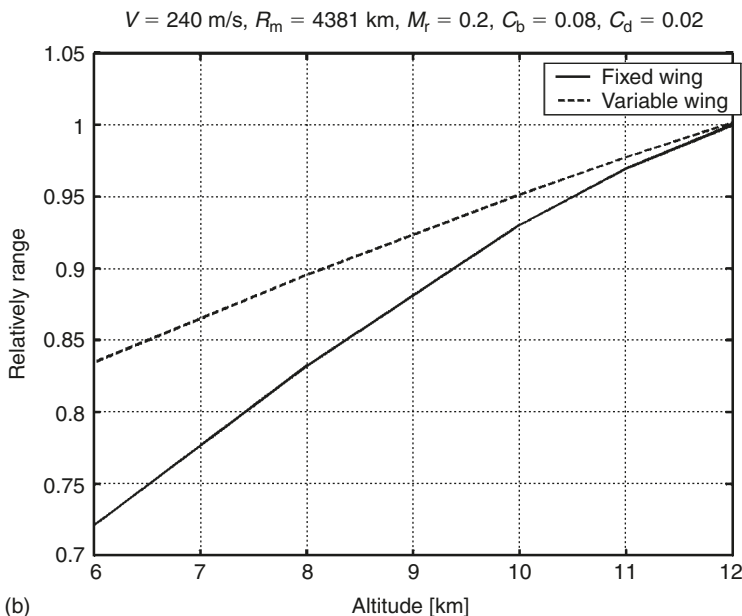
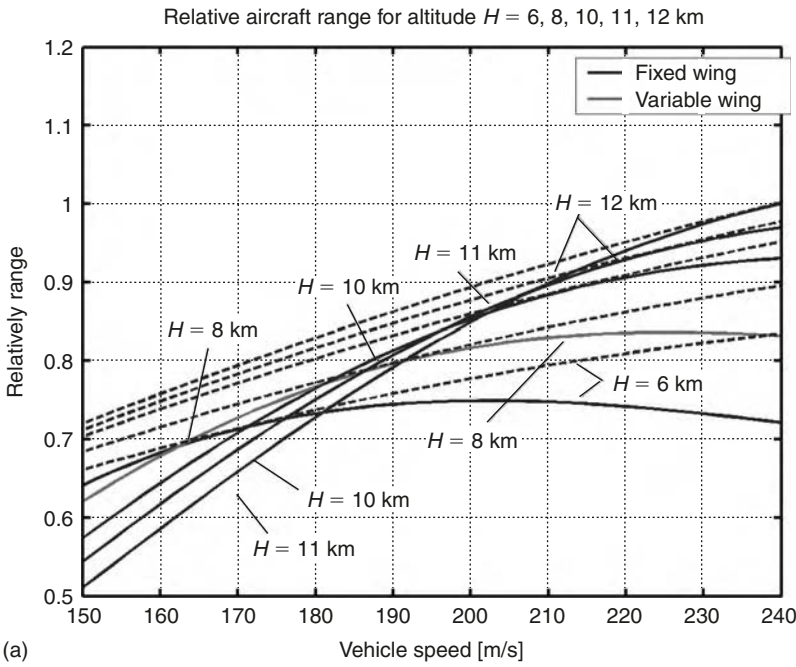


Fig. A4.23. (a) Relative aircraft range for speed $V = 240 \text{ m/s}$, maximum range $R_m = 4381 \text{ km}$, relative fuel mass $M_r = 0.2$, body drag coefficient $C_b = 0.08$, and wing drag coefficient $C_d = 0.02$. (b) Relative aircraft range for altitude $H = 6, 8, 10, 11$, and 12 km , maximum range $R_m = 4381 \text{ km}$, relative fuel mass $M_r = 0.2$, body drag coefficient $C_b = 0.08$, and wing drag coefficient $C_d = 0.02$.

and control devices that can be placed in the cannon projectiles. If we replace our cannon ballistic projectiles with projectiles with a fixed wing, and a control and navigation system, we increase the range 3–9 times (from 35 up to 360 km, see Figs. A4.20 and A4.21). We can use a smooth barrel to increase the nozzle shell speed up to 2000 m/s and range up to 1000 km. These systems can guide the *winged* projectiles and significantly improving their aim. We can reach this result because we use all the *kinetic* energy of the projectile. A conventional projectile cannot remain in the atmosphere and drops at a very high speed. Most of its kinetic energy is wasted. In our case 70–85% of the projectile's kinetic energy is used for support of the moving projectile. This way the projectile range increases 3–9 times or more.

- (c) All aircraft are designed for only one optimal flight regime (speed, altitude, and fuel consumption). Any deviation from this regime decreases the aircraft range. For aircraft like to the Boeing 747 this regime is: altitude $H = 12$ km, speed $V = 240$ m/s, specific fuel consumption $C_s = 0.00019$ kgf/s/kg thrust. If the speed is reduced from 240 to 200 m/s, the range decreases by 15% (Fig. A4.23(a)). Application of the variable wing area reduces this loss from 15 to 10%. If the aircraft reduces its altitude from 12 to 9 km, it loses 12% of its maximum range (Fig. A4.23(b)). If it has a variable wing area, it loses only 7.5% of its maximum range. Civil air vehicles are forced to deviate from the optimal conditions by weather or a given flight air corridor. Military air vehicles sometimes have to make a very large deviation from the optimal conditions (for example, when they fly at low

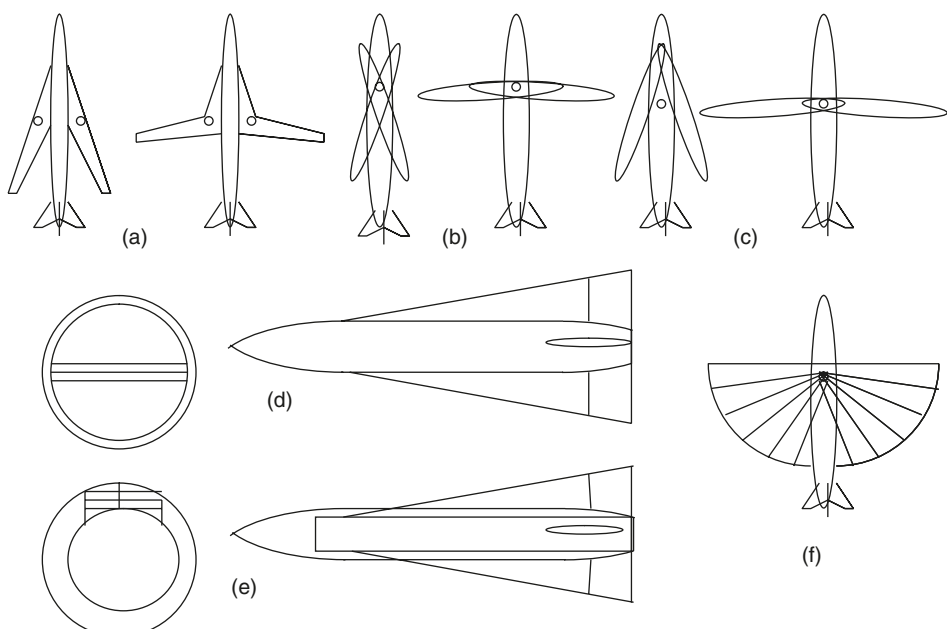


Fig. A4.24. Possible variants of variable wing designs: (a–c) and (f) for aircraft; (d) and (e) for gun projectiles.

altitude, below the enemy radar system). A variable wing area may be very useful for them because it decreases the loss by approximately 50%, improves supersonic flight and taking off and landing lengths.

The author offers some fixed and variable wing designs for air vehicles (Fig. A4.24). Variants (a–c), and (f) are for missiles and warheads, variants (d) and (e) are for shells.

References

1. A. Miele, “General Variable Theory of the Flight Paths of Rocket-Powered Aircraft, Missile and Satellite Carries”, *Astronautica acta*, Vol. 4, 1958, pp. 256–288.
2. A.A. Bolonkin, “Special Extrema in Optimal Control Problems”, Akademiya Nauk, Izvestia, *Theknicheskaya Kibernetika*, No. 2, March–April, 1969, pp. 187–198. See also English translation in *Engineering Cybernetics*, No. 2, March–April 1969, pp. 170–183.
3. A.A. Bolonkin, *New Methods of Optimization and their Application*, Bauman Technical University, Moscow, 1972 (in Russian).
4. A.A. Bolonkin, “A New Approach to Finding a Global Optimum”, *New Americans Collected Scientific Reports*, Vol. 1, 1991, The Bnai Zion Scientists Division, New York.
5. A.A. Bolonkin, “Optimization of Trajectory of Multistage Flight Vehicles”, in *Collection Researches of Flight Dynamics*, Masinobilding, Moscow, 1965, pp. 20–78 (in Russian).
6. A.A. Bolonkin and N.S. Khot, “Method for Finding a Global Minimum”, *AIAA/NASA/ USAF/SSMO Symposium on Multidisciplinary Analysis and Optimization*, 7–9 September 1994, Panama City, FL, USA.
7. A.A. Bolonkin, “Solution Methods for Boundary-Value Problems of Optimal Control Theory”, 1973. Consultants Bureau, a division of Plenum Publishing Corporation, New York. Translation from *Prikladnaya Mekhanika*, Vol. 7, No. 6, 1971, pp. 639–650 (in English).
8. A.A. Bolonkin, “Solution General Linear Optimal Problem with One Control”, *Prikladnaya Mechanika*, Vol. 4, No. 4, 1968, pp. 111–122, Moscow (in Russian).
9. A.A. Bolonkin and N. Khot, “Optimal Structural Control Design”, IAF-94-1.4.206, 45th Congress of the International Astronautical Federation, World Space Congress-1994, 9–14 October, 1994, Jerusalem, Israel.
10. A.A. Bolonkin and N.S. Khot, “Optimal Bounded Control Design for Vibration Suppression”, *Acta Astronautica*, Vol. 38, No. 10, 1996, pp. 803–813.
11. A.A. Bolonkin and D. Jeffcoat, “Optimal Thrust Angle of Aircraft”, 2002 (see Attachment 6).
12. A.A. Bolonkin and R. Sierakowski, “Design of Optimal Regulators”, AIAA-2003-6638, *2nd AIAA “Unmanned Unlimited” Systems, Technologies, and Operations – Aerospace, Land, and Sea Conference and Workshop and Exhibit*, 15–18 September 2003, San Diego, CA.
13. A.A. Bolonkin, “Optimal Trajectories of Air and Space Vehicles”, *Aircraft Engineering and Aerospace Technology*, Vol. 78, No. 2, 2004, pp. 192–214.
14. Bolonkin’s site: <http://Bolonkin.narod.ru>

This page intentionally left blank

ATTACHMENT 5

High-Efficiency Transfer of Mechanical Energy*

Summary

At present, high-voltage electric lines are used for power transfer. This method is expensive and requires complex devices. The author proposes a new method of power transfer (mechanical cable transmission) for long distances in the air. This method does not require electricity transmission lines, high-voltage equipment, large cost, or very much time for construction. It has high efficiency and is cheaper by hundreds of times. In space and on planets without atmosphere this method may be used in very long distance.

A5.1 Introduction

At the current time, turbo, thermo, hydro, and wind power stations produce mechanical energy. This energy is converted into low-voltage electricity by electric generators, then the low-voltage electricity is converted into high-voltage electricity, transferred over middle or long distances, converted back into low-voltage electricity and distributed among customers. Many customers' devices convert the electricity back into mechanical energy (for example, machines, pumps, locomotives, electric motors, etc.). Short electricity lines have length 20–120 km, voltage 110,000 V, and transfer power 35–50 MW; mid-length electricity lines have length 200–300 km, voltage 330,000 V, and transfer power 300–400 MW; long electricity lines have length 800–1500 km, voltage up to 0.75 MV, and transfer power up to 1.8–2.5 GW; and very long electricity lines have length up to 2000 km, voltage 1.15 MV, and transfer power 4–6 GW. The coefficient of efficiency of the transferor is 85–92%. All of the lines are very expensive (tens and hundreds millions of dollars) because they require a lot of expensive, clean, electric copper (wire), a lot of masts, ground to be

*This idea was presented in manuscript by author as “Inexpensive Cable Space Launcher of High Capability”, IAC-02-V.P.07, 53rd International Astronautical Congress. The World Space Congress – 2002, 10–19 October 2002, Houston, TX, USA.

Paper was also presented at the *International Energy Conversion Engineering Conference at Providence*, RI, 16–19 August 2004, as AIAA-2004-5660.

Paper was published as “Air Transfer of Mechanical Energy” in *Actual Problems of Aviation and Aerospace Systems*, Vol. 10, No 1 (19), 2005, pp. 102–110.

found for to put them in, and a long construction time. Terrorists can easily damage the masts and deprive a large region of energy, and capability to work. The detail researches were published in Refs.^{1–4}

A5.2 Description of innovation

The transfer system includes (Fig. A5.1) mechanical stations for transmission and reception, and air transmission, supported by winged devices. The transmitter station may be turbo, hydro, or wind powered. The reception station may include an electric generator, flywheels as accumulators of energy, and an electric and/or mechanical distribution network. Transmission involves a long closed-loop cable made from strong artificial fiber, with the winged devices connected to the cable by rope. The cable is located in the air, and is supported by the winged devices. The cable may be located at high altitude, where the air has low density and low air friction. The cross-section of the cable can be round or rectangular (flat) (Fig. A5.1). The round form has less air drag, and the flat form is better for the drive mechanism.

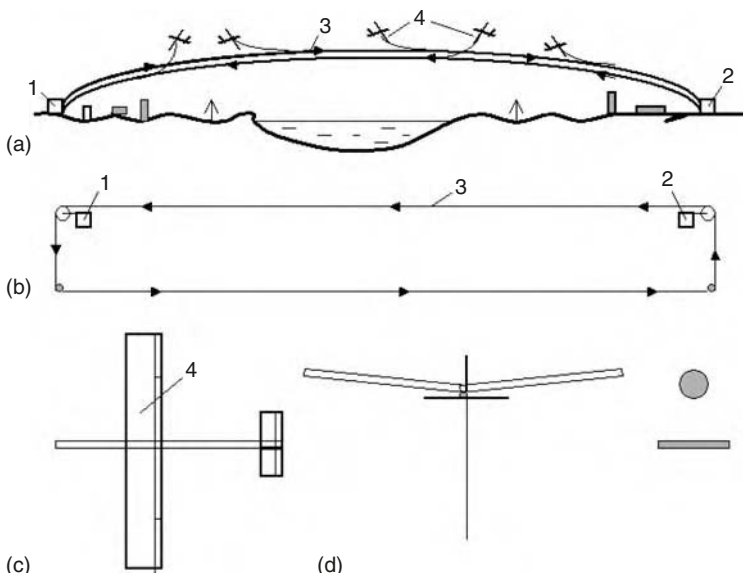


Fig. A5.1. Transferor of mechanical energy. *Notations:* (1) Transmission station; (2) reception station; (3) closed-loop mobile cable; and (4) supporting winged device. (a) Transfer system (side view); (b) transfer system (top view); (c) supporting winged device; and (d) cross-section of the cable.

The energy transferor works in the following way. The transmitter pulls one branch of the closed-loop cable, and rotates the cable and the electricity generator (or wheel) at the reception station.

The cable can be installed by an aircraft (for example, a C-130) or by a helicopter in windy weather, and the winged devices (or small balloons) can keep the cable in the air

until the aircraft finishes the flight and the cable is connected in a loop and begins to rotate and support itself. The winged devices have controls that allow the altitude and cable stress to be changed. There is wind virtually all the time at high altitude. You can see clouds moving at altitude in spite of the fact that there is no wind on the ground.

A5.3 Theory of air energy transfer (in metric system)

1. Maximum transfer energy, E , is:

$$E = TV = 0.24\pi d^2\sigma V, \quad (\text{A5.1})$$

where $T = 0.24\pi d^2\sigma$ is thrust [N]; V is cable speed [m/s]; d is cable diameter [m]; and σ is cable tensile stress [N/m^2].

Results of computations for current fibers, whiskers, and nanotubes are presented in Figs. A5.2–A5.4.

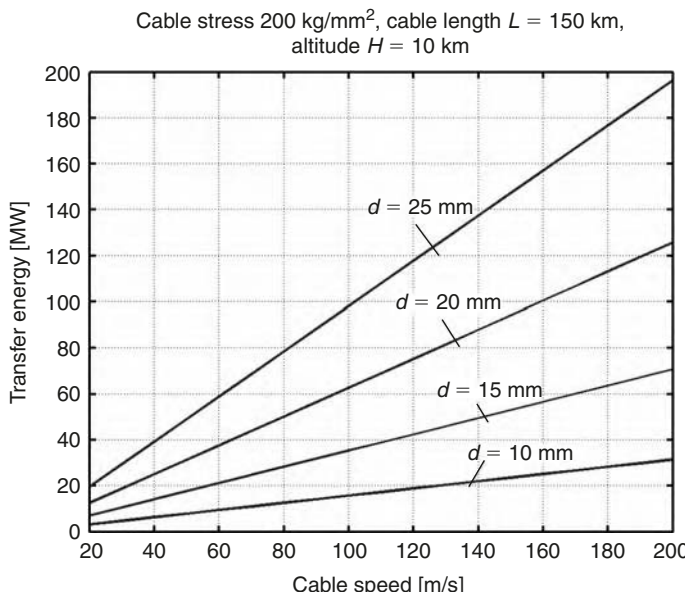


Fig. A5.2. Transfer energy versus cable speed for cable diameter $d = 10\text{--}25 \text{ mm}$, cable stress 200 kg/mm^2 , cable length $L = 150 \text{ km}$, average cable altitude $H = 10 \text{ km}$, and aerodynamic efficiency of winged support devices $k = 25$.

As you see, a large amount of energy (up to 200 MW) can be transferred over a distance of up to 150 km using a fiber cable of diameter 10–25 mm, up to 1.8 GW over a distance of 1000 km using a whisker cable of diameter 15–30 mm, and up to 25 GW over a distance of more than 7000 km, from continent to continent (for example, the USA to Europe) using nanotubes cable. With more power systems then one can transfer more energy over longer distance.

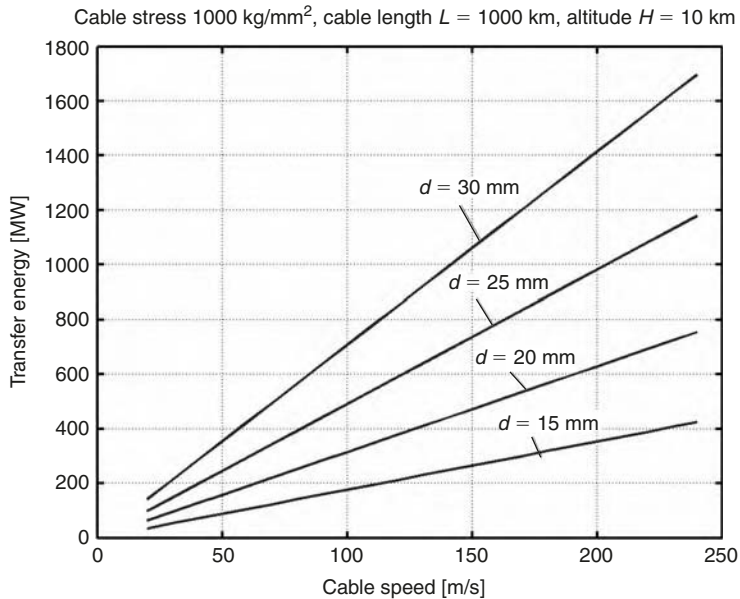


Fig. A5.3. Transfer energy versus cable speed for cable diameter $d = 15\text{--}30 \text{ mm}$, cable stress 1000 kg/mm^2 , cable length $L = 1000 \text{ km}$, average cable altitude $H = 10 \text{ km}$, and aerodynamic efficiency of winged support devices $k = 25$.

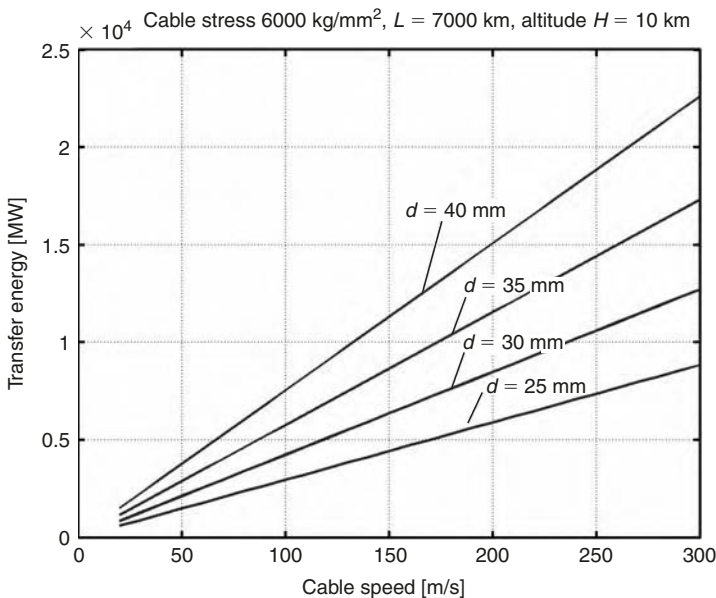


Fig. A5.4. Transfer energy versus cable speed for cable diameter $d = 25\text{--}40 \text{ mm}$, cable stress 6000 kg/mm^2 , cable length $L = 7000 \text{ km}$, average cable altitude $H = 10 \text{ km}$, and aerodynamic efficiency of winged support devices $k = 25$.

2. The air drag of a double cable can be computed by the following equations (Reynolds number is included):

$$\begin{aligned} D_L &= 2.08\rho^{0.5}\mu^{0.5}V^{1.5}L^{0.8}d, & D_T &= 0.2292\rho^{0.8}\mu^{0.2}V^{1.8}L^{0.8}d, \\ D_S &= m/k, & m &= 0.5\pi d^2 L \gamma, & D &= 0.5(D_L + D_T) + D_S, \end{aligned} \quad (\text{A5.2})$$

where D_L is laminar air drag [N]; D_T is turbulent air drag [N]; D_S is drag of wing support devices [N]; D is average air drag [N] (it is impossible to show, but full drag equals half the sum of laminar and turbulent drag); ρ is air density at a given average altitude H (for example, for $H = 10$ km, $\rho = 0.4125$, $\mu = 1.458 \times 10^{-5}$), μ is air viscosity [$\text{kg/s} \times \text{m}$]; L is cable length between the transfer and reception station [m]; m is mass of half the cable [kg]; γ is density of the cable [kg/m^3]; and k is the aerodynamic coefficient ($k = 20\text{--}30$ in our case).

3. Efficiency coefficient of transfer, η , is:

$$\eta = 1 - \frac{D}{T}. \quad (\text{A5.3})$$

Results of computations for current fibers, whiskers, and nanotubes are presented in Figs. A5.5–A5.7.

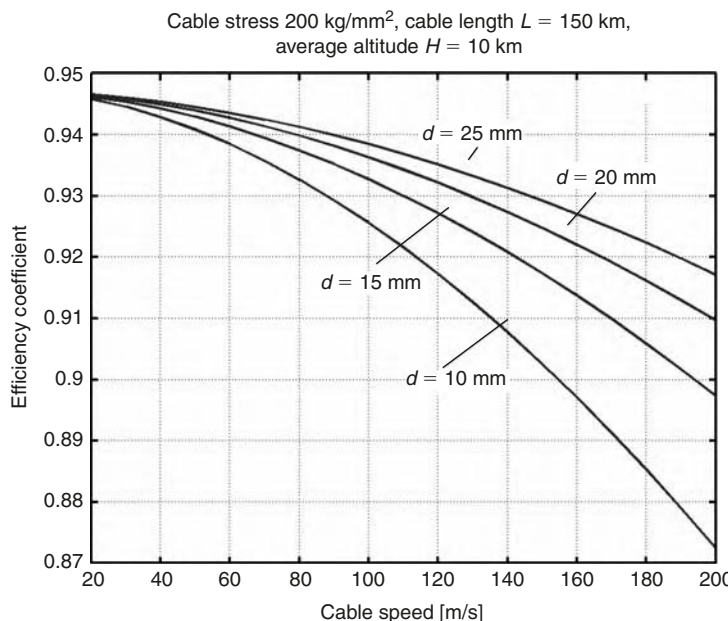


Fig. A5.5. Electrical efficiency coefficient versus cable speed for cable diameter $d = 10\text{--}25$ mm, cable stress 200 kg/mm^2 , cable length $L = 150$ km, average cable altitude $H = 10$ km, and aerodynamic efficiency of winged support devices $k = 25$.

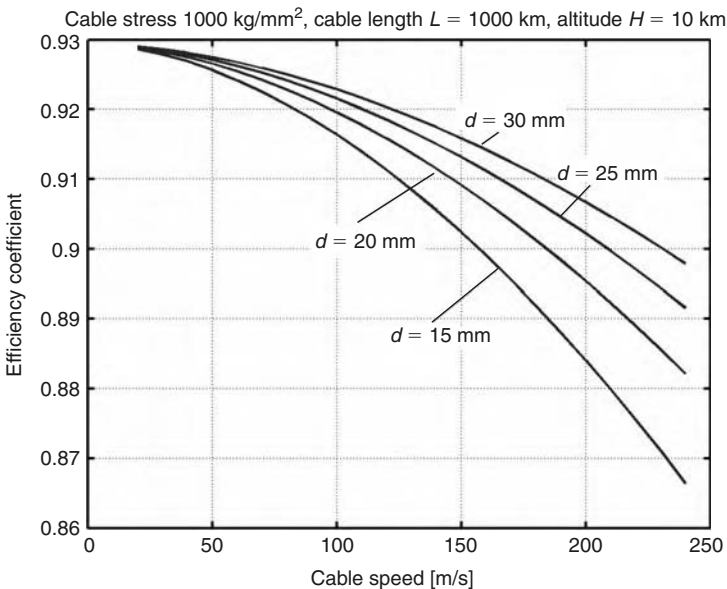


Fig. A5.6. Electric efficiency coefficient versus cable speed for cable diameter $d = 15\text{--}30 \text{ mm}$, cable stress 1000 kg/mm^2 , cable length $L = 1000 \text{ km}$, average cable altitude $H = 10 \text{ km}$, and aerodynamic efficiency of winged support devices $k = 25$.

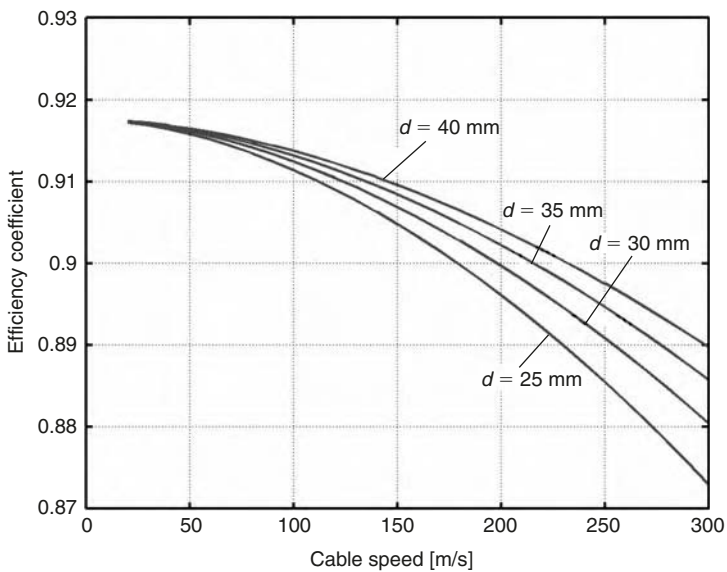


Fig. A5.7. Electric efficiency coefficient versus cable speed for cable diameter $d = 25\text{--}40 \text{ mm}$, cable stress 6000 kg/mm^2 , cable length $L = 7000 \text{ km}$, average cable altitude $H = 10 \text{ km}$, and aerodynamic efficiency of winged support devices $k = 25$.

The transfer efficiency ($\eta = 88\text{--}94.5$) is the same as or better than efficiency of current electricity lines.

4. Maximum energy storage using a 1-kg flywheel from artificial fiber, whisker, or nanotubes is:

$$E_s = \frac{\sigma}{2\gamma}, \quad (\text{A5.4})$$

where γ is wheel tread density [kg/m^3].

5. Minimum energy needed to support the cable in the air when there is no transfer of energy is:

$$E_{\min} = D(V_{\min})V_{\min}. \quad (\text{A5.5})$$

This energy may be estimated using Figs. A5.2–A5.4 if they continue at low cable speed.

A5.4 Discussion

A5.4.1 Cable problem (see also Chapters 1 and 2)

At present, industry produces cheap artificial fibers with a tensile stress, σ , of up to $500\text{--}620 \text{ kg/mm}^2$ and density $\gamma = 970\text{--}1800 \text{ kg/m}^3$. This is enough for a distance up to $150\text{--}300 \text{ km}$. The coefficient of efficiency is about 87%. However, if the cable made the whiskers (for example, C_D with maximum $\sigma = 8000 \text{ kg/mm}^2$), the range increases by $1000\text{--}2000 \text{ km}$ (Figs. A5.3 and A5.6).

The nanotubes created in scientific laboratories promise a revolution in space, aviation, machine-building, and transferring of energy. They increase the transfer distance by up to $7000\text{--}10,000 \text{ km}$ or more in air (in space, without limit). They allow a transfer distance of up to $20,000 \text{ km}$ through space with high cable speed when the cable is supported by centrifugal force.

A5.4.2 Building problems

This problem may be solved by transport airplanes or helicopters as described in the description of the innovation.

A5.4.3 Air traffic problems

Commercial passenger aircraft fly in special air corridors in most cases. The energy lines (winged support devices) will be visible in daytime and can have red lights at night. They can be located at high altitudes (14–15 km), over the conventional aircraft routes. High altitude only improves the parameters.

The proposed design of the air transfer power lines is not optimal. The author's purpose is to show the new method and its possibilities.

The offered method may seem strange to electrical engineers. However, this method can have a big future. The author has more detailed research and can take part in design and testing an experimental installation.

A5.5 Advantages of proposed method

The proposed mid-length energy transferor has large advantages in comparison with equivalent electricity lines.

1. The cable transferor is cheaper than equivalent (equal power) electricity line by tens or hundreds of times (no masts, expensive copper wires, ground costs, high-voltage substations, no additional electricity generator, transformers, etc.). Artificial fibers are cheap and widely produced by current industry, and current fibers may be used for short- and mid-length (up to 300 km) lines.
2. Construction time is reduced from months to days (only line is installed).
3. We can transfer a high energy more than current electric lines.
4. We can transfer a huge amount of energy over a very long distance (7000–10,000 km), from continent to continent (for example, from the USA to Europe and back) with high efficiency (more than electrical line efficiency).
5. The cable transferor can be used for delivery of a payload (for example, mail).
6. The cable transferor can be used as high-altitude communication antenna for radio, TV, and telephone.
7. Nanotubes have an electrical conductivity close to copper and the proposed transferor can be used to deliver electricity and communications.
8. Terrorists cannot damage the line.

A5.6 Defect

1. If no energy is being transferred, it is necessary to expend a small amount of energy for cable rotation (for support in the air if there is no wind).

References

1. A.A. Bolonkin, “Inexpensive Cable Space Launcher of High Capability”, *IAC-02-V.P.07, 53rd International Astronautical Congress. The World Space Congress – 2002*, 10–19 October 2002, Houston, TX, USA.
2. A.A. Bolonkin, “Transmission of Mechanical Energy to Long Distance”, *The International Energy Conversion Engineering Conference at Providence, RI, USA*, 16–19 August 2004, as Paper AIAA-2004-5660.
3. A.A. Bolonkin, “Air Transfer of Mechanical Energy”, *Actual Problems of Aviation and Aerospace Systems*, Vol. 10, No 1 (19), 2005, pp. 102–110.
4. A.A. Bolonkin, “Non-rocket Transportation System for Space Travel”, *Journal of British Interplanetary Society*, Vol. 56, No 7/8, 2003, pp. 231–249.

ATTACHMENT 6

Optimal Aircraft Thrust Angles*

Summary

The optimal angle for an aircraft's thrust vector is derived from first principles. Two equations are shown to encompass six different flight regimes. The main result for take-off and landing is that the optimal thrust angle (OTA) in radians approximately equals the coefficient of rolling friction. For climb, cruise, turn, and descent, the OTA equals the arctangent of the ratio of the drag coefficient to the lift coefficient. The second result differs from the well-known result that OTA equals the arctangent of the partial derivative of drag with respect to lift. The authors discuss this difference.

Nomenclature

B	artificial function, $B = \lambda dx/dt - H$
C_D	drag coefficient
C_L	lift coefficient
D	drag
d	takeoff or landing distance
E	aircraft efficiency, C_L/C_D
F	fuel consumption
f	performance function
g	n -dimensional vector constraint function
g_0	acceleration due to gravity
H	Hamiltonian, $-f + \lambda g$
h	altitude
I	performance index
L	lift force

* This chapter is contributed by Alexander Bolonkin (Senior Research Associate, National Research Council, assigned to Munitions Directorate, Air Force Research Lab, 1310 Avenue R, #6-F, Brooklyn, NY 11229, USA, T/F 718-339-4563, aBolonkin@juno.com) and David Jeffcoat (Principal General Engineer, Munitions Directorate, Air Force Research Lab, 101 W. Eglin Blvd, Ste. 341, Eglin AFB, FL 32542-6810, david.jeffcoat@eglin.af.mil).

M	aircraft mass
OTA	optimal thrust angle
q	dynamic pressure, $\rho V^2/2$
R	range
S	wing area
t	time
T	thrust or time of flight
T_f	friction force
u	m -dimensional control vector
V	aircraft speed
W	aircraft weight
w_f	specific fuel consumption
x	n -dimensional state vector
λ	n -dimensional Lagrange multiplier
γ	thrust angle
μ	friction coefficient
ψ	specific function
ϕ	roll angle

A6.1 Introduction

Aircraft designers must determine the angle of the thrust vector relative to the main horizontal flight direction. When this angle is positive (up from the horizontal plane), an additional lift force is generated, but at the expense of horizontal thrust. In this chapter, the optimal thrust angle (OTA) is derived, using both classical methods and an alternative optimization method developed by the first author.^{1,2} Many methods of deflecting the nozzle exhaust stream of rocket engines to provide thrust vector control have been investigated, including jet vanes, gimbaled or swiveled nozzles, and extendable nozzle deflectors.^{3–6} Jet vanes have been widely applied for the control of solid-rocket engines and for early liquid-rocket engines, including the German V-2 missile.⁷ Ref.⁸ presents metrics for assessing the performance of fighter aircraft implementing thrust vector control.

Refs. [3] and [9] are most closely related to this chapter. Gilyard and Bolonkin³ use numeric calculations to search for the OTA, whereas in this chapter the focus is theoretic, rather than numeric. Miele⁹ presents a basic theory for analyzing the optimum flight paths of rocket-powered vehicles. Miele simultaneously optimizes the time history of lift, thrust modulus and thrust direction, and states that the OTA equals the arctangent of the partial derivative of drag with respect to lift. In this chapter, we provide theory and formulas for the OTA for six primary flight regimes of any aircraft type. The formulas provided are accurate for stable flight conditions, but may be sub-optimal during high dynamic maneuvers. The six flight regimes are listed below, each with one or more optimization objectives:

1. Takeoff, to minimize takeoff distance.
2. Climb, to minimize fuel consumption.

3. Cruise, to minimize fuel consumption or to maximize range.
4. Turn, to minimize fuel consumption or to minimize turn time.
5. Descent, to minimize fuel consumption or to maximize range.
6. Landing, to minimize landing distance.

A6.2 General methodology

Consider the problem of minimizing a performance index I , where:

$$I = \int_0^T f(t, x, u) dt. \quad (\text{A6.1})$$

We wish to minimize I with respect to x and u , subject to the dynamic constraint:

$$\dot{x} = g(t, x, u). \quad (\text{A6.2})$$

We assume an initial condition, $x(0)$, is known. Following the approach described in Ref.¹, we define an artificial function:

$$B = f - \frac{\partial \psi}{\partial x} g(t, x, u) - \frac{\partial \psi}{\partial t}. \quad (\text{A6.3})$$

In particular, the function ψ may be defined by:

$$\psi = \lambda(t)x. \quad (\text{A6.4})$$

If we find:

$$\min_{x,u} B = \min_{x,u} [f(t, x, u) - \lambda(t)g(t, x, u) - \dot{\lambda}(t)x], \quad (\text{A6.5})$$

then the values of x and u that minimize B , subject to the constraint given in equation (A6.2), are optimal control and state vectors for the problem stated in equation (A6.1).

We can also solve this problem by a classical method¹⁰ using the Hamiltonian for this problem, which is given by:

$$H(t, x, u, \lambda) = -f(t, x, u) + \lambda(t)g(t, x, u), \quad (\text{A6.6})$$

and

$$\dot{\lambda} = -\frac{\partial H}{\partial x}.$$

The values of u which maximize the Hamiltonian, subject to the constraint in equation (A6.2), are optimal control vectors for equation (A6.1). That is:

$$\bar{H} = \max_u H(t, x, u, \lambda). \quad (\text{A6.7})$$

When the process does not change with time, we have a more straightforward problem.

Minimize a performance index I , defined by:

$$I = \int_0^T f(x, u) dt, \quad (\text{A6.8})$$

with respect to x and u , subject to the dynamic constraint:

$$\dot{x} = g_i(x, u), \quad \text{for } i = 1, 2, \dots, n \quad (\text{A6.9})$$

$$H(t, x, u, \lambda) = -f(x, u) + \lambda(t)g(x, u) \quad (\text{A6.10})$$

$$\bar{H} = \max_u H(t, x, u, \lambda), \quad \bar{u} = u(t, x) \quad (\text{A6.11})$$

The parameter λ is an n -dimensional unknown Lagrange multiplier and \bar{u} is the optimal control. Equations (A6.4) through equation (A6.6) give the system of equations:

$$\frac{\partial B}{\partial u_j} = \frac{\partial H}{\partial u_j} = 0, \quad j = 1, 2, \dots, m; \quad \frac{\partial B}{\partial x_i} = \dot{\lambda}_i(t) + \frac{\partial H}{\partial x_i} = 0, \quad i = 1, 2, \dots, n. \quad (\text{A6.12})$$

These equations are equivalent to conventional principle of maximum.¹⁰

$$\dot{\lambda}_i(t) = -\frac{\partial H}{\partial x_i}, \quad i = 1, 2, \dots, n; \quad \frac{\partial H}{\partial u_j} = 0, \quad j = 1, 2, \dots, m. \quad (\text{A6.13})$$

These equations, together with equation (A6.2), allow us to find an extreme of the Hamiltonian H , which is optimal if the appropriate second-order sufficient conditions for optimality are satisfied.

A6.3 OTA for takeoff and landing

For takeoff, the performance index is the takeoff distance, described by:

$$d = \int_0^T V dt. \quad (\text{A6.14})$$

The aircraft speed serves as the performance function. The dynamic constraint on acceleration is given by as illustrated in Fig. A6.1:

$$\dot{V} = \frac{1}{M} (T \cos \gamma - D - T_f). \quad (\text{A6.15})$$

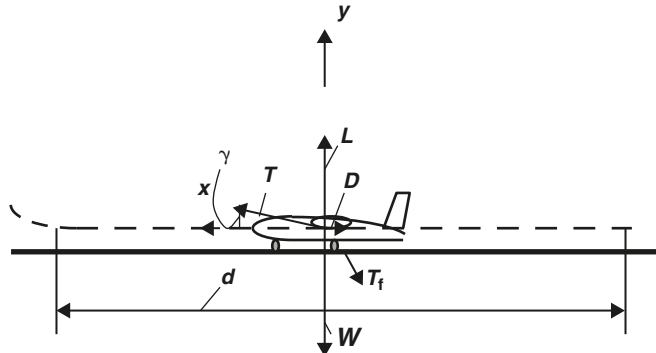


Fig. A6.1. Takeoff.

The friction force is given by:

$$T_f = \mu(Wg_0 - L - T \sin \gamma). \quad (\text{A6.16})$$

We know from aerodynamics and trigonometry that:

$$L = C_L q S, \quad D = C_D q S, \quad \sin \gamma = \sqrt{1 - \cos^2 \gamma}. \quad (\text{A6.17})$$

We consider only the positive root, but the result is the same for the negative root.

To simplify subsequent calculations, make the substitution:

$$u = \cos \gamma, \quad (\text{A6.18})$$

so that

$$\sin \gamma = \sqrt{1 - u^2}. \quad (\text{A6.19})$$

Substituting equations (A6.16)–(A6.19) to equation (A6.15) yields:

$$\dot{V} = \frac{1}{M} [Tu - D - \mu(Wg_0 - L - T\sqrt{1 - u^2})], \quad (\text{A6.20})$$

which leads to function B or the Hamiltonian H :

$$\begin{aligned} B &= f + \dot{\lambda}(t)V + \lambda(t)\dot{V} = V + \dot{\lambda}(t)V + \lambda(t)\frac{1}{M}[Tu - D - \mu(Wg_0 - L - T\sqrt{1 - u^2})] \\ &= \dot{\lambda}(t)V + H, \end{aligned} \quad (\text{A6.21})$$

where

$$H = V + \lambda(t)\frac{1}{M}[Tu - D - \mu(Wg_0 - L - T\sqrt{1 - u^2})]. \quad (\text{A6.22})$$

To find the minimum of B over all admissible u , the necessary condition is that the partial derivative is equal to zero, that is:

$$\frac{\partial B}{\partial u} = 0, \quad (\text{A6.23})$$

or

$$\frac{\partial B}{\partial u} = \frac{\lambda(t)T}{M} \left[1 - \frac{\mu u}{\sqrt{1 - u^2}} \right] = 0. \quad (\text{A6.24})$$

If M, T , and $\lambda \neq 0$, then from equation (A6.24), it must be true that:

$$\mu u = \sqrt{1 - u^2}, \quad (\text{A6.25})$$

or

$$\mu^2 u^2 = 1 - u^2, \quad (\text{A6.26})$$

so that the final result from equation (A6.26) is:

$$u = \pm \frac{1}{\sqrt{1 + \mu^2}}. \quad (\text{A6.27})$$

Returning to the original notation, we have the thrust angle as a function of the coefficient of friction:

$$\cos \gamma = \pm \frac{1}{\sqrt{1 + \mu^2}} \quad \text{or} \quad \gamma = \cos^{-1} \left(\frac{\pm 1}{\sqrt{1 + \mu^2}} \right) \text{rad.} \quad (\text{A6.28})$$

We can use the trigonometric identity:

$$\cos \gamma = \frac{1}{\sqrt{1 + \tan^2 \gamma}}, \quad (\text{A6.29})$$

to get our final result,

$$\tan \gamma = \pm \mu, \quad (\text{A6.30})$$

or, for small μ , say $\mu < 0.2$, we have the design rule-of-thumb that:

$$\gamma \cong \pm \mu, \quad (\text{A6.31})$$

where γ is in radians.

The sign of γ depends on our goal, minimization or maximization of the function, as well as the sign of λ and T in equation (A6.24). Clearly, the thrust must have a forward direction for aircraft takeoff, and the angle γ must be positive. Similarly, for landing, the thrust must have a backward direction to brake the airplane, and the angle γ must be negative, pushing the airplane to the ground, as illustrated in Fig. A6.2.

The angles for takeoff and landing are different, because the coefficients of rolling friction are different for takeoff and landing. For takeoff, the friction coefficient is small ($\mu \approx 0.01\text{--}0.05$); for landing, the coefficient is larger ($\mu \approx 0.3\text{--}0.4$). The direction of thrust is also different for takeoff ($\gamma \approx +1^\circ$ to $+3^\circ$) than for landing ($\gamma \approx -16^\circ$ to -22°). For takeoff, the thrust has a forward direction; for landing the thrust has a backward direction.

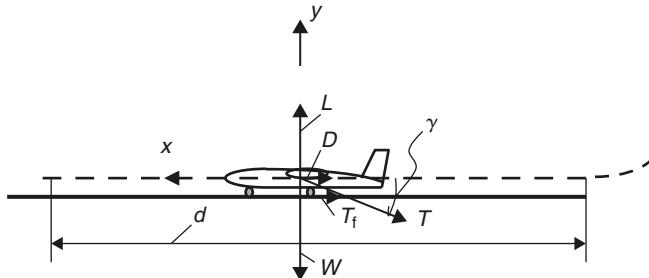


Fig. A6.2. Landing.

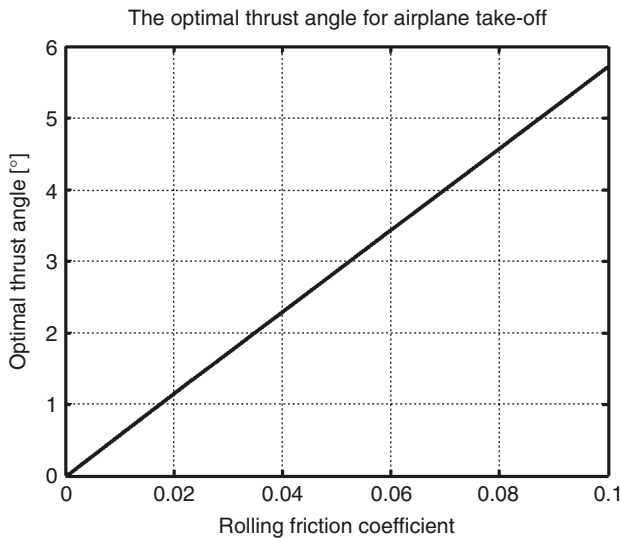


Fig. A6.3. Optima for takeoff.

As a design “rule-of-thumb,” we can say that the OTA in radians is equal to the coefficient of rolling friction for takeoff, and the OTA is within 5% of the coefficient of rolling friction for landing. The expression $\tan \gamma = \mu$ is exact for any rolling friction coefficient.

The optimal angles for takeoff and landing are shown in Figs. A6.3 and A6.4, respectively.

A6.4 Optimal angle of thrust vector in horizontal flight (cruise regime)

Assume that speed, altitude, and direction of flight are constant during horizontal flight time, and that we wish to maximize range, R , of the aircraft over the time interval $[0, T]$. Then:

$$R = \int_0^T V dt. \quad (\text{A6.32})$$

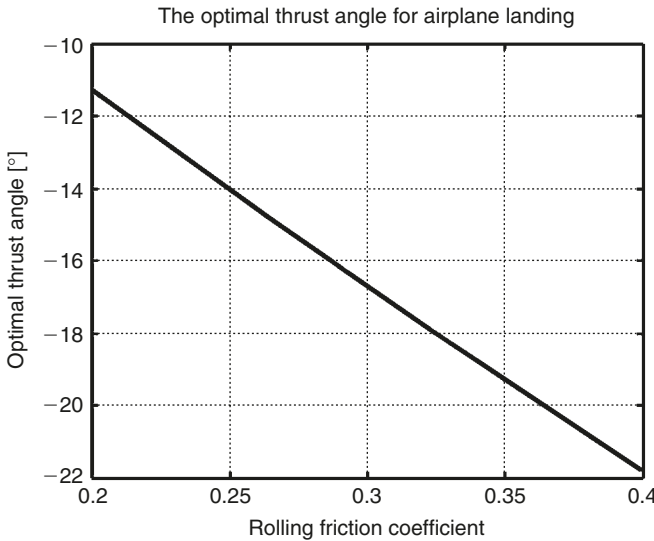


Fig. A6.4. OTA for landing.

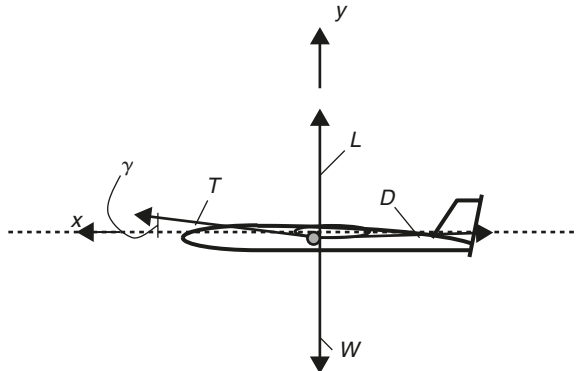


Fig. A6.5 Horizontal flight.

The equilibrium equations of motion (Fig. A6.5) are:

$$T \cos \gamma - D = 0, \quad (\text{A6.33})$$

$$L - W g_0 + T \sin \gamma = 0. \quad (\text{A6.34})$$

Using the notation:

$$E = \frac{L}{D} = \frac{C_L}{C_D}, \quad u = \cos \gamma, \quad \sin \gamma = \sqrt{1 - u^2} = 0, \quad (\text{A6.35})$$

we can substitute D and u from equation (A6.35) and L from equation (A6.34) to equation (A6.33) to obtain:

$$Tu - \frac{Wg_0}{E} + \frac{T}{E} \sqrt{1 - u^2} = 0. \quad (\text{A6.36})$$

Next, compose the Hamiltonian function H , as in equation (A6.10):

$$H = -V + \lambda(Tu - \frac{Wg_0}{E} + \frac{T}{E} \sqrt{1 - u^2}). \quad (\text{A6.37})$$

And find the maximum of this function:

$$\frac{\partial H}{\partial u} = \lambda T \left[1 - \frac{u}{E \sqrt{1 - u^2}} \right] = 0. \quad (\text{A6.38})$$

If we take values for λ and T such that $\lambda T \neq 0$, we find that:

$$u = E \sqrt{1 - u^2}, \quad (\text{A6.39})$$

or

$$u^2 = E^2 (1 - u^2). \quad (\text{A6.40})$$

From equation (A6.40), it follows that:

$$u = \pm \frac{E}{\sqrt{1 + E^2}}, \quad (\text{A6.41})$$

or

$$\cos \gamma = \pm \frac{E}{\sqrt{1 + E^2}} \quad \text{or} \quad \gamma = \arccos \left(\pm \frac{E}{\sqrt{1 + E^2}} \right). \quad (\text{A6.42})$$

Note that γ in degrees given by:

$$\gamma^\circ = 180 \gamma / \pi. \quad (\text{A6.43})$$

From physical conditions, it is evident that angle γ is positive. For fighter aircraft, aerodynamic efficiency, E , ranges from 2 to 10. For transport or passenger aircraft, efficiency

ratios vary from 10 to 20. Using the trigonometric identify in equation (A6.29), we obtain a final result:

$$\tan \gamma = \frac{1}{E} \quad \text{or} \quad \tan \gamma = \frac{C_D}{C_L}. \quad (\text{A6.44})$$

For small γ , say $\gamma < 0.2$ rad, we have the design rule-of-thumb that:

$$\gamma \approx \frac{C_D}{C_L}. \quad (\text{A6.45})$$

The OTA for the cruise regime is shown in Fig. A6.6 for aerodynamic efficiencies ranging from 2 to 10, typical of fighter aircraft.

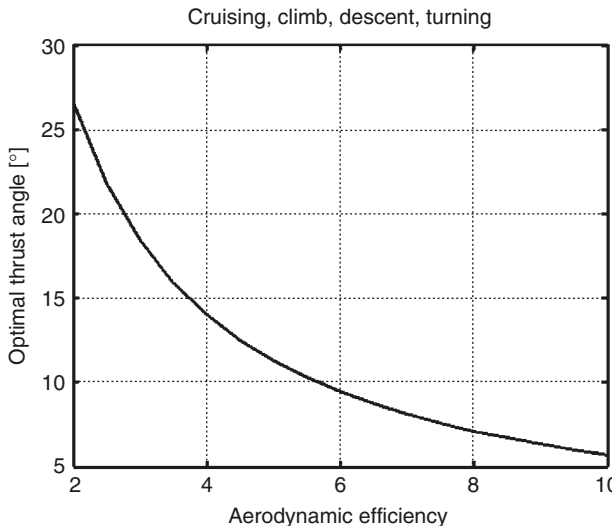


Fig. A6.6. OTA for cruise regime.

So far, we have used as the performance index the maximum range of the aircraft. The results are the same if we minimize fuel consumption:

$$F = \int_0^T w_f dt. \quad (\text{A6.46})$$

Or minimize time:

$$T = \int_0^T dt. \quad (\text{A6.47})$$

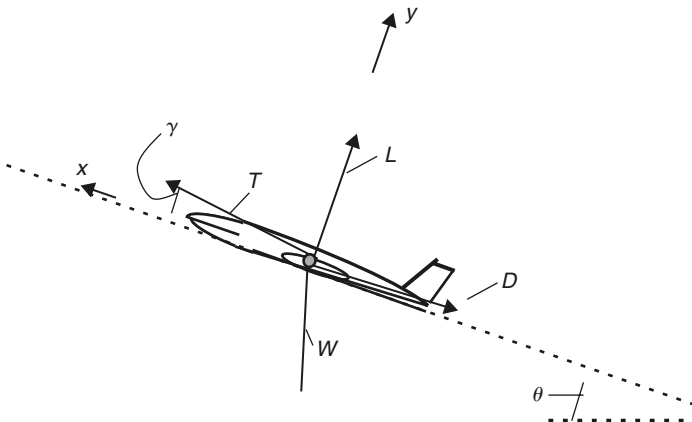


Fig. A6.7. Climb.

A6.5 Climb and descent regimes

Fig. A6.7 illustrates the climb regime.

Let us take as the performance index the range or altitude:

$$R = \int_0^T V dt \quad \text{or} \quad h = \int_0^T V \sin \theta dt. \quad (\text{A6.48})$$

Then the equilibrium equations are:

$$T \cos \gamma - D - W g_0 \sin \theta = 0, \quad (\text{A6.49})$$

$$L + T \sin \gamma - W g_0 \cos \theta = 0, \quad (\text{A6.50})$$

where θ is the angle between the trajectory and the horizon. Using the notation:

$$E = \frac{L}{D} = \frac{C_L}{C_D}, \quad \cos \gamma = u, \quad \sin \gamma = \sqrt{1 - u^2}, \quad (\text{A6.51})$$

and substituting equations (A6.50) and (A6.51) to equation (A6.49), we have:

$$Tu - \frac{W g_0 \cos \theta}{E} + \frac{T}{E} \sqrt{1 - u^2} - W \sin \theta = 0, \quad (\text{A6.52})$$

and

$$H = V + \lambda \left[Tu - \frac{Wg_0 \cos \theta}{E} + \frac{T}{E} \sqrt{1 - u^2} - Wg_0 \sin \theta \right]. \quad (\text{A6.53})$$

The necessary condition for an extreme is:

$$\frac{\partial H}{\partial u} = 0, \quad (\text{A6.54})$$

or

$$\frac{\partial H}{\partial u} = \lambda T \left(1 - \frac{u}{E \sqrt{1 - u^2}} \right) = 0. \quad (\text{A6.55})$$

That is the same as equation (A6.38), which means that the final equation for the optimal angle of thrust vector in climb and descent will be equal to the equation for a cruise regime:

$$\cos \gamma = \pm \frac{E}{\sqrt{1 + E^2}} \quad \text{or} \quad \tan \gamma = \frac{1}{E} = \frac{C_D}{C_L} \quad \text{or} \quad \gamma \approx \frac{C_D}{C_L}. \quad (\text{A6.56})$$

From physical conditions, it is evident that angle γ is positive. The aerodynamic efficiencies are different for climb, descent, and cruise, so that the optimal thrust vector angle will be different, but the equations for the calculation are the same. Again, note that we can use trigonometric equalities to derive the more concise expression, $\cot \gamma = E$, which is exact for any aerodynamic efficiency ratio. The results are the same whether time or fuel consumption is used for the performance index.

A6.6 Turning of airplane

Consider now the turning of an airplane in one plane, with a constant roll angle ϕ .

Our performance index can be distance, minimum time of turn, or fuel consumption:

$$R = \int_0^T V dt, \quad T = \int_0^T dt, \quad F = \int_0^T w_f dt. \quad (\text{A6.57})$$

The equations of motion are:

$$T \cos \gamma - D = 0, \quad (\text{A6.58})$$

$$L + T \sin \gamma - Wg_0 \cos \phi = 0. \quad (\text{A6.59})$$

Using the notation:

$$E = \frac{L}{D} = \frac{C_L}{C_D}, \quad \cos \gamma = u, \quad \sin \gamma = \sqrt{1 - u^2}, \quad (\text{A6.60})$$

and substituting equations (A6.59) and (A6.60) to equation (A6.58), we obtain:

$$Tu - \frac{Wg_0 \cos \phi}{E} + \frac{T\sqrt{1 - u^2}}{E} = 0, \quad (\text{A6.61})$$

and

$$H = V + \lambda \left[Tu - \frac{Wg_0 \cos \phi}{E} + \frac{T}{E} \sqrt{1 - u^2} \right]. \quad (\text{A6.62})$$

The necessary condition for an extreme is:

$$\frac{\partial H}{\partial u} = 0 \quad \text{or} \quad \frac{\partial H}{\partial u} = \lambda T \left(1 - \frac{u}{E\sqrt{1 - u^2}} \right) = 0. \quad (\text{A6.63})$$

Equation (A6.63) is equivalent to equation (A6.38), which means the final equation for the optimal angle of thrust vector in a roll is equal to the equation for a cruise regime:

$$\cos \gamma = \pm \frac{E}{\sqrt{1 + E^2}} \quad \text{or} \quad \tan \gamma = \frac{1}{E} = \frac{C_D}{C_L} \quad \text{or} \quad \gamma \approx \frac{C_D}{C_L}. \quad (\text{A6.64})$$

From physical conditions, it is evident that angle γ is positive.

A6.7 Discussion

The problem of determining an OTA is also discussed in Ref.⁹, in which the OTA for rocket-powered aircraft is given by:

$$\omega = \arctan \frac{\partial D}{\partial L}, \quad (\text{A6.65})$$

where ω is equivalent to our angle γ . In the particular case of a parabolic polar drag coefficient of the form $C_D = C_{D_0}(M) + K(M)C_L^2$, where M is the Mach number, K is the induced drag factor, and C_{D_0} is the zero-lift drag coefficient, equation (A6.65) leads to:

$$\omega = \arctan(2KC_L). \quad (\text{A6.66})$$

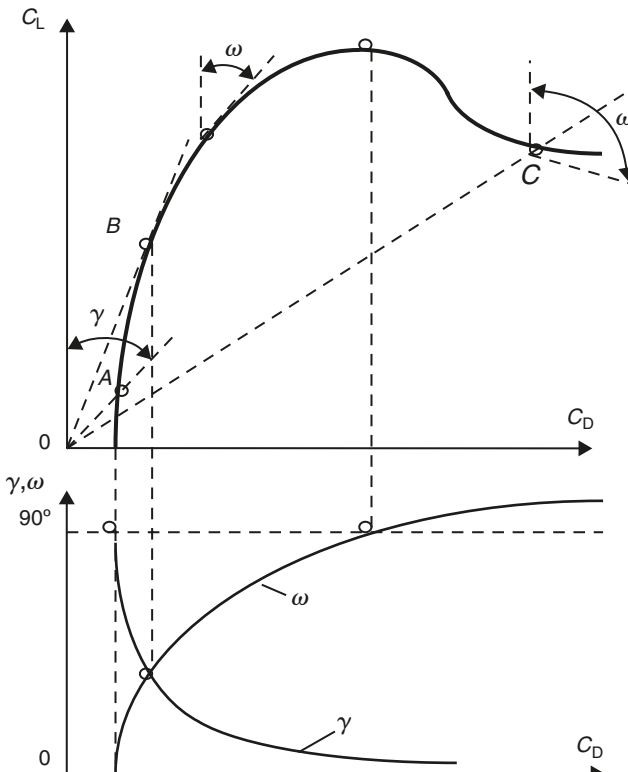


Fig. A6.8. Comparison of γ and ω .

Equations (A6.44) and (A6.66) give very different results (Fig. A6.8). For example, when there is no lift force ($C_L = 0$), equation (A6.44) gives $\gamma = 90^\circ$, meaning that the OTA is strictly vertical (perpendicular to the desired trajectory), while equation (A6.66) gives $\omega = 0$, corresponding to a horizontal thrust. Conversely, when the lift force is maximum, equation (A6.65) gives $\omega = 90^\circ$. We also see in Fig. A6.8 that as the lift force (C_L) decreases after passing through its maximum point, equation (A6.65) yields an OTA greater than 90° , producing a reverse thrust force. So, we conclude that equations (A6.65) and (A.66) do not adequately model the OTA near extreme points.

The angle γ produced by equation (A6.44) also has better trend characteristics, starting at 90° when $C_L = 0$, then decreasing as the lift force is increasing and positive. The angle ω starts at zero when $C_L = 0$, then increases as the aerodynamic lift force increases. Equations (A6.44) and (A6.65) do produce the same result at one point, when the efficiency coefficient, $E = C_L/C_D$ is maximized. Equation (A6.65) was derived for an optimal angle of attack, and the result is valid at the point of optimal aircraft lift. Equation (A6.44) is more general, and may be used at any polar coordinate in any of the four flight regimes: climb, cruise, turn, or descent.

A6.8 Conclusions

In this application, we derived two simple equations for the OTA of an aircraft. One equation is valid for takeoff and landing, the other for climb, cruise, turn, and descent. During takeoff, the OTA is positive, decreases as the coefficient of rolling friction decreases, and is essentially equal to the friction coefficient. During landing, the OTA is negative, increases as the coefficient of rolling friction increases, and is within 5% of the value of the friction coefficient. The simple expression $\tan \text{OTA} = \mu$ provides an exact result for the OTA as a function of the rolling friction coefficient.

In the climb, cruise, turn, or descent flight regimes, the OTA depends only on the coefficient of aerodynamic efficiency. Here, we observe an inverse proportion: the greater the coefficient of aerodynamic efficiency, the smaller the OTA. The OTA is positive in all flight regimes, with the possible exception of air braking, which is not addressed in this research. As in the cases of takeoff and landing, we have a simple expression, $\tan \text{OTA} = 1/E$, relating the OTA to a single parameter, the aerodynamic efficiency. The equations for OTA developed in this attachment were also shown to have more intuitive trends and better behavior at extreme points than the Miele equations.

References

1. A. Bolonkin, "A New Approach to Finding a Global Optimum", *New American's Collected Scientific Reports*, Vol. 1, The Bnai Zion Soviet-American Scientists Division, New York, 1991, pp. 45–50.
2. A. Bolonkin, *New Methods of Optimization and Their Application*, Bauman Technical University, Moscow, 1972 (in Russian).
3. G. Gilyard and A. Bolonkin, "Optimal Pitch Thrust-Vector Angle and Benefits for all Flight Regimes", NASA-TM-2000-209021, March 2000.
4. B. Gal-Or, "Thrust Vectoring for Flight Control and Safety: A Review", *International Journal of Turbo and Jet Engines*, Vol. 11, 1994, pp. 119–136.
5. D.S. Gerren, "Design, Analysis, and Control of a Large Transport Aircraft Utilizing Selective Engine Thrust as a Backup System for the Primary Flight Control", NASA-CR-186035, September 1995.
6. P. Mangold and G. Wedekind, "Inflight Thrust Vectoring: A Further Degree of Freedom in the Aerodynamic/Flight Mechanical Design of Modern Fighter Aircraft", *AGARD, Aerodynamics of Combat Aircraft Controls and of Ground Effects*, April 1990.
7. H.H. Koelle (ed.), *Handbook of Astronautical Engineering*, McGraw-Hill, 1961, New York, pp. 19–38.
8. A. Kutschera and P.M. Render, Performance Assessment of Thrust Vector Controlled Post Stall Manoeuvrable Fighter Aircraft Using Minimal Input Data, AIAA Paper 99-4020, 1999.
9. A. Miele, "General Variational Theory of the Flight Paths of Rocket-Powered Aircraft, Missiles and Satellite Carriers", *Astronautica acta*, Vol. 4, Pergamon Press, New York, 1958, pp. 272–273.
10. L.S. Pontryagin, V.G. Boltyanskii, R.V. Gamkrelidze and E.F. Mischenko, *The Mathematical Theory of Optimal Processes*, Interscience Publishers, Inc., New York, 1962, pp. 17–20.

APPENDIX 1

System of mechanical and electrical units and other useful values

Here there are values useful for calculations and estimations of aerospace projects.

1.1 System of mechanical and electrical units

The following table contains the delivered metric mechanical and the electromagnetic SI units that have been introduced in this text, expressed in terms of the fundamental units *meter*, *kilogram*, *second*, and *ampere*. From these expressions the *dimensions* of the physical quantities involved can be readily determined.

Length	1 meter = 1 m
Mass	1 kilogram = 1 kg
Time	1 second = 1 s
Electric current	1 ampere = 1 A
Force	1 newton = 1 N = 1 kg m/s ²
Pressure	1 N/m ² = 1 kg/m s ²
Energy	1 joule = 1 J = 1 N m = 1 kg m ² /s ²
Power	1 watt = 1 W = 1 J/s = 1 kg m ² /s ³
Rotational inertia	1 kilogram meter ² = 1 kg m ²
Torque	1 meter newton = 1 kg m ² /s ²
Electric charge	1 coulomb = 1 C = 1 As
Electric intensity	1 N/C = 1 V/m = 1 kg m/s ³ A
Electric potential	1 volt = 1 V = 1 J/C = 1 kg m ² /s ³ A
Electric resistance	1 ohm = 1 Ω = 1 V/A = 1 kg m ² /s ² A ²
Capacitance	1 farad = 1 F = 1 C/V = 1 C2/J = 1 s ⁴ A ² /kg m ²
Inductance	1 henry = 1 H = 1 J/A ² = 1 Ωs = 1 kg m ² /s ² A ²
Magnetic flux	1 weber = 1 Wb = 1 J/A = 1 Vs = 1 kg m ² /s ² A
Magnetic intensity	1 tesla = 1 Wb/m ² = 1 Vs/m ² = 1 kg/s ² A

Reluctance 1 ampere-turn/weber = 1 A/Wb = $1 \text{ s}^2 \text{ A}^2/\text{kg m}^2$
 Magnetizing force 1 ampere-turn/meter = 1 A/m
 Kelvin is the fundamental unit of temperature.
 Candela is the fundamental power-like unit of photometry.

1.2 Fundamental physical constants

Standard gravitational acceleration	9.806 65 m/s ²
Standard atmosphere (atm)	101 325 N/m ²
Thermochemical kilocalorie	4184 J
Speed of light in vacuum (c)	$2.997\ 935 \times 10^8 \text{ m/s}$
Electronic charge (e)	$1.602\ 10 \times 10^{-19} \text{ C}$
Avogadro constant (N_A)	$6.0225 \times 10^{26}/\text{kmol}$
Faraday constant (F)	$9.6487 \times 10^7 \text{ C/kmol}$
Universal gas constant (R)	8314 J/kmol
Gravitational constant (G)	$6.67 \times 10^{-11} \text{ N m}^2/\text{kg}^2$
Boltzmann constant (k)	$1.3895 \times 10^{-23} \text{ J/K}$
Stefan–Boltzmann Constant (σ)	$5.670 \times 10^{-8} \text{ W/K}^4 \text{ m}^2$
Rest energy of one atomic mass unit	931.48 MeV
Electron-volt (eV)	$1.602\ 10 \times 10^{-19} \text{ J}$

Rest masses of particles

	u	kg	MeV
Electron	$5.485\ 97 \times 10^{-4}$	9.1091×10^{-31}	0.511 006
Proton	1.002 2766	$1.672\ 52 \times 10^{-27}$	938.26
α -particles	4.001 553	6.6441×10^{-27}	3727.3

1.3 Astronomical data

Space body	Distance from sun (10^6 km)			Period of Revolution (d)	Mean radius (km)	Mass (10^{24} kg)	Mean density (Mg/m^3)	Mean on surface (m/s^2)	Orbital speed (km/s)	Gravity
	Mean	Aphelion	Perithelion							
Sun	–	–	–	–	696,000	–	1.41	274	–	–
Mercury	57.9	69.8	46.0	88.0	2420	3.167	5.46	3.72	48.8	
Venus	108.1	109.0	107.5	224.7	6261	4.870	4.96	8.69	35.0	
Earth	149.5	152.1	147.1	365.2	6371	5.975	5.52	9.78	29.8	
Mars	227.8	249.2	206.6	687.0	3389	0.639	4.12	3.72	24.2	
Jupiter	777.8	815.9	740.7	4333	69,900	1900	1.33	23.01	13.0	
Saturn	1426	1508	1348	10,760	57,500	568.8	0.71	9.14	9.65	
Uranus	2868	3007	2737	30,690	23,700	86.9	1.56	9.67	6.78	
Neptune	4494	4537	4459	60,100	21,500	102.9	2.47	15.0	5.42	
Pluto	5908	7370	4450	90,740	2900	5.37	5.50	8.0	4.75	
Moon	0.384 from Earth			27.322	1737	0.0735	3.34	1.62	1.02	

1.4 Density of gases at normal pressure and temperature 0°C in kg/m³

Air	1.293
Hydrogen	0.08988
Helium	0.1785

1.5 Parameters of earth atmosphere (relative density and temperature)

H km	ρ/ρ_0	T °K	H km	ρ/ρ_0	T °K	H km	ρ/ρ_0	T °K	H km	ρ/ρ_0	T °K
0	0	288.2	5	0.601	255.6	20	0.0725	216.7	50	0.000375	274
1	0.908	281.6	7	0.482	242.6	25	0.0332	216.7	60	0.000271	253.4
2	0.822	275.1	10	0.338	223.1	30	0.0146	230.4	100	0.32×10^{-6}	208.2
3	0.742	268.6	12	0.255	216.7	35	0.00676	244.0	200	0.295×10^{-9}	1227
4	0.669	262.1	15	0.159	216.7	40	0.00327	257.7	300	0.273×10^{-10}	1358

Specific impulse of liquid fuel (nozzle 100:0.1, seconds):

Oxygen–kerosene 372

Oxygen–hydrogen 463

Specific impulse of solid fuel (nozzle 40:0.1, seconds): 228–341.

Heat of combustion (MJ/kg):

Benzene	44	Mazut	30–41	Natural gases	42–47	Firewood	30
Diesel fuel	43	Spirit	27.2	Hydrogen	120	Peat	8–11
Kerosene	43	Bituminous coal	21–24	Acetylene	48	gunpowder	3

This page intentionally left blank

General References

(Part of these works are in <http://Bolonkin.narod.ru/p65.htm>)

1. A.A. Bolonkin, *Theory of Flight Models*, Association of Army, Air Force, and NAVY, Moscow, 1962, p. 328 (in Russian).
2. A.A. Bolonkin, "Theory of Flight Vehicles with Control Radial Force", Collection *Researches of Flight Dynamics*, Mashinostroenie Publisher, Moscow, 1965, pp. 79–118, (in Russian). International Aerospace Abstract A66-23338# (in English).
3. A.A. Bolonkin, Investigation of the Take off Dynamics of a VTOL Aircraft. Collection *Researches of Flight Dynamics*. Mashinostroenie Publisher, Moscow, 1965, pp. 119–147 (in Russian). International Aerospace Abstract A66-23339# (in English).
4. A.A. Bolonkin, "Optimization of Trajectories of Multistage Rockets", *Collection Researches of Flight Dynamics*, Mashinostroenie Publisher, Moscow, 1965, pp. 20–78 (in Russian). International Aerospace Abstract A66-23337# (in English).
5. A.A. Bolonkin, Special extreme in optimal control. Akademia Nauk USSR, Izvestiya. *Tekhnicheskaya Kibernetika*, No. 2, March–April 1969, pp. 187–198. See also English translation in *Engineering Cybernetics*, No. 2, March–April 1969, pp. 170–183 (in English).
6. A.A. Bolonkin, Solution Methods for Boundary-Value Problems of Optimal Control Theory. Translated from *Prikladnaya Mekhanika*, Vol. 7, No. 6, 1971, pp. 639–650 (in English).
7. A.A. Bolonkin, *New Methods of Optimization and their Applications*, Highest Technology University named Bauman, Moscow, 1972, p. 220 (in Russian).
8. A.A. Bolonkin, Installation for Open Electrostatic Field, Russian Patent Application #3467270/21 116676, 9 July 1982 (in Russian), Russian PTO.
9. A.A. Bolonkin, Radioisotope Propulsion. Russian Patent Application #3467762/25 116952, 9 July 1982 (in Russian), Russian PTO.
10. A.A. Bolonkin, Radioisotope Electric Generator. Russian Patent Application #3469511/25 116927, 9 July 1982 (in Russian), Russian PTO.
11. A.A. Bolonkin, Space Propulsion Using Solar Wing and Installation for It, Russian Patent Application #3635955/23 126453, 19 August 1983 (in Russian), Russian PTO.
12. A.A. Bolonkin, Getting of Electric Energy from Space and Installation for It, Russian Patent Application #3638699/25 126303, 19 August 1983 (in Russian), Russian PTO.
13. A.A. Bolonkin, Protection from Charged Particles in Space and Installation for It, Russian Patent Application #3644168 136270, 23 September 1983 (in Russian), Russian PTO.

14. A.A. Bolonkin, Method of Transformation of Plasma Energy in Electric Current and Installation for It, Russian Patent Application #3647344 136681, 27 July 1983 (in Russian), Russian PTO.
15. A.A. Bolonkin, Method of Propulsion using Radioisotope Energy and Installation for It, Plasma Energy in Electric Current and Installation for It, Russian Patent Application #3601164/25 086973, 6 June 1983 (in Russian), Russian PTO.
16. A.A. Bolonkin, Transformation of Energy of Rarefaction Plasma in Electric Current and Installation for It, Russian Patent Application #3663911/25 159775, 23 November 1983 (in Russian), Russian PTO.
17. A.A. Bolonkin, Method of a Keeping of a Neutral Plasma and Installation for It, Russian Patent Application #3600272/25 086993, 6 June 1983 (in Russian), Russian PTO.
18. A.A. Bolonkin, Radioisotope Electric Generator, Russian Patent Application #3620051/25 108943, 13 July 1983 (in Russian), Russian PTO.
19. A.A. Bolonkin, Method of Energy Transformation of Radioisotope Matter in Electricity and Installation for It, Russian Patent Application #3647343/25 136692, 27 July 1983 (in Russian), Russian PTO.
20. A.A. Bolonkin, Method of Stretching of Thin Film. Russian Patent Application #3646689/10 138085, 28 September 1983 (in Russian), Russian PTO.
21. A.A. Bolonkin, "New Way of Thrust and Generation of Electrical Energy in Space", Report ESTI, 1987, (Soviet Classified Projects).
22. A.A. Bolonkin, "Aviation, Motor and Space Designs", *Collection Emerging Technology in the Soviet Union*, Delphic Ass., Inc., Washington, 1990, pp. 32–80 (in English).
23. A.A. Bolonkin, *The Development of Soviet Rocket Engines*, Delphic Ass. Inc., Washington, 1991, p. 122 (in English).
24. A.A. Bolonkin, "A Space Motor Using Solar Wind Energy (Magnetic Particle Sail)", IAF-0615, *The World Space Congress*, 28 August–5 September 1992, Washington, DC, USA.
25. A.A. Bolonkin, "Space Electric Generator, Run by Solar Wing", IAF-92-0604, *The World Space Congress*, 28 August–5 September 1992, Washington, DC, USA.
26. A.A. Bolonkin, "Simple Space Nuclear Reactor Motors and Electric Generators Running on Radioactive Substances", IAF-92-0573, *The World Space Congress*, 28 August–5 September 1992, Washington, DC, USA.
27. A.A. Bolonkin, "The Simplest Space Electric Generator and Motor with Control Energy and Thrust", IAF-94-R.1.368, *45th International Astronautical Congress*, Jerusalem, Israel, 9–14 October 1994.
28. A.A. Bolonkin, "A High Efficiency Fuselage propeller (Fusefan) for Subsonic Aircraft", AIAA, #1999-01-5569, *1999 World Aviation Congress*.
29. A.A. Bolonkin and G.B. Gilyard, Estimated Benefits of Variable-Geometry Wing Camber Control for Transport Aircraft. NASA Center for AeroSpace Information (CASI), NASA/TM-1999-206586; H-2368; NAS 1.15:206586 , 19991001; October 1999.
30. A.A. Bolonkin and G.B. Gilyard, Optimal Pitch Thrust-Vector Angle and Benefits for all Flight Regimes, NASA Center for AeroSpace Information (CASI), NASA/TM-2000-209021; NAS 1.15:209021; H-2402 , 20000301; March 2000.

31. A.A. Bolonkin and G.B. Gilyard, Optimal Pitch Thrust-Vector Angle and Benefits for all Flight Regimes. NASA Dryden Flight Research Center, NASA Technical Memorandum, 2000-03-01.
32. A.A. Bolonkin, “Non-Rocket Space Rope Launcher for People”, IAC-02-V.P.06, *53rd International Astronautical Congress, The World Space Congress – 2002*, 10–19 October, 2002, Houston, TX, US.
33. A.A. Bolonkin, “Non-Rocket Missile Rope Launcher”, IAC-02-IAA.S.P.14, *53rd International Astronautical Congress, The World Space Congress – 2002*, 10–19 October 2002, Houston, TX, USA.
34. A.A. Bolonkin, “Inexpensive Cable Space Launcher of High Capability”, IAC-02-V.P.07, *53rd International Astronautical Congress, The World Space Congress – 2002*, 10–19 October 2002c, Houston, TX, USA.
35. A.A. Bolonkin, “Hypersonic Launch System of Capability up 500 tons per day and Delivery Cost \$1 per Lb”. IAC-02-S.P.15, *53rd International Astronautical Congress, The World Space Congress – 2002*, 10–19 October 2002, Houston, TX, USA.
36. A.A. Bolonkin, “Employment Asteroids for Movement of Space Ship and Probes”, IAC-02-S.6.04, *53rd International Astronautical Congress, The World Space Congress – 2002*, 10–19 October 2002, Houston, TX, USA.
37. A.A. Bolonkin, “Optimal Inflatable Space Towers of High Height”, COSPAR-02 C1.1-0035-02, *34th Scientific Assembly of the Committee on Space Research (COSPAR), The World Space Congress – 2002*, 10–19 October 2002, Houston, TX, USA.
38. A.A. Bolonkin, “Non-Rocket Earth-Moon Transport System”, COSPAR-02 B0.3-F3.3-0032-02, 02-A-02226, *34th Scientific Assembly of the Committee on Space Research (COSPAR), The World Space Congress – 2002*, 10–19 October 2002, Houston, TX, USA.
39. A. A. Bolonkin, “Non-Rocket Earth-Mars Transport System”, COSPAR-02 B0.4-C3.4-0036-02, *34th Scientific Assembly of the Committee on Space Research (COSPAR), The World Space Congress – 2002*, 10–19 October 2002, Houston, TX, USA.
40. A.A. Bolonkin, “Transport System for Delivery Tourists at Altitude 140 km”. IAC-02-IAA.1.3.03, *53rd International Astronautical Congress, The World Space Congress – 2002*, 10–19 October 2002, Houston, TX, USA.
41. A.A. Bolonkin, “Hypersonic Gas-Rocket Launch System”, AIAA-2002-3927, *38th AIAA/ASME/SAE/ASEE Joint Propulsion Conference and Exhibit*, 7–10 July 2002, Indianapolis, IN, USA, 2002.
42. A.A. Bolonkin, “Air Cable Transport”, *Journal of Aircraft*, Vol. 40, No. 2, March–April 2003, pp. 265–269.
43. A.A. Bolonkin, “Optimal Inflatable Space Towers with 3–100 km Height”, *Journal of the British Interplanetary Society*, Vol. 56, No. 3/4, 2003, pp. 87–97.
44. A.A. Bolonkin, “Asteroids as Propulsion Systems of Space Ships”, *Journal of the British Interplanetary Society*, Vol. 56, No. 3/4, 2003, pp. 97–107.
45. A.A. Bolonkin, “Non-Rocket Transportation System for Space Travel”, *Journal of the British Interplanetary Society*, Vol. 56, No. 7/8, 2003, pp. 231–249.
46. A.A. Bolonkin, “Hypersonic Space Launcher of High Capability”, *Actual Problems of Aviation and Aerospace Systems*, Vol. 8, No. 1(15), 2003, pp. 45–58. Kazan Aviation Institute, Kazan.

47. A.A. Bolonkin, "Centrifugal Keeper for Space Stations and Satellites", *Journal of the British Interplanetary Society*, Vol. 56, No. 9/10, 2003, pp. 314–327.
48. A.A. Bolonkin, "Non-Rocket Earth-Moon Transport System", *Advances in Space Research*, Vol. 31/11, 2003, pp. 2485–2490, Elsevier, London.
49. A.A. Bolonkin, "Earth Accelerator for Space Ships and Missiles", *Journal of the British Interplanetary Society*, Vol. 56, No. 11/12, 2003, pp. 394–404.
50. A.A. Bolonkin, "Air Cable Transport and Bridges", TN 7567, International Air and Space Symposium – The Next 100 Years, 14–17 July 2003, Dayton, OH, USA.
51. A.A. Bolonkin, "Air Cable Transport System", *Journal of Aircraft*, Vol. 40, No. 2, March–April 2003, pp. 265–269.
52. A.A. Bolonkin, "Kinetic Space Towers and Launchers", *Journal of the British Interplanetary Society*, Vol. 57, No. 1/2, 2004, pp. 33–39.
53. A.A. Bolonkin, "Optimal trajectory of air vehicles", *Aircraft Engineering and Space Technology*, Vol. 76, No. 2, 2004, pp. 193–214.
54. A.A. Bolonkin, "Long Distance Transfer of Mechanical Energy", AIAA-2004-5660, *International Energy Conversion Engineering Conference at Providence RI, USA*. 16–19 August 2004.
55. A.A. Bolonkin, "Light Multi-Reflex Engine", *Journal of the British Interplanetary Society*, Vol. 57, No 9/10, 2004, pp. 353–359.
56. A.A. Bolonkin, "Kinetic Space Towers and Launchers", *Journal of the British Interplanetary Society*, Vol. 57, No 1/2, 2004, pp. 33–39.
57. A.A. Bolonkin, "Optimal Trajectory of Air and Space Vehicles", *Aircraft Engineering and Aerospace Technology*, No. 2, 2004, pp. 193–214.
58. A.A. Bolonkin, "Hypersonic Gas-Rocket Launcher of High Capacity", *Journal of the British Interplanetary Society*, Vol. 57, No. 5/6, 2004, pp. 167–172.
59. A.A. Bolonkin, "High Efficiency Transfer of Mechanical Energy", AIAA-2004-5660, *International Energy Conversion Engineering Conference at Providence RI, USA*. 16–19 August 2004.
60. A.A. Bolonkin, "Multi-Reflex Propulsion System for Space and Air Vehicles", *Journal of the British Interplanetary Society*, Vol. 57, No. 11/12, 2004, pp. 379–390.
61. A.A. Bolonkin, "High Speed Catapult Aviation", AIAA-2005-6221, *Atmospheric Flight Mechanic Conference – 2005*, 15–18 August USA, 2005.
62. A.A. Bolonkin, "Kinetic Anti-Gravitator", AIAA-2005-4504, *41 Propulsion Conference*, 10–12 July 2005, Tucson, AZ, USA.
63. A.A. Bolonkin, "Electrostatic Solar Wind Propulsion System", AIAA-2005-3857, *41 Propulsion Conference*, 10–13 July 2005, Tucson, AZ, USA.
64. A.A. Bolonkin, "Sling Rotary Space Launcher", AIAA-2005-4035, *41 Propulsion Conference*, 10–13 July 2005, Tucson, AZ, USA.
65. A.A. Bolonkin, "Electrostatic Utilization Asteroids for Space Flight", AIAA-2005-3857, *41 Propulsion Conference*, 10–12 July 2005, Tucson, AZ, USA.
66. A.A. Bolonkin, "Guided Solar Sail and Electric Generator", AIAA-2005-3857, *41 Propulsion Conference*, 10–12 July 2005 Tucson, AZ, USA.

67. A.A. Bolonkin, "Problems of Levitation and Artificial Gravity", AIAA-2005-3365, *41 Propulsion Conference*, 10–12 July 2005, Tucson, AZ, USA.
68. A.A. Bolonkin, "Radioisotope Sail and Electric Generator", AIAA-2005-3653, *41 Propulsion Conference*, 10–12 July, 2005, Tucson, AZ, USA.
69. J.D. Anderson, *Hypersonic and High Temperature Gas Dynamics*. McGraw-Hill Book Co., New York, 1989.
70. M.L. Cosmo and E.C. Lorenzini, *Tethers in Space Handbook*, 3rd edition, Smithsonian Astrophysical Observatory, December 1997.
71. F.E. Calasso, *Advanced Fibers and Composite*, Gordon and Breach Scientific Publisher, New York, 1989.
72. *Carbon and High Performance Fibers*, Directory, 6th edition, Chapman & Hall, New York, 1995.
73. *Concise Encyclopedia of Polymer Science and Engineering*, Ed. J.I. Kroschwitz, New York, 1990.
74. M.S. Dresselhous, *Carbon Nanotubes*, Springer, New York, 2001.
75. L. Funaki, et al., "Trust Production Mechanism of Magnetoplasma Sail", AIAA 2003-4292, *34th AIAA Plasmadynamics and Lasers Conference*, 23–26 June 2003, Orlando, FL, USA.
76. R.L. Forward, "Radioisotope Sails for Deep Space, Propulsion and Electric Power", AIAA 95-2596, *31st AIAA/ASME/SAE/ASEE Joint Propulsion Conference and Exhibit*, 10–12 July 1995, San Diego, CA, USA.
77. R.L. Forward, *Indistinguishable from Magic*, Baen books, New York.
78. J.T. Harris, Advanced Material and Assembly Methods for Inflatable Structures. AIAA, Paper No. 73-448, 1973.
79. R.A. Hyde, "Earthbreak: Earth to Space Transportation", "Defense Science 2003 + Vol. 4," No. 4, 1985, pp. 78–92.
80. R.A. Hyde, "Earthbreak: A Review of Earth-to-Space Transportation", in *Energy in Physics, War and Peace. A Festschrift Celebrating Edward Teller's 80th Birthday*, Eds. H. Mark and L. Wood, Kluwer Academic Publishers, Dordrecht, pp. 283–307.
81. G.A. Landis and C. Cafarelli, The Tsiolkovski Tower Re-Examined, *Journal of the British Interplanetary Society*, Vol. 32, 1999, pp. 176–180.
82. G.A. Landis and C. Cafarelli, (1995), "The Tsiolkovski Tower", paper IAF-95-V.4.07, *46th International Astronautics Federation Congress*, Oslo, Norway, 2–6 October, 1995.
There is also an errata to this paper, which was published in *Journal of the British Interplanetary Society*: G.A. Landis, "Correction", *Journal of the British Interplanetary Society*, Vol. 58, 2005, p. 58.
83. G.A. Landis, "Compression Structures for Earth Launch," AIAA-98-3737, *24th AIAA/ASME/SAE/ASEE Joint Propulsion Conference*, 13–15 July 1998, Cleveland, OH, USA.
84. K. H. Lofstrom, "The Launch Loop", *Magazine "Analog"*, Vol. 103, December 1983, pp. 67–80.
85. K.H. Lofstrom, "The Launch Loop: A Low Cost Earth-to-High Orbit Launch System", AIAA-85-1368, *AIAA 21st Joint Propulsion Conference*, 1985. See also:
<http://www.launchloop.com/launchloop.pdf> (2002).
86. M. Minovich, "Electromagnetic Transport System for Manned Space Travel", US Patent No. 4,795,113, 3 January 1989.

87. N. Omidi and H. Karimabadi, "Electrostatic Plasma Sail", AIAA 2003-5227, 2003. 39th AIAA/ASME/SAE/ASEE Joint Propulsion Conference and Exhibit, 20–23 July 2003, Hurtisville, AL, USA.
88. G. Shortley and D. Williams, *Elements of Physics*, Prentice-Hall Inc., Englewood Cliffs, NJ, USA, 1971.
89. D.V. Smitherman, "Space Elevators". Compiled by NASA/CP-2000-210429, 2000.
90. Space Technology & Application, International Forum (1996–1997), Albuquerque, MN, Part1–3. Collection of Papers.

Russian works:

91. K.E. Tsiolkovski, "Speculations about Earth and Sky on Vesta", Izd-vo AN SSSR, Moscow, 1959; Grezi o zemle i nebe (in Russian), Academy of Sciences, USSR., Moscow, 1999, p. 35.
 92. A. Mayboroda, Zero Gravity on Earth, "Yuniy Tehnik" (Young Technician), No. 10, October 1988, Moscow (in Russian).
 93. G.I. Pokrovskii, Space Tower, TM (Technology for Youth), No. 10 1964 (in Russian).
 94. G. Poliakov, Space Necklace of Earth, TM (Technology for Youth), No. 4, 1977 (in Russian).
 95. A. Yunitskii, "General Planetary Transport System", "TM" (Technology for Youth), No. 6 1982 (in Russian).
- (see last four Rusian works in: <http://www.ipu.ru/stran/bod/ing/sovet2.htm>, Pictures: http://www.ipu.ru/stran/bod/ing/sovet_ris.htm)

NIAC reports:

96. C. Christensen, "Ultralight Solar Sail for Interstellar Travel", <http://NASA-NIAC.narod.ru>
97. S.D. Hose, "Antimatter Drive Sail for Deep Space Missions", <http://NASA-NIAC.narod.ru>
98. G.A. Landis, "Advanced Solar and Laser Pushed Lightsail Concepts", <http://NASA-NIAC.narod.ru>
99. D.W. Miller, "Electromagnetic Formation Flight", <http://NASA-NIAC.narod.ru>
100. R. Zubrin, "The Magnetic Sail", <http://NASA-NIAC.narod.ru>

Bolonkin's Papers are Presented in American Scientific Conferences 2006 or Accepted for Publications:

1. Electrostatic AB-Ramjet engine.
2. Electrostatic Linear Accelerator.
3. Electrostatic MagSail.
4. Electrostatic Solar Sail.

5. Recombination Ramjet Propulsion.
6. New Thermonuclear Reactor.
7. Ramjet Space Propulsion.
8. Organization and Economical Efficiency of Aviation/Space Researches.
9. Space Mirror for Earth Illumination.
10. Suspended Air Surveillance System.
11. Motionless Low Orbit Space Station.
12. Transfer Matter, Energy, and Thrust to Space Ships.

This page intentionally left blank

Index

Entries taken from figures are suffixed with “f” and tables with “t”

- Absorption, 231, 241, 262–263, 375
- Aerodynamic efficiency, 202, 204, 352, 354, 353, 354, 355, 369, 411, 415, 440, 441, 443, 446
- Aerodynamics, of levitated vehicles, 296
- Air bridge, 343, 345, 354–355
- Air cable transport and bridges, 341
 - advantages, 345–346
 - cable problems, 349–352
 - data, 352
 - estimation and computation, 346–349
 - installation, description of, 343–345
 - projects, 352–357
- Air drag, 194, 399
 - of double cable, 427
 - of double subsonic cable, 173–174
 - of supersonic and hypersonic double cable, 174–175
- Air energy transfer
 - air drag, of double cable, 427
 - efficiency coefficient of transfer, 427–429
 - maximum energy storage, 429
 - maximum transfer energy, 425
 - minimum energy, cable, 429
- Air friction, 49, 74, 75, 116, 142, 348
- Air gas line, 346
- Air traffic problems, 429–430
- Air vehicle, optimal trajectories, 383
- Aircraft sling launcher, 191
 - forces, 192f
- Airlines, 345
 - from New York to Paris, 353
 - from New York to Washington, 352–353
- Airplane, turning, 443–444
- Alpha particles, 310–311
 - radioisotopes, 311f
- Amount of sag, of cable, 46–47
- Anchor, 212–214
- Anderson’s equations, 48, 49, 74, 116, 142, 174
- Artificial gravity, for space ships and asteroids, 281
 - electrostatic levitation, 281, 284, 300
- Artificial moon, 325
- Artsutanov, Y.N., 2
- Artsutanov space elevator
 - construction, without rockets, 183–184
- Asteroid rubble/ships garbage, 175
- Asteroids, 8, 281
 - anchor, 212–214
 - circular velocity of ship, 215
 - connection method, 210–218
 - electrostatic utilization, for space flight, 271
 - employment, preparing for, 211f
 - meeting, probability estimation, 220–221, 279
 - as propulsion system of space ships, 209
- Astronomical data, 448
- Atmosphere, 327–328
 - composition, 328
 - layers, 328–329
 - parameters, 249
- Attenuation coefficient, 231, 375

- Aviation, 359
 and energy air transfer, 230
 fuel, 345, 353
- Ball charge
 blockading, 250–251, 279–280
 electrical energy expenditure, 277–278,
 323
- Ball cover
 particles absorption by, 262–263
 thickness, 256–258, 278, 324
- Ball mass, 256–258, 278, 324
- Ball stress, 256–258, 278, 324
- Ballistic Research Laboratory, 126–127
- Ballistic trajectory, 402–403, 411
- Base stations, 3
- Beam, focusing, 228f, 232, 239, 306, 334
- Beam attenuation
 absorption, 231
 scattering process, 231
- Beam power, change, 231
- Beam transfer, 226, 241
 in multi-reflex launching, 230
 space beam transfer, 228–230
- Bridge, 2, 342f, 345
- Cable air drag, 173–175
 energy, 51
- Cable friction, 48, 49–50
 estimation, 74–75, 114–117, 348–349
- Cable launcher
 advantages, 41
 amount of sag, 46–47
 cable friction, 48, 49–50
 cable mass, 50–51
 energy
 for cable air drag, 51
 for rotary flywheel, 46
- flight range, 47
- last drive station, 54–55
- maximum distance, 46
- relative cross-section area, 42–45
- safety cable speed, 46
- speed loss, 48
- subsonic speed, 51
- wave drag, 47
- Cable mass, 50–51, 150, 151, 215, 218
- Cable News Network, 84
- Cable problem, 31–32, 67, 368, 429
- Cable space accelerator, 39
 cable launcher, 42
 launcher, description of, 40–42
 projects, 55–58
- Cable system characteristics, data for
 estimation, 151–154
- Cable transport system, 4–5, 8
 Earth–Mars, 157–163
 Earth–Moon, 147–155
- Cable volume, 151, 160
- Cannon wing projectiles, 403
 optimal trajectories, 416–418
- Carbon nanotubes (CNT), 4
- Cardioids, 212, 213f
- Cell mirrors, 225, 226–227, 241
- Centrifugal force, 193
- Centrifugal space launchers, 8, 187
 innovative launcher, description of,
 189–193
 projects, 197–205
 sling launcher, 193–197
 space elevator, 188–189
- Centrifugal theory, for kinetic anti-
 gravitator, 171–172
- Charged ball
 and charged asteroid, interaction, 274f
 charging, 264–265, 279, 298
 electric intensity, 252, 254f, 283
 electrical energy expenditure, 263–264,
 277–278, 323
- energy accumulator, 298–299
 rocket engine, 300–301
- on high mast/tower, 300
 minimum neutral sphere around, 253
- Circle launcher, 59
 case studies, 75–80
 description, 61–67
 and space keeper, 59
 and space transport system, 62f
 theory, 67–75
- Circular velocity of ship, asteroid, 215
- Clarke, Sir Arthur, 2, 84
- Climb regime, 442–443
- Climbers, 4
- Closed-loop cable circle
 full lift force, 72f
 maximum speed, 71f
- Cone, flight angle, 194–196
- Connection method, 210–218
 equipment, probe trajectory
 change, 211
 theory and computation, 214–218
 utilization, description of, 211–214
- Constant flight pass angle, optimal engine
 control, 405–406
- Constant gravity field
 lift force, 112

- maximum tower height, 113, 114f
 minimum cable speed, 113, 114f
 repulsive force, 172
- Corona* *see* Electric corona
- Cosmos 1, 318
- Coulomb's force, 252
- Counterweight, 2, 4
- Cover mass, of inflatable space towers, 91
- Cover thickness, of inflatable space towers, 91
- Cruise regime, 438–441
- Cumulonimbus, 300
- Current aircraft, optimal trajectory, 418
- Current typical cannons, properties, 416t
- Cylindrical lifting belt, 294–296
- Cylindrical tube, half-life, 290
- Delivery cost, hypersonic launcher, 138
- Descent regime, 442–443
- Double cable, air drag, 63–64, 173–175, 427
- Earth–Mars cable transport system, 157–163
 description, 158–159
 equal stress cable theory, 159–160
 project, 160–162
- Earth–Moon cable transport system, 147
 description, theory and innovations, 148–150
 history, 147–148
 optimal cable, 150–151
 projects, technical parameters, 151–154
 theory, 150–151
- Efficiency coefficient, 232, 427–429
- Electric charge, 285
 half-life, 290
- Electric corona, 285
 corona size, 286–287
 discharging, 288–289
 radius, 287
 safe electrical intensity, for ball, 286–287
- Electric intensity, charged ball, 252, 283, 286
- Electric power, 312–313
 heating, 313
of IsoSail, 314–315
- Electrical energy expenditure, to ball charge, 263–264, 277–278, 323
- Electrical units, 447–448
- Electrodynamic tethers, 34, 35, 36
- Electro-generator and radioisotope space sail, 309–315
- Electronic sail, 334–335
 innovation, description of, 335
- Electrostatic accelerators, 264–265
- Electrostatic force, between charged bodies, 252, 273–274
- Electrostatic levitation, on Earth
 artificial gravity, for space ships and asteroids, 281
- between flat net and ground surface, 290–291
- highway, 299
- innovation, description of, 282–284
- in low cumulonimbus and thunderstorm clouds, 300
- projects, 299–301
- of train, 291
- tube highway, 300
- Electrostatic lift force, 282
 ball material, data, 289
 charged ball, energy accumulator, 298–299
 charging, 298
 control and stability, 298
 cylindrical cable/belt, 287
 cylindrical lifting belt, 294–296, 297f
 electric charge, 285
 half-life, 290
 electric corona, 285, 286–287, 288–289
 electrical field, 285
 insulator, rupture, 290
 levitated vehicles, aerodynamics, 296
 safety, 298
 small spherical lifting balls, 293–294
 spherical main ball and air balloon, 292–293
 thunderstorms, flight, 298
 top tube highway, 291–292
- Electrostatic sail drag, 255–256, 257f
- Electrostatic solar sail, 317–325
 advantages, 319–320
 artificial moon, 325
 ball cover thickness, 324
 ball mass, 324
 ball stress, 324
 electrical energy expenditure, to ball charge, 323
 innovations, description of, 318–320
 technology, 324
- Electrostatic solar wind propulsion, 245
 absorption of particles, by ball cover, 262–263
- ball, charging, 264–265
 ball charge, blockading of, 250–251
 ball cover thickness, 258
 ball discharge, 249–250
 ball mass, 258

- Electrostatic solar wind propulsion (*contd*)
 ball stress, 256
 charged ball, minimum neutral sphere
 around, 253–255
 comparison, 265–266
 description, 247–251
 electrical energy expenditure, ball
 charge, 263–264
 electrostatic sail drag, 255–256
 interstellar propulsion system, 251
 limitations, 265
 probe acceleration, 259
 probe flight time, 259
 probe speed, 259
 space propulsion system, 247, 248f
 steerability, 247–249
 theory, 252–253
 thermonuclear propulsion, 264
- Electrostatic space radiator, 336–337
- Electrostatic utilization
 of asteroids, 271–280
 description, 272–273
 theory and computation, 273–278
- Energy, 138–140, 251, 298, 367
 for cable air drag, 51
 generator, 303–307
 for rotary flywheel, 46, 348
 transfer, 223
- Energy accumulator, 181, 182
 charged ball, 298–299, 300–301
 flywheel, 41, 42, 110, 193
 gas tube hypersonic launcher, 140–141
- Energy generator and solar sail, 303–307
- Energy storage, 80, 145, 249
- Energy transfer, 229–230
 air transfer, 230, 425–429
 beam energy transfer, 230f
 space energy transfer, 8, 229f
- Energy transferor, 424–425
 advantages, 430
- Engine, 8, 30, 41, 110, 144, 344, 369, 405–406
 conventional, 108, 167–168, 189
 light multi-reflex, 371
 ramjet, 396–397
 rocket, 127, 129, 159, 300–301, 392,
 395–396
 space jet propulsion, 327–330
 thermonuclear, 264, 265
 turbo-jet, 392–393
- Engine power, 116–117, 196
- Equilibrium equations, 159–160, 439, 442
- Excess energy, hypersonic launcher,
 138–140
- Fiber, 32, 56, 87–88, 197–199
- Filling gas, for inflatable space towers,
 85–87, 88f
- Fixed wing space vehicle, optimal
 trajectory, 410–411
- Flight
 in thunderstorms, 298
 vehicle mass and path angle, change of,
 386–388
- vehicles
 optimal fuel consumption, 408f
 trajectory, 410f
- Flight range, estimation, 47
 subsonic aircraft, with thrust, 403–405
 without thrust, 401–403
- Flight regimes, 432–433
- Flying superman, 180, 181f
- Flywheel, 46, 57, 180, 189, 196, 348, 429
- Free round trip to Mars, delivery system,
 24–29
- Free trip to Moon, 29–31
 technical parameters, 31
- Free trip to space
 delivery cost, 24
 description, 8–10
 installation costs, 23–24
 space elevator, transport system, 21–23
 theory and computation, 10–21
- Fuel, 139, 345, 368
 consumption optimization, 408–410
 injection programs, for launch system,
 129
- Full lift force, of closed-loop cable circle, 72f
- Gas density, 449
- Gas filling, 85–87
- Gas friction, hypersonic launcher, 142–143
- Gas laser, 372
- Gas line, 356–357
- Gas mass, into inflatable space towers,
 91–92
- Gas pressure, for inflatable space towers, 89
- Gas tube hypersonic launcher, 125
 delivery, production cost of, 138
 description, 127–129
 as energy accumulator, 140–141
 excess energy, 138–140
 gas friction, 142–143
 gun recoil, 141
 high-speed gun, history, 126–127
 load delivered to orbit, 136–137
 missile velocity estimation, 129–132
 space launcher, advantages, 143–145

- tube curvature, 142
- tube length estimation, 132–134
- tube wall thickness, 142
- velocity loss, in atmosphere, 135–136
- Geostationary Earth orbit (GEO), 2, 84
- Geosynchronous orbital tether, 2
- Ground sling launcher, 189–190
 - centrifugal catapults, conventional, 190
- Ground vehicles, 355–356
- Gun recoil, hypersonic launcher, 141
- Gun system, 143–144

- Half-life
 - of charge, 290
 - of cylindrical tube, 290
- High aerodynamic efficiency, 369
- High-altitude crane, 183
- High-altitude mirror, utilization
 - innovations, advantages of, 330
 - local Earth areas, lighting, 330–334
 - method and innovations, description of, 331–334
- High efficiency transfer, of mechanical energy, 230, 423
- High-power weapons-class lasers, 372–373
- High-speed catapult aviation, 359
 - advantages, 365, 367
 - innovation, description of, 360–361
 - KV and flight data estimation, 361–365
 - problems, 368–369
- High-speed gun, history, 126–127
- High tower, 183
- Horizontal flight
 - OTA vector, 438–441
 - in subsonic speed, with thrust, 403–405
- Horizontal turn, of kinetic air vehicles, 364–365
- Hypersonic launcher *see* Gas tube launcher
- Hypersonic glider, 395–396
- Hypersonic speed, 74, 394–397
 - in optimal wing area, 399–400
 - ramjet engine, 396–397
 - rocket engine/hypersonic glider, 395–396
- Hypersonic trajectory, 401

- Inflatable space towers *see* Optimal inflatable space towers
- Innovative launcher, description
 - advantages, 191, 193
 - aircraft sling launcher, 191, 192f
 - ground sling launcher, 189–190
 - shortcomings, 193

- Insulator, rupture of, 290
- Interstellar propulsion system, 251
- Ionosphere, 328–329
 - regions, 329
 - structure, 329
- IsoSail, conventional, 313–315
 - electric power, 314–315
 - heating, 315

- Jumping superman, 181
- Jumping vehicle, 181–182

- Kapton, 304, 331
- Kinetic air vehicles, average speed of, 364, 365f
- Kinetic anti-gravitator, 165
 - advantages, 179
 - applications, 179–184
 - installation, description of, 167–171
 - and Loftstrom installation, differences, 184–185
 - theory, 171–178
- Kinetic lift force, variable gravity field and rotary Earth, 113–114
- Kinetic space towers, 107
 - cable friction estimation, in air, 114–117, 118f–119f
 - lift force, 111–112
 - under constant gravity field, 112
 - under variable gravity field, 113–114, 115f
 - launcher, description of, 108–111
 - maximum height/minimum cable speed, 113, 114f
 - people security, 117–119
 - projects, 121–122
- Kinetic vehicles (KV)
 - average speed, 364, 365f
 - horizontal turn, 364–365, 366f
 - maximum acceleration, 362–363
 - maximum range, 361–362
- Krupp gun, 126

- Laminar boundary layer, 49, 74, 114–116
- Landing, 32, 41, 369, 430
 - OTA, 435, 437–438, 439f
- Laser beam, 4, 223–224, 225, 305, 372
 - long-distance transfer, 228f
- Laser ring, 241, 225–226, 227
- Last drive station, 54–55
- Launcher
 - advantages, 41–42
 - aircraft sling, 191

- Launcher (*contd*)**
- centrifugal space, 187
 - circle, 59, 61
 - as energy accumulator, 140–141
 - gas tube hypersonic, 125
 - installation, 40–41
 - thermodynamic diagram, 139f
- Levitated vehicles, aerodynamics**, 296
- Lift force**
- in constant gravity field, 112
 - electrostatic lift force, 285
 - of kinetic tower, 111–112
 - tower lift force, 90
 - in variable gravity field, 113–114
- Light and light devices**, 224–225, 372–373
- laser beam divergence, 225
- Light engine**, 225, 372
- and sloping reflective cells, 375f
- Light lock**, 226f, 227–228, 373–374
- Light multi-reflex engine**
- history, 371–372
 - innovation, description of, 373–375
 - light and light devices, 372–373
 - theory, 375–381
- Light pressure**, 305, 376–377
- multi-reflex, 231–232, 372
- Light reflection method**, 224
- Light sail**, 304
- design, 305f
- Lishanski, G.**, 171
- Load delivered to orbit**, 136
- Local air friction**, for two-sided plate, 49–50, 74, 116, 142–143, 174
- Loftstrom installation, space launcher**, 184–185
- Long arm/hand**, 182
- Long cylindrical lifting belt**, 294–296
- Lorenz force law**, 252
- Mars transport system, technical parameters of**, 25–29
- Massachusetts Institute of Technology (MIT)**, 298
- Maximum acceleration**, of kinetic vehicles, 362–363
- Maximum distance**, of cable, 46
- Maximum range**, of kinetic vehicles, 361–362
- Maximum safety bending moment**, for inflatable space towers, 91
- Maximum tower height**, in constant gravity field, 113, 114f
- Maximum transfer energy**, 425
- Mechanical energy**
- air energy transfer, 425–429
 - air traffic problems, 429–430
 - building problems, 429
 - cable problem, 429
 - high-efficiency transfer, 423
 - innovation, description of, 424–425
- Mechanical units**, 447
- Mesosphere**, 328
- Minimum cable speed**, in constant gravity field, 113, 114f
- Missile Defense Agency/USAF Airborne Laser (ABL) program**, 372–373
- Missile velocity**, estimation, 129–132
- Moon's trajectory, eccentricity**, 31
- Motion of charged particles**, 252
- Multi-bounce sail**, 240–242
- Multi-reflection system**, 374f
- Multi-reflex engine**, 230, 242, 375–381
- Multi-reflex launching**
- and beam transfer, 230–240
 - installation of space vehicle, 225–228
- Multi-reflex light pressure**, 231–232, 372
- Multi-reflex propulsion systems**
- and energy transfer, 223
 - history, 223–224
 - innovation, description of, 225–230
 - launching and beam transfer, theory, 230–240
 - light and light devices, 224–225
 - for space and air vehicles, 223
 - tasks, 225
- Multi-stage kinetic tower**, 109f
- Mylar**, 304, 331
- Nanotubes**, 32, 41, 430
- NASA**, 304
- National Oceanic and Atmospheric Administration (NOAA)**, 304
- Natural space body**, 211–212, 272
- Non-rocket space apparatus**, 180
- Non-rocket transport system**, 160–162
- One winged cabin**, 352
- Optimal cable**, 150–151, 214
- cable equal stress, 214–215
 - cross-section area, along launch distance, 41f
- Optimal cable theory**, from Earth to Moon
- cable mass, 151, 152f, 153f, 154f
 - cable volume, 151
 - equations, 150–151

- Optimal cover thickness and radius, of inflatable space towers, 89–90
- Optimal engine control, for constant flight pass angle, 405–406
- Optimal fuel consumption, of flight vehicles, 408f
- Optimal inflatable space towers
 - applications, 84–85
 - base area, for top load, 90
 - base radius, 92
 - construction, 89
 - cost, 89
 - cover mass, 91
 - cover thickness, 91
 - Earth's distance, 92
 - filling gas, 85–87
 - gas mass into tower, 91–92
 - gas pressure in column versus altitude, 89
 - history, 83–84
 - lift force, 90
 - mass, 92
 - mass of cover, 91
 - material, 87–88
 - maximum safety bending moment, 91
 - optimal cover thickness and tower radius, 89–90
 - projects, 92
 - safety, 88
 - stability, 89
 - structure, 85
- Optimal relative sling cross-section area, 193–194, 195f
- Optimal thrust angles (OTA), 431
 - airplane, turning, 443–444
 - climb and descent regimes, 442–443
 - methodology, 433–435
 - takeoff and landing, 435–438
 - vector in horizontal flight, 438–441
- Optimal trajectory
 - of air and space vehicles, 383, 410, 418f
 - for air vehicle
 - climb and flight, 389f
 - descent and flight, 390f
 - cannon wing projectiles, application, 416–418
 - current aircraft, application, 418
 - for fixed wing space vehicle, 410–411
 - flight, vehicle mass and path angle, 386–388
 - flight range estimation, 401–405
 - general equations, 385–386
 - necessary condition, 391
- optimal engine control, constant flight pass angle, 405–406
- optimal wing area, 397–400
- path angle and fuel consumption, 408–410
- rocket vehicles and missiles, application, 410–416
- solution, 406–408
- statement of problem, 388–397
- Optimal variable diameter cable, 148–149
- Optimal wing area, 397–400
 - hypersonic speed, 399–400
 - subsonic speed, 398–399
- Path angle and fuel consumption, optimization, 408–410
- Payload, 128–129, 144
- Pearson, J., 2
- People security, 117–119
- Performance index, 434, 435, 442, 433, 443
- Physical constants, 448
- Piezoelectric plate, 227, 229, 374
- Piston and turbo engines with propeller, subsonic speed, 394
- Pogo-stick *see* Jumping superman
- Prism, 226, 373, 374
- Probability estimation, of meeting asteroid, 220–221
- Projectile, 48
 - launcher, sling, 197–199
- Projects
 - in air cable transport and bridges, 352–357
 - in asteroids, 218
 - in cable space accelerator, 55–58
 - in centrifugal space launchers, 197–205
 - in circle launcher and space keeper, 75–80
 - in Earth–Mars cable transport system, 151–154
 - in electrostatic levitation, on earth, 299–301
 - in high-speed catapult aviation, 367–368
 - in kinetic space towers, 121–122
 - in optimal inflatable space towers, 92
 - in space elevator, 8–31
- Propulsion system
 - asteroids, 209
 - electrostatic solar wind propulsion, 245
 - interstellar propulsion system, 251
 - multi-reflex propulsion systems, 223–240
 - recombination space jet propulsion engine, 327–330

- Propulsion system (*contd*)
 space jet propulsion, 327–330
 space propulsion system, 247, 248f
 thermonuclear propulsion, 264
 Push force, for immobile object, 171–173
- Radar, 210
- Radioisotope space sail
 conventional IsoSail, equation, 313–315
 description of method and innovations, 309–310
 electric power, possibility, 312–313
 and electro-generator, 309–315
 improvements, 312
 innovations and advantages, 311–312
 Ramjet engine, hypersonic speed, 396–397
- Recombination space jet propulsion
 engine
 atmosphere, 327–328
 composition, 328
 layers, 328–329
 innovation, description of, 329–330
- Reflection number, limitation, 232
- Relative cable mass, 215, 216
- Relative cross-section area, of cable, 42–45
- Repulsive force, 167–168, 169, 227, 373
 in constant gravity field, 172
 creating methods, 281
 for mobile object, 173
 in space, without gravitation, 171–172
 in variable gravity field and rotary Earth, 172–173
- Restore force, 173
- Rocket engine, 202, 203, 212, 300–301, 400
 subsonic speed, 392
 hypersonic speed, 395–396
- Rocket payload, increasing, 415
- Rocket vehicles and missiles, application, 410–416
 fixed wing space vehicle, optimal trajectory, 410–411, 412f
 variable wing space vehicles, 411, 413f–415f
- Rope circle usage, as propulsion system, 65f
- Rotary earth
 kinetic lift force, 113–114
 repulsive force, 172–173
- Rotary energy, of rotating asteroid, 214f
- Rotary flywheel, 46, 348
- Rotovators, 35–36
- Safety cable speed, 46
- Sag, of cable, 46–47
- Sea space elevator, 4f
- Semi-circle launcher and transport system, 63f
- Shuttle, 48, 136, 206, 368, 369
- Sling launcher, 189, 200, 204, 205
 air drag, 194, 195f
 aircraft sling launcher, 191, 192f
 centrifugal force, 193
 cone, flight angle, 194–196
 engine power, 196
 forces, 192f
 ground sling launcher, 189–190
 optimal relative sling cross-section area, 193–194, 195f
 tourist trajectory, estimation, 196–197
 vacuum, 196
- Slingaton launcher, 205
- Sloping reflective cells and light engine, 375f
- Small spherical lifting balls, 293–294
- Smitherman, D., 2
- Solar cells *see* Light sail
- Solar light pressure, 314, 317, 335
- Solar mirror, 331, 333f
- Solar sail, 223, 317, 334
 conventional, 318
 electronic solar sail, 335
 innovation, 303, 305–306
 method and innovations, description of, 303–305
- Solar wind electron and negatively charged ball, minimum distance, 252
- Solar wind, 246–247, 279, 329, 335
see also Electrostatic solar wind
 propulsion
- Space anchor, 213–214
- Space apparatus, 109, 175, 180, 212–213
 charging, 272, 273
 electrostatic maneuvers, 272f, 273f
 launching and landing, 278
 trajectory, 211, 212, 214, 272, 274–277
- Space beam transfer, 228–230
- Space bridge *see* Space elevator
- Space elevator, 3f, 39, 61, 148, 163, 183–184, 188–189, 209
 cable problems, 31–33
 data for computation, 33
 description, 2–5
 free round trip to Mars, delivery system, 24–29
 free trip to Moon, 29–31

- free trip to space, 8
- history, 1–2
- innovations, objective, 8
- tether system, 34–36
- transport system for, 5–8
- Space flight, 210, 246, 271
 - trajectory, 192f
- Space jet propulsion, 327–330
- Space launcher, 40, 110, 122, 226f
 - advantages, 143–145
 - centrifugal space launcher, 8–9, 187
 - with gas rocket and rocket nozzle, 128f
 - Loftstrom space launcher, 184
- Space mirror, 330, 335
 - conventional, limitations, 333–334
 - current design, 331, 333
 - history, 331
 - innovations and advantages, 334
 - solar mirror, 331, 333f
- Space projectile launcher, with whisker sling, 199–200
- Space propulsion system, 61, 247
 - light, reflecting, 371
- Space suit
 - innovation, description of, 335–336
- Space tourism/scientific laboratory, projects, 75–80
 - economic estimations, 77–78, 79
- Space tourists launcher, sling
 - from nanotubes, 200–202
 - from whiskers, 202–205
- Space vehicle
 - additional velocity, from asteroid, 216–218
 - multi-reflex launch installation, 225
 - cell mirrors, 226–227
 - laser ring, 226f, 227
 - light lock, 226f, 227–228
 - optimal trajectories, 383
 - fixed wing, 410–411
 - variable wing, 411–415
 - tourist trajectory, estimation, 196–197
- Space utilization
 - electronic sail, 334–335
 - electrostatic space radiator, 336–337
 - high-altitude mirror, 330–334
 - recombination jet propulsion engine, 327–330
 - space suit, 335–336
- Speed loss
 - of cable, 48, 49f
 - see also* Velocity loss
- Spherical air balloon, 292–293
- Spherical ball, 290, 293–294
- Spherical main ball, 292–293
- Stratosphere, 328
- Subsonic speed, 391–394
 - of cable, 51
 - in optimal wing area, 398–399
 - piston and turbo engines, 394
 - rocket engine, 392
 - with thrust, 403–405
 - turbo-jet engine, 392–393
- Subsonic trajectory, 402
- Support wings, 344
- Surface transport system, 346
- Takeoff, OTA, 435–438
- Technical parameters
 - cable system characteristics, estimation, 151–154
 - for free trip to Moon, 31
 - for Mars transport system, 25–29
 - for space elevator, transport system, 21–22
- Tensile strength, 3, 4, 32, 33f, 56, 57, 58, 64, 81
- Tesla, N., 1
- Tether system, 148
 - description, 34–36
 - electrodynamic tethers, 35
 - problems, 36
 - rotovators, 35–36
 - space elevators, 36
 - for space vehicles, 147–148
 - tidal stabilization, for altitude control, 35
- Thermodynamic diagram, of launcher, 139f
- Thermonuclear propulsion, 264
- Thermosphere *see* Ionosphere
- Three winged cabins, 353
- Thrust/drag, 247–248, 249f, 256
- Thunderstorms, flight, 298, 300
- Tidal stabilization, for altitude control, 35
- Top tube highway, 291–292
 - tube lift force, 292
- Total internal reflection, 227, 373
- Tourist trajectory, estimation
 - ballistic part, 197
 - vertically accelerated part, 196–197
- Tower cover thickness, in inflatable space towers, 91
- Tower of Babel, 83–84
- Trajectory change, of space vehicles, 7, 209, 211, 272
- Transfer system, 424
 - mechanical energy, transferor, 424f

- Transport system, for space elevator, 5–8, 9f
 - roller, 10f
 - rope length change, mechanisms for, 10f
- Tropopause, 328
- Troposphere, 328
- Tsiolkovsky, K.E., 1, 84
- Tsiolkovsky's tower, 1
- Tube curvature, hypersonic launcher, 142
- Tube highway, levitating, 300
- Tube length, estimation, 132–134
- Tube wall thickness, hypersonic launcher, 142
- Turbo-jet engine, subsonic speed, 392–393
- Turbulent
 - drag, 49, 74, 114–116
 - flow, 49, 50, 74
- Turbulent boundary layer, 74
 - in cable friction, 49, 74, 114–116
- Underground tunnel, 345
- Vacuum, 196
- Variable cable spool, 110f
- Variable gravity field
 - kinetic lift force, 113–114
 - repulsive force, 172–173
- Variable wing designs, variants, 420f
- Variable wing space vehicles, 411
- Vehicle forces and coordinate system, 386f
- Vehicle heating, 368–369
- Vehicle mass and path angle, change of in flight, 386–388
- Velocity loss
 - in atmosphere, 135–136
 - see also* Speed loss
- Vertical takeoff and landing (VTOL), 179–180
- Walking superman, 181
- Wave drag, of cable, 47
- Whiskers, 5, 32, 33f, 179, 199, 202–203, 205, 368
- X-prize flight, 191, 205
- X-rays, 232, 329, 372, 377
- Young's modulus, 22, 32, 33